2-Channel Kondo Scaling in Metal Nanoconstrictions — a Conformal Field Theory Calculation of Scaling Function

A Dissertation

Presented to the Faculty of the Graduate School

of Cornell University

in Partial Fulfillment of the Requirements for the Degree of

Doctor of Philosophy

by

Jan von Delft

August 1995

2-Channel Kondo Scaling in Metal Nanoconstrictions — a Conformal Field Theory Calculation of Scaling Function

Jan von Delft, Ph.D.

Cornell University 1995

This thesis is concerned with experiments done by D.C. Ralph and R.A. Buhrman [RB92,Ralph93] at Cornell University on zero-bias anomalies in conductance signals through metal nanoconstrictions. They have suggested that their data is in accord with the assumption that conduction electrons interact with two-level tunneling systems in the constriction region according to the non-magnetic 2-channel Kondo model.

We quantitatively analyze their data within the theoretical framework of the 2-channel Kondo model, in the regime of very low temperatures (T) and voltages (V). This regime is governed by the strong-coupling $T = V = 0$ fixed point of the 2-channel Kondo model, at which the exact conformal field theory solution of Affleck and Ludwig [AL93] applies.

Near the strong-coupling fixed point, the conductance $G(V,T)$ is predicted [RLvDB94] to obey the following scaling relation:

$$\frac{G(V,T) - G(0,T)}{T^{\alpha}} \;=\; B\,[\Gamma(Ax) - 1] \;\; .$$

Here $\Gamma(x)$ is a universal scaling function, and the universal exponent α is predicted to have the value $\alpha = \frac{1}{2}$. We show that the data of Ralph and Buhrman indeed obey the above scaling relation, with $\alpha = 0.5 \pm 0.05$; this we take as strong evidence that their samples can plausibly be described by a simple one-dimensional 2-channel Kondo model.

The bulk of this thesis is concerned with analytically calculating $\Gamma(x)$, which is a "fingerprint" of the 2-channel Kondo problem, in order to compare it to experiment.

Conceptually new is our treatment of non-equilibrium effects: we show that Hershfield's formulation of non-equilibrium problems [Hers93] can be combined with Affleck and Ludwig's conformal field theory approach to deal with the $V \neq 0$ situation.

When our results for $\Gamma(x)$ are combined with recent numerical (NCA) results [HKH94] for the same model, good quantitative agreement with the data is obtained, indicating that *the 2-channel Kondo model is in accord with* ***all*** *experimental facts*. However, the theoretical justification for the model employed here has recently been called into question [MF95,WAM95], indicating that more theoretical work is needed before the experiment can be regarded as completely understood.

The thesis contains six lengthy appendices, intended as a pedagogical introduction to Affleck and Ludwig's conformal field theory solution of the Kondo problem.

Biographical Sketch

The author was born in 1967 in Bloemfontein, South Africa, where he spent the first 23 years of his life. He obtained a B.Sc. degree in Physics and Mathematics (1987) at the University of the Orange Free State, and a B.Sc. honours (1988) and M.Sc. (1990) degrees in Theoretical Physics from the University of Stellenbosch. The next five years were spent in the United States, where he obtained his Ph.D degree in Theoretical Physics at Cornell University in August 1995. He is currently a post-doc with the group of Prof. G. Schön in Karlsruhe, Germany.

Für meine Eltern, und Karin

Acknowledgments

I would like to sincerely thank Prof. Vinay Ambegaokar for agreeing to be my thesis supervisor, and for the way in which he approached this task. His ability to recognize an experimental phenomenon as interesting and worthy of theoretical study long before it is understood in any detail has served me beyond all expectations: the thesis topic that he suggested to me required a detailed analysis of a recent experiment and intensive interactions with experimentalists, as well as learning and applying theoretical techniques of an unexpected variety and sophistication; in short, it was a "dream topic". I am particularly grateful for the freedom he allowed me to learn and apply conformal field theory to the present problem, despite the fact that "the real world is three-dimensional", but at the same time for his persistent reminders, when my detours into abstract field theory threatened to become a goal unto themselves, that the ultimate goal should be to understand the phenomenon in the lab. His credo, "follow the phenomenon", has made a lasting impression on me.

Apart from the very many hours he devoted to discussions of our research (in particular, trying by example to develop my underdeveloped physical intuition) he has also helped me significantly in a number of non-thesis related ways, including financial support for conferences, and helping to keep my duties as a teaching

assistant light. Finally, I greatly profited from his German connection: I am very grateful for his help in arranging visits at several German universities early in 1994, which ultimately lead to my current position as a post-doc in Karlsruhe.

Of the five most memorable dinners I have enjoyed in Ithaca over the last few years, Vinay's wife Saga has been responsible for at least four; I thank them both for their hospitality in this regard!

I owe many sincere thanks to Prof. Andreas Ludwig, who during the last two years has in effect taken on the role of a second thesis advisor to me. His successful prediction that the experiment studied here should show scaling behavior, and that this could be studied quantitatively using his conformal field theory solution of the Kondo problem, lies at the heart of this thesis. I am very thankful for his offer to collaborate with him to pursue his ideas, and for the large amounts of time and money (financing a substantial number of visits to Princeton) that he invested in this collaboration. I would never have been able to learn the requisite conformal field theory without his detailed and patient explanations (that often lasted until long after midnight!). His ability to find a way around, or if necessary cut right through the most formidable technical complications has impressed me deeply, and played a major role in working out the ideas presented in this thesis.

I thank my experimental colleagues Dan Ralph and Prof. Bob Buhrman for performing such an exciting experiment, and for their patience in explaining to a theorist the intricacies of the real world. Dan has particularly impressed me with his attention to detail, both experimental and theoretical (on more than one occasion, I learned some theory from him!), and with the care in which he weighed *every single word* in the paper we wrote together. To me, he is the

personification of the "ideal experimental collaborator".

My colleagues Matthias Hettler, Hans Kroha and Selman Hershfield deserve many thanks for studying the model employed in this thesis with a different method. Without their results, which are in quantitative agreement with experiment and play an important part in the interpretation presented here, our arguments would loose half their force. I particularly thank them for their permission to use unpublished figures of their results in my thesis.

The research reported here was partially supported by the MRL Program of the National Science Foundation, Award No. DMR-9121654, and Award No. DMR-9407245 of the National Science Foundation.

I would like to thank Prof. Chris Henley for supervising my work on the quantum tunneling of spin systems during the academic year 1992-1993; I found this research very exciting and rewarding, and particularly profited from his tireless efforts to improve the readability of the two papers we wrote together. I am also grateful that he agreed to serve on my committee, gave me an A-exam question directly relevant to my research, and for the care with which he read my thesis.

Likewise, I would like to thank Prof. Jeevak Parpia for serving on my committee, posing an A-exam question related to my research, and involving me in one of his projects as well. Thanks also go to Professors A. LeClair and R. Buhrman for reading my thesis and attending my B-exam.

I am very grateful to Prof. Gerd Schön for very graciously giving me complete freedom to write the appendices to my thesis in Karlsruhe after leaving Cornell, even though the need for this exercise might have seemed mysterious to any observer (including, at times, the author).

I have benefited from discussions with a large number of physicists, including N. Wingreen, D. Fisher and M. Moustakas, whose recent criticism of our work has made matters even more interesting than they seemed; A. Zawadowski, who spent an entire Sunday afternoon answering my endless questions about his model; P. W. Anderson, C. Bruder, S. Coppersmith, T. Costi, K. Dahmen U. Eckern, V. Elser, B. Halperin, K. Ingersent, B. Janko, B. Jones, Y. Kanter, Y. Kondev, R. Konik, A. LeClair, D. Mermin, B. Roberts, A. Rosch, R. Smith, G. Schön, J. Sethna, H. Tye, P. Wölfle, Z. Zimanyi and N. Zimmerman.

I thank my South-African friends Jannie Engelbrecht and Hans Eggers for their advice to follow their example and study in the United States. So far, it has been by far the best career advice I have ever gotten!

The staff in Clark Hall, in particular Deb Hatfield, Douglas Milton and Cindy LeFever, deserve thanks for their help in many administrative tasks.

Over the years, my various officemates have contributed substantially to making life at Cornell an unforgetable experience. In particular I would like to mention Rob Pelak, Barry Winter, Jennifer Hodgdon, Joel Shore, Ragu, Tom Lenosky and Qing Sheng. I have particularly fond memories of my last office, which I shared with Ron Lifshitz, Yané Kondev and Claudia Filippi. Yané's help in conformal field theory deserves special mention. Yakov Kanter and Chen-Yang Tan, comrades in the struggle to pass Quantum II and 510, could always be trusted to solve any math or computer problem, respectively.

I spent many enjoyable hours of chamber music in the company of Susan Stolovy, Sarah Peach, Katerina Hur, Persis Drell and her husband Jim Welch. Olga and Sara Perkovic, Karin Dahmen, Rineke Coumans and Nicole Vogt, Yané

Kondev, Jens Knobloch and Bill Wedemeyer shared in the fun of discovering the joys of dancing, as did the incomparable tanguero, Thomas Baumgarte.

My two roommates Bill Wedemeyer and Thomas Baumgarte became much more than that, and were invaluable in helping me to deal with some of life's tougher aspects. I owe them many thanks. I also thank Bill for proofreading part of my thesis.

My dear friend Karin has enriched my life in innumerable ways; I thank her for her friendship, which has been a blessing in the truest sense of the word.

Finally, the support and encouragement of my parents and my family over the years has been a continuous source of inspiration, and their advice invaluable, in matters both trivial and profound. The constant stream of e-mail messages from Bloemfontein has helped maintain the link to the southern hemisphere and has considerably shortened the distance to home.

Table of Contents

List of Tables

List of Figures

Chapter 1

Introduction and Overview

The work described in this thesis is an attempt to understand certain zero-bias anomalies (ZBA) that were investigated by Dan Ralph and Robert Buhrman [RB92] in the course of their studies of the I-V curves of metallic point contacts. Taking up a suggestion put forth by Ralph and Buhrman, we ascribe the observed anomalies to the scattering of non-equilibrium conduction electrons off degenerate two-level systems, with which they interact according to the non-magnetic 2-channel Kondo model of Zawadowski [VZ83]. Therefore, in this thesis we develop the theory for a (weakly) non-equilibrium 2-channel Kondo problem and apply it to experiment. Combining our results with recent numerical results by Hettler, Kroha and Hershfield [HKH94], we conclude that the 2-channel Kondo model is in qualitative and quantitative agreement with *all* experimental facts, though some questions regarding the theoretical justification for the model remain.

An outline of the thesis itself, and suggestions for "how to read this thesis if you are interested in ...", are given in section 1.6. Let us first outline the main train of thought that underlies this thesis.

1.1 Statement of the Experimental Problem

Ralph and Buhrman have developed a new technique which allows them to probe individual processes that occur on an atomic scale inside metals. They fabricate so-called nanoconstrictions, i.e. metal constrictions of diameters as small as 3 nm (see Fig. 2.1) and study the current I through the constriction as a function of voltage (V), temperature (T) and magnetic field (H). Since their constrictions are so small, they are able to detect electron scattering due to individual impurities or defects in the constriction. The energy dependence of the scattering rate can be extracted from the voltage dependence of the resistance. Thus, they essentially have developed a very-low-energy electron microscope, capable of energy-analyzing electron scattering from single defects within a metal, with which they have already discovered several new and unexpected phenomena [Ralph93].

The particular application of this versatile toy that attracted our interest was in the study of the zero-bias anomalies found for rather clean constrictions. These anomalies showed logarithmic T- and V- dependencies reminiscent of the magnetic Kondo effect. However, Ralph and Buhrman could demonstrate that their devices contained not magnetic impurities but structural defects, such as two-level systems (TLS). It was shown by Zawadowski [Zaw80,VZ83] that the interaction of conduction electrons with TLSs can be described by the so-called *non-magnetic 2-channel Kondo model*, which also gives rise to Kondo logarithms. Therefore *Ralph and Buhrman proposed that their zero-bias anomalies were due to the non-magnetic 2-channel Kondo scattering of conduction electrons off a small number of TLSs in the constriction.*

We set ourselves the task of developing the picture proposed by Ralph and

Buhrman into a theory that could make quantitative predictions, testable against experiment. Specifically, *we decided to calculate the I-V curve*, assuming non-magnetic 2-channel Kondo scattering and drawing upon the vast existing literature on the Kondo problem.

1.2 So what's so new about 2-channel Kondo physics?

The Kondo problem, of course, has enjoyed 30 years of unceasing theoretical attention from theorists as a prototypical quantum impurity problem. Some of the most recent advances were made by Affleck and Ludwig (AL). In a by now lengthy series of papers [Aff90,AL91a,AL91b,AL91c,AL91d,AL92a,AL92b,AL93, AL94,Lud94a,Lud94b,ML95], they developed an exact conformal field theory (CFT) solution for the $T = 0$ fixed point. Amongst many other quantities, it allows the exact analytic calculation of all equilibrium Green's functions in the regime ($T \ll T_K$) governed by the $T = 0$ fixed point.

Moreover, AL showed that in the $T \ll T_K$ regime the 2-channel Kondo model (and other multi-channel versions) display unusual and exotic non-Fermi liquid properties: the presence of a quantum impurity leads to a separation of charge, spin, and flavor degrees of freedom for the conduction electrons, which leads to non-Fermi liquid behavior for various quantities such as the conductivity, susceptibility, specific heat, etc. (It is this non-Fermi liquid behavior that is responsible for the current strong theoretical interest in multi-channel Kondo models, since various tenuous connections to the unusual normal-state properties of high-T_c superconductivity materials have been suggested [CJJ89,EK92,GVR93].) However,

prior to 1993, no convincing experimental realization of the 2-channel Kondo model was known (though some heavy-fermion compounds were under investigation as possible candidates [Cox87,SML91,AT91]), and hence the exotic phenomena that were predicted were yet to be observed.

In the spring of 1993, Andreas Ludwig became involved in our project. He suggested to us that *if one assumed that some of the TLSs were practically degenerate* (with a level splitting of $\Delta < 1\text{K}$), then a regime of lowest temperatures ($T < 5\text{K}$) and voltages ($V < 5\text{meV}$) explored in the Ralph-Buhrman experiment might in fact fall in the regime dominated by the $T = 0$ fixed point of the 2-channel Kondo problem. If correct, this would imply that his exact $T = 0$ solution was directly applicable to the experiment; Ralph and Buhrman would have found the first unambiguous experimental realization of a 2-channel Kondo model, and observed some of its associated exotic behavior; their zero-bias anomaly would be elevated from being a mere anomaly to a beautiful experimental realization of some very exotic theory. The stakes had clearly been raised considerably!

1.3 Scaling Prediction for Conductance

Drawing on his experience with his exact solution, Ludwig immediately made a strong, testable prediction. He predicted that in the regime $T \ll T_K$ and $V \ll T_K$, and assuming degenerate TLSs, the conductance $G(V,T)$ should obey a scaling relation of the following form:

$$\frac{G(V,T) - G(0,T)}{T^{\alpha}} = F(eV/k_{B}T) \tag{1.1}$$

where $F(x)$ is a sample-dependent scaling function. In the 2-channel Kondo problem, the universal scaling exponent α is predicted to have the non-Fermi-

liquid value $\alpha = \frac{1}{2}$. Moreover, by scaling out non-universal constants, it should be possible to extract a universal scaling curve $\Gamma(x)$ from $F(x)$.

It turned out that the data of Ralph and Buhrman indeed obey the above scaling relation, with $\alpha = 0.5 \pm 0.05$, in remarkably good agreement with Ludwig's prediction; furthermore, $\Gamma(x)$ was indeed the same for all three samples studied in detail. We took this as strong evidence that their samples can plausibly be described by the simplest possible one-dimensional 2-channel Kondo model (since Ludwig's prediction was based on such a model).

However, it is quite conceivable that other theories could also reproduce this scaling behavior, in particular since an exponent of $\alpha = \frac{1}{2}$ is not all that uncommon in condensed matter physics. Indeed, an alternative theory that accomplishes this but is based not on Kondo physics but the physics of disorder, has recently been proposed [WAM95] (although we believe it contradicts other important experimental facts, see section 2.4, page 30).

Therefore we decided to calculate the universal scaling function $\Gamma(x)$, and compare it to experiment. This curve is a fingerprint of the 2-channel Kondo problem, and being universal, should be independent of the details of the sample. If agreement were found, the case in favor of the 2-channel Kondo problem would be considerably strengthened. A different (non-Kondo) theory is expected to give a different scaling curve.

1.4 The Non-Equilibrium Problem

The conceptually new aspect of our work is that we need a non-equilibrium theory to describe the non-equilibrium situation found in Ralph and Buhrman's

experiments, whereas the exact conformal field theory solution of AL applies to the equilibrium situation. Thus the conceptual challenge that we had to address (and that is of general interest, beyond that of the present application), was: *how does one approach a strongly interacting non-equilibrium problem of which the equilibrium solution is known exactly?*

We were not able to find a general, exact solution to the particular non-equilibrium generalization of the 2-channel Kondo problem relevant to the experimental situation (though another, related non-equilibrium model can be solved exactly [SH95a]). However, we argue that for our purposes this is not necessary: if one assumes that the experiments are in the regime $V \ll T_K$, i.e. the "weakly non-equilibrium regime", it suffices to extract information for this regime from the exact equilibrium solution of AL. "Truly non-equilibrium" effects need only be treated in perturbation theory in V/T_K.

A description of the "weakly non-equilibrium regime" is achieved by drawing on a recent reformulation of non-equilibrium statistical mechanics by Hershfield [Hers93]. Hershfield showed that certain non-equilibrium problems become much simpler, formally resembling equilibrium, when formulated in the language of scattering states. We show that (to zeroth order in V/T_K) these scattering states can be extracted from the exact theory of AL for the equilibrium problem. Inserting the scattering states into Hershfield's formalism thus yielded a natural description of the "weakly non-equilibrium regime".

Within this formulation, the final calculation of the scaling curve $\Gamma(x)$ actually turned out to be extremely straightforward: the scaling function is given by

[eq. (9.26)]

$$\Gamma(v) = -\gamma_o^{-1} \int dx \tilde{\Gamma}_e \left(x + v/(2\gamma_1)\right) \left[-\partial_x f_o(x)\right] , \tag{1.2}$$

where $v \equiv eV/T$, $x = \varepsilon/T$, $f_o(x) = 1/(e^x + 1)$, γ_0, γ_1 are normalization constants and the function $T^{1/2}\tilde{\Gamma}_e(\varepsilon/T)$ is given by a correction $\delta\Sigma^R(\omega)$ to the retarded electron self-energy that had already been calculated in complete detail in [AL93]. Thus, no challenging new calculations were required. The challenge was mainly the conceptual one of how to best approach a strongly interacting problem out of equilibrium.

1.5 Results and Prognosis

The result of our calculation at first seemed somewhat disappointing: the calculated $\Gamma(x)$ curve does *not* agree with the experimental one (see Fig. 9.6).

However, it was pointed out by Hettler, Kroha and Hershfield [HKH94], who have studied the same model using numerical (NCA) techniques and whose results are in good agreement with ours, that theory and experiment can nevertheless be reconciled: they suggest that the experiment is in fact not in the pure scaling regime as we had assumed it would be. By incorporating corrections of order T/T_K ($\simeq 0.08$ for the lowest T in the experiment), which we had to neglect in our calculation, they achieve good agreement with experiment, using only one adjustable parameter, namely T_K.

Thus, the main conclusion reached in this thesis is that *the 2-channel Kondo model can satisfactorily account for all known experimental facts, both qualitative and quantitative.*

Nevertheless, some open questions remain. Very recently, the theoretical jus-

tification for the 2-channel Kondo model has been criticised. Wingreen, Altshuler and Meir [WAM95] argue that the the presence of static disorder could lead to a significant splitting Δ between the two states of the TLS, and Moustakas and Fisher [MF95] argue that a previously undiscovered relevant operator exists near the fixed point. Both these claims would make it rather unlikely for the system to flow to the $T = 0$ fixed point that is invoked in this thesis to explain the scaling properties of the data.

Therefore, we are faced with the peculiar situation of having a model that beautifully accounts for all experimental facts, but is on somewhat shaky theoretical grounds. In my opinion, this uncertain state of affairs should be an incentive for further theoretical and experimental work.

1.6 Outline of Thesis

In chapter 2 we present all experimental facts relevant to the Ralph-Buhrman experiment, and perform a detailed scaling analysis of the data in chapter 3. In chapter 4 we introduce Zawadowski's non-magnetic Kondo model. Chapter 5 is the heart of the thesis: it shows how one can describe non-equilibrium transport through the nanoconstriction by Hershfield's Y-operator method, and how AL's CFT can be used to calculate the necessary scattering states. This is done in chapter 9, where the scaling curve obtained from CFT is compared with that from Hettler, Kroha and Hershfield's numerical NCA calculations and experiment. A summary and conclusions can be found in chapter 10.

Chapters 6 to 8 and appendices A to F contain a detailed and extensive introduction to Affleck and Ludwig's CFT solution of the Kondo problem, aimed at a

reader with no or very little background in conformal field theory, but interested in mastering the necessary technicalities.

Chapter 6 works through a toy problem, namely the scattering of two species of spinless fermions off a scalar potential, using the same techniques as those used by AL for the Kondo problem, in order to illustrate these techniques in the simplest possible setting.

Chapters 7 and 8 explain AL's approach to the Kondo problem with as little recourse to CFT as possible – a reader familiar with elementary Sugawara technology (derived in detail in appendix A) should be able to follow almost everything in these chapters.

In an extensive set of six appendices, we attempt to provide (almost) all the technical details needed elsewhere. Appendix A uses nothing but Wick's theorem to derive the Sugawara technology necessary for chapters 6 and 7. Appendix B summarizes (without derivation, since they can be found in many reviews) those basic elements of bulk CFT field theory needed for AL's work. Assuming knowledge of appendix B, in appendix C we attempt to derive in quite some detail all elements of Cardy's boundary conformal field theory needed by AL (since to our knowledge, no detailed review of this exists). In appendix D we illustrate these methods by showing how AL calculated the highly non-trivial four-point function $\langle \psi_L \psi_L^\dagger \psi_R \psi_R^\dagger \rangle$, a calculation needed to check whether the all-important $T^{1/2}$ really does show up in the theory. Appendix E summarizes some elements of bosonization, that are used in appendix F to show how AL's theory can also be reformulated in terms of free bosons.

A few suggestions for readers with various interests:

How to read this thesis if you are interested in

- **experimental details:** read chapters 2 and 3, and the final comparison of theory and experiment in section 9.6;
- **the non-equilibrium 2-channel Kondo problem (without CFT):** read chapters 4 (in particular section 4.4), 5 and 9;
- **an introduction to AL's theory with (almost) no CFT:** read, in that order, appendix A, chapters 7 and 8; for a more technical discussion of a simpler toy problem, also read chapter 6 before chapter 7, or at least the summary in section 6.6;
- **a detailed introduction to all relevant technicalities of AL's theory:** read, in that order, appendix A, chapters 6, 7 and 8, and appendices C and D, consulting appendix B where necessary;
- **a bosonic formulation of AL's theory:** read appendices E and F — some familiarity with appendix D may be necessary.

A comment on notation: we in general take $\hbar \equiv 1$, $k_B \equiv 1$ and $v_F \equiv 1$. In chapter 3, however, we display k_B explicitly, because the figures were plotted in corresponding units.

Chapter 2

The Experiment

This chapter contains a presentation of experimental facts, and we attempt to keep it as free from theoretical baggage as possible. The only theory presented is the theory of point contact spectroscopy (section 2.2), needed to understand what kind of spectroscopic information can be extracted from analyzing the non-linear conductance $G(V)$. Apart from that, we deal mainly with matters of device characterization and data analysis and interpretation.

The chapter is organized as follows: In section 2.1 we describe the fabrication and characterization of nanoconstrictions. Section 2.2 deals with the theory of point contact spectroscopy. In section 2.3 we summarize the main experimental facts associated with the zero-bias anomaly (ZBA). Section 2.4 describes Ralph and Buhrman's arguments for ruling out a number of possible explanations for the ZBA and proposing the 2-channel Kondo picture of conduction electrons interacting with TLSs. In section 2.5 we present just enough of a discussion of the interaction of conduction electrons with TLS in metals to be able to draw the analogy with the 2-channel Kondo model. Finally, in section 2.6 we describe in

Figure 2.1 Cross-sectional schematic of a metal nanoconstriction. The hole at the lower edge of the Si_3N_4 is so small that this region completely dominates the resistance of the device.

more detail the physical picture that Ralph and Buhrman have pieced together for what actually occurs inside the nanoconstrictions.

All of this chapter is based on the thesis of Dan Ralph, from which I quote extensively (often verbatim), and to which the reader is referred for a much more extensive and thorough discussion.

2.1 The Nanoconstriction

Dan Ralph has done a great variety of experiments with his nanoconstrictions, most of which differ slightly from each other in details of sample fabrication, etc. We just describe the details relevant to nanoconstrictions with structural defects.

A schematic cross-sectional view of a typical nanoconstriction is shown in Fig. 2.1. The device is made in a sandwich structure. The middle layer is an insulating Si_3N_4 membrane. This contains in one spot a bowl-shaped hole, which just breaks through the lower edge of the membrane to form a very narrow opening, as small as 3 nm in diameter. The narrow neck at the lower opening in the Si_3N_4 membrane is so small that this region completely dominates the resistance,

measured between the top and bottom of the structure. Only metal within a distance equal to a few constriction diameters from the narrowest region contributes significantly to the resistance signal. This means that the device may be used as a kind of microscope. The small physical size of the structure serves to focus electrons so that only atoms in a very small region contribute to the resistance, and the resistance is sensitive to scattering from single defects in the constriction region.

To fabricate the devices, electron beam lithography and reactive ion etching are used to form the bowl-shaped hole in a Si_3N_4 membrane. The secrets for making a bowl-shaped hole that just breaks through the Si_3N_4 membrane (which is essential to obtaining a nano-hole), are described in [Ralph93, section 2.2]. In ultra-high vacuum ($< 2 \times 10^{-10}$ torr) and at room temperature the membrane is then rotated to expose both sides while evaporating metal to fill the hole to form the metal constriction and coat both sides of the membrane. A layer of at least 2000 $\mathring{A}$ of metal is deposited on both sides of the membrane to form clean, continuous films. In the devices studied in this thesis, the metal was always Cu, but similar phenomena have been seen in aluminum, silver and platinum constrictions.

Usually a large number of holes is made in the same Si_3N_4 membrane before evaporation. After evaporation, the membrane is manually disassembled along break lines to separate the different devices. Thus, devices are mass-produced, and then checked for suitability as nanoconstrictions, by measuring their resistance (which should preferably be large). One membrane usually produces 20-30% useful devices, with resistance greater than 5 Ω.

Finally, to obtain devices with structural defects such as TLSs, the devices have to be cooled to cryogenic temperatures within several hours after they are formed by evaporation, before all structural defects can anneal away.

The devices are physically quite robust [Ralph93, p.16]. For example, for samples that are not cooled soon after evaporation, the resistance may wander up or down slightly within the first day after an evaporation, indicating that the metal in the device may anneal or relax at room temperature, but after that the devices are generally stable for years. They may be dropped on the floor without harm, and they almost always survive thermal cycling to helium temperatures.

Conductance measurements are performed by 4-point measurements on current-biased samples[1], using standard lock-in amplifier or DC techniques [Ralph93, p.255].

2.2 Point Contact Spectroscopy

One of the most important characteristics of nanoconstrictions (also called *point contacts* in the literature to be cited in this section), is that the voltage dependence of the conductance may be related directly to the energy dependence of the electron relaxation rate $\tau^{-1}(\varepsilon - \mu)$, within the device, e.g.

$$G(V) = G_o - eK\tau^{-1}(eV) \ , \tag{2.1}$$

for phonon scattering, allowing one to do spectroscopy. In this section we explain how this comes about for *ballistic* constrictions, i.e. constrictions through which the electrons travel ballistically along semi-classical, straight line paths between

[1]To be explicit: a voltage source is connected in series with a large resistor, thus forming a current source that sends a current of specified magnitude I through the sample. Then the corresponding voltage across the sample is measured as a function of I.

collisions with defects or the walls of the constriction. Transport through the constriction can then be described using a Boltzmann formalism. This was first worked out in [KSO77,OKS77]; I found the most careful treatment to be [KOS77], and the best review in [JvGW80]. A more up-to-date review is [DJW89].

Two conditions have to be met for a constriction to be in the ballistic regime. Firstly, it must be possible to neglect effects due to the diffraction of electron waves, i.e. one needs $1/k_F \ll a$, where a = constriction radius. Secondly, the constriction must be rather clean (as opposed to disordered): an electron should just scatter off impurities once or twice while traversing the hole. One therefore needs $a \ll l$, where l is the electron mean free path.

Ralph and Buhrman work with devices with a of order 2-8 nm [as determined from TEM studies and from the Sharvin formula for the resistance, eq. (2.11)]. For clean devices for which all structural defects have annealed away, $l \sim 200$ nm (as determined from the residual bulk resistivity). For devices containing structural defects, l is reduced to about $l \sim 40$ nm (as estimated from a reduction in the phonon peak amplitude, see page 23), which is still about twice the constriction diameter [Ralph93, p.258]. Thus the constrictions can be assumed to be in the ballistic regime.

2.2.1 Boltzmann Equation and Sharvin Resistance

To set up a Boltzmann description of transport through the constriction we follow the presentation of [JvGW80, section 4], where more details may be found. The constriction geometry is modeled as an open, circular hole of radius a in the otherwise non-conducting, infinitely thin x-y plane (representing the insulating membrane) which separates two metallic half-spaces (the two leads, R/L for $z \gtrless$

0). The current through the constriction is given by the integral of the current density over the area of the hole:

$$I = \int_{\text{hole}} dxdy\, j_z(x, y, 0) \ . \tag{2.2}$$

For semi-classical electrons, a position $\vec{r}$ and momentum $\vec{k}$ label can be attached to each electron. Correspondingly, one can define an electron distribution function $f_{\vec{k}}(\vec{r})$ (see Fig. 2.2), in terms of which the current density per unit volume at point $\vec{r}$ is:

$$\vec{j}(\vec{r}) = \frac{2e}{\text{Vol}} \sum_{\vec{k}} \vec{v}_{\vec{k}} f_{\vec{k}}(\vec{r}) \tag{2.3}$$

(where Vol = volume). The task at hand is therefore to find the distribution function $f_{\vec{k}}(\vec{r})$. It is determined by the Boltzmann equation

$$\vec{v}_{\vec{k}} \cdot \vec{\nabla}_r f_{\vec{k}}(\vec{r}) + (e/\hbar)\vec{E} \cdot \vec{\nabla}_k f_{\vec{k}}(\vec{r}) = \left(\frac{\partial f_{\vec{k}}(\vec{r})}{\partial t} \right)_{coll} \ ; \tag{2.4}$$

the right hand side (defined in eq. (2.12) below) describes collisions off defects, phonons, etc. This is supplemented by the charge-neutrality condition

$$2e \sum_{\vec{k}} [f_{\vec{k}}(\vec{r}) - f_o(\varepsilon_{\vec{k}} - \mu)] = 0 \ , \qquad f_o(\varepsilon) \equiv \frac{1}{e^{\beta\varepsilon} + 1} \ . \tag{2.5}$$

Here $\varepsilon_{\vec{k}} \equiv k^2/2m$ is the kinetic energy and $\mu \equiv k_F^2/2m$ the equilibrium chemical potential. The total electron energy is written as

$$E_{\vec{k}}(\vec{r}) \equiv \varepsilon_{\vec{k}} + e\phi(\vec{r}) \tag{2.6}$$

where $e\phi(\vec{r})$ is the electrostatic potential energy, which defines the *bottom* of the conduction band ($e\phi(\vec{r}) \equiv 0$ for $V = 0$). If a bias, $V = -|V|$, is applied across the device, the leads are at different chemical potentials (say $\mu \pm eV/2$ for R/L

leads);[2] this condition is implemented as a boundary condition on $e\phi(\vec{r})$:

$$e\phi(z = \pm\infty) \equiv \pm eV/2 \; . \tag{2.7}$$

Eqs. (2.4), (2.5) and (2.7) are solved iteratively by making the Ansatz

$$f_{\vec{k}}(\vec{r}) \equiv f^{(0)}_{\vec{k}}(\vec{r}) + f^{(1)}_{\vec{k}}(\vec{r}) \qquad \phi(\vec{r}) \equiv \phi^{(0)}(\vec{r}) + \phi^{(1)}(\vec{r}) \; , \tag{2.8}$$

where $f^{(0)}_{\vec{k}}(\vec{r})$ is defined to be the solution of these equations in the absence of any collisions, i.e. with $\left(\frac{\partial f}{\partial t}\right)_{coll} \equiv 0$. The *backscattering correction* $f^{(1)}_{\vec{k}}(\vec{r})$ is then calculated iteratively by using $f^{(1)}_{\vec{k}}(\vec{r})$ in the LHS of eq. (2.4) and $f^{(0)}_{\vec{k}}(\vec{r})$ in its RHS, etc.

The result for $f^{(0)}_{\vec{k}}(\vec{r})$ at $T = 0$ is shown in Fig. 2.2. This figure is a position-momentum space hybrid, showing the momentum-space distribution function $f^{(0)}_{\vec{k}}$ with its origin drawn at the position $\vec{r}$ to which it corresponds. One can understand it almost without calculation, simply by realizing that in the absence of collisions, electrons will maintain a constant total energy $E_{\vec{k}}$. Thus, an electron injected from $z = \pm\infty$ in the R/L lead with total energy $E_{\vec{k}}(z = \pm\infty) = \varepsilon_{\vec{k}} \pm eV/2$, will accelerate or decelerate as its potential energy changes from $e\phi(\pm\infty) = \pm eV/2$ to $e\phi(\mp\infty) = \mp eV/2$ while it traverses the hole, in such a way that $\varepsilon_{\vec{k}} + e\phi(\vec{r}) = E_{\vec{k}}(\vec{r}) = \text{constant}$.

The key feature in Fig. 2.2 is that the distribution of occupied electron states in momentum space, at any point $\vec{r}$ in the vicinity of a ballistic constriction, is highly anisotropic and consists of *two* sectors, denoted by (+) and (−). The (±) sector contains the momenta of all electrons that originate from the $\pm V/2$ side (i.e. R/L side) of the device and can reach $\vec{r}$ along ballistic straight-line paths,

[2] Sign-conventions: following [JvGW80], we take $e = -|e|$, $V = -|V|$, so that $eV > 0$. Then electrons flow from right to left, and the current to the right is positive.

Figure 2.2 [JvGW80, Fig. 7]: The $T = 0$ electron distribution function $f^{(0)}_{\vec{k}}(\vec{r})$ [calculated by neglecting the collision term in eq. (2.7)] shown (a) *at* the hole and (b) at two points near the hole. The picture is a position-momentum space hybrid, showing the momentum-space distribution function $f^{(0)}_{\vec{k}}$ with its origin drawn at the position $\vec{r}$ to which it corresponds. A finite temperature simply smears out the edges of the two (R/L) Fermi seas.

including paths that traverse the hole (the bending of paths due to the electric field is of order eV/ε_F and hence negligible). At a given point $\vec{r}$, the momentum states in the $(\pm)$ sectors are filled up to a maximum energy of $E_{\vec{k}}(\vec{r}) = \mu \pm V/2$, because of energy conservation along trajectories. Thus, for $\vec{k}$ in the $(\pm)$ sector, one finds

$$f^{(0)}_{\vec{k}\in(\pm)}(\vec{r}) \;=\; f_o\Big[E_{\vec{k}}(\vec{r}) - \mu \mp eV/2\Big] = f_o\Big[\varepsilon_{\vec{k}} - \Big(\mu \pm eV/2 - e\phi^{(0)}(\vec{r})\Big)\Big] \qquad (2.9)$$

To zeroth order in the collision term, the electrostatic potential energy can be found by inserting eq. (2.9) into the charge neutrality condition eq. (2.5). The result is

$$e\phi^{(0)}(\vec{r}) = \mathrm{sign}(z)\ \tfrac{1}{2}eV[1 - \Omega(\vec{r})/(2\pi)]\ , \qquad (2.10)$$

where $\Omega(\vec{r})$ is the solid angle at which the hole is seen at position r. Since $\Omega(\vec{r}) \to 0$ as soon as $|\vec{r}| \gg a$, we see that $e\phi^{(0)}(\vec{r})$ changes smoothly from $-eV/2$

Figure 2.3 [JvGW80, Fig. 6]: The electrostatic potential energy $e\phi^{(0)}(\vec{r})$, which defines the *bottom* of the conduction band, near a point contact with radius a, shown along the z-axis. $e\phi^{(0)}(\vec{r})$ changes smoothly from $-eV/2$ to $+eV/2$ within a few radii a from the hole.

to $+eV/2$ within a few constriction radii a from the hole, as shown in Fig. 2.3.

Using these results for $f^{(0)}$ and $\phi^{(0)}$ it is easy to calculate the so-called *Sharvin* resistance, i.e. the "geometrical" resistance that is due solely to the presence of a constriction and independent of the electron mean free path l. From eq. (2.2) one finds [using $e\phi^{(0)}(x,y,0)=0$, $N(\varepsilon)=$ density of state per spin, $eV \ll \varepsilon_F$ and being careful with angular integrals]:

$$\begin{aligned} I_o &= \pi a^2 2e \int d\varepsilon_{\vec{k}} \rho_o \int_{k_z>0} d\Omega_{\vec{k}} |v_{\vec{k}}| \cos\theta_{\vec{k}} \left[f_o(\varepsilon_k - \mu + \tfrac{1}{2}eV) - f_o(\varepsilon_k - \mu - \tfrac{1}{2}eV) \right] \\ I_o &= \pi a^2 |e| v_F) \left(\tfrac{1}{2} eV \rho_o / Vol \right) . \end{aligned} \tag{2.11}$$

Here $\rho_o/Vol = \frac{mk_F}{2\pi^2\hbar^2}$ is the density of states per spin per unit volume. This result is so simple that it explains itself: a current proportional to eV arises simply because near the Fermi surface there are more electrons moving to the left than to the right (hence the - sign), each carrying a current ev_F, the difference in number being $2\frac{1}{2}\frac{1}{2}N(\varepsilon_F)eV$ (2 for two spin directions, $\frac{1}{2}$ from the restriction $k_z > 0$, and $\frac{1}{2}$ from the angular integration over v_z).

The Sharvin formula is used routinely to estimate the area of a nanoconstric-

tion from a measurement of its resistance.

It is worth emphasizing that the electrostatic potential energy $e\phi(\vec{r})$ plays only an indirect role when it comes to calculating low-energy (i.e. $T/\varepsilon_F, V/\varepsilon_F \ll 1$) transport properties.[3] The reason is simply that *the only role of* $e\phi(\vec{r})$ *is to define the bottom of the conduction band*, and hence cause acceleration and deceleration of electrons to maintain $E_{\vec{k}}(\vec{r}) = E$. Low-energy transport properties, however, are determined by what happens at the *top* of the conduction band, in particular by the sharply anisotropic features characterized in Fig. 2.2 and eq. (2.9). This is illustrated by the derivation of the Sharvin formula, where it was the anisotropy in $f^{(0)}_{\vec{k}}(z=0)$ that was crucial [see eq. (2.9)].

We emphasize this conclusion by stating for future reference:

The key non-equilibrium feature of point contacts: *at each point near the point contact, one has effectively two Fermi seas, one consisting (roughly speaking) of L-movers, injected from the R lead with Fermi energy* $\mu + eV/2$*, the other of R-movers, injected from the left lead with Fermi energy* $\varepsilon_F - eV/2$*.*

Any simplified description of non-equilibrium transport through point contacts (such as that used in later chapters) must capture this simple physical picture. [Unfortunately, this also complicates Kondo physics tremendously, as we shall see later.]

[3] When interested in non-equilibrium transport, it is *not* sufficient to simply couple a current to a vector potential, $\int d\vec{r}\ \vec{j}\cdot\vec{A}$, where $\vec{A}$ satisfies $\vec{E} \equiv= -\frac{1}{c}\partial_t\vec{A} = -\vec{\nabla}_r\phi$. This simply does not do full justice to the non-equilibrium aspects introduced by having two distinct R/L Fermi surfaces at $\mu \pm eV/2$ (which took me six months to appreciate fully).

2.2.2 Backscattering Corrections to Current

The corrections (ΔI) to the current through a point contact due to the scattering processes (e.g. off phonons or defects) are negative. This is because electrons that have already traveled through the hole can be scattered back to where they came from. Such scattering processes are incorporated in the collision term in eq. (2.4), which has the general form

$$\begin{aligned}\left(\frac{\partial f_{\vec{k}}(\vec{r})}{\partial t}\right)_{coll} &\equiv Vol^{-1}\sum_{\vec{k}'}\Big[\Gamma(\vec{k}'\to\vec{k};\vec{r})f^{(0)}_{\vec{k}'}(\vec{r})\Big(1-f^{(0)}_{\vec{k}}(\vec{r})\Big)\\ &\quad -\Gamma(\vec{k}\to\vec{k}';\vec{r})f^{(0)}_{\vec{k}}(\vec{r})\Big(1-f^{(0)}_{\vec{k}'}(\vec{r})\Big)\Big]\ , \end{aligned} \tag{2.12}$$

The correction to the current due to scattering is found from the contribution of $f^{(1)}_{\vec{k}}(\vec{r})$ to eq. (2.2), namely

$$\begin{aligned}\Delta I &= \frac{2e}{Vol}\int_{\text{hole}}dxdy\sum_{\vec{k}}\vec{v}_{\vec{k}}f^{(1)}_{\vec{k}}(x,y,0)\\ &= \frac{2e}{Vol}\int_{\text{hole}}dxdy\sum_{\vec{k}}\vec{v}_{\vec{k}}\int_{-\infty}^{0}\frac{ds}{|v_{\vec{k}}|}\left(\frac{\partial f_{\vec{k}}(\vec{r}_s)}{\partial t}\right)_{coll}\ . \end{aligned} \tag{2.13}$$

To understand the second line, note that $f^{(1)}_{\vec{k}}(x,y,0)$ is the correction to $f^{(0)}_{\vec{k}}(x,y,0)$ due to all (single-)scattering processes that an electron could have undergone on its way from $\pm\infty$ to $(x,y,0)$. Hence $f^{(1)}_{\vec{k}}(x,y,0)$ is given by the integral of $\left(\frac{\partial f_{\vec{k}}(\vec{r}_s)}{\partial t}\right)_{coll}$ along all straight-line paths [parameterized by s in eq. (2.13)] parallel to $\vec{k}$ that end at point $(x,y,0)$. (This is Chamber's method of trajectories; for details, see [JvGW80, section 4.3].)

2.2.3 Phonon Scattering

Consider scattering off phonons, at $T=0$. Then $\Gamma(\vec{k}'\to\vec{k};\vec{r})$ has two properties that simplify matters significantly: Firstly, it depends only on $\Delta_\varepsilon \equiv$

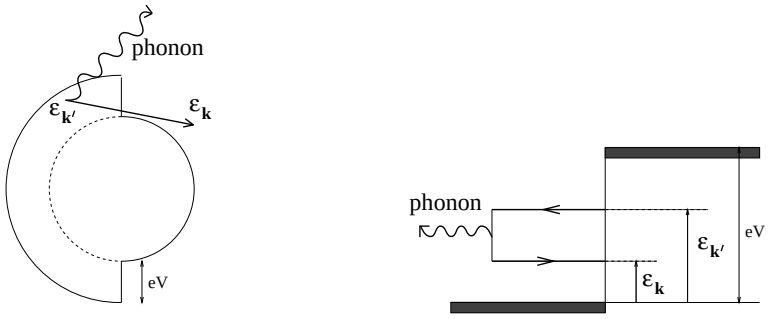

(a) (b)

Figure 2.4 A single-phonon backscattering process in (a) momentum and (b) energy space, where a phonon of energy $\varepsilon_{k'} - \varepsilon_k$ is emitted spontaneously.

$E_k(\vec{r}) - E_{k'}(\vec{r})$ (which means that all $\phi(\vec{r})$-dependence drops out), being proportional to an electron-phonon interaction function $\alpha^2 F_p(\Delta_\varepsilon)$ (which is related to the well-known Eliashberg function). Secondly, it is spatially homogeneous ($\vec{r}$-independent), because phonons are distributed uniformly in space.

It turns out that the backscattering correction at $T = 0$ is [JvGW80, eq.(4.40)]:

$$\Delta I(eV) = -\frac{K}{|e|}\int_0^{eV} d\varepsilon' \int_0^{\varepsilon'} d\Delta_\varepsilon \alpha^2 F_p(\Delta_\varepsilon) \ , \qquad K = \frac{4e^2 m^2 v_F a^3}{3\pi\hbar^4} \ . \tag{2.14}$$

Roughly speaking, at each point along a trajectory, one has to evaluate the probability for inelastic processes of the type shown in Fig. 2.4; since the Pauli principle has to be respected, the upper and lower limits of the relevant energy integral are as in eq. (2.14).

The corresponding correction to the differential conductance is simply

$$\Delta G \equiv -\frac{d\Delta I(V)}{dV} = -K\tau^{-1}(eV) \ , \tag{2.15}$$

where $\tau^{-1}(\varepsilon') \equiv \int_0^{\varepsilon'} d\Delta_\varepsilon \alpha^2 F_p(\Delta_\varepsilon)$ is the relaxation rate for an electron at energy ε' above the Fermi surface. Thus, due to phonon-backscattering processes, the conductance of any point contact has a marked dip at voltages large enough to excite phonons [$V > 5$ meV for Cu, see Fig. 2.5(a)].

Furthermore, $\frac{d^2I}{d(eV)^2}$ is proportional to $\alpha^2F_p(eV)$, which can thus be measured directly from, it turns out,

$$\alpha^2F_p(eV) = -\frac{3}{32\sqrt{2}}\frac{\hbar^2k_F^2}{em}\left(\frac{Re^2}{h}\right)R\frac{d^2I(V)}{dV^2} \quad (2.16)$$

$$= \frac{5.8}{R^{1/2}}\frac{dR(V)}{dV}\,, \quad (2.17)$$

for Cu, where $R = dV/dI$ is in units of Ω and V is in mV. The function on the right hand side of eq. (2.17) is called the *point contact spectrum* (PCS). For any clean, ballistic Cu point contact, it should be a universal function [namely $\alpha^2F_p(eV)$], and indeed measurements of it agree with other determinations of α^2F_p. However, the amplitude of the phonon-induced peaks is reduced dramatically if there is significant elastic scattering due to defects or impurities in the constriction region, as has been modeled theoretically [YS86] and demonstrated experimentally [LYSN80]. Therefore, comparing the PCS of a given point contact to the reference PCS of a clean point contact provides an important and reliable tool for determining whether the point contact is clean or not. (We emphasize this fact, because for our later analysis it will be extremely important to know reliably that the devices of interest to us are in fact very clean.)

2.2.4 Defect scattering

For voltages below the phonon threshold ($V < 5mV$ for Cu), non-linearities in $G(V)$ are due to scattering off defects, which we discuss next.

Consider a set of defects at positions $\vec{R}_i$; furthermore, consider the case (applicable to scattering off degenerate Kondo impurities, for example) that the scattering rate is isotropic and elastic but depends, in the equilibrium case, on

the distance from the Fermi surface, because of many-body effects:

$$\Gamma(\vec{k}' \to \vec{k}; \vec{r}) \propto \sum_i \delta(\vec{r} - \vec{R}_i)\delta(\varepsilon_{\vec{k}} - \varepsilon_{\vec{k}'})\ \tau^{-1}\left(\varepsilon_{\vec{k}'} - \mu\right)\ . \tag{2.18}$$

In general, when a voltage is applied and the Fermi surfaces are distorted as in Fig. 2.2, $\tau^{-1}(\varepsilon_{\vec{k}'} - \mu)$ can become V-dependent. If V is small enough, however, such V-dependent corrections to $\tau^{-1}(\varepsilon_{\vec{k}'} - \mu)$ can be neglected (for Kondo impurities, this requires $eV/T_K \ll 1$, where T_K is the Kondo temperature). We shall call this case, which is the only one considered in this thesis, the *weakly non-equilibrium regime*. In this regime, using eqs. (2.18) and (2.9) in (eq. (2.13)), one finds that the current involves a sum over impurities:

$$\begin{aligned}\Delta I = \frac{\tilde{K}}{|e|}\int d\varepsilon'_k \Big\{ &\sum_i b_i \tau^{-1}(\varepsilon'_k - \mu) \\ &\times \Big[f_o\Big(\varepsilon'_k + e\phi^{(0)}(\vec{r}_i) - \mu + eV/2\Big) - f_o\Big(\varepsilon'_k + e\phi^{(0)}(\vec{r}_i) - \mu - eV/2\Big)\Big]\Big\} \\ = \frac{\hbar\tilde{K}}{|e|}\int d\omega &\left[\sum_i b_i \tau^{-1}\Big(\hbar\omega - e\phi^{(0)}(\vec{r}_i)\Big)\right]\Big[f_o(\hbar\omega + eV/2) - f_o(\hbar\omega - eV/2)\Big]\end{aligned} \tag{2.19}$$

(To obtain the second line, we wrote $\hbar\omega \equiv \varepsilon'_k + e\phi^{(0)}(\vec{r}_i) - \mu$.) Here $\tilde{K} = e^2\tau(0)/h$, the b_i are (unknown) dimensionless constants of order unity that characterize how much an impurity contributes to the backscattering current, and depend on the position of the i-th impurity relative to the hole. The main complication, though, is the $\vec{r}_i$-dependence in the Fermi functions, which enters eq. (2.19) through $e\phi^{(0)}(\vec{r}_i)$. To deal with this, use eq. (2.10) to define "effective voltages" $Va_i^{\pm}$ by writing

$$\tfrac{1}{2}eV \pm e\phi^{(0)}(\vec{r}_i) \equiv \tfrac{1}{2}eVa_i^{\pm}\ , \qquad a_i^{\pm} \equiv 1 \pm \mathrm{sign}(z)[1 - \Omega(\vec{r}_i)/(2\pi)]\ . \tag{2.20}$$

The backscattering correction to the conductance, $\Delta G(V) \equiv -\frac{d\Delta I}{dV}$, then is (after

differentiating and then making shifts $\hbar\omega \to \hbar\omega \pm eV/2$)

$$\Delta G(V) = -\tilde{K}\int d\omega[-\partial_\omega f_o(\hbar\omega)] \sum_i b_i \tfrac{1}{2}\left[\tau^{-1}(\hbar\omega - \tfrac{1}{2}eVa_i^+) + \tau^{-1}(\hbar\omega - \tfrac{1}{2}eVa_i^-)\right] , \tag{2.21}$$

Thus, the contribution of the i-th impurity to $\Delta G(V)$ depends on position-dependent effective voltages $Va_i^\pm$. The reason is that τ^{-1} was assumed to depend on the (energy)-distance from the Fermi surface $[\varepsilon_{k'} - \mu = E_{k'} - \mu - e\phi^{(0)}(\vec{r})]$; for an electron traveling at constant total energy $E_{k'}$, this distance changes with position, since $e\phi^{(0)}(\vec{r})$ changes with position.

However, we know that the conductance is dominated by what happens in the immediate vicinity of the hole; in other words, the b_i will be much larger for impurities close to the hole (for which $e\phi^{(0)}(\vec{r}_i) \simeq 0$ and $a_i^\pm \simeq 1$) than for those further away (for which $e\phi^{(0)}(\vec{r}_i) \simeq \pm eV/2$ and $a_i^\pm \neq 1$). Thus the effect of $e\phi^{(0)}(\vec{r}_i) \neq 0$ terms should not be too disruptive.

Nevertheless, the position-dependence of the impurities has muddied the waters somewhat compared to the case of phonon scattering, and this should be borne in mind when comparing experiment to theory.

2.3 The Zero-Bias Anomaly: Experimental Facts

In this section we summarize in brief all the experimental facts relevant to the zero-bias anomaly. Our interpretation of these facts is postponed to later sections, where some of them will be elaborated upon more fully, and most of the figures quoted below can be found.

The basic phenomenon to be studied is illustrated by the upper conductance

Figure 2.5 A typical conductance curve for a constriction containing structural defects: (a) The upper curve, showing a dip in conductance at $V = 0$ and voltage-symmetric spikes, is the differential conductance for an unannealed Cu sample at 4.2 K. The lower curve shows the conductance of the same device at 4.2 K, after annealing at room temperature for 2 days. The curves are not artificially offset; annealing changes the overall conductance of the device by less than 0.5%. (b) Dashed line: PCS for the device before anneal at 2 K. Solid line: PCS after anneal.

curve in Fig. 2.5. The essential features are the following: Firstly, a drop in the conductance for $|V| > 10$ mV, due to the excitation of phonons, which is well understood (see section 2.2). Secondly, sharp voltage-symmetric conductance spikes at somewhat larger voltages, called *conductance transitions* by Ralph and Buhrman. They are described at length, from an experimental point of view, in [RB95]. However, their detailed origins are as yet a total mystery (though Ralph and Buhrman argue in [RB95] that they probably have the same origin as the zero-bias anomalies, and probably signify the sharp, sudden, "switching off" of whatever had been giving rise to the zero-bias anomaly). They will not be discussed at all in this thesis. Thirdly, the conductance has a voltage-symmetric dip in the conductance near $V = 0$, the so-called *zero-bias anomaly.* This thesis is concerned exclusively with the regime $V < 5$ mV and the zero-bias anomaly.

The zero-bias anomaly (ZBA) has the following properties:

(P1) *Cooling:* It is found only in samples that are cooled to cryogenic temperatures within hours after being formed by evaporation. It is found in about 50% of such samples, and in a variety of materials, such as Al, Ag, Pt and Cu, which was the material used most often.

(P2) *Amplitude:* The amplitude of the ZBA $[G(V = 0) - G_{max}]$ varies from sample to sample, from a fraction of e^2/h to as large as $60e^2/h$.

(P3) *Annealing:* After annealing at room temperature for several days, the ZBA and conductance spikes disappear, and the conductance curve looks like that of a completely clean point contact (see lower curve in Fig. 2.5, and Fig. 2.6). Nevertheless, annealing changes the total conductance by less than 1%.

(P4) *Phonon spectra:* The magnitudes of the phonon peaks in the PCS for the unannealed device are only about 15% smaller than for the annealed device [see Fig. 2.5(b)], for which the phonon peaks have the magnitudes corresponding to a clean, ballistic point contact (refer to the discussion on page 23). From this one can estimate that the mean free path of the unannealed sample is still greater than 30 nm, implying a rather clean, ballistic constriction.

(P5) *Effect of disorder:* If static disorder is intentionally introduced into a nanoconstriction (by adding 1% or more of impurity atoms such as Au to the Cu during evaporation), the the zero-bias conductance dip and conductance spikes *disappear completely* (see Fig. 2.7). When a strongly disordered region is created near the constriction (by electromigration: a high bias (100-500 mV) is applied at low temperatures so that Cu atoms are moved around), the conductance shows no ZBA either, but instead small-amplitude, aperiodic (in V) conductance fluctuations at low voltage due to quantum interference (see Fig. 2.8).

(P6) *Magnetic field:* When a magnetic field (of up to 6 T) is applied, the amplitude of the conductance dip decreases, see Fig. 2.9(b), in other words the magnetoconductance is positive. However, the dip undergoes no Zeeman-splitting, in constrast to the Zeeman splitting that *is* found for devices intentionally doped with magnetic impurities such as Mn [see Fig. 2.9(a)]. The magnetoconductance seems to depend roughly linearly on $|H|$ at fixed T and $V = 0$: $G(H,T) \propto |H|$ (see Fig. 3.11), but not enough data is currently available to establish this beyond doubt.

(P7) *Logarithms:* For V and T not too small and $H = 0$, there are (admittedly rather small) regimes in which the conductance goes like $\log V$ at fixed T, and $\log T$ at $V = 0$, see Fig. 2.10.

(P8) V, T *scaling:* As a function of V and T at $H = 0$, the conductance obeys the following scaling relation if both V and T are small enough, but for arbitrary ratio V/T:

$$\frac{G(V,T) - G(0,T)}{T^{\alpha}} = F(V/T) \ , \tag{2.22}$$

where $\alpha = 0.5 \pm 0.05$ and $F(x) \propto x^{1/2}$ as $x \to \infty$. This relation allows a large number of data curves to be collapsed onto a single, sample-dependent scaling curve, [e.g. see Figs. 3.3 and 3.4(a)].

(P9) *Universality:* By scaling out sample-dependent constants, it is possible to extract from $F(x)$ a "universal" scaling function $\Gamma(x)$, shown in Fig. 3.10(b). $\Gamma(x)$ is universal in the sense that it is indistinguishable for all three devices for which a scaling analysis was carried out (they are called sample 1,2 and 3 below).

Any theory that purports to explain the zero-bias anomaly must be consistent with all of the above experimental facts.

2.4 Eliminating various possibilities

In this section we present the arguments by which Ralph and Buhrman eliminate all the obvious candidate causes for the ZBA that come to mind.

Since the ZBAs only occur in samples that are cooled shortly after evaporation (P1), and since ZBAs anneal away at room temperature (P2), one concludes that

Figure 2.6 Differential conductance versus voltage at 4.2 K for a Cu sample which underwent repeated thermal cycling. The time sequence runs from the bottom curve to the top. Curves are artificially offset. The first 2 excursions were to 77 K, the next 5 to room temperature.

they must be *due to structural defects or disorder that can anneal away at high temperatures*. However, only a small amount of such disorder can be present, for two reasons: Firstly, annealing changes the total conductance by less than 1% (P3) indicating that the unannealed device could not have been strongly disordered to begin with. Secondly, comparison of the phonon peaks in the PCS spectra of annealed and unannealed samples indicate that in the unannealed devices the mean free path l is still greater than 30 nm, implying a rather clean, ballistic constriction (P4).

Could the anomalies be due to static disorder? For example, both weak localization due to disorder [Berg84] and disorder-enhanced electron-electron interactions [LR85] could be considered candidate mechanisms to explain the decreased conductance near $V = 0$. In fact, Wingreen, Altshuler and Meir (WAM) [WAM95] have recently strongly advocated the latter possibility: they pointed out that strong static disorder (mean free path $l \simeq 3$nm) give rise to a depression $\delta N(\varepsilon - \varepsilon_F) \propto T^{1/2}\Gamma\left(\frac{\varepsilon-\varepsilon_F}{T}\right)$ in the density of states near the Fermi surface, which

Figure 2.7 (a) Differential conductance and (b) PCS curve for a Cu sample intentionally doped with 6 % Au. Static impurities reduce the electronic mean free path but completely eliminate the zero-bias anomaly of interest to us.

Figure 2.8 (a) Differential conductance at 1.8 K for a Cu device in which disorder has been created by electromigration (which means that a high bias (100-500 mV) has been applied at low temperatures so that Cu atoms moved around). (b) Phonon spectrum for this device, averaged over 25 different defect configurations (for details, see Fig. 4.3 of [Ralph93]).

Figure 2.9 Conductance signals for 500 ppm magnetic Mn impurities in Cu at 100 mK, showing Zeeman splitting in an applied magnetic field. (b) The zero-bias signals from the unannealed metal samples exhibit no Zeeman splitting, demonstrating that they are not due to a magnetic impurity.

Figure 2.10 (a) V-dependence of the differential conductance for $B = 0$ and $T = 100$ mK. (b) T-dependence of the conductance for $B = 0$ and $V = 0$. Straight lines illustrate regions of logarithmic V and T dependencies.

explains the scaling property (P8), and in fact quantitatively reproduces the scaling curve $F(x)$ of eq. (2.22) (see [WAM95, Fig.1]). However, Ralph and Buhrman have several arguments that rule out scenarios due to disorder [Ralph93, section 6.6.1]:

1. According to (P5), upon the intentional introduction of static disorder (by coevaporation of 1 % or more of impurity atoms such as Au with the Cu) the ZBAs are not enhanced, as one would have expected if the anomalies had been due to static disorder, but disappear completely. If one increases the disorder even more, using for example electromigration, all one finds are small-amplitude, aperiodic conductance fluctuations at low voltage due to quantum interference.

2. Signals due to weak localization or disorder-enhanced electron-electron scattering are limited to amplitudes of order $1e^2/h$ (except in the inapplicable case of a long 1-dimensional wire); they cannot account for ZBAs with amplitudes as large as 10's of e^2/h (P2).

3. As already argued above, the electronic mean free path l is not short, but > 30 nm, even in the unannealed samples. In other words, *the devices really are rather clean*; whatever amount of disorder is present, it is doubtful that this could be enough for weak localization or disorder-enhanced electron-electron scattering to be important.

4. Property (P3), namely the disappearence of the zero-bias anomalies under annealing, might be interpreted to imply that static disorder has annealed away. If the bowl of the nano-constriction had been filled with a disor-

dered region with disorder as strong as suggested by WAM, and if all this disorder is assumed to disappear under annealing, then a simple Drude-model estimate of the disorder-induced resistance shows that the overall resistance should change by tens of percents. However, under such annealing, the overall amplitude of the effect does not change by more than 1 or 2% [RLvDB95].

If not static disorder, what else? A clue may be found from Fig. 2.10, which shows that there are (admittedly rather small) regimes in which the conductance goes like $\log V$ at fixed T, and $\log T$ at $V = 0$. This is reminiscent of the magnetic Kondo effect, where the resistance increases as $\log T$ with decreasing T (as long as $T > T_K$). However, there are several arguments that rule out magnetic impurities as the source of the anomalies:

1. An effect due to magnetic impurities would not anneal away at higher temperatures (P3).

2. If the magnetic Kondo effect were at work, a magnetic field (P6) would cause a well-known Zeeman splitting in the zero-bias conductance dip. In fact, a Zeeman splitting has been observed in nanoconstrictions intentionally doped with the magnetic impurity Mn [Ralph93, section 5.2], as shown in Fig. 2.9(a). However, in the devices under present consideration, a Zeeman splitting has never been observed, although a magnetic field does decrease the amplitude of the conductance dip somewhat, see Fig. 2.10(a).

3. For a magnetic Kondo effect, the anomaly would behave like $\Delta G \propto T^2$, $\Delta G \propto V^2$ for very small T and V [GW78]. However, as will be demon-

strated in detail in chapter 3, the conductance obeys instead the scaling form eq. (2.22), which implies $\Delta G \propto T^{1/2}$, $\Delta G \propto V^{1/2}$.

However, one does not necessarily need magnetic impurities to get a Kondo effect. Zawadowski [Zaw80, VZ83] showed that in a metal, the interaction of conduction electrons with certain type of structural defects, namely a two-level systems (TLSs), can be described by the so-called *non-magnetic* or *orbital Kondo model*, which also results in a logarithmic T and V dependence for the conductance (as long as $T, eV > T_K$). Zawadowski's model was later shown to be equivalent to the 2-channel Kondo model [MG86]. This led Ralph and Buhrman to propose in 1992 the following scenario:

The 2-channel Kondo picture:

The ZBAs are due to structural defects, namely TLSs, that interact with conduction electrons according to the non-magnetic 2-channel Kondo model.

As will be seen later, the following assumptions are also needed: To account for the size of the signals, one needs several, sometimes tens of TLS in the constriction. Moreover, their asymmetry energies Δ [see eq. (2.23)] have to be very small ($\Delta < 1K$), and interactions between the various TLSs must be negligible.

This proposal is described at length in subsequent sections. Let us end this section by remarking that in his thesis, Dan Ralph has also considered and ruled out [Ralph93, section 6.6] as causes for the observed ZBAs a number of other mechanisms: charge traps in the Si_3Ni_4 membrane, electronic surface states or quasi-localized states within the metal, defect rearrangement, mechanical instabilities, superconducting phases and heating effects (see footnote on p. 56 for ruling out heating).

2.5 TLSs in metals

The term two-level system refers to an atom or group of atoms that can hop between two different positions inside a material (more correctly, it should be called a *tunneling center*, since in general it can have more than two energy levels, see section 4.2). Its behavior is governed by a double well potential, generically depicted in Fig. 2.11, with asymmetry energy Δ. If the energy barrier between the two wells is low enough to allow *tunneling* between them, with a tunneling matrix element Δ_o, the system is known as a two-level tunneling system (TLS). If all relevant energies are much smaller than that of the first excited states in the double well (with energy on the order of the Debye frequency), the Hilbert space of the TLS can be truncated to consist of only the lowest two, near-degenerate states (this restriction is relaxed in section 4.2). Thus, the TLS can be described in terms of an (Ising) spin variable (described by Pauli matrices τ^i below and often called *impurity pseudospin*), with Hamiltonian

$$H_{TLS} = \frac{1}{2} \begin{pmatrix} \Delta & \Delta_o \\ \Delta_o & -\Delta \end{pmatrix} = \frac{1}{2} \left(\Delta \tau^z + \Delta_o \tau^x \right) . \tag{2.23}$$

The concept of the TLS was first introduced to explain the low-temperature thermal and acoustic properties of amorphous solids or glasses [AHV72,Phil72], in which they occur because some groups of atoms are likely to have more than one accessible low-energy configuration, due to the disordered arrangement of atoms. Their concentration is roughly 10^{-5} to 10^{-4} per atom, with a wide distribution of energy splittings and tunneling times [Phil81,HR86,Phil87], and the interesting properties arise from the coupling of TLSs to phonons.

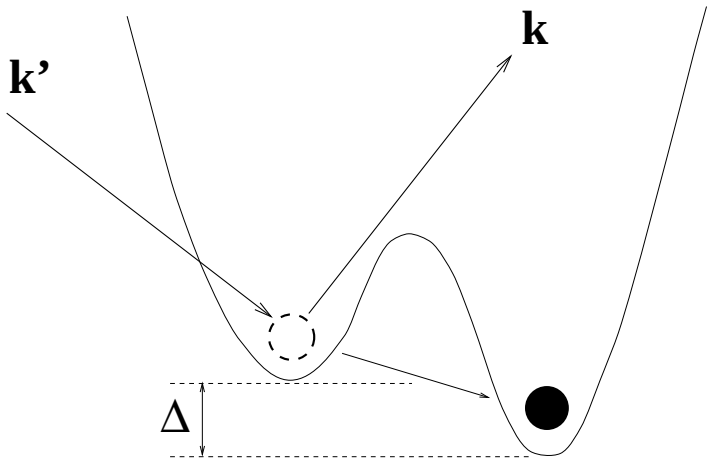

Figure 2.11 A generic two-level-system, with (bare) energy asymmetry Δ and tunneling rate Δ_0. An electron-assisted tunneling event is depicted: an electron scatters of the TLS and induces the atom to tunnel.

However TLSs are also known to exist in polychrystalline metals, with concentrations only a factor of 25-100 less than in fully amorphous materials [EKP92]. In such materials, the microscopic origin of TLSs is probably due to the movement of atoms along grain boundaries or due to the motion of dislocation segments.

How does the presence of conduction electrons influences a TLS? The TLS-electron interaction is usually modeled by

$$\begin{aligned} H_{int} &= \sum_{\vec{k}\vec{k}'} \left[V^o_{\vec{k}\vec{k}'} \begin{pmatrix} 1 & 0 \\ 0 & 1 \end{pmatrix} + V^z_{\vec{k}\vec{k}'} \begin{pmatrix} 1 & 0 \\ 0 & -1 \end{pmatrix} + V^x_{\vec{k}\vec{k}'} \begin{pmatrix} 0 & 1 \\ 1 & 0 \end{pmatrix} \right] c^\dagger_{\vec{k}\sigma} c_{\vec{k}'\sigma} \\ &= \sum_{\vec{k}\vec{k}'} \sum_{i=0,z,x} c^\dagger_{\vec{k}\sigma} \left[V^i_{\vec{k}\vec{k}'} \tau^i \right] c_{\vec{k}'\sigma} \ . \end{aligned} \tag{2.24}$$

where $c^\dagger_{\vec{k}\sigma}$ creates an electron with momentum $\vec{k}$ and spin σ. The terms $V^o\sigma^o$ and $V^z\sigma^z$ describe *diagonal* scattering events in which the TLS-atoms do not tunnel between wells. The term $V^x\sigma^x$ (first written down by Zawadowski [Zaw80]), describes so-called *electron-assisted tunneling* processes; during these, electron scattering does lead to tunneling, and hence the associated bare matrix elements

are much smaller than for diagonal scattering: $V^x/V^z \simeq 10^{-3}$.

In certain parts of the parameterspace (one needs "fast" TLSs, see section 2.6), the TLS-electron interaction can lead to complicated many-body effects, since the TLS allows the conduction electrons to effectively interact with each other: when one electron flips the TLS, the next electron knows about this.

The properties of this model will be discussed extensively in chapter 4. For now, note that its generic behavior can be understood by noting the analogy to the magnetic Kondo model, where a magnetic impurity (spin $\frac{1}{2}$, described by $\vec{S}$) interacts with conduction electrons through

$$H_{Kondo} = \sum_{\vec{k}\vec{k}'} c^\dagger_{\vec{k}\sigma} \left[\sigma^i_{\sigma\sigma'} S^i\right] c_{\vec{k}'\sigma'} \ . \tag{2.25}$$

In both cases one has a dynamic defect with two spin states (magnetic spin up/down, or TLS in left or right well), whose coupling to conduction electrons can cause scattering-induced spin-flips for the defect.

It has been shown [VZ83, MG86] that as the temperature is lowered, the coupling constant V^x and an analogous V^y grow to values comparable to V^z, and the TLS-electron model renormalizes to an isotropic 2-channel Kondo model. The 2 channels are the Pauli spin up and down ($\sigma = \uparrow, \downarrow$) of the conduction electrons, which are *not* flipped by the interaction (2.24). Hence, *the small-T behavior of the TLS-electron system can be understood in terms of that of the 2-channel Kondo model* (see chapter 4 for details).

Since the 2-channel Kondo model has been studied extensively, this means that some powerful predictions for the small-T, small-V behavior of the conductance in Ralph and Buhrman's nanoconstrictions can be made. They are the subject of chapter 3.

2.6 TLSs in nanoconstrictions

In this section we discuss in some detail the physical picture that Dan Ralph has pieced together [Ralph93] for what actually occurs inside his nanoconstrictions. We believe, and try to convey this belief to the reader, that the rather numerous assumptions that need to be made about the TLSs to make the 2-channel Kondo picture work, are all reasonable, given the lack of information on the microscopic details about what is *really* going on in the nanoconstrictions.

Direct Observation of two-level systems: It is a well-established experimental fact that two-level systems can occur in metal nanoconstrictions, and can influence the conductance. Ralls and Buhrman [RB88,RRB89] have observed slow, time-resolved fluctuations of the conductance between several discrete values (see Fig. 2.12). They ascribe these fluctuations to *slow* two-level systems [called two-level fluctuators (TLF)] in the constriction region that hop between their two wells; the conductance fluctuates (by an amount of order e^2/h), depending on which well they are in. These kind of signals occur in well-annealed devices in a range of temperatures and voltages where the TLF-motion occurs due to thermally activated hopping "over" the barrier, not tunneling through the barrier, i.e. they are "slow" two-level systems (hopping rates $\tau^{-1} < 10^8 s^{-1}$ [CZ95]) with large inter-well barriers.

The two-level systems that are proposed to give rise to the zero-bias anomaly in the unannealed devices are, in contrast, "fast" TLSs with small inter-well barriers, through which tunneling can occur (at rates $10^8 s^{-1} < \tau^{-1} < 10^{12} s^{-1}$). However, these defects presumably have the same microscopic nature as the slow fluctuators, being composed of atoms or small groups of atoms which move be-

Figure 2.12 Resistance vs. time in copper nanobridges [RB88] for $T < 150$ K showing several types of behavior. Fluctuations studied range from 0.005% to 0.2% of the total resistance. Time scales are somewhat arbitrary, as they depend on the temperature at which the fluctuation is observed. (a) A single TLF. (b) Two independent TLF's. (c) Amplitude modulation. Notice that the amplitude of the small TLF is larger when the large TLF is down than when it is up. (d) Frequency modulation of one TLF by another.

tween two metastable configurations. Therefore, Ralph and Buhrman suggest [RB92], [Ralph93, p. 265] that before annealing, each constriction may contain some fast, low-barrier tunneling states of the kind that cause a zero-bias anomaly; annealing would then tend to leave the sample only with two-level systems having high potential barriers, so that only slow, thermally activated transitions of the kind seen by Ralls *et al.* occur.

How many TLS? The maximum amplitude of the ZBA $[G(V = 0) - G_{max}]$ varies from sample to sample, from a fraction of e^2/h to as large as $70e^2/h$. This indicates that more than one TLS is probably contributing to the conductance. Assuming that a TLS composed of a single atom will not produce a scattering cross-section larger than approximately $8\pi/k_F$, one can estimate from eq. (2.21) its contribution to the conductance to be at most $\sim 4e^2/h$ [Ralph93, p.276]. To account for the largest signals, more than 10 such 1-atom TLSs would have to contribute to the signal. However, since a real TLS may well involve the

simultaneous small motion of tens of atoms, the corresponding signal per defect may well be substantially larger, and the required number of multi-atom TLSs smaller. Nevertheless, we shall see later in chapter 4 that even if many channels scatter off a single defect, only two pseudo-spin channels eventually dominate the low-energy physics. Therefore, we probably do need to assume a substantial number of TLSs in the constriction to explain the size of the signals.

It would not be unreasonable to expect tens of defects in the constriction region [Ralph93, p.277]: for example, the 6.4Ω constriction studied in [RB92] has a diameter of $\sim$ 13 nm [estimated via the Sharvin formula eq. (2.11)], and there are 10^5 Cu atoms within a sphere of this diameter about the constriction. Assuming $\sim$10 active TLSs to account for a ZBA of $\sim 70e^2/h$, their density is therefore roughly of order 10^{-4}/atom, about the same as estimates for the total density of TLSs in glassy systems.

Dislocation kinks: What could the microscopic nature of the TLSs be in the present case? Transmission electron microscopy studies of silicon constrictions with a similar geometry indicate that dislocation networks may form in the constriction region during fabrication [Theo91]. Thus, dislocation kinks could act as TLSs. This would explain property (P5), namely that the addition of even small (1 %) concentrations of impurities completely eliminates the ZBAs: the impurities would act as pinning sites for the dislocation kinks, disrupting their fluctuations between two equivalent positions (see also [RB95, p.3564]).

Asymmetry energy Δ: It will be argued in section 3.4 (and was mentioned on p.37) that for the 2-channel Kondo picture to make sense, the asymmetry energy Δ of all the active TLSs has to be $\Delta \lesssim 1$ K, which is a rather small splitting.

However, dislocation segments in a rather crystalline material would probably move in a rather symmetric environment, due to the surrounding crystal lattice. This might be one reason why TLSs with such small Δs are apparently possible (see also the *autoselection* argument below).

It is worth noting that tunneling centers with very small splittings have in fact been observed in polychrystalline Bi films. Zimmerman *et al.* [GZC92,ZGH91] were able to measure directly the parameters of a single slow-tunneling TLS (i.e. of the kind studied by Ralls and Buhrman), and found values as small as $\Delta = 0.08$ K [with coupling strengths $\rho_o J \simeq 0.7$ ($= \sqrt{2\alpha}$ there)]. Unfortunately, since these were *slow* tunneling centers, and the samples were strongly disordered, it is not clear that the samples of Ralph and Buhrman (fast tunneling, clean constriction) necessarily will have the same parameters. Nevertheless, the fact that tunneling centers with very small splittings do exist in some systems is encouraging.

Finally, it should be mentioned that Wingreen, Altshuler and Meir have recently argued [WAM95] that such splittings can not occur at all in a disordered material if the TLS-electron coupling has the large values that apply to the over-screened 2-channel Kondo fixed point. Their arguments, which I do not find entirely convincing, are presented in section 4.3.

Interactions between TLSs: In principle, TLSs should interact with each other, due to the strain fields caused around them, and the change in electron density around them. In fact, Ralls and Buhrman [RB88] have directly observed the modulation of the conductance signal from one TLSs due to the motion of another [see Fig. 2.12(c) and (d)]. Unfortunately, very little is known about the strength

of the interactions between TLSs in systems such as those of Ralph and Buhrman.

The scaling analysis presented in chapter 3 requires interactions to be negligible (because it assumes Kondo scattering off each individual impurity as though the others were not present). The success of the scaling analysis implies that interactions only set in at very low temperatures. Of course, it would be nice to have some independent way to estimate whether this is a reasonable assumption.

Autoselection: By now it should be evident that a TLS is required to have some rather special properties in order to contribute to a ZBA. Nevertheless, ZBAs are seen rather frequently. This might be due to the fact that experiment autoselects only "interesting" TLS. Those with inappropriate parameters (too large Δ, too strongly interacting with each other, etc.), simply do not flow to the strong-coupling 2-channel Kondo fixed point. Hence they do not give rise to an interesting T- and V-dependence, and only contribute to the boring background signal. The ZBA arises only from those TLS which happen to have parameters appropriate for scaling to the strong-coupling 2-channel Kondo fixed point.

Universality: At present, the 2-channel Kondo picture seems to be the only one that is consistent with all the experimental facts that have been accumulated. We shall therefore henceforth assume that the 2-channel Kondo picture as the orrect and appropriate one, and try to extract more quantitative predictions from it, for direct comparison with experiment. Indeed, some powerful predictions are possible, as we shall see in chapter 3. These predictions are based on the assumption that the experiment is in the universal scaling regime of the $T = 0$ fixed point of the 2-channel Kondo picture. It is important to emphasize that this means that the predictions are *universal,* i.e. *independent of which particular*

realization of the 2-channel Kondo model one has in mind. It does not matter whether the TLS is a dislocation kink (as proposed above) or something else, as long as it is governed by a 2-channel Kondo model in the universal scaling regime.

Chapter 3

Scaling Analysis

In this chapter we carry out a scaling analysis of the conductance $G(V,T)$ in the absence of a magnetic field, and demonstrate that it obeys the scaling relation eq. (2.22) of (P8):

$$\frac{G(V,T)-G(0,T)}{T^{\alpha}} = F(eV/k_BT)\ , \tag{3.1}$$

with $\alpha = 0.5 \pm 0.05$. This is simply an experimental fact, independent of any theoretical interpretation.[1] Nevertheless, this relation was predicted (before its experimental verification) by Andreas Ludwig on the basis of his conformal field theory (CFT) solution of the 2-channel Kondo model, and we shall present our analysis within this framework.

Section 3.1 gives a general scaling argument and a back-of-the-envelope calculation to motivate Ludwig's scaling Ansatz for the conductance $G(V,T)$. Section 3.2 presents a scaling analysis of the data, verifying that the data indeed

[1] Indeed, an explanation completely different from our's has recently been proposed by Wingreen *et al.* [WAM95]. They attribute the ZBA to disorder-enhanced electron-electron interactions, but in our opinion their explanation is at odds with some of the other experimental facts, in particular (P5) on page 28, as was argued on page 30.

does obeys Ludwig's scaling Ansatz. In section 3.3 we discuss the magnetic field dependence of the conductance, and in section 3.4 we obtain an experimental upper bound on the asymmetry energy Δ. Finally, we summarize the results of this chapter in section 3.5.

3.1 Ludwig's Scaling Ansatz

The 2-channel Kondo model is known [NB80] to flow to a non-trivial, non-Fermi-liquid fixed point at $T = 0$. This fixed point governs the physics in the so-called small-T, small-V regime, which is defined by the conditions $T \ll T_K$, $eV \ll k_B T_K$, where T_K is the Kondo temperature (the characteristic energy scale in the problem below which perturbation theory breaks down). Affleck and Ludwig have solved the k-channel Kondo problem exactly at $T = 0$, using conformal field theory [AL93].

In the spring of 1993, Andreas Ludwig suggested that in *the regime of smallest T and V in the Ralph-Buhrman experiment the TLSs that contribute to the zero-bias anomaly are all in the scaling regime of the $T = 0$ fixed point of the 2-channel Kondo model.* Based on this suggestion he predicted that the conductance should obey the scaling relation eq. (3.1), with $\alpha = \frac{1}{2}$.

3.1.1 Ludwig's original argument

Ludwig's argument leading to eq. (3.1), as originally presented in [RLvDB94], is as follows: Consider first the conductance signal $G_i(V, T)$ due to a single TLS (labeled by the index i) with $T \ll T_K^i$, $eV \ll k_B T_K^i$, $\Delta_i = 0$, but *arbitrary* ratio $eV/k_B T$. According to the general theory of critical phenomena, one expects that physical quantities will obey scaling relations in the neighborhood of any fixed

point.[2] For the conductance in the present case, a natural scaling Ansatz is:

$$G_i(V,T) = G_i(0,0) + B_i T^\alpha \, \Gamma\!\left(\frac{A_i eV}{(k_B T)^{\alpha/\beta}}\right) . \tag{3.2}$$

The parameters A_i and B_i are non-universal, positive constants, analogous to the $a_i^\pm$ and b_i of eq. (2.21), which may vary, for instance, as a function of the distance between the TLS and the narrowest point of the constriction. However, the function $\Gamma(v)$ should be a *universal function,* a fingerprint of the 2-channel Kondo model that is the same for *any* microscopic realization thereof. It must have the asymptotic form $\Gamma(v) \propto v^\beta$ as $v \to \infty$, so that $G(V,T)$ is independent of T for $eV \gg k_B T$. Due to the arbitrariness of A_i and B_i, we are free to use the normalization conventions that

$$\Gamma(0) \equiv 1 , \qquad \Gamma(v) \text{ vs. } v^\beta \text{ has} \quad \text{slope=1} \quad \text{as } v^\beta \to \infty . \tag{3.3}$$

Now, if V is small enough, its only effect will be to create a slightly non-equilibrium electron distribution in the leads. In particular, effects that directly affect the impurity itself, like V-dependent strains, or the "polarization" of the TLS in one well due to the non-equilibrium electron distribution, etc. can then be neglected. In this case, which we shall call the *weakly non-equilibrium regime,* V only enters in the Fermi functions of the leads, in the form $[e^{\beta(\varepsilon - eV/2)} + 1]^{-1}$, i.e. in the combination $eV/k_B T$, implying $\alpha = \beta$.

For a constriction with several defects, the conductance signal will be additive, i.e. (now using α=β):

$$G(V,T) = G(0,0) + T^\alpha \sum_i B_i \, \Gamma\!\left(\frac{A_i eV}{k_B T}\right) . \tag{3.4}$$

[2] This is discussed in detail in chapter 8.

Subtracting $G(0,T)$ from this to eliminate $G(0,0)$ then immediately gives the scaling relation eq. (3.1); $F(v)$ is non-universal, since it depends on the A_i and B_i.

This is as far as general scaling arguments will take one; a specific theory is needed to predict α. To this end, Ludwig proposed an analogy with the conductivity of a *bulk* metal containing 2-channel Kondo impurities. There the bulk conductivity $\sigma(T)$ is determined, via the Kubo formula,

$$\sigma(T) = 2\frac{e^2}{3m^2}\int \frac{d^3p}{(2\pi)^3}\left[-\partial_{\varepsilon_p} f_o\right]\vec{p}^{\,2}\tau(\varepsilon_p)\ , \tag{3.5}$$

by the elastic scattering life-time $\tau^{-1}(\omega) = -2\mathrm{Im}\ \Sigma^R(\omega)$, where $\omega \equiv \varepsilon_p - \mu$, and $\Sigma^R(\omega)$ is the retarded electron self-energy. Affleck and Ludwig have calculated $\Sigma^R(\omega)$ exactly, using CFT, and found that τ^{-1} has the following scaling form for $T \ll T_K$:

$$\tau^{-1}(\omega) \equiv -2\mathrm{Im}\Sigma^R(\omega) = \tau_o^{-1} + \tilde{b}\ T^{1/2}\ \tilde{\Gamma}(\omega/T)\ . \tag{3.6}$$

Here $\tilde{b}$ is a non-universal (positive) constant and $\tilde{\Gamma}(x)$ a universal function (given in [AL93, eq.(3.50)] and eq. (8.38)]), with the properties $\tilde{G}amma(x) < 0$, $\tilde{\Gamma}(x) = \tilde{\Gamma}(-x)$, $\tilde{\Gamma}(x) \propto x^{1/2}$ as $x \to \infty$, (the proportionality constant being negative).

It follows immediately from the Kubo formula that the bulk conductivity has the form

$$\sigma(T) = \sigma_o + \left(\frac{T}{T_K}\right)^{1/2}\sigma_1\ . \tag{3.7}$$

The power law $T^{1/2}$ is a signature of the non-Fermi-liquid nature of the $T = 0$ fixed point. For a Fermi liquid, one would have had T^2.

By analogy with the bulk case, Ludwig proposed that the bulk conductivity exponent $\alpha = \frac{1}{2}$ should also apply to the conductance in the nanoconstriction geometry, i.e. in eq. (3.2) one should also have $\alpha = \frac{1}{2}$.

3.1.2 Back-of-the-envelope calculation of $\Gamma(v)$

The above argument by analogy with the bulk conductivity has since been turned into a calculation tailored to the nanoconstriction geometry, which is presented in chapter 9. It turns out that the main idea can be summarized on the proverbial back of an envelope, if one is willing to gloss over some important subtleties:

The change in conductance due to back-scattering off defects in a nanoconstriction is given by eq. (2.21). The main difference between a bulk metal and a nanoconstriction is that the latter represents a decidedly non-equilibrium situation. However, in the weakly non-equilibrium regime, i.e. if the voltage is small enough, it is a reasonable guess (which is verified in later chapters) that the scattering rate of electrons off a TLS in the nanoconstriction is not all that different as when the TLS are in the bulk (provided one ignores interactions between different TLSs, which we always do). Hence, let us boldly use[3] the *equilibrium* form for τ^{-1}, namely eq. (3.6), in eq. (2.21) for ΔG, thus obtaining:

$$G(V,T) = G(0,0) - \tilde{K}\tilde{b}T^{1/2}\int d\omega[-\partial_\omega f_o(\omega)]\sum_i b_i \tfrac{1}{2}\left[\tilde{\Gamma}(\omega - \tfrac{1}{2}eVa_i^+) + \tilde{\Gamma}(\omega + \tfrac{1}{2}eVa_i^-)\right] \tag{3.8}$$

Now write $\omega/k_BT \equiv x$, $eV/k_BT \equiv v$, $f_o(v) \equiv [e^v+1]^{-1}$, and define a (universal) function $\Gamma(v)$ by:

$$\gamma_o\Gamma(\gamma_1 v) \equiv -\int dx[-\partial_x f_o(x)]\tilde{\Gamma}(x + v/2)\ . \tag{3.9}$$

Here γ_o and γ_1 are universal (positive) constants, chosen such that $\Gamma(v)$ is normalized as in eq. (3.3). Using the property $\tilde{\Gamma}(x) = \tilde{\Gamma}(-x)$ in the first term of

[3]The justification for this assumption is explained in section 9.3, page 250.

eq. (3.8), we find

$$G(V,T) = G(0,0) + T^{1/2} \sum_i (\tilde{K}\tilde{b} b_i \gamma_o) \, \tfrac{1}{2}\Big[\Gamma(a_i^+ \gamma_1 v) + \Gamma(a_i^- \gamma_1 v)\Big] \, . \tag{3.10}$$

Eq. (3.10) is precisely of the form eq. (3.4), and thus, assuming eq. (3.6) for $\tau^{-1}(\omega)$ as given, we have found a "derivation" for Ludwig's scaling Ansatz.[4] Moreover, this little calculation has furnished us with an expression, namely eq. (3.9), for the universal scaling function $\Gamma(v)$, in terms of the exactly known universal function $\tilde{\Gamma}(x)$.

This, in a nutshell, is all there is to the scaling prediction. The reader not interested in the technicalities of CFT and non-equilibrium quantum statistical mechanics can, with sigh of relief, disregard all subsequent chapters without fear of missing out on anything but mathematical physics. The origin of $T^{1/2}$ and of the scaling relations, and the calculation of $\tilde{\Gamma}(\omega)$, of course, will then forever remain a mystery to her.

3.2 Scaling Analysis of Experimental Data

In this section we present a careful scaling analysis of the experimental data. The analysis was done by Dan Ralph, in close collaboration with Andreas Ludwig and myself. I thank Dan Ralph for his kind permission to directly quote (indicated by " ") substantial portions of the text, and all the figures, from section 6.4.2 of his thesis for the present section.

[4] Note though that eq. (3.2) is actually a little too simplistic, since in eq. (3.10) each defect gives rise to two terms with different a_i^+ and a_i^-. Note also that $\tilde{K}$, b_i, γ_o are by definition all positive constants. However, it turns out that the sign of $\tilde{b}$ is not determined by CFT (see [AL93, after eq. (3.64)]). To explain the observed increase of $G(V,T)$ relative to $G(V,0)$ as T is increased, we have to choose $\tilde{b} > 0$.

"In general, the zero-bias signals always have the sign corresponding to a decrease in conductance at low T and low V. The signals are temperature-dependent, growing larger in amplitude with decreasing temperature. As a sample is cooled, the temperature at which the zero-bias features become measurable varies from sample to sample, ranging from 10 K to 100 mK. The amplitude of the signals may also vary over a large range, from less than 1 e^2/h to as much as 70 e^2/h at 100 mK."

3.2.1 First Test of $T^{1/2}$ and $V^{1/2}$ Behavior

"Fig. 3.1 shows the temperature dependence of the $V = 0$ conductance for 4 different samples on semi-log and $T^{1/2}$ scales. Fig. 3.2 displays the voltage dependence of the differential conductance for 3 of the samples at 100 mK (the fourth was not measured to such low temperatures). At high T and V, the conductance is approximately logarithmic. The range of logarithmic behavior varies from sample to sample, but may extend almost a decade in V or T. As T or V is lowered, the conductance on the semi-log plots crosses over from a logarithmic to a slower dependence. Crossover temperatures for these samples are in the range of a few K, while crossover voltages are a few tenths of mV."

At lower T and V, both the V and T behavior may be accurately described by a square root dependence.[5] This is in agreement with the scaling relation eq. (3.4) and the prediction $\alpha = \frac{1}{2}$, which give (using eq. (3.3)):

$$G(0,T) \;=\; G(0,0) + B_\Sigma T^{1/2}\,, \qquad B_\Sigma \equiv \sum_i B_i\,; \tag{3.11}$$

[5] "The size of deviations from $T^{1/2}$ behavior in Figs. 3.1(b) (1 part in 3000) is consistent with the magnitude of amplifier drift in these measurements, as they were performed over several days. The V-dependent measurements are less subjective to such drift problems, as they are taken over a much shorter time span."

Figure 3.1 Temperature dependence of the $V = 0$ conductance for 4 unannealed Cu samples, plotted on (a) a semi-log scale and (b) versus $T^{1/2}$. The values of the conductance for the different samples, extrapolated to $T = 0$ as shown are for sample #1: 2829 e^2/h, sample #2: 3973 e^2/h, sample #3: 30.8 e^2/h, and sample #4: approximately 2810 e^2/h.

Figure 3.2 Voltage dependence of the differential conductance at $T = 100$ mK for some of the same samples as in Fig. 3.1.

$$G(V,T_o) \;=\; const + F_o\,(eV/k_B)^{1/2} \qquad \text{at} \quad \text{fixed } T_o \ll eV/k_B\,. \quad (3.12)$$

Values for B_Σ and F_o can be obtained from straight-line fits in Figs. 3.1(b) and Figs. 3.2(b), and are listed in table 3.1.

However, "the data is such that, at this stage of the analysis, other functional forms cannot be ruled out. At low V, the voltage dependence could be consistent with power laws ranging from $V^{0.25}$ to $V^{0.75}$. Much more stringent tests of the theory are provided by the tests of the scaling properties of the V and T dependence of the conductance," which are described in the next section.

3.2.2 Scaling Collapse

The most stringent test of the exponent α of the conductance signals is provided by the scaling properties of the *combined* V and T dependence of $G(V,T)$. It is convenient to rewrite the scaling Ansatz eq. (3.4) to eliminate $G(0,0)$, which is not measured directly:

$$\frac{G(V,T)-G(0,T)}{T^\alpha} \;=\; \sum_i B_i\,[\Gamma(A_i v)-1] \;\equiv\; F(v)\,, \quad (3.13)$$

where $v = eV/k_BT$. To check this relation, one should plot the left hand side vs. v. Provided that one has chosen the correct value of α, the low-T curves for a given sample should all collapse, with no further adjustment of free parameters, onto the sample-specific scaling curve $F(v)$ vs. v. Furthermore, when $F(v)$ is plotted vs. v^α, the resulting curve is expected be linear for large v^α. By adjusting α to obtain the best possible collapse, one can determine α from the data quite accurately. 2-channel Kondo theory, of course, predicts $\alpha = \frac{1}{2}$.

The raw data for the differential conductance $G(V,T)$ of sample #1 is shown[6]

[6] "For eV much greater than k_BT, the conductance curves approach each other, but do

in Fig. 3.3, for T ranging from 100 mK to 5.7 K. "After rescaling as in eq. (3.13) and plotting the left-hand side vs. v, these data have the form shown in Fig. 3.4(a). The data at low V and low T collapse remarkably well onto one curve. Furthermore, $F(v)$ vs. v^α has linear asymptote as $v \to \infty$ [Fig. 3.4(b)], illustrating eq. (3.12).

The lowest curves in the figure, which deviate from scaling, correspond to the highest temperatures. These deviations from scaling at high V and T are expected, since if either V or T becomes too large ($\geq T_K$), the scaling Ansatz is expected to break down. We estimate T_K as that T for which the rescaled data already deviate from the scaling curve at $eV/k_BT \leq 1$. This gives $T_K \geq 5$ K for the defects of sample 1.

The quality of the scaling provides an exacting test of the exponent in the scaling Ansatz. Substitution of $T^{0.4}$ or $T^{0.6}$ for $T^{1/2}$ in eq. (3.13) produces a clear worsening of the collapse of the data. Fig. 3.5 and 3.6 show the poor collapse of the data for exponents other than $\alpha = \frac{1}{2}$.

As a more quantitative measure of the quality of scaling, we define the parameter $D(\alpha)$, which is the mean square deviation from the average scaling curve $\bar{F}(v) \equiv \frac{1}{N}\sum_{k=1}^{N} F_k(v)$ (where k labels the different experimental curves), integrated over small values of $v = eV/k_BT$ ($< v_{max}$):

$$D(\alpha) \equiv \frac{1}{N}\sum_{k=1}^{N}\int_{-v_{max}}^{v_{max}} dv \left[F_k(v) - \bar{F}(v)\right]^2 \ . \qquad (3.14)$$

not cross, in the range of voltages that are displayed. This demonstrates that the voltage dependence of the conductance is not purely a heating effect. If the only effect of an applied voltage were to cause the sample to heat, the currents through the sample at different T would converge at high V (because V would determine the effective temperature). This would require that the differential conductance curves at different T would cross, in order that the area under the curves would be equal at high V. This does not occur in the range of V displayed in Fig. 3.3."

Figure 3.3 Voltage dependence of the differential conductance for sample #1 of 3.1, plotted for temperatures ranging from 100 mK (bottom curve) to 5.7 K (top curve).

Figure 3.4 (a) The data of Fig. 3.3 for sample #1, rescaled according to eq. (3.13) and plotted vs. $v = eV/k_BT$. The low-temperature, low-voltage data collapse onto a single curve, with deviations when the voltage exceeds 1 mV. (b) When plotted against $v^{1/2}$, the resulting scaling curve is linear for large $v^{1/2}$, in agreement with eq. (3.12) .

Figure 3.5 Attempts at rescaling the data of Fig. 3.3 for sample #1, using temperature exponents of 0.3 and 0.4, showing that the collapse of the data does not work as well as for an exponent of 0.5.

Figure 3.6 Attempts at rescaling the data of Fig. 3.3 for sample #1, using temperature exponents of 0.6 and 0.7, showing that these do not collapse the data as well as 0.5 either.

$D(\alpha) = 0$ would signify perfect scaling. Taking the 5 lowest T ($\leq$ 1.4 K), and $v_{max} = 8$ (these are the data which *a priori* would be expected to be most accurately within the scaling regime, since they are closest to the $T = 0$ fixed point), one obtains Fig. 3.7(a). Evidently the best scaling of the data requires $\alpha = 0.48 \pm 0.05$ (the estimated uncertainty of ± 0.05 comes from the uncertainty in the exact minimum in the curve in Fig. 3.7(a)). This is in good agreement with the CFT prediction of $\alpha = \frac{1}{2}$.

We have also tested the more general scaling form of Eq. (3.2), and have observed scaling for $0.2 < \alpha < 0.8$, with $(\beta - 0.5) \approx (\alpha - 0.5)/2$, with best scaling for $\alpha = 0.5 \pm 0.05$. But as argued earlier on page 49, one expects $\alpha = \beta$ on general grounds.

The scaling Ansatz has also been tested on two other Cu samples. The rescaled data for sample 2 (Fig. 3.8) collapse well onto a single curve at low V and T, for $\alpha = 0.52 \pm 0.05$ [Fig. 3.7(b)] and with $T_K \geq 3.5$ K. At high V and high T the non-universal conductance spikes, discussed previously [RB92, Ralph93,RB95], are visible. The data for sample #3 do not seem to collapse as well (Fig. 3.9) (illustrating how impressively accurate by comparison the scaling is for samples #1 and #2). However, we suggest that this sample in fact displays two separate sets of scaling curves (see arrows), one for $T \leq 0.4$ K and one for 0.6 K $\leq T \leq 5$ K, with interpolating curves in between. This could be due to defects with a distribution of T_K's, some having $T_K \simeq 0.4$ K and others having $T_K \geq 5$ K. The second (higher-T) set of curves do not collapse onto each other as well as the first, presumably because there is still some (approximately logarithmic) contribution from the $T_K \simeq 0.4$ K defects.

Figure 3.7 The deviation parameter $D(\alpha)$ of eq. (3.14), which quantifies the quality of scaling, for (a) sample #1 and (b) sample #2. The minimum of $D(\alpha)$ defines the value of α that gives the best scaling, giving $\alpha = 0.48 \pm 0.05$ for sample #1 and $\alpha = 0.52 \pm 0.05$ for sample #2.

Figure 3.8 Differential conductance data for sample #2 of Fig. 3.1, at temperatures from 200 mK to 5.7 K, rescaled according to eq. (3.13). The low-voltage, low-temperature data collapse well onto one curve.

Figure 3.9 Differential conductance data for sample #3 of Fig. 3.1, at temperatures from 50 mK to 7.6 K. The data do not collapse onto one curve for this sample, possibly due to the existence of TLSs with Kondo temperatures in (rather than above) the temperature range of the measurement.

"A somewhat complimentary estimate for the highest Kondo temperatures of the TLSs in these samples comes from the temperature at which the zero-bias signals first become visible as the samples are cooled. For all 3 samples featured here, this value is approximately 10 K.

"The magnitudes of the Kondo temperatures, being in the few K range, are rather large relative to the earliest theoretical predictions of 0.01-0.1 K [VZ83, ZV92]. However, they are not out of line with more recent speculations that virtual excitations to higher-lying energy levels in the double-well potential of a TLS may increase the Kondo temperature above previous estimates, to around 1-10 K" [ZZ94a].

3.2.3 Universality

If for any sample all the A_i in Eq. (3.13) were equal, one could directly extract the universal scaling curve from the data. The curve obtained by plotting

$$\frac{G(V,T)-G(0,T)}{B_\Sigma T^{1/2}} \quad \text{vs.} \quad (AeV/k_BT)^{1/2}\ , \tag{3.15}$$

with A determined by the requirement that the asymptotic slope be equal to 1 (compare eq. (3.3)), would be identical to the universal curve $[\Gamma(x)-1]$ vs. $x^{1/2}$. Such plots are shown in Fig. 3.10(b). The fact that the scaling curves for all three samples are indistinguishable indicates that the distribution of A_i's in each sample is quite narrow, and is a measure of the universality of the observed behavior.

To make possible quantitative comparisons of the data with the CFT prediction of eq. (3.9), we now proceed to extract from the data the value of one universal (sample-independent) constant and an upper bound on another (es-

Figure 3.10 Representative conductance curves which lie along the scaling curves for each of the 3 samples in Fig. 3.4, Fig. 3.8 and Fig. 3.9. For sample #1, the curve corresponds to T=1.1 K, for sample #2 1.4 K, and for sample #3 250 mK. These curves were chosen because they had the best signal-to-noise ratio for each sample, for those lying along the scaling curve. (a) The y-axis is scaled by the value of B_Σ determined from the temperature dependence of the $V = 0$ conductance for each sample (values listed in Table 6.1). (b) In addition, the x-axis scaled with a number a_i for each sample. The scaling curves for all three samples seem to lie on one universal curve.

sentially Taylor coefficients of $\Gamma(v)$). The procedure by which we extract these parameters is independent of the possible distribution of A_i's and B_i's.

Consider the sample-specific scaling function $F(v)$ defined in Eq. (3.13). By construction, $F(0) = 0$, and if $F(v)$ is symmetric and analytic at $v = 0$ (as the data suggest) one also has $F'(0) = 0$. The second derivative, $F''(0) = \Gamma''(0) \sum_i B_i A_i^2$, may be measured directly from the low eV/k_BT portion of the scaling curve.

Next, consider the regime $v \gg 1$. As argued earlier, here $\Gamma(v) \simeq v^\beta$, and since β=α=1/2, with our normalization conventions eq. (3.3) we can write, asymptotically

$$\Gamma(v) - 1 \equiv v^{1/2} + \Gamma_1 + O(v^{-1/2}) \,. \tag{3.16}$$

It follows from Eq. (3.13) that

$$F(v) = v^{1/2} F_0 + F_1 + O(v^{-1/2}) \,, \tag{3.17}$$

where $F_0 \equiv \sum_i B_i A_i^{1/2}$ and $F_1 \equiv \Gamma_1 B_\Sigma$. Values for F_0 and F_1 may be determined from the conductance data by plotting F versus $(eV/k_BT)^{1/2}$ and fitting the data for large $(eV/k_BT)^{1/2}$ to a straight line. For samples 1 and 2 we fit between $(eV/k_BT)^{1/2}$=2 and 3, and for sample 3 (using only the curves below 250 mK) between 2 and 2.5. Values for $F''(0)$, F_0, and F_1 are listed in Table 3.1. The uncertainties listed are standard deviations of values determined at different T within the scaling regime for each sample.

From these quantities, we obtain an experimental determination of the universal number $\Gamma_1 = F_1/B_\Sigma$ and an upper bound on the universal number $\Gamma''(0)$:

$$\frac{F''(0) B_\Sigma^3}{F_0^4} \;=\; \frac{\Gamma''(0) \left[\sum_i B_i A_i^2\right] B_\Sigma^3}{\left[\sum_i B_i A_i^{1/2}\right]^4} \geq \Gamma''(0) \,. \tag{3.18}$$

Table 3.1 Measured parameters of the scaling functions for the Kondo signals in 3 Cu samples. B_Σ, $F''(0)$, F_o and F_1 have units $K^{-1}e^2/h$, and Γ_1 and $\frac{F''(0)B_\Sigma^3}{F_0^4} \geq \Gamma''(0)$ are dimensionless.

#	B_Σ	$F''(0)$	F_0	F_1	$\Gamma_1 = \frac{F_1}{B_\Sigma}$	$\frac{F''(0)B_\Sigma^3}{F_0^4}$
1	7.8 ± 0.2	0.55 ± 0.04	4.2 ± 0.3	-5.7 ± 0.9	-0.73 ± 0.11	0.8 ± 0.3
2	25.2 ± 0.7	1.03 ± 0.09	12.8 ± 0.8	-19.7 ± 1.5	-0.78 ± 0.06	0.6 ± 0.2
3	10.3 ± 0.4	0.82 ± 0.06	6.0 ± 0.6	-7.7 ± 1.6	-0.75 ± 0.16	0.7 ± 0.3

Values for Γ_1 and this ratio are listed in Table 3.1 and are consistent among all 3 samples.

3.3 Magnetic Field Dependence

Since the electron-TLS interaction is non-magnetic, it is not entirely obvious in what way a magnetic field (H) couples to the system. However, at least two possibilities come to mind, both of which drive the system away from the fixed point, but not in precisely the same manner. Firstly, due to Pauli paramagnetism, a magnetic field *breaks channel symmetry* (recall that the channel index i labels Pauli spin $\uparrow, \downarrow$), since it causes a net magnetic moment $M = \mu_0^2 H N(\varepsilon_F)$ [Ziman, eq, (10.11)]. Secondly, it has been argued theoretically [AS89] and demonstrated experimentally [ZGH91,GZC92] that the asymmetry energy of a TLS is a random function[7] of the magnetic field, $\Delta = \Delta(H)$. The reason is, roughly, that Δ depends on the difference $\delta\rho$ in the local electron density at the two minima of the TLS potential; due to quantum interference effects, $\delta\rho$ can change in a random

[7]It may be, though, that this effect occurs only for strongly disordered systems, such as those studied in [ZGH91,GZC92], where there is a large amount of impurity scattering, but not in clean systems. In this case it would not apply to the present experiment, and the analysis below would not be applicable.

way when H is changed, so that Δ depends on H too. Thus in general $\Delta(H)$ is a non-monotonic, random function of H. However, for a TLS that started out with $\Delta \simeq 0$, Δ will in general increase as H is turned on (see [ZGH91, Fig. 4]).

A magnetic field will affect the conductance via its effect on the self-energy [since $\tau^{-1}(\omega) = -2\mathrm{Im}\,\Sigma^R(\omega)$]. For small values of H and Δ, the distance in the (T, H, Δ) parameter space that the system has been displaced away from the $(T, H, \Delta) = (0, 0, 0)$ fixed point due to channel anisotropy (CA) and asymmetry energy (AE), is proportional to H and Δ, respectively. Now, it can be shown that both channel anisotropy and asymmetry energy (which corresponds to a local magnetic field $h = \Delta$ in the language of the magnetic Kondo problem) are, in the RG sense, *relevant perturbations with scaling dimensions* $\frac{1}{2}$ (see eqs. (3.15) and (3.19) of [AL92b], or [CZ95, section 3.4.1 (e)]). That means that the self-energy and hence τ^{-1} is a function of $\left(\frac{H^2}{k_B T E_{CA}}\right)$ and $\left(\frac{\Delta^2}{k_B T E_{AE}}\right)$, where E_{CA} and E_{AE} are constants that set the energy scales for channel anisotropy and asymmetry energy to become important:[8]

$$\tau^{-1}(\omega, H, \Delta, T) = \tau_o^{-1} + \tilde{b} T^{1/2} \tilde{\Gamma}\left(\frac{\omega}{T}, \frac{H^2}{k_B T E_{CA}}, \frac{\Delta^2}{k_B T E_{AE}}\right) . \tag{3.19}$$

Since τ^{-1} must be T-independent in the limit $T \to 0$, we must have asymptotically:

$$\tilde{\Gamma}(x, y, z) \sim y^{1/2} \qquad \text{for} \quad x, z \lesssim 1, \quad \text{and}\, y \to \infty\ ; \tag{3.20}$$

$$\tilde{\Gamma}(x, y, z) \sim z^{1/2} \qquad \text{for} \quad x, y \lesssim 1, \quad \text{and}\, z \to \infty\ . \tag{3.21}$$

[8] This can be proved using finite-size scaling arguments: for a system of fermions, all fields must be anti-periodic, with period $\beta = 1/k_B T$, in the imaginary time direction, i.e. they live on a strip of width $L \equiv \beta$. Therefore the limit $T \to 0$ corresponds to the customary $L^{-1} \to 0$ in finite-size scaling arguments, i.e. T is a relevant perturbation with scaling dimension 1 (see section 8.4).

Using these results in eq. (3.9) for $\Gamma(v)$ and eq. (3.10), we can make the following predictions, at $V = 0$ and in the limit $T \to 0$:

If the channel anisotropy effect of H dominates the asymmetry energy effect (i.e. $E_{CA} \ll E_{EA}$), but H is still small enough that one is close to the 2-channel fixed point, then at $V = 0$, and in the limit $T \to 0$,

$$G(H,T) - G(0,0) \propto |H| \; . \tag{3.22}$$

On the other hand, if the effects of a change in asymmetry energy $\Delta(H)$ with H dominate the channel anisotropy effect, (i.e. $E_{EA} \ll E_{CA}$), then

$$G(H,T) - G(0,0) \propto \sum_i \tilde{B}_i |\Delta_i(H)| \; . \tag{3.23}$$

In the latter case, the detailed H-dependence is essentially unknown, since nothing is known about the random functions $\Delta_i(H)$, apart from the fact that they probably increase with $|H|$ for small H.

Unfortunately, in the absence of a microscopic model for the TLSs, it seems impossible to predict from first principles which of the 2 effects will dominate the other. The experimental H-dependence is shown in Fig. 3.11, which shows the non-analyticity at $H = 0$ predicted by eq. (3.22), suggesting that channel anisotropy effects are dominant at small H. On the other hand, the non-universal non-monotonic features seen at large H for sample #2 (which is also the one containing the conductance spikes), could possibly be due to the non-monotonic features of $\Delta(H)$ becoming important at large H. Thus, while it would be an exaggeration to claim that the 2-channel Kondo model correctly "predicts" the observed H-dependence, it evidently *is* possible to accommodate the observed H-dependence within the 2-channel Kondo phenomenology.

Figure 3.11 Magnetic field dependence of the V=0 conductance for the 3 unannealed Cu samples at 100 mK. (a) Absolute magnetoconductance. (b) Magnetoconductance scaled by the value of B_Σ for each sample. (c) Magnetoconductance relative to the change in conductance between 100 mK and 6 K. An applied magnetic field alters, but does not eliminate, the zero-bias conductance signal due to TLSs.

If H is made large enough, the polarization of the Fermi sea will become so strong that one channel of conduction electrons (the one with higher Zeeman energy) will decouple from the impurity altogether, and the system will cross over to the one-channel Kondo fixed point, at which the conductance T-exponent is $\alpha = 2$. In this scenario, the conductance, at fixed, large H, should obey the scaling relation eq. (3.13), with $\alpha = 2$ [AL93, eq. (D29)]. Dan Ralph performed such a V, T scaling analysis for sample #2 at fixed $H = 6$ T (Fig. 3.12). The data do not collapse with $\alpha = \frac{1}{2}$ and also not with $\alpha = 2$, meaning that the system is neither at the 2-channel fixed point nor at the 1-channel fixed point. A reasonable collapse is obtained for $\alpha = 0.3$ [Fig. 3.12(b)]. This might mean that the data in Fig. 3.12 correspond to some complicated crossover regime, between the limits of 1-channel and 2-channel behavior. Alternatively, since $H = 6$ T is a very large field, and for sample #2 non-monotonic features, that are presumably non-universal, have already set in at fields as small as 1 T, the 6 T data might simply be in the non-universal regime at which no scaling *should* be expected.

It would be interesting to perform a V, T scaling analysis for a set of *small* H-fields, between 0 and 1 T, which are presumably still in the universal regime. This would allow a systematic analysis of the flow away from the 2-channel Kondo fixed point as a function of H. Unfortunately the experiments were done 2 years ahead of the theory, and hence not enough data is available to carry through such an analysis.

If one assumes channel anisotropy to be the dominant effect of H, then in principle it should be possible to calculate exactly, using Bethe-Ansatz techniques, the cross-over scaling function $G(H, T)$ from the 2-channel to the 1-channel fixed

Figure 3.12 (a) Differential conductance at 6 Tesla for sample #2 of Fig. 3.1, rescaled according to eq. (3.13), for temperatures from 100 mK to 1.1 K. The data no longer collapse onto one curve, indicating that at high fields the system is no longer governed by the $T = 0$ fixed point of the two-channel kondo model. (b) The low-temperature data collapse reasonably well for a temperature exponent of 0.3. The curve which does not collapse corresponds to 1.1 K.

point [Lud95]. This would be a very interesting theoretical challenge, since such cross-over functions are in general hard to calculate. However, the theorist setting out to calculate this cross-over function should be aware of the uncertainty as to which effect, channel anisotropy or energy asymmetry, dominates in the actual experiment (in particular since non-monotonic behavior is observed for $G(H)$ in some samples). Unfortunately, this uncertainty may somewhat limit the applicability to experiment of such a calculation.

3.4 Asymmetry energy Δ

The analysis of the previous section enables us to estimate an upper bound on the asymmetry energy Δ (at H=0) in our samples. Our scaling analysis (at H=0) assumes that $\frac{\Delta^2}{TE_{AE}}$ is small enough that the scaling form eq. (3.19) is essentially independent of this argument. This implies that $\frac{\Delta^2}{TE_{AE}} \lesssim 1$, i.e. $T \gtrsim \frac{\Delta^2}{T_K}$, where we have assumed that $E_{AE} \simeq T_K$ (since at H=0 and $V \ll T_K$, the only characteristic energy scale in the problem is T_K).

The fact that the data for samples 1 and 2 show pure $(T/T_K)^{1/2}$ scaling for 0.4 $K < T < T_K$ implies that any non-zero Δ must be rather small: for $T_K \approx 5$ K, good scaling down to 0.4 K implies $\frac{\Delta^2}{T_K} < 0.4$ K and hence $\Delta < 1.4$ K. We suggest that the defects that are selected by (i.e. dominate) our transport measurements are those with a strong V, T-dependence. Such TLSs must have significant tunneling amplitudes, and hence cannot have large Δ [Zaw80, (b) p.1599–1600]. Also, the microscopic origin of our TLSs, likely dislocations in clean metal, may well produce lower asymmetry energies than for TLSs in glassy materials. A longer discussion of the likelihood of finding TLSs with $\Delta \lesssim 1$ K in

a nanoconstriction may be found in section 2.6 on page 43.

3.5 Summary

We have shown in this chapter that V, T scaling of the conductance $G(V,T)$, with a T-exponent $\alpha = \frac{1}{2}$, is an established experimental fact. We have argued that this scaling behavior can be understood naturally within the phenomenology of the $T = 0$ fixed point of 2-channel Kondo model. Breakdown of scaling for larger T and V values is explained too, since for these the system is no longer fine-tuned to be close to the $T = 0$ fixed point, so that scaling is spoiled. Estimates of T_K in the range 1-5 K, which is reasonable, were obtained. The magnetic field dependence for small H can also be understood within this framework, though an unambiguous scaling analysis has not been possible, due to lack of data, and it remains an open question whether it is channel anisotropy or asymmetry energy effects that are dominant. Finally, a rather small but in our opinion reasonable upper bound for the asymmetry energy $\Delta \lesssim 1$ K has been obtained.

We hope to have persuaded the reader that the 2-channel Kondo model, at its $T = 0$ fixed point, is in rather good agreement with the observed phenomenology, and that quantitative calculations based on this model are therefore warranted. The remainder of this thesis is devoted to a quantitative calculation of the scaling function $\Gamma(v)$, to be compared with the experimental curve in Fig. 3.10(b). The final result is shown in 9, Fig. 9.6.

The theoretical framework needed to perform this calculation, namely conformal field theory, may seem rather formidable to the uninitiated reader. Some may have their doubts whether it is sensible to apply such elaborate theoretical tools

to the present experimental system, given the lack of microscopic information about it. Our attitude is: once a model has been deemed worthy of careful consideration, and in the present chapter we have tried to argue that the 2-channel Kondo model certainly qualifies, one should fearlessly employ whatever tools necessary, be they ever so involved, to extract from it quantitative predictions. In particular when interested, as we are, in universal properties close to a critical point, microscopic details should not matter.

Chapter 4

The Non-Magnetic Kondo Problem

The goal of this chapter is to describe the orbital (non-magnetic) Kondo model of Zawadowski and coworkers [Zaw80,BVZ82,VZ83,VZ85,VZZ86,VZZ88,Zar93, ZZ94a,ZZ94b,Zar95], that describes the interaction of a tunneling center (TC) with conduction electrons in a metal. As an introduction, in section 4.1 we define the multi-channel (magnetic) Kondo model of Nozières and Blandin [NB80] and discuss the physical picture developed by Nozières for the $T \to 0$ regime. Section 4.2 is devoted to Zawadowski's model. In particular, we outline in some detail the poor man's scaling RG analysis that determines the nature of the RG flow away from the weak-coupling regime. In section 4.3, we briefly discuss and comment on some recent criticism of this model by [WAM95] and [MF95]. Finally, in section 4.4 we discuss the complications that occur when considering a non-equilibrium version of the orbital Kondo model.

The main result of this chapter is that the non-magnetic Kondo model flows to an isotropic, 2-channel Kondo fixed point, described by the effective Hamiltonian H_{int}^{eff} of eq. (4.23). The non-equilibrium version (4.27) of this Hamiltonian is used in chapter 9 as starting point [see eq. (9.6)] for our calculation of the conductance through Ralph and Buhrman's nanoconstrictions.

4.1 The Multi-channel Kondo Model

In this section, we define the magnetic multi-channel Kondo model of Nozières and Blandin and discuss the physical picture developed by Nozières for the $T \to 0$ regime. The material can be found in any number of reviews, see e.g. the book by Hewson [Hew93], or [Lud94a, p. 359].

4.1.1 Definition of the Model

The magnetic multi-channel Kondo problem was introduced by Nozières and Blandin [NB80]. They consider the general case of a spin-s magnetic impurity, coupled anti-ferromagnetically to k degenerate bands (called *channels* or flavors) of electrons in an $SU(2)^{(spin)} \times SU(k)^{(flavor)}$ invariant way. In the so-called *weak-coupling limit*, where perturbation theory holds, the Hamiltonian is defined as

$$H = \sum_{p\alpha i} \varepsilon_p c^\dagger_{p\alpha i} c_{p\alpha i} \; + \; \lambda_K \sum_{pp'} \sum_{\alpha\alpha' i} c^\dagger_{p\alpha i} \tfrac{1}{2} \vec{\sigma}_{\alpha\alpha'} c_{p'\alpha' i} \cdot \vec{S} \; , \qquad (\lambda_K > 0) \; . \tag{4.1}$$

Here the operators $\vec{S} \equiv b^\dagger_a \vec{S}_{ab} b_b$ describe the local spin-s impurity, where $[S^A, S^B]_{ab}$ $= i\varepsilon^{ABC} S^C_{ab}$ and $|a\rangle = b^\dagger_a |0\rangle$ (for $a \in [-s, \ldots + s]$) are the $2s+1$ spin states of the magnetic impurity. Electrons are described by the second-quantized operators $c^\dagger_{p\alpha i}$, where p is the magnitude of its momentum, $\alpha, \beta = \pm$ labels the electron

spin[1], and $i = 1, \ldots, k$ labels the k channels. Note that H is diagonal in channel indices, which are therefore "spectator" indices.

In Nozières and Blandin's original work they considered an impurity with angular momentum l, to which only electrons with angular momentum l, described by the operators $c^\dagger_{plm,\alpha}$ can couple. The channel index i then corresponds to $m_l \in [-l, \ldots + l]$, i.e. there are $k = 2l + 1$ channels. However, more generally, the channel index i can correspond to any quantum number in which the interaction is diagonal.

Kondo became famous for showing that the second-order vertex correction [see Fig. 4.4(a)], calculated in perturbation theory in λ_K, depends on $\log T/D$, where D is the band-width and T the temperature [Kon64], [Hew93, section 2.4]. This means that as T is lowered below a characteristic cross-over temperature T_K, called the Kondo temperature, perturbation theory breaks down, because $\log T/D$ becomes so large that the expansion coefficient in the perturbation series is no longer small.

The break-down of perturbation theory indicates that complicated many-body physics is at work: the interaction with a dynamical impurity, whose spin can flip, implies that the electrons are no longer independent: (very) loosely speaking, when an electron interacts with the impurity and flips its spin, the next electron notices that the spin has flipped, and hence is affected by the previous electron, leading to an effective electron-electron interaction.

Subsequent work by Anderson and coworkers [And70,YA70,AYH70] and Wil-

[1]In this section we use the terminology that is appropriate to the *magnetic* multi-channel Kondo problem, i.e. "spin" (α, β) refers to the Pauli spin that couples to the magnetic impurity. In later sections (and chapter 9) the notation α, β for the pseudo-spin index (that couples to the dynamic impurity) and i for the channel index (the spectator) will be maintained, but the physical quantum numbers that these indices are associated with will be different.

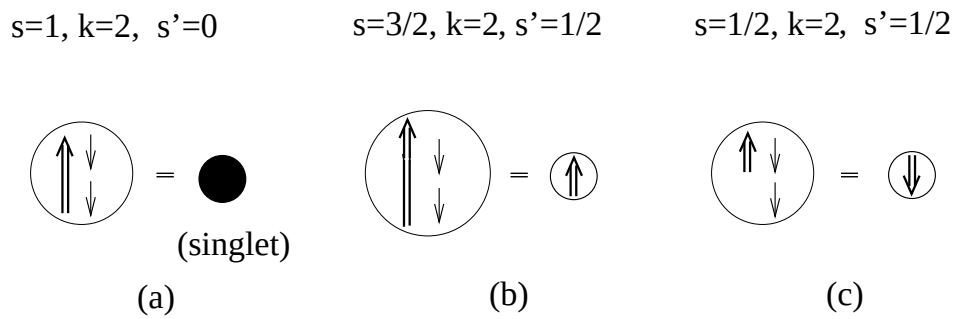

Figure 4.1 (a) Completely screened Kondo problem ($s = k/2$): k conduction electrons of the same spin form an inert singlet ($s' = 0$) with the impurity spin. (b) Underscreened Kondo problem ($s > k/2$): k electrons of the same spin cannot completely compensate the spin of the local impurity of spin s: a residual unscreended spin of $s' = s - k/2$ remains, which is coupled *ferro*magnetically to the remaining conduction electrons. (c) Overscreened Kondo problem ($s < k/2$): k electrons overcompensate the spin s of the impurity. An overscreened object of spin $s' = k/2 - s$ remains, which is coupled *anti*-ferromagnetically to the remaining conduction electrons.

son [Wil75] has shown that the regime $T < T_K$ can be understood within the framework of the renormalization group: the presence of $\log T/D$-terms implies that the effective coupling constant grows as one renormalizes to smaller temperatures, and flows out of the weak-coupling $\lambda_K \ll 1$ regime. For example, for $k = 1$, it was shown that $\lambda_K \to \infty$ as $T \to 0$, i.e. the problem flows towards the so-called *strong-coupling* fixed point.

4.1.2 Nozières' Physical Picture at Strong Coupling

In general, depending on the values of s and k, the coupling can flow to one of three qualitatively different fixed points, called *completely screened* ($s = k/2$), *under-screened* ($s > k/2$) and *over-screened* ($s < k/2$) [shown in Fig. 4.1, with flow diagrams given in Fig. 4.2]. Nozières has developed a very simple intuitive picture for these fixed points [Noz74,Noz75,Noz78,NB80]. We now briefly summarize his arguments, which have been completely confirmed by detailed numerical

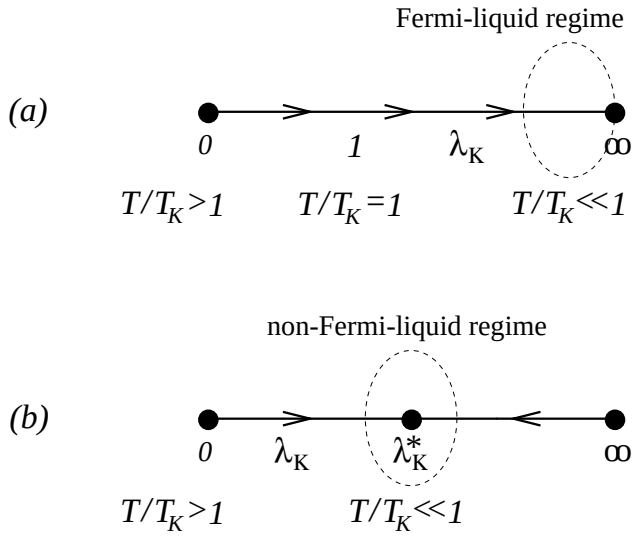

Figure 4.2 Flow-diagrams for the Kondo coupling constant for (a) the completely screened ($s = k/2$) and under-screened ($s > k/2$) cases, and (b) the over-screened case ($s < k/2$).

renormalization group calculations [Wil75,KWW80,CLN80,PC91,AL92b].

First consider the case $s = k/2$ (*complete screening*), in which case $\lambda_K \to \infty$. Because λ_K is becomes large, the state in which $\langle H_{int} \rangle$ is minimized is strongly favored. Hence, k conduction electrons "get trapped" at the origin, coupled together to a total spin of $k/2$, to form a *singlet* ($s' = 0$) with the impurity spin [Fig. 4.1(a)]. Being a singlet, this new composite object at the origin is no longer a dynamical object, but simply an "inert lump", which may be visualized as a bound state consisting of the impurity and a *screening cloud* of k electrons. Since the remaining conduction electrons cannot occupy the origin (that would break the singlet and cost a large energy of order $\lambda_K \to \infty$), the inert singlet acts as an infinitely repulsive, *non-magnetic* scattering potential, which merely causes a phase-shift when other electrons scatter off it. The fact that this scattering is non-magnetic implies that $\lambda_K = \infty$ is a *stable* fixed point, at which the physics

is simple. Nozières has shown [Noz74] that it can be described by a Fermi liquid theory.

Consider next the case $s > k/2$ (*underscreening*). Because of the Pauli principle, the largest spin that can be formed by conduction electrons at the origin is $k/2$, which is too small to be coupled to a singlet with s. Hence, an (unscreened) free impurity spin of size $s' = s - k/2$ remains [Fig. 4.1(b)]. The effective interaction between the remaining conduction electrons and this unscreened remaining spin s' can be shown to be *ferro*magnetic (roughly speaking, if s is up then s' is up, and the conduction sea also has net spin up (of size $k/2$), since $k/2$ spin down electrons have been coupled to the original spin s up). Since ferromagnetic couplings are known to be irrelevant, $\lambda_K = \infty$ is a stable fixed point in this case too, and the physics is again simple.

Finally, consider $s < k/2$ (*overscreening*). As λ_K becomes large, the impurity (say of spin up) will at first attempt to capture k conduction electrons (of spin down), forming an overscreened composite object of spin $s' = k/2 - s$ (down) [Fig. 4.1(c)]. It cannot capture *less* than k electrons at a time, since that would break channel symmetry, which was taken to be an exact bulk symmetry of the system and cannot be broken in the bulk by a single local impurity. Having spin s', this composite object is not inert but still dynamical. It forms another Kondo problem with the remaining conduction electrons, with a coupling that is again *anti*-ferromagnetic (roughly speaking, if s is up then then s' is down, but the conduction sea has net spin up [of size $k/2$]). Hence, similar to the $\lambda_K = 0$ fixed point, the $\lambda_K = \infty$ fixed point is also unstable. Since both $\lambda_K = 0$ and $\lambda_K = \infty$ are unstable, there must be a *stable* fixed point in between, at some intermediate

value[2] of the coupling (first identified by Nozières and Blandin in the limit of a large number of bands ($k \to \infty$) but with s kept fixed). This is called the *over-screened* (or sometimes also *strong-coupling*) fixed point. Using an analogy due to Wilson, it may be visualized as an onion of ever-increasing size, the layers of which correspond to layers of conduction electrons of alternating spins, each layer trying (unsuccessfully) to screen the dynamical composite object within.

The physics at this fixed point is highly non-trivial, and cannot be described by a Fermi liquid theory – it exhibits so-called *non-Fermi-liquid*-like behavior. For example, exact values of some thermodynamic exponents at finite values of $s < k/2$ have been obtained by the Bethe Ansatz [AD84,WT85], exhibiting non-Fermi-liquid critical exponents unlike those found for the underscreened or completely screened cases. The CFT solution of AL gives a complete description of this fixed point, enabling one to compute all thermodynamic quantities and Green's functions exactly (their methods of course also work for the under- and completely screened cases [Aff90,AL91a], although the details are somewhat different). The transport coefficients, too, show anomalous non-Fermi-liquid behavior. For example, for $k = 2$, AL showed that the conductivity at very low temperatures behaves as $\sigma(T) = \sigma_o + BT^\alpha$, with $\alpha = 1/2$. In contrast, for a Fermi liquid, one always has $\alpha = 2$, as was indeed found by Noziéres [Noz74] for the case $k = 1$.

The rest of this chapter is devoted to showing that a two-level system interacting with conduction electrons can be described, at low temperatures, by the 2-channel Kondo problem, and should hence display non-Fermi-liquid properties.

[2] It turns out that $\lambda_K^* = \frac{2}{2+k}$, see just before eq. (7.35).

4.2 The Non-Magnetic Kondo Problem

The theory of a tunneling center (TC) [simply called a two-level system (TLS) in the other chapters of this thesis] interacting with metallic conduction electrons within the framework of the non-magnetic or orbital Kondo model, is due to Zawadowski and coworkers. Zawadowski proposed his model in [Zaw80], subsequently developed it with his coworkers in [BVZ82,VZ83,VZ85,VZZ86,VZZ88], and rather recently, together with Zaránd, introduced some important refinements [Zar93, ZZ94a, ZZ94b, Zar95]. This work has been reviewed in [ZV92], and an exhaustive review is currently being written by Zawadowski and Cox [CZ95]. Our discussion mainly follows the recent papers by Zaránd and Zawadowski [ZZ94a,ZZ94b] and Zaránd [Zar95].

4.2.1 General Considerations

Consider a tunneling center in a metal, i.e. an atom or group of atoms that can hop between two different positions inside the metal, modelled by a double-well potential [see Fig. 2.11, page 39, and Fig. 4.3]. At low enough temperatures and if the barrier is sufficiently high, hopping over the barrier through thermal activation becomes negligible. However, if the separation between the wells is sufficiently small, the atom can still move between them by tunneling.

If the tunneling is *slow* (hopping rates $\tau^{-1} < 10^8 s^{-1}$ [CZ95]), the atom is coupled only to the density fluctuations of the electron sea, which can be described by a bosonic heat bath [YA84,HMG84]. The tunneling is then mainly incoherent, and the only effect of the electron bath is then to "screen" the tunneling center: an electron screening cloud builds up around the center and moves adiabatically

with it, which leads to a reduced tunneling rate due to the non-perfect overlap of the two screening clouds corresponding to the two positions of the tunneling center.

We are interested only in the case where the tunneling is *fast* (at rates $10^8 s^{-1} < \tau^{-1} < 10^{12} s^{-1}$ [CZ95]), so that the energy corresponding to the tunneling rate, determined by the uncertainty principle, is in the range 1 mK to 10 K. (If the tunneling is "ultra-fast" ($\tau^{-1} > 10^{12} s^{-1}$), the energy splitting $\Delta = E_2 - E_1$ between the lowest two eigenstates due to tunneling becomes too large ($> 10K$) and the interesting dynamics is frozen out.) Moreover, the TC-electron coupling is assumed strong enough that in addition to screening, electron density fluctuations can *directly induce* transitions between the wells: they can either induce direct tunneling through the barrier (*electron-assisted tunneling*), or excite the atom to an excited state from where it can decay to the other well (*electron-assisted hopping* over the barrier).

In this scenario, the interaction of the conduction electrons with the dynamical impurity is analogous to the Kondo interaction with magnetic impurities, in that the impurity undergoes electron-induced "spin-flip" transitions, leading to complicated many-body physics. In fact, it is shown below that at low temperatures, the model renormalizes to an isotropic 2-channel Kondo problem: two of the orbital (angular momentum) indices of the electrons play the role of pseudospin indices, coupled to the impurity, whereas their Pauli spins $\uparrow$ and $\downarrow$, which are not flipped by the interaction, become the "spectator" channel indices of the 2-channel Kondo problem. [An interpretation of the electronic pseudospin index is given after eq. (4.23).]

Hence, a strongly correlated Kondo-type ground state develops, characterized by logarithmic T-dependences for $T > T_K$, and non-Fermi liquid behavior for $T \ll T_K$. Of course, the flow toward the isotropic 2-channel Kondo model only happens provided that all relevant perturbations that would drive the system away from this fixed point are negligbly small – this is an implicit assumption made in the subsequent development, that will be critically discussed in section 4.3.

4.2.2 Definition of the Non-Magnetic Kondo Model

We describe the most general version [ZZ94a,ZZ94b] of Zawadowski's model for a heavy particle moving in a double-well potential and interacting with a band of conduction electrons. The Hamiltonian is the sum of three terms:

$$H = H_{TC} + H_{el} + H_{int} \ . \tag{4.2}$$

The first term describes the motion of the heavy particle in the double well, in the absence of electrons [see Fig. 2.11 and Fig. 4.3]:

$$H_{TC} = \sum_a E_a b_a^\dagger b_a \ . \tag{4.3}$$

This problem is considered to be already solved: the energies E_a ($E_1 < E_2 < \ldots$) are the exact eigenenergies of the exact eigenstates $|\Psi_a\rangle = b_a^\dagger|0\rangle$ of the TC, with corresponding wave-functions $\varphi_a(\vec{R})$. The spectrum will contain two nearly-degenerate energies E_1 and E_2, split by an amount $\Delta = E_2 - E_1$, corresponding to even and odd linear combinations of the lowest-lying eigenstates of each separate well; the remaining energies, collectively denoted by E_{ex}, correspond to excited states in the well, with $E_{ex} - E_2$ typically on the order of the Debye temperature of the metal, i.e. several hundred Kelvin.

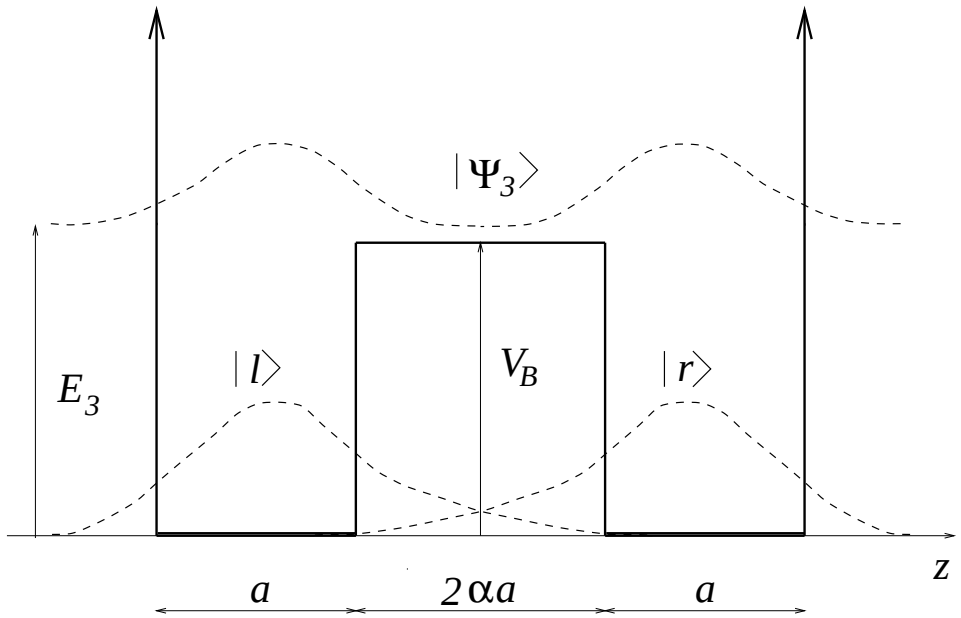

Figure 4.3 A symmetrical square double well potential (heavy line), and the wave-functions for the states $|r\rangle$, $|l\rangle$ and the first excited state $|\Psi_3\rangle$. We show a square well to illustrate the parameters chosen by Zaránd and Zawadowski for their model calculations [ZZ94b]. The choices most favorable for obtaining a large Kondo temperature were [ZZ94a, Table I]: $a = 0.1\mathring{A}$, $\alpha = 2.5$; the choices $V_B = 494$ K or 740 K then gave $E_3 = 245$ K or 456 K, and $T_K = 2.76$ K or 3.19 K, respectively. The effective couplings v^x, v^y and v^z, all equal to v_K at the 2-channel fixed point [see eq. (4.23)], are then on the order of $v_K \simeq 0.1 - 0.2$. The parameter that most strongly influences T_K is α, because it affects the overlap between the states $|r, l\rangle$, and $|\Psi_3\rangle$.Even though the barrier is very high relative to the other energy scales, Kondo temperatures in experimentally accessible ranges result.

The free-electron band is described by

$$H_{el} = \sum_{\vec{p}i} \varepsilon_{\vec{p}} c^{\dagger}_{\vec{p}i} c_{\vec{p}i} \ , \tag{4.4}$$

where $\varepsilon_{\vec{p}}$ is the energy, measured from the Fermi energy ε_F, of an conduction electron with momentum $\vec{p}$ and Pauli spin i (we use the index i because this will turn out to be the channel index). For simplicity, the electron energies are usually assumed to lie within a band of width $2D$, symmetric about ε_F, with constant density of states ρ_o per spin.

The TC-electron interaction is described by a pseudo-potential $U(\vec{R} - \vec{r})$, which describes the change in energy of the heavy atom at position $\vec{R}$ due to electronic density fluctuations at position $\vec{r}$, and is assumed to depend only on the relative coordinate $\vec{R} - \vec{r}$:

$$H_{int} = \sum_{\vec{p}\vec{p}'} \sum_{aa'i} V^{a,a'}_{\vec{p},\vec{p}'} \ c^{\dagger}_{\vec{p}i} c_{\vec{p}'i} \ b^{\dagger}_{a} b_{a'} \ , \tag{4.5}$$

where the coupling constants $V^{a,a'}_{\vec{p},\vec{p}'}$ are given in terms of the Fourier transform $U(\vec{p})$ of $U(\vec{R})$ by[Zar93]

$$V^{a,a'}_{\vec{p},\vec{p}'} = U(\vec{p} - \vec{p}') \int d\vec{R} \, e^{i(\vec{p}-\vec{p}')\cdot\vec{R}} \varphi^{*}_{a}(\vec{R}) \varphi_{a'}(\vec{R}) \ . \tag{4.6}$$

We are interested in the regime where $\Delta \ll T \ll E_{ex} \ll D$. Hence we take $\Delta \simeq 0$, i.e. consider a symmetrical double well with a two-fold degenerate ground state. (Experimental arguments in favor of this assumption in the case of the Ralph-Buhrman experiment are given on page 43 and in sections section 3.4; criticism of the assumption is discussed in section 4.3). It is then convenient to make a change of basis from the exact symmetrical and anti-symmetrical ground states $|\Psi_1\rangle$ and $|\Psi_2\rangle$ to the right and left states $|r\rangle$ and $|l\rangle = \frac{1}{\sqrt{2}} (|\Psi_1\rangle \pm |\Psi_2\rangle)$.

Note that, since a non-zero bare tunneling matrix element (Δ_0) between the wells always leads to a splitting $E_1 - E_2 \simeq \Delta_o$, we are also implicitly assuming that $\Delta_o \ll T$. This means that direct tunneling events are very unlikely, raising the question of whether Kondo-physics will occur at all.[3] However, the inclusion of excited states in the model overcomes this potential problem as follows [ZZ94a, ZZ94b]: a careful estimate of the coupling constants [Zar93] in terms of the overlap integrals (4.6) has shown that

$$|V^{r,l}| \simeq 10^{-3}|V^{l,l} - V^{r,r}| \,, \qquad |V^{l,ex}| \simeq |V^{r,ex}| \simeq |V^{l,l} - V^{r,r}| \,. \tag{4.7}$$

The first relation reflects the fact that direct electron-assisted tunneling, parameterized by $|V^{r,l}|$, is proportional to the bare tunneling rate Δ_o and hence very small. However, the matrix elements for electron-assisted transistions to excited states, parametrized by $|V^{l,ex}|$ and $|V^{r,ex}|$, are of the same order of magnitude as for the usual "screening term" $|V^{l,l} - V^{r,r}|$ [this is because the overlap integrals in (4.6) are larger for $\varphi_{ex}\varphi_{r,(l)}$ than for $\varphi_r\varphi_l$, since the excited state wave-function spreads over both wells (see Fig. 4.3)]. Although the amplitudes for such processes are proportional to the factor $1/E_{ex}$ (which is small, since E_{ex} is large), Zaránd and Zawadowski showed that such terms also grow under scaling [see eq. (4.11) below], and eventually lead to a renormalized model which has sufficiently large effective tunneling amplitudes to display Kondo physics.

[3] This was a serious limitation of Zawadowski's original model, which did not include excited states: to give non-trivial many-body physic (i.e. a sufficiently large Kondo energy T_K), the bare tunneling rate Δ_o could not be too small; yet at the same time, the model only flows to the interesting non-Fermi liquid fixed point if $E_1 - E_2 \ll T$. This would have required a rather delicate and perhaps questionable fine-tuning of parameters. This problem has been overcome by including excited states in the model [ZZ94a,ZZ94b], as explained above.

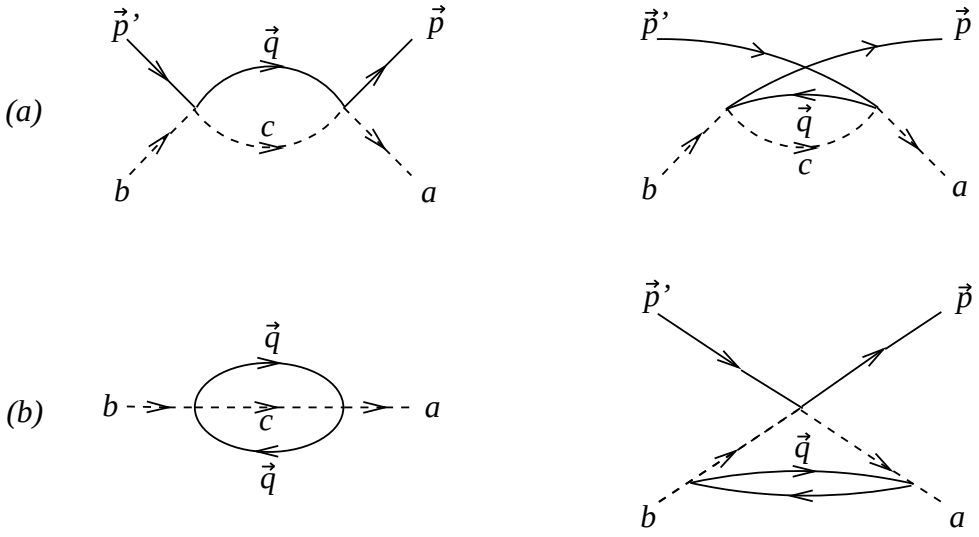

Figure 4.4 (a) The second-order vertex corrections that contribute to eq. (4.8) and generate the leading order scaling equation (4.11). (b) The impurity self-energy correction and the third-order next-to-leading-logarithmic vertex correction that generate the subleading terms in the second-order scaling equation (4.17). (Note that subleading diagrams that are generated by the leading-order scaling relation derived from the diagrams in (a) have to be omitted.) Dashed and solid lines denote impurity and electron Green's functions, respectively.

4.2.3 Poor Man's Scaling RG

The interaction vertex, calculated second order in perturbation theory from to the diagrams in Fig. 4.4(a), is given by the following expression:

$$\begin{aligned}\Gamma^{a,b}_{\vec{p}\vec{p}'} = V^{a,b}_{\vec{p},\vec{p}'} \; + \; \int \frac{d\Omega_{\hat{q}}}{4\pi} \sum_c \rho_o \int_{-D}^{D} d\varepsilon_{\vec{q}} \times \qquad (4.8)\\ \left[V^{a,c}_{\vec{p},\vec{q}} V^{c,b}_{\vec{q},\vec{p}'} \frac{1-f_q}{\varepsilon_{p'}+E_b-(\varepsilon_q+E_c)} \; - \; V^{a,c}_{\vec{q},\vec{p}'} V^{c,b}_{\vec{p},\vec{q}} \frac{f_{\vec{q}}}{\varepsilon_{p'}+E_b-(-\varepsilon_q+\varepsilon_{p'}+\varepsilon_p+E_c)} \right] \\ = \; V^{a,b}_{\hat{p},\hat{p}'} \; + \; \int \frac{d\Omega_{\hat{q}}}{4\pi} \sum_c \rho_o \ln\left[\max\{E_b, E_c, T, \varepsilon_p, \varepsilon_{p'}\}/D\right] \; \left[V^{a,c}_{\hat{p},\hat{q}} V^{c,b}_{\hat{q},\hat{p}'} - V^{c,b}_{\hat{p},\hat{q}} V^{a,c}_{\hat{q},\hat{p}'} \right] \; ,\end{aligned}$$

where in the second line it was assumed that the couplings only depend on the direction $\hat{p}$ of $\vec{p}$ (the dependence on $|\vec{p}|$ is negligible sufficiently close to the Fermi surface), and only the logarithmic terms were retained.

Note the occurence of the "commutator" $\left[V^{a,c}_{\hat{p},\hat{q}} V^{c,b}_{\hat{q},\hat{p}'} - V^{c,b}_{\hat{p},\hat{q}} V^{a,c}_{\hat{q},\hat{p}'}\right]$; the fact that

this is in general non-zero, due to the non-trivial angular dependence of the coupling constants, is crucial for the presence of logarithmic corrections (and is the reason why this model is sometimes called a *non-commutative* model).

One proceeds by introducing a new set of dimensionless couplings $v^{a,b}_{\alpha\alpha'}$ in terms of an orthogonal set of angular functions $f_\alpha(\hat{p})$ (e.g. $f_\alpha(\hat{p}) = \sqrt{4\pi}Y_{lm}(\hat{p})$, but any set of orthogonal angular functions will do):

$$v^{a,b}_{\alpha\alpha'} \;=\; \rho_o \int \frac{d\Omega_{\hat{p}}}{4\pi} \int \frac{d\Omega_{\hat{p}'}}{4\pi} f^*_\alpha(\hat{p}) V^{a,b}_{\hat{p},\hat{p}'} f_{\alpha'}(\hat{p}') \; . \tag{4.9}$$

In terms of these eq. (4.8) takes the form:

$$\Gamma^{a,b}_{\alpha\alpha'} = v^{a,b}_{\alpha\alpha'} \;+\; \sum_{c,\beta} \ln\left[\max\{E_b, E_c, T, \varepsilon_p \varepsilon_{p'}\}/D\right] \left[v^{a,c}_{\alpha\beta} v^{c,b}_{\beta\alpha'} - v^{c,b}_{\alpha\beta} v^{a,c}_{\beta\alpha'}\right] \; . \tag{4.10}$$

Now Anderson's poor man's scaling RG [And70] is implemented (very nicely explained in [CZ95, sections 3.2.2]): particle or hole excitations with large energy values do not directly participate in *real* physical processes; their only effect occurs through virtual excitions of the low-energy states to intermediate high-energy states. Hence such processes may be taken into account by introducing renormalized coupling parameters, which sum up all the virtual processes between a new, slightly smaller cut-off D' and the original D. In other words, all virtual processes between the energies D' and D are integrated out and their contributions incorportated in new, D'-dependent coupling constants. This procedure is repeated for smaller and smaller D' until D' becomes on the order of $\max\{E_c, T, \varepsilon_{p'}\}$.

Concretely, this is done by writing $v^{a,b}_{\alpha\alpha'} = v^{a,b}_{\alpha\alpha'}(x)$, where $x = \ln(D'/D)$ and x-dependence of the coupling constants is determined by the requirement that the interaction vertex be invariant under poor man's scaling, i.e. $\partial_x \Gamma^{a,b}_{\alpha\alpha'} = 0$. By

eq. (4.10), this leads to the following *leading-order scaling equation*:

$$\partial_x \underline{v}^{a,b}(x) = \sum_c \theta(D' - E_c)[\underline{v}^{a,c}(x), \underline{v}^{c,b}(x)] \ , \tag{4.11}$$

where we have adopted the matrix notation $v^{a,b}_{\alpha\alpha'} \equiv \underline{v}^{a,b}$. [The significance of $\theta(D' - E_c)$ is explained in section 4.2.7.] This equation, to be solved with the boundary condition $\underline{v}^{a,b}(0) = (\underline{v}^{a,b})_{bare}$, determines the nature of the RG flow away from the weak-coupling limit.

In the following two sections we outline the results obtained by Zawadowski and co-workers concerning the nature of the fixed point that the Hamiltonian flows towards as it scales out of the weak-coupling region. However, the arguments that are to follow all have a somewhat heuristic character: since they are based on scaling equations that were derived in the weak-coupling limit, based on perturbation theory in the coupling constants, in principle they cease to be strictly valid as soon as one scales into strong-coupling regions of parameter space. (The only method that gives quantitatively reliable results for the cross-over region is Wilson's numerical NRG [Wil75,KWW80,CLN80,AL92b,PC91].) Many of the results obtained below are therefore of mainly qualitative value, and not expected to be quantitatively accurate.

4.2.4 Scaling to 2-D Subspace

Let us for the moment consider the model without any excited TC states, i.e. with $\sum_c = \sum_{r,l}$ (as was done in the first papers [Zaw80,BVZ82,VZ83]), postponing the more general case to section 4.2.7. In this case, the coupling constants $\underline{v}^{a,b}(x)$ can be expanded in terms of Pauli matrices in the 2-dimensional space of the TC:

$$v^{a,b}_{\alpha\alpha'}(x) = \sum_{A=0}^{3} \tilde{v}^{A}_{\alpha\alpha'}(x)\sigma^{A}_{a,b} \ , \qquad a, b = l, r \ , \tag{4.12}$$

where $A = (0,1,2,3) = (0,x,y,z)$ and $\sigma^0_{AB} \equiv \delta_{AB}$. The v^z term is called the *screening* term, and characterizes the difference in scattering amplitudes for processes in which an electron scatters from the atom in the right or left well *without* inducing a transition to the other well. The v^x and v^y terms are called *electron-assisted tunneling* terms, and describe the amplitude for processes in which the scattering of an electron induces the TC to make a transition to the other well. According to eq. (4.7), $\underline{\tilde{v}}^x \simeq \underline{\tilde{v}}^y \ll \underline{\tilde{v}}^z$. If one chooses the wave-functions of the TC to be real, and time-reversal invariance requires $\underline{\tilde{v}}^y = 0$ (see [VZ83, (a), eq.(2.11)]).

The problem is now formally analogous to a (very anisotropic) magnetic Kondo problem in which a spin-$\frac{1}{2}$ impurity is coupled to a conduction electron with very large pseudo-spin (since α takes on a large number of values). However, Vladár and Zawadowski (VZ) have shown [VZ83, (a), section III.C] that (with realistic choices of the initial parameters) the problem always scales to a 2-dimensional subspace in the electron's α-index, so that the electrons have pseudo-spin $S_e = \frac{1}{2}$ (this happens indepedent of the signs of the initial couplings, see section 4.2.5). Their argument goes as follows:

In the notation of eq. (4.12), the scaling equation (4.11) takes the form [VZ83, p.1573, eq.(3.3)]

$$\frac{\partial \underline{v}^A}{\partial x} \;=\; -2i \sum_{BC} \varepsilon^{ABC}\; \underline{v}^B \underline{v}^C \;. \tag{4.13}$$

Since $\underline{\tilde{v}}^x \ll \underline{\tilde{v}}^z$ and $\underline{\tilde{v}}^y = 0$, eq. (4.13) can be linearized in $\underline{v}^x$ and $\underline{v}^y$. VZ solved the linearized equations in a basis in α-space in which $\tilde{v}^z_{\alpha\beta}(0)$ is diagonal $[\tilde{v}^z_{\alpha\beta}(0) = \delta_{\alpha\beta}\tilde{v}^z_\alpha(0)]$, and obtained the following solution [VZ83, p.1576, eq.3.17]:

$$\tilde{v}^z_{\alpha\beta}(x) \;=\; \delta_{\alpha\beta}\tilde{v}^z_\alpha(0) \tag{4.14}$$

$$\tilde{v}^x_{\alpha\beta}(x) = \tilde{v}^x_{\alpha\beta}(0)\cosh 2x\left[\tilde{v}^z_\beta(0) - \tilde{v}^z_\alpha(0)\right] , \quad (4.15)$$

$$\tilde{v}^y_{\alpha\beta}(x) = i\tilde{v}^x_{\alpha\beta}(0)\sinh 2x\left[\tilde{v}^z_\beta(0) - \tilde{v}^z_\alpha(0)\right] . \quad (4.16)$$

Barring unforeseen degeneracies in the matrix $\underline{\tilde{v}}^z$, this shows that the two elements of $\underline{\tilde{v}}^z$ which produce the largest difference $|\tilde{v}^z_\beta(0) - \tilde{v}^z_\alpha(0)|$ will generate the most rapid growth in the corresponding couplings $\tilde{v}^x_{\alpha\beta}(x)$ and $\tilde{v}^y_{\alpha\beta}(x)$. In fact, since this growth is exponentially fast, any couplings with only slightly smaller $|\tilde{v}^z_\beta(0) - \tilde{v}^z_\alpha(0)|$ will grow much slower and hence decouple. Thus, we conclude that according the the leading-order scaling equations, the system *always renormalizes to a 2-D subspace in which the electrons have pseudo-spin* $S_e = \frac{1}{2}$.

The argument just presented is not quite waterproof, though. Firstly, it depends on the assumption of extreme initial anisotropy in the couplings, and secondly, it is based only on the leading-order scaling equations. As one scales towards larger couplings, sub-leading terms in the scaling equations can conceivably become important. Zaránd has investigated this issue by including next-to-leading-order logarithmic terms [generated by the diagrams in Fig. 4.4(b)] in the scaling equations, which turn out to be [Zar95, eq.(2.6)]:

$$\partial_x \underline{v}^A = -2i\sum_{BC}\varepsilon^{ABC}\underline{v}^B\underline{v}^C - 2N_f\sum_{B\neq A}\left[\underline{v}^A\mathrm{Tr}[(\underline{v}^B)^2] - \underline{v}^B\mathrm{Tr}[\underline{v}^A\underline{v}^B]\right] \quad (4.17)$$

Note that the number of channels, N_f (equal to 2 for the case of interest), shows up here for the first time in the next-to-leading order, since each electron loop [see Fig. 4.4(b)] carries a factor N_f. Performing a careful analysis of the stability of the various fixed points that occur, he concluded that the above-mentioned $S_e = \frac{1}{2}$ fixed point is the only *stable* fixed point in of these equations. Since this result is independent of the value of N_f and the number of orbital channels

considered, and his analysis is exact in the limit $N_f \to \infty$, one would expect his results to also be valid for $N_f = 2$. (However, no completely rigorous proof exists yet for this expectation; in particular, his analysis assumes $\Delta = 0$, and the case $\Delta \neq 0$ is substantially more complicated, see [VZ83, (b), section III]. For another, symmetry-based argument in favor of $S_e = \frac{1}{2}$, see [CZ95, section 3.3.2 (iii)].)

4.2.5 The fixed point is Pseudo-Spin Isotropic

Next we show, following [Zar95, section III], that the $S_e = \frac{1}{2}$ fixed point is actually *isotropic* in pseudo-spin space.

The last term in eq. (4.17) can be eliminated from the fixed-point analysis by making a suitable orthogonal transformation $\underline{v}^A \to \sum_B O_{AB}\underline{v}^B$. Therefore, it is sufficient to consider the first two terms on the right-hand side of eq. (4.17). At the fixed point, where $\partial_x \underline{v}^A = 0$, we have

$$\sum_{BC} \varepsilon^{ABC} \underline{v}^B \underline{v}^C \;=\; iN_f \underline{v}_A \sum_{B\neq A} \mathrm{Tr}[(\underline{v}^B)^2] \; . \tag{4.18}$$

Multiplying by $\underline{v}^A$ and taking the trace, one obtains the three relations

$$iN_f \boldsymbol{\alpha}^A(\boldsymbol{\alpha}^B + \boldsymbol{\alpha}^C) = \boldsymbol{\beta} \; , \quad \text{where} \quad \{A,B,C\} = \{x,y,z\} \quad \text{(cyclically)} \; , \tag{4.19}$$

where we have defined $\boldsymbol{\alpha}^A \equiv \mathrm{Tr}[(\underline{v}^A)^2]$ and $\boldsymbol{\beta} \equiv \mathrm{Tr}(\underline{v}^A\underline{v}^B\underline{v}^C - \underline{v}^C\underline{v}^B\underline{v}^A)$. This immediately implies one of two possibilities: either at least two of the $\boldsymbol{\alpha}^A$'s are zero, which is the trivial (commutative) case without electron-assisted tunneling ($\underline{v}^x = \underline{v}^y = 0$); or else they are all equal:

$$\boldsymbol{\alpha}^A = \boldsymbol{\alpha}^B = \boldsymbol{\alpha}^C = \boldsymbol{\alpha} \; . \tag{4.20}$$

Figure 4.5 Scaling trajectories of the matrix norms $\boldsymbol{\alpha}^A \equiv \mathrm{Tr}[(\underline{\mathrm{v}}^A)^2]$ $(A = x, y, z)$, calculated numerically for the case $N_f = 3$. All three norms tend to the same value, in accord with eq. (4.20). Consult [Zar95], from which this figure was taken, for details regarding the initial parameters used.

The latter case is the one of present interest. The conclusion that the couplings are all equal (i.e. the effective Hamiltonian isotropic) was checked numerically by Zaránd [Zar95, Fig.4], and is illustrated in Fig. 4.5.

What is the matrix structure of the $\underline{v}^A$'s? Introducing the notation $J^A = \frac{1}{2N_f \boldsymbol{\alpha}} \underline{v}^A$, eqs. (4.18) and (4.20) imply that the J^A satisfy the $SU(2)$ Lie algebra,

$$[J^A, J^B] = i\varepsilon^{ABC} J^C \ , \tag{4.21}$$

which means that they must be a direct sum of irreducible $SU(2)$ representations:

$$J^A = \sum_{\oplus k=1}^{n} S^A_{(k)} \ . \tag{4.22}$$

According to the analysis of Zaránd mentioned in the previous section, only a single subspace $S_e = \frac{1}{2}$ in this sum corresponds to a stable fixed point (all the others correspond to unstable fixed points), in the vicinity of which we can therefore write $J^A_{\alpha\alpha'} = \frac{1}{2}\sigma^A_{\alpha\alpha'}$.

4.2.6 Effective Hamiltonian

After a rotation in α-space to line up the quantization axis of the pseudospins of the impurity and the electrons, the effective Hamiltonian to which (4.5) renormalizes can be written as:

$$\boxed{H_{int}^{eff} = \frac{\rho_o v_K}{V_{ol}} \int d\varepsilon_p \int d\varepsilon_{p'} \sum_{\alpha\alpha'=1,2} \sum_{aa'=1,2} \sum_{i=\uparrow,\downarrow} \left(c^\dagger_{p\alpha i} \tfrac{1}{2}\vec{\sigma}_{\alpha\alpha'} c_{p'\alpha' i}\right) \left(b^\dagger_a \tfrac{1}{2}\vec{\sigma}_{aa'} b_{a'}\right) ,} \tag{4.23}$$

Here V_{ol} is the volume (inserted for dimensional reasons) and v_K is the magnitude of the effective TC-electron coupling (and estimated to be of order $v_K \simeq 0.1 - 0.2$ [ZZ94a, Table 1]). This is the main result of the RG analysis: *The effective Hamiltonian has exactly the form of the isotropic, magnetic 2-channel Kondo problem; the two surviving orbital indices $\alpha = 1, 2$ play the role of pseudo-spin indices and the Pauli spin indices $i = \uparrow, \downarrow$ the role of channel indices.* When, in subsequent chapters, we apply Affleck and Ludwig's conformal field theory results on the 2-channel Kondo model to TC-physics, the effective Hamiltonian H_{int}^{eff} will always be regarded as the starting point.

It is tempting to propose the following physical interpretation of the effective Hamiltonian (it is given in this form by [MF95], and can be viewed as complimentary to Zawadowski's picture of electron-induced tunneling). A charged impurity in a metal will be screened by a screening cloud of electrons, which can be thought of as part of the "dressed" impurity. If the impurity is a tunneling center, it will drag along its tightly bound screening cloud as it tunnels between the wells. In doing so, it will redistribute the low-energy excitations near the Fermi surface. In particular, it will likely interact most strongly with two spherical waves of low-energy electrons, "centered" on the two impurity positions in well 1 and 2

[VZ83, p.1575], with which one can associated a pseudospin index $\alpha = 1, 2$. Now, when the impurity tunnels from well 1 to 2, low-energy electrons around well 2 (with $\alpha = 2$) will move in the opposite direction to well 1, to compensate the movement of electronic charge bound up in the screening cloud that moved with the impurity from well 1 to 2, and thereby to decrease the orthogonality between the pre- and post-hop configurations. Thus, a flip in the impurity pseudospin is always accompanied by a flip in electron pseudospin, as in eq. (4.23).

In two very recent papers [MF95], Moustakas and Fisher have used this interpretation as a starting point for a related but not quite equivalent description of the TC-electron system (to be mentioned again in section 4.3).

We conclude this section with a number of miscellaneous comments:

The fact that one always scales towards an *isotropic* effective Hamiltonian is rather remarkable (though in accord with the conformal field theory results that show that anisotropy is an irrelevant perturbation [AL92b, eq.(3.17)]): the initial extreme anisotropy of the couplings is dynamically removed, and a $SU(2)$ symmetry emerges that is not present in the original problem!

Note that the initial signs of the anisotropic coupling constants did not matter in the above arguments. A more careful argument [CZ95, section 3.3.2 (ii)] shows that the flow toward this fixed point indeed occurs irrespective of the initial signs of the coupling constants.

Relevant perturbations: When the initial splitting Δ is non-zero, the 2-nd order RG is considerably more complicated [VZ83, (b), section III]. The result is that Δ gets normalized downward by about two orders of magnitude [VZ83, (b), Fig.3]. However, as emphasized in [CZ95, section 3.4.1 (c)], *the splitting* Δ

is nevertheless a relevant perturbation: it can be shown to scale downward much slower than the bandwidth D', so that $\Delta(D')/D'$ *grows* as D' is lowered.

By analyzing the stability of the fixed point equations against a perturbation that breaks *channel* symmetry, it can likewise be shown that *channel anisotropy* is a relevant perturbation [CZ95, section 3.4.1 (c)].

Kondo temperature: The Kondo temperature is the cross-over temperature at which the couplings begin to grow rapidly. It can be estimated from an approximate solution of the second order scaling equation (4.17).[4] The result found for T_K by VZ [VZ83, p.1590, eq.(4.11)] is

$$T_K = D\left[v^x(0)v^z(0)\right]^{1/2}\left(\frac{v^x(0)}{4v^z(0)}\right)^{\frac{1}{4v^z(0)}} \quad . \tag{4.24}$$

Note that the factor $\left[v^x(0)v^z(0)\right]^{1/2}$ is absent[5] if one estimates T_K only from the leading-order scaling equation (4.11) [VZ83, p.1577, eq.(4.11)]. Since the bare $v^x(0) \ll 1$, this factor causes a substantial suppression of T_K (by about two orders of magnitude), if one simply inserts $v^x(0)$ into eq. (4.24), leading to pessimistically small values of $T_K \simeq 0.01 - 0.1$ K [ZZ94a,ZZ94b]. However, the inclusion of excited states remedy this problem, in that excited states renormalize v^x to larger values by about two orders of magnitude (see below).

4.2.7 The Role of Excited States

Let us now return to the more general problem where the excited states with energies E_{ex} are not neglected from the beginning.

[4] Since T_K is only a statement about the *onset* of rapid growth of coupling constants, the value obtained from scaling equations derived by perturbation theory is expected to give approximately the correct scale even though the scaling equations themselves become invalid when the couplings become too large [Wil75].

[5] The presence of the prefactor to the exponent in (4.24) is of course a well-known feature of second-order scaling, see e.g. [Hew93, eq.(3.47)].

The first important consequence of including excited states in the model has already been discussed in section 4.2.2: electron-assisted hopping transitions between the two wells *via excited states* allow Kondo physics to occur even if the barrier is so large that direct and electron-assisted tunneling through the barrier is negligible (i.e. $\Delta_o \simeq 0$). This is good news, since the energy splitting $\Delta = E_1 - E_2$ is limited from below by Δ_o, but simultaneously Δ (being a relevant perturbation) needs to be very small if scaling to the 2-channel fixed point is to take place.

Secondly, in the presence of excited states, poor man's scaling towards strong-coupling, based on eq. (4.11), has to proceed in several steps: the excited state $|\Psi_c\rangle$ only contributes as long as the effective bandwidth D' is larger than E_c, as is made explicit by the $\theta(D' - E_c)$ in eq. (4.11). As soon as $D' < E_c$, the excited state decouples.

Assuming that the presence of excited states does not affect the result found in section 4.2.4, namely that the effective Hamiltonian scales towards a 2-D subspace in which the electrons have pseudo-spin $S_e = \frac{1}{2}$, Zaránd and Zawadowski [ZZ94a,ZZ94b] have analyzed the successive freezing out of excited states. They concluded that when D' becomes smaller than the smallest excited-state energy E_3, one ends up with a TC of formally exactly the same nature as the one discussed in sections 4.2.4 and 4.2.5, *but with renormalized couplings.*

The renormalized couplings turn out to be still small, which means that the perturbative scaling analysis of sections 4.2.4 and 4.2.5 still applies; however, v^x and v^y are renormalized upward by a factor of up to 50 from their bare values (which were three orders of magnitude smaller than v^z see eq. (4.7)). This

has very important consequences for the Kondo temperature eq. (4.24), which strongly depends on v^x: with realistic choices of parameters (given in the caption to Fig. 4.3) the Kondo temperature turns out to be about 2 orders of magnitude larger with than without excited states in the model, and Kondo temperatures in the experimentally relevant range of 1 to 3 K were obtained [ZZ94b, table II].

To summarize: the inclusion of excited states in the model leads to more favorable estimates of the important parameters Δ_o (can be zero) and T_K (larger); but since the excited states eventually decouple for small enough effective bandwidths, they do not affect the flow toward the 2-channel Kondo fixed point in any essential way.

4.3 Recent Criticism of the 2-Channel Kondo Scenario

Very recently, the claim that the non-magnetic Kondo problem will renormalize to the 2-channel Kondo model at sufficiently low temperatures, has been criticized in two separate papers [WAM95,MF95]. We describe the points of contention, and our attitude to them, below.

4.3.1 Large Δ due to Static Impurities

Wingreen, Altshuler and Meir have recently argued [WAM95] that TC with very small splittings ($\Delta < 1K$) can not occur at all in a disordered material if the TLS-electron coupling has the large values that apply to the over-screened 2-channel Kondo fixed point. Their argument goes as follows:

Ordinary elastic scattering of electrons off other defects in the system will cause Friedel oscillations (wavelength $1/k_F$) in the electron density (see e.g.

[KV60]). This in turn will cause a typical splitting $\bar{\Delta}$ of a TLS, because the depth of each well is affected by the *local* electron density, which differs from well to well if there are strong density fluctuations. (In the language of the magnetic Kondo problem, the Friedel oscillations produce a random "magnetic field" at the impurity site).

Although the random contributions to the splitting from the various static impurities will cancel to a large extent, WAM argued that there will nevertheless be a residual typical splitting, $\bar{\Delta}$. The crucial question is: how large is this typical splitting?

By doing simple 2nd-order perturbation theory in the coupling between the electrons and static impurities to estimate the magnitude in the resulting electron density fluctuations between the neigbouring wells, WAM produced the estimate[6]

$$\bar{\Delta} \simeq \varepsilon_F v \sqrt{k_F \ell}\,, \tag{4.25}$$

where ℓ is the mean free path (a measure of the concetration of static impurities) and v_K the effective TLS-electron coupling strength in eq. (4.23). Moreover, WAM, predict zero probability to find zero splitting.

Since according to eq. (4.25) $\bar{\Delta}$ is proportional to ε_F, it is typically a rather large number, quite independent of the detailed values for the parameters one uses. WAM found a value of $\Delta \simeq 100K$ by using $l \simeq 30\mathring{A}$ and employing the strong-coupling value $v_K \simeq 0.1$ appropriate for the 2-channel Kondo fixed point (see caption of Fig. 4.3; this number also follows using a Kondo temperature of about 4K in the standard formula $v_K = \log(k_B T_K/\epsilon_F)$ obtained from the leading-order scaling equations.)

[6]Cox has reproduced this result [Cox95] by a simple calculation analogous to the one by which one obtains the RKKY interaction between two magnetic impurities.

Since 100 K is a huge energy scale compared to all other scales of interest, WAM argued that the 2-channel Kondo physics evoked in this thesis to explain the Ralph-Buhrman experiment would never occur. Instead, they proposed an alternative explanation of the experiment based on disorder-enhanced electron interactions. The latter suggestion, which we believe contradicts several experimental facts [RLvDB95], is critically discussed section 2.4. Here we briefly comment on their estimate of $\bar{\Delta}$, following [RLvDB95].

We believe that WAM are correct in pointing out that the interaction of a two-level tunneling system (TLS) with elastically-scattered electron waves can act to increase the energy splitting, Δ, of the TLS. However, we suggest that their method of estimating the average $\bar{\Delta}$ is oversimplified, and that the result, ~ 100 K, may be a considerable overestimate.[7]

As explained in the preceding sections, large TLS-electron couplings are produced at low temperatures only after renormalizing smaller high-T bare couplings. The WAM estimate of Δ attempts to simply use a large low-T value of the coupling to determine the effects of elastic scattering in isolation, and this is done without considering possible counteracting effects that might favor smaller splittings. Instead, we believe that the mechanism desribed by WAM should be included from the beginning in the renormalization analysis. An extra term, including the effects of static disorder, should be added to the Hamiltonian, and then an RG analysis should be performed to determine *self-consistently* how the couplings, Δ, and the electronic energy evolve together at low T. While the effect

[7] This result seems particularly suspect in the light of the fact that TLS-splittings as small as $\Delta = 0.08$K have been directly measured in strongly disordered bismuth films [GZC92,ZGH91], even though the effective electron-TLS coupling was large [$v \simeq 0.7$ ($= \sqrt{2\alpha}$ there)]; see page 44. Unfortunately, the bismuth experiments studied slow tunneling centers, whereas here we are dealing with fast ones, and it is not clear which properties of the one carry over to the other.

proposed by WAM may act to increase Δ at low T, other effects in the scaling analysis [VZ83] act to decrease Δ strongly [compare the comments on page 99], and may therefore prevent any growth of Δ during renormalization and favor instead the formation of TLSs with $\Delta \simeq 0$.

Futhermore, it was pointed out to us by A. Moustakas that WAM's use of ε_F in eq. (4.25) might be suspect: in this formula, ε_F plays the role of an effecitve bandwith D, but as one flows to strong coupling, the effective bandwidth is renormalized to D', which eventually becomes replaced by V or $T \ll \varepsilon_F$. This argument underscores the need to carefully investigate the effect pointed out by WAM within an RG framework.

Finally, with regard to the interpretation of the experiments put forth in this thesis, we point out the following:

Firstly, WAM's prediction of large average splittings $\bar{\Delta}$ assumes sufficient disorder to create strong density fluctuations. However, the samples of Ralph and Buhrman are believed to be rather clean and crystalline, with long mean free paths ($l > 30$ nm, see 35). Therefore, it is incorrect to view the constrictions as strongly disordered. — Scattering off the walls of the constriction could have an effect similar to static impurities; however, an explanation that has to evoke scattering off the walls cannot account for the fact that the zero-bias anomalies disappear when the system is heated and recooled (point (P3) in section 2.3).

Secondly, WAM's estimate only concerns the *typical* splitting Δ. [They do claim that the probability for zero splitting is zero; however (in the absence of published details of their calculation) this seems rather unnatural for any effect that is the sum of many random contributions; for example, it contradicts the

standard picture of TLS in glasses, in which TLS are assumed to have a broad, almost flat distribution of splittings [AHV72,Phil72]]. However, as emphasized in [RLvDB94] and on page 45, the conductance measurements probably are not sensitive to the "typical" TLSs. Instead, within the 2-channel Kondo picture a conductance measurement is *preferentially* sensitive to TLSs with small Δ, as only these TLSs will produce large V-dependent signals. Therefore, even if on average the splitting $\bar{\Delta}$ is rather large, such impurities only contribute to the background signal, and we believe it is not unreasonable to propose that a small number of them *do* have sufficiently small splittings to give rise to the anomalous behavior.

4.3.2 Another Relevant Operator

Very recently, the theoretical justification for the non-magnetic Kondo model proposed by Zawadowski has been questioned by Moustakas and Fisher (MF) [MF95]. Reexamining a degenerate two-level system interacting with conduction electrons, they argued that the model (4.5) and (4.6) used by Zawadowski is incomplete, because it neglects subleading terms in the TLS-electron interaction that have the same symmetries as the leading terms.

These subleading terms are initially small when the coupling is small, and moreover are RG irrelevant. Therefore, neglecting them is perfectly valid for the purpose for which Zawadoski constructed his model, namely estimating the Kondo temperature at which the leading terms in H_{int} begin to grow. However, such subleading terms *can* become important when investigating the nature of the fixed point towards which the system flows under renormalization. MF show that when combined in certain ways, they generate an extra *relevant* operator,

not present in Zawadowski's analysis, which in general prevents the system from flowing to the $T = 0$ fixed point. Therefore, unless a fine-tuning of parameters miraculously causes this relevant operator to vanish, it will eventually always become large, and the system will never reach the $T = 0$ fixed point.

What is the nature of the terms neglected by Zawdowski? Formally, he estimates the electron-assited tunneling terms by expanding the WKB exponent for tunneling through the barrier in powers of the barrier potential $\mathcal{V} = \mathcal{V}_o + \delta\mathcal{V}$, where $\delta\mathcal{V}$ is the fluctuation in this potential due to fluctuations $\delta\rho$ in the electron density. However, he keeps only leading terms in $\delta\mathcal{V}$, whereas MF argue that sub-leading terms should also be kept, because they can give rise to terms that grow rapidly when the coupling constants (and hence $\delta\mathcal{V}$ too) begin to grow rapidly.

MF set up their model in a somewhat different way than Zawadowski. In their model, electron-assisted tunneling processes are viewed as follows: the TLS (together with its dressing cloud of electrons) hops from well 1 to well 2, and at the same time one or two electrons hop from well 2 to well 1. This, they argue, will happen because such electron-hopping events lower the total amount of electron charge that gets shifted during the tunneling process and hence help to decrease the orthogonality between the initial and final electron states. In this language, Zawadowski's electron-assisted tunneling term corresponds to the hopping of a single electron, and the terms which he neglected correspond to the simultaneous hopping of two electrons.

In our opinion, the work of MF points out a serious problem with the assumption that the system will flow to the $T = 0$ fixed point. However, in the

same spirit as that adopted when arguing that the experiment self-selects only impurities with very small splittings, one could argue that it also only selects impurities for which this extra relevant operator happens to be very small.

4.4 The Non-Equilibrium Orbital Kondo Problem

In this section we take a preliminary look at the orbital Kondo problem out of equilibrium. The purpose of this excercise is to develop some intuitition for the complications that arise when $V \neq 0$. The most important result is that the flow to the 2-channel fixed point is not disrupted, as long as $V < T_K$, and that the physics in this regime is governed by the $T = 0, V = 0$ fixed point of the 2-channel Kondo model. We also cite some instructive results derived by Gan for the case of large channel number [Gan94], for later comparison with Affleck and Ludwig's CFT results.

4.4.1 Definition of the Non-Equilibrium Model

We shall use the same model as that to be employed in chapter 9 [see eq. (9.6) and table 9.1], where the assumptions made below are motivated in more detail. We envision a single (degenerate) TC at the center of the nanoconstriction (see Fig. 2.2). The electrons incident towards the constriction from the right and left leads will be called L- and R-movers, respectively (although the angle of incidence can of course be arbitrary), and will be distinguished by an additional *species index* $\sigma = (+,-) = (L,R)$. For convenience we also introduce the collective notation $\nu \equiv (p, \sigma, \alpha, i)$ for the electron's quantum numbers of momentum p, L/R-mover σ, pseudospin α (orbital index) and Pauli spin i (channel index).

Now, intuitively speaking, the regime of low energies should still be described by a Hamiltonian of the form eq. (4.23): there should still be two pseudospin channels of conduction electrons, consisting of electron waves "centered" at the minima of the two wells of the TLS,[8] that couple most strongly to the TC at low temperatures. As in the equilibrium case, they will give rise to an effective 2-channel Kondo interaction, with pseudospin $S_e = \frac{1}{2}$. However, they are built from both L- and R-movers,[9] and in the nanoconstriction geometry one has to distinguish between these (since they originate from different baths), and between forward and backward scattering (since these contribute with different signs to the current). During a scattering event, an electron can be scattered either backward or forward (σ does or does not change); simultaneously, the impurity can either tunnel or not, and correspondingly the electronic pseudospin either flips or does not flip the TC (α does or does not change).

To describe this situation, we therefore adopt the following Hamiltonian:

$$H = H_o + H_{int}^{eff} \ , \qquad H_o = \sum_{\nu} \varepsilon_\nu c_\nu^\dagger c_\nu \ , \tag{4.26}$$

where $\sum_\nu \equiv \rho_o \int d\varepsilon_\nu \sum_{\sigma\alpha i}$ with interaction given by

$$H_{int}^{eff} = \frac{1}{V_{ol}\rho_o} \sum_{\nu a, \nu' a'} c_\nu^\dagger b_a^\dagger \left(H_{1\,\nu\nu'}^{aa'}\right) c_{\nu'} b_{a'} \ , \qquad \text{where} \quad H_{1\,\nu\nu'}^{aa'} \equiv v_K V_{\sigma\sigma'} \left(\tfrac{1}{2}\vec{\sigma}_{\alpha\alpha'} \cdot \tfrac{1}{2}\vec{\sigma}_{aa'}\right) \ , \tag{4.27}$$

This is just eq. (4.23), but with an extra factor $V_{\sigma\sigma'} \equiv \frac{1}{2}\begin{pmatrix} 1 & 1 \\ 1 & 1 \end{pmatrix}_{\sigma\sigma'}$. This factor ensures that during scattering events a L-mover can be scattered into either a L- or a R-mover, at the same time as its pseudo-spin index α and that of the TC

[8] These waves will not be spherical, due to the presence constriction, but probably rather shaped like p-orbitals.

[9] Loosely speaking, waves that in a bulk situtation were associated with the pseudospin index α now have to be divided into L, α and R, α components, depending on the direction of propagation of the component.

do or do not flip. That the simple form of $V_{\sigma\sigma'}$ used here is sufficiently general is explained on page 245; note that it ensures that ${H_1}_{\nu\nu'}^{aa'}$ is actually independent of σ, σ', which is a major simplification.

The L- and R-movers that are incident on the TC originate from the R- and L leads, which are at chemical potentials $\mu + \frac{1}{2}eV$ and $\mu - \frac{1}{2}eV$ respectively (see Fig. 2.2). Therefore,

$$\langle c_\nu^\dagger c_{\nu'} \rangle = f_{\sigma_\nu}(\varepsilon_\nu)\delta_{\nu\nu'} = \frac{\delta_{\nu\nu'}}{e^{\beta(\varepsilon_\nu - \mu_\nu)} + 1} \ , \qquad \text{where} \quad \mu_\nu \equiv \sigma_\nu \tfrac{1}{2}eV \ , \tag{4.28}$$

i.e. $\mu_\pm = \pm\frac{1}{2}eV$ for L/R-movers, respectively.

The backscattering current ΔI (to the right), i.e. the negative contribution to I (which flows to the left) due to the scattering events of H_1, is given quite generally by

$$\begin{aligned} \Delta I \ &= \ \frac{\tilde{K}\rho_o b}{|e|} \int d\varepsilon_\nu \int d\varepsilon_{\nu'} \Big(f_R(\varepsilon_{\nu'})(1 - f_L(\varepsilon_\nu))\Gamma(\varepsilon_{\nu'}, R \to \varepsilon_\nu, L) \qquad (4.29) \\ &\quad - f_L(\varepsilon_\nu)(1 - f_R(\varepsilon_{\nu'}))\Gamma(\varepsilon_\nu, L \to \varepsilon_{\nu'}, R) \Big) \ , \qquad (4.30) \end{aligned}$$

where here $\sigma_\nu = L$ and $\sigma_{\nu'} = R$, and

$$\Gamma(\varepsilon_{\nu'}, R \to \varepsilon_\nu, L) = 2\pi/\hbar \, \delta(\varepsilon_{\nu'} - \varepsilon_\nu) \, \rho_o^{-2} \, \tfrac{1}{2} \sum_{\alpha i a, \alpha' i' a'} |\Gamma_{\nu\nu'}^{aa'}|^2 \ . \tag{4.31}$$

In writing down eq. (4.29), the fact that the Fermi functions do not depend on the indices that appear in the sums $\sum_{\alpha i a, \alpha' i' a'}$ has been exploited to pull them out to the front. The factor $\frac{1}{2}$ in eq. (4.31) is due to an average over the initial states of the TC, and $T_{\nu\nu'}^{aa'}$ is the generalization of the interaction vertex $\Gamma_{\eta\eta'}^{aa'}$ of Eq. (4.10) to all orders of perturbation theory. The factor $\tilde{K} \equiv e^2\tau(0)/h$ ($\tau(\varepsilon)$ is defined below) is included in Eq. (4.29) for dimensional reasons, and b is a dimensionless, geometric constant (compare section 2.2.4).

Now, since $H_1{}^{aa'}_{\nu\nu'}$ is independent of the indices σ, σ', the same is true for $|\Gamma^{aa'}_{\nu\nu'}|^2$, so that it follows immediately that[10]

$$\Gamma(\varepsilon_{\nu'}, R \to \varepsilon_\nu, L) = \Gamma(\varepsilon_\nu, L \to \varepsilon_{\nu'}, R) \equiv \tfrac{1}{2}\Gamma(\varepsilon_{\nu'} \to \varepsilon_\nu) \ . \tag{4.32}$$

Exploiting eq. (4.32) and the $\delta(\varepsilon_{\nu'} - \varepsilon_\nu)$ function in $\Gamma(\nu' \to \nu)$, the backscattering current can be simplified to

$$\Delta I = \frac{\tilde{K}}{|e|} \int d\varepsilon_{\nu'} \left[f_R(\varepsilon_{\nu'}) - f_L(\varepsilon_{\nu'}) \right] \tfrac{1}{2} \sum_{\alpha', i'} \frac{1}{\tau_{\nu'}(\varepsilon_{\nu'})} \ , \tag{4.33}$$

where the scattering rate $\frac{1}{\tau_{\nu'}(\varepsilon_{\nu'})}$ for a particle with quantum numbers ν' is defined by

$$\frac{1}{\tau_{\nu'}(\varepsilon_{\nu'})} \equiv \rho_o^{-2} \sum_\nu 2\pi/\hbar \delta(\varepsilon_{\nu'} - \varepsilon_\nu) \tfrac{1}{2} \sum_{aa'} |T^{aa'}_{\nu\nu'}|^2 = (2/\rho_o) \sum_{\alpha i} 2\pi/\hbar \tfrac{1}{2} \sum_{aa'} |T^{aa'}_{\nu\nu'}|^2 \tag{4.34}$$

4.4.2 Poor Man's Scaling unaffected by V

Consider the interaction vertex $\Gamma^{aa'}_{\nu\nu'}$ in the poor man's scaling approach, as in section 4.2.3. The only difference from the equilibrium case discussed there (apart from the extra index σ) is that here *the Fermi functions in the intermediate states in eq. (4.8) are V-dependent*, see eq. (4.28). In principle, this is a considerable complication, since one now has to keep track of two different kinds of Fermi functions, f_L and f_R.

Fortunately, though, the poor man's scaling equations are not affected by this complication. Since they are derived by adjusting the cut-off from D to D', which are both $\gg V, T$, they are independent of V for the same reason as that they are independent of T. In other words, the scaling equations for $V \neq 0$ are the same

[10] The factor $\frac{1}{2}$ is because $\Gamma(\varepsilon_{\nu'} \to \varepsilon_\nu) = \Gamma(\varepsilon_{\nu'}, R \to \varepsilon_\nu, L) + \Gamma(\varepsilon_{\nu'}, R \to \varepsilon_\nu, R)$.

as for $V = 0$. Thus, we arrive at the important conclusion that *the initial RG flow is unaffected by* $V \neq 0$.

Eventually, the RG flow is cut off by either V or T, whichever is larger; however, if both are $\ll T_K$, the RG flow will terminate in the close vicinity of the $T = 0, V = 0$ fixed point, even if $V \neq 0$. Thus we obtain the second important conclusion that *for* $V \ll T_K$*, which we will call the* **weakly non-equilibrium regime***, the low-energy physics is governed by the same fixed point as for* $V = 0$.

Actually, the preceding argument has to be refined a little. It is shown in section 9.4 that $V \neq 0$ introduces is a marginally relevant perturbation to the fixed point Hamiltonian (proportional to V/T_K). Therefore, even if $V \ll T_K$, if T/V is made sufficiently small the system will eventually flow away from the $T = 0, V = 0$ fixed point (at a crossover temperature T_V^*, say). However, since this perturbation is marginal, it only grows logarithmically slowly as T is decreased, so that T_V^* will be *very* small. Therefore, there should exist a rather large regime in which one can have both $V, T \ll T_K$ and $T > T_V^*$, and this regime is governed by the 2-channel Kondo, $T = 0, V = 0$ fixed point.

The above two conclusions are the justification for the strategy followed in subsequent chapters, namely to apply conformal field theory, which is an equilibrium theory, governed by the $T = 0$, $V = 0$ fixed point, to the Ralph-Buhrman experiment, which is non-equilibrium, but has $V < T_K$ in the scaling regime [see the discussions in sections 5.1 (point 3) and section 5.4.5].

The poor man's scaling argument also shows, however, that the effective Hamiltonian that the system renormalizes to is V-dependent if $V > T$. The reason is simply that when one has scaled down to $D' = V > T$, one has to

replace D' by V in the effective interaction vertex. This complication (which will influence the argumentation in section 5.4.5) reflects the presence of the marginal operator mentioned above. However, the complication disappears in the regime $V \ll T_K$ and $T > T_V^*$, where the V-dependence becomes negligible.

4.4.3 Gan's Results for Large Channel Number

As a check on the CFT calculation of the backscattering current to be performed in chapter 9, we briefly cite some results obtained by Gan [Gan94] for the isotropic k-channel Kondo model in the limit of a large number of channels, $k \to \infty$.

In the limit $k \to \infty$, the poor man's scaling approach becomes exact. The reason is that (for the isotropic model) the over-screened fixed point occurs when the coupling constant has the special value $v^* = \frac{2}{2+k}$ [see eq. (7.35)], which $\to 0$ as $k \to \infty$. Thus, in this limit one never scales into a "strong-coupling" regime, and the perturbative expressions from which the scaling equations are derived retain their validity throughout. Thus, in the limit $k \to \infty$, results from the poor man's scaling approach should agree with exact results from CFT, which serves as a useful check on both methods. Gan calculated the imaginary part of the electron self-energy, $\Sigma^I(\omega, D, g)$, perturbatively[11] to order k^{-4}, and was able to reproduce exact results to order k^{-2}. (We cite only the lowest relevant terms.)

In order to apply Gan's calculation to the model defined by eq. (4.27), one first has to diagonalize $V_{\sigma\sigma'}$ by the unitary transformation[12] $c_{p\sigma\alpha i} \equiv \frac{1}{\sqrt{2}} \begin{pmatrix} 1 & 1 \\ 1 & -1 \end{pmatrix}_{\sigma\bar{\sigma}} \bar{c}_{p\bar{\sigma}\alpha i}$. Since the eigenvalues of $V_{\sigma\sigma'}$ are 1 and 0, one set of channels in the new basis

[11] Since the coupling constant $v \sim 1/k$, and closed electron loops get a factor k, Gan had to include up to 8-th order diagrams!

[12] The fact that the Fermi functions associated with the states that are mixed by this transformation are not equal, $f_L \neq f_R$, does not matter, since the poor man's scaling equations for $V \neq 0$ are the same as for $V = 0$, as emphasized in section 4.4.2.

decouples (with $\bar{\alpha}$=odd, say) and we have the conventional 2-channel Kondo problem in the $\bar{\alpha}$=even channel (see section 9.2 for details), to which Gan's results can be applied.

Gan obtained the following expression for the self-energy at $T = 0$, $V = 0$, to next-to-leading logarithmic order (below, $c_1, c_2 \ldots$ are constants):

$$\Sigma^I(\omega, D, v) = c_1\, v^2 \Big[1 - 2v \ln(\omega/D) + v^2 k \ln(\omega/D)\Big] \,. \tag{4.35}$$

The requirement that this be invariant under band-width rescaling reads

$$(\partial_x + \beta(v)\partial_v)\, \Sigma^I(\omega, D', v) = 0, \qquad \text{where} \quad \beta(v) \equiv \partial_x v(x) \,, \tag{4.36}$$

and $x = \ln(D'/D)$. This implies $\beta(v) = -v^2 + \frac{1}{2}kv^3$, so that the fixed point condition $\beta(v^*) = 0$ gives $v^* = 2/k$, which agrees to order $O(k^{-1})$ with the exact result $v^* = \frac{2}{2+k}$ [see eq. (7.35)]. Solving the second of eqs. (4.36) for $v(x)$, with the boundary condition $v(0) = v$ gives, for $v(x)$ close to v^*,

$$v(x) = v^* - c_2 \left(\frac{D'}{T_K}\right)^{\Delta} \,, \qquad \text{where} \quad T_K = D v^{k/2} e^{-1/v} \,, \tag{4.37}$$

and $\Delta = 2/k$. Finally, use this result in $\Sigma^I(\omega, D, v) = \Sigma^I(\omega, D', v(x))$, and choose $D' = \omega$ so that the logarithms $\ln \omega/D'$ in eq. (4.35) are zero, to obtain:

$$\Sigma^I(\omega, D, v) = c_1 v^2(x) = c_1 (v^*)^2 \left[1 - \frac{2c_2}{v^*} \left(\frac{\omega}{T_K}\right)^{\Delta}\right] \,. \tag{4.38}$$

This is the desired result. Since $\frac{1}{\tau(\omega)} = -2\Sigma^I(\omega)$, it can be used[13] in eq. (4.33) to obtain asymptotic expressions for the backscattering conductance $\Delta G(V, T) =$

[13]It has to be admitted that some "fudging", typical of the poor man's scaling approach, is involved in doing this: the scaling relations were derived under the assumption $\omega \gg V, T \sim 0$ (without which they are intractable). However, in the integral (4.33) this condition is not satisfied. Therefore, the answers obtained by such an approach only hold with logarithmic accuracy (in which $\ln \omega$ and $\ln 2\omega$ are treated as "equal").

$\partial_V \Delta I(V,T)$. One readily obtains

$$\Delta G(V,0) \propto V^{\Delta} \qquad \text{and} \qquad \Delta G(0,T) \propto T^{\Delta} \; . \tag{4.39}$$

The corresponding expressions that we shall obtain in chapter 9 from our CFT approach have the same form, but with $\Delta = \frac{2}{2+k}$, see eq. (9.28). (Actually, in chapter 9 we always use $k = 2$, and hence $\Delta = \frac{1}{2}$ in eq. (9.28).) This reduces to $2/k$ as $k \to \infty$, which is a useful check on the methods developed in subsequent chapters.

Chapter 5

Scattering State Theory

In chapter 2, section 2.2, we presented the standard theory [KSO77, OKS77, KOS77,JvGW80] of transport through ballistic nanoconstrictions, which employs a semi-classical Boltzmann equation for the distribution function $f_{\vec{k}}(\vec{r})$. In chapter 3, we demonstrated that the conductance data obey a scaling relation in accord with conformal field theory predictions for the $T = 0$ fixed point of the 2-channel Kondo model, and extracted from the data a universal scaling curve $\Gamma(v)$. Our ultimate goal is to calculate $\Gamma(v)$. We therefore need a formulation of transport through a nanoconstriction that meets two requirements: Firstly, it must apply to the weakly non-equilibrium regime, i.e. must go beyond linear response; and secondly, it must be tailor-made for a direct application of results from CFT.

The central idea of the approach by which we achieve this is as follows: *We adopt Hershfield's Y-operator approach* [Hers93], *which formulates a non-equilibrium problem in terms of* **scattering states**, *and obtain these scattering states from Affleck and Ludwig's CFT solution of the 2-channel Kondo problem.*

The present chapter lays the groundwork for this scheme, by describing the basics of the scattering state approach, and Hershfield's Y-operator formalism. Only elementary quantum mechanics is needed. Our main goal is to find an expression for the current in terms of scattering states [eq. (5.52)], and a formula expressing these scattering states in terms of an exactly known Green's function [eq. (5.60)]. The application of AL's CFT to find these scattering states is presented in chapters 7 and 8.

In section 5.1 we outline the proposed scattering state strategy in more detail. In sections 5.2 to 5.3 we develop a rather general (i.e. model-independent) description of nanoconstriction scattering states for the equilibrium situation. Section 5.4 considers the non-equilibrium case $V \neq 0$, with particular emphasis on the Y-operator formulation developed by Hershfield. In sections 5.5 and 5.6 we reexpress the problem as a 2-D field theory, and arrive at an expression, eq. (5.52), for the current in terms of scattering states. Section 5.7 shows how these scattering states can be extracted from a Green's function. In section 5.8 we illustrate the formalism by discussing a simple example, that of 2 species of spinless electrons scattering off a scalar potential.

5.1 General Strategy

Consider a free Hamiltonian H_o with a set of "free" eigenstates $\{|\varepsilon\eta\rangle_o\}$. If a scattering term H_{scat} is turned on adiabatically, the $\{|\varepsilon\eta\rangle_o\}$ will adiabatically develop into a new set of states, $\{|\varepsilon\eta\rangle\}$, which are eigenstates of the full Hamiltonian, $H = H_o + H_{scat}$. These are called the *scattering states* (SSs) of H.

Hershfield has shown recently [Hers93] that non-equilibrium problems, even

strongly interacting ones, become in principle very simple when formulated in terms of SSs, *provided these are known.* In terms of SSs, a non-equilibrium problem can be cast in a form that is formally equivalent to an equilibrium problem. In particular, it is not necessary to resort to the usual non-equilibrium calculational tools, such as the Keldysh technique, which become very complicated for strongly interacting systems.

However, for Hershfield's formulation to be useful, one needs to know the SSs explicitly. Our new proposition is that *the SSs can be extracted from Affleck and Ludwig's CFT solution of the equilibrium 2-channel Kondo problem.* It is then straightforward to insert these SS into Hershfield's non-equilibrium theory to calculate the non-equilibrium conductance, from which the scaling function $\Gamma(v)$ will be extracted.

In making this proposition, we immediately have to address three obvious concerns:

1. *Does CFT make sense for a nanoconstriction?*

After all, CFT is a field theory in 1+1 dimensions, based on an infinite symmetry group, that of all conformal transformations. A nanoconstriction exists in 3+1 dimensions, and does not even have left-right symmetry. How can the former possibly apply to the latter, even in the absence of any impurity and in equilibrium?

The key to this riddle is to formulate the problem (without impurity and at $V = 0$) not in real space, where it is intractable (because of the complicated geometry of the nanoconstriction), *but in energy space, where it becomes simple at low enough energy scales* (see section 5.5). The point is that all one needs

in order to arrive at a CFT of free fermions is a set of one-dimensional, gapless excitations with linear dispersion relation and hence a constant density of states. Now, no matter how complicated the constriction geometry, gapless excitations are always provided by the *geometrical scattering states* (GSS) of the nanoconstriction. These are simply the single-particle states $\{|\varepsilon,\eta\rangle_o = c^\dagger_{o\varepsilon\eta}|0\rangle\}$ that correspond to the complete set of solutions $\{\Phi^o_{\varepsilon,\eta}(\vec{x})\}$ of the free Schrödinger equation in the constriction geometry. The requisite one-dimensionality of the excitations is provided by the constriction itself, which allows one to classify all excitations as either left-moving or right-moving. A linear dispersion relation and constant density of states come for free if we are close enough to the Fermi surface. A (conformally invariant) (1+1)-dimensional field theory can then be constructed by Fourier-transforming, $\psi_\eta(\tau, ix) \equiv \int d\varepsilon\; e^{-i\varepsilon x}\, c_{o\varepsilon\eta}(\tau)$, see eq. (5.30).

Thus the geometrical scattering states can be used in a natural way to construct a (1+1)-dimensional field theory of free fermions. Next we postulate, solely on the basis of the observed phenomena (in particular, the observed $T^{1/2}$ scaling behavior), that these interact with TLSs via a 2-channel Kondo interaction.[1] Switching on such an interaction with an impurity maps the original geometrical scattering states into a new set of *impurity scattering states* $\{|\varepsilon,\eta\rangle\}$ [see eq. (5.9)]. We shall show that these can be extracted from AL's exact CFT solution of the 2-channel Kondo problem [see eqs. (5.60) and (5.59)]. In other words, once the

[1] Of course, historically things happened in exactly the opposite order, as described in the introduction: first Ralph and Buhrman suggested that 2-channel Kondo physics is at work [RB92], (on the basis of $\log V$ and $\log T$ behavior for G and the disappearance of the effect upon annealing, which indicated that structural disorder was important); then Ludwig predicted $T^{1/2}$ scaling behavior; and subsequent analysis of the data indeed showed this behavior. Nevertheless, since other explanations should not be ruled out *a priori*, in constructing the argument above the logic is: "The experiment shows a list of properties, including $T^{1/2}$ scaling; which model can reproduce them all? Let us try the 2-channel Kondo model and see how well it does in reproducing the scaling curve quantitatively."

theory has been defined in energy space, CFT is simply a fancy way of extracting its properties.

At this point, the second concern arises:

2. *Do scattering states make sense for a dynamical impurity problem?*

After all, a *dynamical* impurity is constantly flipping its spin. Can one even define scattering states for such a problem? Would the scattering states not have to "flip along" with the impurity, in some way or other?[2]

However, as is explained in great length in chapter 7, section 7.4.1, in the conformal field theory formulation of the overscreened fixed point, the impurity completely disappears from the formulation: it is absorbed in the definition of a new spin current spin current, $\vec{\mathcal{J}}(x) \equiv \vec{J}_L(ix) + 2\pi\delta(x)\vec{S}$, see eq. (7.36) – this is the technical way of expressing the loose statement "the impurity is screened by conduction eletrons". In terms of the new currents $\vec{\mathcal{J}}$, the Hamiltonian takes the form of a free Hamiltonian, for which one *can* meaningfully define scattering states. These scattering states can be extracted from exactly known two-point functions (which, in a sense, can be viewed Green's functions for which the impurity has been "integrated out").

The third concern is possibly the most serious:

3. *Does is it make sense to extract SSs, to be used in a non-equilibrium problem, from an* **equilibrium** *theory such as CFT?*

After all, it is obvious that in general the SSs must depend on V in some way or other: it is known [MWL93,WM94] that in the "extremely non-equilibrium regime" defined by $V \gg T_K$, the density of states no longer shows a single Kondo

[2] I thank P. Wölfle for pointing out this potential concern to me.

peak at the Fermi energy μ of the equilibrium bath, as it did for $V = 0$, but instead two separate Kondo peaks at $\mu \pm \frac{1}{2}eV$, the separate Fermi energies of the two baths.[3] This is clearly illustrated in Fig. 9.3(b) in chapter 9, obtained by [HKH95]. Thus, the low-T physics for the case $V \gg T_K$ clearly is different from that of $V = 0$.

However, the scaling regime of the Ralph-Buhrman experiments correspond to the opposite limit, $V \ll T_K$, which defines what will be termed the *weakly non-equilibrium regime*. In this limit the physics *is* governed by the $V = 0$ fixed point: since the width of the equilibrium Kondo peak in the density of states is $\sim T_K$ [Hew93, eq.(5.22)], for $V \ll T_K$ the above-mentioned peak-splitting effects are not yet important. Intuitively speaking, by simple "continuity" there must exist a regime in which V is so small that the actual SSs are indistinguishable from the $V = 0$ scattering states, because the V-dependent corrections, of order V/T_K (since T_K is the only energy scale in the problem) are negligible. [Indeed, in Fig. 9.3(b), the Kondo peak shows no signs of splitting for $eV < T_K$.] Clearly, in this regime it *is* valid to extract the SSs from an equilibrium theory such as CFT. Corrections in V/T_K can always be calculated later, if desired [in the framework of the AL theory, this is done by adding operators proportional to V/T_K to the fixed point Hamiltonian (see section 9.4)].

The fact that for small enough V the physics does not differ significantly from that at $V = 0$ also follows from a poor man's scaling argument: it is easy to show [see section 4.4.2] that the poor man's scaling RG equations are completely independent of V (for the same reason as that they are independent of T, namely

[3] This result was obtained in [MWL93,WM94] using the NCA method to study an Anderson model out of equilibrium.

that the bandwidth D is $\gg V, T$). Therefore, the RG flow is initially unaffected by $V \neq 0$. Of course the RG flow is eventually cut off by either V or T, whichever is larger; however, if both are $\ll T_K$, the RG flow will terminate in the close vicinity of the $T = 0, V = 0$ fixed point, even if $V \neq 0$. Thus it makes sense to use AL's equilibrium theory for this fixed point to calculate the SSs.

5.2 Geometrical Scattering States

In this section we formulate the problem in terms of geometrical scattering states.

Consider the problem of free electrons moving ballistically through a nanoconstriction. Ultimately, we have to include 2-channel Kondo scattering off TLSs in our model. For the moment, however, consider such 2-channel Kondo scattering to be switched off. The electrons scatter only off static impurities and the insulating material.

In principle, we have to solve the Schrödinger equation for free electrons and some random static impurities, with boundary conditions that all electron wavefunctions vanish on the metal-insulator boundary. Evidently, this is an intractable problem.[4] Nevertheless, in principle there exists a complete set of single-particle solutions to the Schrödinger equation, $\{\Phi^o_{\varepsilon\eta}(\vec{x})\}$. They are labeled by a continuous eigenenergy ε (measured relative to the Fermi energy), and a set of discrete quantum numbers, denoted collectively by $\eta \equiv (\sigma_\eta, \alpha, i)$. In this chapter, the indices i and α will be called *channel indices:* $i = \uparrow, \downarrow$ is the Pauli electron spin, and α is a discrete index associated with the "non-radial" variables, depending on the coordinate system used. α roughly corresponds to the index α introduced

[4] Even if one ignores scattering off static impurities, and describes the nanoconstriction as a circular hole in a flat, insulating sheet, the resulting problem of wave diffraction through a circular aperture is notoriously difficult to solve [Som54,Born64,Jack75].

in chapter 4, eq. (4.9) (and in chapter 9 will become a pseudospin index). For example, in spherical (r, θ, ϕ), cylindrical (z, ρ, ϕ) or Cartesian (x, y, z) coordinates (with origin $\vec{x} = \vec{0}$ at the center of the hole), α would label complicated linear combinations of angular harmonics $Y_{l,m}(\theta, \phi)$, or Bessel functions $B(\rho, \phi)$, or transverse standing waves $e^{i(k_m x + k_n y)}$, respectively, whereas the "radial" coordinate would be r, z and z, respectively. Finally, $\sigma_\eta = (+, -) = (L, R)$, the *species index,* denotes the direction of propagation of the incident wave: left-moving waves incident from $z = +\infty$ in the right lead towards the left have $\sigma_\eta = L = +$; those incident from $z = -\infty$ in the left lead towards the right have $\sigma_\eta = R = -$. The asymptotic behavior of the incident (or transmitted) parts of such a wave-function $\Phi^o_{\varepsilon\eta}(\vec{x})$ will roughly be (in spherical coordinates) e^{-ikr}/r (or e^{ikr}/r) as $r \to \infty$.

The single-particle eigenstates $\{|\varepsilon, \eta\rangle_o = c^\dagger_{o\varepsilon\eta}|0\rangle\}$ (where $|0\rangle$ = vacuum) of the free Hamiltonian corresponding to these wave-functions will be called *geometrical scattering states,* since they are determined solely by the geometry of the nanoconstriction. We shall use them as a basis of "free" states in terms of which to formulate the scattering of electrons off impurities in the nanoconstriction.

Measuring all energies relative to the equilibrium Fermi energy, for each η, the $T = 0$ Fermi sea is filled up to $\varepsilon = 0$. Since ε is continuous, *for each η we thus have a channel of gapless excitations.* The transport physics is governed by excitations with ε of order T from the Fermi surface. For T small enough ($\ll \mu$), we may thus take the density of states in the η-channel to be energy-independent, $N_\eta(\varepsilon) = N_\eta(0)$ [to order $O(T/\mu)$]. Consequently, such density of states factors can be absorbed into matrix elements [see eq. (5.2)] and the normalization of the

$c^\dagger_{o\varepsilon\eta}$'s, for which we take

$$\{c_{o\varepsilon\eta}, c^\dagger_{o\varepsilon\eta}\} = \delta_{\eta\eta'}\delta(\varepsilon - \varepsilon') \; . \tag{5.1}$$

Hence no explicit $N_\eta(0)$'s appear in the energy integrals below. Also, energy integrals will be taken from $-\infty$ to $+\infty$, since they are cut off by T in any case.[5]

With these conventions, any operator $\hat{O}$ may be expressed in second-quantized form as:

$$\hat{O} = \sum_{\eta\eta'} \int d\varepsilon \int d\varepsilon' \; {}_o\langle \varepsilon\eta | O | \varepsilon'\eta' \rangle_o \; c^\dagger_{o\varepsilon\eta} c_{o\varepsilon'\eta'} \; , \tag{5.2}$$

In particular, the free Hamiltonian is diagonal:

$$H_o = \sum_{\eta} \int d\varepsilon \; \varepsilon \; c^\dagger_{o\varepsilon\eta} c_{o\varepsilon\eta} \, , \tag{5.3}$$

The operator for the current (to the left, say) can be written as

$$I = (e v_{_F}) \sum_{\eta\eta'} \int d\varepsilon \int d\varepsilon' \; \langle \varepsilon\eta | I | \varepsilon'\eta' \rangle \; c^\dagger_{o\varepsilon\eta} c_{o\varepsilon'\eta'} \; . \tag{5.4}$$

What will the coefficients $\langle \varepsilon\eta | I | \varepsilon'\eta' \rangle$ look like? In general, the current does not have to be strictly diagonal in η; in spherical coordinates, for example, it certainly has off-diagonal elements. However, roughly speaking, the current to the left is the difference between the number of left-moving and right-moving transmitted electrons, and hence the largest contribution will come from terms diagonal in η. Thus we write

$$\langle \varepsilon\eta | I | \varepsilon'\eta' \rangle = \frac{1}{v_{_F} h} \sigma_\eta T_\eta \delta_{\eta\eta'} \delta(\varepsilon - \varepsilon') \; , \tag{5.5}$$

where the $\sigma_\eta = \pm$ in front ensures that L/R-movers are counted with opposite signs, and we have neglected the ε-dependence of the "geometrical transmission

[5] Strictly speaking, the $\int d\varepsilon$ integrals have to be cut-off, $\int_{-\Lambda}^{\Lambda} d\varepsilon$, at an energy Λ satisfying $T \ll \Lambda \ll \mu$. However, when interested in low-T physics, we may take $\Lambda \to \infty$ in integrals such as in eq. (5.2), since the corrections thereby neglected are of order $O(T/\Lambda)$.

coefficients" T_η. Since a typical "open" channel has conductance of about 1 e^2/h, we expect $T_\eta \simeq 1$ for transmitting channels, and $T_\eta \simeq 0$ for reflecting channels. For a device with conductance of about 4000 e^2/h, about 4000 channels will be "open" (i.e. transmitting electrons through the hole), while the others will be closed (reflecting).

Suppose a device has an observed ZBA with maximum amplitude of about 10 e^2/h. This means that about 10 of the transmitting channels interact strongly with defects, which induce a non-trivial energy- and temperature dependence in their transmission coefficients. We write the corresponding scattering potential generically as

$$H_{scat} = \sum_{\eta\eta'} \int d\varepsilon d\varepsilon' c^\dagger_{o\varepsilon\eta} V_{\eta\eta'}(\varepsilon, \varepsilon') c_{o\varepsilon'\eta'} \ , \tag{5.6}$$

For Kondo impurities, $V_{\eta\eta'}$ has additional 2×2 matrix structure corresponding to the dynamics of the impurity; however, in the present chapter this need not be made explicit.

5.3 Impurity Scattering States

The so-called *impurity scattering states* are defined to be the set of states $\{|\varepsilon\eta\rangle \equiv c^\dagger_{\varepsilon\eta}|0\rangle\}$ into which the geometrical scattering states $\{|\varepsilon\eta\rangle_o\}$ "develop" when H_{scat} is turned on adiabatically, and which diagonalize the full Hamiltonian H:

$$H \equiv H_o + H_{scat} = \sum_\eta \int d\varepsilon \varepsilon c^\dagger_{\varepsilon\eta} c_{\varepsilon\eta} \ . \tag{5.7}$$

Since both sets of states span the same Hilbert space, they are related by a unitary transformation,[6] $U_{\eta'\eta}(\varepsilon',\varepsilon) \equiv {}_o\langle\varepsilon'\eta'|\varepsilon\eta\rangle$:

$$|\varepsilon\eta\rangle = \sum_{\eta'}\int d\varepsilon' \; |\varepsilon'\eta'\rangle_o U_{\eta'\eta}(\varepsilon',\varepsilon) \; , \tag{5.8}$$

$$c_{\varepsilon\eta} = \sum_{\eta'}\int d\varepsilon' \; U^\dagger_{\eta\eta'}(\varepsilon\varepsilon') c_{o\varepsilon'\eta'} \; ; \tag{5.9}$$

$$\delta_{\eta\eta'}\delta(\varepsilon-\varepsilon') = \sum_{\bar\eta}\int d\bar\varepsilon \; U^\dagger_{\eta\bar\eta}(\varepsilon,\bar\varepsilon) U_{\bar\eta\eta'}(\bar\varepsilon,\varepsilon') \; . \tag{5.10}$$

Note that $U_{\eta'\eta}(\varepsilon',\varepsilon)$ is not quite the same as the usual scattering matrix $S_{\eta\eta'}(\varepsilon',\varepsilon)$, defined by $|\varepsilon\eta\rangle^{(+)} \equiv \sum_{\eta'}\int d\varepsilon' |\varepsilon\eta'\rangle^{(-)} S_{\eta'\eta}(\varepsilon',\varepsilon)$ [Merz70, eq. (19.48)] (in that language $|\varepsilon\eta\rangle^{(+)}$ corresponds to our $|\varepsilon\eta\rangle$). $S_{\eta'\eta}(\varepsilon'\varepsilon)$ maps two sets of eigenstates of the *full* Hamiltonian onto each other, namely "incoming" states $\{|\varepsilon\eta'\rangle^{(-)}\}$ onto "outgoing" ones $\{|\varepsilon\eta\rangle^{(+)}\}$. In contrast, $U_{\eta'\eta}(\varepsilon',\varepsilon)$ maps eigenstates $\{|\varepsilon'\eta'\rangle_o\}$ of H_o onto "outgoing" eigenstates $\{|\varepsilon\eta\rangle\}$ of H.

Since the scattering state operators diagonalize H, their equilibrium thermal expectation values are extremely simple:

$$\langle c^\dagger_{\varepsilon\eta}(\tau) c_{\varepsilon'\eta'}(\tau')\rangle = \delta_{\eta\eta'}\delta(\varepsilon-\varepsilon') e^{\varepsilon(\tau-\tau')} f_o(\varepsilon) \; , \tag{5.11}$$

where $f_o(\varepsilon) = \frac{1}{e^{\beta\varepsilon}+1}$ is the equilibrium Fermi function.

The task at hand, therefore, is to find the $\{c_{\varepsilon\eta}\}$ in terms of the $\{c_{o\varepsilon\eta}\}$. The standard textbook approach is to observe that

$$H_o|\varepsilon\eta\rangle_o = \varepsilon|\varepsilon\eta\rangle_o \quad \text{and} \quad (H_o + H_{scat})\,|\varepsilon\eta\rangle = \varepsilon|\varepsilon\eta\rangle \tag{5.12}$$

[6] It was pointed out to us by A. Stern that the argument below seems to make an implicit assumption that the scattering states can be written as a sum of single-particle states; for a many-body problem such as the Kondo problem, in which particle-hole excitations can be created upon scattering, this might not seem quite appropriate. However, it is known that the scattering matrix for free particles incident on a Kondo impurity is unitary, if the Hilbert space is appropriately enlarged to include "spinor-electrons" (see section 7.5.2 and appendix F). Thus, when applying the formalism below to the Kondo problem in later sections, the unitary transformation in eq. (5.8) is understood to act in this enlarged Hilbert space.

imply

$$|\varepsilon\eta\rangle = |\varepsilon\eta\rangle_o \; + \; \frac{1}{\varepsilon - H_o + i\alpha} H_{scat} |\varepsilon\eta\rangle \tag{5.13}$$

as can be verified by acting on the left-hand-side with $(\varepsilon - H_o)$. This is the *Lippmann-Schwinger* equation for $|\varepsilon\eta\rangle$, see e.g. [Merz70, eq. (19.20)] or [Sak85, eq. (7.1.6)]. When iterated, eq. (5.13) evidently gives $|\varepsilon\eta\rangle$ in terms of $|\varepsilon\eta\rangle$, i.e. it gives a perturbative expression for the operator $U_{\eta'\eta}(\varepsilon', \varepsilon)$ in eq. (5.8).

However, for any Kondo problem perturbation theory is known to break down at low T, so that we have to adopt a different approach. Fortunately, for the 2-channel Kondo problem we have the exact field-theoretic solution of AL at our disposal, which gives exact expression for all Green's functions. Therefore, in section 5.5 we shall transcribe the present problem into a 2-dimensional field theory, and show in section 5.7 how $U_{\eta'\eta}(\varepsilon', \varepsilon)$ can be extracted from an exactly known Green's function [see eqs. (5.59) and (5.60)].

Before turning to field theory, though, we explain in the next section Hershfield's Y-operator approach to non-equilibrium problems, in which the usefulness of scattering states becomes dramatically clear.

5.4 The Non-Equilibrium Case

In this section, we describe how to incorporate a non-zero voltage into the problem. First we scetch in section 5.4.1 the physical situation that applies to a non-equilibrium nanoconstriction without backscattering. Then we explain how the non-equilibrium problem in the presence of backscattering can be treated in terms of Hershfield's formulation of non-equilibrium quantum statistical mechanics.

5.4.1 The Non-Equilibrium Nanoconstriction without Backscattering

Suppose $H_{scat} = 0$, and turn on a voltage, so that the right and left leads have chemical potentials $\mu + eV/2$ and $\mu - eV/2$, respectively. As discussed in section 2.2.1, this causes a gradual drop in the electrostatical potential $e\phi(\vec{r})$ (i.e. the bottom of the conduction band) across the nanoconstriction (see Fig. 2.3), from $+eV/2$ on the right to $-eV/2$ on the left. Consequently L- (or R-) moving electrons traveling at total constant energy E are accelerated (or decelerated) as they approach the constriction. The details of their motion might be complicated, but the result is simple (see page 20): *At each point near the point contact, one has effectively two Fermi seas, one consisting (roughly speaking) of L-movers, injected from the R lead with Fermi energy $\mu + eV/2$, the other of R-movers, injected from the left lead with Fermi energy $\mu - eV/2$* (Fig. 2.2).

Thus, the essence of the non-equilibrium nature of the problem will be captured correctly if we adopt the following simplified picture: ignore the spatial variation of the electrostatic potential $e\phi(\vec{r})$ altogether, and simply consider two leads (R/L) with chemical potentials $\mu \pm \frac{1}{2}eV$, that inject L/R-moving ballistic electrons into each other.

Formally, this means that in the absence of any scattering potential, thermal weighting is done with the following density matrix $\rho_o(V)$:

$$\langle O \rangle \equiv \frac{\mathrm{Tr}\rho_o(V)O}{\mathrm{Tr}\rho_o(V)} , \qquad \text{where} \qquad \rho_o(V) \equiv e^{-\beta[H_o - Y_o(V)]} , \tag{5.14}$$

and the *weighting operator* Y_o is defined as

$$Y_o(V) \equiv \tfrac{1}{2}eV\,(N_L - N_R) \;=\; \tfrac{1}{2}eV \sum_{\eta} \sigma_\eta \int d\varepsilon\, c^\dagger_{o\varepsilon\eta} c_{o\varepsilon\eta} . \tag{5.15}$$

Here N_L and N_R denote the total number of L- and R-moving electrons (recall that $\sigma_\eta = (+,-)$ for (L,R)-movers).

The task at hand is to now incorporate the effect of backscattering at the center of the constriction due to H_{scat}.

5.4.2 The Kadanoff-Baym Ansatz for $V \neq 0$

Let us formulate the problem in general terms: we are confronted with a non-equilibrium problem whose dynamics is described by a Hamiltonian $H = H_o + H_1$, whereas the statistical (thermal weighting) properties are governed by heat baths at chemical potentials $\mu \pm eV/2$. H_1 contains all many-body interactions and scattering terms between baths [in our case there are no many-body interactions, and $H_1 = H_{scat}$.] The heat baths are assumed infinitely large and hence "independent and unperturbed", in the sense that their thermal distribution properties are not perturbed when a small number of particles are transferred from one to the other. A well-known example of such a system consists of two heat-baths, L and R, separated by a tunnel barrier, and H_1 contains a tunneling Hamiltonian H_{tun} that transfers L- and R particles between the two baths, which are otherwise disconnected (apart from a battery of course, to maintain a steady state). In our present system, where the two baths are a bath of L-movers and one of R-movers, H_{scat} plays the role of H_{tun}, which converts the L- to R-movers and vice versa. In our case, the physical left and right leads are of course *not* disconnected, in contrast to the typical tunnel barrier case, and particles freely pass from one lead into the other, with or without scattering. However, we assume that the leads are large enough that none of these processes disturb the equilibrium in each of them, in the sense that each still has a definite well-defined chemical potential,

which governs the distribution of electrons injected towards the lead.

How does one calculate thermal averages for such a system? The main complication that has to be confronted is that the number of particles in each bath is not conserved, in that $[N_{L,R}, H_1] \neq 0$. Therefore, any attempt to simply replace $\rho_o(V)$ in eq. (5.14) by $e^{-\beta(H-Y_o)}$ will (apart from lacking first-principles justification) quickly run into problems: since $[H, Y_o] \neq 0$, many of the standard properties of equilibrium Green's functions (e.g. $G(\tau+\beta) = \pm G(\tau)$), no longer hold.

Kadanoff and Baym have shown how such a general problem is to be dealt with [KB62, eq.(6.20)]: Thermal weighting has to be done at some early time $t_o \to -\infty$, at which all interactions H_1 are switched off, and then H_1 is adiabatically turned on [$H_1(t) \equiv H_1 e^{\alpha t}$, with $\alpha \to 0^+$] while the system is time-evolved to the time t of interest. Concretely, in taking the thermal trace, one uses the thermal weighting factors $e^{-\beta[E_o - \frac{1}{2}eV(N_L-N_R)]_n}$ appropriate to a trace $\sum_n \langle n, t_o|\quad |n, t_o\rangle$ taken at some early time $t_o \to -\infty$; the actual trace, however, is taken between the time-evolved versions of these states $|n,t\rangle = U(t,t_o)|n,t_o\rangle$, where $U = e^{-iH(t-t_o)}$ is the Heisenberg time-evolution operator:[7]

$$\langle O(t)\rangle_V \equiv \frac{\sum_n e^{-\beta[E_o - \frac{1}{2}eV(N_L-N_R)]_n}\langle n,t|O|n,t\rangle}{\sum_n e^{-\beta[E_o - \frac{1}{2}eV(N_L-N_R)]_n}} = \frac{\mathrm{Tr}\,\rho_o(V,t_o)\,U^\dagger(t,t_o)OU(t,t_o)}{\mathrm{Tr}\,\rho_o(V,t_o)}\,, \tag{5.16}$$

where in the second equality the trace is taken between the states $|n,t_o\rangle$. This is the defining prescription for taking non-equilibrium expectation values in the presence of interactions.

Since steady-state expectation values of a single operator are time-independent,

[7] No time-ordered exponential is needed here, because H is assumed to be time-independent.

t is here just a dummy variable, and is often taken to be 0.

5.4.3 Recovering Standard Results for $V = 0$

Of course, for $V = 0$ the prescription (5.16) has to reduce to the standard equilibrium prescription:[8]

$$\langle O \rangle_{V=0} \equiv \frac{\mathrm{Tr}\rho(0,t_o)O}{\mathrm{Tr}\rho(0,t_o)} , \qquad \text{where} \qquad \rho(0,t_o) \equiv e^{-\beta H} . \tag{5.17}$$

To show that this is indeed the case is actually not completely trivial, though intuitively plausible (it is done explicitly in [Hers93]). Adopting the interaction representation with respect to H_1, in which

$$U(t,t_o) = e^{-iH_o(t-t_o)}U_I(t) , \qquad \text{with} \quad U_I(t) = Te^{-i\int_{t_o}^{t} dt' H_{1I}(t')} , \tag{5.18}$$

one expands eq. (5.16) in powers of H_{1I}, and compares the resulting perturbation expansion to that obtained by expanding eq. (5.17) in powers of H_{1I}. If one assumes that a physical relaxation process exists that causes correlation functions to decay in time, so that

$$\lim_{t_o \to -\infty} \frac{\mathrm{Tr}\,\rho_o(0,t_o)B_I(t_o)C_I(t)}{\mathrm{Tr}\,\rho_o(0,t_o)} = \frac{\mathrm{Tr}\,\rho_o(0,t_o)B}{\mathrm{Tr}\,\rho_o(0,t_o)} \, \frac{\mathrm{Tr}\,\rho_o(0,t_o)C}{\mathrm{Tr}\,\rho_o(0,t_o)} , \tag{5.19}$$

then one can set the convergence factor $\alpha = 0$, since its only role was to regulate the $t_0 \to -\infty$ limit, and terms of the form (5.19) arise from the lower limit of the $\int_{t_o}^{t} dt'$ integrals. They turn out to exactly cancel the terms that arise from an expansion of the denominator in eq. (5.17), and the perturbation expansions of eqs. (5.16) and (5.17) indeed turn out to be the same.

Eq. (5.17) is of course the starting point for familiar equilibrium statistical mechanics. One of its most useful features is that the thermal weighting factor

[8] The second argument t_o in $\rho(0,t_o)$ is superfluous; it is retained here only for the sake of notational consistency with the $V \neq 0$ case.

$e^{-\beta H}$ and the dynamical time-evolution factor $U(t,t_o) = e^{-iH(t-t_o)}$ commute; Green's functions therefore have the periodicity property $G(\tau+\beta) = \pm G(\tau)$, which makes it convenient to formulate perturbation expansions in H_1 along the negative imaginary axis, $t = -i\tau \in [0, -i\beta]$.

5.4.4 Hershfield's Formulation of the case $V \neq 0$

If $V \neq 0$ so that eq. (5.16) and not eq. (5.17) is the starting point, there are no obvious periodicity properties along the imaginary time axis, and the conventional approach, due to Keldysh, is to formulate perturbation expansions in H_1 along the real axis [Kel64,RS86]. The various diagrammatic techniques that have been devised are simply ways of doing the real-time integrals $\int_{t_o}^{t} dt'$ that result from the expansion of $U(t,t_o)$. However, for our purposes such expansions are inconvenient: firstly, perturbation expansions have limited use in the Kondo problem, and secondly, we would in the end like to apply Affleck and Ludwig's non-perturbative CFT results.

Hershfield has recently shown that eq. (5.16) can be rewritten in a way that exactly meets our needs (what follows is a simplified version of his arguments): By using the cyclical property of the trace to pull $U(t,t_o)$ to the front, eq. (5.16) can be written as

$$\langle O(t)\rangle_V \equiv \frac{\mathrm{Tr}\rho(V,t)O}{\mathrm{Tr}\rho(V,t)}\,, \tag{5.20}$$

where

$$\frac{\rho(V,t)}{\mathrm{Tr}\rho(V,t)} \equiv \frac{U(t,t_o)\rho_o(V,t_o)U^\dagger(t,t_o)}{\mathrm{Tr}\rho_o(V,t_o)} \tag{5.21}$$

$$\rho(V,t) \equiv e^{-\beta[H-Y(V,t)]}\,, \tag{5.22}$$

The formal definition (5.21) makes it clear that $\rho(V,t)$ is the density operator

that $\rho_o(V, t_o)$ develops into as the interaction is switched on and the system time-evolves from t_o to t, with appropriately changing normalization. Eq. (5.22), purposefully written in a form resembling that of $\rho_o(V, t_o)$ in eq. (5.14), *defines* the operator Y.

What are the properties of $\rho(V, t)$? To gain some intuition, we shall glibly pretend that the denominators in eq. (5.21) are equal [which they are not quite — for a more careful but also more technical treatment of the denominators, relying on the relaxation assumption of eq. (5.19), refer to [Hers93]]. The definition eq. (5.21) then implies that $\rho(V, t)$ satisfies the following differential equation in the interaction picture:[9]

$$i\partial_t \rho_I(V, t) = -[\rho_I(V, t), H_{1I}(t)] \tag{5.23}$$

By expanding in powers of H_1, $\rho_I(V, t) \equiv \sum_{n=0}^{\infty} \rho_{I,n}(V, t)$, and using the fact that each term in the expansion has time-dependence $\rho_{I,n}(V, t) = e^{iH_o(t-t_o)}\ \rho_{I,n}(V, t)\ e^{-iH_o(t-t_o)} e^{\alpha t}$, we find the relation

$$[\rho_{I,n}(V, t), H_o] + i\alpha\rho_{In}(V, t) = -[\rho_{I,n-1}(V, t), H_{1I}(t)]\ , \tag{5.24}$$

which, when summed over n, gives

$$[\rho(V, t), H] = i\alpha\Big(\rho_o(V, t_o) - \rho(V, t)\Big)\ . \tag{5.25}$$

The positive infinitessimal here makes the operator equation well-defined, but can be taken to zero if a relaxation process is assumed and eq. (5.19) holds [Hers93]. Therefore we find, reassuringly, that $[\rho(V, t), H] = 0$, which means that the density matrix is conserved, as it should be.

[9] Note the extra $-$ sign that is characteristic of the time-evolution of the density operator [Sak85, chapter 2].

In a similar fashion, Hershfield showed that the operator Y defined in eq. (5.22) can be characterized as follows:

(P) Y is the operator into which Y_o evolves as the interactions are turned on [as is suggested by a comparison of eqs. (5.21) and (5.14)]. It satisfies the relation

$$[Y, H] = i\alpha(Y_o - Y) \ , \qquad \text{where} \quad \alpha \to 0^+ \ , \tag{5.26}$$

which implies that Y *is a conserved quantity.*

Using this property [and the relaxation assumption eq. (5.19)], Hershfield showed explicitly that eq. (5.22), expanded in powers of H_1, reproduces the Keldysh perturbation expansion obtained from the Kadanoff-Baym Ansatz (5.16).

The fact that the Y-operator is a conserved quantity is the great advantage of the Y-operator approach. It implies that the problem is now formally equivalent to an equilibrium one, where one has μN (N= total particle number) instead of Y, and $[H, N] = 0$. Once the scattering states have been found, one can therefore apply the usual methods of *equilibrium* statistical mechanics,[10] using the density matrix $\rho \equiv e^{-\beta(H-Y)}$ and Heisenberg time-development $\hat{O}(\tau) = e^{H\tau}\hat{O}e^{-H\tau}$.

The fact that Y evolves from Y_o as H_1 is turned on implies that Y can be obtained from Y_o by *replacing*[11] the $c_{o\varepsilon\eta}$ in eq. (5.15) by the scattering-state

[10] By comparing eq. (5.7) and eq. (5.27), it is clear that Y can actually be shifted away in $\rho = e^{-\beta(H-Y)}$ by defining new energies $\varepsilon' \equiv \varepsilon - \mu_\eta$ associated with $c_{\varepsilon\eta}$, i.e. measuring the energy of an excitation relative to the Fermi surface of the bath from which it originates. This brings the weighting factor into a truly equilibrium form, but because $c_{\varepsilon\eta}(\tau) = c_{\varepsilon\eta}e^{-\tau(\varepsilon'+\mu_\eta)}$, it will produce extra factors of $e^{\pm\tau 2\mu_\eta}$ on some operators that are not diagonal in σ_η, such as H_{scat}. We shall not follow this approach here.

[11] Note that Y is *not* simply equal to the Y_o of eq. (5.15), rewritten in terms of the scattering-state basis via eq. (5.9): $Y \neq Y_o$. Y is obtained from Y_o not by rewriting the $c_{o\varepsilon\eta}$ in terms of the $c_{\varepsilon\eta}$, but by *replacing* the former by the latter.

operators $c_{\varepsilon\eta}$ into which the latter evolve:

$$Y \equiv \tfrac{1}{2}eV \sum_{\eta} \sigma_{\eta} \int d\varepsilon \, c^{\dagger}_{\varepsilon\eta} c_{\varepsilon\eta} \qquad (\neq Y_o) \; . \tag{5.27}$$

It follows that non-equilibrium thermal expectation values of the $c_{\varepsilon\eta}$'s have the standard form:

$$\langle c^{\dagger}_{\varepsilon\eta}(\tau) c_{\varepsilon'\eta'}(\tau') \rangle = \delta_{\eta\eta'} \delta(\varepsilon - \varepsilon') e^{\varepsilon(\tau - \tau')} f(\varepsilon, \eta). \tag{5.28}$$

The *only* difference between this equation and its equilibrium version (5.11) is that $f_o(\varepsilon)$ is here replaced by

$$f(\varepsilon, \eta) \equiv \frac{1}{e^{\beta(\varepsilon - \mu_\eta)} + 1} \; = \; f_o(\varepsilon - \mu_\eta) \; , \qquad \text{where} \quad \mu_\eta \equiv \sigma_\eta eV/2 \; , \tag{5.29}$$

(i.e. $\mu_\eta = \pm eV/2$ for scattering states originating from the right or left bath). A remarkably simple result!

The main message of Hershfield's Y-operator formalism is that non-equilibrium problems become simple when formulated in terms of scattering states. The crucial question now becomes: how does one calculate these scattering states for a complicated, many-body problem?

5.4.5 Applying the Y-Operator Approach to the Kondo Problem

Although Hershfield derived his Y-operator approach using arguments based on perturbation theory, he proposed that the formulation that he arrived at can also be used as starting point for non-perturbative calculations. In other words, if it is possible to calculate the scattering states non-perturbatively, and to somehow find an operator Y that is conserved and reduces to Y_o when H_{scat} is turned off,

one can simply insert these into the density matrix ρ of eq. (5.22), and proceed to use relations such as eq. (5.28) and (5.29).

How readily this works in practice depends on the details of the problem. Let us classify a given problem as being of type I if its scattering states are independent of V and T, and of type II if they do explicitly depend on V and T.

"Sufficiently simple" problems will be of type I. For such problems, one can proceed in two separate steps:

(1) First find a basis that diagonalizes the Hamiltonian (i.e. the $c_{\varepsilon\eta}$'s), by the procedure described in section 5.3. By definition, for type I problems this process is independent of whether the system is in equilibrium or not, because it simply amounts to finding a convenient basis for one's Hilbert space (and hence the scattering states are V-independent).

(2) *Thereafter* construct the Y-operator and density matrix ρ directly from the eigenstates of H (not H_o); this means that in doing the thermal weighting in the baths, one specifies the Boltzmann weights associated with the scattering states (not the original free states).

This order of steps, namely first finding a convenient basis, then specifying their thermal weighting, is intuitively plausible: after all, thermal weighting is nothing but a specification of the occupation probabilities of the *eigenstates* of the full Hamiltonian. If one has two leads at different chemical potentials, those states "originating" from the R/L lead should have Boltzmann weights reflecting from which lead they originated, since the thermal equilibration that leads to the Boltzmann factors happens deep inside the leads, before the particles are injected and scattered by H_{scat}.

An example of a problem of type I can be found in [SH95a],[12] where Schiller and Hershfield solve a certain non-equilibrium Kondo problem exactly using Emery-Kivelson bosonization techniques. The scattering states that they calculate explicitly [SH95b] are V- (and T-) independent. Unfortunately it is not suitable for our purposes, because it does not give a $T^{1/2}$ contribution to the conductance [see section 9.1, page 242].

On the other hand, "sufficiently complicated" problems will be of type II, and the Kondo model that we use in chapter 9 falls in this category. In such problems, because of many-body effects the scattering states depend on the occupation of other states, and hence become T and V-dependent. Then the low-energy physics is described by an effective Hamiltonian that is explicitly V- and T-dependent. That this is the case for a typical Kondo problem follows from poor man's scaling: the effective Hamiltonian depends on the rescaled cut-off D', which has to be replaced by $\max(V,T)$ at low energies (this is because the logarithms that arise in perturbation theory will contain $\log[\max(V,T)]$, because the Fermi functions for intermediate states also depend on V, see section 4.4.2).

Intuitively speaking, the Kondo problem is very sensitive to what happens close to the Fermi surface. If the Fermi surface "splits in two" due to a non-zero voltage, this must somehow influence matters. Indeed, in the extreme limit $V \gg T_K$, the Kondo resonance actually splits in two, as mentioned on page 121, and illustrated in Fig. 9.3(b) of chapter 9.

Thus, for a type II problem one cannot first diagonalize H^{eff} and then construct Y^{eff}, because H^{eff} depends on V. Instead H^{eff} and Y^{eff} have to be found

[12]The preprint of [SH95a] inspired the approach proposed below. I would like to thank its authors for making it available to me prior to its publication.

simultaneously and self-consistently, a complicated procedure that has never been attempted so far, to my knowledge (though the non-equilibrium, Keldysh-NCA calculations of [MWL93,WM94] and [HKH94] can be considered to be an indirect way of doing this).

However, in the weakly non-equilibrium regime where $V \ll T_K$, the situation becomes tractable again. As was argued in section 5.1, page 120, in this regime the Kondo peaks have not yet begun to split and the V-dependence of the SSs will only be of order V/T_K, and hence negligible. Hence, in this regime we may use the *equilibrium* version of the SSs, and calculate corrections in perturbation theory in V/T_K, if desired.

We propose (and that is one new aspect of our work) that for the Kondo problem, *the exact equilibrium scattering states* $\{c_{\varepsilon\eta}\}$ *can be obtained from conformal field theory, by extracting them from an equilibrium Green's function* [see eq. (5.60)].[13] These equilibrium SSs are then to be used in a non-equilibrium expression for the current. The conductance so obtained will still be non-linear in V, because the expression for the current contains V-dependent Fermi functions.

The rest of this chapter is devoted to formulating the nanoconstriction problem as a 2-D conformal field theory, and deriving the relation [eq. (5.60)] that gives the scattering states in terms of an exactly known Green's function. The formalism below is valid for arbitrary $V \neq 0$ (only in chapter 9, when applying the formalism to Kondo Green's functions to obtain Kondo SSs, will we have to take $V = 0$).

[13] As argued above [see page 120], in Affleck and Ludwig's conformal field theory approach, the impurity is completely screened (technically, it is absorbed in the spin current) and disappears from the formulation, so that it *is* possible to meaningfully speak of scattering states even for a problem that initially involved a dynamical impurity.

5.5 Transcription to a 2-D Field Theory

In this section we formulate the problem in terms of a set of 2-dimensional, second-quantized fields, $\psi_\eta(\tau, ix)$, one for each channel. They can be expressed either in terms of geometrical or impurity scattering states [eqs. (5.30) or (5.41)]. If the Green's function $G_{\eta\eta'} \equiv -\langle \psi_\eta \psi^\dagger_{\eta'} \rangle$ is known exactly, one can therefore extract from it a relation between $c_{o\varepsilon\eta}$ and $c_{\varepsilon\eta}$, and hence find $U_{\eta'\eta}(\varepsilon', \varepsilon)$.

We initially defined all physical operators in terms of $c_{o\varepsilon\eta}$'s [eq. (5.2)]. A natural way to rewrite them in terms of second-quantized fields is to define, for each channel η, the field $\psi_\eta(\tau, ix)$ (with $x \in [-l, l]$, $l \to \infty$) as a Fourier-integral over all ε: [14]

$$\psi_\eta(ix) \equiv \int_{-\infty}^{\infty} d\varepsilon \; e^{-i\varepsilon x} \, c_{o\varepsilon\eta} \; , \tag{5.30}$$

$$c_{o\varepsilon\eta} = \int_{-\infty}^{\infty} \tfrac{dx}{2\pi} e^{i\varepsilon x} \psi_\eta(ix) \; , \tag{5.31}$$

$$\{\psi_\eta(ix), \psi^\dagger_{\eta'}(ix)\} = 2\pi \delta_{\eta\eta'} \delta(x - x') \; . \tag{5.32}$$

Several comments are in order:

1. Note that $\psi_\eta(ix)$ is *not* the usual electron field $\Psi(\vec{x})$, which is constructed from the (unknown) wave-functions $\Phi^o_{\varepsilon,\eta}(\vec{x})$ through $\Psi(\vec{x}) \equiv \sum_\eta \int d\varepsilon \Phi^o_{\varepsilon,\eta}(\vec{x}) c_{o\varepsilon\eta}$. Instead, $\psi_\eta(ix)$ is best thought of simply as the Fourier transform of $c_{o\varepsilon\eta}$, this being a convenient way of rewriting the problem in field-theoretical language. Nevertheless, the role of x is strongly analogous to that of the "radial" coordinate of the actual wave-function $\Psi_{\varepsilon\eta}(\vec{x})$.

2. If $H_{scat} = 0$, then the $\psi_\eta(ix)$ are *free* fields, that have the following three

[14] As mentioned in footnote 5, the $\int d\varepsilon$ integrals strictly speaking have to be cut-off, $\int_{-\Lambda}^{\Lambda} d\varepsilon$, at an energy Λ satisfying $T \ll \Lambda \ll \mu$, but we take $\Lambda \to \infty$ (which allows us to invert relations such as (5.30) straightforwardly).

properties:

2(a): $c_{o\varepsilon\eta}(\tau) = c_{o\varepsilon\eta}e^{-\varepsilon\tau}$ in the Heisenberg picture (in imaginary time, $t \to -i\tau$), implying that $\psi_\eta(\tau, ix) = \psi_\eta(u)$, where $u \equiv \tau + ix$. [The u dependence of free fields ψ_η of course also follows from the Heisenberg equation of motion for free fields, $(\partial_\tau + i\partial_x)\psi_\eta = 0$.] This is the reason for writing the argument of ψ_η as (ix) in eq. (5.30), since the τ dependence of ψ_η can then simply be obtained by analytic continuation $(ix \to \tau + ix)$.

2(b): *By construction*, all free fields are "mathematical left-movers", since upon continuation to real time, $\tau \to it$, they depend only on $i(t + x)$ [the distinction between *physical* L- and R-movers is carried in the index $\sigma_\eta = \pm 1$]. The reason for choosing such a construction is explained below, just after eq. (5.39).

2(c): If $H_{scat} = 0$, then $c_{o\varepsilon\eta}(\tau) = c_{\varepsilon\eta}(\tau)$ and hence obeys eq. (5.28). This means that the free Green's function G_o is given by [see eq. (A.36)]:

$$G_{\eta\eta'}(u - u') \equiv -\langle T\psi_\eta(u)\psi^\dagger_{\eta'}(u')\rangle \tag{5.33}$$

$$= \frac{-\delta_{\eta\eta'}e^{-\mu_{\eta'}(u-u')}}{\frac{\beta}{\pi}\sin\frac{\pi}{\beta}(u-u')} \xrightarrow{T\to 0} \frac{-\delta_{\eta\eta'}}{u-u'}e^{-\mu_{\eta'}(u-u')} . \tag{5.34}$$

It is straightforward to rewrite any operator $\hat{O}$, expressed as in eq. (5.2), in terms of $\psi_\eta(ix)$:

$$\hat{O} = \sum_{\eta\eta'}\int\tfrac{dx}{2\pi}\int\tfrac{dx'}{2\pi}\ \psi^\dagger_\eta(ix)O_{\eta\eta'}(x,x')\psi_{\eta'}(ix') \tag{5.35}$$

where

$$O_{\eta\eta'}(x,x') \equiv \int d\varepsilon \int d\varepsilon'\ {}_o\langle\varepsilon\eta|O|\varepsilon'\eta'\rangle_o\, e^{-i(\varepsilon x - \varepsilon' x')} \tag{5.36}$$

In particular, the Hamiltonian becomes

$$H \equiv H_o + H_{scat} = \sum_{\eta\eta'}\int_{-\infty}^{\infty}\tfrac{dx}{2\pi}\psi^\dagger_\eta(ix)H_{\eta\eta'}(x)\psi_{\eta'}(ix) , \tag{5.37}$$

$$H_{\eta\eta'}(x) \equiv \delta_{\eta\eta'}i\partial_x + 2\pi\delta(x)V_{\eta\eta'} . \tag{5.38}$$

We have neglected the energy-dependence of the matrix elements in H_{scat}, taking $V_{\eta\eta'}(\varepsilon, \varepsilon') \equiv V_{\eta\eta'}$; this corresponds to assuming a short-range interaction, as is evident in eq. (5.38).

By simple Fourier transformation, we have hence arrived at a 2-dimensional field theory, defined by eqs. (5.37) and (5.38). The reason why this (and not a 3+1 dimensional theory) resulted, is essentially that there is only *one* continuous quantum number, namely ε, in the problem, with respect to which we can Fourier transform. This in turn is a result of the constriction geometry, which defines a definite and unique origin, and consequently a notion of a single "radial" coordinate, r or z, depending on the coordinate system used, to which our x roughly corresponds.

5.6 Scattering State Wave-Functions

In this section we reexpress the field $\psi_\eta(ix)$ in terms of the $\{c_{\varepsilon\eta}\}$, and derive a convenient expression for the current, namely eq. (5.52). In the process we shall naturally be lead to define an important quantity, the scattering amplitude $\tilde{U}_{\eta\eta'}(\varepsilon)$ for an incoming particle with quantum numbers (ε, η') to emerge with quantum numbers (ε, η). This is the quantity that can most easily be extracted from an exact Green's function.

The Heisenberg equation for $\psi_\eta(\tau, ix)$ is

$$-\partial_\tau \psi_\eta(u) = [\psi_\eta(u), H] = H_{\eta\eta'}(x)\psi_{\eta'}(u) \tag{5.39}$$

Now, we emphasized on page 140, point 2(b), that *all* our fields (both for $\sigma_\eta = L$ and R) are mathematical left-movers, incident from $x = \infty$ and traveling toward $x = -\infty$. When a scattering term $H_{scat} = V_{\eta\eta'}\delta(x)$ is turned on, the scattered

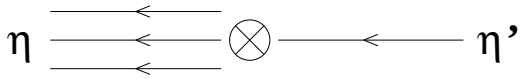

Figure 5.1 A one-dimensional scattering problem: Free fields are incident from the right, scattered at the origin and outgoing to the left.

fields will be different from free fields only for $x < 0$. Thus, *we have turned our problem into a one-dimensional scattering problem,* with *all* free fields incident from the right, and *all* scattered ones outgoing to the left (see Fig. 5.1). This is the reason for introducing both L- and R-movers as "mathematical left-movers". L-R backscattering is described by the $\sigma_\eta \neq \sigma_{\eta'}$ terms in $V_{\eta\eta'}$.

It is convenient to express this scattering problem in terms of the $\{c_{\varepsilon\eta}\}$, since the full H is diagonal in terms of these. Inserting the inverse of eq. (5.9) into eq. (5.30) and defining

$$\phi_{\varepsilon'\eta'}(ix,\eta) \equiv \int d\varepsilon e^{-i\varepsilon x} U_{\eta\eta'}(\varepsilon,\varepsilon') \ , \tag{5.40}$$

we find

$$\psi_\eta(\tau,ix) = \sum_{\eta'} \int d\varepsilon' \phi_{\varepsilon'\eta'}(ix,\eta) c_{\varepsilon'\eta'}(\tau) \ , \tag{5.41}$$

$$c_{\varepsilon'\eta'}(\tau) = \sum_{\eta} \int \tfrac{dx}{2\pi} \phi^*_{\varepsilon'\eta'}(ix,\eta) \psi_\eta(\tau,ix) \ . \tag{5.42}$$

The function $\phi_{\varepsilon'\eta'}(ix,\eta)$ may be thought of as the "wave-function" for the impurity scattering state $|\varepsilon'\eta'\rangle$:[15] it gives the amplitude for an electron, injected in state $|\varepsilon'\eta'\rangle_o$, to be found at x with quantum number η. The unitarity (5.10) of

[15]This interpretation of $\phi_{\varepsilon'\eta'}(ix,\eta)$ as a wave-function is meant as a mnemonic and should not be taken literally; as mentioned on page 139, point 1, the actual wave-functions are intractably complicated.

$U_{\eta\eta'}(\varepsilon,\varepsilon')$ guarantees orthonormality and completeness of the $\phi_{\varepsilon'\eta'}(ix,\eta)$'s:

$$\sum_{\bar\eta}\int\tfrac{d\bar x}{2\pi}\;\phi^*_{\varepsilon\eta}(i\bar x,\bar\eta)\phi_{\varepsilon'\eta'}(i\bar x,\bar\eta) \;=\; \delta_{\eta\eta'}\delta(\varepsilon-\varepsilon')\;, \tag{5.43}$$

$$\sum_{\bar\eta}\int d\bar\varepsilon\;\phi^*_{\bar\varepsilon\bar\eta}(ix,\eta)\phi_{\bar\varepsilon\bar\eta}(ix',\eta') \;=\; 2\pi\;\delta_{\eta\eta'}\delta(x-x')\;. \tag{5.44}$$

The advantage of the representation (5.41) of $\psi_\eta(\tau,ix)$ is that $c_{\varepsilon\eta}(\tau)=c_{\varepsilon\eta}e^{-\tau\varepsilon}$, because $c_{\varepsilon\eta}$ diagonalizes H [eq. (5.7)]. Therefore the Heisenberg equation (5.39) reduces to an eigenvalue equation for $\phi_{\varepsilon'\eta'}(ix,\eta)$:

$$H_{\eta\bar\eta}(x)\phi_{\varepsilon'\eta'}(ix,\bar\eta)=\varepsilon'\phi_{\varepsilon'\eta'}(ix,\eta)\;. \tag{5.45}$$

Since the solutions of eq. (5.45) must correspond to the free wave-function $e^{-i\varepsilon' x}$ of the state $|\varepsilon'\eta'\rangle_o$ for all $x>0$ (before the scatterer is encountered), they will in general have the following form: [16]

$$\phi_{\varepsilon'\eta'}(ix,\eta)\equiv e^{-i\varepsilon' x}\left[\tilde U_{\eta\eta'}(\varepsilon')\theta(-x)+\delta_{\eta\eta'}\theta(x)\right]\;. \tag{5.46}$$

This relation defines the matrix $\tilde U_{\eta\eta'}(\varepsilon')$, which clearly can be interpreted as a scattering amplitude, since it specifies the amplitude for an electron incident with quantum numbers $(\varepsilon'\eta')$ to emerge with quantum numbers $(\varepsilon'\eta)$.

The relation between the scattering amplitude $\tilde U_{\eta\eta'}(\varepsilon')$ and the matrix $U_{\eta\eta'}(\varepsilon,\varepsilon')$ can be found by inserting eq. (5.46) into the inverse of eq. (5.40):

$$U_{\eta\eta'}(\varepsilon,\varepsilon') \;=\; \int\tfrac{dx}{2\pi}e^{i\varepsilon x}\phi_{\varepsilon'\eta'}(ix,\eta) \tag{5.47}$$

$$\;=\; \frac{1}{2\pi i}\left[\frac{\tilde U_{\eta\eta'}(\varepsilon')}{\varepsilon-\varepsilon'-i\alpha}\;-\;\frac{\delta_{\eta\eta'}}{\varepsilon-\varepsilon'+i\alpha}\right]. \tag{5.48}$$

[16] In writing eq. (5.46), we have assumed elastic scattering ($\varepsilon_{in}=\varepsilon_{out}$). For a 2-channel Kondo model this means that we assume that the impurity energy splitting $\Delta=0$, so that electrons cannot exchange energy with the impurity (experimental evidence that Δ is indeed small ($\lesssim 1$ K) is presented in section 3.4).

The unitarity condition eq. (5.10) on $U_{\eta\eta'}(\varepsilon,\varepsilon')$ then immediately implies unitarity for $\tilde{U}_{\eta\eta'}(\varepsilon')$ (the $\int d\bar{\varepsilon}$ integral can trivially be done by contour methods):

$$\sum_{\bar{\eta}} \tilde{U}_{\eta\bar{\eta}}(\varepsilon')\tilde{U}^{\dagger}_{\bar{\eta}\eta'}(\varepsilon') \equiv \delta_{\eta\eta'} \ . \tag{5.49}$$

The unitarity of $\tilde{U}_{\eta\bar{\eta}}(\varepsilon')$ could of course have been anticipated from eq. (5.46): it ensures that scattering conserves probability, i.e. that $\sum_{\eta} |\phi_{\varepsilon'\eta'}(ix,\eta)|^2$ is the same for $x>0$ and $x<0$.

As a consistency check, note that by using $\frac{1}{\varepsilon-i\alpha}+\frac{1}{\varepsilon+i\alpha}=2\pi i\delta(\varepsilon)$, eq. (5.48) can be written in the form

$$U_{\eta'\eta}(\varepsilon',\varepsilon) = \delta_{\eta\eta'}\delta(\varepsilon'-\varepsilon) \ + \ \frac{1-\tilde{U}_{\eta'\eta}(\varepsilon)}{\varepsilon-\varepsilon'+i\alpha} \tag{5.50}$$

which has the form of (an iterated version of) the Lippmann-Schwinger eq. (5.13).

Using eq. (5.41) and eq. (5.46), any operator written in the form (5.35) can be expressed in terms of $\tilde{U}_{\eta\eta'}(\varepsilon)$. In particular, the current density becomes

$$\begin{aligned} I \equiv \lim_{l\to\infty} \tfrac{1}{2l}\langle \hat{I}(\tau)\rangle \ &= \ \tfrac{2\pi e}{h}\sum_{\eta\eta'} \tfrac{1}{2l}\int_{-l}^{l}\tfrac{dx}{2\pi}\sum_{\bar{\eta}\bar{\eta}'}\!\!\int d\bar{\varepsilon}d\bar{\varepsilon}' e^{(\tau+ix)(\bar{\varepsilon}-\bar{\varepsilon}')}\langle c^{\dagger}_{\bar{\varepsilon}\bar{\eta}}c_{\bar{\varepsilon}'\bar{\eta}'}\rangle \\ &\quad \times \ \Big[\tilde{U}^{\dagger}_{\bar{\eta}\eta}(\bar{\varepsilon})\sigma_\eta T_\eta \tilde{U}_{\eta\bar{\eta}'}(\bar{\varepsilon}')\ \theta(-x) \ + \ \delta_{\bar{\eta}\bar{\eta}'}\sigma_{\bar{\eta}}T_{\bar{\eta}}\theta(x)\Big] \ , \end{aligned} \tag{5.51}$$

where we used eq. (5.5) in eq. (5.36) to obtain $I_{\eta\eta'}(x,x') = \frac{2\pi}{v_F h}\sigma_\eta T_\eta \delta_{\eta\eta'}\delta(x-x')$. Using eq. (5.28), the thermal expectation value of the current density becomes

$$\boxed{I \ = \ \tfrac{e}{h}\textstyle\sum_{\bar{\eta}\eta}\!\int d\bar{\varepsilon}\tfrac{1}{2}\left[\tilde{U}^{\dagger}_{\bar{\eta}\eta}(\bar{\varepsilon})\sigma_\eta T_\eta \tilde{U}_{\eta\bar{\eta}}(\bar{\varepsilon}) \ + \delta_{\bar{\eta}\eta}\sigma_{\bar{\eta}}T_{\bar{\eta}}\right] f(\bar{\varepsilon},\bar{\eta})} \tag{5.52}$$

The problem of calculating the current has thus been reduced to that of finding the scattering amplitude $\tilde{U}_{\eta\eta'}(\varepsilon)$.

5.7 Extracting $\tilde{U}$ from a Green's Function

We show in this section that $\tilde{U}_{\eta\eta'}(\varepsilon)$ can readily be extracted from the thermal Green's function in Matsubara space, $G_{\eta\eta'}(\omega_n; x, x')$, and illustrate this with the simplest possible example.

5.7.1 General Derivation

First note that the discontinuity at $x = 0$ of $\phi_{\varepsilon'\eta'}(ix, \eta)$ [see eq. (5.46)] implies that $\psi_\eta(\tau, ix)$, too, is discontinuous at $x = 0$. Therefore we write it in terms of two pieces that are separately continuous in their domains of definition, $x \gtrless 0$:

$$\psi_\eta(\tau, ix) \equiv \psi_{\substack{\eta> \\ \eta<}}(\tau, ix) \equiv \psi_{\eta L/R}(\tau \pm ir) \ , \qquad \text{for } x \gtrless 0; \quad r \equiv |x| \ , \tag{5.53}$$

with $\psi_{\eta<}(\tau, i0^-) \neq \psi_{\eta>}(\tau, i0^+)$. In the second equality we used the index L/R to denote *mathematical L/R-movers,* (since the corresponding fields depend on $t \pm r$ when $\tau \to it$), thus introducing a notation that is used extensively by Affleck and Ludwig.

The thermal Green's function is defined by

$$G_{\eta\eta'}(\tau, ix; \tau', ix') \equiv -\langle T\psi_\eta(\tau, ix)\psi^\dagger_{\eta'}(\tau', ix')\rangle \ . \tag{5.54}$$

For $x' \equiv r' > 0$ and $x \equiv -r < 0$, it gives the amplitude that an incident η-electron will emerge from the scattering process with quantum number η'. Using eqs. (5.41), (5.46) and (5.28), the corresponding Green's function is found to be

$$\begin{aligned} G^{RL}_{\eta\eta'}(\tau - ir\,; \tau' + ir') &\equiv G_{\eta\eta'}(\tau, -ir; \tau', ir') \qquad (5.55) \\ &= -\sum_{\bar\eta\bar\eta'} \int d\bar\varepsilon \, d\bar\varepsilon' \, \tilde{U}_{\eta\bar\eta}(\bar\varepsilon)\delta_{\bar\eta'\eta'} \, \langle c_{\bar\varepsilon\bar\eta}(\tau) c_{\bar\varepsilon'\bar\eta'}(\tau')\rangle \, e^{-i(-\bar\varepsilon r - \bar\varepsilon' r')} \\ &= -\int d\bar\varepsilon \, \tilde{U}_{\eta\eta'}(\bar\varepsilon) \, \frac{e^{-\bar\varepsilon[(\tau-\tau') - i(r+r')]}}{e^{-\beta(\bar\varepsilon - \mu_{\eta'})} + 1} \ . \qquad (5.56) \end{aligned}$$

It can be checked that this function has the periodicity property

$$G^{RL}_{\eta\eta'}(\tau+\beta) = -e^{-\mu_\eta \beta} G^{RL}_{\eta\eta'}(\tau) \ , \tag{5.57}$$

[see, e.g. (5.62) below], which means that its Matsubara transform must be defined with an extra factor of $e^{-\mu_{\eta'}\tau}$ (see e.g. [Amb69, p.266, eq.(51)]):

$$G^{RL}_{\eta\eta'}(\tau - ir\,;\tau' + ir') \equiv \sum_m e^{-i(\omega_n - i\mu_{\eta'})\tau} G^{RL}_{\eta\eta'}(i\omega_n; r, r') \ , \tag{5.58}$$

where $\omega_n = 2\pi(n+\frac{1}{2})/\beta$. Writing the Matsubara transform of eq. (5.56) in spectral form,

$$G^{RL}_{\eta\eta'}(i\omega_n; r, r') \equiv \int_{-\beta/2}^{\beta/2} d\tau e^{i(\omega_n - i\mu_{\eta'})\tau} G^{RL}_{\eta\eta'}(\tau, r; 0, r') \ \equiv \ \int \tfrac{d\varepsilon}{2\pi} \frac{\mathcal{A}^{RL}_{\eta\eta'}(\varepsilon; r, r')}{i\omega_n - (\varepsilon - \mu_{\eta'})} \ , \tag{5.59}$$

one finds that $\tilde{U}_{\eta\eta'}(\varepsilon)$ is related as follows to the spectral function $\mathcal{A}^{RL}_{\eta\eta'}(\varepsilon; r, r')$:

$$\boxed{\tilde{U}_{\eta\eta'}(\varepsilon) = \tfrac{1}{2\pi} \mathcal{A}^{RL}_{\eta\eta'}(\varepsilon; r, r') e^{-i\varepsilon(r+r')} \ .} \tag{5.60}$$

Thus, *if $G_{\eta\eta'}$ is known exactly* (e.g. from AL's conformal field theory for the 2-channel Kondo problem), *then $\tilde{U}_{\eta\eta'}(\varepsilon)$ can be obtained directly by calculating its spectral function $\mathcal{A}^{RL}_{\eta\eta'}(\varepsilon; r, r')$.*

Equations (5.60) and (5.52) are the main results of this chapter, and will be used in chapter 9 to calculate the scaling curve $\Gamma(v)$.

5.7.2 Simplest Possible Example

As the simplest possible example, suppose that at $T = 0$, $G_{\eta\eta'}$ has the form

$$G^{RL}_{\eta\eta'}(\tau - ir, \tau' + ir') = \frac{-\tilde{U}_{\eta\eta'} e^{-\mu_{\eta'}[\tau - \tau' - i(r+r')]}}{[\tau - \tau' - i(r+r')]} \ , \tag{5.61}$$

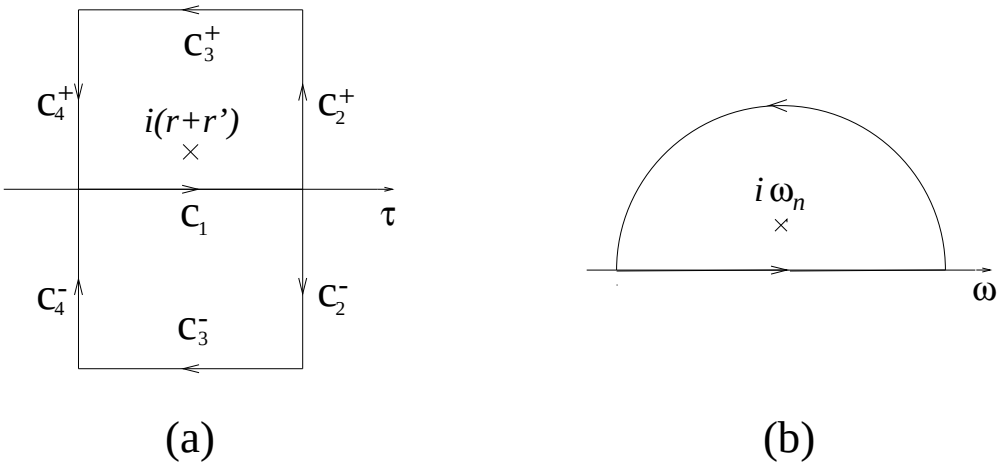

Figure 5.2 Integration contours useful for performing (a) the $\int d\tau$ integral in eq. (5.59); (b) the $\int d\omega$ integral in eq. (5.64).

where $\tilde{U}_{\eta\eta'}$ is a constant. (If $\tilde{U}_{\eta\eta'} = \delta_{\eta\eta'}$, this is the case of free fermions with no scattering, see eq. (5.34).) This is a case that occurs often in subsequent chapters. The corresponding $T \neq 0$ Green's function then is[17]:

$$G^{RL}_{\eta\eta'}(\tau - ir, \tau' + ir') = \frac{-\tilde{U}_{\eta\eta'} e^{-\mu_{\eta'}[\tau - \tau' - i(r+r')]}}{\frac{\beta}{\pi} \sin \frac{\pi}{\beta}[\tau - \tau' - i(r + r')]} \ . \tag{5.62}$$

Calculate $G^{RL}_{\eta\eta'}(i\omega_n; r, r')$ from eq. (5.59). Since the extra factor $e^{\mu_{\eta'}\tau}$ in eq. (5.59) ensures that the integrand is periodic in τ, the $\int d\tau$ integral can readily be done by contour methods: for $\omega_n \gtrless 0$, the integral can be closed in the upper (lower) half-plane of the complex τ plane [see Fig. 5.2(a)]. This is possible because the portions $C_2^{\pm} + C_4^{\pm}$ cancel due to the periodicity of the integrand, and the contributions along $C_3^{\pm}$ vanish for $\omega_n \gtrless 0$ as $\mathrm{Im}(\tau) \to \pm\infty$. Thus one obtains

$$G^{RL}_{\eta\eta'}(i\omega_n; r, r') = -\theta(\omega_n)\, 2\pi i\, e^{-(\omega_n - i\mu_{\eta'})(r+r')}\, \tilde{U}_{\eta\eta'} \ . \tag{5.63}$$

The spectral form for this expression is

$$G^{RL}_{\eta\eta'}(i\omega_n; r, r') = \tilde{U}_{\eta\eta'} \int_{-\infty}^{\infty} d\omega \frac{e^{i\omega(r+r')}}{i\omega_n - (\omega - i\mu_{\eta'})} \ , \tag{5.64}$$

[17] See eq. (5.33), and for a general argument (for $V = 0$) describing how to obtain $T \neq 0$ Green's functions from $T = 0$ ones in CFT, see section 8.1, eq. (8.7).

as follows by closing the $\int d\omega$ integral as in Fig. 5.2(b). Comparing this expression with eqs. (5.59) and (5.60), we deduce that

$$U_{\eta\eta'}(\varepsilon) = \tilde{U}_{\eta\eta'} \ . \tag{5.65}$$

Thus, for simple Green's functions such as eq. (5.61), $U_{\eta\eta'}(\varepsilon)$ is energy-independent, and can be read off directly from eq. (5.61). This will be useful in later chapters.

5.8 Example: 2-species Scalar Scattering

In this section we illustrate[18] the formalism developed so far by considering a very simple scattering problem, namely the scattering of only two species of (spinless) electrons off a scalar scattering potential. We take η equal to the species index, $\eta \equiv \sigma_\eta = (L, R) = (+, -)$ (i.e. η contains no extra channel indices i or n, and L/R denotes physical L/R movers), and our Hamiltonian [compare eqs. (5.37) and (5.38)] is:

$$H = \sum_\sigma \int \tfrac{dx}{2\pi} \psi^\dagger_\sigma(ix) H_{\sigma\sigma'}(x) \psi_{\sigma'}(ix') \ , \tag{5.66}$$

$$H_{\sigma\sigma'}(x) \equiv \delta_{\sigma\sigma'} i\partial_x + 2\pi\delta(x) V_{\sigma\sigma'} \ . \tag{5.67}$$

Here $V_{\sigma\sigma'}$ is simply a hermitian 2×2 matrix representing potential scattering of the two species into each other (i.e. the impurity is not a dynamical object with internal degrees of freedom). Since V is Hermitian, we can diagonalize the scattering term by making a unitary transformation of the form

$$\overline{\psi}_\sigma \equiv N_{\sigma\sigma'} \psi_{\sigma'} \ , \tag{5.68}$$

[18] This problem is also discussed at length in chapter 6 to illustrate the CFT methods needed for the Kondo problem.

with N chosen such that

$$H_{\rm scat} = \sum_{\sigma\sigma'} \overline{\psi}^\dagger_\sigma(0) \left(NVN^{-1}\right)_{\sigma\sigma'} \overline{\psi}_\sigma(0) \equiv \overline{\psi}^\dagger_\sigma(0) \left(v_o \tfrac{1}{2}\delta_{\sigma\sigma'} + v_3 \tfrac{1}{2}\sigma^3_{\sigma\sigma'}\right) \overline{\psi}_\sigma(0) \ . \quad (5.69)$$

Since the scattering term is now diagonal, its only effect on the $\overline{\psi}_\sigma$-fields can be to cause a phase shift of the outgoing fields relative to the incident ones:

$$\overline{\psi}_{\sigma<}(ix) = P_{\sigma\sigma'}\overline{\psi}_{\sigma'>}(ix) \qquad \text{for } x < 0 \ , \quad (5.70)$$

$$\text{where} \qquad P_{\sigma\sigma'} = \delta_{\sigma\sigma'} e^{-i(\phi_o + \sigma\phi_3)} \ . \quad (5.71)$$

and the phase shifts ϕ_0 and ϕ_3 are functions of v_o and v_3 (this is discussed at length in chapter 6). Rotated back into the ψ_σ-basis, this phase shift of course becomes an actual $[SU(2)]$ rotation of the two species into each other:

$$\psi_{\sigma<}(ix) = \tilde{U}_{\sigma\sigma'}\psi_{\sigma'>}(ix) \ , \quad (5.72)$$

where

$$\tilde{U}_{\sigma\sigma'} \equiv \left(N^{-1}PN\right)_{\sigma\sigma'} \equiv \begin{pmatrix} \mathcal{T} & \mathcal{R} \\ -\mathcal{R}^*\mathcal{T}/\mathcal{T}^* & \mathcal{T} \end{pmatrix} , \qquad [|\mathcal{T}|^2 + |\mathcal{R}|^2 \equiv 1] \ , \quad (5.73)$$

is a unitary matrix. Comparing eq. (5.72) with eq. (5.46) and eq. (5.41), we see that $\tilde{U}_{\sigma\sigma'} = \tilde{U}_{\sigma\sigma'}(\varepsilon')$, i.e. in this simple case $\tilde{U}$ is ε'-independent. Physically, this rotation of physical L- and R-movers into each other simply reflects the fact that H_{scat} causes backscattering: an incoming L-mover has amplitude $\mathcal{T}$ to undergo forward scattering and emerge as a L-mover, and $\mathcal{R}$ to be backscattered into a R-mover (this is how backscattering is possible despite our formulation of both $\sigma = L$ and $\sigma = R$ as mathematical L-movers, for which both the transmitted ($\mathcal{T}$) and reflected ($\mathcal{R}$) parts of ψ_σ live at $x < 0$).

As a concrete example, we give the matrices N and $\tilde{U}$ corresponding to a very simple case. If $V_{\sigma\sigma'} \equiv \frac{1}{2}(v_o\delta_{\sigma\sigma'} + v_1\sigma^x_{\sigma\sigma'})$, then

$$N = \tfrac{1}{\sqrt{2}} \begin{pmatrix} 1 & 1 \\ 1 & -1 \end{pmatrix} \quad \text{and} \quad \tilde{U} = e^{-i\phi_o} \begin{pmatrix} \cos\phi_3 & -i\sin\phi_3 \\ -i\sin\phi_3 & \cos\phi_3 \end{pmatrix}. \tag{5.74}$$

To calculate the current, insert eq. (5.73) into eq. (5.52), and for simplicity assume $T_\eta = 1$ for the geometrical transmission coefficients. One readily finds [using eq. (5.29) for the second line]:

$$\begin{aligned} I &= \tfrac{e}{h}\sum_{\bar{\sigma}}\int d\bar{\varepsilon}\ |\mathcal{T}|^2\ \bar{\sigma}\ f(\bar{\varepsilon},\bar{\sigma}) && (5.75)\\ &= \tfrac{e^2}{h}|\mathcal{T}|^2 V\ . && (5.76) \end{aligned}$$

As expected, the conductance $G \equiv \partial_V I = \frac{e^2}{h}|\mathcal{T}|^2$ is reduced from its customary value for a single channel in the absence of scattering, namely $\frac{e^2}{h}$, by the transmission coefficient squared $|\mathcal{T}|^2$.

Eq. (5.75) can also be used to illustrate that the conductance assumes a V/T *scaling* form if the transmission coefficient $\mathcal{T}$ is energy dependent. Assume that for some reason the $\mathcal{T}$ in eq. (5.75) depends on the distance from the Fermi surface, and can be expanded as $|\mathcal{T}|^2 \equiv A_o + (\varepsilon/\varepsilon_{_F})A_1 + (\varepsilon/\varepsilon_{_F})^2A_2 + \ldots$ Then the conductance $G = \partial_V I$ is readily found to be

$$\begin{aligned} G(V,T) &= \tfrac{e^2}{h}\int d\varepsilon \left(A_o + (\varepsilon/\varepsilon_{_F})A_1 + (\varepsilon/\varepsilon_{_F})^2A_2 + \ldots\right) \\ &\quad \times(-\tfrac{1}{2})\left[\partial_\varepsilon f_o(\varepsilon - eV/2) + \partial_\varepsilon f_o(\varepsilon - eV/2)\right] && (5.77)\\ &= \tfrac{e^2}{h}\left[A_o\ +\ A_2\tfrac{\pi^2}{3}\left(\frac{T}{\varepsilon_{_F}}\right)^2\left(1\ +\ \tfrac{3}{4\pi^2}\left(\frac{eV}{T}\right)^2\right)\right]. && (5.78) \end{aligned}$$

This has the scaling form $G(V,T) = G(0,0) + BT^2\Gamma(v)$, where $\Gamma(v) = \left(1 + \frac{3}{4\pi^2}v^2\right)$ is a universal function, and $v \equiv eV/T$.

In the 2-channel Kondo case, *a scaling form for the conductance will arise in a similar fashion, namely from an energy-dependence in the transmission coefficient,* the non-trivial difference being that there we shall find $|\mathcal{T}(\varepsilon)|^2 = A_o + A_1 T^{1/2}\tilde{\Gamma}(\varepsilon/T)$ [compare eqs. (3.6) and (9.12)]. This will be demonstrated in chapter 9, for which one needs to understand the main features of Affleck and Ludwig's CFT solution of the 2-channel Kondo problem. The following several chapters are therefore devoted to an introduction to the Kondo problem, and in particular its CFT solution.

Chapter 6

Scalar Scattering as a Boundary Conformal Field Theory

This chapter serves a purely pedagogical purpose. We introduce the reader to elements of Cardy's boundary conformal field theory that were used by Affleck and Ludwig in their solution of the Kondo problem. Instead of directly starting with the AL theory, we discuss here a far simpler case, namely the calculation of the Green's function G^{RL} for the scattering of two species of spinless fermions off a diagonal scalar scatterer at the origin. This problem, already solved in section 5.8, is so simple that it certainly does not need the elaborate treatment to be presented here. However, we hope that due to the very simplicity of this problem the reader will be able to follow the (rather) technical details below with reasonable ease. We have attempted to make the presentation as self-contained as possible; however, if need be, the reader is encouraged to consult appendix C for a general discussion of the techniques used here.

Our discussion of the Kondo problem will then proceed mainly by analogy to

the arguments presented in this chapter. The reader not interested in technical details can skip to the summary in section 6.6, and then proceed to chapter 7.

The problem to be studied here arose in section 5.8 in the study of the scattering of two species of spinless electrons, ψ^α, with $\alpha = (+,-)$, off a scalar potential $2\pi\delta(x)V_{\alpha\alpha'}$.[1] A rotation to new fields, $\overline{\psi}^\alpha \equiv N_{\alpha\alpha'}\psi^{\alpha'}$ was made in order to diagonalize $V_{\alpha\alpha'}$. It is the resulting problem, defined by [see eqs. (5.66) and (5.69)]

$$H = \sum_\alpha \int \tfrac{dx}{2\pi} \overline{\psi}^{\dagger\alpha}(x) H_{\alpha\alpha'}(x) \overline{\psi}^{\alpha'}(x') \,, \tag{6.1}$$

$$H_{\alpha\alpha'}(x) \equiv \delta_{\alpha\alpha'} i\partial_x + 2\pi\delta(x)\left(v_o \tfrac{1}{2}\delta_{\alpha\alpha'} + v_3 \tfrac{1}{2}\sigma^3_{\alpha\alpha'}\right) \,. \tag{6.2}$$

that we shall study in this chapter.

We argued in section 5.8 that the only effect of a diagonal scattering potential can be to cause a phase shift of the outgoing fields relative to the incident ones:

$$\overline{\psi}^\alpha_<(ix) = e^{-i(\phi_o + \alpha\phi_3)} \overline{\psi}^{\alpha'}_>(ix) \qquad \text{for } x < 0 \,. \tag{6.3}$$

However, we did not explain in section 5.8 how to calculate the phase shifts ϕ_o and ϕ_3 in terms of the parameters v_o and v_3. In this chapter we discuss three increasingly elaborate ways of doing this calculation [resulting in eqs. (6.38), (6.47)].

The main idea is the following: The scatterer at $x = 0$ can be thought to induce a specific *boundary condition* on the fermion fields at $x = 0$ (in a way to be made precise below). The simplest way to *characterize* this boundary condition is to analyze the *finite-size spectrum* of the theory, or equivalently, the

[1] Upper and lower indices, ψ_α and ψ^α, are used interchangeably in this thesis, and have the same meaning.

partition function. When the scattering interaction is switched on, the finite-size spectrum and the partition function are modified in a very particular way, from which one can deduce the resulting effective boundary condition on $\psi_\alpha(x)$ at $x = 0$, which indeed turns out to have the form of eq. (6.3).

The chapter is organized as follows. In section 6.1 we analyze the finite-size spectrum of a free theory: we separate spin and charge degrees of freedom by rewriting the Hamiltonian in a $U^{(c)}(1) \times U^{(s)}(1)$ Sugawara form. In section 6.2 we explain how the impurity term can be "absorbed" by making a shift in the $U(1)$ currents J_o and J_3. Section 6.3 shows how the fermion phase shift $\phi_o + \alpha\phi_3$ can be obtained from this shift in the $U(1)$ currents. In section 6.4 we tackle the real technicalities of boundary conformal field theory, and show how this phase shift can also be derived using Cardy's methods to calculate the Green's function G^{RL}. Finally, in section 6.5 we consider a special value of the coupling constant at which the full $U(1) \times SU(2)$ symmetry of the free problem reemerges, and discuss the consequences of this additional symmetry. A summary of the strategy followed in order to calculate the Green's function G^{RL} by Cardy's methods is given in section 6.6.

It will be assumed that the reader is familiar with the contents of appendix A for sections 6.1, appendix E for section 6.3, and appendix C (mainly section C.4.2) for sections 6.4 and 6.5. If this is not the case, at least a cursory glance through these appendices at this stage is highly recommended.

6.1 $U^{(c)}(1) \times U^{(s)}(1)$ Bosonization of Free Theory

In this section we recall some elementary facts of the abelian bosonization of two species of spinless, left-moving fermions (more details can be found in appendix A, sections A.6 and A.7).

There are two equivalent Abelian bosonization schemes possible, which we denote by $U^{\uparrow} \times U^{\downarrow}$ (up-down scheme) and $U^{(c)} \times U^{(s)}$ (charge-spin scheme). We have to use the latter scheme, since it is the one that is compatible with the symmetry of our interaction eq. (6.2). However, we start our discussion by stating some basic facts of the up-down scheme, since this allows a natural derivation of the so-called "gluing condition" [see eq. (6.19)] that is an essential ingredient in the charge-spin scheme.

First a comment about terminology: in the up-down scheme, we call the species index $\alpha = \uparrow, \downarrow$, "up-down" merely for convenience; our original electrons were spinless, and α originally indicated physical L- and R-movers. Similarly, in the charge-spin scheme, "spin" does not mean Pauli spin, but simply half the difference between the number of $\uparrow$ and $\downarrow$ electrons [see eq. (6.11)].

Throughout, we take all fields to be defined on a line $x \in [-l, l]$, with anti-periodic boundary conditions for the fermion fields:[2]

$$\psi^{\alpha}(il) = -\psi^{\alpha}(-il) \; . \tag{6.4}$$

Furthermore, we consider finite temperatures, $T \neq 0$, and hence work on the imaginary time-axis, $t = -i\tau$, $\tau \in [0, \beta]$, with $\psi^{\alpha}(0) = -\psi^{\alpha}(\beta)$.

[2] In appendix A, we take $x \in [0, l]$; therefore, remember to replace $l \to 2l$ when using formulas from the appendix A here.

In the up-down scheme, one introduces the currents $J^{\uparrow(\downarrow)}$ and their Fourier components through:

$$J^{\alpha}(ix) \equiv :\overline{\psi}^{\alpha\dagger}(ix)\overline{\psi}^{\alpha}(ix): \qquad (\alpha=\uparrow,\downarrow, \text{ not summed}) ; \tag{6.5}$$

$$J^{\alpha}_{m} \equiv \int_{-l}^{l}\tfrac{dx}{2\pi}e^{i\pi mx/l}J^{\alpha}(ix) . \tag{6.6}$$

In terms of these, the Hamiltonian takes the following Sugawara form [see eq. (A.53)]:

$$H_o = H^{\uparrow}+H^{\downarrow} = \int_{-l}^{l}\tfrac{dx}{2\pi}\ \tfrac{1}{2}\left[:J^{\uparrow}J^{\uparrow}:+:J^{\downarrow}J^{\downarrow}:\right] . \tag{6.7}$$

As shown in appendix A, the eigenstates of H_o can be arranged into direct products of $\uparrow$ and $\downarrow$ towers, labeled by $(Q^{\uparrow},Q^{\downarrow})$. All states in the $(Q^{\uparrow},Q^{\downarrow})$ tower by definition have the same number of α-electrons, namely Q_{α} $(\in Z)$ (the $T=0$ Fermi sea has $(Q^{\uparrow},Q^{\downarrow})=(0,0)$ by definition); in other words, all states in the tower satisfy

$$J^{\uparrow(\downarrow)}_{o}|Q^{\uparrow},d^{\uparrow};Q^{\downarrow},d^{\downarrow}\rangle_{\uparrow\downarrow} = Q^{\uparrow(\downarrow)}|Q^{\uparrow},d^{\uparrow};Q^{\downarrow},d^{\downarrow}\rangle_{\uparrow\downarrow} , \tag{6.8}$$

where $\{d^{\uparrow},d^{\downarrow}\}$ labels the states of an orthonormal basis in the tower.

The energy of a typical state in the $(Q^{\uparrow},Q^{\downarrow})$ tower has the form

$$E_{Q^{\uparrow}Q^{\downarrow}}-E_{00} = \tfrac{\pi}{l}\left[\left(\tfrac{1}{2}Q^{\uparrow 2}+m^{\uparrow}\right)+\left(\tfrac{1}{2}Q^{\downarrow 2}+m^{\downarrow}\right)\right] , (m^{\alpha}\in Z) . \tag{6.9}$$

The partition function in this basis has a particularly simple form (see section A.4):

$$Z_o = Tr\ e^{-\beta H_o} = \eta^{-2}(q)\sum_{Q^{\uparrow},Q_{\downarrow}\in Z} q^{\frac{1}{2}\left[Q^{\uparrow 2}+Q^{\downarrow 2}\right]} \qquad \text{where} \quad q\equiv e^{-\pi\beta/l} . \tag{6.10}$$

The sum over the charge towers is explicit; the sum over the excited states (descendants) in each tower has already been done and gives rise to the factor $\eta^{-1}\equiv q^{-1/24}\frac{1}{\prod_{n=1}^{\infty}(1-q^n)}$ per tower (see eq. (A.41)).

Now let us rewrite the above in terms of the charge and spin $[U^{(c)} \times U^{(s)}]$ currents J^o and J^3, defined as follows:

$$\begin{aligned} J^o(ix) &\equiv \tfrac{1}{2}\left(J^{\uparrow} + J^{\downarrow}\right) = \textstyle\sum_\alpha \tfrac{1}{2} : \overline{\psi}^{\alpha\dagger}(ix)\overline{\psi}^{\alpha}(ix) : ; \\ J^3(ix) &\equiv \tfrac{1}{2}\left(J^{\uparrow} - J^{\downarrow}\right) = \textstyle\sum_{\alpha\alpha'} \tfrac{1}{2} : \overline{\psi}^{\alpha\dagger}(ix)\sigma^3_{\alpha\alpha'}\overline{\psi}^{\alpha'}(ix) : \ . \end{aligned} \tag{6.11}$$

[Note that we have adopted a somewhat unconventional normalization for J^0 (usually the $\frac{1}{2}$ is omitted, see e.g. eq. (A.74), with N=2); this we do purely for the sake of notational convenience, since many of our formulas then are symmetrical under $0 \leftrightarrow 3$, and can be written in terms of an index $a = 0, 3$.] In terms of these currents, the Hamiltonian eq. (6.7) clearly becomes

$$H_o = H_o^o + H_o^3 = \int_{-l}^{l} \tfrac{dx}{2\pi} \left[: J^o J^o : + : J^3 J^3 : \right] \ . \tag{6.12}$$

The discussion of the spectrum of H_o that follows below parallels that of appendix A. However, there we bosonize according to the $U(1) \times SU(2)$ scheme, which means that there we work with *three* spin currents, J^a, $(a = 1, 2, 3)$, instead of just J^3. This means that the states in the spectrum are grouped together in a different way than below (into $U(1)$-charge and $SU(2)$-spin towers, instead of $U^{(c)} \times U^{(s)}$-towers). Nevertheless, the spectra are of course the same. This can be seen by comparing eqs. (A.81) to (A.83) (with $N = 2$) to eq. (6.12), and realizing that for $SU(2)$, $: J^1 J^1 := : J^2 J^2 := : J^3 J^3 :$ (as can be verified directly from eq. (A.78)).

The structure of the spectrum can be determined by studying the commutation relations of the Fourier components J^a_m and L^a_m of $J^a(ix)$ and $: J^a J^a : (ix)$ ($a, b = 0, 3$ in all subsequent formulas):

$$J^a(ix) \equiv \tfrac{\pi}{l} \sum_{m \in Z} e^{-i\pi m x/l} J^a_m \ ; \qquad J^a_m \equiv \int_{-l}^{l} \tfrac{dx}{2\pi} e^{i\pi m x/l} J^a(ix) \ ; \tag{6.13}$$

$$\tfrac{\pi}{l} L^a_m \equiv \int_{-l}^{l} \tfrac{dx}{2\pi} e^{i\pi m x/l} \left[: J^a J^a : (ix) + \left(\tfrac{\pi}{l}\right)^2 \tfrac{c_a}{24} \right] \;=\; \tfrac{\pi}{l} \sum_{n\in Z} {}^{*}_{*} J^a_n J^a_{m-n*}{}^{*} \,. \qquad (6.14)$$

[Here c_a is the central charge, with the usual value $c_a = 1$ for each bosonic current.] In terms of these, the Hamiltonians H^a_o are

$$H^a_o \equiv \tfrac{\pi}{l}\left[-\tfrac{c_a}{24} + L_o\right] = \tfrac{\pi}{l}\left[-\tfrac{c_a}{24} + \sum_{n\in Z} {}^{*}_{*} J^a_n J^a_{-n*}{}^{*}\right] , \qquad (\text{for } a = 0, 3) \,, \qquad (6.15)$$

and the following commutation relations, which we list for future reference, hold:[3]

$$\begin{aligned} [L^a_n, L^b_m] &= \left[(n-m)L^a_{n+m} + \tfrac{c_a}{12}(n^3 - n)\delta_{n+m,0}\right]\delta_{ab} \,; \\ [L^a_n, J^b_m] &= -m J^a{}_{n+m}\delta_{ab} \,; \\ [J^a_n, J^b_m] &= \tfrac{1}{2} n \delta_{n+m,0}\delta_{ab} \,. \end{aligned} \qquad (6.16)$$

From these one can deduce (see appendix A, page 298) that the spectrum is organized into direct products of "charge" and "spin" towers, labeled by charge and spin quantum numbers (Q_0, Q_3). These are half the total number of electrons in the tower and half the difference between them, since [by eq. (6.11)] they are related to $(Q^\uparrow, Q^\downarrow)$ through

$$Q_o \equiv \tfrac{1}{2}(Q^\uparrow + Q^\downarrow) \equiv c_o + s_o \,, \qquad Q_3 \equiv \tfrac{1}{2}(Q^\uparrow - Q^\downarrow) \equiv c_3 + s_3 \,, \qquad (6.17)$$

$$\text{where} \qquad Q_a \in Z/2, \qquad s_a \in Z \,, \qquad c_a = 0, \tfrac{1}{2} \,. \qquad (6.18)$$

Note that we wrote Q_a in terms of an integer part s_a and a "remainder", $c_a = 0, \frac{1}{2}$. Since $Q^\uparrow$ and $Q^\downarrow$ are integers, it follows immediately that $c_0 = c_3$. This relation is formalized by introducing a set of numbers, $\{n_0^{c_o c_3}\}$, known as the *gluing condition,* that are either zero or one, and given here simply by

$$n_o^{c_o c_3} = \delta_{c_o c_3} \,. \qquad (6.19)$$

[3] For $a = 3$, they can be found from eq. (A.89), with $a = b = 3$; those for $a = 0$ are identical to those for $a = 3$.

The gluing condition specifies which combination of charge and spin towers can occur together in a free-fermion theory. The need for such a condition arises, formally, because our Hilbert space is a direct product of charge and spin subspaces, and thus also contains unphysical states [e.g. pure "chargons" or "spinons", for which $(Q_o, Q_3) = (\frac{1}{2}, 0)$ or $(0, \frac{1}{2})$]. These are unphysical, since adding or removing one electron always changes *both* Q_o and Q_3 by $\frac{1}{2}$, and the $T = 0$ Fermi sea has $(Q_o, Q_3) = (0, 0)$. Any physical (i.e. free-fermion) state must always have $c_0 = c_3$, and the gluing condition formalizes this requirement.

All states in the (Q_o, Q_3)-th tower satisfy

$$J_o^a |Q_o, d_o; Q_3, d_3\rangle_{03} = Q_a |Q_o, d_0; Q_3, d_3\rangle_{03} \ , \tag{6.20}$$

and [from eq. (6.15)] the energy of a typical such state is

$$E_{Q_0 Q_3} - E_{00} = \tfrac{\pi}{l} \left[(Q_0^2 + m_o) \ + \ (Q_3^2 + m_3) \right] \ , \qquad (m_a \in Z) \ . \tag{6.21}$$

When calculating the partition function in this basis, one has to be careful to take the trace only over physical states allowed by the gluing condition:

$$\begin{aligned} Z_o &= \sum_{Q_o, Q_3 \in Z/2} \sum_{\{d_o, d_3\}} n_o^{c_o c_3} \langle Q_o, d_o; Q_3, d_3 | e^{-\beta \left[H_o^o + H_o^3 \right]} | Q_o, d_o; Q_3, d_3 \rangle & (6.22) \\ &= \eta^{-2}(q) \sum_{Q_o, Q_3 \in Z/2} n_o^{c_o c_3} q^{\left[Q_o^2 + Q_3^2 \right]} & (6.23) \end{aligned}$$

Eq. (6.22) also follows directly from eq. (6.10) by just redoing the sum on $(Q^\uparrow, Q^\downarrow)$ in terms of (Q_0, Q_3).

6.2 Absorbing the Interaction

Let us now turn on the scattering term of eq. (5.67) (our discussion will follow that of Callan *et al.* [CKLM94, section 4]). As a result of our judicious choice of

the charge-spin bosonization scheme, it has an extremely simple form in terms of the $U^{(c)}(1) \times U^{(s)}(1)$ currents:[4]

$$H_{\rm scat} \equiv H^o_{\rm scat} + H^3_{\rm scat} = v_o J^o(0) + v_3 J^3(0) \; , \tag{6.24}$$

$$= \tfrac{\pi}{l} \sum_m \left[v_o J^o_m + v_3 J^3_m \right] \; . \tag{6.25}$$

Next, note that one can formally absorb the scattering terms by simply "completing the square": Let us introduce new currents,

$$\mathcal{J}^a(ix) \equiv J^a(ix) + \tfrac{1}{2} v_a 2\pi\delta(x) \; ; \tag{6.26}$$

$$\mathcal{J}^a_m \equiv \int_{-l}^{l} \tfrac{dx}{2\pi} e^{i\pi m x/l} \mathcal{J}^a(ix) = J^a_m + \tfrac{1}{2} v_a \; . \tag{6.27}$$

In terms of these the *full* Hamiltonian has the same form as a free Hamiltonian [compare with eq. (6.15)]:

$$\begin{aligned} H^a \equiv H^a_o + H^a_{\rm scat} &= \textstyle\int_{-l}^{l} \frac{dx}{2\pi} : \mathcal{J}^a \mathcal{J}^a : (ix) \; ; \\ &= \tfrac{\pi}{l} \left[-\tfrac{c_a}{24} + \textstyle\sum_{n \in Z} {}^*_* \mathcal{J}^a_n \mathcal{J}^a_{-n} {}^*_* \right] \; . \end{aligned} \tag{6.28}$$

The impurity has "disappeared", or been "absorbed".

Now, we know from eq. (5.53) that in the presence of a scatterer, the fields $\overline{\psi}^\alpha(ix)$ and hence the old currents $J^a(ix)$ are non-analytic at the origin: $J^a_<(\tau, i0^-) \neq J^a_>(\tau, i0^+)$. In contrast, the new $\mathcal{J}^a(ix)$'s are analytic at $x = 0$:

$$\mathcal{J}^a_<(\tau + i0^-) = \mathcal{J}^a_>(\tau + i0^+) \; . \tag{6.29}$$

The reason is simply that the full Hamiltonian H^a looks like a free Hamiltonian when expressed in terms of $\mathcal{J}^a$'s. This implies immediately (e.g. from Heisen-

[4] There are some subtleties involved in writing down eq. (6.24): Since we know from eq. (5.46) that the presence of a scatterer causes discontinuities in the fermion fields at $x = 0$, we have to define what is meant by $\overline{\psi}_\alpha(x = 0)$. This issue was discussed by Polchinsky and Thorlacius [PT94, sec.3], who argued that the prescription $\psi^\alpha(0) \equiv \frac{1}{2}\left(\psi^\alpha(0^-) + \psi^\alpha(0^+)\right)$ is equivalent to using eq. (6.24).

berg equations of motion) that the $\mathcal{J}^a$'s will behave like *free* currents, which are analytic functions of $\tau + ix$ for all τ and x.

Since the $\mathcal{J}^a$'s behave like free currents, it is straightforward to analyze the spectrum of the full H: introduce the Fourier components $\mathcal{L}^a_m$ of $:\mathcal{J}^a\mathcal{J}^a:$ in analogy with eq. (6.14), then it follows immediately that the $\mathcal{L}^a_m$ and $\mathcal{J}^a_n$'s obey commutation relations that are identical to those of the the original L^a_m and J^a_n's (for a free theory), namely eq. (6.16). Hence, the structure of the spectrum (i.e. the organization into towers, and the spacing and degeneracy of energy levels within the towers) must also be identical to that of a free theory. (This is a strong statement, and illustrates the power of the algebraic approach!) The only but crucial difference is in the allowed values of the $U(1)$ charges (i.e. eigenvalues of $\mathcal{J}^a_0$): from eq. (6.20) and eq. (6.27) we conclude that

$$\mathcal{J}^a_o|Q_o;Q_3\rangle_{03} = (Q_a + \tfrac{1}{2}v_a)|Q_o;Q_3\rangle_{03}\ . \tag{6.30}$$

Hence, the scatterer shifts the allowed charges: $Q_a \to Q_a + \frac{1}{2}v_a$.

This is its only effect on the spectrum. Since the level spacings and degeneracies in each tower remain unaffected, it follows immediately from eq. (6.23) that the partition function in the presence of a scatterer is:

$$Z = \eta^{-2}(q) \sum_{Q_o,Q_3\in Z/2} n_o^{c_o c_3}\ \ q^{\left[\left(Q_o+\frac{1}{2}v_o\right)^2+\left(Q_3+\frac{1}{2}v_3\right)^2\right]}\ . \tag{6.31}$$

A beautifully simple result!

The shift in the currents thus allows us to find the spectrum and partition function very straightforwardly. In the next two sections, we show how it also gives the fermion phase shifts $\phi_0 + \alpha\phi_3$.

Before addressing that issue, however, one more comment on our bosonization approach is in order. Strictly speaking, the Sugawara form eq. (6.12), which for

free fields is an identity, has to be modified as soon as one switches on an interaction: an additional term, which we denote by δH_o, should occur on the right-hand side of eq. (6.12). To understand this statement, recall [from appendix A] that the Sugawara form was derived using the point-splitting prescription

$$: A(u)B(u) : \equiv \lim_{\delta \to 0} \left[A(u+\delta)B(u) - \langle A(u+\delta)B(u) \rangle \right] , \tag{6.32}$$

which requires one to subtract off point-split expectation values. However, these are strictly speaking expectation values of the fully interacting fields, not the free fields, if one considers the interaction turned on. In particular, the result $\lim_{\delta \to 0} \langle \psi^{\alpha\dagger}(\tau, x+\delta)\psi^{\alpha}(\tau, x) \rangle = \frac{\delta_{\alpha\alpha'}}{i\delta}$, needed to derive equations like (6.12) [e.g., see derivation of eq. (A.83)], holds only for *free* fields. Using the results of section 5.8, in particular eq. (6.3), it can easily be shown that additional contributions to this expectation value arise when one evaluates it in the presence of an interaction, though these extra terms are non-singular in δ [i.e. $O(1)$ or $O(\delta)$].

The extra terms $\delta \widehat{H}_o$ can be calculated explicitly in this way; however, we shall here follow the usual practice of neglecting them, with the argument that they represent irrelevant terms (in the renormalization group sense) that vanish as $T \to 0$. Nevertheless, it is worth noting that in the presence of a voltage, such terms can also depend on V, since then the subtracted $\langle A(u+\delta)B(u) \rangle$ in eq. (6.32) can be V-dependent.

6.3 Phase Shift via Bosonization of Fermion Fields

The simplest way to find the fermion phase shift $\phi_0 + \alpha\phi_3$ of eq. (6.3) is to express the fermion fields in terms of two boson fields, X^0 and X^3, using the standard

bosonization formula [see eq. (E.25) for notational details]:

$$\overline{\psi}^{\alpha}(ix) = a_{\alpha} :e^{-i\frac{1}{\sqrt{2}}[X^{o}(ix)+\alpha X^{3}(ix)]}: \ . \tag{6.33}$$

In terms of the X^a's, the currents take the form

$$\begin{aligned}
J^{o}(ix) &\equiv \sum_{\alpha} \tfrac{1}{2} :\overline{\psi}^{\alpha\dagger}(ix)\overline{\psi}^{\alpha}(ix): &&= \tfrac{1}{\sqrt{2}} :\partial_x X^{o}(ix): ; \\
J^{1}(ix) &\equiv \sum_{\alpha\alpha'} :\overline{\psi}^{\alpha\dagger}(ix)\tfrac{1}{2}\sigma^{2}_{\alpha\alpha'}\overline{\psi}^{\alpha'}(ix): &&= a_3 :\sin\sqrt{2}X^{3}(ix): ; \\
J^{2}(ix) &\equiv \sum_{\alpha\alpha'} :\overline{\psi}^{\alpha\dagger}(ix)\tfrac{1}{2}\sigma^{2}_{\alpha\alpha'}\overline{\psi}^{\alpha'}(ix): &&= -a_3 :\cos\sqrt{2}X^{3}(ix): ; \\
J^{3}(ix) &\equiv \sum_{\alpha\alpha'} :\overline{\psi}^{\alpha\dagger}(ix)\tfrac{1}{2}\sigma^{3}_{\alpha\alpha'}\overline{\psi}^{\alpha'}(ix): &&= \tfrac{1}{\sqrt{2}} :\partial_x X^{3}(ix): \ .
\end{aligned} \tag{6.34}$$

For future reference, we have also displayed the off-diagonal currents J^1 and J^2 that we have not needed so far. [The three currents J^1, J^2 and J^3 are called $SU(2)$ currents, since they are the Nöther currents for the $SU(2)$ spin symmetry of the free theory.] Similarly, the new currents $\mathcal{J}^a$ can be represented as

$$\mathcal{J}^{a}(ix) \equiv \tfrac{1}{\sqrt{2}}\partial_x \mathcal{X}^{a}(ix) \ , \qquad (\text{for } a = 0, 3) \ , \tag{6.35}$$

where $\mathcal{X}^a$ are boson fields that are analytic at $x = 0$, $\mathcal{X}^{a}_{<}(\tau + i0^-) = \mathcal{X}^{a}_{>}(\tau + i0^+)$ [since the $\mathcal{J}^a$'s are analytic at $x = 0$, recall eq. (6.29)].

Now insert eqs. (6.35) and (6.34) into eq. (6.26), and integrate, with boundary condition $\mathcal{J}^a(ix) = J^{a}_{<}(ix)$ for $x > 0$ [since the incident part of the new current should not differ from the old one; compare the $\theta(x)$ term in eq. (5.46)]. This gives the following relation between X^a and $\mathcal{X}^a$:

$$X^{a}(ix) = \mathcal{X}^{a}(ix) + v_a \pi\sqrt{2}\,\theta(-x) \ , \qquad \text{for all } x \ , \tag{6.36}$$

and in particular

$$X^{a}_{<}(ix) = \mathcal{X}^{a}(ix) + v_a\pi\sqrt{2} = X^{a}_{>}(ix) + v_a\pi\sqrt{2} \ , \qquad \text{for } x < 0 \ . \tag{6.37}$$

Inserting eq. (6.37) into eq. (6.33) then gives

$$\overline{\psi}^{\alpha}_{<}(ix) =: e^{-i\frac{1}{\sqrt{2}}[X^{o}_{<}(ix)+\alpha X^{3}_{<}(ix)]} : = e^{-i\pi(v_o+\alpha v_3)}\overline{\psi}^{\alpha}_{>}(ix) \tag{6.38}$$

from which we read off the desired phase shift in eq. (6.3), namely $\phi_0 + \alpha\phi_3 = \pi(v_o + \alpha v_3)$.

For future reference, note also that eq. (6.37), inserted into eq. (6.34), gives

$$\begin{aligned}
J^{o}_{<}(ix) &= \tfrac{1}{\sqrt{2}} :\partial_x X^{o}_{>}(ix): &&= J^{o}_{>}(ix)\ , \\
J^{1}_{<}(ix) &= a_3 :\sin\left(\sqrt{2}X^{3}_{>}(ix) + 2\pi v_3\right): &&\neq J^{1}_{>}(ix)\ , \\
J^{2}_{<}(ix) &= -a_3 :\cos\left(\sqrt{2}X^{3}_{>}(ix) + 2\pi v_3\right): &&\neq J^{2}_{>}(ix)\ , \\
J^{3}_{<}(ix) &= \tfrac{1}{\sqrt{2}} :\partial_x X^{3}_{>}(ix): &&= J^{3}_{>}(ix)
\end{aligned} \tag{6.39}$$

These relations reflect the fact that the interaction breaks the $U(1)\times SU(2)$ Kac-Moody symmetry of the bulk theory down to $U^{(c)}(1) \times U^{(s)}(1)$: we find that the L, R components of the SU(2) currents J^1 and J^2 are *unequal* at the boundary ($x = 0$), $J^{a}_{>}(i0^+) \neq J^{a}_{<}(i0^-)$ for $a = 1, 2$; in the language of appendix C [see eq. (C.2)] this implies that the boundary is not $SU(2)$ invariant. However, the boundary *is* $U^{(c)}(1) \times U^{(s)}(1)$ invariant (since $J^{a}_{>}(\tau + i0^+) = J^{a}_{<}(\tau + i0^-)$ for $a = 0, 3$); of course, we knew this all along, since the boundary term does not break the $U^{(c)}(1) \times U^{(s)}(1)$ symmetry.

6.4 Phase Shift via Boundary States

In section 6.3 we found the fermion phase shift directly by exploiting a bosonized representation for the fermion fields. Unfortunately, this simple procedure does not work for the Kondo problem. Hence we shall now rederive it by using the techniques of boundary conformal field theory due to Cardy [Car84a, Car84b,

Car86a,Car86a,Car87,Car89,CL91] to calculate the Green's function G^{RL}. These are the techniques used by Affleck and Ludwig in solving the Kondo problem. We shall attempt to outline the essential ingredients of their approach by treating the present simple problem in considerable detail. Our presentation is modeled on that given by Affleck and Ludwig in appendix F of [AL94], and also draws on [CKLM94]. The general strategy is summarized section 6.6, which might be worth a glance before proceeding.

Before delving into details, we begin by summarizing some essential ingredients of Cardy's approach. (More details on the general philosophy of Cardy's approach, and some of the technicalities, can be found in appendix C.)

To cast our theory in the form of a boundary conformal theory, we shall henceforth adopt Cardy's terminology. Write

$$u \equiv \tau + ix \equiv \begin{cases} z \equiv \tau + ir & \text{for } x > 0 \ , \\ \bar{z} \equiv \tau - ir & \text{for } x < 0 \ , \end{cases} \tag{6.40}$$

where $r \equiv |x|$. Then define [comparing with eq. (5.53)]:

$$\begin{aligned} \overline{\psi}^{\alpha}(\tau + ix) &\equiv \overline{\psi}^{\alpha}_{\gtrless}(\tau + ix) \equiv \overline{\psi}^{\alpha}_{L/R}(\tau \pm ir) \qquad \text{for } x \equiv \pm r \gtrless 0 \ . \\ J^{a}(\tau + ix) &\equiv J^{a}_{\gtrless}(\tau + ix) \equiv J^{a}_{L/R}(\tau \pm ir) \qquad \text{for } x \equiv \pm r \gtrless 0 \ . \end{aligned} \tag{6.41}$$

The incident and outgoing fields and currents are henceforth to be called left- and right-movers, respectively.[5] Since $0 < r < l$, all fields are defined on a strip of width l in the upper half of the $\tau + ir$ plane, with $\overline{\psi}^{\alpha}_{L}(z)$ depending on $z \equiv \tau + ir$ and $\overline{\psi}^{\alpha}_{R}(\bar{z})$ on $\bar{z} = \tau - ir$. At zero temperature, the length of the strip is infinite, $\tau \in [-\infty, \infty]$. At finite temperatures (the case were are interested in),

[5] As explained in section 5.7, these are "mathematical" L- and R-movers, not to be confused with physical L- and R-movers, which are distinguished from each other by a separate index (e.g. α_η in chapter 5.)

the fermion fields are anti-periodic on an interval $\tau \in [0, \beta]$, which means that this strip gets bent around into a cylinder of circumference β [see Fig. 6.1].

The boundary conditions on these fields at $r = 0$ and l are as follows: In eq. (6.4), we agreed to take anti-periodic boundary conditions on the fermion fields at $x = \pm l$, which translates into $\psi_L^\alpha(\tau + il) = -\psi_R^\alpha(\tau - il)$. This will be called the "free boundary condition at $r = l$", and denoted by F_- (the subscript – denotes anti-periodicity). In the absence of any scattering terms, we know that $\psi_>^\alpha(\tau + i0^+) = \psi_<^\alpha(\tau - i0^+)$, i.e. $\psi_L^\alpha(\tau) = \psi_R^\alpha(\tau)$. This is called the "free boundary condition at $r = 0$", and denoted by F. However, in the presence of a scatterer at $r = 0$ the behavior of $\psi_<^\alpha = \psi_R^\alpha$ gets modified (by a phase shift, as we happen to know). This is formalized by saying that the boundary interaction induces a new $r = 0$ boundary condition, denoted by B, on the fields.

To summarize, the basic geometry on which our fields live is that of a cylinder of circumference β and length l, with boundary conditions F_-F (for free fields) or F_-B (with scatterer) at $r = l$ and $r = 0$, respectively (see Fig. 6.1, taken from [AL94, App. F]).

Cardy's approach requires all boundary conditions to be conformally invariant under conformal transformations that "leave the boundary invariant" (i.e. map the boundary onto itself [Car84b]). In the present case, we know that the scattering term also has a $U^{(c)}(1) \times U^{(s)}(1)$ symmetry (a so-called Kac-Moody (KM) symmetry), which means that both boundaries are KM invariant (see eqs. (6.69) and (6.70) for the mathematical expression of this fact).

We are interested in the two-point functions of the fermion fields $\overline{\psi}_{L/R}^\alpha$ and currents $J_{L/R}^a$. These are examples of so-called chiral primary fields of scaling

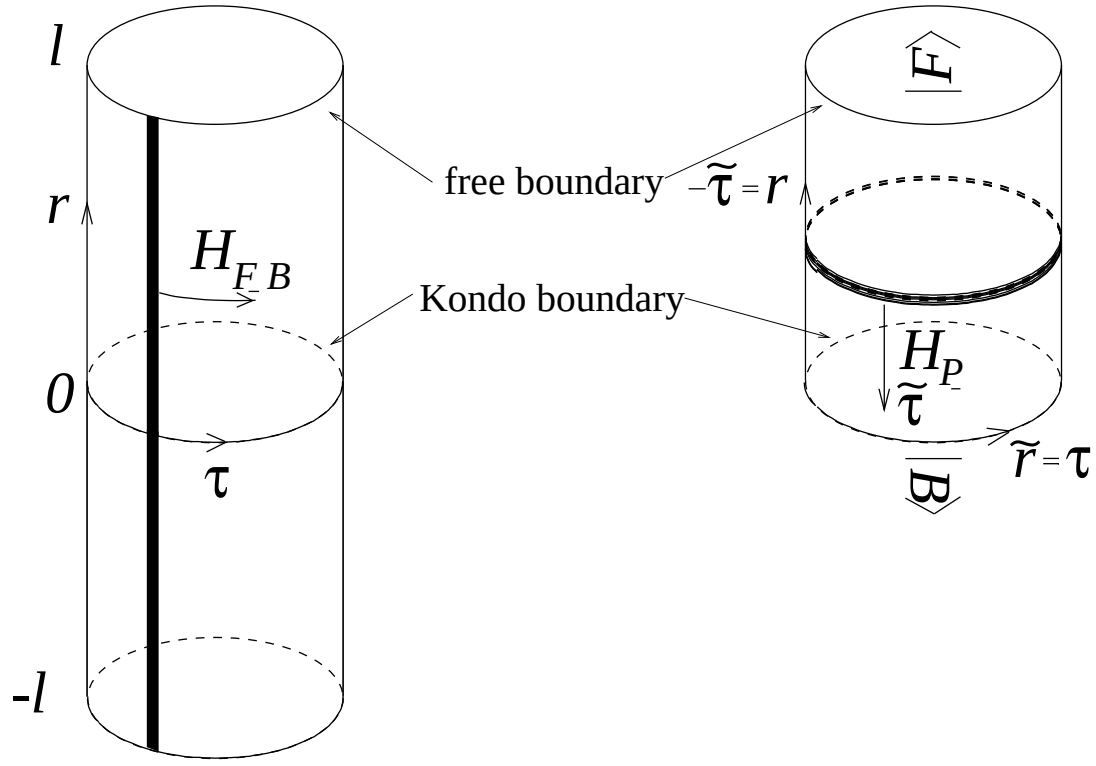

Figure 6.1 The partition function Z on a cylinder of circumference β and length l, with Kac-Moody invariant boundary conditions B and F_- at $r = 0$ and l respectively, can be written in two different ways: 1) Using the Hamiltonian H_{F_-B} generating translations in the τ-direction; 2) After relabeling space and time coordinates as in eq. (6.62), using the Hamiltonian H_P, generating translations in the $\tilde{\tau} = -r$ direction. The equivalence of the two descriptions leads to the Cardy formula, eq. (6.74).

dimension $\frac{1}{2}$ and 1 respectively (chiral, since they only depend on z or $\overline{z}$; see appendix B for questions of CFT terminology). Cardy has shown [Car84b, section 4], [CL91] that for the present geometry, the two-point functions of any chiral primary operator O_i with scaling dimension x_i have the following for at $T = 0$:[6]

$$-G_i^{LL}(z_1, z_2) = \langle O_{iL}(z_1) O_{iL}^\dagger(z_2) \rangle_{\text{bound}} = \frac{1}{(z_1 - z_2)^{2x}} ; \tag{6.42}$$

$$-G_i^{RR}(\bar{z}_1, \bar{z}_2) = \langle O_{iR}(\bar{z}_1) O_{iR}^\dagger(\bar{z}_2) \rangle_{\text{bound}} = \frac{1}{(\bar{z}_1 - \bar{z}_2)^{2x}} ; \tag{6.43}$$

$$-G_i^{RL}(\bar{z}_1, z_2) = \langle O_{iR}(\bar{z}_1) O_{iL}^\dagger(z_2) \rangle_{\text{bound}} = \frac{\tilde{U}_B(O_i)}{(\bar{z}_1 - z_2)^{2x}} . \tag{6.44}$$

Note that the L-L and R-R Green's functions are exactly the same as for a free theory; note in particular that they are translationally invariant (depending only on $r_1 - r_2$). Therefore, their amplitudes are fixed by the requirement that they coincide with the bulk normalization, which is set to = 1 (this is because when one takes the limit $r_1 \to \infty, r_2 \to \infty$ at fixed $r_1 - r_2$, one has to recover free Green's functions, because the effects of the boundary cannot extend to ∞ [AL94, p.556]).

The G_i^{RL} Green's function, on the other hand, depends on $r_1 + r_2$ and hence is not translationally invariant. Its amplitude $\tilde{U}_B(O_i)$ depends on the particular boundary interaction (or boundary condition). Cardy has shown [Car89] that to each boundary condition B allowed by conformal symmetry, one can associate a boundary state $|B\rangle$ in the Hilbert space of the bulk Hamiltonian (called the "closed-string" Hilbert space in the present context, as explained below). Similarly, to each primary operator O_i can be assigned a state $|O_i\rangle$ in the same Hilbert

[6]These Green's functions are defined in the so-called "closed string" picture, a concept introduced and explained below. It is sufficient to calculate them at $T = 0$, because the $T \neq 0$ form can be obtained from that at $T = 0$ by a straightforward conformal transformation, described in section 8.1.

space. Using conformal mappings, it can be shown [CL91, eq.(6)] that the amplitude $\tilde{U}_{_B}(O_i)$ in eq. (6.44) is given simply by the following ratio of "boundary matrix elements":

$$\tilde{U}_{_B}(O_i) = \langle O_i|B\rangle / \langle \mathbf{1}\ |B\rangle\ , \tag{6.45}$$

Here $\mathbf{1}$ denotes the identity operator.

Our aim in this section is to calculate $\tilde{U}_{_B}(O_i)$ for the fermion fields and currents. We shall find [see eq. (6.77)] the result

$$\tilde{U}_{_B}(\overline{\psi}^{\alpha}) = e^{i\pi(v_0+\alpha v_3)}\,; \qquad \tilde{U}_{_B}(J^{\pm}) = e^{\pm i2\pi v_3}\ ; \qquad \tilde{U}_{_B}(J^3) = 1\ , \tag{6.46}$$

where $J^{\pm} \equiv J^1 \pm iJ^2$. Inserted into eq. (6.44) and recalling definition (6.41), this is in agreement with eq. (6.38) for the fermion fields, and eqs. (6.39) for the currents. In particular

$$-G^{RL}_{\alpha\alpha'}(\bar{z}_1, z_2) \equiv \langle \psi^{\alpha}_{_R}(\bar{z}_1)\psi^{\alpha'\dagger}_{_L}(z_2)\rangle = \frac{e^{i\pi(v_0+\alpha v_3)}\delta^{\alpha\alpha'}}{(\bar{z}_1 - z_2)}\ . \tag{6.47}$$

This illustrates how the desired phase shifts can be obtained from knowledge of the boundary state $|B\rangle$, and hence G^{RL}.

What is this boundary state? Cardy pointed out [Car86a] that in 2-D conformal field theories it should be possible to calculate the partition function in two equivalent ways. The first is just the standard one, namely:

$$Z \equiv \mathrm{Tr} e^{-\beta H_{F_-B}} \tag{6.48}$$

Here H_{F_-B} is the usual Hamiltonian that generates translations in the τ-direction; the subscripts remind us of the fact that this Hamiltonian "knows" about the boundary conditions F_- and B, since it is an integral (indicated by a heavy line

in fig. 6.1) of the Hamiltonian densities $\mathcal{H}_L$ and $\mathcal{H}_R$ from $r = 0$ (*on* the boundary) to l:

$$H_{F\_B} = \int_0^l \tfrac{dr}{2\pi} \left[\mathcal{H}_L(\tau + ir) + \mathcal{H}_R(\tau - ir)\right] \qquad \text{(independent of } \tau\text{)} \; . \tag{6.49}$$

The Hilbert space on which H_{F_B} acts is called the *open string* Hilbert space by string theorists, because the boundary conditions on the fields at $r = 0$ and $r = l$ are not simply periodic or anti-periodic.

We have already calculated the partition function of eq. (6.48) explicitly, including the effects of the interaction, in section 6.2, eq. (6.31).

The second way of calculating Z exploits the fact that for a "Lorentz"-invariant theory (i.e. one with linear dispersion, where all fields depend only on $\tau \pm ix$), one can exchange the role of space and time [see eq. (6.62)], and quantize all operators along lines of constant r in the $\tau + ir$ plane, called the *closed string picture,* instead of the usual way of quantizing along lines of constant τ (the open string picture). Thus, one can also calculate the partition in the closed string picture by making the following Ansatz:

$$Z \equiv \langle F_- | e^{-l\tilde{H}_{P-}} | B \rangle \; . \tag{6.50}$$

Here $\tilde{H}_{P\_}$ is a purely bulk Hamiltonian, that generates translations in the *space* direction [see eq. (6.64)]:

$$\tilde{H}_{P\_} = \int_0^\beta \tfrac{d\tau}{2\pi} \left[\mathcal{H}_{oL}(\tau + ir) + \mathcal{H}_{oR}(\tau - ir)\right] \qquad \text{(independent of } \tau\text{)} \; . \tag{6.51}$$

The Hilbert space upon which $\tilde{H}_{P\_}$ acts is called the closed string Hilbert space (and is different from the open string Hilbert space on which H_{F_B} acts, as explained below). The bulk fermion fields have anti-periodic boundary conditions

between $\tau = 0, \beta$, hence the subscript P_- (this is also the reason for the nomenclature "closed" string picture).

Note that since $\tilde{H}_{P_-}$ is an integral of the free Hamiltonian densities $\mathcal{H}_{oL}$ and $\mathcal{H}_{oR}$ from $\tau = 0$ to $\tau = \beta$ for arbitrary $r(\neq 0)$, it cannot "know" *anything* about what happens at the boundaries at $r = 0, l$ (see fig. 6.1). This is the chief advantage of the open string picture: *there is no impurity term in the Hamiltonian.* Instead, one may think of the impurity as having been "integrated out",[7] and information about the effects of the impurity, i.e. about the boundary condition B, is encoded in the so-called *boundary state* $|B\rangle$. Similarly, $|F_-\rangle$ is a boundary state that encodes the trivial boundary condition eq. (6.4) at $r = l$. $|B\rangle$ and $|F_-\rangle$ are basically infinite sums [to mimic a trace, see eq. (6.71)] over all states in the closed string Hilbert space on which $\tilde{H}_{P_-}$ acts, with coefficients determined by the requirement that the two ways of calculating the partition function give the same result. The detailed properties of $|F_-\rangle$ and $|B\rangle$ will become clear in the course of the calculation (see also appendix C).

Loosely speaking, $|B\rangle$ ($|F_-\rangle$) determines how L- (R-) moving fields, incident on the boundary at $r = 0$ ($r = l$), are reflected into R- (L-) moving fields. Whereas the reflection at $r = l$ is trivial, merely representing the trivial boundary condition eq. (6.4), the reflection at $r = 0$ can be decidedly non-trivial, because it represents the effect of the boundary interaction on the fermions (see the discussion after eq. (6.71) for a "physical" interpretation of $|B\rangle$).

Let us now get down to business and go through the required calculation.

[7] The phrase "integrating out the impurity" is borrowed here from the Kondo problem, where the impurity is a dynamic degree of freedom that indeed has to be integrated out. For a static (i.e. non-dynamic) impurity one does not really need to integrate out anything, and we use this phrase here merely to indicate that $\tilde{H}_{P_-}$ does not contain an explicit $\tilde{H}_{scat}$ term.

It turns out that we actually need the *extended* ("grand-canonical") partition function,[8] defined by

$$Z(\theta_0,\theta_3) \equiv \tag{6.52}$$

$$\sum_{Q_o,Q_3\in Z/2} n_o^{c_o c_3} \sum_{\{d_o,d_3\}} \langle Q_o,d_o;Q_3,d_3| \prod_{a=0,3} e^{-\beta\left[H_o^a+H_{\rm scat}^a-\theta_a(J_o^a+\frac{1}{2}v_a)\right]} |Q_o,d_o;Q_3,d_3\rangle$$

$$= \eta^{-2}(q) \sum_{Q_o,Q_3\in Z/2} n_o^{c_o c_3} \prod_{a=0,3} \left[q^{(Q_a+\frac{1}{2}v_a)^2} e^{\beta\theta_a(Q_a+\frac{1}{2}v_a)}\right] , \tag{6.53}$$

where $q \equiv e^{-\pi\beta/l}$. Here we have introduced extra "fugacities" (θ_o,θ_3), keeping track of constants of the motion other than the energy. The second equality was obtained by analogy with eq. (6.31), and using eq. (6.20) for the fugacity terms.

Now, the boundary-state expression for Z, eq. (6.50), which needs to be compared to eq. (6.53), is expressed in terms of $\tilde{q}$. Therefore, it is necessary to rewrite eq. (6.53) in terms of the parameter $\tilde{q} \equiv e^{4\pi l/\beta}$ instead of $q = e^{-\pi\beta/l}$. To do this, proceed as follows:

It is useful to break up the double summation in eq. (6.53), which is constrained by the gluing condition $n_o^{c_o c_3}$, by writing $\sum_{Q_a\in Z/2} = \sum_{c_a=0,\frac{1}{2}} \sum_{s_a\in Z}$. Then eq. (6.53) becomes:

$$Z(\theta_0,\theta_3) = \sum_{c_o,c_3=0,\frac{1}{2}} n_o^{c_o c_3} \sum_{s_o,s_3\in Z} \prod_{a=0,3} \left[\frac{q^{(c_a+s_a)^2} e^{\beta(\theta_a-\pi v_a/l)(c_a+s_a)}}{\eta^2(q)} e^{-\frac{\pi\beta}{l}(v_a^2/4-\theta_a v_a l/2\pi)} \right] . \tag{6.54}$$

The $\sum_{s_a\in Z}$ sums can be written in terms of so-called non-specialized $U(1)$ characters, defined by

$$\chi_{2c}^{(c)}(q,y) \equiv \eta^{-1}(q) \sum_{s\in Z} q^{(c+s)^2} e^{2y(c+s)} , \qquad c = 0, \tfrac{1}{2} . \tag{6.55}$$

[8] One needs to use the extended partition function whenever the spectrum is "degenerate" (i.e. there are different primary states with the same energy), because the characters of degenerate primary states are not linearly independent [see page 177].

These are basically extended partition functions, but constrained to one of the two allowed values of $c = 0, \frac{1}{2}$. Using $y = \frac{1}{2}\beta(\theta_a - \pi v_a/l)$, we thus get

$$Z(\theta_0, \theta_3) = \sum_{c_o, c_3 = 0, \frac{1}{2}} n_o^{c_o c_3} \prod_{a=0,3} \left[e^{-\frac{\pi\beta}{l}(v_a^2/4 - \theta_a v_a l/2\pi)} \ \chi^{(c)}_{2c_a}\left(q, \tfrac{1}{2}\beta(\theta_a - \pi v_a/l)\right)\right] \qquad (6.56)$$

Now, the $U(1)$ characters have the following useful mathematical property, known as a *modular transformation*, when rewritten in terms of $\tilde{q}$:

$$\chi^{(c)}_{2c}(q, y) \ = \ \tilde{q}^{-\left(\frac{y}{2\pi}\right)^2} \sum_{\tilde{c}=0,\frac{1}{2}} S^{(c)}_{c\tilde{c}} \ \chi^{(c)}_{2\tilde{c}}(\tilde{q}, -i2ly/\beta) \qquad \tilde{q} \equiv e^{4\pi l/\beta} \quad (6.57)$$

$$\text{where} \qquad S^{(c)}_{c\tilde{c}} \ \equiv \ \tfrac{1}{\sqrt{2}} e^{i4\pi c\tilde{c}} \ = \ \tfrac{1}{\sqrt{2}} \begin{pmatrix} 1 & 1 \\ 1 & -1 \end{pmatrix}_{c\tilde{c}} \qquad (6.58)$$

It is easy to check this by simply using the Poisson resummation formula

$$\sum_{k \in Z} e^{-(ak^2 + bk + c)} = \sqrt{\tfrac{\pi}{a}} e^{\left(\frac{b^2}{4a} - c\right)} \sum_{m \in Z} e^{-\frac{1}{a}(\pi^2 m^2 + i\pi m b)} \qquad (6.59)$$

and the property $\eta(q) = \sqrt{2l/\beta}\ \eta(\tilde{q})$ (see [Gins87, eq. 7.33]). Eq. (6.57) tells us that $\chi^{(c)}_{2c}(q, y)$ can be written as a linear combination of $\chi^{(c)}_{2\tilde{c}}(\tilde{q}, -i2ly/\beta)$'s, where the coefficients are given by the so-called *modular S-matrix*, $S^{(c)}_{c\tilde{c}}$ (which has nothing do with the physical S-matrix of scattering theory). (For some more comments about modular transformations, see [Gins87, section 7.3].)

Using eq. (6.57) in eq. (6.56), we obtain

$$\begin{aligned} Z(\theta_0, \theta_3) &= \sum_{c_o, c_3 = 0, \frac{1}{2}} n_o^{c_o c_3} \prod_{a=0,3} \left[\tilde{q}^{-(\frac{\theta_a \beta}{4\pi})^2} \sum_{\tilde{c}=0,\frac{1}{2}} S^{(c)}_{c_a \tilde{c}_a} \ \chi^{(c)}_{2\tilde{c}_a}\left(\tilde{q}, i(-l\theta_a + \pi v_a)\right)\right] \\ &= \ \eta^{-2}(\tilde{q}) \sum_{c_o, c_3 = 0, \frac{1}{2}} n_o^{c_o c_3} \prod_{a=0,3} \left[\tilde{q}^{-(\frac{\theta_a \beta}{4\pi})^2} \sum_{\tilde{Q}_a \in Z/2} S^{(c)}_{c_a \tilde{c}_a} \tilde{q}^{\tilde{Q}_a^2} e^{i2(-l\theta_a + \pi v_a)\tilde{Q}_a}\right] \end{aligned} \qquad (6.60)$$

where we have recombined the sums $\sum_{\tilde{c}_a, s_a} = \sum_{\tilde{Q}_a}$ in the last step. The result is the desired expression for $Z(\theta_0, \theta_3)$ as a function of $\tilde{q}$.

We now turn to the task of recalculating $Z(\theta_0, \theta_3)$ in terms of boundary states. The general strategy for this procedure is described in appendix C, section C.4.2, with which the reader is assumed to be familiar. The starting point is the following Ansatz (a generalization of eq. (6.50)):

$$Z(\theta_0,\theta_3) \equiv \tilde{q}^{-(\frac{\beta}{4\pi})^2(\theta_0^2+\theta_3^2)} \langle F_-| \prod_{a=0,3} e^{-l\left[(\tilde{H}^a_{oL}+\tilde{H}^a_{oR})+\theta_a i(\tilde{J}^a_{oL}-\tilde{J}^a_{oR})\right]} |B\rangle \ , \tag{6.61}$$

[We have included a (for our purposes uninteresting) factor $\tilde{q}^{-(\frac{\beta}{4\pi})^2(\theta_0^2+\theta_3^2)}$, arising from the vacuum fluctuations of the operators $e^{-il\theta_a(\tilde{J}^a_{oL}-\tilde{J}^a_{oR})}$; see [AL94, eq.(F.8)].]

In the boundary-state description, the role of space and time coordinates have been interchanged, by introducing new coordinates $(\tilde{\tau}, \tilde{r})$, defined by

$$\tilde{r} = \tau \ , \qquad \tilde{\tau} = -r \ . \tag{6.62}$$

This is nothing but a conformal transformation, $\tilde{z} \equiv iz$. Thus, the operators $\tilde{H}^a$ and $\tilde{J}^a_0$ in eq. (6.61), which are quantized along lines of constant $\tilde{\tau}$ in the $\tilde{\tau} + i\tilde{r}$)-plane, are related as follows to the H^a and J^a_0 of eq. (6.52):

$$J^a_L(\tau + ir) = i\tilde{J}^a_L(\tilde{\tau} + i\tilde{r}) \ , \qquad J^a_R(\tau - ir) = -i\tilde{J}^a_R(\tilde{\tau} - i\tilde{r}) \, ; \tag{6.63}$$

$$\beta H^a_o = \int_0^\beta d\tau \int_0^l \tfrac{dr}{2\pi} \left[H^a_{oL}(\tau + ir) + H^a_{oR}(\tau - ir)\right] = l(\tilde{H}^a_{oL} + \tilde{H}^a_{oR}) \tag{6.64}$$

$$\beta J^a_o = \int_0^\beta d\tau \int_0^l \tfrac{dr}{2\pi} \left[J^a_L(\tau + ir) + J^a_R(\tau - ir)\right] = -il\left(\tilde{J}^a_{oL} - \tilde{J}^a_{oR}\right) \ ; \tag{6.65}$$

$$\tilde{J}^a_{oL/R} \equiv \int_o^\beta \tfrac{d\tilde{r}}{2\pi} \tilde{J}^a_{L/R}(\tilde{\tau} \pm i\tilde{r}) \qquad (= \text{independent of } \tilde{\tau}). \tag{6.66}$$

Note that only $\tilde{H}^a_0$'s appear here in eq. (6.61), no $\tilde{H}^a_{\rm scat}$: as remarked above, the reason is that $\tilde{H}^a_0$ generates translations in the $\tilde{\tau} = -r$ direction *and hence knows nothing about the boundary terms.*

The closed-string Hilbert space on which these operators act (not to be confused with the usual open-string Hilbert space on which the H^a and J^a act) has

the same structure of charge and spin towers as that outlined in section 6.1. The only additional feature is that we now have both R and L-moving fields, so that a typical basis state in the closed-string Hilbert space has the following form:

$$n_o^{\tilde{c}_0\tilde{c}_3} n_o^{\tilde{c}'_0\tilde{c}'_3} |\tilde{Q}_0, \tilde{d}_0; \tilde{Q}_3, \tilde{d}_3\rangle_L \otimes |\tilde{Q}'_0, \tilde{d}'_0; \tilde{Q}'_3, \tilde{d}'_3\rangle_R \ , \tag{6.67}$$

where $\tilde{Q}_a \equiv \tilde{c}_a + \tilde{s}_a$, $\tilde{c}_a \in Z$, $\tilde{s}_a = 0, \frac{1}{2}$. Note in particular the presence again of *free*-fermion gluing conditions; they are needed to ensure that the closed string theory describes free fermions, because, as emphasized above, $\tilde{H}_{F\_P}$ is a bulk, free-fermion Hamiltonian without any $\tilde{H}_{scat}$.

The energy of a state such as eq. (6.67) has the form

$$\tilde{E}_{\tilde{Q}_0\tilde{Q}_3} - \tilde{E}_{00} \ = \ \tfrac{2\pi}{\beta}\left[\tilde{Q}_0^2 + \tilde{Q}_3^2 + \tilde{Q}_0'^{\,2} + \tilde{Q}_3'^{\,2} + \tilde{m}\right], \qquad (\tilde{m} \in Z) \ , \tag{6.68}$$

where the factor $\frac{2\pi}{\beta}$ arises because the $\tilde{J}^a_{L/R}$ currents live on a line of length β (instead of $2l$).

Now, as mentioned above, we know that the boundary term is $U^{(c)}(1) \times U^{(s)}(1)$ invariant. Formally, this is reflected in the fact that the L- and R parts of the corresponding KM currents J^0 and J^3 become equal at the boundary, as we have verified explicitly in eqs. (6.39):

$$J^a_L(\tau + i0^+) = J^a_R(\tau - i0^+) \qquad \text{for } a = 0, 3 \tag{6.69}$$

A similar condition (trivially) holds at $r = l$, due to the periodic boundary conditions on the currents. These conditions immediately translate into operator conditions in the new coordinates:

$$\left\{\int_0^\beta d\tilde{r} e^{i2\pi n\tilde{r}/\beta}\left(\tilde{J}^a_L(i\tilde{r}) + \tilde{J}^a_R(-i\tilde{r})\right)\right\}|B\rangle = 0 \ , \qquad \text{for } \ n \in Z \text{ and } a = 0, 3 \, , \tag{6.70}$$

with a similar equation for $|F_-\rangle$. Now, it can be shown [Ishi89] that the most general solution of eq. (6.70) is of the form:

$$|B\rangle = \sum_{\tilde{Q}_0,\tilde{Q}_3\in Z/2} n_o^{\tilde{c}_0\tilde{c}_3}\, B(\tilde{Q}_0,\tilde{Q}_3) \left(\sum_{\{\tilde{d}_0,\tilde{d}_3\}} |\tilde{Q}_0,\tilde{d}_0;\tilde{Q}_3,\tilde{d}_3\rangle_L \otimes |\tilde{Q}_0^*,\tilde{d}_0^*;\tilde{Q}_3^*,\tilde{d}_3^*\rangle_R \right) \ , \quad (6.71)$$

The state $|F_-\rangle$ has a similar structure. There are two crucial properties here: Firstly, all states in the same tower $(\tilde{Q}_o,\tilde{Q}_3)$ get the same weight (i.e. the coefficients $B(\tilde{Q}_0,\tilde{Q}_3)$ do not depend on the descendant labels $\{\tilde{d}_0,\tilde{d}_3\}$). Secondly, the quantum numbers of the R-tower are linked to (and not independent of) those of the L-tower, which is a direct consequence of eq. (6.70) (* denotes complex conjugation). This linking of the L-R quantum numbers has a "physical" interpretation. It means that the states propagating between the boundaries at $r = 0, l$ always come in L-R pairs (created from the vacuum by a $c_L^\dagger c_R^\dagger$ combination). Loosely speaking, the wave-function associated with this pair-state can be thought of as a particular standing wave between the two boundaries, the coefficient $B(\tilde{Q}_0,\tilde{Q}_3)$ giving the amplitude (at $r = 0$) of the R-moving (reflected) component of this standing wave relative to the L-moving (inciident) component.

Now we know all the ingredients of eq. (6.61). The next step is to insert into it a complete set of states of the form (6.67), and simplify. The result is

$$Z(\theta_o,\theta_3) \ = \quad (6.72)$$
$$\tilde{q}^{-(\frac{\beta}{4\pi})^2(\theta_0^2+\theta_3^2)} \sum_{\tilde{Q}_0,\tilde{Q}_3\in Z/2} n_o^{\tilde{c}_0\tilde{c}_3} \prod_{a=0,3} \left[\frac{\tilde{q}^{\tilde{Q}_a^2} e^{-i2\theta_a l\tilde{Q}_a}}{\eta^2(\tilde{q})} \right] \cdot \langle F_-|\tilde{Q}_0;\tilde{Q}_3\rangle\langle\tilde{Q}_0;\tilde{Q}_3|B\rangle \ .$$

Here we have exploited the fact that due to the equal-weight sum over descendants in $|B\rangle$, the matrix element

$${}_L\langle\tilde{Q}_0,\tilde{d}_0;\tilde{Q}_3,\tilde{d}_3| \otimes {}_R\langle\tilde{Q}_0',\tilde{d}_0';\tilde{Q}_3',\tilde{d}_3'|B\rangle \ \equiv \ \delta_{\tilde{Q}_0^*\tilde{Q}_0'}\delta_{\tilde{Q}_3^*\tilde{Q}_3'}\delta_{\tilde{d}_0^*\tilde{d}_0'}\delta_{\tilde{d}_3^*\tilde{d}_3'} \ \langle\tilde{Q}_0;\tilde{Q}_3|B\rangle \quad (6.73)$$

is independent of the descendant labels. This allows one to perform the sums over all states in a given tower, obtaining the familiar η^{-2} factor. Furthermore, the δ-functions in eq. (6.73) force all L- and R quantum numbers to be the same (up to complex conjugation) thus giving the extra 2 in $\tilde{q} = e^{-2\cdot 2\pi l/\beta}$.

Now we are ready to compare our two expressions for $Z(\theta_o, \theta_3)$, namely eqs. (6.60) and eq. (6.72). Comparing powers of $\tilde{q}e^{\theta_a}$, we deduce that

$$n_o^{\tilde{c}_0\tilde{c}_3}\ \langle F_-|\tilde{Q}_0;\tilde{Q}_3\rangle\langle\tilde{Q}_0;\tilde{Q}_3|B\rangle\ =\sum_{c_0,c_3=0,\frac{1}{2}} n_o^{c_0c_3}\ S^{(c)}_{c_0\tilde{c}_0}\ S^{(c)}_{c_3\tilde{c}_3}\ e^{i2\pi(v_0\tilde{Q}_0+v_3\tilde{Q}_3)} \tag{6.74}$$

This central result is known as a Cardy formula (first derived in [Car89, eq.(18)]). It determines the boundary matrix elements in terms of known quantities, namely the modular S-matrix and the gluing condition.

For the present problem, $S^{(c)}_{c_0\tilde{c}_0}$ and $n_o^{c_0c_3}$ are so simple that a further simplification follows immediately:

$$\sum_{c_0,c_3=0,\frac{1}{2}} n_o^{c_0c_3} S_{c_0\tilde{c}_0} S_{c_3\tilde{c}_3}\ =\ \tfrac{1}{2}\left(1+e^{i4\pi(\frac{1}{2}\tilde{c}_0+\frac{1}{2}\tilde{c}_3)}\right)\ =\ n_o^{\tilde{c}_0\tilde{c}_3}\ . \tag{6.75}$$

Thus we obtain

$$n_o^{\tilde{c}_0\tilde{c}_3}\langle\tilde{Q}_0;\tilde{Q}_3|B\rangle\ =\ n_o^{\tilde{c}_0\tilde{c}_3}\ e^{i2\pi(v_0\tilde{Q}_0+v_3\tilde{Q}_3)}\ . \tag{6.76}$$

Here we have exploited the $v_0 = v_3 = 0$ version of Cardy's formula, namely $\langle F_-|\tilde{Q}_0;\tilde{Q}_3\rangle\langle\tilde{Q}_0\tilde{Q}_3|F\rangle = 1$, to conclude that we may take $\langle\tilde{Q}_0;\tilde{Q}_3|F_-\rangle \equiv 1$.

All that remains is to find the coefficients $\tilde{U}_B(\overline{\psi}^\alpha)$, $\tilde{U}_B(J^\pm)$ and $\tilde{U}_B(J^3)$ from eq. (6.45). To this end, we have to identify the $(\tilde{Q}_0, \tilde{Q}_3)$ quantum numbers of the fields $\overline{\psi}^\alpha$, $J^\pm$ and J^3 in the *closed* string picture (because the correlation functions of eq. (6.44) are defined in the closed string picture, see footnote 6 on page 168). Now, the identity operator **1** corresponds to the "vacuum state" (i.e. the $T = 0$ Fermi sea), $|\tilde{Q}_0, \tilde{Q}_3\rangle = |0, 0\rangle$. The fermion fields $\overline{\psi}^\pm$ correspond to

the $|\frac{1}{2},\pm\frac{1}{2}\rangle$ KM primary state, because they have $(\tilde{Q}^{\uparrow},\tilde{Q}^{\downarrow})=(1,0)$ or $(0,1)$, and hence $(\tilde{Q}_0,\tilde{Q}_3)=(\frac{1}{2},\pm\frac{1}{2})$. The current J^3 is diagonal in fermion fields, $[J^3=\frac{1}{2}:\overline{\psi}^{1\dagger}\overline{\psi}^{1}-\overline{\psi}^{\dagger 2}\overline{\psi}^{2}:]$, i.e. has the same number of fermions as the vacuum; therefore, it also has $(\tilde{Q}_0,\tilde{Q}_3)=(0,0)$, which means that it corresponds to a descendant of the $|0,0\rangle$-vacuum state. The currents $J^+=\overline{\psi}^{1\dagger}\overline{\psi}^{2}$ and $J^-=\overline{\psi}^{2\dagger}\overline{\psi}^{1}$ have $(\tilde{Q}_0,\tilde{Q}_3)=(0,\pm 1)$, and are descendants in the $(0,\pm 1)$ KM towers, respectively.

Using this information in eqs. (6.76) and (6.45), we find

$$\tilde{U}_{B}(\overline{\psi}^{\alpha})=e^{i\pi(v_0+\alpha v_3)}\,;\qquad \tilde{U}_{B}(J^{\pm})=e^{\pm i2\pi v_3}\,;\qquad \tilde{U}_{B}(J^{3})=1\,, \tag{6.77}$$

This, finally, is the result promised above [in eq. (6.46)].

Note that on the right-hand-side of eq. (6.76), the *free*-fermion gluing conditions reappear. Thus, our calculation has explicitly justified an assumption that was made when we wrote down eq. (6.67) for the basis states of the Hilbert space in the closed-string picture, namely that they only occur in *free-fermion* combinations, as indicated by the n_o's in eq. (6.67).

The preceding presentation might have been painfully detailed; however, the methods are well worth learning, for they are very powerful, and easily applied to other theories that have a similar structure. The details need to be digested only once. Once the exact partition function is known, an aficionado could find the desired result eq. (6.77) on the proverbial back of an envelope: all he would do is take one glance at the partition function, written in the form of eq. (6.53), look up the relevant modular transformation properties of the appropriate characters [eq. (6.57)] to arrive at eq. (6.60), and then directly read off Cardy's formula eq. (6.74).

The generalization of these methods to the Kondo problem will indeed be very

straightforward, as will be explained in chapter 7. However, in that context the role of symmetries is much more important than can be gleaned from the present example. Therefore, in the next section, we shall discuss a special value of the coupling constants, namely $v_0 = 0$ and $v_3 = 1$, at which the theory suddenly has a larger symmetry, $U^{(c)} \times SU(2)$. We shall exploit this to redo the above calculation more efficiently, and in closer analogy to the Kondo problem.

Before proceeding, however, let us briefly remark that for the present problem there actually exists a short-cut to obtaining $|B\rangle$. The boundary terms $H^a_{\rm scat}$ that appear in eq. (6.52), but not in eq. (6.61), may be thought of as acting on a free boundary state $|F_+\rangle$ at $r = 0$, to produce $|B\rangle$ (compare [CKLM94, eq.(2.23)]):

$$|B\rangle \equiv \prod_{a=0,3} \left[e^{-\int_0^\beta d\tau v_a J^a_L(\tau+i0)} \right] |F_+\rangle \;=\; \prod_{a=0,3} \left[e^{i2\pi v_a \tilde{J}^a_{oL}(\tilde{\tau}=0)} \right] |F_+\rangle \; . \tag{6.78}$$

For the second equality we used eq. (6.65). Now, $|F_+\rangle$ has the structure of eq. (6.71), with all coefficients $F(\tilde{Q}_0, \tilde{Q}_3) = 1$. Therefore eq. (6.76) immediately follows, since $\tilde{J}^a_{oL}|\tilde{Q}_0;\tilde{Q}_3\rangle_L = \tilde{Q}_a|\tilde{Q}_0;\tilde{Q}_3\rangle_L$. Unfortunately, this simple trick does not generalize to the more complicated case in which the boundary operator involves a Kondo impurity.

6.5 Restoration of $SU(2)$-symmetry at $v_3 = 1$

In this section, we examine the case that the coupling constant v_3 has the special values $v_3 = 1$. We shall call this the "strong-coupling fixed point", in analogy with terminology used for the Kondo problem. It turns out that at this point the $SU(2)$ symmetry (in the spin sector) that the free theory possesses is restored. This has two important consequences: Firstly, the spectrum turns out to look exactly

like that of a free theory, but with a modified gluing condition [see eq. (6.79)]. Secondly, the boundary state $|B\rangle$ now also has to respect this $SU(2)$ symmetry. These two facts allow one to calculate the boundary-state matrix elements more efficiently (using the same ideas as those developed above, but exploiting the additional $SU(2)$ symmetry). Moreover, they illustrate quite explicitly in a simple setting the ideas that are also at the heart of Affleck and Ludwig's solution of the Kondo model: namely the (in their case dynamical) restoration of the original symmetry of the free theory at the strong-coupling fixed point, accompanied by a modified gluing condition.

For simplicity, we shall take $v_0 = 0$ in this section, but (with some obvious changes) the entire discussion holds also for arbitrary v_0 (since apart from the gluing condition, the charge and spin sectors are decoupled).

Why is $v_3 = 1$ special? At this value, we note two facts: Firstly, we learn from eq. (6.27), with $m = 0$, that the boundary interaction shifts the charges by exactly $\frac{1}{2}$: $c_3 = 0$ is simply replaced by $c_3 = \frac{1}{2}$, and $c_3 = \frac{1}{2}$ by $c_3 = 0$. Thus, *the spectrum is essentially that of a free theory, but with modified gluing condition,* namely:

$$n_*^{c_0 c_3} \equiv \begin{cases} 1 & \text{if} \quad c_o \neq c_3 \ , \\ 0 & \text{if} \quad c_o = c_3 \ , \end{cases} \tag{6.79}$$

We shall call this the "strong-coupling" gluing condition.

Secondly, we see from eq. (6.76) that $\langle Q_0, Q_3|B\rangle = e^{i2\pi c_3}$, (since $e^{i2\pi s_3} = 1$); in other words, the s_3-dependence of these matrix elements disappears completely, which means that *all* the descendants in a tower get the same phase. This is a hint that *at the strong-coupling fixed point the system has more symmetry than at other values of* v_3. In what follows, we describe how the modification of the

gluing condition and the emergence of a larger symmetry are related, and how these features can be exploited to compute $|B\rangle$, which also has more symmetry, more efficiently.

To illustrate the significance of the new gluing condition, we reconsider the partition function $Z(\theta_0, \theta_3)$. For the special choice $v_0 = 0, v_1 = 1$ (indicated by the subscript 1 on Z_*), eq. (6.53) can be rewritten as follows:

$$\begin{aligned} & Z_*(\theta_0,\theta_3)\eta^{-2}(q) \sum_{Q_o,Q_3\in Z/2} n_o^{c_o c_3}\; q^{\left[Q_0^2+(Q_3+\frac{1}{2})^2\right]} e^{\beta\left[\theta_0 Q_0+\theta_3(Q_3+\frac{1}{2})\right]} \\ &= \eta^{-2}(q) \sum_{Q_o,Q_3\in Z/2} n_*^{c_o c_3}\; q^{(Q_0^2+Q_3^2)} e^{\beta(\theta_0 Q_0+\theta_3 Q_3)} \qquad (6.80) \\ &= \sum_{Q_o,Q_3\in Z/2} n_*^{c_o c_3} \sum_{\{d_o,d_3\}} \langle Q_o,d_o;Q_3,d_3| \prod_{a=0,3} e^{-\beta(H_o^a-\theta_a J_o^a)} |Q_o,d_o;Q_3,d_3\rangle \qquad (6.81) \end{aligned}$$

Compare eq. (6.81) with eq. (6.53): in eq. (6.53), the partition function is expressed in terms of the *full* Hamiltonian $H_o^3+H_{\rm scat}^3$, and the trace is taken over the *free-electron* subspace (characterized by the free-fermion gluing condition $n_o^{c_o c_3}$) of the tensor product of the charge and spin Hilbert spaces. In eq. (6.81), the partition function is expressed in terms of only the *free* Hamiltonian H_o, but now the trace is over a *different* subspace of the full Hilbert space, characterized by the strong-coupling gluing condition $n_*^{c_o c_3}$.

Thus we come to the following remarkable conclusion: *at the strong-coupling fixed point, the boundary condition is* **completely** *characterized by the strong-coupling gluing condition $n_*^{c_o c_3}$; no* further information is needed beyond these numbers.

Now, the free Hamiltonian H_o has a larger symmetry than the $U^{(c)}(1)\times U^{(s)}(1)$ symmetry that we have been exploiting so far. It is also invariant under $U^{(c)} \times SU(2)$ transformations of the form $\psi^\alpha \to e^{i\phi_o} R^{SU(2)}_{\alpha\alpha'}$. The fact that at the strong-

coupling fixed point the partition function can again be expressed purely in terms of H_o means that this larger symmetry must somehow be hidden in Z_* too. In fact, it should be possible to exploit this larger symmetry to calculate Z_* and $|B\rangle$ more efficiently. We now describe how this works.

Consider the interaction switched off for the moment. As described in appendix A (section A.7), the free Hamiltonian can also be written in a Sugawara form that reflects its $U(1) \times SU(2)$ symmetry [eq. (A.83)]. In terms of the $U(1)$ and $SU(2)$ Nöther currents J^0 and $\vec{J}$ defined in eq. (6.34), one finds [see eqs. (A.81) and (A.83), with J^0-normalization differing by $\frac{1}{2}$],

$$H_o = H_o^{(c)} + H_o^{(s)} = \int_{-l}^{l} \frac{dx}{2\pi} \left[: J^o J^o : + \tfrac{1}{3} : \vec{J}\vec{J} : \right] , \tag{6.82}$$

with spectrum given by eq. (A.94):

$$E_{Q_0 j} - E_{00} = \tfrac{2\pi}{l} \left[\left(Q_0^2 + m^c \right) + \left(\frac{j(j+1)}{3} + m^s \right) \right] . \tag{6.83}$$

The spectrum is arranged into towers labeled by a charge and a spin quantum number, (Q_0, j) [section A.7.2]. Here the charge, $Q_0 \in Z/2$, is the same quantum number as that used above. However, the spin j is restricted to the values $j = 0, \frac{1}{2}$, and plays the role of c_3 (and not Q_3). The tower (Q_0, j) can be thought of as a combination, into a single tower, of all (Q_0, Q_3) towers with the same $c_3 = j$: $(Q_0, j) = \{(Q_0, j + s_3),\ s_3 \in Z\}$. The reason for combining all these towers together is that they are related to each other by $SU(2)$ symmetry, in the sense that $SU(2)$ transformations mix all their states together. For more discussion, see appendix A, page 300.

Since j plays the role of c_3, the free-fermion gluing condition eq. (6.19) for gluing charge and spin towers together is simply $n_0^{c_0 j} = \delta_{c_o j}$ [where $2c_0 = Q \bmod(1)$].

In terms of the $|Q_0, j\rangle$ basis, the free-fermion partition function of eq. (6.23) can also be rewritten in the equivalent form

$$Z_o(\theta_0, \theta_3) \;=\; \sum_{Q_o \in Z/2} \sum_{j=0,\frac{1}{2}} n_o^{c_o j}\; \chi^{(c)}_{2c_0}(q, \beta\theta_0/2)\;\; \chi^{(s)}_j(q, \beta\theta_3) \tag{6.84}$$

Here $\chi^{(s)}_j$ are the so-called non-specialized $SU(2)_1$ characters, defined by

$$\chi^{(s)}_j(q, \beta\theta_3) \equiv \sum_{\{r_j\}} \langle j, r_j | e^{-\beta\left(H_o^{(s)} - \theta_3 J_0^3\right)} | j, r_j \rangle \;. \tag{6.85}$$

Since the states $|j, d_j\rangle$ span the same Hilbert space as the states $\{|j + s_3, d_3\rangle\}$, it follows (by comparing eq. (6.84) to eq. (6.23)) that the following character identity holds:

$$\chi^{(c)}_{2j}(q, \beta\theta/2) = \chi^{(s)}_j(q, \beta\theta) \;. \tag{6.86}$$

Let us now switch the interaction back on, with $v_0 = 0$ and $v_3 = 1$, and reexamine the partition function Z_*. By writing eq. (6.80) in terms of $\chi^{(c)}$'s [defined in eq. (6.55)], and then using eq. (6.86), it immediately follows that Z_* can also be written as

$$Z_*(\theta_0, \theta_3) = \sum_{c_0 j = 0, \frac{1}{2}} n_*^{c_o j}\; \chi^{(c)}_{2c_0}(q, \beta\theta_0/2)\;\; \chi^{(s)}_j(q, \beta\theta_3) \;. \tag{6.87}$$

The fact that the partition function can be expressed in terms of $SU(2)_1$ characters is quite startling – it implies that despite the presence of a boundary interaction that seems to break $SU(2)$ symmetry, this symmetry somehow reemerges at $v_3 = 1$.

The reason for the reemergence of this $SU(2)$ symmetry can be understood as follows: note from eq. (6.39) that at $v_3 = 1$, J^0 and also *all three* the $SU(2)$ Nöther currents become analytic at the boundary:

$$J^a_L(0) = J^a_R(0) \;, \qquad \text{for } a = 0, 1, 2, 3 \;. \tag{6.88}$$

But this is exactly the condition that guarantees that the boundary will be $U^{(c)}(1) \times SU(2)$ invariant; therefore, both bulk and boundary are $U^{(c)}(1) \times SU(2)$ invariant, and the effect of the boundary interaction *cannot* be anything more than to simply modify the gluing conditions.

Since we intend to compare Z_* to a closed-string expression depending on $\tilde{q}$ below [eq. (6.93)], let us rewrite Z_* in terms of $\tilde{q}$. This is done using the modular transformation properties of $\chi^{(c)}$ and $\chi^{(s)}$, given by eq. (6.57) and

$$\chi_j^{(s)}(q,y) \;=\; \tilde{q}^{-\left(\frac{y}{4\pi}\right)^2} \sum_{\tilde{j}=0,\frac{1}{2}} S^{(s)}_{j\tilde{j}}\, \chi^{(s)}_{\tilde{j}}(\tilde{q}, -i2ly/\beta)\;, \tag{6.89}$$

$$\text{where} \qquad S^{(s)}_{j\tilde{j}} \;\equiv\; \tfrac{1}{\sqrt{2}} \sin\Big((2j+1)(2\tilde{j}+1)\pi/4\Big) \;=\; \tfrac{1}{\sqrt{2}} \begin{pmatrix} 1 & 1 \\ 1 & -1 \end{pmatrix}_{j\tilde{j}} \tag{6.90}$$

(see eqs. (F.21) and (3.5) of [AL94]). Thus, eq. (6.87) can also be written as:

$$Z_*(\theta_o,\theta_3) = \tilde{q}^{-(\frac{\beta}{4\pi})^2(\theta_0^2+\theta_3^2)} \sum_{c_o,j=0,\frac{1}{2}} n_*^{c_0 j} \sum_{\tilde{c}_o,\tilde{j}=0,\frac{1}{2}} S^{(c)}_{c\tilde{c}_0} S^{(s)}_{j\tilde{j}}\; \chi^{(c)}_{2\tilde{c}_0}(\tilde{q}, -i\theta_0 l)\; \chi^{(s)}_{\tilde{j}}(\tilde{q}, -i2\theta_3 l)\;. \tag{6.91}$$

Now turn to the closed string picture. The $U^{(c)}(1) \times SU(2)$ symmetry of the boundary can be exploited to calculate $|B\rangle$ in a "more efficient" way: the boundary condition (6.88) on the currents translates in the $|Q_0, j\rangle$ basis into conditions on $|B\rangle$ and $|F_-\rangle$ that have precisely the form of eq. (6.70), but now holding for $a = 0, 1, 2, 3$ (instead of just $a = 0, 3$). This implies that $|B\rangle$ and $|F_-\rangle$ can be constructed from Ishibashi states that respect $U^{(c)}(1) \times SU(2)$ symmetry:

$$|B\rangle = \sum_{\tilde{Q}_0 \in Z/2} \sum_{\tilde{j}=0,\frac{1}{2}} n_o^{\tilde{c}_0 \tilde{c}_3}\; B(\tilde{Q}_0, j) \left(\sum_{\{\tilde{d}_0, \tilde{r}_j\}} |\tilde{Q}_0, \tilde{d}_0; \tilde{j}, \tilde{r}_j\rangle_L \otimes |\tilde{Q}_0^*, \tilde{d}_0^*; \tilde{j}^*, \tilde{r}_j^*\rangle_R \right)\;. \tag{6.92}$$

The difference from eq. (6.71) is that now $B(\tilde{Q}_0, \tilde{j} + \tilde{s_0}) \equiv B(\tilde{Q}_0, \tilde{j})$ for all $\tilde{s}_3 \in Z$, i.e. the additional $SU(2)$ symmetry has constrained an infinite number of B-coefficients to all have the same value (this is why the calculation is "more

efficient"). Consequently, the partition function, expressed in terms of $|F_-\rangle$ and $|B\rangle$, is

$$Z_*(\theta_o,\theta_3) = \tag{6.93}$$
$$\tilde{q}^{-(\frac{\beta}{4\pi})^2(\theta_0^2+\theta_3^2)}\sum_{\tilde{Q}_0\in Z/2}\sum_{\tilde{j}=0,\frac{1}{2}} n_*^{\tilde{c}_0\tilde{j}}\ \chi^{(c)}_{2\tilde{c}_0}(\tilde{q},-i\theta_0 l)\ \ \chi^{(s)}_{\tilde{j}}(\tilde{q},-i2\theta_3 l)\cdot\langle F_-|\tilde{Q}_0;\tilde{j}\rangle\langle\tilde{Q}_0;\tilde{j}|B\rangle\ .$$

Since the products of non-specialized characters are linearly independent, we can equate their coefficients in eqs. (6.91) and (6.93), to obtain the following Cardy formula:

$$\boxed{n_o^{\tilde{c}_0\tilde{j}}\ \langle F_-|\tilde{Q}_0;\tilde{j}\rangle\langle\tilde{Q}_0\tilde{j}|B\rangle\ =\ \textstyle\sum_{c_0,j=0,\frac{1}{2}} n_*^{c_0 j}\ S^{(c)}_{c_0\tilde{c}_0}\ S^{(s)}_{j\tilde{j}}\ =\ n_o^{\tilde{c}_0\tilde{j}}\ (-1)^{\tilde{j}}\ .} \tag{6.94}$$

Thus we find, remarkably, that *the boundary matrix elements are given purely in terms of the strong-coupling gluing conditions and modular S-matrix elements!* It turns out that an entirely analogous statement holds for the Kondo effect (which is the reason why we discussed the $v_3 = 1$ case in so much detail).

The last equality in eq. (6.94) follows from simply inserting eqs. (6.58), (6.79) and (6.90), and is in agreement with eq. (6.76). Since fermion fields correspond to $|Q_0, j\rangle = |\frac{1}{2},\frac{1}{2}\rangle$, and the currents J^0 and $J^\pm$ to (KM descendants of) $|0,0\rangle$ and $|0,1\rangle$ we immediately recover eq. (6.77) too.

Note again how the strong-coupling gluing conditions n_* in the open string expression (the middle expression) in eq. (6.94) emerge as free-fermion gluing conditions in the closed string expressions (the left- and right expressions) of eq. (6.94). It turns out that this is a general phenomenon: whenever the effect of some boundary interaction can completely be described, in the open string picture, by merely changing the gluing condition from n_o for free fermions to a

modified gluing condition n_*, then in the closed string picture, the *free*-fermion gluing condition n_o reemerges.[9] In particular, this also happens in the Kondo problem [see eq. (7.64)].

6.6 Summary

Let us take a step back and summarize the procedure by which the boundary interaction was treated and the Green's function G^{RL} was found in this chapter.

The general framework for the calculation rests on the equivalence of two different ways of viewing the theory:

(a) *Open string picture:* The system is quantized on lines of constant τ in the upper half of the $\tau + ir$ plane. Besides the bulk-fermion term H_o, the Hamiltonian also contains a scattering term H_{scat}, which *explicitly* represents the effects of the impurity. This impurity term can be absorbed by making appropriate shifts in the currents. At the strong-coupling fixed point, this shift is equivalent to a change from a free-fermion to a strong-coupling gluing condition ($n_o \to n_*$).

(b) *Closed string picture:* The system is quantized on lines of constant r. The Hamiltonian contains *only* a bulk, free-fermion term H_{F_P}. The impurity has been effectively "integrated out", and its effects are encoded in the boundary state $|B\rangle$, which determines how free L-moving fields are reflected into free R-moving fields at $r = 0$.

Since the closed string picture is a theory in which the impurity has been effectively "integrated out" and one is left with a theory of *free* fermions being

[9] Technically, this is a consequence of the Verlinde formula [Ver88].

reflected off a boundary, it provides a description that, once $|B\rangle$ is known, is in many ways simpler than the open string picture. This is why Green's functions are best calculated in the closed string picture. For the Kondo problem, where the impurity is dynamical, this simplification of effectively having integrated out the impurity will be even more signicant; Kondo Green's functions in the closed string picture indeed represent correlation functions in which the impurity degrees of freedom have been traced out already.

The boundary state $|B\rangle$ is determined by requiring the open and closed string partition functions to be the same, and once known, immediately gives G^{RL}. Below we summarize the steps involved in the form of a cook-book recipe, formulated in a way that also applies to Affleck and Ludwig's solution of the Kondo problem, discussed in chapter 7:

Recipe for Calculating G^{RL}:

1. Start with a free Hamiltonian H_0, which has a certain symmetry $\mathcal{G}[= U^{(c)}(1) \times SU(2)]$.

2. The impurity at the origin breaks this down to a smaller symmetry $\mathcal{G}_i[= U^{(c)}(1) \times U^{(s)}(1)]$. Therefore, choose a bosonization scheme which is compatible with this smaller symmetry [namely the charge-spin scheme].

3. Find the free-fermion gluing condition n_o [eq. (6.19)], the finite-size spectrum [eq. (6.21)] and the free-fermion partition function $Z_o(q)$ [eq. (6.23)].

4. Absorb the impurity completely by making appropriate shifts in the currents [eq. (6.26)].

5. Calculate the new partition function $Z(q)$ exactly in terms of the new currents, in the open string picture [eq. (6.31)], and make a modular transformation, thus replacing q by $\tilde{q}$, to obtain $Z(\tilde{q})$ [eq. (6.60)].

6. Alternatively, in the closed string picture, express the partition function $Z(\tilde{q})$ as an expectation value [eq. (6.72)] between two boundary states, $\langle F_-|$ and $|B\rangle$, which respect the (smaller) symmetry $[U^{(c)}(1) \times U^{(s)}(1)]$.

7. Equate the two expressions for $Z(\tilde{q})$, and read off Cardy's formula [eq. (6.74)] for the boundary matrix elements $\langle \tilde{Q}_0; \tilde{Q}_3|B\rangle$.

   At Strong-Coupling Fixed Point:

8. At the so-called strong-coupling fixed point ($v_0 = 0$, $v_3 = 1$), the original symmetry $\mathcal{G}$ reemerges. This implies that the *only* effect of the scatterer is to change the free-fermion gluing conditions n_o to strong-coupling ones, n_* [eq. (6.79)].

9. Exploit this restored symmetry to express the partition function $Z_*(q)$ in terms of $\mathcal{G}$-characters and the strong-coupling gluing conditions [eq. (6.87)], and modular transform to get $Z_*(\tilde{q})$ [eq. (6.91)].

10. Since $|B\rangle$ also respects the restored symmetry, find an expression for $Z_*(\tilde{q})$ in terms of $\langle F_-|$, $|B\rangle$ and $U^{(c)}(1) \times SU(2)$ [eq. (6.93)].

11. Compare the two expressions for $Z_*(\tilde{q})$ to deduce Cardy's formula [eq. (6.94)]. We find the remarkable result that *at the strong-coupling fixed point, Cardy's formula gives the boundary matrix elements purely in terms of the strong-coupling gluing condition and modular S-matrix elements.*

12. The boundary-state matrix elements $[\langle \tilde{Q}_0; \tilde{Q}_3 | B \rangle]$ directly give the Green's function G^{RL} [eq. (6.47)], and hence the transmission matrix elements $\tilde{U}$ that determine the scattering states [eq. (5.60)].

The strategy for solving the Kondo problem at its strong-coupling fixed point, and in particular for finding the scattering states, is of an entirely analogous nature: at this point, the full symmetry of the original free Hamiltonian reemerges. The impurity spin disappears altogether, and the only trace it leaves behind is a modified gluing condition. Thus, most of the above steps can be repeated for the Kondo problem at its strong-coupling fixed point [see chapter 7]. Not surprisingly, therefore, the boundary state matrix elements are given by a Cardy formula [eq. (7.61)] that has precisely the structure of eq. (6.94) above.

Due to the simplicity of the present problem, we were able to demonstrate the reemergence of the $U^{(c)}(1) \times SU(2)$ at the strong-coupling fixed point explicitly [e.g. by proving that $J^a_L(\tau) = J^a_R(\tau)$ for $a = 0, 1, 2, 3$, eq. (6.88)]. For the Kondo problem, such a direct demonstration of the reemergence of the full symmetry of H_0 seems not to be possible. Therefore, the reemergence of this symmetry, accompanied by new strong-coupling gluing conditions, is stated as a hypothesis. The consequences of this hypothesis are then worked out, and compared with other well-established results, obtained using Wilson's numerical renormalization group approach and the Bethe Ansatz. The agreement is excellent and exact, respectively, and serves as *a posteriori* validification of the strong-coupling hypothesis.

Chapter 7

CFT treatment of k-channel Kondo problem

In this chapter we describe some of the main aspects of the conformal field theory (CFT) solution to the over-screened[1] k-channel Kondo problem developed by Affleck and Ludwig (AL) [Aff90,AL91a,AL91b,AL91c,AL91d,AL92a,AL92b,AL93, AL94,Lud94a,Lud94b,ML95]. It is impossible to give a comprehensive account of their work in the space of one chapter. Instead, we shall restrict our attention to the calculation of the simplest non-trivial Green's function in the theory,

$$G^{RL}(\bar{z}, z') \equiv -\langle \psi_R(\bar{z}) \psi_L^\dagger(z') \rangle \ , \tag{7.1}$$

which, according to eqs. (5.52) and (5.60), is needed for the nanoconstriction current. Nevertheless, even this calculation, presented in [AL93], requires thorough familiarity with substantial parts of AL's theory.

This chapter is intended as an introduction to AL's theory that is accessible

[1]The completely screened and under-screened Kondo problems can be solved by the same methods but many of the details are different [Aff90,AL91a].

to a reader not thoroughly familiar with CFT, but willing to learn what is needed along the way.[2] Our presentation is not self-contained, but should be viewed as a "road map" to the papers of AL; therefore, particularly at the beginning of each section, we shall provide detailed references, including specific page and eqation numbers, for the reader interested in the finer details. Some technicalities are also discussed in the appendices.

The strategy followed in this chapter is roughly the same as that of the previous chapter. It is organized as follows. In section 7.1, we present the mapping of the (3+1)-D k-channel Kondo problem theory to an effective (1+1)-D field theory, whose properties in the weak-coupling regime are discussed in section 7.2. Section 7.3 shows how the free theory can be written in a Sugawara form, which is essential for understanding the absorption of the impurity spin at strong-coupling, discussed in section 7.4. Finally, in section 7.5, we implement the recipe for calculating G^{RL} presented in chapter 6, page 188, points 8 to 12, for calculating the Kondo Green's function G^{RL} at $T = 0$. The $T \neq$ calculation is reserved for chapter 8.

7.1 Mapping to a 2-D Field Theory

[AL91b], appendix A; [Lud94a], section 2.1; [AL94], appendix A.

The k-channel Kondo problem of Nozières and Blandin [NB80] has been introduced in section 4.1. It describes a spin-s magnetic impurity, coupled anti-

[2] I found that most of what I needed to know about "basic" CFT was contained in just the two seminal papers [BPZ84,KZ84], and Ginsparg's excellent review [Gins87]. For a concise summary, see [GW86, section 3] or my section B.1. In addition, familiarity with Cardy's *boundary* CFT is also essential [Car84a,Car84b,Car86a,Car86b,Car89,CL91]; an introduction to this material can be found in C.

ferromagnetically to k degenerate bands (called *channels* or flavors) of electrons in an $SU(2)^{(spin)} \times SU(k)^{(flavor)}$ invariant way. Written in position space, the Hamiltonian density (4.1) in the so-called *weak-coupling limit* takes the form

$$H = \Psi^{\dagger\alpha i}(\vec{x}) \left(-\frac{\nabla^2}{2m} \right) \Psi_{\alpha i}(\vec{x}) \; + \; \lambda_K \delta^3(\vec{x}) \Psi^{\dagger\alpha i}(\vec{x}) \tfrac{1}{2} \vec{\sigma}^{\beta}_{\alpha} \Psi_{\beta i}(\vec{x}) \cdot \vec{S} \; . \tag{7.2}$$

Here the operators $\vec{S}$ describes the local spin-s impurity, with $[S^i, S^j] = i\varepsilon^{ijk} S^k$. Electrons are described by three-dimensional non-relativistic fermion fields $\Psi_{\alpha i}(\vec{x})$, where $\alpha, \beta = \pm$ labels the electron spin[3], and $i = 1, \ldots, k$ labels the k channels. Note that H is diagonal in channel indices.

Nozières arguments about the nature of the fixed points were discussed in chapter 4.

The Hamiltonian clearly has a radial symmetry about the origin, hence it is convenient to expand $\Psi_{\alpha i}(\vec{x})$ in spherical harmonics about the origin:[4]

$$\Psi_{\alpha i}(\vec{x}) = \psi_{\alpha i}(r) + \text{ higher} \quad \text{harmonics} \; ; \tag{7.3}$$

Since the $\delta(\vec{x})$-interaction has "zero" range, it only couples to $\psi_{\alpha i}(r)$, the angular momentum $l = 0$ part ("s-wave-projected" part) of $\Psi_{\alpha i}(\vec{x})$. Thus one has effectively a one-dimensional (radial) problem in terms of $\psi_{\alpha i}(r)$, with two Fermi points, at $|k| = k_F$, for incident and outgoing radial waves. To describe the universal low-temperature, large-distance physics, it is sufficient to linearize the

[3]Following AL, we shall use in this chapter the terminology that is appropriate to the *magnetic* multi-channel Kondo problem, i.e. "spin" (α, β) refers to the Pauli spin that couples to the magnetic impurity. In later chapters, the index that couples to the dynamic impurity will still be called a "spin" (or sometimes "pseudospin") index and denoted by α, β, but it will not always be the Pauli spin.

[4]The mapping from a 3- to a 1-dimensional problem is worked out in detail in Appendix A of [AL94], whose sign-conventions for $e^{\mp i k_F r} \psi_{L/R}(ir)$ we use; see also Appendix A of [AL91b] and section 2 of [Lud94a] where the sign conventions are slightly different – but all that really matters are the signs in $\pm i\partial_r$ in eq. (7.7).

dispersion relation about these points ($\varepsilon_{\vec{k}} = k^2/2m = v_{_F}|k|$). Thus one writes

$$\psi_{\alpha i}(r) \propto \left[-e^{-ik_{F}r}\psi_{L\alpha i}(ir) + e^{+ik_{F}r}\psi_{R\alpha i}(ir)\right] . \tag{7.4}$$

where the radial fields $\psi_{_{L/R}}(ir)$ (called L/R movers on the positive r-axis) are composed of low-energy incoming/outgoing radial excitations about the Fermi sea,

$$\psi_{_{L/R}\alpha i}(ir) \equiv \int_{-\Lambda}^{\Lambda} dk e^{\mp ikr} c_{o\alpha i}(k_{_F} + k) \tag{7.5}$$

[$c_o(k)$ creates a radial wave with radial momentum $k \equiv |k|$, and Λ is a cut-off satisfying $T \ll v_{_F}\Lambda \ll \varepsilon_{_F}$]. The radial multi-channel Kondo problem is then defined, in the weak-coupling limit, by the following Hamiltonian:

$$\begin{aligned} H(\lambda_{_K}) &= H_o + H_{_K} , & (7.6)\\ H_o &\equiv v_{_F}\int_0^{\infty}\tfrac{dr}{2\pi}\left[\psi_{_L}^{\alpha i\dagger}(ir) i\partial_r \psi_{L\alpha i}(ir) - \psi_{_R}^{\alpha i\dagger}(ir) i\partial_r \psi_{R\alpha i}(ir)\right] , & (7.7)\\ H_{_K}(\lambda_{_K}) &\equiv v_{_F}\lambda_{_K}\vec{S}\cdot\tfrac{1}{2}\Big(\psi_{_L}^{\alpha i\dagger}(0) + \psi_{_R}^{\alpha i\dagger}(0)\Big)\Big(\tfrac{1}{2}\vec{\sigma}_{\alpha}^{\ \beta}\Big)\tfrac{1}{2}(\psi_{L\beta i}(0) + \psi_{R\beta i}(0)) & (7.8) \end{aligned}$$

The normalization employed by AL is

$$\{\psi_{_X}^{\alpha i\dagger}(ir), \psi_{X'\beta j}(ir')\} = 2\pi\delta_{XX'}\delta_{\beta}^{\alpha}\delta_{j}^{i}\delta(r - r') \qquad (X, X' = L, R);. \tag{7.9}$$

The Hilbert space on which H acts is a tensor product of free fermion states and the $(2s + 1)$ states of the impurity spin.

This problem can be viewed as a 2-dimensional field theory in the complex plane. We adopt again the notation of eq. (6.40):

$$u \equiv \tau + ix \equiv \begin{cases} z \equiv \tau + ir & \text{for } x > 0 , \\ \bar{z} \equiv \tau - ir & \text{for } x < 0 , \end{cases} \tag{7.10}$$

where $r \equiv |x|$, and $\tau(= it)$ is the imaginary time. Also, write $\partial_z \equiv \frac{1}{2}(\partial_\tau - i\partial_r)$, $\partial_{\bar{z}} \equiv \frac{1}{2}(\partial_\tau + i\partial_r)$. The Heisenberg equations of motion for $r \neq 0$ are

$$\partial_{\bar{z}}\psi_{L\alpha i}(\tau, ir) = 0 \ , \qquad \partial_z\psi_{R\alpha i}(\tau, ir) = 0 \ , \qquad \text{for } r \neq 0 \ . \tag{7.11}$$

They imply that

$$\psi_{L\alpha i}(\tau, ir) = \psi_{L\alpha i}(z) \ , \qquad \psi_{R\alpha i}(\tau, ir) = \psi_{R\alpha i}(\bar{z}) \ , \tag{7.12}$$

and similarly for $\psi^\dagger_L(z)$ and $\psi^\dagger_R(\bar{z})$. Thus, $\psi_L(z)$ is an analytic function of u in the upper half of the complex u-plane (where $u = z$), and $\psi_R(\bar{z})$ can be viewed in two ways, either as an anti-analytic function of u in the upper half of the u-plane, or as an analytic function of u in the lower half of the u-plane (where $u = \bar{z}$) [see Fig. 7.1].

For future reference, let us define the *charge, spin* and *flavor* currents, J^o, J^a and I^b [compare eqs. (A.99) to (A.101)]:

$$J^o_L(z) \ \equiv \ :\psi^{\dagger\mu i}_L(z)\psi_{L\mu i}(z): \tag{7.13}$$

$$J^a_L(z) \ \equiv \ :\psi^{\dagger\alpha i}_L(z)\ \tfrac{1}{2}(\sigma^a)_\alpha{}^\beta\ \psi_{L\beta i}(z): \qquad (a = x, y, z = 1, 2, 3) \tag{7.14}$$

$$I^b_L(z) \ \equiv \ :\psi^{\dagger\alpha i}_L(z)(T^b)_i{}^j\psi_{L\alpha j}(z): \qquad (b = 1, \ldots, k^2 - 1) \ . \tag{7.15}$$

Here : : denotes point-splitting [defined in eq. (A.9)], and the matrices $(T^b)_i{}^j$ are $SU(k)$ generators in the fundamental $k \times k$-dimensional representation [obeying relations like eqs. (A.72), (A.73), with $N \to k$]. For $k = 2$, $(T^b)_i{}^j = \frac{1}{2}(\sigma^b)_i{}^j$.

Right-moving currents $J_R(\bar{z})$ are defined similarly in terms of $\psi_R(\bar{z})$. We shall denote these currents collectively by J^X_L and J^X_R, where x denotes o, a or b.

Eq. (7.12) ensures that these currents are conserved for $r \neq 0$, i.e. $\partial_{\bar{z}}J^X(z) = 0$, $\partial_z J^X(\bar{z}) = 0$. They generate so-called $\mathcal{G} = U(1) \times SU(2)_k \times SU(k)_2$ Kac-Moody

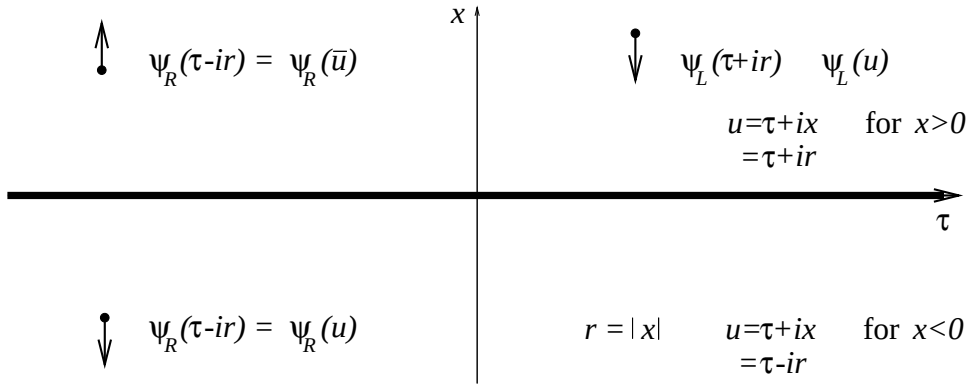

Figure 7.1 .

L- and R-moving fields in the complex plane. The boundary is at $x = 0$. $\psi_L(z)$ is an analytic function of u in the upper half of the complex u-plane (where $u = z$), and $\psi_R(\bar{z})$ can be viewed in two ways, either as an anti-analytic function of u in the upper half of the u-plane, or as an analytic function of u in the lower half of the u-plane (where $u = \bar{z}$).

gauge transformations, parametrized by infinitesimal *analytic* functions $\omega_L^X(z)$ and $\omega_R^X(\bar{z}) \equiv [\omega_L^X(z)]^*$ through:[5]

$$\delta O(\tau, ir) = \int_0^l \frac{dx'}{2\pi} \{\omega_L^X(z')[J_L^X(z'), O(\tau, ir)] \ + \omega_R^X(\bar{z}')[J_R^X(\bar{z}'), O(\tau, ir)]\} \quad (7.16)$$

[see section A.2, especially eq. (A.12) for a discussion of Kac-Moody symmetry transformations].

7.2 Weak-Coupling Description

[AL91b], section 2.1; [Lud94a], section 2.1.

The behavior of the fields $\psi_{L,R}$ and currents $J_{L/R}^X$ at $r = 0$ is determined by the presence or absence of a *boundary interaction,* $H_K \propto \lambda_K \delta(r)$, which may be thought of as a boundary condition on the fields at $r = 0$ (in a sense to be made precise below). In this section we consider the weak-coupling limit ($\lambda_K \ll 1$), in which the boundary condition is trivial [see eq. (7.17)]. However it is highly non-trivial at the over-screened fixed point to which the system flows when $T/T_K \to 0$, which is discussed in subsequent sections.

7.2.1 Weak-Coupling Boundary Conditions

The weak-coupling limit is applicable if $T \gg T_K$ and $\lambda_K \ll 1$. One envisions doing perturbation theory in H_K, and hence expresses all quantities, including H_K, in terms of *free* fields, obeying free Heisenberg equations of motion (with $\lambda_K = 0$). Then it follows from the 3-D to 1-D mapping [see eq. (7.5)] that $\psi_L(z)$ and $\psi_R(\bar{z})$ satisfy the following so-called *weak-coupling boundary condition* at $r = 0$:

$$\psi_{L\alpha i}(\tau + i0) \ = \ \psi_{R\alpha i}(\tau - i0) \ , \quad (7.17)$$

[5] Transformations obeying $\omega_R^X(\bar{z}) \equiv [\omega_L^X(z)]^*$ can be shown to be sufficiently general. For details, see appendix C, section C.1.1.

Since $\psi_L(z)$ and $\psi_R(\bar{z})$ are analytic functions of their arguments and equal to each other on an open domain (the τ-axis), $\psi_R(\bar{z})$ must be the analytic continuation of $\psi_L(z)$ to the lower half of the u plane (where $x = -r < 0$), and hence can be expressed as

$$\psi_{R\alpha i}(\bar{z}) = \psi_{L\alpha i}(\bar{z}) \; . \tag{7.18}$$

It follows immediately from their definition that the currents obey a similar boundary condition,

$$J^X_L(\tau + i0) \;=\; J^X_R(\tau - i0) \; , \qquad\qquad (x = o, a, b) \; , \tag{7.19}$$

which means that "no current of any type flows accross the boundary" [AL91b, p. 653]. To borrow a metaphor from electromagnetism, whatever charge $J^X_L(z)$ carries towards the boundary is carried away again by $J^X_R(\bar{z})$. It follows that $J^X_R(\bar{z})$ must be the analytic continuation of $J^X_L(z)$ into the lower half-plane:

$$J^X_R(\bar{z}) = J^X_L(\bar{z}) \qquad\qquad (x = o, a, b) \; . \tag{7.20}$$

The boundary condition eq. (7.19) is extremely important, because without it, the free theory would be $\mathcal{G} = U(1) \times SU(2) \times SU(k)$ Kac-Moody gauge invariant only "in the bulk" (i.e. for $r \neq 0$), but not on the boundary ($r = 0$). The reason is that surface terms that usually can be neglected when proving the invariance of the action under symmetry transformations, no longer vanish automatically in the presence of a boundary [AL91b, p. 653]. It is shown in detail in Appendix C, section C.1.3, that under spatially varying, analytic, infinitesimal KM gauge transformation such as eq. (7.16), the action $\mathcal{A}$ picks up a surface correction [see second eq. in section C.1.3]:

$$\delta\mathcal{A} \;=\; \int_{-\infty}^{\infty} d\tau \omega^X_L(\tau + i0) \, [J^X_L(\tau + i0) - J^X_R(\tau - i0)] \tag{7.21}$$

Eq. (7.20) ensures that $\delta\mathcal{A} = 0$, so that "the boundary is also KM invariant", and not only the bulk. In general, a boundary CFT is only KM invariant if the currents that generate KM transformations satisfy $J_L^X = J_R^X$ on the boundary.

7.2.2 Weak-Coupling Hamiltonian

The boundary conditions eqs. (7.17) and (7.19) can be used to write $\psi_{R\alpha i}(\bar{z})$ in terms of $\psi_{L\alpha i}(\bar{z})$, and to rewrite the weak-coupling Hamiltonian in the form:

$$H_o = v_F \int_{-\infty}^{\infty} \frac{dx}{2\pi}\, \psi_L^{\alpha i\dagger}(ix)\, i\partial_x\, \psi_{L\alpha i}(ix) \tag{7.22}$$

$$H_K = v_F \lambda_K \vec{S}\cdot \psi_L^{\alpha i\dagger}(i0) \left(\tfrac{1}{2}\vec{\sigma}_\alpha{}^\beta\right) \psi_{L\beta i}(i0) \;=\; v_F \lambda_K \vec{S}\cdot \vec{J}_L(i0)\;. \tag{7.23}$$

This is the form encountered in chapter 5, eq. (5.37), and to be used in chapter 9. It demonstrates two important facts:

(i) Instead of considering R- and L-movers in the upper half of of the complex $u = \tau + ix$ plane ($x > 0$), one can consider L-movers only, but in the full u plane ($x \gtrless 0$);

(ii) In the weak-coupling limit, the effect of the Kondo interaction can be entirely expressed in terms of a coupling to the left-moving $SU(2)$ current $\vec{J}_L(ix)$.

The presence of H_K of course modifies the boundary condition eqs. (7.17), as we know from chapter 5. Therefore, strictly speaking the step of using a weak-coupling boundary condition to write H_K in the form of eq. (7.23) only makes sense in perturbation theory, where by definition one expresses the interaction in terms of free fields. In the strong-coupling regime, one has to follow a different approach. Nevertheless, the weak-coupling form of eqs. (7.22) and (7.23) is very useful, and will be studied at some length in the next section in order to gain the intuition needed to eventually write down the strong-coupling solution.

7.3 Sugawara form for H_o

[AL91b], section 2.1; [Lud94a], section 3.

In this section we write the free Hamiltonian H_o in Sugawara form, discuss the structure of the finite-size spectrum, and write down an expression for the free-electron partition function Z_o. These are steps 1 to 3 of the program outlined in section 6.6, and are prerequisites for understanding the strong-coupling solution. The Sugawara technology used in this section is discussed in detail in Appendix A, especially section A.8, with which the reader is assumed to be familiar. Here we merely summarize the main conclusions.

Since we are interested in the finite-size spectrum, we put the system in a spherical box of radius l, so that $\psi_{\alpha i L}(ix)$ lives on a line of length $2l$, $x \in [-l, l]$. Hence the weak-coupling form eq. (7.22) for H_o becomes (with $v_F \equiv 1$ henceforth)

$$H_o = \int_{-l}^{l} \tfrac{dx}{2\pi}\ \psi_L^{\alpha i\dagger}(ix) i\partial_x \psi_{L\alpha i}(ix). \tag{7.24}$$

It is convenient to impose an anti-periodic[6]. boundary condition on $\psi_{\alpha i L}(ix)$, so that the single-particle eigenenergies of H_o will be of the form $E - E_o = \frac{\pi}{l}(m + \frac{1}{2})$, with $m \in Z_+$ (Z_+ denotes the non-negative integers, and E_o is the energy of the $T = 0$ Fermi sea).

Since the impurity couples only to $\vec{J}_L$ in H_K, i.e. only to the spin degrees of freedom, it is convenient to write H_o in a form in which charge, spin and flavor degrees of freedom are separated, and the $\mathcal{G} = U(1) \times SU(2)_k \times SU(k)_2$ KM gauge symmetry becomes explicit. This can be achieved by writing H_o in a Sugawara form in terms of the currents J_L^o, J_L^a and I_L^b of eqs. (7.13) to (7.15. The Sugawara

[6]This choice of boundary condition is motivated in appendix A, footnote 7.

form is derived in appendix A and given by eq. (A.102) (with $l \to 2l$, $\tilde{N} = 2$ and $c_{tot} = 2k$):

$$\begin{aligned} H_o &= H^c + H^s + H^f \\ &= \int_{-l}^{l} \frac{dx}{2\pi} \left[\frac{1}{4k} :J_L^o J_L^o: + \frac{1}{2+k} :J_L^a J_L^a: + \frac{1}{k+2} :I_L^b I_L^b: \right] , \\ &= -\frac{\pi}{l}\frac{c_{tot}}{24} + \frac{\pi}{l} \sum_{n\in Z} \left[\frac{1}{4k} {}^{*}_{*} J^o_{nL} J^o_{-nL} {}^{*}_{*} + \frac{1}{2+k} {}^{*}_{*} J^a_{nL} J^a_{-nL} {}^{*}_{*} + \frac{1}{k+2} {}^{*}_{*} I^b_{nL} I^b_{-nL} {}^{*}_{*} \right] , \end{aligned} \tag{7.25}$$

Here ${}^{*}_{*}\ {}^{*}_{*}$ denotes normal ordering in momentum space [see eq. (A.58)], and the Fourier modes of current J_L^X are defined by

$$J^X_{nL} \equiv \int_{-l}^{l} \frac{dx}{2\pi} e^{i\pi nx/l} J^X_L(ix) \; ; \qquad J^X_L(ix) \equiv \frac{\pi}{l} \sum_{n\in Z} e^{-i\pi nx/l} J^X_{nL} \; . \tag{7.26}$$

Since H^c, H^s and H^f commute, the representation space of the group $\mathcal{G}$, i.e. the Hilbert space $HS(\mathcal{G})$ on which H_o acts, decomposes into a direct product of charge, spin and flavor towers, denoted by $T^{(c)}_Q$, $T^{(s)}_j$ and $T^{(f)}_\rho$. They are labeled by (Q, j, ρ), the charge, spin and flavor quantum numbers of the corresponding primary states. $Q \in Z$ are the possible charges of the charge primary states $|Q\rangle$; The spin, j, restricted[7] to $j = 0, 1/2, \ldots, k/2$, labels the possible $SU(2)$ representations according to which the spin primary states $|j, j_z\rangle$ can transform. The flavor quantum number ρ labels the $SU(k)$ representations for the flavor primary states $|\rho\rangle$ [for $k = 2$, $\rho \equiv j_f =$ "flavor-spin", with $j_f = 0, 1/2, 1$]. Thus, $HS(\mathcal{G})$ can be represented as follows:

$$HS(\mathcal{G}) := \sum_{\oplus Q} \sum_{\oplus j} \sum_{\oplus \rho} \left[T^{(c)}_Q \otimes T^{(s)}_j \otimes T^{(f)}_\rho \right] \; . \tag{7.27}$$

The internal structure of these towers (discussed in appendix A, sections A.6.2 and A.7.2), is determined by the commutation relations satisfied by the current

[7] The important restriction $0 \le j \le k/2$ for $SU(2)_k$ is derived in [Gins87, eq.(9.30)].

modes J^X_{mL} [given in eqs. (A.103) to (A.105)]. In particular, the spin current modes satisfy

$$\left[J^a_{nL}, J^b_{mL}\right] = i\varepsilon^{abc} J^c_{n+mL} + \tfrac{1}{2} kn\delta^{ab}\delta_{n+m,0} \ , \tag{7.28}$$

known as the $SU(2)_k$ ($SU(2)$-level-k) Kac-Moody algebra.

The energy eigenvalues for a state with charge, spin and flavor quantum numbers (Q, j, ρ) are given by [eq. (A.108)]

$$E_{Qj\rho} - E_{ooo} = \tfrac{\pi}{l}\left[\left(\frac{Q^2}{4k} + m_c\right) + \left(\frac{j(j+1)}{2+k} + m_s\right) + \left(\frac{C_f(\rho)}{k+2} + m_f\right)\right] \tag{7.29}$$

where (m_c, m_s, m_f) are non-negative integers characterizing the energy levels within each tower (the level of the KM descendants). $C_f(\rho)$ is the quadratic Casimir eigenvalue in the flavor sector; for $k = 2$, one has $C_f(\rho) = j_f(j_f + 1)$.

However, we know that in a free-electron theory with anti-periodic boundary conditions and single-particle eigenenergies $E - E_o = \frac{\pi}{l}(m + \frac{1}{2})$ [with $m \in Z_+$], all eigenenergies must be of the form [eq. (A.70)]

$$E_{Qj\rho} - E_{ooo} = \begin{cases} \frac{2\pi}{l} m & \text{for} \quad Q = \text{ even} \ , \\ \frac{2\pi}{l}(m + \frac{1}{2}) & \text{for} \quad Q = \text{ odd} \ , \end{cases} \qquad \text{with } m \in Z_+ \ , \tag{7.30}$$

The spectrum of eq. (7.29) clearly contains many eigenvalues that are not of this form. The reason is that in breaking up H_o into charge, spin and flavor degrees of freedom, we have embedded the free-electron Hilbert space $[HS(\lambda_K = 0)]$ into the much larger Hilbert space $HS(\mathcal{G}) \supset HS(\lambda_K = 0)$, in which charge, spin and flavor excitations are independent – we have effectively "unglued" free electrons into their constituent excitations.

To recover a free-electron theory, these excitations have to be glued back together to form free electrons. This is done by specifying a *free-electron gluing*

condition, i.e. a set of numbers $\{n_o^{(Qj\rho)}\}$, either 0 or 1, that determine which combinations of charge, spin and flavor excitations are allowed in a free electron spectrum [by selecting only those (Q, j, ρ) for which eq. (7.29) is compatible with eq. (7.30)]. For $k = 2$, these numbers were derived in section A.8.2 and are summarized in table A.2.

The structure of the free-electron Hilbert space $[HS(\lambda_K = 0)]$ can be thus be represented symbolically as follows:

$$HS(\lambda_K = 0) := \sum_{\oplus Q} \sum_{\oplus j} \sum_{\oplus \rho} n_o^{(Qj\rho)} \left[T_Q^{(c)} \otimes T_j^{(s)} \otimes T_\rho^{(f)} \right] . \tag{7.31}$$

This is clearly a subspace of $HS(\mathcal{G})$ of eq. (7.27).

The free-electron partition function Z_o is defined as $Z_o = \mathrm{Tr}'\ e^{-\beta H_o}$, where the prime on Tr' indicates that the trace is only over free-electron states. This condition is enforced by inserting the free-electron gluing condition $n_o^{(Q,j,\rho)}$ into the sum over states. Since H^c, H^s and H^f commute, the partition function factorizes:

$$Z_o = \sum_{Q,j,\rho} n_o^{(Q,j,\rho)} \chi_Q^{(c)}(q)\ \chi_j^{(s)}(q)\ \chi_\rho^{(f)}(q) , \qquad \text{where } q \equiv e^{-\pi\beta/l} . \tag{7.32}$$

Here $\chi_Q^{(c)}(q)$ $[\chi_j^{(s)}(q),\ \chi_\rho^{(f)}(q)]$ is a charge [spin, flavor] character,[8] i.e. a partition function over all states within the single tower labeled by Q $[j, \rho]$. The dependence of these quantities on q follows by inspection from the typical form eq. (7.29) of the eigenenergies.

[8] (Non-specialized) $U(1)$-characters are defined in eq. (6.55). See also [AL94], appendix F [eq. (F.23) and the eq. after (F.5)], and [Gep87, eq. (25)].

7.4 Over-Screened Fixed Point: λ_K^*

If one were interested in doing $T \ll T_K$ physics, one would do weak-coupling perturbation theory in $\lambda_K \ll 1$. However, we know that perturbation theory breaks down for $T \lesssim T_K$, and that when $T \to 0$, the system flows to a strong-coupling fixed point (more specifically, an over-screened fixed point, if $s < k/2$) at λ_K^* [NB80] that is inaccessible to perturbation theory (see section 4.1). According to the Kondo lore discussed in section 4.1.2, at the over-screened fixed point the impurity spin is in a sense "absorbed" by the conduction electrons, and the electron fields get "renormalized". The great accomplishment of AL was to make this mathematically precise: they show how the spin is "absorbed", and explicitly construct the new fields into which the old ones "renormalize". However, this comes at a cost: there is no continuous interpolation between the weak-coupling and over-screened theories. The over-screened theory is written down as an Ansatz, based on an inspired hypothesis, which has to be checked *a posteriori* against other methods.

Nevertheless, *a priori* the over-screened fixed point is known from the work of Nozières and Blandin to have the following properties [as summarized by [AL91b, p. 650]]:

1. The theory has global $U(1) \times SU(2) \times SU(k)$ symmetry, since the Kondo interaction H_K does not break this symmetry of H_o.

2. Far away from the boundary we recover the free electron theory as described by the free Hamiltonian H_o of eq. (7.24).

3. The entire system, and boundary the bondary in particular, is scale invari-

ant at $\lambda_K = \lambda_K^*$, since this is a *fixed* point.

7.4.1 Absorption of the Impurity Spin at λ_K^*

[AL91b], section 2.1, [Lud94a], section 3.

To arrive at the over-screened solution of AL, it is useful to adhere to the weak-coupling description of section 7.2 a little longer, to gain some intuition for the effects of H_K (our discussion follows [AL91b, section 2.1]; see also [Lud94a], section 2).

It is clear from eq. (7.23) that the impurity couples only to the spin current $\vec{J}_L$; hence the charge and flavor sectors of the theory are completely unaffected by H_K. The spin part of H takes the following form:

$$H^s = H_o^s + H_K = \int_{-l}^{l} \frac{dx}{2\pi} \left[\frac{1}{2+k} : \vec{J}_L \cdot \vec{J}_L : + 2\pi\lambda_K \vec{J}_L(ix) \cdot \vec{S}\delta(x) \right] \quad (7.33)$$

$$= \frac{\pi}{l} \sum_{n\in Z} \left[\frac{1}{2+k^*} \vec{J}_{nL} \cdot \vec{J}_{-nL^*}^* + \lambda_K \vec{J}_{nL} \cdot \vec{S} \right] . \quad (7.34)$$

Now consider a special value of the coupling, $\lambda_K^* \equiv \frac{2}{2+k}$ (to be identified with the intermediate-coupling fixed point of Nozières and Blandin). Define a new (shifted) spin current, $\vec{\mathcal{J}}_L$, which may be interpreted as the *total spin current* of the combined electron and impurity system, through:

$$\vec{\mathcal{J}}_{nL} \equiv \vec{J}_{nL} + \vec{S} \quad (7.35)$$

$$\vec{\mathcal{J}}_L(ix) \equiv \frac{\pi}{l} \sum_{n\in Z} e^{-i\pi nx/l} \vec{\mathcal{J}}_{nL} = \vec{J}_L(ix) + 2\pi\delta(x)\vec{S} . \quad (7.36)$$

Now "complete the square" and write H^s in terms of $\vec{\mathcal{J}}$:

$$H^s - const = \frac{\pi}{l} \sum_{n\in Z} \frac{1}{2+k^*} \vec{\mathcal{J}}_{nL} \cdot \vec{\mathcal{J}}_{-nL^*}^* = \int_{-l}^{l} \frac{dx}{2\pi} \frac{1}{2+k} : \vec{\mathcal{J}}_L \cdot \vec{\mathcal{J}}_L : , \quad (7.37)$$

where *const* is an (infinite) constant. Thus we see that H^s takes the form of a *free* spin Hamiltonian when written in terms of the new currents: $H^s[\vec{J}] = H_o[\vec{\mathcal{J}}]$.

Now AL made the crucial observation that eq. (7.28) and $[S^a, S^b] = i\varepsilon^{abs}S^c$ imply that

$$[\mathcal{J}^a_{nL}, \mathcal{J}^b_{mL}] = i\varepsilon^{abc}\mathcal{J}^c_{n+mL} + \tfrac{1}{2}kn\delta^{ab}\delta_{n+m,0} \ , \tag{7.38}$$

i.e. *the Fourier modes $\vec{\mathcal{J}}_{nL}$ of the shifted spin current obey the* **same** *KM $SU(2)_k$ commutation relations [compare eq. (7.28)] as the $\vec{J}_{nL}$ of the old spin current!*[9] Consequently the spin current $\vec{\mathcal{J}}^X_L(ix)$, defined as the Fourier transform of these modes $\vec{\mathcal{J}}^X_{nL}$, acts as the generator of KM gauge transformations on the combined electron plus impurity system in the same way as $\vec{J}^X_L(ix)$ did for the free-electron system.[10]

This means that at the over-screened point, the $\mathcal{G} = U(1) \times SU(2) \times SU(k)$ KM gauge invariance that the free theory had (both in the bulk and on the boundary), is restored. To see this in detail, we now show that the theory can completely be brought in the form of a free theory, as follows;

Since the impurity has been completely absorbed and H^s has the form of a free Hamiltonian in terms of $\vec{\mathcal{J}}_L$, it follows (e.g. from Heisenberg equations of motion) that the new spin currents are continuous at $x = 0$, $\vec{\mathcal{J}}_L(\tau + i0^+) = \vec{\mathcal{J}}_L(\tau - i0^+)$. The charge and flavor currents are unaffected by our manipulations in the spin sector, so if we define for convenience $\mathcal{J}^o_L(ix) \equiv J^o_L(ix)$ and $\mathcal{I}^b_L(ix) \equiv I^b_L(ix)$, *all* the $\mathcal{J}^X_L$ currents obey $\mathcal{J}^X_L(\tau + i0^-) = \mathcal{J}^X_L(\tau - i0^+)$. Thus, we can reintroduce right-moving spin currents as in eq. (7.20), by defining

$$\mathcal{J}^X_R(\bar{z}) = \mathcal{J}_L(\bar{z}) \ , \qquad \text{with} \qquad \mathcal{J}^X_R(\tau - i0^+) = \mathcal{J}^X_L(\tau + i0^+) \ , \tag{7.39}$$

[9] This is the reason why we need $\lambda_K = \lambda^*_K$. The "square can be completed" for arbitrary λ_K, using $\vec{\mathcal{J}}_{nL} \equiv \vec{J}_{nL} + \frac{1}{2}(2+k)\lambda_K\vec{S}$, but eq. (7.38) holds only if $\frac{1}{2}(2+k)\lambda_K = 1$.

[10] It is worth emphasizing the logic here: the fundamental definition of the shifted current is eq. (7.35), in terms of Fourier modes $\vec{\mathcal{J}}_{nL}$; once these have been found to obey the KM algebra eq. (7.38), one knows that the currents $\vec{\mathcal{J}}^X_L(ix)$, constructed from them by Fourier transformation, will be KM generators in coordinate space.

and write the over-screened Hamiltonian in the form of L- and R-moving free Hamiltonians:

$$H(\lambda_K^*) = \int_0^l \tfrac{dr}{2\pi} \left[\mathcal{H}_{oL}(ix) + \mathcal{H}_{oR}(ix)\right];, \tag{7.40}$$

$$\mathcal{H}_{oL/R}(ix) = \tfrac{1}{4k} :\mathcal{J}^o_{L/R}\mathcal{J}^o_{L/R}: + \tfrac{1}{2+k} :\mathcal{J}^a_{L/R}\mathcal{J}^a_{L/R}: + \tfrac{1}{k+2} :\mathcal{I}^b_{L/R}\mathcal{I}^b_{L/R}: \tag{7.41}$$

In analogy to our discussion for H_o on p. 197, eqs. (7.40) and (7.39) imply together that $H(\lambda_K^*)$ is invariant, both in the bulk em and on the boundary, under $\mathcal{G} = U(1) \times SU(2)_k \times SU(k)_2$ KM gauge transformations generated by the currents $\mathcal{J}^X(ix)$ which act on the combined electron plus impurity system. Thus, as a direct consequence of the KM commutation relations eq. (7.38), *KM gauge invariance is restored at the over-screened fixed point,* in agreement with requirement 1 on page 203 above.

7.4.2 Over-Screened Gluing Conditions

[AL91b], section 4; [AL92b], section III.B.

Another consequence of eq. (7.38) is that the spin spectrum in the spin sector again has the form

$$E_{j'} - E_o = \tfrac{\pi}{l}\left[\frac{j'(j'+1)}{2+k} + m_s\right] \;, j' = 0, \tfrac{1}{2}, \ldots, k/2\,; \quad m_s \in Z_+\,, \tag{7.42}$$

because the spectrum is completely determined by the $SU(2)_k$ KM algebra. Consequently, the possible eigenenergies at the over-screened fixed point are again precisely of the form of eq. (7.29).

However, this does *not* mean that the over-screened spectrum is the same as the free spectrum, since the gluing condition is not the same. At the over-screened fixed point one has a new *over-screened gluing condition,* denoted by a

set of integers $\{n_*^{(Qj\rho)}\}$, instead of the free-electron gluing condition $\{n_o^{Qj\rho)}\}$. It is in writing down this new over-screened gluing condition that AL had to make a hypothesis that can not be proven *a priori* (but has been convincingly verified *a posteriori*). We now describe in some detail the argument that leads to their hypothesis.

The manipulations in section 7.4 may appear to be rather straightforward. However, eq. (7.35) is more subtle than it appears at first sight, since $\vec{J}_{nL}$ and $\vec{\mathcal{J}}_{nL}$ obey a different algebra than $\vec{S}$ [$SU(2)_k$ vs. $SU(2)$], and correspondingly, $\vec{\mathcal{J}}_L(ix)$ and $\vec{J}_L(ix)$ are conformal fields, while $\vec{S}$ is a local object. Thus we are adding apples and oranges to get apples, which clearly needs to be thought through carefully.

Said differently, the operators in eq. (7.35) act on two different Hilbert spaces. The Hilbert space $HS(\vec{J}+\vec{S})$ on which $\vec{J}_{nL}+\vec{S}$ acts can be represented by

$$HS(\vec{J}+\vec{S}) := \left[\sum_{\oplus j=0}^{k/2} T_j^{(s)}\right] \otimes \mathcal{D}_s \ , \tag{7.43}$$

where $\mathcal{D}_s$ represents the $(2s+1)$-dimensional impurity Hilbert space. However, the Hilbert space $HS(\vec{\mathcal{J}})$ on which $\vec{\mathcal{J}}_{nL}$ acts is simply

$$HS(\vec{\mathcal{J}}) := \left[\sum_{\oplus j'=0}^{k/2} T_{j'}^{(s)}\right] \ , \tag{7.44}$$

[This is because the $\vec{\mathcal{J}}_{nL}$ satisfy the same $SU(2)_k$ KM algebra as the $\vec{J}_{nL}$, so that the space of possible representations must be the same.] Therefore we have to speficy how $HS(\vec{\mathcal{J}})$ and $HS(\vec{J}+\vec{S})$ are related.

Now, *if* we restrict our attention to the $n=0$ modes, then $\vec{\mathcal{J}}_o$, $\vec{J}_o$ and $\vec{S}$ are all ordinary angular momentum operators,[11] acting on $SU(2)$ representations

[11]This so is because the $\vec{J}_o$ and $\vec{\mathcal{J}}_o$ satisfy the ordinary $SU(2)$ algebra.

denoted by $\mathcal{D}_{j'}$, $\mathcal{D}_j$ and $\mathcal{D}_s$, respectively. Eq. (7.35) then simply is the familiar angular momentum coupling of electron spin $\vec{J}_o$ and impurity spin $\vec{S}$ to form a total spin $\vec{\mathcal{J}}_o$, governed by the Clebsch-Gordan series

$$\mathcal{D}_j \otimes \mathcal{D}_s = \sum_{\oplus j'} \tilde{N}_{js}^{j'} \mathcal{D}_{j'} \ , \tag{7.45}$$

where the integers $\tilde{N}_{js}^{j'}$ indicate which representations can occur in the Clebsch-Gordan series:

$$\tilde{N}_{js}^{j'} = \begin{cases} 1 & \text{if} \quad j' \in \{|j-s|, |j-s|+1, \ldots, j+s\} \ ; \\ 0 & \text{otherwise} \ . \end{cases} \tag{7.46}$$

Similarly, in CFT the direct product of two towers can be decomposed into a direct sum of towers according to a "conformal Glebsch-Gordan series", which is called a *fusion rule*. Let $T_j^{(s)}$ and $T_s^{(s)}$ be conformal spin towers of spin j and s, both carrying representations of the $SU(2)_k$ KM algebra [eq. (7.28)]. Then the number of distinct ways in which the spin tower $T_{j'}^{(s)}$ of spin j' occurs in the decomposition of their direct product,

$$T_j^{(s)} \otimes T_s^{(s)} = \sum_{\oplus j'=0}^{k/2} N_{js}^{j'} T_{j'}^{(s)} \ , \tag{7.47}$$

is specified by a set of integers, $\{N_{js}^{j'}\}$, given by[12]

$$N_{js}^{j'} = \begin{cases} 1 & \text{if} \quad j' \in \{|j-s|, |j-s|+1, \ldots, \min\left[j+s, k-j-s\right]\} \ ; \\ 0 & \text{otherwise} \end{cases} \ . \tag{7.48}$$

[12]Eq. (7.48)is the fusion rule for specifically the $SU(2)_k$ KM algebra. However, *any* KM algebra has an associated "conformal Clebsch-Gordan series" or fusion rule of the form eq. (7.47). This fusion rule also acts as a selection rule for OPE coefficients: Let $O_j(z)$ denote a primary field transforming in the j-representation, and write the OPE of two such fields as $O_j(z)O_s(z') = \sum_{j'} C_{js}^{j'}(z')O_{j'}(z')$; then the OPE coefficient functions $C_{js}^{j'}(z')$ can be non-zero only if the corresponding $N_{js}^{j'} \neq 0$.

which constitute the $SU(2)_k$ KM fusion rule. Note that in contrast to eq. (7.46), this fusion rule ensures that no towers with $j > k/2$ ever occur, as required for $SU(2)_k$ towers [compare footnote 7].

However, the situation at hand corresponds neither to pure angular momentum coupling nor to pure $SU(2)_k$ fusion, since in eq. (7.43) $T_j^{(s)}$ is an $SU(2)_k$ spin tower, but $\mathcal{D}_s$ an ordinary $SU(2)$ representation; *a priori* it is not clear what their direct product is. Likewise, $\vec{J}(ix)$ is a conformal current, $\vec{S}$ an ordinary angular momentum operator; *a priori* it is not clear what their sum $\vec{\mathcal{J}}(ix)$ really is. AL cut through this Gordian knot by proposing[13] [AL91b, section 4] (see also [AL92b, III.B] and [Lud94a, p. 19]) the following so-called

Fusion Hypothesis: The "screening or absorption" of an impurity of spin s by k channels of conduction electrons is technically implemented by replacing each spin tower $T_j^{(s)}$ by a set of new spin towers $\{T_{j'}^{(s)}\}$ according to the $SU(2)_k$ KM fusion rule:

$$T_j^{(s)} \otimes \mathcal{D}_s :\rightarrow \sum_{\oplus j'=0}^{k/2} N_{js}^{j'} T_{j'}^{(s)} \tag{7.49}$$

In other words, "fuse" $T_j^{(s)}$ with the impurity spin s as though $\mathcal{D}_s$ were a spin tower $T_s^{(s)}$, which it of course is not — this is why this is a hypothesis and not a derivation.

To be explicit, for $k = 2$ (i.e. $j = 0, \frac{1}{2}, 1$) and $s = \frac{1}{2}$, the fusion hypothesis implies the following replacements:

$$\begin{aligned} T_0^{(s)} \otimes \mathcal{D}_{1/2} &:\rightarrow T_{1/2}^{(s)} \\ T_{1/2}^{(s)} \otimes \mathcal{D}_{1/2} &:\rightarrow T_0^{(s)} \oplus T_1^{(s)} \\ T_1^{(s)} \otimes \mathcal{D}_{1/2} &:\rightarrow T_{1/2}^{(s)} \end{aligned} \tag{7.50}$$

[13] In this thesis, the fusion hypothesis is discussed only for the overscreened case $k/2geqs$, but similar arguments apply to the exactly and underscreened cases, see [Aff90,AL91a].

(Note the absence of any $T^{(s)}_{3/2}$, which would have occured for ordinary $SU(2)$ coupling.)

The fusion rule hypothesis implies that the structure of the Hilbert space at over-screening, $HS(\lambda^*_K)$, is to be obtained from that of the free-electron Hilbert space $HS(\lambda_K = 0)$ of eq. (7.31) by applying the replacement eq. (7.49) to $HS(\lambda_K = 0) \otimes \mathcal{D}_s$:

$$HS(\lambda^*_K) :\equiv \sum_{\oplus Q} \sum_{\oplus j'} \sum_{\oplus \rho} n_*^{(Qj'\rho)} \left[T_Q^{(c)} \otimes T_{j'}^{(s)} \otimes T_\rho^{(f)} \right] , \tag{7.51}$$

were

$$\boxed{n_*^{(Qj'\rho)} \equiv \textstyle\sum_j n_o^{(Qj\rho)} N_{js}^{j'} .} \tag{7.52}$$

The numbers $\{n_*^{(Qj'\rho)}\}$ (either 0 or 1) constitute the *over-screened gluing condition* that governs the physics at the over-screened fixed point.

Clearly $HS(\lambda^*_K)$ is a subspace of $HS(\mathcal{G}$, but it is a *different* subspace than $HS(\lambda_K = 0)$. New *non-Fermi-liquid* combinations of (Q, j', ρ) are allowed by the $\{n_*^{(Qj'\rho)}\}$ that would never occur in a free-electron theory. For example, the Fermi sea, $(0, 0, 0)$ gets mapped onto a "pure spinon", $(0, \frac{1}{2}, 0)$. As AL phrase it, the charge-spin-flavor excitations that are confined or bound together to form free electrons in a free-electron theory, are "deconfined" by the presence of an impurity, and exotic new non-Fermi-liquid combinations arise.

The over-screened spectrum is given by eq. (7.29), subject to the over-screened gluing condition $\{n_*^{(Qj'\rho)}\}$. For $k = 2$ and $s = \frac{1}{2}$, the new set of primary states, and their eigenenergies, are listed in table 7.1, which is obtained from from table A.2 by fusion according to eq. (7.50). Clearly, non-Fermi-liquid eigenenergies (e.g. $\frac{1}{8}, \frac{5}{8}$) show up in the spectrum. These "anomalous" numbers also govern the leading powerlaws of many physical quantities, giving rise to non-Fermi-liquid

exponents[14] (see section 7.4.3 for an example).

As should be clear from our discussion, AL's fusion hypothesis represents an intuitive leap of faith that, though seemingly plausible, has no rigorous *a priori* justification. However, once made, it can and has been tested extensively against other results. The most direct test is to compare the finite-size spectrum with numerical renormalizations [CLN80, AL92b]. The agreement is excellent [Lud94a, table 2], serving as *a posteriori* confirmation of the validity of the fusion hypothesis. Further corroborating evidence is listed in [Lud94a, p. 19].

Summary: Let us summarize the over-screened picture that has emerged as a consequence of the intuitive leap of AL's fusion hypothesis. The over-screened fixed point is described by a *free* Hamiltonian, $\mathcal{H}_{oL} + \mathcal{H}_{oR}$, eq. (7.40), composed of L- and R-moving currents $\mathcal{J}_L^X$ and $\mathcal{J}_R^X$, living in the upper half-plane. The currents obey the over-screened boundary condition $\mathcal{J}_L^X(\tau + i0) = \mathcal{J}_R^X(\tau - i0)$ [eq. (7.39)], which means that the system is $\mathcal{G} = U(1) \times SU(2)_k \times SU(k)_2$ Kac-Moody gauge invariant not only in the bulk, but also on the boundary (just as the free theory was). The Hilbert space is a direct product space of charge, spin and flavor towers [eq. (7.51)] (*without* an extra $\mathcal{D}_s$ impurity Hilbert space), with eigenenergies given by eq. (7.29). *The only difference from the free theory is that these towers are glued together by a over-screened gluing condition* $n_*^{(Qj'j_f)}$ *instead of a free-electron gluing condition* $n_o^{(Qjj_f)}$.

[14] Eigenenergies are related to power-law exponents, since for every tower (say T_j), the lowest eigengenergy of the tower, say $E_j - E_o$, is related to the scaling dimension Δ_j of a primary field $\phi_i(u)$ through $E_j - E_o = \frac{\pi}{l}\Delta_j$ [see appendix C, eq. (B.94)], and Δ_j appears in the correlation function $\langle \phi_i(u)\phi^\dagger(u') = (u - u')^{-2\Delta_j}$.

Table 7.1 Weak- and over-screened spectra, and boundary operator content for $k = 2$, $s = \frac{1}{2}$ (from [Lud94a], Tables 1a, 1b & 1c). The left three columns correspond to free fermions and are derived in appendix A [and taken from table A.2]. They show $\Delta_{Qjj_f} \equiv \frac{l}{\pi}(E_{Qjj_f} - E_{000})$ for those combinations of primary states for which $n_o^{(Qjj_f)} \neq 0$. All other combinations for which $n_o^{(Qjj_f)} \neq 0$ can be obtained from the above by letting $Q \to Q + 4m$ ($m \in Z$). The middle three columns show the over-screened spectrum, i.e. $\Delta_{Qj'j_f} \equiv \frac{l}{\pi}(E_{Qj'j_f} - E_{0\frac{1}{2}0})$ for those combinations of primary fields for which $n_*^{(Qj'j_f)} \neq 0$. These are obtained from the left columns by fusion according to eq. (7.50). The right three columns show the primary boundary operator content of the theory, with $\Delta_{Qj''j_f} \equiv \frac{l}{\pi}(E_{Qj''j_f} - E_{000})$, obtained from the left columns by double fusion according to eq. (7.53).

Free spectrum			Single Fusion			Double Fusion		
$Q\ \ j\ \ j_f$	Δ_{Qjj_f}	n_0	$Q\ \ j'\ \ j_f$	$\Delta_{Qj'j_f}$	n_*	$Q\ \ j''\ \ j_f$	$\Delta_{Qj''j_f}$	n_{KK}
$0\ 0\ 0$	0	1	$0\ \ \frac{1}{2}\ \ 0$	0	1	$0\ 0\ 0$	0	1
						$0\ 1\ 0$	$\frac{1}{2}$	1
$\pm1\ \ \frac{1}{2}\ \ \frac{1}{2}$	$\frac{1}{2}$	1	$\pm1\ \ 0\ \ \frac{1}{2}$	$\frac{1}{8}$	1	$\pm1\ \ \frac{1}{2}\ \ \frac{1}{2}$	$\frac{1}{2}$	1
			$\pm1\ \ 1\ \ \frac{1}{2}$	$\frac{5}{8}$	1	$\pm1\ \ \frac{1}{2}\ \ \frac{1}{2}$	$\frac{1}{2}$	1
$0\ 1\ 1$	1	1	$0\ \ \frac{1}{2}\ \ 1$	$\frac{1}{2}$	1	$0\ 0\ 1$	$\frac{1}{2}$	1
						$0\ 1\ 1$	1	1
$2\ 1\ 0$	1	1	$2\ \ \frac{1}{2}\ \ 0$	$\frac{1}{2}$	1	$2\ 0\ 0$	$\frac{1}{2}$	1
						$2\ 1\ 0$	1	1
$2\ 0\ 1$	1	1	$2\ \ \frac{1}{2}\ \ 1$	1	1	$2\ 0\ 1$	1	1
						$2\ 1\ 1$	$\frac{3}{2}$	1

7.4.3 Boundary Operator Content

[AL91b, p.681], [Lud94a, appendix A.2]

Though the impurity spin has been formally absorbed, it nevertheless causes some Green's functions to behave anomalously when evaluated near $r = 0$: Consider for example the function $G^{(4)} = \langle \psi_L(z_1)\psi_L^\dagger(z_2)\psi_R(z_2^*)\psi_R^\dagger(z_1^*)\rangle$. As shown by AL [AL94, eq.(4.5)] [and in my appendix D, eq. (D.32)], when $r_1 \to 0$, $r_2 \to 0$, this function decays with time like $|\tau_1 - \tau_2|^{-2\Delta}$, where $\Delta = \frac{2}{2+k}$, which is an anomolous, non-Fermi-liquid exponent (and in fact related to the $T^{\frac{2}{2+k}}$ behavior of the conductivity).

This kind of anomalous behavior is analyzed in CFT by introducing the concept of *boundary operators* (introduced in detail in section C.3). These are operators $\Phi_n(\tau)$ that live only at the boundary, at $r = 0$. They can have anomalous scaling dimensions, and govern the behavior of correlation functions close to the boundary.

For future reference, it will be important to have a list of all possible KM primary boundary operators, i.e. to know the *boundary operator content* for the Kondo problem. Using tricks due to Cardy [Car84b], AL showed [AL91b, p.681] [Lud94a, eq.(A.14)] that this list can be given in terms of a set of integers, $\{n_{KK}^{(Qj''\rho)}\}$, that are obtained from the free-fermion gluing conditions by "double fusion" [this formula is derived[15] in section C.5, see eq. (C.80)]:

$$n_{KK}^{(Qj''\rho)} \equiv \sum_j n_o^{(Qj\rho)} N_{js}^{j'} N_{j's}^{j''} \,. \tag{7.53}$$

For each $n_{KK}^{(Qj''\rho)} \neq 0$, a boundary operator with quantum numbers (Q, j'', ρ) exists

[15] In section C.5, the double fusion formula is derived for an arbitrary boundary CFT governed by a fusion principle. Eq. (7.53) follows from eq. (C.80) by applying double fusion in the spin sector while leaving the charge and flavor sectors unchanged.

in the theory. For the case $k = 2$, $s = \frac{1}{2}$, we can obtain these integers by simply applying the fusion replacements (7.50) a second time to the middle section of table 7.1. The resulting non-zero $n_{KK}^{(Qj''\rho)}$ are listed on the right side of table 7.1, together with their scaling dimensions.

7.5 G^{RL} Green's function at $T = 0$

In this section we calculate, at $T = 0$, the G^{RL} Green's function that we are ultimately interested in. The $T \neq 0$ calculation is discussed in chapter 8. The necessary concepts, namely that of boundary states $|K\rangle$ and $|F_-\rangle$ in the closed string picture, were introduced in sections 6.4, and our discussion here parallels that given in section 6.5 and summarized in section 6.6.

We are interested in "impurity-averaged" Green's functions G^{RL}, in the sense that the degrees of freedom of the impurity have been traced out,[16] so that G^{RL} only carries electron indices:

$$G_{\alpha i}^{RL\alpha' i'}(\bar{z}, z') \equiv -\langle \psi_{\alpha i R}(\bar{z}) \psi_L^{\dagger \alpha' i'}(z') \rangle \tag{7.54}$$

As emphasized in chapter 6, page 186, such Green's functions are best calculated in the closed string picture, in which the impurity does not enter explicitly the description at all. The ingredients of the closed string picture are simply L- and R-moving free electron fields $\psi_{\alpha i L}(z)$ and $\psi_{\alpha i R}(\bar{z})$, with, even at the over-screened fixed point, *free*-fermion gluing conditions $n_o^{(Qj\rho)}$ [as emphasized on page 186, and as shown below, eq. (7.64)]. These fields are incident upon boundaries at

[16] Loosely speaking, if we label the local impurity states by $\mu = -s, \ldots, +s$, and the electron quantum numbers by η, then the "impurity-averaged" Green's function can be thought of as $G_{\eta\eta'}^{RL}(\bar{z}, z') \equiv \frac{1}{2s+1} \sum_{\mu\mu'} G_{\eta\mu,\eta'\mu'}^{RL}(\bar{z}, z')$, i.e. average over initial and sum over final impurity states.

$r = 0, l$, and their reflection into each other by these boundaries is characterized by a *Kondo boundary state* $|K\rangle$ at $r = 0$ and a free boundary state $|F_-\rangle$ at $r = l$.

7.5.1 Boundary State Matrix Elements

[AL93], section II; [Lud94a], appendices A, B; [AL94], appenix F.

We now need an important result of boundary CFT, discussed in appendix C, section C.4.1: Cardy showed that *R-L* Green's functions at $T = 0$[17] for KM primary fields $O_{\tilde{a}}(z)$ with quantum numbers $\tilde{a} \equiv (\tilde{Q}, \tilde{j}', \tilde{\rho})$ and scaling dimension $x_{\tilde{a}}$ have the form [eq. (C.55)]

$$-G^{RL}_{\tilde{a}\tilde{b}}(\bar{z}, z') \equiv \langle O_{R\tilde{a}}(\bar{z}) O^{\dagger}_{\tilde{b}L}(z') \rangle \;=\; \frac{\tilde{U}_{K}(\tilde{a})\delta_{\tilde{a}\tilde{b}}}{(\bar{z} - z')^{2x_{\tilde{a}}}} \tag{7.55}$$

where

$$\tilde{U}_{K}(\tilde{a}) = \frac{\langle \tilde{a}|K\rangle}{\langle \mathbf{1}|K\rangle} \; . \tag{7.56}$$

Here $|\mathbf{1}\rangle \equiv |0, 0, 0\rangle$ is the vacuum state, denoted by $|0\rangle$ in appendix C. For a *free* theory ($\lambda_{K} = 0$ and a trivial boundary state $|F\rangle$ at $r = 0$), we have to recover free, trivial *R-L* Green's functions, which means that $\langle \tilde{a}|F\rangle / \langle \mathbf{1}|F\rangle = 1$ for *all* $\tilde{a}$. It follows that $\tilde{U}_{K}(\tilde{a})$ can be written as

$$\tilde{U}_{K}(\tilde{a}) = \frac{\langle \tilde{a}|K\rangle}{\langle \tilde{a}|F\rangle} . \frac{\langle \mathbf{1}|F\rangle}{\langle \mathbf{1}|K\rangle} \; , \tag{7.57}$$

which can be calculated from a knowledge of $\langle \tilde{a}|K\rangle / \langle \tilde{a}|F\rangle$. We now proceed to calculate this ratio, following [AL93, section II] (or [Lud94a, appendix A.2]). The general strategy for finding the Kondo boundary state $|K\rangle$ is the same as in chapter 6, page 188, points 8 to 12 (which might be worth a glance at this

[17] the $T \neq 0$ form can be obtained from that at $T = 0$ by a straightforward conformal transformation, described in section 8.1.

point). Therefore, we merely outline the argument here. A completely detailed derivation is given in [AL94, appendix F].

The boundary state $|K\rangle$ is determined by equating the partition functions calculated in the open string picture $[Z_*(q)]$ and the closed string picture $[Z_*(\tilde{q})]$.[18] In the open-string picture of section 7.4.2, the only difference between the spectrum for $\lambda_K = \lambda_K^*$ and 0 is that different gluing conditions, n_* instead of n_o, select which eigenergies in eq. (7.29) are allowed. Therefore, the over-screened partition function Z_* has exactly the same form as the free partition function Z_o of eq. (7.32), but with the n_o replaced by n_* [compare eq. (6.87)]:

$$Z_*(q) = \sum_{Q,j',\rho} n_*^{(Qj'\rho)} \chi_Q^{(c)}(q)\ \chi_{j'}^{(s)}(q)\ \chi_\rho^{(f)}(q)\ , \qquad \text{where } q \equiv e^{-\pi\beta/l}\ . \tag{7.58}$$

Express this in terms of $\tilde{q} \equiv e^{-4\pi l/\beta}$ by using the modular transformation properties [$\chi_a(q) = S_a{}^{\tilde{a}} \chi_{\tilde{a}}(\tilde{q})$] of the characters,[19] obtaining [compare eq. (6.91)]:

$$Z_*(q) = \sum_{Q,j',\rho} \sum_{\tilde{Q},\tilde{j},\tilde{\rho}} n_*^{(Qj'\rho)} S_Q{}^{\tilde{Q}} S_{j'}{}^{\tilde{j}} S_\rho{}^{\tilde{\rho}} \chi_{\tilde{Q}}^{(c)}(\tilde{q})\ \chi_{\tilde{j}}^{(s)}(\tilde{q})\ \chi_{\tilde{\rho}}^{(f)}(\tilde{q})\ . \tag{7.59}$$

Alternatively, $Z_*(\tilde{q})$ can be expressed as follows in the closed string picture [compare eqs. (6.61) and (6.93)]:

$$\begin{aligned} Z_*(\tilde{q}) &= \langle F_-|e^{-l\tilde{H}_{P-}}|K\rangle \\ &= \sum_{\tilde{Q},\tilde{j},\tilde{\rho}} n_o^{(Qj\rho)} \chi_{\tilde{Q}}^{(c)}(\tilde{q})\ \chi_{\tilde{j}}^{(s)}(\tilde{q})\ \chi_{\tilde{\rho}}^{(f)}(\tilde{q})\ \langle F_-|\tilde{Q},\tilde{j},\tilde{\rho}\rangle\langle\tilde{Q},\tilde{j},\tilde{\rho}|K\rangle\ . \end{aligned} \tag{7.60}$$

Comparing eqs. (7.59) and (7.60),[20] we arrive at a Cardy formula for the boundary

[18] A more careful derivation requires using a "grand-canonical" partition function and non-specialized characters, as we did in chapter 6. This is done in [AL94, appendix F].

[19] For example, the modular transformation properties of $U(1)$ and $SU(2)_1$ characters are given by eqs. (6.57)and (6.89); see also [AL94, eqs. (F.20) - (F.22)], and [Gep87, eq. (25)].

[20] This step assumes that the characters are linearly independent, which is strictly speaking only true if one employs non-specialized characters, as in [AL94, appendix F].

matrix elements [compare eq. (6.94)]:

$$n_o^{(\tilde{Q}\tilde{j}\tilde{\rho})}\langle F_-|\tilde{Q},\tilde{j},\tilde{\rho}\rangle\langle\tilde{Q},\tilde{j},\tilde{\rho}|K\rangle = \sum_{Q,j',\rho} n_*^{(Qj'\rho)} S_Q^{\tilde{Q}} S_{j'}^{\tilde{j}} S_\rho^{\tilde{\rho}} \,. \tag{7.61}$$

Of course, a similar (trivial) relation holds for a free-electron theory ($n_* \to n_o$ and $|K\rangle \to |F\rangle$):

$$n_o^{(\tilde{Q}\tilde{j}\tilde{\rho})}\langle F_-|\tilde{Q},\tilde{j},\tilde{\rho}\rangle\langle\tilde{Q},\tilde{j},\tilde{\rho}|F\rangle = \sum_{Q,j',\rho} n_o^{(Qj'\rho)} S_Q{}^{\tilde{Q}} S_{j'}{}^{\tilde{j}} S_\rho{}^{\tilde{\rho}} \,. \tag{7.62}$$

To simplify this important result, insert eq. (7.52), which gives n_* in terms of the fusion rule coefficients $\left\{N_{js}^{j'}\right\}$, into eq. (7.61). Using a useful mathematical property, known as Verlinde's formula [Ver88],

$$\sum_{j'} N_{js}^{j'} S_{j'}{}^{j} = S_j{}^{\tilde{j}} S_s{}^{\tilde{j}} / S_o{}^{\tilde{j}} \,, \tag{7.63}$$

which expresses the fusion rule coefficients in terms of $SU(2)_k$ modular S-matrix elements, one then finds

$$\begin{aligned} n_o^{(\tilde{Q}\tilde{j}\tilde{\rho})}\langle F_-|\tilde{Q},\tilde{j},\tilde{\rho}\rangle\langle\tilde{Q},\tilde{j},\tilde{\rho}|K\rangle &= \left(S_s{}^{\tilde{j}}/S_o{}^{\tilde{j}}\right) \sum_{Q,j,\rho} n_o^{(Qj\rho)} S_Q{}^{\tilde{Q}} S_j{}^{\tilde{j}} S_\rho{}^{\tilde{\rho}} \\ &= \left(S_s{}^{\tilde{j}}/S_o{}^{\tilde{j}}\right) n_o^{(\tilde{Q}\tilde{j}\tilde{\rho})}\langle F_-|\tilde{Q},\tilde{j},\tilde{\rho}\rangle\langle\tilde{Q},\tilde{j},\tilde{\rho}|F\rangle \end{aligned} \tag{7.64}$$

[using eq. (7.62) for the last line]. Note the emergence of the free-electron gluing condition n_o on the right hand side of this result, which illustrates a general point already emphasized in chapter 6, page 186: whenever the effect of some boundary interaction can completely be described, in the open string picture, by merely changing the gluing condition from n_o for free fermions to a modified gluing condition n_*, obtained from n_o through a fusion rule, then in the closed string picture the *free*-fermion gluing condition n_o reemerges, due to the Verlinde formula, in the Cardy formula for boundary matrix elements. This proves the

assertion made earlier (page 214) that in the closed string picture, one really does only have free electrons fields glued by n_o (and not unusual non-Fermi-liquid excitations of n_* that occur in the closed string picture).

It follows from eq. (7.64) that the desired ratio of boundary matrix elements is

$$\frac{\langle \tilde{Q}, \tilde{j}, \tilde{\rho} | K \rangle}{\langle \tilde{Q}, \tilde{j}, \tilde{\rho} | F \rangle} = S_s{}^{\tilde{j}} / S_o{}^{\tilde{j}} \ . \tag{7.65}$$

Remarkably, these boundary matrix elements differ only by a number given as a ratio of modular S-matrix elements, which, for $SU(2)_k$, are given by [KP84]

$$S^j_{j'} = \sqrt{2/(2+k)} \sin\left[\pi(2j+1)(2j'+1)/(2+k)\right] \ . \tag{7.66}$$

Finally, inserting this result into eq. (7.57), we obtain our final result for the scattering amplitude:

$$\tilde{U}_K(\tilde{Q}, \tilde{j}, \tilde{\rho}) \ = \ \frac{\langle \tilde{(}\tilde{Q}, \tilde{j}, \tilde{\rho}) | K \rangle}{\langle \mathbf{1} | K \rangle} \ = \ \frac{S_s{}^{\tilde{j}}}{S_o{}^{\tilde{j}}} \frac{S_o{}^0}{S_s{}^0} \ . \tag{7.67}$$

7.5.2 Unitarity Paradox

Equiped with eqs. (7.67) and (7.55), let us now calculate the desired electron Green's function $G^{RL\alpha' i'}_{\alpha i}(\bar{z}, z')$ of eq. (7.54). In the closed string picture, the indices of the fermion field $\psi^\dagger$ are $(\tilde{Q}, \tilde{j}, \tilde{\rho}) = (1, \frac{1}{2}, \tilde{\rho}^e)$ (where for $k = 2$, $\rho^e = \frac{1}{2}$), hence

$$\tilde{U}_K(\psi^\dagger) \ = \ \frac{\cos\left[\pi(2s+1)/(2+k)\right]}{\cos\left[\pi/(2+k)\right]} \ . \tag{7.68}$$

Now, since $k \geq 2s$ (for the over- of completely screened case we are considering), we see immediately that $|\tilde{U}_K(\psi^\dagger)|^2 \leq 1$. This means that the scattering matrix for scattering of incident L-moving electrons into outgoing R-moving electrons is not unitary! For the case of interest to us, namely $k = 2$, $s = \frac{1}{2}$, we find the

particularly dramatic result that $\tilde{U}_K(\psi) = 0$, i.e.

$$\langle \psi_{\alpha i R}(\bar{z}) \psi_L^{\dagger \alpha' i'}(z') \rangle \;=\; 0 \tag{7.69}$$

This means that when an incident electron scatters off the impurity, the amplitude to observe an outgoing electron is strictly zero!

The result that $|\tilde{U}_K(\psi^\dagger)|^2 \leq 1$ is known as the *unitarity paradox*. It is a paradox, since on general grounds, we know that the scattering matrix *must* be unitary: when you send in an electron, *something* must come out, with probability one when summed over all possible final states.

For $k = 2$, the resolution of this paradox has very recently been found by Maldacena and Ludwig (ML) [ML95]. Their work demonstrates in a particularly striking way the fact that the $T = 0$ fixed point cannot be understood purely in terms of free electrons. They showed that the free-electron field $\psi^{\dagger \alpha i}$ is not the only field in the theory with quantum numbers $(\tilde{Q}, \tilde{j}, \tilde{\rho}) = (1, \frac{1}{2}, \frac{1}{2})$. There is another field, which we shall call a *spinor-electron* field and denote by $S^{\dagger \alpha i}$, which *also* has $(\tilde{Q}, \tilde{j}, \tilde{\rho}) = (1, \frac{1}{2}, \frac{1}{2})$, but cannot exist in a free-fermion theory. ML showed that (at $T = 0$)

$$\langle S_{\alpha i R}(\bar{z}) \psi_L^{\dagger \alpha' i'}(z') \rangle = \frac{\delta_\alpha^{\alpha'} \delta_i^{i'}}{(\bar{z} - z')} \;, \tag{7.70}$$

which means that an incident L-moving *free* electron scatters with probability 1 into a outgoing R-moving *spinor*-electron.

The spinor-electron field has well-defined mathematical properties, which are summarized in appendix F, where we also attempt to interpret it physically. For the purposes of our calculation of the current in chapter 9, though, all we need to know about it are the following two facts:

1. Spinor-electrons have the same charge, spin and flavor quantum numbers, hence they carry the same amount of current, ev_F per quantum.

2. In order to obtain a unitary scattering matrix, the closed-string Hilbert space, which hitherto had been taken to include only free electron states, has to be *enlarged* to also include spinor-electron states.

3. Spinor-electrons are *only* created upon scattering from the impurity. – The leads inject only free electrons into the system, and no spinor electrons at all.

In the notation of chapter 5, we therefore have to include an extra index $a \equiv f/s$ into our generic index $\eta \equiv (\alpha, i, a)$, to distinghuish free ($a = f$) and spinor- ($a = s$) electrons from each other. Thus we write

$$\psi_\eta \equiv \psi_{\alpha i a} = \begin{cases} \psi_{\alpha i} & \text{if} \quad a = f \quad \text{for free electrons ,} \\ S_{\alpha i} & \text{if} \quad a = s \quad \text{for spinor-electrons .} \end{cases} \tag{7.71}$$

[However $\psi_{\alpha i}$ (without the extra index a) will always refer to free electrons.] Thus, eq. (7.70) implies that (at $T = 0$)

$$-(G^{RL})_\eta{}^{\eta'}(\bar{z}, z') \equiv \langle \psi_{\eta R}(\bar{z}) \psi_L^{\eta'}(z') \rangle = \frac{\delta_\alpha{}^{\alpha'} \delta_i{}^{i'} (\sigma^x)_a{}^{a'} \delta_{a'f}}{(\bar{z} - z')} \ . \tag{7.72}$$

The $\delta_{a'f}$ enforces condition 3 above. Evaluating the $T = 0$ transmsission matrix $\tilde{U}_\eta{}^{\eta'}(\varepsilon)$ of eq. (5.60) from eq. (7.72), using eq. (5.59), gives the following result for the $T = 0$ scattering matrix:

$$\boxed{(\tilde{U}_{oK})_\eta^{\eta'}(\varepsilon) = \delta_\alpha{}^{\alpha'} \delta_i{}^{i'} (\sigma^x)_a{}^{a'} \delta_{a'f}} \tag{7.73}$$

This important result will be used in chapter 9, and concludes our discussion of $T = 0$ Green's functions. In the next chapter, we discuss the effect of taking $T \neq 0$.

Chapter 8

Finite Temperature Kondo Green's Functions

The mechanism through which a change from $T = 0$ to $T \neq 0$ manifests itself in a conformal field theory is through a *change in the geometry* of the manifold on which the theory is defined. In order to ensure the requisite (anti)-periodicity of Green's functions in the τ direction for $T \neq 0$, the underlying geometry changes from being infinite (plane or half-plane) to being finite (cylinder or half-cylinder). This has two consequences:

1. The form of all Green's functions changes; this change is rather trivial, since it can be found by making a conformal transformation that maps the plane to the cylinder.

2. T-dependent finite-size corrections to the fixed point action occur: $S_*(0) \stackrel{T\neq 0}{\longrightarrow} S_*(T) + \delta S(T)$. Their effect can be analyzed by using the concepts of finite-size scaling.

In section 8.1 we explain the plane-to-cylinder mapping of point 1. The rest of the chapter is devoted to discussing point 2. In section 8.2 we state the general renormalization group framework applicable near any critical point, and apply this in section 8.3 to the $T = 0$ strong-coupling Kondo problem. In section 8.4 we consider $T \neq 0$, and show how finite-size scaling arguments[1] can be used to deduce the existence of T-scaling relations in any physical quantity near $T = 0$, and apply this in section 8.5 to the $T \neq 0$ Green's function G^{RL} that is of interest to us.

Strictly speaking, it is not necessary to go through a general RG discussion to find G^{RL} for $T \neq 0$, since one can simply calculate it directly [AL93]. However, we feel that a general discussion will help to elucidate the origin of the scaling relation more clearly than an overly detailed specific calculation.

8.1 Conformal Mapping from Plane to Cylinder

At $T = 0$, the underlying geometry is the infinite (or semi-infinite) complex plane: $u = \tau + ix$, with $\tau \in [-\infty, \infty]$ and $x \in [-\infty, \infty]$ (or $x \in [0, \infty]$).[2] Let us consider for the moment the infinite plane, without any special boundary at $x = 0$. Let $O_i(u, \bar{u})$ be a (Virasoro) primary field of scaling dimension $(x_i, \bar{x}_i)$. This means, by definition, that under a conformal transformation $\tilde{u} = w(u)$ (where $w(u)$ is an

[1] For an extensive discussoin of the use of finite-size scaling arguments inthe application of CFT to lattice models in 2-dimensional statistical mechanics, see [CH93].

[2] In previous chapters, we considered a finite size in the x direction, $x \in [0, l]$. However, this was done only as a tool to find the boundary state $|B\rangle$ by calculating the finite-size spectrum and the partition function. If one is interested in calculating Green's functions, then once $|B\rangle$ is known, one always takes $l \to \infty$.

analytic function) it transforms as follows [see eq. (B.2)]:

$$\tilde{u} = w(u) \ : \qquad O_i(u,\bar{u}) = \left(\frac{\partial\tilde{u}}{\partial u}\right)^{x_i}\left(\frac{\partial\tilde{\bar{u}}}{\partial\bar{u}}\right)^{\bar{x}_i}\tilde{O}_i(\tilde{u},\tilde{\bar{u}})\ . \tag{8.1}$$

The L- and R-moving fields that we have encountered so far are chiral fields, depending only on u (or $\bar{u}$), and hence have $\bar{x}_i = 0$ (or $x_i = 0$). Conformal invariance alone is sufficient to completely determine the form of all two- and three-point functions of such (Virasoro) primary fields to be [Gins87, eqs. (2.4), (2.5)]:

$$\langle O_i(u_1,\bar{u}_1)O_j(u_2,\bar{u}_2)\rangle_o = \frac{\delta_{ij}C_i}{u_{12}^{2x_i}\bar{u}_{12}^{2\bar{x}_i}} \tag{8.2}$$

$$\langle O_i(u_1,\bar{u}_1)O_j(u_2,\bar{u}_2)O_k(u_3,\bar{u}_3)\rangle_o = \frac{C_{ijk}}{u_{12}^{\Delta_{ijk}}u_{23}^{\Delta_{jki}}u_{13}^{\Delta_{kij}}\bar{u}_{12}^{\bar{\Delta}_{ijk}}\bar{u}_{23}^{\bar{\Delta}_{jki}}\bar{u}_{13}^{\bar{\Delta}_{kij}}} \tag{8.3}$$

where $u_{12} \equiv u_1 - u_2$, $x_{ijk} \equiv x_i + x_j - x_k$, etc. and C_i and C_{ijk} are constants.

Now, for $T \neq 0$, we know that two-point functions of (fermion) boson fields become (anti)-periodic in the imaginary time direction, with period $\beta = 1/T$. This means that the geometry changes from the infinite plane (parametrized by $u = \tau + ix$) to a cylinder of radius β [Fig. 8.1] Choose $\tilde{u} = \tilde{\tau} + i\tilde{x}$ as coordinates parametrizing the cylinder, then there is a "seam" on the cylinder, at which $\tilde{\tau} = -\beta/2$ and $\tilde{\tau} = \beta/2$ are identified.

If a theory is conformally invariant, any $T \neq 0$ Green's function can be obtained from the corresponding $T = 0$ one by the following conformal transformation, which maps the infinite plane (or half-plane) onto the infinitely long cylinder (or half-cylinder):

$$u = \tan\tfrac{\pi}{\beta}\tilde{u}\ , \qquad \frac{du}{d\tilde{u}} = \tfrac{\pi}{\beta}(1+u^2) = \tfrac{\pi}{\beta}(1+\tan^2\tfrac{\pi}{\beta}\tilde{u}) \tag{8.4}$$

This maps the τ-axis ($r = 0$) onto the $\tilde{\tau}$-axis ($\tilde{r} = 0$), and $\tau = \pm\infty$ onto $\tilde{\tau} = \pm\beta/2$. Using eq. (8.1), we can immediately find the form of any $T \neq 0$

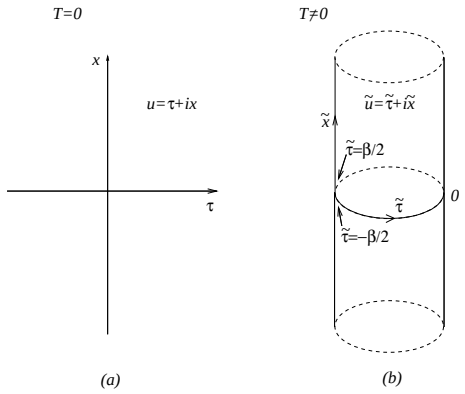

Figure 8.1 (a) At $T = 0$, the theory is defined on the infinite plane of half-plane, parametrized by $z = \tau + ix$. (b) At $T \neq 0$, the theory is defined on the infinite cylinder or half-cylinder, parametrized by $\tilde{u} = \tilde{\tau} + i\tilde{x}$. The two geometries are related through the comformal map: $z = \tan\frac{\pi}{\beta}\tilde{u}$.

2-point function of (Virasoro) primary fields from eq. (8.2):

$$\begin{aligned}
&\langle \tilde{O}_i(\tilde{u}_1, \bar{\tilde{u}}_1)\tilde{O}_j(\tilde{u}_2, \bar{\tilde{u}}_2)\rangle_T \\
&= \left(\frac{\partial u_1}{\partial \tilde{u}_1}\right)^{x_i}\left(\frac{\partial \bar{u}_1}{\partial \bar{\tilde{u}}_1}\right)^{\bar{x}_i}\left(\frac{\partial u_2}{\partial \tilde{u}_2}\right)^{x_j}\left(\frac{\partial \bar{u}_2}{\partial \bar{\tilde{u}}_2}\right)^{\bar{x}_j}\langle O_i(u_1, \bar{u}_1)O_j(u_2, \bar{u}_2)\rangle_o \qquad (8.5)\\
&= \delta_{ij}\frac{\left[\frac{\pi}{\beta}(1+u_1^2)\right]^{x_i}\left[\frac{\pi}{\beta}(1+\bar{u}_1^2)\right]^{\bar{x}_i}\left[\frac{\pi}{\beta}(1+u_2^2)\right]^{x_j}\left[\frac{\pi}{\beta}(1+\bar{u}_2^2)\right]^{\bar{x}_j}}{u_{12}^{2x_j}\bar{u}_{12}^{2\bar{x}_j}} \qquad (8.6)\\
&= \frac{\delta_{ij}}{s_{12}^{2x_i}\bar{s}_{12}^{2\bar{x}_j}} \qquad (8.7)
\end{aligned}$$

where we have defined $s_{12} \equiv \frac{\beta}{\pi}\sin\frac{\pi}{\beta}(\tilde{u}_1 - \tilde{u}_2)$, and the fourth line follows from the third using standard trigonometric identities. Eq. (8.7) agrees with the result eq. (A.36) found in appendix A by more elementary means. Likewise, for any $T \neq 0$ three-point function of (Virasoro) primary fields one finds

$$\langle \tilde{O}_i(\tilde{u}_1, \bar{\tilde{u}}_1)\tilde{O}_j(\tilde{u}_2, \bar{\tilde{u}}_2)\tilde{O}_k(\tilde{u}_3, \bar{\tilde{u}}_3)\rangle_T = \frac{C_{ijk}}{s_{12}^{\Delta_{ijk}}s_{23}^{\Delta_{jki}}s_{13}^{\Delta_{kij}}\bar{s}_{12}^{\bar{\Delta}_{ijk}}\bar{s}_{23}^{\bar{\Delta}_{jki}}\bar{s}_{13}^{\bar{\Delta}_{kij}}} \qquad (8.8)$$

This result will be used in section 8.5.

8.2 General RG Framework near $T = 0$

We have repeatedly stated that the $T = 0$ strong-coupling Kondo problem is at a fixed (and hence critical) point. In this and subsequent sections, we explain how the behavior of the model near its $T = 0$ fixed point fits into the conceptual framework of critical phenomena. In particular, we show how the effects of taking $T \neq 0$ can be analyzed using concepts of finite size scaling.

Let us introduce the standard terminology of the renormalization group to analyze the neighborhood of this fixed point. We shall consider the properties of the action, $S = \int dx d\tau \mathcal{L}$, instead of the Hamiltonian, because the behavior of the correlation functions that we are interested in is governed by S via a path-integral, written symbolically as

$$\langle O_i(u_i) \dots O_j(u_j) \rangle = \int \mathcal{D}O_i \dots \int \mathcal{D}O_j \left[e^{-S} O_i(u_i) \dots O_j(u_j) \right] . \tag{8.9}$$

If we place ourselves sufficiently close to the fixed point in parameter space, the system is governed by an action of the form

$$S(\{\lambda_m\}) = S_* + \sum_m \lambda_m \delta S_m . \tag{8.10}$$

Here $S_* = S(\{0\}) = \int dx d\tau \mathcal{L}_*$ is the action at the critical point (corresponding to the Hamiltonian H_*), the parameters λ_m determine the distance from the critical point, and the δS_m are eigenvectors of the RG transformation: Under an RG transformation that shrinks all length scales by a factor $b > 1$, $x \xrightarrow{RG} x = b\tilde{x}$ (this notation means that expressions are rewritten by substituting $b\tilde{x}$ for x), we have

$$\lambda_m \delta S_m \xrightarrow{RG} \tilde{\lambda}_m \delta S_m \qquad \text{with} \quad \tilde{\lambda}_m = b^{\alpha_m} \lambda_m . \tag{8.11}$$

We shall denote relevant and irrelevant perturbations by superscripts $^{(r)}$ and $^{(i)}$ where necessary, i.e. $\alpha_m^{(r)} > 0$, $\alpha_m^{(i)} < 0$.

To place the system at the physical critical point, one has to fine-tune the relevant perturbations to zero (set $\lambda_m^{(r)} = 0$, i.e. place the system on the critical manifold). Under repeated RG transformations, the irrelevant perturbations will then decrease ($\lambda_m^{(i)} \to 0$) and the system will flow to S_*. If, however, one starts with some $\lambda_m^{(r)} \neq 0$ (though small), it will grow under RG transformations, and the system will eventually flow away from S_*.

8.3 Application to $T = 0$ Kondo problem

How does all this apply to the 2-channel Kondo problem?

The reason why the $T = 0$ strong-coupling Kondo problem is at a fixed point is simple:[3] it is described by a conformal field theory, which is conformally invariant at $T = 0$, and hence *scale invariant* (since scale transformations are a subset of conformal transformations). Therefore, it must be exactly *at* a fixed point.

To be more explicit, we have seen in section 7.4 that the strong-coupling theory at $T = 0$ can be described by a conformal field theory in the complex upper half-plane, defined by the strong-coupling Hamiltonian H_* of eq. (7.40) (in which we may take $l = \infty$ for present purposes), with the currents satisfying the boundary condition eq. (7.39). This manifestly has the Hamiltonian of a free theory (the fact that one has to use strong-coupling gluing conditions $n_*^{(Qj'\rho)}$ is inconsequential here). Hence it is invariant[4] under all conformal transformations that *preserve the geometry* of the system, i.e. that map the upper half-plane, and in particular the boundary, onto itself. In particular, it is scale invariant, and hence at a fixed

[3] Perhaps it would be more accurate to say it the other way round: the reason why the strong-coupling Kondo problem at $T = 0$ can be described by a conformal field theory is that at $T = 0$, it is at a critical point.

[4] This is demonstrated explicitly in section A.2, eq. (A.18), in the fermionic representation.

point. However, as we shall see in the next section, transformations which change the geometry in a way that introduces a new length scale into the problem (such as the one that maps the plane onto the cylinder, in which case the new length scale is the radius of the cylinder), break scale invariance, because of the presence of this new length scale. Hence, such transformations take the system away from the fixed point.

The strong-coupling model we have written down may be thought of as a fine-tuned version of some much more general model. In particular, we have fine-tuned to zero the temperature T, the magnetic field H, the asymmetry energy Δ of the impurity,[5] and all anisotropies $\delta\lambda_K^a$ $(a = x, y, z)$ in the coupling between local spin and electron spin. It can be shown [AL92b] that the $\delta\lambda_K^a$ are irrelevant perturbations, but H and Δ are relevant; T is also relevant, in a finite-size scaling sense, as we shall see.

To make these statements precise, we have to define an RG transformation for our problem. An RG is designed to drive the system away from criticality by shrinking all length scales, in an attempt to reduce the correlation length (if it is not ∞). Thus it involves a rescaling transformation $x \xrightarrow{RG} x = b\tilde{x}$ with $b > 1$. Usually, the step of shrinking length scales is preceded by a coarse-graining step, designed to eliminate graininess on the smallest length scales in the problem (which would not bear shrinking).

However, for a conformal field theory, one does not need such a coarse-graining step, because the system is *by definition* scale-invariant on all length scales – it does not have any graininess that needs to be integrated out. Of course, in

[5] In the magnetic Kondo model, Δ corresponds to a local magnetic field that only acts on the impurity

converting some initial model, defined on a lattice, to a CFT, one has to introduce a cut-off, in our case the bandwidth Λv_F, which determines the graininess in the theory. However, we are considering temperatures $T \ll \Lambda v_F$ and hence neglect all terms of order $T/\Lambda v_F$. Therefore correlation functions at a given $T \ll \Lambda v_F$ would not notice if we coarse-grained by reducing the cut-off from Λ to $\tilde{\Lambda}$ during an RG transformation.

In a conformal field theory, therefore, an RG transformation is extremely simple. Writing $u = \tau + ix$ and $\tilde{u} = \tilde{\tau} + i\tilde{x}$, it is nothing more than a rescaling coordinate transformation, combined with a corresponding rescaling of all conformal fields:

$$u = \stackrel{RG}{\longrightarrow} u = b\tilde{u} \ , \qquad \text{with} \quad b > 1 \ . \tag{8.12}$$

$$O_i(u, \bar{u}) \stackrel{RG}{\longrightarrow} O_i(u, \bar{u}) = b^{-(x_i + \bar{x}_i)} \tilde{O}_i(\tilde{u}, \tilde{\bar{u}}) \ . \tag{8.13}$$

The notation $\stackrel{RG}{\longrightarrow}$ means: *rewrite* x by substituting $b\tilde{x}$ for it, and $O_i(u, \bar{u})$ by substituting $b^{-(x_i+\bar{x}_i)}\tilde{O}_i(\tilde{u}, \tilde{\bar{u}})$ for it. The reason why the fields have to be rescaled too, is simply that eq. (8.12) is a conformal transformation (albeit an exceedingly trivial one), under which all conformal fields $O_{iL}(u)$, $O_{iR}(\bar{u})$, have to be rescaled according to their scaling dimensions $x_i + \bar{x}_i$ [compare eq. (8.1)] to ensure that correlation functions are invariant, in the sense of eq. (8.5). Thus, eq. (8.13) is a relation that is true whenever used inside correlation functions $\langle O_i(u) \ldots \rangle$.

Now, in a boundary CFT, a perturbation δS_m in eq. (8.10) can be either a bulk or a boundary perturbation. Consider first the case $T = 0$ for the Kondo problem, where the boundary ($r = 0$) is the entire τ axis. A bulk *bulk perturbation* consists

of some operator, i.e. some conformal field, integrated over all of the half-plane:

$$\delta S_m^{(bulk)}[O_n(u,\bar{u})] = \int_0^\infty dx \int_{-\infty}^\infty d\tau O_n(u,\bar{u}) \tag{8.14}$$

However, it can also be a *boundary perturbation*, depending on a *boundary operator*, which by definition is a field $O_m(\tau)$ that lives only on the boundary. Such a field transforms as $\tilde{O}_m(\tilde{\tau}) = \left(\frac{\partial\tau}{\partial\tilde{\tau}}\right)^{x_m} O_m(\tau)$ under conformal transformations $\tilde{z} = \tilde{z}(z)$ *that map the boundary onto itself*, i.e. for which $\tilde{\tau} = \tilde{\tau}(\tau)$. In this case the boundary perturbation is simply a single $\int d\tau$ integral:

$$\delta S_m^{(bnd)}[O_m(\tau)] = \int_{-\infty}^\infty d\tau O_m(\tau) \tag{8.15}$$

Applying the RG transformation, eqs. (8.12) and (8.13) to these perturbations

$$\begin{aligned}
\delta S_m^{(bulk)}[O_m(u,\bar{u})] &\xrightarrow{RG} b^{2-x_m-\bar{x}_m}\int_0^\infty d\tilde{x}\int_{-\infty}^\infty d\tilde{\tau}\,\tilde{O}_m(\tilde{u},\tilde{\bar{u}}) \\
&= b^{2-x_m-\bar{x}_m}\,\delta\tilde{S}_m^{(bulk)}[\tilde{O}_m(\tilde{u},\tilde{\bar{u}})] \qquad (8.16)\\
\delta S_m^{(bnd)}[O_m(\tau)] &\xrightarrow{RG} b^{1-x_m}\int_{-\infty}^\infty d\tilde{\tau}\tilde{O}_n(\tilde{\tau}) \;=\; b^{1-x_m}\delta\tilde{S}_m^{(bnd)}[O_m(\tau)] \qquad (8.17)
\end{aligned}$$

it follows immediately that the scaling exponents α_m in eq. (8.11) are $\alpha_m^{(bulk)} = 2 - x_m - \bar{x}_m$ for a bulk perturbation, and $\alpha_m^{(bnd)} = 1 - x_m$ for a boundary perturbation. Hence, we come to the important conclusion that the RG relevance or not of a perturbation δS_m in the action is determined directly by the scaling dimension x_m of the corresponding field $O_m(u)$: a bulk perturbation is relevant if $(x_m + \bar{x}_m) < 2$, and a boundary perturbation is relevant if $x_m < 1$.

8.4 $T \neq 0$: Finite Size Scaling

We wrote down eqs. (8.14) and (8.15) at $T = 0$. At finite $T \neq 0$, an important new ingredient enters the analysis: as discussed in the previous section, the underlying

geometry then is the cylinder, with radius $\beta = 1/T$, instead of the plane. Thus, our fields now live on a system of finite size ("L"$= \beta$), and the temperature plays the role of L^{-1}.

Every $T = 0$ time integral $\int_{-\infty}^{\infty} d\tau$ in the action becomes $\int_0^{\beta} d\tau$ at $T \neq 0$. Therefore, the RG coordinate transformation eq. (8.12) involves rewriting β in terms of a new $\tilde{\beta} = \beta/b$:

$$\int_0^{\beta} d\tau \xrightarrow{RG} b \int_0^{\beta/b} d\tilde{\tau} \equiv b \int_0^{\tilde{\beta}} d\tilde{\tau} \ , \tag{8.18}$$

in other words

$$\beta \xrightarrow{RG} \beta = b\tilde{\beta} \ . \tag{8.19}$$

This means that the action S is no longer form-invariant under RG-transformations (even if all $\lambda_m = 0$), since it explicitly depends on β through the upper limit in $\int_0^{\beta} d\tau$. Likewise, the perturbations δS_m about the fixed point also become explicitly β-dependent. Thus, for $T \neq 0$, an explicit T-dependence shows up in all terms in eq. (8.10), which hence has to be written as

$$S(\{\lambda_m\}, T) = S_*(T) + \sum_m \lambda_m \delta S_m(T) \ . \tag{8.20}$$

Eq. (8.19) means that temperature behaves like a relevant perturbation, which means that it must be fine-tuned (to be very small) by the experimenter in order to place the system at the physical critical point. If experimentally we place ourselves close to but not at the fixed point, with $T \neq 0$, then T will grow under application of the RG ($\tilde{T} > T$), and one will flow away from the fixed point.

Within the above framework, it is now easy to understand the occurence of scaling relations near $T = 0$. Consider any physical quantity, G, expressed as an expectation value of fields, integrated over space and/or time. (As a concrete

example, consider the Green's function of eq. (8.26) below.) In general, G will depend on T and the parameters λ_m: $G = G(\lambda_m, T)$. Under the RG transformation of eqs. (8.12) and (8.13), which simply constitutes a *rewriting* of G in terms of new variables, we obtain

$$G(\{\lambda_m\}, T) \xrightarrow{RG} G(\{\lambda_m\}, T) = b^{-\Delta} G(\{b^{\alpha_m}\lambda_m\}, bT) \ , \tag{8.21}$$

where Δ is the scaling dimension of G. Choosing $b = T^{-1}$, we find the scaling form

$$\boxed{G(\{\lambda_m\}, T) = T^{\Delta} G(\{T^{-\alpha_m}\lambda_m\}, 1) \ .} \tag{8.22}$$

Thus, the existence of scaling forms near $T = 0$ in the Kondo problem can be understood in a straight-forward way as a finite-size scaling effect.

8.5 Example: Finite-Size Scaling for the Green's Function G^{RL}

[AL93]

In this section and the next, we explain how AL calculated the $T \neq 0$ correction to the two-point function G^{RL} [AL93]. This serves as an explicit illustration of the general finite-size scaling arguments presented in the previous section. The final result, eqs. (8.36) and (8.38, will be used in chapter 9.

In chapter 7 we found the $T = 0$ form for G^{RL} to be given by eq. (7.72). To find its $T \neq 0$ form, view $\psi_R(\bar{z})$, which is an anti-analytic function of $z = \tau + ir$ in the upper half plane, as the analytic continutation of $\psi_L(z)$ into the lower half plane, i.e. $\psi_R(\bar{z}) = \psi_L(\bar{z})$, which is an analytic function of $\bar{z} = \tau - ir$ in the lower half plane (the general theory behind this construction is due to Cardy and is

reviewed in appendix C, section C.1). Then, using eq. (8.7) with $x_\psi = \frac{1}{2}$, the $T \neq 0$ version of eq. (7.72) is

$$G_o^{RL}{}_{\eta\eta'}(\bar{z}, z') = -\langle \psi_{\eta R}(\bar{z}) \psi^\dagger_{\eta' L}(z') \rangle = \frac{-\tilde{U}_{\eta\eta'}}{\frac{\beta}{\pi} \sin \frac{\pi}{\beta}(\bar{z} - z')} , \tag{8.23}$$

where $\bar{z} = \tau - ir$ and $z' = \tau' + ir'$, and $\tilde{U}_{\eta\eta'}$ is given by eq. (7.73). Now suppose that $\lambda_m \neq 0$ for one of the boundary perturbations in eq. (8.20), and consider the correction δG_m^{RL} to this function that arises due to the presence of the boundary perturbation

$$\lambda_m \delta S_m = \lambda_m \int_0^\beta d\tau' O_m(\tau') . \tag{8.24}$$

where $O_m(\tau')$ is a boundary operator of scaling dimension x_m. For the moment we consider a general boundary operator; later we shall specialize to a particular case. Thus, write

$$G^{RL}_{\eta\eta'}(\bar{z}, z') \equiv G_o^{RL}{}_{\eta\eta'}(\bar{z}, z') + \delta G_m^{RL}{}_{\eta\eta'}(\bar{z}, z') \tag{8.25}$$

where, doing first-order perturbation theory in λ_m in eq. (8.9), the correction is given by

$$\delta G_m^{RL}{}_{\eta\eta'}(\bar{z}, z') \equiv \langle \psi_{\eta R}(\bar{z}) \left[\lambda_m \int_0^\beta d\tau'' O_m(\tau'') \right] \psi^\dagger_{\eta' L}(z') \rangle \tag{8.26}$$

Henceforth we shall suppress all indices on $\delta G_m^{RL}{}_{\eta\eta'} \equiv \delta G$.

For the purposes of chapter 9, we need the transmission coefficient $\tilde{U}_{\eta\eta'}(\epsilon)$, given in terms of the spectral function $\mathcal{A}^{RL}_{\eta\eta'}(\varepsilon; r, r')$ of $G^{RL}_{\eta\eta'}$ through eq. (5.60). Due to the boundary perturbation, $\tilde{U}_{\eta\eta'}(\epsilon)$ will pick up a correction term:

$$\tilde{U}_{\eta\eta'}(\epsilon) = \tilde{U}_{\eta\eta'} + \frac{1}{2\pi} \delta \mathcal{A}^{RL}_{\eta\eta'}(\epsilon, r, r') e^{-i\epsilon(r+r')}. \tag{8.27}$$

The boundary-term correction to the spectral function, $\delta\mathcal{A}$, can be found from the Matsubara transform of δG [compare eq. (5.59), with $\mu_{\eta'} = 0$, since AL's G^{RL}

is an equilibrium Green's function],

$$\delta G(i\omega_n, r, r'; T) = \int_0^\beta d\tau e^{i\omega_n \tau} \delta G(\tau - ir, ir') = \int \frac{d\epsilon}{2\pi} \frac{\delta \mathcal{A}(\epsilon, r, r')}{i\omega_n - \epsilon} \quad (8.28)$$

$$= \lambda_m \int_0^\beta d\tau e^{i\omega_n \tau} \int_0^\beta d\tau'' \langle \psi_{\eta R}(\tau - ir) O_m(\tau'') \psi^\dagger_{\eta' L}(ir') \rangle \quad (8.29)$$

which is therefore the quantity we shall calculate.

Let us first illustrate the finite-size scaling arguments of section 8.4 by showing that $\delta G(i\omega_n)$ obeys a scaling form: Rewrite eq. (8.29) in terms of new coordinates $\tilde{u}$ and fields $\tilde{O}(\tilde{u})$, related to the old through the RG coordinate transformation of eqs. (8.12) and (8.13),

$$\bar{z} = b\tilde{\bar{z}}\,, \qquad r' = b\tilde{r}'\,, \qquad \tau' = b\tilde{\tau}'\,, \quad (8.30)$$

$$\psi_{\eta R}(\bar{z}) = b^{-1/2}\tilde{\psi}_{\eta R}(\tilde{u})\,, \qquad \psi^\dagger_{\eta' L}(ir') = b^{-1/2}\tilde{\psi}^\dagger_{\eta' L}(i\tilde{r}')\,, \qquad O_m(\tau'') = b^{-x_m}\tilde{O}_m(\tilde{\tau}'')$$

to obtain

$$\delta G(\omega_n, r, r'; T) = \left[b^{1-1/2-1/2}\right]\left[b^{1-x_m}\lambda_m\right] \quad (8.31)$$

$$\times \int_0^{\beta/b} d\tilde{\tau} e^{i\omega_n b\tilde{\tau}} \int_0^{\beta/b} d\tilde{\tau}'' \langle \tilde{\psi}_{\eta R}(\tilde{\tau} - i\tilde{r}) \tilde{O}_m(\tilde{\tau}'') \tilde{\psi}^\dagger_{\eta' L}(i\tilde{r}') \rangle$$

$$= (b^{1-x_m}) \delta G(b\omega_n, \tilde{r}, \tilde{r}'; bT)\,. \quad (8.32)$$

Setting $b = T^{-1}$, which simply means choosing units in which the cylinder has circumference 1, we obtain the desired scaling form for δG,

$$\boxed{\delta G(\omega_n, r, r'; T) = T^{(x_m - 1)} \delta G(\omega_n/T, rT, r'T; 1)} \quad (8.33)$$

in agreement with our general expectations based on eq. (8.22). Moreover, the scaling function $\delta G(\omega_n/T, rT, r'T; 1)$ can be calculated from the $T = 1$ version of eq. (8.28),

$$\delta G(\tilde{\omega}_n, \tilde{r}, \tilde{r}'; 1) \equiv \int_0^1 d\tilde{\tau} e^{i\tilde{\omega}_n \tilde{\tau}} \delta G(\tilde{\bar{z}}, \tilde{z}')_{T=1} \quad (8.34)$$

where the $T = 1$ Green's function of eq. (8.26) needed here is an example of the finite-T 3-point functions whose general form is given by eq. (8.8) (with $x_\psi = \frac{1}{2}$, and provided that O_m is Virasoro primary):

$$\delta G(\tilde{\tilde{z}}, \tilde{z}')_{T=1} = \int_0^1 d\tilde{\tau}'' \frac{C^K_{\psi m}\ (\pi^{-1} \sin \pi[\tilde{\tau} - i(\tilde{r} + \tilde{r}')])^{x_m - 1}}{(\pi^{-1} \sin \pi[\tilde{\tau} - \tilde{\tau}'' - i\tilde{r}]\ \pi^{-1} \sin \pi[\tilde{\tau}'' - i\tilde{r}'])^{x_m}} \tag{8.35}$$

where $C^K_{\psi m}$ is a constant [corresponding to C_{ijk} in eq. (8.8)].

Eqs. (8.34) and (8.35) completely and exactly determine the scaling function. Its calculation therefore is merely a matter of doing the two integrals $\int_0^1 d\tilde{\tau} e^{i\tilde{\omega}_n \tilde{\tau}} \int_0^1 d\tilde{\tau}''$, which is a straight-forward though rather non-trivial exercise in complex analysis (see [AL93]).

8.6 Leading Irrelevant Correction

Depending on whether $x_m < 1$ or > 1, the boundary perturbation δS_m is relevant or irrelevant, and will grow or die out as the temperature is lowered. To determine whether a certain perturbation δH_m that may be present in the weak-coupling Hamiltonian (e.g. anisotropic Kondo couplings or an asymmetry splitting Δ of the two levels of the impurity), will drive the system away from the fixed point or not, one must identify the boundary operator $O_m(\tau)$ that is the "strong-coupling version" of δH_m, and check whether $x_m \gtrless 1$.

How does one know which strong-coupling boundary operators $O_m(\tau)$ correspond to a given weak-coupling δH_m? In brief, three steps are involved.

1. Make a list of all possible boundary operators. This has been done in section 7.4.3, using the general method explained in section C.5.2, and the resulting list of primary boundary operators is contained in the right part of table 7.1.

2. Since the RG cannot generate a strong-coupling operator with a symmetry different from the one initially present at weak-coupling, pick from this list the most relevant operator that has the *same symmetries* as the weak-coupling perturbation δH_m. This symmetry analysis is also straightforward, and discussed, for the so-called leading irrelevant operator, in section D.5. [A number of other δH_m's are also discussed in [AL92b].]

3. Check whether the corresponding 3-point function $\langle \psi_R O_m \psi_L^\dagger \rangle$ vanishes identically or not, i.e. whether the coefficient $C^K_{\psi m}$ in eq. (8.35) vanishes identically or not. This is in general a highly non-trivial question, since its answer requires the analysis of four-point functions. We introduce the necessary techniques (due to [CL91]) in appendix C, and show in appendix D how Affleck and Ludwig calculated [AL94] the function $\langle \psi_L \psi_L^\dagger \psi_R \psi_R^\dagger \rangle$. A list of all boundary operators with $x_m \leq \frac{3}{2}$ for which $C^K_{\psi m} \neq 0$ is given in table D.1.

Suppose that all relevant couplings have been fine-tuned to zero. The leading $T \neq 0$ correction to G, namely $\delta G(T)$, will then arise from the so-called *leading irrelevant operator*, i.e. the operator with smallest scaling dimension $x_m (> 1)$. According to eq. (8.33), $\delta G(T)$ will be proportional to $T^{(x_m - 1)}$; all other more irrelevant perturbations will give corrections to δG proportional to subleading powers of T.

AL have shown ([AL91b, p. 657], [AL93, eq. (3.26)] and [AL94, eq. (4.6)]) that for the overscreened k-channel Kondo problem ($k/2 > s$), the leading irrelevant operator, which they denote by $\vec{\mathcal{J}}_{-1} \cdot \vec{\phi}$, is Virasoro primary with scaling dimension $x_\Delta \equiv 1 + \Delta$, where $\Delta \equiv \frac{2}{2+k}$. [We recapitulate their argument in appendix D, section D.5.] Thus, $\delta G \propto T^\Delta$, and for $k = 2$, we have $\delta G \propto T^{1/2}$. This, therefore,

is the origin of the $T^{1/2}$ scaling exponent in the 2-channel Kondo problem.

AL have calculated the scaling function of eq. (8.34) corresponding to an insertion of the leading irrelevant operator in complete detail [AL93], by explicitly performing the integrals in eqs. (8.34) and (8.35) for $x_m = 1+\Delta$. This calculation is an impressive display of complex-analysis skills, but is conceptually straightforward and will not be repeated here. Instead, we merely cite the final result of interest to us. After all necessary manipulations have been performed to extract the spectral function $\delta\mathcal{A}$ of eq. (8.28) from their result [AL93, eq. (3.48)], the transmission coefficient of eq. (8.27) takes the following form, for $k = 2$:

$$\tilde{U}_{\eta\eta'}(\varepsilon, T) = \delta_{\alpha\alpha'}\delta_{ii'}\left[\sigma^x_{aa'} + \delta_{aa'}\mathcal{U}\right] e^{i\phi} \ , \tag{8.36}$$

where

$$\mathcal{U}(\varepsilon, T) = \lambda_{1/2} T^{1/2} \tilde{\Gamma}(\varepsilon/T) \ . \tag{8.37}$$

The first term in eq. (8.36) follows from eq. (7.73), and in the second term, the scaling function $\tilde{\Gamma}(x)$ is given by [AL93, eq. (3.50)][6]

$$\begin{aligned} \tilde{\Gamma}(x) \ = \ & \left\{ \tfrac{3}{2\sqrt{2}} (2\pi)^{\Delta} 2 \sin(\pi\Delta) \int_0^1 du [u^{(-ix)/(2\pi)} u^{-1/2} (1-u)^{\Delta} F(u) \right. \\ & \left. - \frac{\Gamma(1+2\Delta)}{\Gamma^2(1+\Delta)} u^{(\Delta-1)} (1-u)^{-(1+\Delta)}] \right\} \end{aligned} \tag{8.38}$$

$[F(u) \equiv F(1+\Delta, 1+\Delta, 1; u)$ is a hypergeometric function.] The $\int du$ integral can be done numerically for any value of x, thus giving us an explicit expression for the scaling function (the real part of which turns out to be negative definite). This is the result we were after. It will be used in chapter 9 to calculate the universal scaling curve $\Gamma(v)$ that is our ultimate goal. It is interesting to note

[6] Writing $u^{ix} = \cos x \ln u - i \sin x \ln u$, it follows that the real and imaginary parts of $\tilde{\Gamma}(x)$ are even and odd in x, respectively.

that

$$\mathcal{U}(\varepsilon,T) \propto 2\mathrm{Im}\left(\Sigma^R(\varepsilon,T) - \mathrm{Im}\Sigma^R(\varepsilon,0)\right) = -\left(\tau^{-1}(\varepsilon,T) - \tau^{-1}(\varepsilon,0)\right) \ , \quad (8.39)$$

where $\delta\Sigma^R(\varepsilon,T)$ is the retarded bulk electron self-energy calculated by AL [AL93, eq. (3.50)], and $\tau^{-1}(\varepsilon,T)$ the corresponding scattering rate.

Finally, let us say a few words about relevant perturbations. In [AL92b], it was shown that a for the 2-channel, $s = \frac{1}{2}$ Kondo problem, an impurity asymmetry energy (AE) with $\lambda_{AE} \propto \Delta$, and a channel anisotropy (CA) with $\lambda_{CA} = H$, are relevant perturbations, with scaling dimensions $x_{AE} = \frac{1}{2}$ and $x_{CA} = \frac{1}{2}$. According to the general scaling relation eq. (8.22), this immediately implies that

$$\delta G(T,H,\Delta) = T^{1/2}\delta G\left(1, H/T^{1/2}, \Delta/T^{1/2}\right) \ . \quad (8.40)$$

This is the scaling result that was used in section 3.3, eq. (3.19), to analyze the magnetic field dependence of the conductance.

It should be emphasized that the scaling relation found here is only expected to hold for $T/T_K \ll 1$. The reason is that we really are doing perturbation theory in T. There are of course many other irrelevant operators, that give subleading corrections in T/T_K, which are small relative to the leading one that we have calculated only if $T/T_K \ll 1$. However, since each of these enters with a different, unknown universal prefactor, it is not very meaningful to explicitly calculate their contributions. For each new term added, one would get one extra unknown parameter, which one would have to treat as a fitting parameter when comparing theory to experiment. However, the more fitting parameters, the less meaningful the comparison.

Chapter 9

Calculation of scaling curve

In this chapter we compute the scaling curve $\Gamma(v)$ and compare it to the experimental curve of Fig. 3.10(b), and to numerical calculations by Hettler, Kroha and Hershfield (HKH) [HKH94].

Our strategy is straightforward. We calculate the current $I(V,T)$ through the nanoconstriction from the general expression, eq. (5.52) (and eq. (9.1) below), derived in chapter 5. The main ingredients of this formula are the scattering amplitudes $\tilde{U}_{\tilde{\eta}\eta}(\varepsilon)$. In chapters 7 and 8, we showed how these could be extracted, for the magnetic 2-channel Kondo problem, from the CFT solution of Affleck and Ludwig, and found a scaling form [see eq. (8.37)]. In section 9.1 we define a model that describes non-magnetic 2-channel Kondo scattering, in the sense proposed by Zawadowski [Zaw80,VZ83] and discussed in chapter 4, and calculate in section 9.2 the corresponding $\tilde{U}_{\tilde{\eta}\eta}(\varepsilon)$'s from AL's theory. In section 9.3, these are inserted into eq. (9.1); the differential conductance, $G(V,T) = \partial_V I(V,T)$, is found to obey a scaling relation [see eq. (9.28)], with the scaling function $\Gamma(v)$ completely determined by AL's theory [see eq. (9.26)]. In section 9.4 we show

that in general the scattering amplitudes will have V-dependent corrections, but argue that these are of order V/T_K. Finally, after a few words about the NCA calculations of HKH in section 9.5, in section 9.6, we compare the CFT result for the scaling curve with experiment and NCA calculations by Hettler, Kroha and Hershfield [HKH94].

9.1 The Nanoconstriction 2-Channel Kondo Model

The general expression for the current through a nanoconstriction derived in chapter 5, eq. (5.52), is

$$I \;=\; \tfrac{e}{h} \sum_{\tilde{\eta}\eta} \!\!\int\! d\varepsilon \tfrac{1}{2} \left[\tilde{U}^{\dagger}_{\eta\tilde{\eta}'}(\varepsilon) I_{\tilde{\eta}'\tilde{\eta}} \tilde{U}_{\tilde{\eta}\eta}(\varepsilon) \;+\; \sigma_{\tilde{\eta}} \delta_{\tilde{\eta}\eta} \right] f(\varepsilon, \eta) \tag{9.1}$$

where for simplicity we have taken the geometrical transmission coefficients $T_{\tilde{\eta}} = 1$, and have written $I_{\tilde{\eta}'\tilde{\eta}} \equiv \sigma_{\tilde{\eta}} \delta_{\tilde{\eta}'\tilde{\eta}}$. As a reminder, $\eta = (\sigma_\eta, n, i)$ is a collective index labeling the various discrete quantum numbers of the electrons (see section 5.2, page 122): n lables various discrete orbital channels, $i = \uparrow, \downarrow$ is the Pauli electron spin, and the index $\sigma_\eta = \pm$ distinguishes physical L-movers ($\sigma_\eta = +$) from physical R-movers ($\sigma_\eta = +$). The right and left leads are at chemical potentials $\mu_\pm = \mu_\eta$, with $\mu_\eta = +eV/2$ and $-eV/2$ for the R- and L-leads, respectively. They inject L-moving and R-moving electrons, with energy ε and quantum number η, into the system from the right and left, traveling toward the constriction [Fig. 9.1], weighted according to the distribution function for free electrons in the corresponding lead,

$$f(\varepsilon, \eta) = f_o(\varepsilon - \mu_\eta) = \frac{1}{e^{\beta(\varepsilon - \mu - \eta)} + 1} \; . \tag{9.2}$$

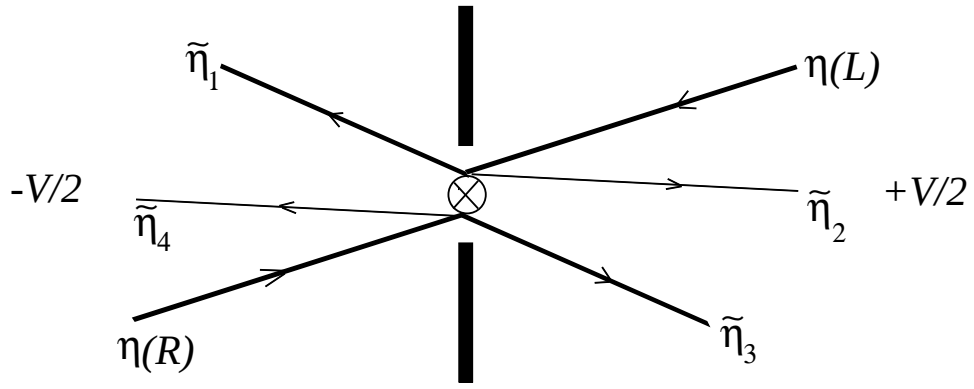

Figure 9.1 L-and R-moving electrons ($\sigma_\eta = \pm$) are injected towards a nanoconstriction from right and left leads, that are at chemical potentials $\mu_\pm = \mu \pm eV/2$. They are scattered by impurities in the nanoconstriction from state η to state $\tilde{\eta}$ with amplitude $\tilde{U}_{\tilde{\eta}\eta}$.

Expression eq. (9.1) for the current counts the difference between the number of L- and R-moving electrons of index $\tilde{\eta}$, weighting them with $\sigma_{\tilde{\eta}} = \pm$; the second term corresponds to incident electrons that have not yet been scattered, the first to electrons that have been scattered from their initial state η to a final state $\tilde{\eta}$, with scattering amplitude $\tilde{U}_{\tilde{\eta}\eta}$.

Before defining the model we intend to use to describe the electron-TLS scattering, some comments about the properties it should have are in order. The main feature of the data that we have to account for is the occurence of a scaling form for the conductance, and in particular, of a scaling exponent $T^{1/2}$. As Ludwig first pointed out, scaling forms and a scaling exponent $T^{1/2}$ appear naturally in the 2-channel Kondo problem at its $T = 0$ fixed point: As we saw in chapter 8, for 2-channel Kondo scattering, the scattering amplitudes extracted from AL's theory have the following scaling form [see eqs. (8.36) and (8.36)]:

$$\tilde{U}_{\eta\eta'}(\varepsilon, T) = \delta_{\alpha\alpha'}\delta_{ii'}\left[\sigma^x_{aa'} + \delta_{aa'}\mathcal{U}\right] e^{i\phi} \ , \qquad \text{where} \quad \mathcal{U} = \lambda T^{1/2}\tilde{\Gamma}(\varepsilon/T) \ , \qquad (9.3)$$

where $\alpha = \pm$ is the (pseudo)-spin index that couples to the impurity, $i = 1, 2$

is a channel index and $a = f/s$ distinguishes "free" from "spinor"-electrons (the latter had to be introduced to ensure that $\tilde{U}_{\eta\eta'}$ is unitary). This is the result we would wish to employ in eq. (9.1) to obtain a scaling form for $I(V,T)$.

In the spirit of Zawadowski's non-magnetic Kondo theory [chapter 4], we envision now that in general, the many discrete orbital channels, labeled by η, can be scattered into each other when an electron scatters off a TLS, and that at the same time, the TLS can change its state (labeled by $\mu = \uparrow, \downarrow$). A corresponding Hamiltonian would have matrix elements $\langle \eta\mu | H_{scat} | \eta'\mu' \rangle$ that are non-zero (but diagonal in the Pauli spin i, which cannot be flipped by scattering off a TLS) for a large number of combinations of states $\langle \eta, \mu |$ and $| \eta'\mu' \rangle$. As explained in chapter 4, Zawadowski has shown that such a Hamiltonian gives rise to a non-magnetic Kondo effect. As the temperature is lowered, the coupling constants generally grow, and perturbation theory breaks down. Moreover, Zawadowski has shown [section 4.2.4] that in general, for each value of $i = \uparrow, \downarrow$, there will be two linear combinations of the various η-channels, which we denote by $\alpha = 1, 2$, for which the effective coupling constants $\langle \alpha i, \mu | H_{scat} | \alpha' i', \mu' \rangle$ grow more rapidly than for any other combination of channels. (Heuristically, these may be thought of as electron waves "centered" on the two impurity positions.) Therefore, if the temperature is small enough, all other channels decouple from the impurity (and hence merely contribute to the large boring background signal), and one is left with an effective Hamiltonian with matrix elements [see eq. (4.23)]

$$\langle \alpha i, \mu | H_{scat} | \alpha' i', \mu' \rangle = \lambda_K \delta_{ii'} \tfrac{1}{2} \vec{\sigma}_{\alpha\alpha} \cdot \vec{S}_{\mu\mu'} \ . \tag{9.4}$$

Thus, one ends up with a 2-channel Kondo problem, α being the pseudospin and i the channel index, to which the AL theory can be applied if $T/T_K \ll 1$.

We have written down an expression that is isotropic in pseudospin space [see section 4.2.5], because it is known that pseudospin anisotropies are irrelevant perturbations near the strong-coupling fixed point [AL92b, p. 7924], and hence negligible for sufficiently small temperatures.

One might hope that eq. (9.3), inserted into eq. (9.1), would immediately give a scaling contribution to I with scaling exponent $T^{1/2}$. However, this is not true, due to an important subtlety: in eq. (9.3), the leading term in $\tilde{U}_{\eta\eta'}(\varepsilon)$ is purely *off-diagonal* in the index a (this is the so-called unitarity paradox), which means that $U^\dagger U$ does not have a term linear in $\mathcal{U}$, and instead $U^\dagger U = 1 + \mathcal{U}^2$. Therefore it seems as though the current, being *quadratic* in $\tilde{U}$, will not have a scaling exponent of $T^{1/2}$, but of T. This, incidentally, is the reason why the exactly solvable non-equilibrium Kondo model studied by Schiller and Hershfield [SH95a] is not useful for our purposes.

The key to resolving this potential problem is contained in AL's calculation of the bulk linear response conductivity [AL93], which, using a Kubo formula, they show to be $\sigma(T) = \sigma_o + \sigma_1(T/T_K)^{1/2}$. However, they show that the $T^{1/2}$ occurs only if one takes into account *cross-terms* [AL93, eq. (C7)] between scattering channels that undergo Kondo scattering (s-wave scattering in their case) and channels that only undergo trivial (non-Kondo) scattering ($l \neq 0$ angular momentum channels in their case). Thus, a model which is to yield $T^{1/2}$ as conductance exponent has to contain cross-terms between Kondo scattering channels and trivial scattering channels.

The ingredient that is missing in the discussion above is forward and backward scattering between L- and R-movers. As was emphasized in section 4.4.1,

Table 9.1 Meaning of indices $\eta \equiv (\sigma_\eta, \alpha, i, a)$ used in non-equilibrium 2-channel Kondo problem

σ_η:	$(L,R) = (+,-)$	=	L/R movers	=	species index
α:	$(1,2)$	=	discrete orbital channels	=	pseudospin index
i:	$\uparrow, \downarrow$	=	Pauli spin	=	channel index
a:	f/s	=	free/spinor-electrons	=	"unitarity" index

in a nanoconstriction geometry, the two pseudospin channels $\alpha = 1, 2$ are both comprised of L- and R-movers, and the Hamiltonian must describe backward and forward scattering between these in addition to (or simultaneously with) pseudospin scattering [see page 109 for the detailed argument]. As we shall see below, incorporating this additional L-R scattering automatically leads to a model that does contain the abovementioned cross-terms. [After taking even and odd linear combinations of L- and R-moving electrons, it turns out (see section 9.2) that the even channels undergo Kondo scattering, and the odd channels only trivial scattering.]

The model that we adopt is defined by the following Hamiltonian (in weak-coupling language) [compare eq. (4.27)]:

$$H_o = v_F \sum_\eta \int_{-\infty}^{\infty} \tfrac{dx}{2\pi} \psi_\eta^\dagger(ix) i\partial_x \psi_\eta(ix) \,, \tag{9.5}$$

$$H_{scat} = \lambda_K \psi_{\sigma\alpha i}^\dagger(0) \left[V_{\sigma\sigma'} \, (\tfrac{1}{2}\vec{\sigma}_{\alpha\alpha'} \cdot \vec{S}) \right] \psi_{\sigma'\alpha' i}(0) \,. \tag{9.6}$$

The meaning of the indices $\eta = \{\alpha, \tau, \sigma, (a)\}$ carried by the electron field $\psi_\eta(x)$ are summarized in table 9.1: $\sigma_\eta = (L,R) = (+,-)$, the *species index*, distinguishes L- from R-movers; $\alpha = (1,2)$ is the orbital *pseudospin* index that Kondo-couples to the TLS-spin $\vec{S}$; and $i = \uparrow, \downarrow$, the Pauli spin, is a *channel* index. In addition, we

shall need below the "unitarity"-index $a = f/s$ that distinguishes free electrons ($a = f$) from the "spinor"-electrons ($a = s$) that can be created upon scattering off the impurity [see section 7.5.2]. However, since this index is a feature of the strong-coupling solution, it enters only in the scattering amplitudes $\tilde{U}_{\tilde{\eta}\eta}$, and is not needed in writing down the weak-coupling Hamiltonian eq. (9.6) that defines the model.

The scattering Hamiltonian H_{scat} describes processes in which the pseudospin of electrons and TLS can be flipped by $(\frac{1}{2}\vec{\sigma}_{\alpha\alpha'} \cdot \vec{S})$, but simultaneously L- and R-movers can also undergo forward- and backscattering into each other through $V_{\sigma\sigma'}$. In general, $V_{\sigma\sigma'}$ can be any Hermitian 2×2 matrix. However, it is actually sufficient to consider only the very simple case

$$V_{\sigma\sigma'} = \tfrac{1}{2} \begin{pmatrix} 1 & 1 \\ 1 & 1 \end{pmatrix}_{\sigma\sigma'} , \tag{9.7}$$

for reasons to be explained below. With this choice, our model is equivalent (after a Schrieffer-Wolf transformation) to a model recently studied by Hettler *et. al.* using numerical NCA techniques, with whose results we shall compare our own.

The Hamiltonian introduced above is strictly speaking not a 2-channel Kondo Hamiltonian, since $\sigma_\eta = \pm$ and $i = \uparrow, \downarrow$ give *four* different combinations of indices that do not Kondo-couple to $\vec{S}$. However, the equilibrium model can be mapped onto a 2-channel model by making a unitary transformation,

$$\overline{\psi}_{\bar{\eta}} = N_{\bar{\eta}\eta}\psi_\eta , \qquad N_{\bar{\eta}\eta} \equiv N_{\bar{\sigma}\sigma}\delta_{\bar{\alpha}\alpha}\delta_{\bar{i}i} , \tag{9.8}$$

chosen such that it diagonalizes $V_{\sigma\sigma'}$. We shall refer to the fields ψ_η as L/R fields and the $\overline{\psi}_{\bar{\eta}}$ as even/odd fields, and always put a bar over all indices and matrices refering to the even/odd basis. For our present choice eq. (9.7) for $V_{\sigma\sigma'}$, $N_{\bar{\sigma}\sigma}$ is

given by

$$N_{\bar{\sigma}\sigma} = \frac{1}{\sqrt{2}} \begin{pmatrix} 1 & 1 \\ 1 & -1 \end{pmatrix}_{\bar{\sigma}\sigma} , \qquad \left(NVN^{-1}\right)_{\bar{\sigma}\bar{\sigma}'} \equiv \overline{V}_{\bar{\sigma}\sigma} = \begin{pmatrix} 1 & 0 \\ 0 & 0 \end{pmatrix}_{\bar{\sigma}\bar{\sigma}'} . \tag{9.9}$$

Thus H_{scat} becomes

$$H_K = \lambda_k \, \overline{\psi}^{\dagger}_{\bar{\sigma}\bar{\alpha}\bar{i}}(0) \begin{pmatrix} \frac{1}{2}\vec{\sigma}_{\bar{\alpha}\bar{\alpha}'} \cdot \vec{S} & 0 \\ 0 & 0 \end{pmatrix}_{\bar{\sigma}\bar{\sigma}'} \overline{\psi}_{\bar{\sigma}'\bar{\alpha}'\bar{i}}(0) \, . \tag{9.10}$$

Thus, in the $\overline{\psi}_{\bar{\eta}}$ basis, one set of channels, which we shall call the *odd channels* ($\bar{\sigma} = o$), completely decouples from the impurity. The other set of channels, which we shall call the *even channels*, constitute a true 2-channel Kondo problem, to which we shall apply AL's solution.

If one chooses a more general $V_{\sigma\sigma'}$ than eq. (9.7), the odd channel will not completely decouple, but (barring some accidental degeneracies) the even and odd channels will always couple to $\vec{S}$ with different strenghts. At low enough temperatures, the one coupled more weakly can be assumed to decouple completely (à la Zawadowski [VZ83], see section 4.2.4), leaving again a 2-channel Kondo problem for the even channel. This is the reason why it is sufficient to take $V_{\sigma\sigma'}$ as in (9.7), and not necessary to consider the more general case.

9.2 Scattering Amplitudes

We are interested only in the *weakly non-equilibrium* regime of very small voltages, $V/T_K \ll 1$. In this regime, it is by definition sufficient to calculate the scattering states and scattering amplitudes from the *equilibrium* theory of AL (see the discussion in section 5.4.5). Hence, the $\tilde{U}_{\tilde{\eta}\eta}$ will be V-independent, and the only V-dependence enters in the Fermi-functions $f(\varepsilon, \eta)$ of eq. (9.2). V-

dependent corrections to $\tilde{U}_{\tilde{\eta}\eta}$ can then in principle be calculated in perturbation theory in V/T_K, which will be done in section 9.4.

Since Kondo scattering generates spinor-electrons (see eq. (9.12) below), we henceforth have to extend our index η to include the index $a = f/s$, i.e. $\eta = (\sigma_\eta, \alpha, i, a)$. However, spinor-electrons are only created *upon scattering* off the TLS, and are certainly not injected from the leads. Thus, only free electrons with $a = f$ are injected by the leads. This requirement will be enforced by writing $f(\varepsilon, \eta) \equiv \delta_{af} f(\varepsilon, \eta)$ for the thermal weighting functions that govern how electrons are injected from the leads.

Since even and odd channels are decoupled in the even/odd basis, the scattering amplitudes, denoted by $\overline{U}_{\bar{\eta}\bar{\eta}'}(\varepsilon)$, have the form

$$\overline{U}_{\bar{\eta}\bar{\eta}'}(\varepsilon) = \delta_{\bar{\alpha}\bar{\alpha}'}\delta_{\bar{i}\bar{i}'} \begin{pmatrix} \overline{U}^{(e)}_{\bar{a}\bar{a}'} & 0 \\ 0 & \overline{U}^{(o)}_{\bar{a}\bar{a}'} \end{pmatrix}_{\bar{\sigma}\bar{\sigma}'} , \tag{9.11}$$

where $\overline{U}^{(e)}$ and $\overline{U}^{(o)}$ are the scattering amplitudes in the even and odd channels, respectively. In the even channel, we have 2-channel Kondo scattering, with $\overline{U}^{(e)}$ given by eq. (8.36), but in the odd channel, no scattering takes place at all. Therefore, we have

$$\overline{U}^{(e)}_{\bar{a}\bar{a}'} = [\sigma^x_{\bar{a}\bar{a}'} + \delta_{\bar{a}\bar{a}'}\,\mathcal{U}]\, e^{i\phi_e} \qquad \text{where } \mathcal{U}(\varepsilon, T) = \lambda T^{1/2}\tilde{\Gamma}(\varepsilon/T) \tag{9.12}$$

$$\overline{U}^{(o)}_{\bar{a}\bar{a}'} = \delta_{\bar{a}\bar{a}'} , \tag{9.13}$$

where $e^{i\phi_e}$ is a trivial phase shift that can occur in the Kondo channel in the absence of particle-hole symmetry (see [AL93, section IV]).

To find the scattering amplitudes $\tilde{U}_{\tilde{\eta}\eta}(\varepsilon)$ in the L-R basis in terms of the $\overline{U}_{\bar{\eta}\bar{\eta}'}(\varepsilon)$ in the e/o basis, note that they are derived from the corresponding L-R

and e/o Greens's functions through

$$\tilde{U}_{\tilde{\eta}\eta}(\varepsilon) \propto \langle \psi_{\tilde{\eta}R} \psi^\dagger_{\eta L} \rangle \ , \qquad \overline{U}_{\bar{\eta}\bar{\eta}'}(\varepsilon) \propto \langle \overline{\psi}_{\bar{\eta}R} \overline{\psi}^\dagger_{\bar{\eta}'L} \rangle \ , \tag{9.14}$$

hence

$$\tilde{U}_{\tilde{\eta}\eta}(\varepsilon) = N^\dagger_{\tilde{\eta}\bar{\eta}} \overline{U}_{\bar{\eta}\bar{\eta}'}(\varepsilon) N_{\bar{\eta}'\eta} \ . \tag{9.15}$$

Inserting eq. (9.15) into eq. (9.1), we can thus write the current as

$$I \ = \ \tfrac{e}{h} \sum_\eta \int d\varepsilon \tfrac{1}{2} \left[P_\eta(\varepsilon) \ + \ \sigma_\eta \right] f(\varepsilon, \eta) \tag{9.16}$$

where

$$P_\eta(\varepsilon) \equiv \sum_{\tilde{\eta}'\tilde{\eta}} \left(N^\dagger \overline{U}^\dagger N \right)_{\eta\tilde{\eta}'} I_{\tilde{\eta}'\tilde{\eta}} \left(N^\dagger \overline{U} N \right)_{\tilde{\eta}\eta} \tag{9.17}$$

Let us analyze this matrix product index by index. All matrices are diagonal in α, i, hence the sums $\sum_{\tilde{\alpha}\tilde{i}}$ in P_η are trivial. Next consider matrix multiplication in the index σ. Using eq. (9.9), we find

$$\left(N^\dagger \overline{U} N \right)_{\tilde{\sigma}\sigma} = \tfrac{1}{2} \begin{pmatrix} [\overline{U}^{(e)} + \overline{U}^{(o)}] & [\overline{U}^{(e)} - \overline{U}^{(o)}] \\ [\overline{U}^{(e)} - \overline{U}^{(o)}] & [\overline{U}^{(e)} + \overline{U}^{(o)}] \end{pmatrix}_{\tilde{\sigma}\sigma} \tag{9.18}$$

The fact that this has off-diagonal elements in the L/R-basis is extremely important, because it implies that P_η will have $\overline{U}^{\dagger(o)} \overline{U}^{(e)}$ cross-terms, in spite of the fact that the current operator $I_{\tilde{\eta}'\tilde{\eta}}$ is diagonal. Indeed, eq. (9.17) reduces to[1]

$$P_\eta = \sigma_\eta \mathrm{Re} \left(\overline{U}^{\dagger(o)} \overline{U}^{(e)} \right) \ . \tag{9.19}$$

Now $\overline{U}^{(e)}$, describing Kondo scattering in the even channel, has a $T^{1/2}$ contribution, but $\overline{U}^{(o)}$, describing no scattering at all in the odd channel, does not. Thus we see that this model indeed *does* contain a $T^{1/2}$ (and not T) contribution to the

[1]Here we have assumed that the phase shift ϕ_e is energy-independent. In general, it can have an energy-dependence, $\phi_e = \phi_e^{(0)} + \frac{\varepsilon}{\varepsilon_F} \phi_e^{(1)} + \ldots$, but this will be very weak, and only give rise to subleading corrections in the conductance, i.e. terms of the form $T^{3/2} \Gamma_{(1)}(V/T)$.

current, as a direct consequence of e/o cross terms in P_η. Physically, the reason why this comes about is that the probability of finding a current-carrying particle with index $\tilde{\eta}$ *after* scattering is a *square* of the sum over all scattering amplitudes into state $\tilde{\eta}$. Since we have two sets of transmission channels, e-channels with Kondo scattering (and $T^{1/2}$) and o-channels without, cross terms between these simply give $T^{1/2}$.

Finally, consider the sums $\sum_{\tilde{a}=f/s}$ in P_η. As mentioned above, for the "incident index" η, we have $a = f$ in eq. (9.17), since the leads inject only free electrons, no spinors. Since all matrices in eq. (9.17) except $\overline{U}^{(e)}$ are proportional to $\delta_{aa'}$, the only component of $\overline{U}^{(e)}_{\bar{a}\bar{a}'}$ that survives the $\tilde{a}$ matrix multiplications is $\overline{U}^{(e)}_{ff}$, giving:

$$P_\eta \equiv \sigma_\eta \mathrm{Re}\left(\overline{U}^{\dagger(o)}_{ff}\overline{U}^{(e)}_{ff}\right) = \sigma_\eta \mathrm{Re}\left[\mathcal{U}e^{i\phi_e}\right] \ . \tag{9.20}$$

Hence, the spinor terms [the $\sigma^x_{\bar{a}\bar{a}'}$ in eq. (9.12)] in fact do not contribute anything after all. The reason is that no spinors are created in the odd channel, and since the current turns out to be composed purely of e-o cross terms, it therefore gets no contributions from spinors, since those created in the even channel cannot be contracted against any in the odd channel. However, for choices for $V_{\sigma\sigma'}$ more general than eq. (9.7), there will be a spinor-contribution in eq. (9.20) too.

9.3 Scaling Form for Conductance

We now have gathered all the ingredients to derive the sought-after scaling form for the current and conductance. Inserting eq. (9.20) into eq. (9.16) gives:

$$I \ = \ \tfrac{e}{h} 4 \int d\varepsilon \tfrac{1}{2} \left\{ \mathrm{Re}\left[\mathcal{U}e^{i\phi_e}\right] + 1 \right\} \left[f_o(\varepsilon - eV/2) - f_o(\varepsilon + eV/2) \right] \ , \tag{9.21}$$

where the factor 4 comes from $\sum_{\alpha i}$ and the sum $\sum_{\sigma_\eta}$, written out explicitly, gives the two terms in the last factor. This is of the form

$$I = \int d\varepsilon g(\varepsilon) \left[f_o(\varepsilon - eV/2) - f_o(\varepsilon + eV/2) \right] , \tag{9.22}$$

which means that only the even part $g_e(\varepsilon) \equiv \frac{1}{2}[g(\varepsilon) + g(-\varepsilon)]$ of the function $g(\varepsilon)$ contributes to the conductance:

$$G = \frac{\partial I}{\partial V} = \int d\varepsilon g_e(\varepsilon + eV/2) \left[-\partial_\varepsilon f_o(\varepsilon) \right] . \tag{9.23}$$

Now, from eq. (8.37) we know that the real and imaginary parts of $\mathcal{U}$ are respectively even and odd in ε (see footnote 6 on page 236):

$$\mathcal{U} = \lambda T^{1/2} \left[\tilde{\Gamma}_e(\varepsilon/T) + i \tilde{\Gamma}_o(\varepsilon/T) \right] , \tag{9.24}$$

with $\tilde{\Gamma}_{e/o}(x) = \pm \tilde{\Gamma}_{e/o}(-x)$. Thus, G reduces to

$$G = 2\tfrac{e}{h} \left[1 - \lambda \gamma_o \cos\phi_e T^{1/2} \Gamma(\gamma_1 eV/T) \right] , \tag{9.25}$$

Here we have defined the universal scaling function $\Gamma(v)$ by

$$\gamma_o \Gamma(\gamma_1 v) \equiv - \int dx \tilde{\Gamma}_e \left(x + v/2 \right) \left[-\partial_x f_o(x) \right] , \tag{9.26}$$

where $v \equiv eV/T$, $x = \varepsilon/T$, $f_o(x) = 1/(e^x + 1)$, and the $-$ sign has been included since $\tilde{\Gamma}$ is negative definite (see page 236). The positive constants γ_o, γ_1 are to be chosen such that $\Gamma(v)$ obeys the normalization conditions used in chapter 3 [compare eq. (3.3)]:

$$\Gamma(0) \equiv 1 , \qquad \Gamma(v) \text{ vs. } v^{\frac{1}{2}} \text{ has} \quad \text{slope=1} \quad \text{as } v^{\frac{1}{2}} \to \infty . \tag{9.27}$$

Thus, we have shown that within the present model, the conductance obeys the scaling relation[2]

$$\boxed{G(V,T) = G_o + BT^{1/2}\Gamma(\gamma_1 eV/T)}\,, \tag{9.28}$$

($B = -2e\lambda\gamma_o \cos\phi_e/2$) with the universal scaling function $\Gamma(v)$, given by eq. (9.26), known exactly. This function is the same as that found in section 3.1.2, eq. (3.9), by a back-of-the-envelope calculation. The reason for this agreement is eq. (8.39), which relates $\mathcal{U}(\varepsilon, T)$ to the bulk scattering rate $\frac{1}{2}\tau^{-1}(\varepsilon, T)$, and justifies the assumption made in section 3.1.2, namely that the nanoconstriction conductance will be governed by $\tau^{-1}(\varepsilon, T)$.

It should be emphasized that the scaling relation found here is only expected to hold for $T/T_K \ll 1$ and $eV/T_K \ll 1$. The first restriction follows from the fact that we really are doing perturbation theory in T, as emphasized at the end of chapter 8, page 237. If T/T_K is not $\ll 1$, the subleading powers of T/T_K that have been neglected in the calculation of will become important, and will give deviations from scaling. As argued at the end of chapter 8, page 237, though, it would not be meaningful to calculate these deviations within our CFT approach. The reason is that each subleading term that is added introduces one more fitting parameter, leading to more freedom than one would want for a meaningful comparison of theory and experiment.

[2]Note that consistency with the sign of the experimental zero-bias anomaly requires $B > 0$, i.e. $\lambda \cos\phi_e < 0$. This is in agreement with AL [AL93, p. 7309], who concluded (for the case $\phi_e = 0$) that $\lambda < 0$ in the regime where the Kondo coupling constant is below its critical value, $\lambda_K < \lambda_K^*$, i.e. if one flows towards λ_K^* from the weak-coupling regime.

9.4 V-dependent Corrections to Scattering Amplitude

In the preceding sections, we used an expression for the scattering amplitudes [eq. (9.3)] that was obtained from a purely equilibrium theory, namely CFT. They were thus V-independent. However, as discussed at some length in section 5.4.5, in principle one expects that the scattering states *will* have some kind of V-dependence: when $V \neq 0$, the "Fermi surface splits in two", and this must somehow show up in the scattering amplitudes. In this section, we analyse the V-dependent corrections to the scattering amplitudes.

In the absence of any kind of scattering, the thermal weighting operator Y_o of eq. (5.15) for the present problem is given by

$$Y_o = \tfrac{1}{2}eV \sum_\eta \int_{-\infty}^{\infty} \tfrac{dx}{2\pi} \psi_\eta^\dagger(ix)\sigma_\eta \psi_\eta(ix) \ , \qquad (\sigma_\eta = \pm \ \text{for} \ \ L/R-\text{movers}) \ . \quad (9.29)$$

After rotating to the even-odd basis according to eq. (9.8), it takes the form

$$Y_o = \tfrac{1}{2}eV \sum_{\bar\alpha\bar i} \int_{-\infty}^{\infty} \tfrac{dx}{2\pi} \left[\overline{\psi}^\dagger_{e\bar\alpha\bar i}(ix)\overline{\psi}_{o\bar\alpha\bar i}(ix) \ + \ \overline{\psi}^\dagger_{o\bar\alpha\bar i}(ix)\overline{\psi}_{e\bar\alpha\bar i}(ix) \right] \ , \quad (9.30)$$

since $(N\sigma^z N^{-1})_{\bar\sigma\bar\sigma'} = \sigma^x_{\bar\sigma\bar\sigma'}$. This shows that Y_o mixes even and odd channels! Since the CFT solution was formulated only in the even sector, the present model[3]

[3]However, related models exist which can be treated exactly by CFT even if $V \neq 0$, for example the the model used by Schiller and Hershfield in [SH95b]. There, the pseudo-spin index is also the L-R index (i.e. the interaction matrix elements are $\frac{1}{2}\vec\sigma_{\sigma\sigma'} \cdot \vec S$), which means that

$$Y_o = \tfrac{1}{2}eV \sum_{\alpha i} \int_{-\infty}^{\infty} \tfrac{dx}{2\pi} \psi^\dagger_{\alpha i}(ix)\sigma^z_{\alpha\alpha'}\psi_{\alpha' i}(ix) = \ eV \int_{-\infty}^{\infty} \tfrac{dx}{2\pi} J^z_s(ix) \ ,$$

where $\vec J_s$ is the spin current. Now, in this case it is easy to find the exact Y-operator in the presence of the Kondo interaction. Y must both commute with H and reduce to Y_o when the interaction is switched off. This is evidently satisfied by $Y = eV\int_{-\infty}^{\infty}\frac{dx}{2\pi}\mathcal{J}^z_{sL}$, where $\mathcal{J}^z_{sL}$ is the z-component of the new spin current $\vec{\mathcal{J}}_s(ix) = \vec J_s(ix) + 2\pi\delta(x)\vec S$ of eq. (7.36). Thus, in the combination $H - Y$ that occurs in the density matrix ρ, eV simply plays the role of a *bulk* magnetic field in the z-direction, which can be gauged away exactly by a gauge transformation [AL91b, eq. (3.37)]. Hence in this model, non-equilibrium properties can be calculated exactly using CFT [vDLA95].

can not be solved exactly by CFT for $V \neq 0$.

Nevertheless, we can analyze Y_o's effects in the limit $V \ll T_K$: Y_o breaks a $U_e(1) \times U_o(1)$ symmetry that the equilibrium model possessed. The breaking of a symmetry will in general allow boundary operators to appear at the fixed point that had been previously forbidden (for extensive applications of this principle, see [AL92b, section III.C]). Evidently, the boundary perturbation to the fixed point action corresponding to Y_o will be[4] [compare eq. (8.15)]:

$$\delta S_V \propto \frac{V}{T_K} \sum_{\bar{\alpha}\bar{i}} \int_0^\beta d\tau \left[\overline{\psi}^\dagger_{e\bar{\alpha}\bar{i}}(\tau) \overline{\psi}_{o\bar{\alpha}\bar{i}}(\tau)) \; + \; \overline{\psi}^\dagger_{o\bar{\alpha}\bar{i}}(\tau) \overline{\psi}_{e\bar{\alpha}\bar{i}}(\tau) \right] \; \equiv \; \frac{V}{T_K} \int_0^\beta d\tau J_{eo}(\tau) \; . \tag{9.31}$$

Since the "even-odd" current J_{eo} has scaling dimension 1, δS_V has scaling dimension zero [see eq. (8.17)], and is therefore a marginal perturbation. As discussed in section 4.4.2, this means that for any $V \neq 0$, there will exist a cross-over temperature T_V^* below which the system flows away from the $V = 0$, $T = 0$ fixed point. However, since this perturbation is marginal, it only grows logarithmically slowly as T is decreased, so that T_V^* will be *very* small. The lack of deviations from scaling in the data for the low-T regime indicate that T_V^* is smaller than the lowest temperatures obtained in the experiment.

How does δS_V affect the scattering amplitudes? δS_V will simply cause a

[4]It is easy to check that the operator J_{eo} is indeed allowed at the boundary: it must be the product $\Phi_e \Phi_o$ of boundary operators in the even and odd sectors, with quantum numbers $(Q_e, j_e, f_e) = (-Q_o, j_o, f_o) = (\pm 1, \frac{1}{2}, \frac{1}{2})$. Φ_o, which lives on a free boundary, since the odd sector is free, is simply the free fermion field in the leftmost column of table A.2; Φ_e must live on a Kondo boundary; indeed boundary operators with the desired quantum numbers do occur in the rightmost column of table 7.1, which lists the operators allowed on the Kondo boundary.

rotation of the e/o indices of the outgoing fields relative to the incident ones by[5]

$$\overline{R}_{\bar{\eta}\bar{\eta}'}(V) = \delta_{\bar{\alpha}\bar{\alpha}'}\delta_{\bar{i}\bar{i}'} \begin{pmatrix} \cos\theta_V & -i\sin\theta_V \\ -i\sin\theta_V & \cos\theta_V \end{pmatrix}_{\bar{\sigma}\bar{\sigma}'} , \qquad \text{where} \quad \theta_V \equiv \arctan\left(\frac{cV}{T_K}\right) . \tag{9.32}$$

Here θ_V is simply a convenient way to parametrize the rotation [CKLM94]. Thus, the effect of δS_V can be incorporated by replacing the scattering amplitude $\overline{U}_{\bar{\eta}\bar{\eta}'}(\varepsilon)$ of eq. (9.11) by $\overline{R}_{\bar{\eta}\bar{\eta}''}(V)\overline{U}_{\bar{\eta}''\bar{\eta}'}(\varepsilon)$. Evidently, the final scattering amplitude $\tilde{U}_{\bar{\eta}\eta}(\varepsilon)$ of eq. (9.15) will now be V-dependent.

It turns out that for the simple form (9.7) used for the backscattering matrix $V_{\sigma\sigma'}$, this extra V-dependence "accidentally" cancels out[6] in eq. (9.17) for $P_\eta(\varepsilon)$. However, for more general forms of $V_{\sigma\sigma'}$, it survives. To lowest order in V/T_K, there will be a contribution to the conductance of the form $(V/T_K)T^{1/2}\Gamma_1(V/T) = T^{3/2}\Gamma_2(V/T)$. This is therefore a *subleading* correction to the scaling function of eq. (9.28). It is of the same order as corrections arising from subleading irrelevant operators of the equilibrium theory, that we have argued [p. 250] are not worth while calculating since there are too many independent ones.

9.5 The NCA approach

In the next section, we shall compare our results to recent numerical calculations by Hettler, Kroha and Hershfield (HKH) [HKH94], who used the non-crossing-

[5] See, for example, [CKLM94]. At $T = 0$, one can prove that δS_V generates such a rotation by closing the $\int_{-\infty}^{\infty} d\tau$ integral along an infinite semi-circle in the lower half-plane (this is allowed, because according to eq. (B.30), $J_{eo}(z) \sim z^{-2} \to 0$ along such a contour); having closed the contour, δS_V has precicely the form (B.14) required for a generator of e/o rotations.

[6] This can be seen from by replacing $\overline{U}$ by $\overline{RU}$ in eq. (9.17) for $P_\eta(\varepsilon)$, and checking that $\overline{R}^\dagger N\sigma^z N^\dagger \overline{R} = \overline{R}^\dagger \sigma^x \overline{R} = \sigma^x$, which is independent of V because $\overline{R}$ generates rotations around the x-axis in the e/o indices. However, if V and N are more complicated than in eqs. (9.7) and (9.9), the V-dependence will clearly not cancel out.

approximation (NCA) approach to the Kondo problem. Therefore a few words about their work are in order here.

9.5.1 Anderson model used for NCA

HKH represent the system by the following infinite-U Anderson Hamiltonian in a slave boson representation:

$$H_1 = \sum_{p,\sigma,\alpha,i} (\varepsilon_p - \mu_\sigma) c^\dagger_{p\sigma\alpha i} c^\dagger_{p\sigma\alpha i} + \varepsilon_d \sum_\alpha f^\dagger_\alpha f_\alpha + \sum_{p,\sigma,\alpha,i} \mathcal{V}_\sigma \left(f^\dagger_\alpha \, b_i c_{p\sigma\alpha i} + \text{H.c.} \right) \ . \quad (9.33)$$

The first term describes conduction electrons in two leads, $\sigma = (L, R) = (+, -)$, separated by a barrier and at chemical potentials $\mu_\sigma = \mu + \sigma \frac{1}{2} eV$. The electrons are labeled by a momentum p, the lead index σ, a pseudospin index $\alpha = (1, 2)$, and their Pauli spin $i = (\uparrow, \downarrow)$. The barrier is assumed to contain an impurity level ε_d far below the Fermi surface, hybridizing (with matrix elements $\mathcal{V}_\sigma$, with $\mathcal{V}_{_L} = \mathcal{V}_{_R}$ for our purposes) with the conduction electrons, which can get from one lead to the other only by hopping via the impurity level. f and b are slave fermion and slave boson operators, and the physical particle operator on the impurity is represented by $d^\dagger_\alpha b_i$, supplemented by the constraint $\sum_\alpha f^\dagger_\alpha f_\alpha + \sum_i b^\dagger_i b_i = 1$.

Although this picture of two disconnected leads communicating only via hopping through an impurity level does not directly describe the physical situation of ballistic transport through a hole accompanied by scattering off two-level systems, the Hamiltonian (9.33) can be mapped by a Schrieffer-Wolff transformation onto the more physical one [eq. (9.6)] used in previous sections. It is therefore in the same universality class and describes the same low-energy physics, provided that one identifies the impurity-induced "tunneling current" I_{tun} in the HKH model with the impurity-induced backscattering current ΔI in the actual

nanoconstriction.

HKH calculate the tunneling current,

$$I_{tun}(V,T) = \int d\omega A_d(\omega)[f_o(\omega - eV/2) - f_o(\omega + eV/2)] \ , \qquad (9.34)$$

where $f_o(\omega) = 1/(e^{\beta\omega} + 1)$, by calculating the impurity spectral function $A_d(\omega)$ using the NCA approximation, generalized to $V \neq 0$ using Keldysh techniques. The NCA technique [Bic87] is a self-consistent summation of an infinite set of selected diagrams (which becomes exact in the limit $N \to \infty$, where N is the number of values the pseudo-spin quantum number can assume), and in that sense it is not an "exact" solution of the model. However, it has been shown [CR93] that for a $U(1) \times SU(N)_s \times SU(M)_f$ Kondo model (i.e. M channels of electrons, each with N possible pseudo-spin values, here we have $N = M = 2$), the NCA approach gives leading critical exponents for $A_d(\omega)$ *identical* to those of conformal field theory for *all* N and M (with $M > 2$). Hence the NCA method can be regarded as a useful interpolation between the high-T regime where any perturbative scheme works, and the low-T regime where it gives the correct exact critical exponents. Moreover, when combined with the Keldysh technique, it deals with the non-equilibrium aspects of the problem in a more direct way than our CFT approach, and is able to go beyond the weakly non-equilibrium regime ($V \ll T_K$).

Therefore, it is certainly meaningful to compare the NCA results of HKH to ours. CFT serves as a check on how well the NCA does at $V = 0$ and very low temperatures, where CFT is exact and NCA only an uncontrolled approximation. Conversely, if this check confirms the reliability of the NCA method in the low-energy regime, the latter can be used as a check on our use of CFT for $V \neq 0$

Figure 9.2 Here $\Sigma(\omega, T)$ is the imaginary part of the retarded self-energy for conduction electrons at $V = 0$, calculated using CFT and the NCA [HKH95]. For the NCA curves, temperatures are given in units of $.001T_K$. The CFT curve corresponds to $T/T_K \to 0$. The asymmetry in the NCA curves is a result of using the asymmetric Anderson model. The CFT and lowest-T NCA curves have been rescaled such that the asymptotic slope of the $\omega < 0$ function is 1, i.e. the CFT curve corresponds to the function $(\tilde{\Gamma}(\tilde{\gamma}_1 x)/\tilde{\Gamma}(0) - 1)$ of eq. (8.38), with $\tilde{\gamma}_1$ an appropriately chosen constant.

situations, where NCA presumably does the more reliable job.

9.5.2 Electron Self-Energy

One would expect that the most direct comparison between CFT and the NCA could be obtained by comparing [see Fig. 9.2] the retarded self-energy $\Sigma^R(\omega)$ for conduction electrons at $V = 0$, calculated from the NCA with that from CFT [essentially the function $\tilde{\Gamma}(x)$ of eqs. (8.38) and (8.39]. However, the usefulness of this comparison is somewhat diminished by the fact that the NCA self-energy is not a symmetric function of frequency, which is a result of using the asymmetric Anderson model. This asymmetry disappears when calculating the conductance,

because $I_{tun}(V) = I_{tun}(-V)$ in eq. (9.34) even if $A_d(\omega) \neq A_d(\omega)$, meaning that the zero-bias conductance is the more meaningful quantity to compare (see next section). Nevertheless, for $\omega < 0$, the CFT and NCA results agree very well [Fig. 9.2].

9.5.3 Impurity Spectral Function $A_d(\omega)$

Figure 9.3 is very instructive, in that it illustrates what happens to the Kondo resonance when T or V become $> T_K$, a regime not accessible to CFT. [T_K is defined as the width at half maximum of the $V = 0$ impurity spectral function at the lowest calculated T.] For $V = 0$ [Fig. 9.3(a)], the Kondo peak spreads out as T is increased, though this spreading only starts to become significant for $T \simeq T_K$. For $T/T_K \simeq 0$, the Kondo peak splits into two when $eV \gg T_K$ [Fig. 9.3(b)], (as also found in [WM94] for a related model). However, note that even for $V \simeq T_K$, this splitting has not yet set in, illustrating that non-equilibrium effects are not important for $eV < T_K$. This is the main justification for the the approach followed in the previous sections of calculating the scattering states from CFT and neglecting their V-dependence (see also the discussion in section 5.1 (point 3), and in section 5.4.5).

9.5.4 NCA Conductance Curves

The NCA results of HKH for the conductance $G(V, T)$, obtained from eq. (9.34) and rescaled according to eq. (3.15), are shown in Fig. 9.4(a). The curves are obtained without any adjustable parameters, since the rescaling of the horizontal axis (by a constant A to get an asymptotic slope 1) that we employed elsewhere was not performed here. The experimental data for sample #1 (which has $T_K \simeq$

Figure 9.3 The Kondo resonance in the impurity spectral function $A_d(\omega)$, calculated at (a) $V = 0$ and (b) $T/T_K = 0.001$ using the NCA [HKH95]. For our purposes the most important feature of this figure is that the Kondo peak does not start to split for $eV < T_K$.

Figure 9.4 Scaling plots of the conductance for (a) the NCA calculations of Hettler *et al.* [HKH94] and (b) experiment (sample #1). With B_Σ determined from the zero-bias conductance, $G(0,T) = G(0,0) + B_\Sigma T^{1/2}$, [eq. (3.11)], there are no adjustable parameters. The temperatures in the NCA and experimental plots are in units of T_K and Kelvin, respectively.

$8K$) are shown for comparison in Fig. 9.4(b).

The lowest T/T_K values in Fig. 9.4(a) show good scaling, in accord with the CFT prediction. However, for larger T-values, marked deviations from scaling occur, just as seen in the experimental curves of Fig. 9.4(b). It is one of the strengths of the NCA method that deviations from scaling are automatically obtained, without the need for making a systematic expansion in powers of T/T_K.

The striking qualitative similarity between the two sets of curves in Fig. 9.4 can be made quantitative by using T_K as a fitting parameter: the choice of T_K determines which curves in fig:NCAcurves(a) and (b) are to be associated with each other. Choosing $T_K = 8K$ for sample 1, HKH are able to get "quite good" [HKH94] simultaneous agreement between a significant number of the individual experimental data curves and their NCA curves of corresponding temperature. This is illustrated in Fig. 9.5 [HKH95] for 3 curves from sample # 1. In other words, *by using a single fitting parameter, HKH can obtain good quantitative agreement between the NCA and experimental conductance curves for a whole set of curves.*

9.6 Comparison with Experimental Curve and NCA Calulation

In this section we compare the CFT prediction of eq. (9.26) for the universal scal ing curve $\Gamma(v)$ to that obtained by HKH via the NCA, and to the experimental scaling curve of Fig. 3.10(b). For the NCA scaling curve we take the lowest T/T_K calculated by HKH, namely $T/T_K = 0.003$, since for this curve the T/T_K deviations from perfect scaling, which are neglected in the CFT calculation, are

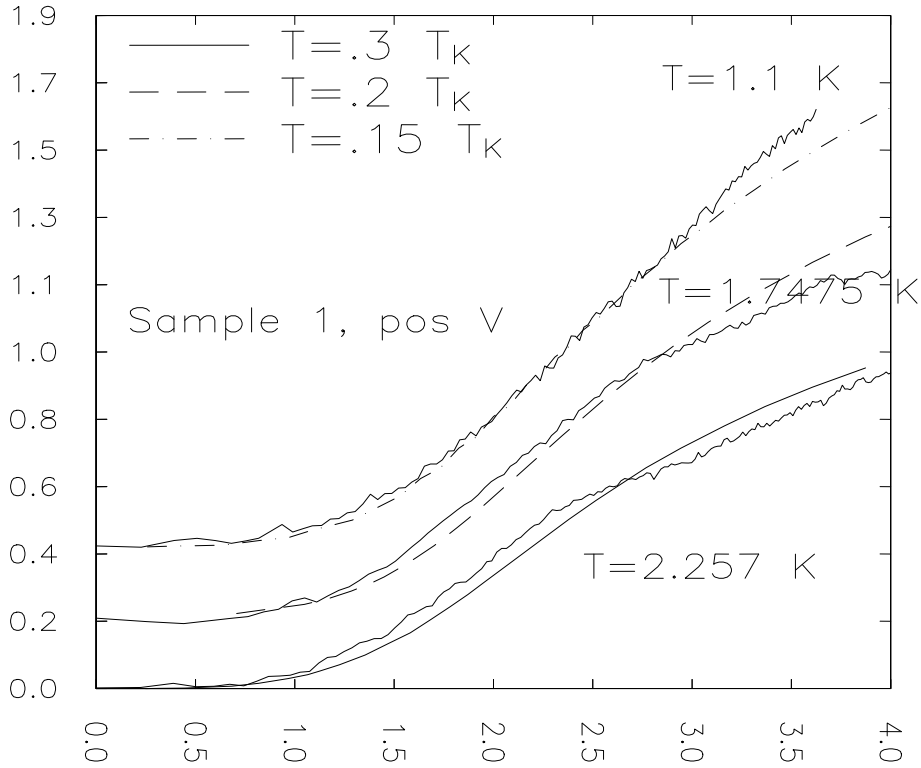

Figure 9.5 Comparison between NCA theory and experiment for three individual conductance curves from sample # 1. By using T_K as a single fitting parameter and choosing $T_K = 8K$ for sample 1, this kind of agreement is achieved simultaneously for a significant number of individual curves [Hettler, private communication], [HKH95]. The NCA curves shown here correspond to $T = 0.3T_K = 2.4$K, $0.2T_K = 1.6$K and $0.15T_K = 1.2$K (NCA curves for the actual experimental temperatures of $T = 2.257$K, 1.745K and 1.1K were not calculated.)

smallest.

In Fig. 9.6 we show the three experimental scaling curves of Fig. 3.10 (curves 1-3), the CFT prediction for $\Gamma(u)$ from eq. (9.26) (curve 4), and the NCA result for $\Gamma(u)$, for $T/T_K = 0.003$ (curve 5) and $T/T_K = 0.08$ (curve 6). All these curves have been rescaled into the "maximally normalized form" of eq. (9.27).

We see that the CFT scaling curve does not agree quantitatively with the experimental curves, but that there is rather good agreement between the CFT curve and the $T/T_K = 0.003$ NCA result. However, the $T/T_K = 0.08$ NCA curve,

Figure 9.6 The conductance scaling function $\Gamma(v)$. Curves 1,2,3 are the experimental curves of Fig. 3.10 (b). Curve 4 is the CFT prediction from eq. (9.26). Curves 5 and 6 are the NCA results of HKH, with $T/T_K = 0.003$ and 0.08, respectively. All curves have been rescaled in accordance with eq. (9.26).

which for $T_K = 8$K corresponds to $T = 0.6$K, the lowest temperature measured in the experiment, agrees remarkably well with the experimental scaling curves.

To make these statements quantitative, we compare the values for the universal constant Γ_1, defined as follows from the asymptotic large-v expansion of $\Gamma(v)$ [compare eq. (3.16)]:

$$\Gamma(v) - 1 \equiv v^{1/2} + \Gamma_1 + O(v^{-1/2})\,. \tag{9.35}$$

Γ_1 is the y-intercept of the asymptotic slope of the curve $\Gamma(v) - 1$ vs. $v^{1/2}$, extrapolated back to $v = 0$. It measures "how soon the scaling curve bends up" towards linear behavior, and is the single parameter that most strongly characterizes the scaling function (which is otherwise rather featureless). We find the following values for Γ_1:

$$\begin{aligned} \Gamma_1^{EXP} &= -0.75 \pm 0.16\,, & \Gamma_1^{CFT} &= -1.14 \pm 0.10\,, \\ \Gamma_1^{NCA}(0.003) &= -1.12 \pm 0.10\,, & \Gamma_1^{NCA}(0.08) &= -0.74 \pm 0.10\,. \end{aligned} \tag{9.36}$$

Hence, *the CFT and NCA calculations agree rather well, which inspires confidence in the general reliability of the NCA method at very low energies*. The fact that both disagree by more than 30 % with experiment is explained by the excellent agreement of the $T/T_K = 0.08$ NCA curve with experiment. As first pointed out by HKH, this simply means that *in the experimentally relevant temperature range, the T/T_K-corrections to the universal curve are apparently not neglibible*, in contrast to the assumptions made by the CFT calculation. In other words, the experimental scaling curve is not the truly universal one, since non-universal correction-to-scaling terms are important too.

From a theorist's point of view, this is a somewhat disappointing conclusion, since for a system about whose microscopic nature so little is known, the only

quantities that allow a truly meaningful comparison between theory and experiment are universal quantities, which are independent of the unknown details. However, disappointing or not, this is the message of Fig. 9.6.

Nevertheless, the good agreement between the CFT and NCA scaling curves, which confirms the reliability of the NCA method, combined with the good quantitative agreement between the NCA and the experimental conductance curves when T_K is used as fitting parameter, allows the main conclusion of this thesis:

- *The 2-channel Kondo model is in quantitative agreement with the experimental $G(V,T)$ data.*

However, as was discussed in section 4.3, the theoretical justification for the simple 2-channel Kondo model used in this thesis has recently been challenged. Therefore, the Ralph-Buhrman experiments can not be regarded as completely understood. Rather, the question that remains is: why does the 2-channel Kondo model seem to describe this experiment so well despite the fact that the theoretical derivation of the model is on shaky grounds? In view of the fact that no alternative explanation for the experiment is known that is in agreement with all experimental facts, this question worthy of further investigation.

Chapter 10

Summary and Conclusions

10.1 Summary

Let us briefly summarize what has been done in this thesis.

1. Chapters 2 and 3 contain a detailed account of all experimental facts relevant to the Ralph-Buhrman experiment (summarized in points (P1) to (P9) in section 2.3), with the following conclusions: the zero-bias anomalies disappear under annealing, and hence must be due to *structural* disorder; they disappear when static disorder is added, and hence cannot be due to static disorder – instead they must be due to *dynamical* impurities; they show no Zeeman splitting in a magnetic field, and hence must be of *non-magnetic* origin; they show V/T scaling with scaling exponent $\alpha = \frac{1}{2}$, and a universal scaling curve $\Gamma(x)$ that was identical for all three samples investigated in detail. These observations lead to the proposal [RB92] that *the zero-bias anomalies are due to degenerate two-level systems, interacting with conduction electrons according to the non-magnetic 2-channel Kondo model of*

Zawadowski [ZZ94a], introduced in chapter 4. Within this interpretation, the observed scaling was explained by assuming that the system is in the vicinity of the $T = V = 0$ fixed point of the 2-channel Kondo problem.

2. In order to quantitatively investigate the consequences of this proposal, we decided to analytically calculate the universal scaling curve $\Gamma(x)$, which is a fingerprint of the 2-channel Kondo model, using the conformal field theory solution of Affleck and Ludwig [AL93] for the 2-channel Kondo problem near $T = 0$. In order to describe properly the non-equilibrium aspects of the problem, we adopted Hershfield's Y-operator formalism [Hers93], which shows that non-equilibrium problems become formally simple when formulated in terms of scattering states. We showed in chapter 5 how Affleck and Ludwig's conformal field theory solution can be used to obtain the requisite exact scattering states, provided that one is willing to neglect their V-dependence (which is of order V/T_K in the weakly non-equilibrium scaling regime of the experiment, and hence indeed negligble).

3. With this method, in chapter 9 the universal scaling curve was calculated exactly to leading order in T/T_K and zeroth order in eV/T_K, but for arbitrary eV/T. The result does not agree with the experimental scaling curve, because a careful analysis shows that subleading corrections of order T/T_K are *not* negligible. However, numerical NCA calculations by Hettler, Kroha and Hershfield [HKH94], which incorporate such corrections automatically, are in good quantitative agreement with experiment; they also agree with CFT in the limit $T/T_K \to 0$, which inspires confidence that the NCA is indeed a reliable tool for describing the low-energy regime of this problem.

4. Chapters 6 to 8 and appendices A to F contain a detailed and extensive introduction to Affleck and Ludwig's CFT solution of the Kondo problem, aimed at a reader with no or very little background in conformal field theory.

10.2 Conclusions

Let us now briefly summarize our conclusions about the 2-channel Kondo interpretation of Ralph and Buhrman's zero-bias anomalies.

Ralph and Buhrman have accumulated a large number of experimental facts about the zero-bias anomaly, summarized in points (P1) to (P9) in chapter 2. Some of these are qualitative (e.g. the signals disappear upon annealing and the existance of scaling properties), others are quantitative (e.g. the conductance exponent $\alpha = \frac{1}{2}$ and the shape of the universal scaling curve). To find an interpretation for their data that simultaneously is in reasonable agreement with *all* the experimental facts is quite a challenge.

In our opinion, the experimental evidence that the zero-bias anomaly is due to some kind of *structural, dynamical* impurities interacting with conduction electrons is very compelling. The difficult question is to find a reasonable model that captures the relevant physics. In this thesis, we adopted the 2-channel Kondo model of Zawadowski, which, at the time this work was started, was the standard and accepted model for describing 2-level systems interacting with conduction electrons.

In this thesis, it is demonstrated that *the 2-channel Kondo model can satisfactorily account for all known experimental facts, both qualitative and quantitative.* In particular, it correctly predicts the scaling exponent $T^{1/2}$ that has been con-

vincingly demonstrated in the data, and a combination of CFT and the NCA calculations of Hettler, Kroha and Hershfield yield good quantitative agreement with the $G(V,T)$ conductance data.

However, very recently the theoretical justification for the 2-channel Kondo model has come under increased scrutiny [see section 4.3]. The criticism has mainly been concerned with the question whether in realistic situations the system will in fact flow toward the $T = 0$ fixed point that is invoked in this thesis to explain the scaling properties of the data.

1. Wingreen, Altshuler and Meir [WAM95] have pointed out that the presence of static disorder could lead to a significant splitting Δ between the two states of the TLS. Since the splitting is a relevant perturbation near the $T = 0$ fixed point, this would mean that the system could never flow into the vicinity of this fixed point. — While we believe that their method of estimating Δ is overly crude and their result unrealistically large (namely $\Delta = 100\text{K}$), we do agree that they have pointed out an important effect, worthy of more careful consideration. Indeed, the assumption that $\Delta < 1\text{K}$ that we have to make in order to explain the experiment is probably the weakest point in the 2-channel Kondo scenario. Unfortunately, there does not seem to be an independent way to experimentally determine what values for Δ could reasonably be expected.

2. Moustakas and Fisher [MF95] have very recently argued that Zawadowski's non-orbital Kondo model is not sufficiently general: they argued that subleading terms in the TLS-electron interaction have to be included, and show that, even if $\Delta = 0$, these give rise to an extra relevant perturbation.

This will prevent flow towards the $T = 0$ fixed point, unless some coupling constants are fine-tuned such that this term vanishes.

It should be pointed out that the CFT approach is more vulnerable to these arguments than the NCA, because the CFT calculation explicitly has to assume that one is in the vicinity of the fixed point, whereas the NCA calculation needs to make no such assumptions, and is completely defined once the Hamiltonian has been written down. Nevertheless, the NCA uses an Anderson Hamiltonian that is physically unrealistic for the present problem, and draws its justification only from the argument that its universal low-energy behavior will be the same as that of the 2-channel Kondo model. Therefore, the NCA approach too implicitly assumes closeness to the fixed point.

Thus, we seem to be faced with the following situation: the 2-channel Kondo model qualitatively and quantitatively agrees with all experimental facts, which cannot be said of any other interpretation of the experiment known to date. However, the theoretical justification for the model is currently on somewhat shaky grounds. In our opinion, this should be regarded as an incentive for furhter theoretical work — perhaps a way around the recently discovered problems can still be found.

On the experimental side, it would be very helpful to get more "handles" on the system. Additional measurements on the magnetic field dependence of the conductance would certainly be welcome. It would be extremely interesting to know the conductance $G(V, H, T)$ as a function of all three arguments. However, as argued in section 3.3, the lack of detailed microscopic understanding for how a magnetic field couples to the system, and experimental evidence (from other

systems [GZC92]) that its effect might be of a rather random nature, might place limits on how much reliable information the magnetic field dependence can yield.

Another handle seems to have been discovered in the second generation of experiments that are currently being done on this system at Cornell by Shashikant Upadhyay and R.A. Buhrman, who are investigating the same system, but with superconducting leads. They are studying the dramatic effects that the presence of a zero-bias anomaly in the normal state has on the system in the superconducting state.

The insights gleaned from these experiments will certainly be useful. Perhaps, with more experimental and theoretical work, it will eventually be possible to establish *conclusively* what is *really* giving rise to the zero-bias anomalies inside these nanoconstrictions!

Appendix A

Sugawara technology

In this appendix we review some aspects of the abelian and non-abelian bosonization of a system of N species of spinless, chiral (left-moving) fermions with linear dispersion relation. Our aim is to derive the Sugawara form of the Hamiltonian for free fermions [eqs.(A.53), or (A.81) to (A.83), or (A.102)]. Our presentation follows the beautifully detailed treatment of Ludwig, [Lud94b], which is well worth reading carefully. Our aim here is to present the important results and outline their derivation. However, we do not attempt a completely self-contained treatment here, and refer the reader to Ludwig's article for some of the more technical issues.

No knowledge of conformal field theory is presumed – familiarity with Wick's theorem suffices.

In section A.1 we define the system to be studied, and in section A.2 discuss the various global (gauge and scaling) symmetries of the action, as well as their generalizations to analytic local (Kac-Moody and conformal) symmetries. This symmetry analysis is really at the heart of all that is to follow, since it explains the

origin of all the structure in the theory that is to be uncovered later. In section A.3 we introduce the notation to be used for analyzing the finite-size spectrum of the system. In section A.4 we derive the partition function for N species of free chiral fermions with anti-periodic boundary conditions. In section A.5 we derive the operator product expansion of two general currents, using nothing but Wick's theorem. Section A.6 discusses the $[U(1)]^N$ abelian bosonization scheme, section A.7 the $U(1) \times SU(N)$ non-abelian bosonization scheme, and section A.8 the $U(1) \times SU(\tilde{N}) \times SU(k)$ non-abelian bosonization scheme for $\tilde{N}k = N$. The important concept of a gluing condition is also introduced in sections A.7 and A.8, and illustrated in detail for the cases $U(1) \times SU(2)$ and $U(1) \times SU(\tilde{2}) \times SU(2)$.

A.1 Introduction

We consider N species of spinless, chiral (left-moving) fermions $\psi^\alpha(\tau, ix)$, with and $\alpha = 1, \ldots, N$ and $x \in [-\infty, \infty]$. Right-moving fermions can be treated in exact analogy to left-moving ones, and hence will not be discussed here (see [Lud94b] for details). To study the low-energy behavior of such fermions, it suffices to restrict attention to momenta within a cut-off energy $\Lambda v_{_F}$ from the left Fermi point, where $T \ll \Lambda v_{_F} \ll \varepsilon_{_F}$. For momenta in the range $p \in [-p_{_F} - \Lambda, -p_{_F} + \Lambda]$, the dispersion relation can be linearized:

$$\varepsilon_k \equiv \frac{p^2}{2m} - \frac{p_{_F}^2}{2m} \simeq v_{_F} k \; . \tag{A.1}$$

Here $k \equiv -(p_{_F} + p)$ is the momentum measured relative to $-p_{_F}$, and the Fermi level is taken at $\varepsilon_k = 0$. (Note that our definition for k for our left-movers is chosen such that $k > 0$ implies $\varepsilon_k > 0$, which is the convention that Ludwig uses for his right-movers.) We set $v_{_F} \equiv 1$ throughout.

Using the normalization

$$\{\psi^\dagger(ix), \psi(iy)\} = 2\pi\delta(x-y) \ , \tag{A.2}$$

we thus consider the free Hamiltonian

$$H = v_{_F} \int_{-\infty}^{\infty} \tfrac{dx}{2\pi} \sum_\alpha \psi^{\alpha\dagger}(\tau, ix) i\partial_x \psi^\alpha(\tau, ix) \ . \tag{A.3}$$

The Heisenberg equations of motions,

$$(\partial_\tau + i\partial_x)\, \psi^\alpha(\tau, ix) = 0 \ , \qquad \text{imply} \qquad \psi^\alpha(\tau, ix) = \psi^\alpha(z) \ , \tag{A.4}$$

where $z \equiv \tau + ix$. Thus, the Heisenberg fields $\psi^\alpha(z)$ can be obtained from their Schrödinger cousins $\psi^\alpha(ix)$ simply by analytic continuation, $ix \to z \equiv \tau + ix$, which is the motivation for writing the argument of the Schrödinger field as ix in eq. (A.2). Whenever the argument is written as only ix, the Schrödinger picture will be implied.

The fact that the free fields only depend on z is extremely important, since it implies invariance of the system under gauge and scale transformations that are *analytic* functions of z. In the next section, we discuss these in some detail.

A.2 Lagrangian Description and Symmetries

The symmteries of the system are best analyzed in a Lagrangian description of the system, which follows from the action (at $T = 0$)[1]

$$\mathcal{S} = \int_{-\infty}^{\infty} d\tau \int_{-\infty}^{\infty} \tfrac{dx}{2\pi} \sum_\alpha \psi^{\alpha\dagger}(\tau, ix) \partial_\tau \psi^\alpha(\tau, ix) + \int_{-\infty}^{\infty} d\tau H(\tau) \tag{A.5}$$

$$= \int_{-\infty}^{\infty} d\tau \int_{-\infty}^{\infty} \tfrac{dx}{2\pi} \sum_\alpha \psi^{\alpha\dagger}(\tau, ix) 2\partial_{\bar{z}} \psi^\alpha(\tau, ix) \ , \tag{A.6}$$

where $\partial_{\bar{z}} = \frac{1}{2}(\partial_\tau + i\partial_x)$.

[1] We choose the sign of $\mathcal{S}$ such that the weighting factor in path-integral expressions is $e^{-\mathcal{S}}$, see e.g. [NO88], eq. (2.66).

A.2.1 Global Gauge Symmetries

The action is form-invariant (i.e. $\mathcal{S}[\psi] = \mathcal{S}[\tilde{\psi}]$) under the following global (i.e. parametrized by constants) symmetry operations:

1. Global overall abelian $U(1)$ gauge transformations, $\psi^\alpha = e^{i\phi}\tilde{\psi}^\alpha$, i.e. one overall constant (global) phase change, whose associated conserved current we denote by J^o.

2. Global abelian $U(1)\times U(1)\ldots U(1)$ gauge transformation, $\psi^\alpha = e^{i\phi_\alpha}\tilde{\psi}^\alpha$, i.e. individual global phase changes of each species, with associated conserved currents J^α.

3. Global $SU(N)$ gauge transformations, $\psi^\alpha = \left[e^{i\theta^a T^a}\right]_{\alpha\alpha'}\tilde{\psi}^{\alpha'}$, where the matrices $T^a_{\alpha\alpha'}$ ($a = 1,\ldots,N^2-1$) are the $SU(N)$ generators in the fundamental ($N\times N$-dimensional) representation.[2] There are N^2-1 associated conserved currents, one for each generator, denoted by J^a.

Using a general notation, let $\mathcal{G}$ denote any of the above global gauge groups, and the matrices $T^X_{\alpha\alpha'}$ be the corresponding generators in an $N\times N$-dimensional representation [with $x = 1,\ldots,\dim(\mathcal{G})$]. Then the action is invariant under

$$\psi^\alpha(z) = \left[e^{-i\theta^X T^X}\right]_{\alpha\alpha'}\tilde{\psi}^{\alpha'}(z)\ , \qquad \psi^{\dagger\alpha}(z) = \left[e^{i\theta^X T^{X*}}\right]_{\alpha\alpha'}\tilde{\psi}^{\alpha'\dagger}(z)\ , \tag{A.7}$$

where the θ^X are real constants, and T^{X*} is the complex conjugate of T^X (which is hermitian). This implies via Nöther's theorem that the currents

$$J^X(z) \equiv \sum_{\alpha,\alpha'=1}^{N} :\psi^{\alpha\dagger}(z)T^X_{\alpha\alpha'}\psi^{\alpha'}(z): \qquad [x = 1,\ldots,\dim(\mathcal{G})]\ . \tag{A.8}$$

[2]Some properties of the $T^a_{\alpha\alpha'}$ are summarized in eqs. (A.72)and (A.73).

are conserved, i.e. satisfy $\partial_{\bar{z}} J^X(z) = 0$. Here the symbol : : denotes the point-splitting operation in coordinate space:

$$: O_1(z)O_2(z) : \equiv\ O_1(z+\delta)O_2(z) - \langle O_1(z+\delta)O_2(z)\rangle\ , \tag{A.9}$$

which is used to subtract off the divergence that arises when two quantized fields sit at the same point.[3] The corresponding conserved charges

$$Q^X \equiv \int_{-\infty}^{\infty} \tfrac{dx}{2\pi} J^X(z)\ , \tag{A.10}$$

are time-independent constants, i.e. satisfy $\partial_\tau Q^X(\tau) = 0$. They act as generators of infinitesimal global gauge transformations through

$$\begin{aligned} \delta\psi^\alpha(z) &= \tilde{\psi}^\alpha(z) - \psi^\alpha(z) &&= -i\theta^X[Q^X, \psi^\alpha(z)] &&= i\theta^X T^X_{\alpha\alpha'}\psi^{\alpha'}(z)\ , \\ \delta\psi^{\alpha\dagger}(z) &= \tilde{\psi}^{\alpha\dagger}(z) - \psi^{\alpha\dagger}(z) &&= -i\theta^X[Q^X, \psi^{\alpha\dagger}(z)] &&= -i\theta^X T^{X*}_{\alpha\alpha'}\psi^{\alpha'\dagger}(z)\ , \end{aligned} \tag{A.11}$$

as can directly be verified using eq. (A.2).

A.2.2 Kac-Moody Gauge Symmetries

Now note the following very important fact, which is a direct consequence of the linearization of the dispersion relation and hence the appearance of the very simple derivative $\partial_{\bar{z}}$ in the action: Whenever the action is invariant under eqs. (A.11), it is automatically also is invariant under the infinitesimal *local but analytical* gauge transformations that are obtained by replacing the constant parameters

[3] It sometimes happens that $\langle O_1(z+\delta)O_2(z)\rangle$ does not subtract off all the divergent terms; in that case, $: O_1(z)O_2(z) :$ should still be interpreted as $[O_1(z+\delta)O_2(z)$ – all divergent terms]. It can be shown (see [Lud94b, section 1.5]) that point-splitting in coordinate space is equivalent to normal ordering in momentum space.

θ^X by spatially varying *analytic*[4] functions $\theta^X(z)$ that are real on the real axis.[5] This is an immediate consequence of the fact that if $\theta^X(z)$ is analytic, then the derivative $\partial_{\bar{z}}$ in $\mathcal{S}$ commutes with $\theta^X(z)$. Thus, $\mathcal{S}$ is invariant under the following generalization of eq. (A.11):

$$\begin{aligned} \delta\psi^\alpha(z) &= -i\int_{-\infty}^{\infty}\tfrac{dx'}{2\pi}\theta^X(z')[J^X(z'),\psi^\alpha(z)] \quad = \quad i\theta^X(z)T^X_{\alpha\alpha'}\psi^{\alpha'}(z)\ , \\ \delta\psi^{\alpha\dagger}(z) &= -i\int_{-\infty}^{\infty}\tfrac{dx'}{2\pi}\theta^X(z')[J^X(z'),\psi^{\alpha\dagger}(z)] \ = \ -i\theta^X(z)T^{X*}_{\alpha\alpha'}\psi^{\alpha'\dagger}(z)\ . \end{aligned} \tag{A.12}$$

This conclusion is so important that it deserves a general formulation:

To each of the global gauge symmetries of the action there corresponds a **local** *gauge symmetry, obtained by allowing the parameters of the transformation to become* **analytic functions** *of z, i.e. $\theta^X = \theta^X(z)$. Such transformations leave the action form-invariant, since the derivative $\partial_{\bar{z}}$ commutes with any analytic function [$\partial_{\bar{z}}\phi(z) = \phi(z)\partial_{\bar{z}}$]. The corresponding local analytical gauge symmetries are called* **Kac-Moody (KM) gauge symmetries**.

Since the space of all analytic functions is infinite-dimensional, there are an infinite number of independent symmetry transformations, hence an infinite number of conserved Nöther currents. For example, if we put the system in a box, $x \in [0, l]$, with periodix boundary conditions on the currents $J^X(ix)$, then the $\theta^X(z)$ can be expanded in a Fourier series,

$$\theta^X(z') = \tfrac{2\pi}{l}\sum_{n\in Z} e^{2\pi n z'/l}\theta^X_n\ . \tag{A.13}$$

[4]Actually one has to be a little careful: since any analytic function that is not a constant is unbounded in the full complex plane, an analytic gauge transformation will diverge somewhere in the complex plane. Therefore one has to restrict attention to a bounded domain $\mathcal{D}$, and require $\theta^X(\tau, ix)$ to be analytic [$= \theta(z)$] inside $\mathcal{D}$, and non-analytic but bounded outside $\mathcal{D}$. This is discussed in more detail in appendix C.

[5]This condition, i.e. $\theta^X(\tau) = [\theta^X(\tau)]^*$, is necessary to ensure that on the real axis, where $z = \tau$ (so that all factors of ix are absent), eq. (A.12) reduces to the standard form (A.11), in which the θ^X are real. It implies that $\theta^X(z)$ must be the analytical continuation into the full complex plane ($\tau \to \tau + ix$) of some real function $\theta^X(\tau)$ (i.e. in the Taylor series $\theta^X(z)\sum_n a_n z^n$, all a_n are real).

Each term in this series, inserted into eq. (A.12), corresponds to a conserved current, whose conserved charge,

$$J_m^X(\tau) \equiv \int_0^l \tfrac{dx}{2\pi} e^{2\pi m z/l} J^X(z) \,, \tag{A.14}$$

satisfies $\partial_\tau J_m^X(\tau) = 0$ [see also eq. (A.67)].

The presence of an infinite number of conserved quantities of course allows one to extract an enormous amount of detailed information from the theory, and is at the heart of all that follows. For example, this appendix is concerned with analyzing the structure of the finite-size spectrum in ways that reflect these infinite symmetries. This is will be done by analysing the algebra satisfied by the generators $\{J_m^X\}$, which is called a Kac Moody algebra.

A.2.3 Conformal Symmetry

Finally, by inspection, the action is invariant under a global rescaling of coordinates, $\tau = a\tilde{\tau}$ and $x = a\tilde{x}$, accompanied by a rescaling of fields, $\psi^\alpha(\tau, ix) = a^{-1/2}\tilde{\psi}^\alpha(\tilde{\tau}, i\tilde{x})$. The simple nature of the derivative $\partial_{\bar{z}}$ in the action implies that this symmetry, too, has a local analytic version, namely *conformal symmetry* (see [Lud94b, section 2.1]). Make a change of coordinates by writing $z = \tau + ix$ as an arbitrary analytic function of a new variable $w = \tilde{\tau} + i\tilde{x}$:

$$z(w) = \tau(w) + ix(w) \,, \qquad [\text{and} \quad \bar{z}(\bar{w}) = \tau(\bar{w}) - ix(\bar{z}) \,] \,, \tag{A.15}$$

and define new fermion fields $\tilde{\psi}^\alpha(\tilde{\tau}, i\tilde{x})$, via

$$\psi^\alpha(\tau, ix) \equiv \left(\frac{dw}{dz}\right)^{1/2} \tilde{\psi}^\alpha\left(\tilde{\tau}, i\tilde{x}\right) , \qquad \psi^{\dagger\alpha}(\tau, ix) \equiv \left(\frac{dw}{dz}\right)^{1/2} \tilde{\psi}^{\dagger\alpha}(\tilde{\tau}, i\tilde{x}) \,. \tag{A.16}$$

In terms of the new coordinates the measure becomes[6]

$$d\tau dx \;=\; \left|\begin{smallmatrix} \frac{d\tau}{d\tilde{\tau}} & \frac{dx}{d\tilde{\tau}} \\ \frac{d\tau}{d\tilde{x}} & \frac{dx}{d\tilde{x}} \end{smallmatrix}\right| d\tilde{\tau}\, d\tilde{x} \;=\; \left|\begin{smallmatrix} \frac{dz}{dw} & \frac{d\bar{z}}{dw} \\ \frac{dz}{d\bar{w}} & \frac{d\bar{z}}{d\bar{w}} \end{smallmatrix}\right| d\tilde{\tau}\, d\tilde{x} \;, \tag{A.17}$$

and, for analytic transformations such as eq. (A.15), the second determinant simplifies to $\frac{dz}{dw}\frac{d\bar{z}}{d\bar{w}}$. Therefore, under this transformation, the action of eq.(A.6) becomes:

$$\begin{aligned} \mathcal{S} \;&=\; \int d\tilde{\tau} \int \tfrac{d\tilde{x}}{2\pi} \sum_\alpha \left|\frac{dw}{dz}\right|^{-2} \left[(\frac{dw}{dz})^{1/2} \tilde{\psi}^{\dagger\alpha}(\tilde{\tau}, i\tilde{x}) \frac{d\bar{w}}{d\bar{z}} 2\partial_{\bar{w}} \left((\frac{dw}{dz})^{1/2} \tilde{\psi}^{\alpha}(\tilde{\tau}, i\tilde{x}) \right) \right] \\ &=\; \int d\tilde{\tau} \int \tfrac{d\tilde{x}}{2\pi} \sum_\alpha \tilde{\psi}^{\alpha\dagger}(\tilde{\tau}, i\tilde{x}) 2\partial_{\bar{w}} \tilde{\psi}^{\alpha}(\tilde{\tau}, i\tilde{x}) \;. \end{aligned} \tag{A.18}$$

All derivatives cancel, and the action in terms of the new variables has the same form as the action eq.(A.6) in terms of the old variables. In other words, *the action* (A.6) *is invariant under conformal transformations* eq. (A.15). Note once again the importance of the tranformation being *conformal*: without the requirement that $w(z)$ be an analytic function of z, one would have had $\partial_{\bar{z}}(\frac{dw}{dz})^{1/2} \neq 0$, and $\mathcal{S}$ would not have been invariant.

The new equations of motion, $\partial_{\bar{w}}\tilde{\psi}^{\alpha}(\tilde{\tau}, i\tilde{x})$, imply that the new fields are again analytic functions, $\tilde{\psi}^{\alpha}(\tilde{\tau}, i\tilde{x}) = \tilde{\psi}^{\alpha}(w)$.

For future reference, let us find the generator for conformal transformations. Consider an infinitesimal conformal transformation, written in the form

$$w(z) = z - \varepsilon(z) \;, \tag{A.19}$$

where $\varepsilon(z)$ is small (footnote 4 applies here too). Eq. (A.16) implies that to order $O(\varepsilon)$, the infinitesimal change in $\psi^{\alpha}(z)$ is given by

$$\delta\psi^{\alpha}(z) \equiv \tilde{\psi}^{\alpha}(z) - \psi^{\alpha}(z) = \left[\tfrac{1}{2}\partial_z \varepsilon(z) + \varepsilon(z)\partial_z \right] \psi^{\alpha}(z) \;. \tag{A.20}$$

[6]The second equality follows by using $\binom{d\tau}{dx} = \frac{1}{2}\left(\begin{smallmatrix} 1 & 1 \\ -i & i \end{smallmatrix}\right)\binom{dz}{d\bar{z}}$ and $\binom{d\tilde{\tau}}{d\tilde{x}} = \frac{1}{2}\left(\begin{smallmatrix} 1 & 1 \\ -i & i \end{smallmatrix}\right)\binom{dw}{d\bar{w}}$ to rewrite the Jacobian determinant in terms of $dz, d\bar{z}, dw, d\bar{w}$.

Such infinitesimal conformal transformations on $\psi^\alpha(z)$ are generated by the so-called *stress-energy tensor* $T(z)$,

$$T(z) = \tfrac{1}{2} : \left\{ \left[\partial_z \psi^{\alpha\dagger}(z) \right] \psi^\alpha(z) - \psi^{\alpha\dagger}(z) \partial_z \psi^\alpha(z) \right\} : \ , \tag{A.21}$$

through the relation

$$\delta\psi^\alpha(z) = \int_{-\infty}^{\infty} \tfrac{dx'}{2\pi} \varepsilon(z') [T(z'), \psi^\alpha(z)] \ , \tag{A.22}$$

as can directly be verified using the anti-commutation relations (A.2).

A.2.4 Discussion

All of the above symmetries have profound implications for the structure of the theory. These were explored in a systematic fashion in the seminal work of Belavin, Polyakov and Zamolodchikov [BPZ84] for conformal invariance, and by Knizhnik and Zamolodchikov [KZ84] for Kac-Moody invariance. They are summarized in appendix B, and illustrated for free fermions in section B.2 of that appendix, where the equations of the preceding section will be found to be specific realizations of a much more general theory.

However, in the present appendix, we do not need these general results. Here we restrict our attention to the structure of the Hilbert space on which the Hamiltonian acts. Formally, whenever the Lagrangian is invariant under some symmetry, it must be possible to group the eigenstates of H together into subsets that transform into each other in a well-defined way under symmetry operations: the Hilbert space must carry a representation of the corresponding symmetry group.

To analyze the structure of the Hilbert space, it is convenient to put the system in a finite box, $x \in [0, l]$, so that the energy levels are quantized and one

has well-defined eigenstates to work with, and to study the structure of the finite-size spectrum. At first, this seems like a trivial question: the spectrum consists of (highly degenerate) energy levels spaced at uniform intervals, $\varepsilon_{n+\frac{1}{2}} = \frac{2\pi}{l}(n+\frac{1}{2})$. However, we are interested in more detail in the symmetry properties of the spectrum. We would like to answer the following question: How do the states of H transform under the symmetry operations that leave the action invariant? In other words, *how can the Hilbert space be organized into representations of some or other of the above symmetry groups?*

The possible representation can be found via algebraic techniques by rewriting the Hamiltonian in Sugawara form, and studying the commutation relations of the conserved charges. The various bosonization schemes that exist are simply ways of rewriting the Hamiltonian in terms of bosonic currents (expressions quadratic in the ψ's) in ways that make explicit the various symmetries of H and are adaptable to the particular symmetries that a given perturbation might have.

A.3 Finite Size System: Definitions

In this section we summarize the definitions we shall use for our analysis of the finite-size spectrum.

Impose anti-periodic[7] boundary conditions in the space direction on the fermion fields: $\psi^\alpha(\tau, x = l) \equiv -\psi^\alpha(\tau, x = 0)$, so that momenta and energies are quantized at $\varepsilon_{n+\frac{1}{2}} \equiv k_{n+\frac{1}{2}} = \frac{2\pi}{l}(n+\frac{1}{2})$. Let $\psi^{\alpha\dagger}_{n+\frac{1}{2}}$ create an electron of species α and

[7]The reason for choosing anti-periodic instead of periodic boundary conditions is to obtain a non-degenerate ground state, which simplifies the subsequent analysis considerably. With periodic boundary conditions, $\varepsilon_k = 0$ is an allowed energy value. Hence the ground state is 2^N fold degenerate, since the $\varepsilon_k = 0$ state of each of the N species can be either empty or occupied. This case is discussed in [AL92b, section V].

momentum $k_{n+\frac{1}{2}}$. Then the $T=0$ Fermi sea is characterized by

$$\psi^{\alpha}_{n+\frac{1}{2}}|0\rangle = \ 0 \qquad \text{if } \varepsilon_{n+\frac{1}{2}} > 0, \quad i.e. \text{ if } n \geq 0 \ , \tag{A.23}$$

$$\psi^{\alpha\dagger}_{n+\frac{1}{2}}|0\rangle = \ 0 \qquad \text{if } \varepsilon_{n+\frac{1}{2}} < 0, \quad i.e. \text{ if } n < 0 \ . \tag{A.24}$$

Normal ordering of operators in momentum space is consequently defined as follows:

$${}^{*}_{*}\psi^{\alpha\dagger}_{m+\frac{1}{2}}\psi^{\alpha}_{n+\frac{1}{2}}{}^{*}_{*} \equiv \begin{cases} \psi^{\alpha\dagger}_{m+\frac{1}{2}}\psi^{\alpha}_{n+\frac{1}{2}} & \text{if} \quad m \neq n \ , \\ \psi^{\alpha\dagger}_{m+\frac{1}{2}}\psi^{\alpha}_{m+\frac{1}{2}} & \text{if} \quad m = n \geq 0 \ ; \\ -\psi^{\alpha}_{m+\frac{1}{2}}\psi^{\alpha\dagger}_{m+\frac{1}{2}} & \text{if} \quad m = n < 0 \ . \end{cases} \tag{A.25}$$

The second-quantized field $\psi^{\alpha}(ix)$ in the Schrödinger picture are related to the $\psi^{\alpha\dagger}_{n+\frac{1}{2}}$ through a Fourier sum:

$$\psi^{\alpha}(ix) \ = \ \tfrac{2\pi}{l}\sum_{n\in Z} e^{-i2\pi(n+\frac{1}{2})x/l}\psi^{\alpha}_{n+\frac{1}{2}} \ , \tag{A.26}$$

$$\psi^{\alpha}_{n+\frac{1}{2}} \ = \ \int_0^l \tfrac{dx}{2\pi} e^{i2\pi(n+\frac{1}{2})x/l}\psi^{\alpha}(ix) \tag{A.27}$$

with

$$\int_0^l \tfrac{dx}{2\pi} e^{i2\pi nx/l} = \tfrac{l}{2\pi}\delta_{n,0} \ , \qquad \sum_{n\in Z} e^{-i2\pi nx/l} = l\delta(x) \ , \tag{A.28}$$

or, in the continuum limit,

$$\tfrac{2\pi}{l}\sum_{n\in Z} \to \int dp \ , \qquad \tfrac{l}{2\pi}\delta_{n,n'} \to \delta(p-p') \, . \tag{A.29}$$

Having chosen the normalization for the canonical anti-commutation relations as

$$\{\psi^{\dagger}(ix), \psi(iy)\} = 2\pi\delta(x-y) \qquad \{\psi^{\dagger}_{n+\frac{1}{2}}, \psi_{m+\frac{1}{2}}\} = \tfrac{l}{2\pi}\delta_{n,m} \ , \tag{A.30}$$

the free Hamiltonian is

$$H \ = \ \int_0^l \tfrac{dx}{2\pi} : \psi^{\alpha\dagger}(ix)\, i\partial_x\, \psi^{\alpha}(ix) : \tag{A.31}$$

$$= \frac{2\pi}{l} \sum_{n\in Z} \sum_{\alpha=1}^{N} \varepsilon_{n+\frac{1}{2}} {}^{*}_{*} \psi^{\alpha\dagger}_{n+\frac{1}{2}} \psi^{\alpha}_{n+\frac{1}{2}} {}^{*}_{*} \tag{A.32}$$

$$\tag{A.33}$$

The time-dependence of the Fourier modes in the Heisenberg picture is simply $\psi^{\alpha}_{n+\frac{1}{2}}(\tau) = \psi^{\alpha}_{n+\frac{1}{2}} e^{-\tau\varepsilon_{n+\frac{1}{2}}} = \psi^{\alpha}_{n+\frac{1}{2}} e^{-2\pi\tau(n+\frac{1}{2})/l}$. Thus eq. (A.26) implies $\psi^{\alpha}(\tau, ix) = \psi^{\alpha}(z)$, as we already know from eq. (A.4).

For future reference, let us calculate the free Green's function at $T \neq 0$. Thermal expectation values have their usual form (written in the continuum limit)

$$\langle \psi^{\alpha\dagger}_{p} \psi^{\alpha}_{p} \rangle = \delta_{\alpha\alpha'} \delta(p - p') f_{\varepsilon_p \alpha} \ , \qquad f_{\varepsilon_p \alpha} = \frac{1}{e^{\beta(\varepsilon_p - \mu_\alpha)} + 1} \ , \tag{A.34}$$

(for generality we show its form for $\mu_\alpha \neq 0$, although we use only $\mu = 0$ in this appendix). Using this, it is straightforward to obtain the finite-temperature Green's function for the fermions:

$$G_{\alpha\alpha'}(z - z') \equiv -\langle T\psi^{\alpha}(z) \psi^{\alpha'\dagger}(z') \rangle \tag{A.35}$$

$$= -\delta_{\alpha\alpha'} \int dp e^{-\varepsilon_p (z - z')} \left[\theta(\tau - \tau')(1 - f_{\varepsilon_p \alpha}) - \theta(\tau' - \tau) f_{\varepsilon_p \alpha} \right]$$

$$= -\delta_{\alpha\alpha'} \frac{e^{-\mu_\alpha (z - z')}}{\frac{\beta}{\pi} \sin \frac{\pi}{\beta}(z - z')} \ . \tag{A.36}$$

The last line can be obtained from standard tables, e.g. [Bate54, p.120, eq.(14)], or by doing the integral by contour methods.[8]

A.4 Free Fermion Partition Function

In this section we calculate the partition function for a single species of free, chiral fermions from first principles, following [Gins87, p.101]. This is an elementary

[8] Make a shift $p' = p - \mu_\alpha$, and close the $\int dp'$ integral along a semi-circle in the lower (or upper) half-plane for $(x - x') > 0$ (or < 0). There are an infinite number of poles at $p' = 2\pi(n + \frac{1}{2})/\beta$; their contributions can be summed up to give $\sin^{-1}$.

exercise, but instructive, since it sheds some light on what we can expect to find from more sophisticated approaches.

We take as Hamiltonian eq. (A.31) with $N = 1$ (and the index α suppressed). Since

$$Q \equiv \int_0^l \frac{dx}{2\pi} : \psi^\dagger(ix)\psi(ix) : \tag{A.37}$$

is the total number of particles relative to the Fermi surface (which has $Q = 0$), Q has integer eigenvalues, $Q \in Z$. The set of all eigenstates of H that have the same Q is called a *tower* of charge Q and denoted by $\{|Q, a\rangle\}$ (with a labelling the states within the tower). The partition function is sum over all towers:

$$Z = \text{Tr } e^{-\beta H} \equiv \sum_{Q \in Z} \chi_Q \tag{A.38}$$

$$\text{where} \qquad \chi_Q \equiv \sum_{\{a\}} \langle Q, a | e^{-\beta H} | Q, a \rangle \tag{A.39}$$

χ_Q, the partition function for the tower with charge Q, is called a *character* in group theory language.

The lowest state in the charge-Q tower is called the charge-Q *primary* state and denoted by $|Q\rangle$. It is the state in which all energy levels up to level Q are occupied and all higher levels are empty, and hence does not contain any particle-hole excitations. Hence its energy is

$$E_{oQ} - E_{oo} = \frac{2\pi}{l} \sum_{j=1}^{|Q|} (j - \tfrac{1}{2}) = \tfrac{2\pi}{l} Q^2/2 \,, \tag{A.40}$$

(the sum here is only over positive energies, since an electron that is added to the j-th level above the ground state, or a hole that is created in the j-th level below the ground state, both have energy $\frac{2\pi}{l}(|j| - \frac{1}{2})$.

The set of all particle-hole excitations that can be created from $|Q\rangle$ constitute the excited states, called *descendants*, in the tower. At energy $E_M = \frac{2\pi}{l} M$ above

E_{oQ} these states are described by a set of integers $k_1 \geq k_2 \geq ...k_l \geq 0$, with $\sum_{i=1}^{l} = M$ (these numbers specify the levels occupied by the uppermost l particles in that particular state, starting from the top). The total number of such states for given M is just the number of partitions $P(M)$ of M, a number that can be obtained from the generating function

$$\frac{1}{\prod_{n=1}^{\infty}(1-q^n)} \equiv \sum_{M=0}^{\infty} P(M)q^M \equiv q^{1/24}\eta^{-1}(q) \; , \tag{A.41}$$

where $\eta(q)$ is known as the Dedekind function. Defining $q \equiv e^{-2\pi\beta/l}$, the contribution from the Q-th tower to the partition function is;

$$\chi_Q \; = \; \sum_{M=0}^{\infty} P(M)e^{-\beta(E_{oQ}+2\pi M/l]} \; = \; \frac{q^{Q^2/2}e^{-\beta E_{oo}}}{\prod_{n=1}^{\infty}(1-q^n)} \; = \; \eta^{-1}(q)q^{Q^2/2}. \tag{A.42}$$

For the last equality, we used the fact that $E_{00} = -\frac{p}{l}\frac{c}{24}$, with c=1; this result can be found using more sophisticated CFT treatments of free fermions (see next section), where E_{00} arises as a finite-size correction to the ground state energy [BCN86,Aff86a].

The partition function itself thus is simply:

$$Z = \frac{1}{\eta(q)} \sum_{Q=-\infty}^{\infty} q^{Q^2/2} \; . \tag{A.43}$$

Using some standard identities [Gins87, eq.(7.13a), (7.29)], it can readily be checked that this result is identically equal to $Z = q^{-1/24}\prod_{n=0}^{\infty}\left(1+q^{(n+\frac{1}{2})}\right)^2$, which is the perhaps more familiar way of summing over all electron and hole states.

The following features of the above calculation will emerge again in subsequent sections:

(a) It is possible to classify or group states into towers, each labelled by a (or

several) quantum number(s) (Q in this case).

(b) In a given tower, the states with the lowest energy are called the primary states of the tower. All other states in the tower are called descendants, and are particle-hole excitations created from the primary states.

(c) When calculating the partition function, the contribution from the excited states (descendants) within any tower simply involves a sum over particle-hole excitations, and always yields a factor $\eta^{-1}(q)$.

(d) What remains is a contribution from the primary state(s) of each tower, summed over all towers ($\sum_{Q\in Z} q^{Q^2/2}$ in this case).

Grouping states together into towers is natural in CFT, since (as will be argued below (see page 293), a conformal transformation reshuffles states within a tower, but not among different towers; hence, *each tower carries an infinite-dimensional* (since arbitrarily high energies are involved) *representation of the conformal algebra, and, in our case, of some KM algebra.*

To make these statements explicit, one has to introduce some more technology. The reward for our extra labors will be that we shall find an algebraic way of classifying the free-fermion spectrum. Moreover, the method will be generalizable to the other, less trivial bosonization schemes, and allow us to uncover some less obvious features of the free fermion spectrum.

A.5 Current OPEs from Wick's theorem

Aff86b

The general strategy in all subsequent section will be to find the commutation relations obeyed by the conserved charges J_n^X of one of the Kac-Moody

gauge symmetries discussed in section A.2, and to analyze the representations of the resulting algebra. The desired commutation relations can be found in a straightforward way from those of the $\psi^{\alpha}_{n+\frac{1}{2}}$. Here we follow a slightly different strategy. We find the operator product expansion (OPE) of any two currents J^A and J^B explicitly, using nothing but the point-splitting prescription and Wick's theorem. From these one can then use a general result [eq. (A.62)] to read off the desired commutation relations. Moreover, the current OPEs allow a direct way of finding various Sugawara forms for the free Hamiltonian.

Consider again the system of N species of free, chiral fermions ψ^{α} introduced in section A.2. Let $A_{\alpha\alpha'}$ be an arbitrary $N \times N$ matrix, and define the current

$$J^A(z) \equiv \sum_{\alpha\alpha'} : \psi^{\alpha\dagger}(z) A_{\alpha\alpha'} \psi^{\alpha'}(z) : \ . \tag{A.44}$$

Using Wick's theorem and [from eq. (A.36)]

$$\langle \psi^{\alpha\dagger}(z+\delta)\psi^{\alpha'}(z)\rangle = \langle \psi^{\alpha}(z+\delta)\psi^{\alpha'\dagger}(z)\rangle = \frac{\delta_{\alpha\alpha'}}{\delta} \ , \tag{A.45}$$

it is straightforward to evaluate the product of two such currents:

$$\begin{aligned} J^A(z+\delta)J^B(z) \ &\equiv \sum_{\alpha\alpha'\beta\beta'} : \psi^{\alpha\dagger}(z+\delta) A_{\alpha\alpha'} \psi^{\alpha'}(z+\delta) : : \psi^{\beta\dagger}(z) B_{\beta\beta'} \psi^{\beta'}(z) : \\ &= \sum_{\alpha\alpha'\beta\beta'} A_{\alpha\alpha'} B_{\beta\beta'} \left[\frac{\delta_{\alpha\beta'}\delta_{\alpha'\beta}}{\delta^2} + \ : \psi^{\alpha\dagger}(z)\psi^{\alpha'}(z)\psi^{\beta\dagger}(z)\psi^{\beta'}(z) : \right. \\ &\qquad \left. + \ \tfrac{1}{\delta}\left(\delta_{\alpha'\beta} : \psi^{\alpha\dagger}(z+\delta)\psi^{\beta'}(z) : + \delta_{\alpha\beta'} : \psi^{\alpha'}(z+\delta)\psi^{\beta\dagger}(z) : \right) \right] \end{aligned} \tag{A.46}$$

The first and third terms arise from double and single Wick contractions. Note that terms that arise from contracting operators within the same : : do not contribute, since they are automatically subtracted by the point-splitting subtraction prescription. Now add $0 = (1-1)\frac{1}{\delta}\left[: \psi^{\alpha\dagger}(z)(AB-BA)_{\alpha\beta}\psi^{\beta\dagger}(z) : \right]$ and

rearrange, remembering that fermion fields inside : : anti-commute:

$$\begin{aligned} J^A(z+\delta)J^B(z) \;&=\; \tfrac{1}{\delta^2}\mathrm{Tr}[AB] \;+\; \tfrac{1}{\delta}\Big[:\psi^{\alpha\dagger}(z)(AB-BA)_{\alpha\alpha'}\psi^{\alpha'}(z):\Big] \\ &+\; :\Big(\partial_z\psi^{\alpha\dagger}(z)\Big)(AB)_{\alpha\alpha'}\psi^{\alpha'}(z): - :\psi^{\alpha\dagger}(z)(BA)_{\alpha\alpha'}\partial_z\psi^{\alpha'}(z): \\ &+\; :\psi^{\alpha\dagger}(z)A_{\alpha\alpha'}\psi^{\alpha'}(z)\psi^{\beta\dagger}(z)B_{\beta\beta'}\psi^{\beta'}(z): \quad . \end{aligned} \tag{A.47}$$

This result is an example of an OPE, the general form of which is:

$$A(z_1)B(z_2) = \frac{C(z_2)}{(z_1-z_2)^2} + \frac{D(z_2)}{(z_1-z_2)} + O(1)\ldots \tag{A.48}$$

We have displayed only the leading divergent terms as $z_1 \to z_2$; $O(1)$ denotes all terms that remain finite in this limit. An OPE expresses the product of two operators, in the limit that their arguments approach each other, in terms of a sum over local operators $C(z_2)$, $D(z_2)$, etc. Such an OPE is understood to become a true equation when inserted into *any* correlation function of other fields $O_j(z_j)$ in the theory under consideration, in the limit where the distance between z_1 and z_2 becomes much smaller than the distance between z_1 and z_2 and the arguments z_j of all the other fields O_j. (For a review of the concept of an OPE see e.g. [Car87].)

Eq.(A.47) will be very useful in subsequent sections for finding various equivalent expressions for the free-fermion Hamiltonian of eq. (A.31) in terms of expressions that are quadratic in various currents.

A.6 Abelian Bosonization

A.6.1 Tomonaga form of Hamiltonian

As discussed in section A.2, the action is invariant under phase changes of the form $\psi^\alpha \to e^{i\phi_\alpha}\psi^\alpha$. the corresponding N abelian conserved currents $J^\alpha(z)$ and

charges Q^α are:

$$J^\alpha(z) \equiv :\psi^{\alpha\dagger}(z)\psi^\alpha(z): \qquad (\alpha \text{ not summed}), \tag{A.49}$$

$$Q^\alpha \equiv \int_0^l \tfrac{dx}{2\pi} J^\alpha(z) \qquad (\alpha \text{ not summed}). \tag{A.50}$$

[i.e. $A_{\beta\beta'} = \delta_{\alpha\beta}\delta_{\alpha\beta'}$ in eq. (A.44)].

From eq. (A.47) the mutual OPEs of the currents are:

$$\begin{aligned} J^\alpha(z+\delta)J^{\alpha'}(z) &= \delta_{\alpha\alpha'}\left[\frac{1}{\delta^2} + :\left(\partial_z\psi^{\alpha\dagger}(z)\right)\psi^\alpha(z): - :\psi^{\alpha\dagger}(z)\partial_z\psi^\alpha(z):\right] \\ &\quad + :\psi^{\alpha\dagger}(z)\psi^\alpha(z)\psi^{\alpha'\dagger}(z)\psi^{\alpha'}(z): \end{aligned} \tag{A.51}$$

The second term in eq. (A.47) is zero, because $A = B$. If $\alpha = \alpha'$, the last is also zero because the ψ's anti-commute within the normal ordering symbol, and $\psi^\alpha(z)\psi^\alpha(z) = 0$, due to Fermi statistics. Consequently, we have the important result

$$\tfrac{1}{2} :J^\alpha(z)J^\alpha(z): := \tfrac{1}{2}\left[:\left(\partial_z\psi^{\alpha\dagger}(z)\right)\psi^\alpha(z): - :\psi^{\alpha\dagger}(z)\partial_z\psi^\alpha(z):\right], \tag{A.52}$$

the : : subtracting out the $\frac{1}{\delta^2}$ divergence.

Now note that the Hamiltonian eq. (A.31) may be written in the so-called Tomonaga form:

$$H = \sum_{\alpha=1}^N H^\alpha, \qquad H^\alpha = \int_0^l \tfrac{dx}{2\pi}\ \tfrac{1}{2} :J^\alpha(ix)J^\alpha(ix): \tag{A.53}$$

$$[H^\alpha, H^{\alpha'}] = [H^\alpha, Q^{\alpha'}] = [Q^\alpha, Q^{\alpha'}] = 0\,. \tag{A.54}$$

This scheme is known as abelian bosonization, because H is written in terms of the abelian currents J^α. The associated charges Q^α are the generators of the abelian $U_1(1) \times \ldots \times U_N(1)$ symmetry group of independent phase changes on each of the N species ψ^α.

A.6.2 Algebraic Analysis of Spectrum

Since the H^α and J^α for different α commute, we shall analyze the spectrum for a given H^α on its own, and hence suppress the index α in this subsection. Unraveling the structure of the spectrum is straightforward but instructive (we shall of course rediscover the tower structure introduced in section A.4). We follow the presentation of [Lud94b, sections 1.7, 1.8].

It is instructive to write H in terms of the Fourier modes of the current J:

$$J(ix) \equiv \tfrac{2\pi}{l} \sum_{m\in Z} e^{-i2\pi mx/l} J_m \tag{A.55}$$

$$J_m \equiv \int_0^l \tfrac{dx}{2\pi} e^{i2\pi mx/l} J(ix) \qquad \left[= \tfrac{2\pi}{l} \sum_{n\in Z} {}^*_*\psi^\dagger_{n+\frac{1}{2}}\psi_{n+m+\frac{1}{2}}{}^*_* \right] . \tag{A.56}$$

(These conventions are those of [Lud94b, Appendix]. Also, see [Lud94b, sections 1.5] for a discussion of the subtleties involved in going from point-splitting $(:\quad:)$ in position space to normal ordering $({}^*_*\quad{}^*_*)$ in momentum space.) We see from eq. (A.56) that J_m is built from an infinite sum of electron-hole excitations. Moreover, all non-negative Fourier modes $m > 0$ annihilate the Fermi sea,

$$J_m|0\rangle = 0 \qquad \text{if } m > 0 \, , \tag{A.57}$$

due to the definition (A.25) of ${}^*_*\quad{}^*_*$. Thus, normal ordering for the currents can be defined as follows

$${}^*_*J_m J_n{}^*_* \equiv \begin{cases} J_m J_n & \text{if } n \neq -m \, , \\ J_{-n} J_n & \text{if } n = -m > 0 \, , \\ J_n J_{-n} & \text{if } n = -m < 0 \, . \end{cases} \tag{A.58}$$

Next, introduce the so-called stress-energy tensor T, of central importance in

CFT, because it is the generator of coordinate transformations:[9]

$$T(z) \equiv \tfrac{1}{2} : J(z)J(z) : + (\tfrac{2\pi}{l})^2 \tfrac{c}{24} \ , \qquad c \equiv 1 \ . \tag{A.59}$$

Its Fourier modes are defined through

$$\tfrac{2\pi}{l} L_m \ \equiv \ \int_0^l \tfrac{dx}{2\pi} e^{i2\pi nx/l} T(ix) \ + \ \tfrac{2\pi}{l} \delta_{m,o} \tfrac{c}{24} \ = \ \tfrac{2\pi}{l} \sum_{n \in Z} \tfrac{1}{2}{}^*_* J_n J_{m-n}{}^*_* \ . \tag{A.60}$$

It follows from the 2nd equation in (A.53) that the Hamiltonian is related to L_o:

$$H = \tfrac{2\pi}{l} \left[-\tfrac{c}{24} + L_o \right] = \tfrac{2\pi}{l} \left[-\tfrac{c}{24} + \sum_{n \in Z} \tfrac{1}{2}{}^*_* J_n J_{-n}{}^*_* \right] \ . \tag{A.61}$$

The extra term $-\frac{2\pi}{l}\frac{c}{24}$ in eq. (A.61) arises from a careful treatment of the transition from point-splitting to normal ordering that occurs when rewriting H in Fourier space. Adding such a term in the definition (A.59) of the stress-energy tensor ensures that eqs. (A.60) and (A.61) are consistent (see [Lud94b, section 1.6]). This term turns out to be universal, in the sense that it is independent of the way one chooses to regularize the theory. Its value is always $-\frac{2\pi}{l}\frac{c}{24}$, where c, the so-called *central charge*, is a parameter of the theory. $c = 1$ for a theory of a single species of Dirac fermions, as in the present case of eqs. (A.59) to (A.61) (and hence $c_{\rm tot} = N$ if one considers all N species of fermions together).

The fact that the magnitude of the finite-size corrections in eqs. (A.59) to (A.61) depend only on the central chare c, can be used to interpret it as follows: it characterizes the magnitude of the "response" of the stress-energy tensor and the ground state energy to imposing a finite size on the system (see [Aff86a] and [BCN86], and for a nice summary, [CH93], p. 37).

[9] Note that eq. (A.52) ensures that the definitions eqs. (A.59) and (A.21) are consistent, up to the constant $(\frac{2\pi}{l})^2 \frac{c}{24}$, which is a finite-size effect that vanishes as $l \to \infty$. However, eq. (A.59) is a much more general definition of the stress-energy tensor – see [Gins87, section 9.2] for a general discussion of this construction, which we summarize in appendix B, section B.3.

The commutation relations of the J_m and L_m are found most easily by using the following result (proven in [Lud94b, eq.(1.40)]): if two operators $A(u_1)$ and $B(u_2)$ depend analytically on their arguments and have the OPE of eq. (A.48), then their commutation relations in Fourier space are

$$[A_n, B_m] = n\tfrac{2\pi}{l} C_{n+m} + D_{n+m} \ , \tag{A.62}$$

$$\text{where} \qquad A_m \equiv \int_0^l \tfrac{dx}{2\pi} e^{i2\pi mx/l} A(ix) \, . \tag{A.63}$$

Using point-splitting techniques such as those illustrated in section A.5, one readily finds the following OPEs:

$$T(z_1)J(z_2) = \frac{J(z_2)}{(z_1-z_2)^2} + \frac{\partial_{z_2} J(z_2)}{(z_1-z_2)} + \ldots \ ; \tag{A.64}$$

$$J(z_1)J(z_2) = \frac{1}{(z_1-z_2)^2} + \ldots \ . \tag{A.65}$$

where the $\ldots$ denote terms that are regular in the limit $z_1 \to z_2$. These relations translate into the following commutation relations for the currents (for the first of eq. (A.66), a generalization of eq. (A.62) is needed, see [Gins87, eq.(3.8a)]):

$$\begin{aligned} [L_n, L_m] &= (n-m)L_{n+m} + \tfrac{c}{12}(n^3-n)\delta_{n+m,0} \ ; \\ [L_n, J_m] &= -mJ_{n+m} \ ; \\ [J_n, J_m] &= n\delta_{n+m,0} \ . \end{aligned} \tag{A.66}$$

The first and third equations define the so-called *Virasoro* and $U(1)$ *Kac-Moody* algebras, respectively [they are a special case (namely $k=1$, $f=0$, $c=1$) of the general form of these relations, which will be encountered in eq. (A.105)]. They play a central role in CFT, since very many general properties can be deduced from them.

In close analogy to the representation theory of angular momenta, we can deduce the structure of the spectrum as follows:[10] Eq. (A.66a) and (A.66b), with $n = 0$, imply that

$$[H, L_m] = -\tfrac{2\pi}{l} m L_m \; ; \qquad [H, J_m] = -\tfrac{2\pi}{l} m J_m \; . \tag{A.67}$$

This implies that there are an infinite number of conserved quantities, namely[11] $J_m(\tau) \equiv e^{2\pi m\tau/l} e^{\tau H} J_m e^{-\tau H}$, all satisfying $\partial_\tau J_m(\tau) = 0$. As explained in section A.2, this is a consequence of the fact the action is invariant under an infinite set of Kac-Moody symmetry transformations, generated by the J_m. Furthermore, eq. (A.67) implies that (for $m > 0$) the L_{-m} and J_{-m} act as raising operators, and L_{+m} and J_{+m} as lowering operators (in units of $\frac{2\pi}{l}$), for the Hamiltonian H. Furthermore, we find that $[L_n, J_o] = [J_n, J_o] = 0$, hence all states related to each other by raising and lowering operations through L_n's or J_n's have the same charge, say Q. For any given Q, there is a so-called "primary state $|Q\rangle$ of charge Q", which by definition obeys

$$J_o|Q\rangle = Q|Q\rangle \qquad \text{and} \qquad J_m|Q\rangle = 0 \qquad \text{for all} \quad m > 0 \; . \tag{A.68}$$

Since for $m > 0$ the $J_m = \frac{2\pi}{l} \sum_{n \in Z} {}^*_* \psi^\dagger_{n+\frac{1}{2}} \psi_{n+m+\frac{1}{2}} {}^*_*$ [see eq. (A.56)] are (energy-) lowering operators, the second equation of (A.68) implies that $|Q\rangle$ has no particle-hole excitations and hence is the charge-Q state of lowest energy. Thus it is precisely the primary state of charge Q encountered in section A.4 (compare with point (b) on p. 285). All descendant (higher-energy) states $\{|Q, a\rangle\}$ in the

[10] For a systematic discussion of the representation theory of the Virasoro algebra, see [Gins87], section 3.3, or [CH93], chapter 4.

[11] The extra factor of $e^{2\pi m\tau/l}$ is needed to compensate for the fact that $[H, J_m] \neq 0$ if $m \neq 0$; it also follows naturally from general considerations of $J_m(\tau)$ as the conserved charge of a KM symmetry, see eq. (A.14).

charge-Q tower can be obtained from the primary state by application of all possible combinations of (energy-) raising operators J_m ($m < 0$). Thus they are essentially particle-hole excitations on $|Q\rangle$, and hence their energies are of the form

$$E_Q - E_o = \tfrac{2\pi}{l}(Q^2/2 + m) \ , \qquad m \in Z_+ \ , \tag{A.69}$$

where Z_+ denotes the non-negative integers.

A partition-function sum over the Q-th tower is simply equal to the character χ_Q of eq. (A.42). Note that eq. (A.69) implies the general rule

$$E_Q - E_o = \begin{cases} \tfrac{2\pi}{l} m & \text{for} \quad Q = \text{ even} \ , \\ \tfrac{2\pi}{l}(m + \tfrac{1}{2}) & \text{for} \quad Q = \text{ odd} \ , \end{cases} \qquad \text{with } m \in Z_+ \ , \tag{A.70}$$

as one would expect for Q free fermions with energies $\varepsilon_{n+\frac{1}{2}} = \frac{2\pi}{l}(n + \frac{1}{2})$.

Since the L_n are the Fourier components of the stress-energy tensor T which generates coordinate transformations, they play the role of generators of conformal transformations (on the strip of width l that we are considering). (To be precise, $(1 + \sum_n a_n L_n)$ is the generator of an infinitesimal conformal transformation characterized by the parameters a_n.) Now recall that $[L_m, J_o] = 0$ for *all* m. This means that conformal transformations don't change the charge Q of a state, i.e. they only mix state within the same tower. In other words, each tower $\{|Q, a\rangle\}$ is an infinite-dimensional representation of the conformal group, the primary state $|Q\rangle$ being the so-called highest weight state from which all other states in the tower can be generated.

Finally, note that eq. (A.66c), rewritten in position space, implies that

$$[J(ix), J(iy)] = -i\partial_x \delta(x - y) \ . \tag{A.71}$$

Thus, the current does not commute with itself! This is a consequence of vacuum fluctuations and is called the Schwinger or chiral anomaly.

Combining the $\alpha = 1, \ldots, N$ species at the end, the complete Hilbert space is a direct product of N copies of the one described above. In particular, a general primary state will be labelled by N charges, $|Q_1, \ldots, Q_N\rangle$.

To summarize this section, we have algebraically analyzed the spectrum of N species of free, chiral fermions, and found that it can be organized into (a direct product of) conformal towers, labelled by charges Q_α, each of which carries a representation of the conformal group.

For a detailed physical interpretation of the various states in a tower, see [Lud94b, section 1.8]. For a more systematic discussion of the properties of towers, primary states and descendants, see [BPZ84] or [Gins87, chapter 3].

A.7 $U(1) \times SU(N)$ Non-Abelian Bosonization

Under $SU(N)$ transformations that transform the various species ψ^α into each other, the abelian charge towers discussed above do not transform into each other in a simple way. Finding a classification of the spectrum in terms of $SU(N)$ multiplets is the subject of this section.

A.7.1 $SU(N)$ currents and OPEs

Let $T^a_{\alpha\alpha'}$, $A = 1, \ldots, N^2 - 1$ denote the generators of $SU(N)$ transformations in the fundamental ($N \times N$-dimensional) representation, and $f^{abc}_{(N)}$ the $SU(N)$ structure constants. Using the normalization $\mathrm{Tr}(T^a T^b) = \frac{1}{2}\delta^{ab}$, the following

properties hold:

$$[T^a, T^b] = f^{abc}_{(N)}\, T^c; \qquad \mathrm{Tr}(T^a) = 0; \qquad \sum_{a=1}^{N^2-1} (T^a T^a) = \frac{N^2-1}{2N}\ ; \tag{A.72}$$

$$\sum_{a=1}^{N^2-1} T^a_{\alpha\alpha'} T^a_{\beta\beta'} = \tfrac{1}{2}\left(\delta_{\alpha\beta'}\delta_{\alpha'\beta} - \tfrac{1}{N}\delta_{\alpha\alpha'}\delta_{\beta\beta'}\right)\ . \tag{A.73}$$

[The latter result can be obtained from noting that the left-hand side is an $SU(N)$-invariant tensor, and hence necessarily of the form $c_1\delta_{\alpha\beta'}\delta_{\beta\alpha'} + c_2\delta_{\alpha\alpha'}\delta_{\beta\beta'}$. The coefficients c_1 and c_2 are then obtained by enforcing the second and third equalities listed in eq. (A.72).]

The conserved current J^o and charge Q^o associated with total phase transformations ($\psi^\alpha \to e^{i\phi}\psi^\alpha$), and J^a, Q^a associated with $SU(N)$ transformations ($\psi^\alpha \to (R_N)_{\alpha\alpha'}\psi^{\alpha'}$), are constructed as follows:

$$J^o(z) \equiv \sum_{\alpha=1}^{N} :\psi^{\alpha\dagger}(z)\psi^\alpha(z): \qquad \left[= \sum_{\alpha=1}^{N} J^\alpha\right] \tag{A.74}$$

$$J^a(z) \equiv \sum_{\alpha,\alpha'=1}^{N} :\psi^{\alpha\dagger}(z) T^a_{\alpha\alpha'} \psi^{\alpha'}(z): \qquad (a = 1, \ldots, N^2-1)\ . \tag{A.75}$$

The corresponding charges are

$$Q^o \equiv \int_0^l \tfrac{dx}{2\pi} J^o(z)\ ; \qquad Q^a \equiv \int_0^l \tfrac{dx}{2\pi} J^a(z)\ . \tag{A.76}$$

Using the properties eq. (A.72) in the general OPE eq. (A.47), one immediately finds the following OPEs:

$$\begin{aligned} J^o(z+\delta)J^o(z) &= \tfrac{N}{\delta^2} + \sum_\alpha \left[: \left(\partial_z \psi^{\alpha\dagger}(z)\right)\psi^\alpha(z): - :\psi^{\alpha\dagger}(z)\partial_z\psi^\alpha(z):\right] \\ &\quad + \sum_{\alpha\beta} :\psi^{\alpha\dagger}(z)\psi^\alpha(z)\psi^{\beta\dagger}(z)\psi^\beta(z):\ ; \end{aligned} \tag{A.77}$$

$$J^a(z+\delta)J^{a'}(z) = \frac{\frac{1}{2}\delta^{aa'}}{\delta^2} + \tfrac{1}{\delta} f^{aa'c}_{(N)} J^c(z)$$

$$+\sum_{\alpha\alpha'}\Big[:\Big(\partial_z\psi^{\alpha\dagger}(z)\Big)\,(T^aT^{a'})_{\alpha\alpha'}\psi^{\alpha'}(z):-:\psi^{\alpha\dagger}(z)(T^{a'}T^a)_{\alpha\alpha'}\partial_z\psi^{\alpha'}(z):\Big]$$
$$+\sum_{\alpha\alpha'\beta\beta'}:\psi^{\alpha\dagger}(z)T^a_{\alpha\alpha'}\psi^{\alpha'}(z)\psi^{\beta\dagger}(z)T^{a'}_{\beta\beta'}\psi^{\beta'}(z):\quad. \tag{A.78}$$

Eq. (A.77) is very similar to eq. (A.51); however, the last term is non-zero even if $a = a'$, since $\psi^\alpha(z)\psi^\beta(z) \neq 0$ if $\alpha \neq \beta$. In eq. (A.78), the non-abelian nature of the $SU(2)$ currents manifests itself in the 2nd term (which was zero for $U(1)$ currents).

The OPEs again contain $:\psi^\dagger\partial_z\psi:$ terms, hence one can construct the free-fermion Hamiltonian eq. (A.31) from current bilinears. However, a very particular linear combination of J^oJ^o and J^aJ^a is needed to eliminate the non-zero $:\psi^\dagger\psi\psi^\dagger\psi:$ terms in eqs. (A.77) and (A.78). Using eq. (A.73) in eq. (A.78) it follows that

$$\begin{aligned}\sum_a :J^a(z)J^a(z): \;&=\; \left(\frac{N^2-1}{2N}\right)\sum_\alpha\Big[:\Big(\partial_z\psi^{\alpha\dagger}(z)\Big)\,\psi^\alpha(z):-:\psi^{\alpha\dagger}(z)\partial_z\psi^\alpha(z):\Big]\\ &\quad -\tfrac{1}{2}\Big(1+\tfrac{1}{N}\Big)\sum_{\alpha\alpha'}:\psi^{\alpha\dagger}(z)\psi^\alpha(z)\psi^{\alpha'\dagger}\psi^{\alpha'}(z):\;,\end{aligned} \tag{A.79}$$

which implies that the needed linear combination is

$$-\sum_\alpha :\psi^{\alpha\dagger}(z)\partial_z\psi^\alpha(z): = \tfrac{1}{2N}:J^oJ^o:(z)+\tfrac{1}{N+1}\sum_a :J^aJ^a:(z) \tag{A.80}$$

[compare [AL91b], eq.(2.8), or [KZ84], eq. (4.31)]. Consequently, the free fermion Hamiltonian (A.31) can be written in the following so-called *Sugawara form*, in which a separation of charge and spin degrees of freedom is manifest [Aff86a, eq.(2.32b)]:

$$H \;=\; H^c + H^s \tag{A.81}$$
$$H^c \;=\; \int_0^l \tfrac{dx}{2\pi}\tfrac{1}{2N}:J^oJ^o:(z) \tag{A.82}$$
$$H^s \;=\; \int_0^l \tfrac{dx}{2\pi}\tfrac{1}{N+1}\sum_a :J^aJ^a:(z)\,. \tag{A.83}$$

A.7.2 Algebraic Analysis of Spectrum

Since $[H^c, H^s] = 0$, we can again analyze the spectra of the "charge" and "spin" Hamiltonians H^c and H^s separately. For H^c, the analysis is identical to that presented in section A.6.2, and the central charge is again $c_c = 1$. Consequently, the charge spectrum is organized into charge towers labelled by a charge $Q \in Z$. The energies within a charge-Q tower are

$$E^c_Q - E^c_o = \tfrac{2\pi}{l}\left[\frac{Q^2}{2N} + m_c\right], \qquad (m_c \in Z_+)\ , \tag{A.84}$$

with characters

$$\chi^c_Q = \eta^{-1}(q) q^{\frac{Q^2}{2N}}\ . \tag{A.85}$$

To understand the structure of the spin spectrum, one uses the OPEs of T^s and J^a to calculate the commutation relations of the corresponding L^s_n and J^s_m. We adopt definitions analogous to eqs. (A.59), (A.60) and (A.56):

$$T^s(z) \equiv \tfrac{1}{N+1}\sum_a :J^aJ^a:(z) + (\tfrac{2\pi}{l})^2\tfrac{c_s}{24} \qquad c_s \equiv \tfrac{N^2-1}{N+1}\ ; \tag{A.86}$$

$$\begin{aligned} \tfrac{2\pi}{l}L^s_m &\equiv \int_0^l \tfrac{dx}{2\pi} e^{i2\pi mx/l} T(ix) \ + \ \tfrac{2\pi}{l}\delta_{m,o}\tfrac{c_s}{24} \ = \tfrac{2\pi}{l}\sum_{n\in Z}\sum_a \tfrac{1}{1+N}{}^*_*J^a_n J^a_{m-n}{}^*_*\ ; \\ J^a_m &\equiv \int_0^l \tfrac{dx}{2\pi} e^{i2\pi mx/l} J^a(ix) \qquad \left[= \tfrac{2\pi}{l}\sum_{n\in Z} {}^*_*\psi^{\alpha\dagger}_{n+\frac12} T^a_{\alpha\alpha'} \psi^{\alpha'}_{n+m+\frac12}{}^*_*\right]\ . \end{aligned} \tag{A.87}$$

$$H^s = \tfrac{2\pi}{l}\left[-\tfrac{c_s}{24} + L^s_o\right] = \tfrac{2\pi}{l}\left[-\tfrac{c_s}{24} + \sum_{n\in Z}\sum_a \tfrac{1}{1+N}{}^*_*J^a_n J^a_{-n}{}^*_*\right]\ . \tag{A.88}$$

Note, however, that the central charge in the spin sector, $c_s \equiv \frac{N^2-1}{N+1}$, is different from the charge case. Its value can be obtained by being careful about point-splitting and normal ordering when writing H^s in Fourier space (see [Lud94b, section 1.6]). A consistency check is always that the central charges of the various sectors of the theory have to add up to that of N free fermions: $c^{tot} = c_c + c_s = N$.)

The commutation relations that follow from the OPEs of T^s and the J^as are

$$\begin{aligned} [L^s_n, L^s_m] &= (n-m)L^s_{n+m} + \tfrac{c_s}{12}(n^3-n)\delta_{n+m,0}\ ; \\ [L^s_n, J^a_m] &= -mJ^a_{n+m}\ ; \\ [J^a_n, J^b_m] &= f^{abc}_{(N)}J^c_{n+m} + \tfrac{1}{2}n\delta^{ab}\delta_{n+m,0}\ . \end{aligned} \tag{A.89}$$

Eq. (A.89a) is again the Virasoro algebra, and eq. (A.89c) the so-called $SU(N)_1$ ($SU(N)$-level-1) Kac-Moody algebra. [The general meaning of "level-1" will become clear in section A.8, where the more general case of $SU(n)_k$ is discussed; eq. (A.89) is a special case of eq. (A.105), with $n = N$ and $k = 1$.]

Without going into details (which are analogous to those presented in section A.6.2), let us consider only the case $N = 2$, for which the structure constants are $f^{abc}_{(2)} = i\varepsilon^{abc}$. The spectrum is organized into 2 "spin" towers, labelled by a spin quantum number $j = 0, \frac{1}{2}$. These towers are built upon primary states $|j, j_z\rangle$ (explicitly: $|0, 0, \rangle$, $|\frac{1}{2}, \frac{1}{2}\rangle$ and $|\frac{1}{2}, -\frac{1}{2}\rangle$), which, by definition, satisfy

$$\sum_{a=1}^{3}(J^a_o J^a_o)|j, j_z\rangle = j(j+1)|j, j_z\rangle, \qquad j = 0, \tfrac{1}{2}\ , \tag{A.90}$$

$$J^3_o|j, j_z\rangle = j_z|j, j_z\rangle\ , \qquad (|j_z| \le j)\ , \tag{A.91}$$

$$L^s_m|j, j_z\rangle = J^a_m|j, j_z\rangle = 0 \qquad \text{for} \quad m > 0\ . \tag{A.92}$$

Eqs. (A.90) and (A.91) reflect the fact that the J^a_o satisfy an ordinary $SU(2)$ algebra (the restriction $j \le \frac{1}{2}$ is explained in footnote 12). For $m > 0$, the J^a_m are (energy-) raising operators, as follows from the second eq. (A.87). Therefore eq. (A.92) states that the primary states don't contain any particle-hole excitations, so that they are the lowest-energy states in the tower. Descendants are obtained by acting on $|j, j_z\rangle$ with the raising operators J^a_n, $n < 0$, and can have arbitrarily large energies and $|j_z|$. The energy of a state in the j-th tower has the

form

$$E_j^s - E_o^s = \tfrac{2\pi}{l}\left[\frac{j(j+1)}{3} + m_s\right] , \qquad (m_s \in Z_+) . \tag{A.93}$$

A.7.3 Gluing Conditions for $U(1) \times SU(2)$

According to eqs. (A.93) and (A.84), a direct product state $|Q, m_c; j, m^j\rangle$ has energy

$$E_{Qj} - E_{oo} = \tfrac{2\pi}{l}\left[\left(\frac{Q^2}{4} + m_c\right) + \left(\frac{j(j+1)}{3} + m_s\right)\right] , \tag{A.94}$$

with $m_c, m_s \in Z_+$. Note that for general combinations of (Q, j), $E_{Qj} - E_{oo}$ does not have the general property, specified by eq. (A.70), that a free fermion spectrum must always have, namely that all eigenenergies are multiples of $\frac{2\pi}{l}\frac{m}{2}$, with $m \in Z_+$. The reason is that we have decomposed our free fermions into charge and spin excitations. By themselves, however, these are unphysical, in the sense that they can not occur independently in a free fermion theory. To recover a free fermion spectrum from a Sugawara construction, one has to *glue together* charge and spin excitations in such way that the resulting eigenenergies conform to the free-fermion form of eq. (A.70). This is done by introducing a so-called *gluing condition*; this is a set of numbers $\{n_o^{Qj}\}$, which specify which combinations of charge and spin towers are allowed ($n_o^{Qj} = 1$) or not allowed ($n_o^{Qj} = 0$) in a free fermion spectrum. Since j is restricted to $j = 0, \frac{1}{2}$, we find (by simply inspecting eq. (A.94) for compatibility with eq. (A.70)):

$$n_o^{Qj} = \begin{cases} 1 & \text{if} \quad Q = \text{even} \quad \text{and} \quad j = 0 \ ; \\ 1 & \text{if} \quad Q = \text{odd} \quad \text{and} \quad j = \frac{1}{2} \ ; \\ 0 & \text{otherwise} \ . \end{cases} \tag{A.95}$$

The physical interpretation of this gluing condition is very simple: whenever one adds or removes one free fermion from the system, one changes *both* Q by 1 *and* j by $\frac{1}{2}$.

A quicker (if less general) way to derive this rule is as follows: From $U(1) \times U(1)$ bosonization (eq. (A.53), we know that

$$H|Q_1, Q_2\rangle = \tfrac{1}{2}\left(Q_1^2 + Q_2^2\right)|Q_1, Q_2\rangle \tag{A.96}$$

for a primary state with (Q_1, Q_2) electrons of species $(1, 2)$. Now, define

$$Q \equiv Q_1 + Q_2 \ , \qquad j \equiv \tfrac{1}{2}(Q_1 - Q_2) \ , \tag{A.97}$$

which implies

$$\tfrac{1}{2}\left(Q_1^2 + Q_2^2\right) \ = \ Q^2/4 + j^2 \qquad \left[= \ Q^2/4 + j(j+1)/3 \quad \text{for} \ \ j = 0, \tfrac{1}{2}\right] \ . \tag{A.98}$$

But, since (Q_1, Q_2) are integers, the gluing condition eq. (A.95) follows directly from eq. (A.97).

A primary state $|Q, j\rangle$ can thus be visualized as follows: If Q is even, it consists of $Q/2$ pairs of electrons of opposite species, filling up the lowest $Q/2$ levels, one pair per level, each pair coupled to spin $j = 0$ (since no $j > \frac{1}{2}$ states are allowed in the theory, as mentioned above). Hence the total spin of such a state is $j = 0$. If Q is odd, one simply adds one more electron at the next unfilled level, so that the total spin is $j = \frac{1}{2}$.

Finally, let us compare this organization of the spectrum into $U(1) \times SU(2)$ towers with the abelian $U(1) \times U(1)$ structure: In the former case there are $\infty \times 2$ towers, in the latter $\infty \times \infty$. How did this come about? Note that in the $U(1) \times SU(2)$ scheme, an *infinite number* of $U(1) \times U(1)$ towers are *combined*

together into only two multiplets: For any given $(Q_1 + Q_2) = Q$= even (or odd), the $|Q, j = 0\rangle$ (or $|Q, j = \frac{1}{2}\rangle$) tower consists of all combinations of $U(1) \times U(1)$ towers for which $Q_1 - Q_2$= even (or odd). The reason why it is possible to thus combine them is that it is possible to obtain all such states from each other by acting with J^a_m (which indeed is the reason why they are grouped into a single $U(1) \times SU(2)$ tower). For a very detailed description of how this happens, see [Lud94b, section 3.4].

The moral of the story is: if one considers a larger symmetry group, many more states become related to each other through symmetry operations, and the Kac-Moody towers are much "larger".

A.8 $U(1) \times SU(\tilde{N}) \times SU(k)$ Non-Abelian Bosonization

In the multi-channel Kondo problem, one needs to employ yet another non-abelian bosonization scheme. Suppose that the N species of electrons hitherto considered are labelled by two separate indices, $\psi^\alpha = \psi^{\mu i}$, with $\mu = 1, \ldots, \tilde{N}$ (spin index) and $i = 1, \ldots, k$ (flavor index), with $\tilde{N}k = N$. (In the k-channel Kondo problem, i is the channel index and μ the spin index, with $\tilde{N} = 2$.) Then the free-fermion H of eq. (A.31) is invariant under separate $SU(\tilde{N})$ transformations on the μ indices and $SU(k)$ transformations on the k indices. It is useful to employ a bosonization scheme which preserves these separate symmetries (because the Kondo interaction breaks the full $SU(\tilde{N}k)$ symmetry but not the smaller $SU(\tilde{N}) \times SU(k)$ symmetry). The techniques are identical to the ones outlined above; we therefore just outline the starting point and state the main results.

A.8.1 Sugawara form for H_o

Let $T^a_{\mu\mu'}$ and T^b_{ij} be the generators of $SU(\tilde{N})$ and $SU(k)$ in their respective fundamental representations, obeying relations like eqs. (A.72), (A.73), for $SU(N)$, with $N \to \tilde{N}$ or k, respectively. Define the conserved charge current J^o, $\tilde{N}^2 - 1$ spin currents J^a ($a = 1, \ldots, \tilde{N}^2 - 1$) and $k^2 - 1$ flavor currents I^b ($b = 1, \ldots, k^2 - 1$), as follows:

$$J^o(z) \equiv \sum_{\mu i} : \psi^{\mu i\dagger}(z)\psi^{\mu i}(z) : \qquad \left[= \sum_\alpha J^\alpha\right] \tag{A.99}$$

$$J^a(z) \equiv \sum_{\mu\mu' i} : \psi^{\mu i\dagger}(z) T^a_{\mu\mu'} \psi^{\mu' i}(z) : \qquad (a = 1, \ldots, \tilde{N}^2 - 1)\ , \tag{A.100}$$

$$I^b(z) \equiv \sum_{\mu i j} : \psi^{\mu i\dagger}(z) T^b_{ij} \psi^{\mu j}(z) : \qquad (b = 1, \ldots, k^2 - 1)\ , \tag{A.101}$$

The charge currents have the OPE eq. (A.77). The spin currents J^a have OPEs that are identical to eq. (A.78), except for the first term, where the trace over i produces an extra factor of k, to give a leading term of $\left(\frac{k/2}{\delta^2}\right)\delta_{aa'}$ [likewise for the flavor currents I^b, with leading term $\left(\frac{\tilde{N}/2}{\delta^2}\right)\delta_{bb'}$]. This implies immediately that the Sugawara form for H is [Aff86a, eq.(2.75)]:

$$\begin{aligned} H &= H^c + H^s + H^f \\ &= \int_0^l \tfrac{dx}{2\pi} \left[\tfrac{1}{2k\tilde{N}} : J^o J^o : \ + \tfrac{1}{\tilde{N}+k} : J^a J^a : \ + \tfrac{1}{k+\tilde{N}} : I^b I^b : \right]\ , \end{aligned} \tag{A.102}$$

The coefficients in the second line are determined by the requirement that the quartic terms $: \psi^\dagger\psi\psi^\dagger\psi :$ from the charge, spin and flavor sectors cancel each other identically.

The Hilbert space decomposes into a direct product of charge, spin and flavor towers. The spectrum of H^c can be organized into charge towers, labeled by $Q \in Z$, as before. The spin and flavor sectors of the theory can be organized into spin

and flavor towers, labeled by labels ρ_s (ρ_f) denoting the possible $SU(\tilde{N})$ [$SU(k)$] representations according to which the primary states of the corresponding spin (flavor) tower can transform. The internal structure of these towers is determined by the algebra satisfied by the $\{J^a_m\}$ and $\{I^b_m\}$. The OPEs in the spin sector translates (via eq. (A.62)) into

$$[L^s_n, L^s_m] = (n-m)L^s_{n+m} + \tfrac{c_s}{12}(n^3-n)\delta_{n+m,0}\ ; \tag{A.103}$$

$$[L^s_n, J^a_m] = -mJ^a_{n+m}\ ; \tag{A.104}$$

$$[J^a_n, J^{a'}_m] = f^{aa'c}_{(\tilde{N})}J^c_{n+m} + \tfrac{1}{2}kn\delta^{aa'}\delta_{n+m,0}\ . \tag{A.105}$$

Eq. (A.105) is known as the $SU(\tilde{N})_k$ ($SU(\tilde{N})$-level-k) Kac-Moody algebra (level k means that each field ψ^μ that carries a representation of $SU(\tilde{N})$ has k extra degrees of freedom, labelled by i, that are spectators under $SU(\tilde{N})$ transformations). The $[L^s_m, J^a_n]$ and $[L^s_m, L^s_n]$ commutation relations are as in eq. (A.89), but with central charge $c_s = \frac{k(\tilde{N}^2-1)}{\tilde{N}+k}$. Identical relations hold in the flavor sector, except that $\tilde{N}$ and k are interchanged, so that one obtains an $SU(k)_{\tilde{N}}$ algebra.

As a consistency check, note that the central charges do add up to N as they must [Aff86a, eq.(2.83)]:

$$c_{tot} = c_c + c_s + c_f = 1 + \tfrac{k(\tilde{N}^2-1)}{\tilde{N}+k} + \tfrac{\tilde{N}(k^2-1)}{k+\tilde{N}} = k\tilde{N} = N\ . \qquad \surd \tag{A.106}$$

This decomposition of the theory is denoted by

$$G = U(1) \times SU(\tilde{N})_k \times SU(k)_{\tilde{N}} \tag{A.107}$$

A.8.2 The case $\tilde{N} = 2$, $k = 2$

Finally, let us consider the case that is relevant to the 2-channel Kondo problem, namely $\tilde{N} = 2$, $k = 2$. Then both spin and flavor towers are governed by a

$SU(2)_2$ KM algebra. The spin and flavor primary states are denoted by $|j, j_z\rangle$ and $|j_f, j_{fz}\rangle$. By definition, the $|j, j_z\rangle$ satisfy eqs. (A.90) to eq. (A.92) (and likewise for $|j_f, j_{fz}\rangle$, with $J^a \to I^b$). However, the allowed spin (and channel) quantum nubmers are now[12] $j = 0, \frac{1}{2}, 1$ (and $j_f = 0, \frac{1}{2}, 1$).

The energy eigenvalues for states in a tower with charge, spin and flavor quantum numbers (Q, j, j_f) are given by

$$E_{Qjj_f} - E_{ooo} = \frac{2\pi}{l}\left[\left(\frac{Q^2}{8} + m_c\right) + \left(\frac{j(j+1)}{4} + m_s\right) + \left(\frac{j_f(j_f+1)}{4} + m_f\right)\right], \tag{A.108}$$

with $m_c, m_s, m_f \in Z_+$. Of course, to recover a free fermion spectrum, a free-fermion gluing condition has to be specified, i.e. a set of numbers $\{n_o^{(Q,j,j_f)}\}$, either 0 or 1, that determine which combinations of charge, spin and flavor excitations satisfy the free-fermion condition eq. (A.70) and hence are allowed in a free fermion spectrum. Finding these numbers for general values of k and $\tilde{N}$ is a complicated mathematical problem solved in [ABI90]. For the case $k = \tilde{N} = 2$ of present interest, however, working out the gluing condition is straightforward [AL92b, section 5, Table 1]: all we have to do is to analyze for which combinations of (Q, j, j_f) eq. (A.108) is compatible with the free-fermion condition of eq. (A.70).

First note that when specifiying the gluing condition, Q only needs to be

[12] In general, for $SU(2)_k$, the allowed values of j are $j = 0, 1/2, \ldots, k/2$. Physically, the reason why *primary* states with $j > k/2$ cannot occur is due to Fermi statistics [GW86, p.514-515]: to construct a state with $j > k/2$ and *without* particle-hole excitations, one has to use (partially) *symmetrized* (as opposed to completely antisymmetric) combinations of the avaible k different flavors of spin 1/2 states, all with the same particle number (else there would be particle-hole excitations). However, any such combination will vanish identically, since only completely anti-symmetric combinations of fermion states with identical quantum numbers can be non-zero. For an explicit illustration of this argument, see [Lud94b, section 3.4]. For an algebraic proof, see [Gins87], eq.(9.30), or [GW86], p.514-515.

Table A.1 Eigenenergies (in units of $\frac{2\pi}{l}$) of charge, spin and flavor primary states. At the same time, these numbers are also the scaling dimensions of the corresponding quantum fields.

$q = Q \mathrm{mod} 4$	:	0	± 1	2	j	:	0	$\frac{1}{2}$	1	j_f	:	0	$\frac{1}{2}$	1
$\frac{1}{8}q^2$	:	0	$\frac{1}{8}$	$\frac{1}{2}$	$\frac{1}{4}j(j+1)$	:	0	$\frac{3}{16}$	$\frac{1}{2}$	$\frac{1}{4}j_f(j_f+1)$	:	0	$\frac{3}{16}$	$\frac{1}{2}$

specified up to multiples of 4, i.e. we may write

$$Q \equiv q + 4n, \qquad n \in Z, \qquad q = -1, 0, 1, 2, \tag{A.109}$$

since

$$\tfrac{1}{8}Q^2 = \tfrac{1}{8}(q+4n)^2 = \tfrac{1}{8}q^2 \ + \ \text{integer} \ . \tag{A.110}$$

The values that the various terms in eq. (A.108) can take on are listed in table A.1. Simple inspection of this table shows that the only combinations (Q, j, j_f) for which eq. (A.108) is compatible with eq. (A.70), and hence for which $n_o^{(Q,j,j_f)} = 1$, are those listed in table A.2. The last column indicates generically what combinations of free fermion operators create from the $T = 0$ Fermi sea (denoted by $|0\rangle$) the primary state of the corresponding tower. For the lower three rows, involving two fermion operators, Clebsch-Gordan coefficients are needed (but not shown) in order to couple the $(\mu\mu')$ and (ii') indices together to the corresponding values of $j, j_f = 0, 1$.

Table A.2 Free-electron gluing condition for primary fields for $k = 2$, $\tilde{N} = 2$. All other combinations for which $n_o^{(Q,j,j_f)} \neq 0$ can be obtained from the above by letting $Q \to Q + 4m$ ($m \in Z$). For the lower three rows, involving two fermion operators, Clebsch-Gordan coefficients are needed (but not shown) in order to couple the $(\mu\mu')$ and (ii') indices together to the corresponding values of $j, j_f = 0, 1$.

Q	j	j_f	$\frac{l}{2\pi}(E_{Qjj_f} - E_{ooo})$	$n_o^{(Q,j,j_f)}$	state
0	0	0	$0+0+0 = 0$	1	$\|0\rangle$
$+1$	$\frac{1}{2}$	$\frac{1}{2}$	$\frac{1}{8}+\frac{3}{16}+\frac{3}{16} = \frac{1}{2}$	1	$\psi^{\mu i\dagger}_{\frac{1}{2}}\|0\rangle$
-1	$\frac{1}{2}$	$\frac{1}{2}$	$\frac{1}{8}+\frac{3}{16}+\frac{3}{16} = \frac{1}{2}$	1	$\psi^{\mu i}_{-\frac{1}{2}}\|0\rangle$
0	1	1	$0+\frac{1}{2}+\frac{1}{2} = 1$	1	$\psi^{\mu i\dagger}_{\frac{1}{2}}\psi^{\mu' i'}_{-\frac{1}{2}}\|0\rangle$
2	0	1	$\frac{1}{2}+0+\frac{1}{2} = 1$	1	$\psi^{\mu i\dagger}_{\frac{1}{2}}\psi^{\mu' i'\dagger}_{\frac{1}{2}}\|0\rangle$
2	1	0	$\frac{1}{2}+\frac{1}{2}+0 = 1$	1	$\psi^{\mu i\dagger}_{\frac{1}{2}}\psi^{\mu' i'\dagger}_{\frac{1}{2}}\|0\rangle$

Appendix B

Basic Facts of Bulk 2-D Conformal Field Theory

In this appendix we summarize the axioms of 2-dimensional quantum field theories that are invariant with respect to conformal (Virasoro) and non-abelian current (Kac-Moody) algebras.

Our reasons for presenting these here, despite not really having used them in the main part of the thesis, are the following: Firstly, in appendix A we analyzed in quite some detail the properties of free fermion theories, written in Sugawara form. However, our presentation was rather pedestrian, intended for a reader without any background in CFT. In the summary of the main axioms of CFT that is to follow, in particular in section B.3, the reader will recognize many of the results found in appendix A, which should give her a feeling for how these results fit into the general framework of CFT.

Secondly, whereas the methods of appendix A were sufficient to analyze the spectrum of the Kondo coupling at both weak and strong coupling, they are not

sufficient for calculating Green's functions. For this purpose, one has to take recourse to Cardy's boundary conformal field theory [described in appendix C], which in turn presupposes knowledge of the concepts summarized below.

Thirdly, by writing down the axioms that are needed for our purposes, and providing detailed references to where derivations may be found, we hope to inform the reader as to precicely what is needed in order to understand the technicalities of Affleck and Ludwig's treatment of the Kondo problem. Hopefully this will allow the reader to be more selective when learning this material from the standard references.

The material to follow was developed in the seminal papers by Belavin, Polyakov and Zamolodchikov [BPZ84] (on conformal symmetry) and Knizhnik and Zamolodchikov [KZ84] (on Kac-Moody symmetry). Detailed pedagogical presentations are given, for example, by Ginsparg [Gins87], Christe and Henkel [CH93] or Polchinski [Pol94, section 1]. Our summary is essentially plagiarises that given by Gepner and Witten [GW86, section 3] (which contains a number of minor typographical errors).

B.1 The Axioms of Bulk 2-D Conformal Field Theory

[BPZ84], [KZ84], [GW86, section 3], [Gins87], [CH93], [Pol94, section 1].

Consider a field theory in 2 dimensions, consisting of an infinite set of local fields, $\{A_i(z,\bar{z})\}$, that depend on two complex variables z and $\bar{z}$, which are kept as distinct variables.[1] The set of fields is assumed to be complete in the following

[1]To obtain the "physical" section of the theory, one can in the end treat them as complex conjugates of each other, as we did in eq. (A.15), by setting $z = \tau + ix$, $\bar{z} \equiv z^* = \tau - ix$ [BPZ84,

sense [BPZ84, eq.(1.6)]: it contains the identity operator, $A_o = I$, as well as all coordinate derivatives of each field involved. Furthermore, the operator product expansion of any two fields, $A_i(z,\bar{z})$ and $A_j(z',\bar{z}')$ can be written in terms of other local fields $A_k(z',\bar{z}')$:

$$A_i(z,\bar{z})A_j(z',\bar{z}') = \sum_k C_{ij,k}(z-z',\bar{z}-\bar{z}')A_k(z',\bar{z}') \ , \tag{B.1}$$

where the structure constants $C_{ij,k}$ are single-valued c-number functions. The operator algebra eq. (B.1) is assumed to have the associativity property. This places such stringent constraints on the $C_{ij,k}$ that if the theory has conformal or Kac-Moody symmetry, these functions can be determined exactly.

The theory is assumed to be invariant under a general analytic (conformal) transformation, in which one makes a change of coordinates from $(z,\bar{z})$ to $(\xi,\bar{\xi}) = (f(z),\bar{f}(\bar{z}))$, and expresses all field $A(z,\bar{z})$ in terms of new fields $\tilde{A}(\xi,\bar{\xi})$. Here f and $\bar{f}$ are any two, generally unrelated, analytic functions. Under such transformations, a *Virasoro primary field* is a field that is expressed as follows in terms of a new field $\tilde{\phi}(\xi,\bar{\xi})$:[2]

$$\phi(z,\bar{z}) = \left(\frac{\partial f}{\partial z}\right)^{\Delta_\phi}\left(\frac{\partial \bar{f}}{\partial \bar{z}}\right)^{\bar{\Delta}_\phi}\tilde{\phi}(\xi,\bar{\xi}) \ . \tag{B.2}$$

Here Δ and $\bar{\Delta}$ denote the left and right dimensions of the field. $\Delta+\bar{\Delta}$ is the conventional dimension, whereas $\Delta-\bar{\Delta}$ is the spin of the field. [The fields used

p. 335]. Once the physical section has been taken, the notation $A_i(z,\bar{z})$ may seem redundant, since then the value of z determines the value of $\bar{z}$, but it is useful to reserve the notation $A(z)$ or $A(\bar{z})$ for fields whose equations of motion make them *analytic* in z or $\bar{z}$, respectively.

[2]We employ the notation of [Lud94a], eq. (1.67), where the "passive" form of the transformation properties of primary fields is given. In many texts, the "active" form $\phi(z,\bar{z}) \to \left(\frac{\partial f}{\partial z}\right)^{\Delta_\phi}\left(\frac{\partial \bar{f}}{\partial \bar{z}}\right)^{\bar{\Delta}_\phi}\phi(\xi,\bar{\xi})$ is given, which in a sense corresponds to the inverse of eq. (B.2), with corresponding sign changes $\varepsilon \to -\varepsilon$ for the infinitesimal transformations discussed below.

in the Kondo problem are purely chiral, with $\bar{\Delta} = 0$ for L-movers and $\Delta = 0$ for R-movers.]

The theory is also assumed to possess a symmetry under a certain Lie algebra G. Under "isospin rotations", a *Kac-Moody primary field* $\varphi(z, \bar{z})$ of the Kac-Moody algebra is expressed in terms of a new field $\tilde{\varphi}(\xi, \bar{\xi})$ by[3]

$$\varphi(z, \bar{z}) = \Omega(z)\bar{\Omega}(\bar{z})\tilde{\varphi}(z, \bar{z}) \ , \tag{B.3}$$

and this is assumed to be a symmetry of the theory. In general $\Omega(z)$ and $\bar{\Omega}(\bar{z})$ may belong to any two representations of the Lie algebra, denoted by R and $\bar{R}$ respectively. Note that Ω ($\bar{\Omega}$) operates on the left (right) indices of the primary fields $\varphi(z, \bar{z})$, which indices take their values in the representation R ($\bar{R}$). [For the N species of free fermions of appendix A, the algebra is $SU(N)$, and for left-moving fermions R is the fundamental representation and $\bar{R}$ is the singlet representation; the representations are interchanged for right-moving fermions.] Note also that Ω and $\bar{\Omega}$ are analytic functions of z and $\bar{z}$, respectively.

Infinitesimal versions of the above transformations are generated by

$$\xi = f(z) = z - \varepsilon(z) \ , \qquad \bar{\xi} = \bar{f}(\bar{z}) = \bar{z} - \bar{\varepsilon}(\bar{z}) \ ; \tag{B.4}$$

$$\Omega(z) = I - \omega^a t^a \ , \qquad \bar{\Omega}(\bar{z}) = I - \bar{\omega}^a \bar{t}^a \ ; \tag{B.5}$$

where ε, $\bar{\varepsilon}$, ω^a and $\bar{\omega}^a$ are small, and t^a ($\bar{t}^a$) is an antihermitian matrix in the appropriate representation R ($\bar{R}$) of the algebra G, with $[t^a, t^b] = f_{abc}t^c$. Under

[3] In the original literature [KZ84, GW86] this law is written in the form $\varphi(z, \bar{z}) \to \Omega(z)\varphi(z, \bar{z})\bar{\Omega}^{-1}(\bar{z})$, i.e. the action on right-handed isospin indices occurs from the right. However, in the applications of interest to us, it is more natural to act on both left and right-handed isospin indices from the left (see e.g. eqsB.KM and (B.54) below), which leads to minor notational differences from [KZ84,GW86].

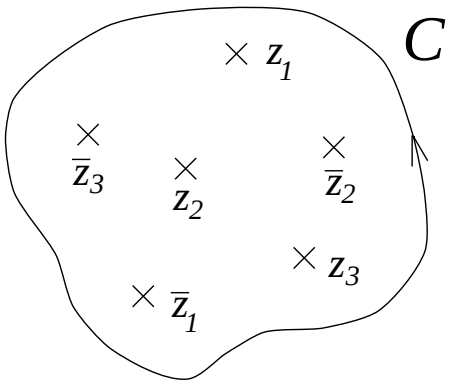

Figure B.1 A contour C that encloses all the points $z_1, \ldots, z_n,\ \bar{z}_1, \ldots, \bar{z}_n$ of the correlation function X of eq. (B.10).

such transformations, eqs. (B.2) and (B.3) become

$$\delta_{\varepsilon,\bar{\varepsilon}}\phi(z,\bar{z}) \equiv \tilde{\phi}(z,\bar{z}) - \phi(z,\bar{z}) \tag{B.6}$$

$$= \left[\Delta_\phi \varepsilon'(z) + \varepsilon(z)\partial_z + \bar{\Delta}_\phi \bar{\varepsilon}'(\bar{z}) + \bar{\varepsilon}(\bar{z})\partial_{\bar{z}}\right]\phi(z,\bar{z})\ ; \tag{B.7}$$

$$\delta_{\omega,\bar{\omega}}\varphi(z,\bar{z}) \equiv \tilde{\varphi}(z,\bar{z}) - \varphi(z,\bar{z}) \tag{B.8}$$

$$= \left[\omega^a(z)t^a + \bar{\omega}^a(\bar{z})\bar{t}^a\right]\varphi(z,\bar{z})\ . \tag{B.9}$$

Consider a correlation function of some fields, not necessarily Virasoro or Kac-Moody primary:

$$\langle X\rangle = \langle A_1(z_1,\bar{z}_1)\ldots A_n(z_n,\bar{z}_n)\rangle\ . \tag{B.10}$$

Let C be a contour that encloses all the points $z_1, \ldots, z_n,\ \bar{z}_1, \ldots, \bar{z}_n$, and let the conformal transformations $\varepsilon(z)$ and $\bar{\varepsilon}(\bar{z})$ be analytic in z and $\bar{z}$, respectively, inside C, and arbitrary but small outside C. These transformations are generated by the left-handed and right-handed components $T(z)$ and $\bar{T}(\bar{z})$ of the energy momentum tensor, which are analytic functions in z and $\bar{z}$ respectively due to the conservation laws $\partial_{\bar{z}}T(z) = \partial_z\bar{T}(\bar{z}) = 0$. The change in $\langle X\rangle$ due to such

conformal transformations is given by[45] (for a very nice discussion, see [Pol94, section 1.2]):

$$\langle \delta_{\varepsilon,\bar{\varepsilon}} X\rangle = \oint_C \tfrac{d\xi}{2\pi i}\, \varepsilon(\xi)\langle T(\xi)X\rangle \;-\; \oint_C \tfrac{d\bar{\xi}}{2\pi i}\, \bar{\varepsilon}(\bar{\xi})\langle \bar{T}(\bar{\xi})X\rangle \;. \tag{B.11}$$

For a single (arbitrary) field $A(z,\bar{z})$, this implies the transformation law

$$\delta_{\varepsilon,\bar{\varepsilon}} A(z,\bar{z}) = \oint_C \tfrac{d\xi}{2\pi i}\, \varepsilon(\xi)T(\xi)A(z,\bar{z}) \;-\; \oint_C \tfrac{d\bar{\xi}}{2\pi i}\, \bar{\varepsilon}(\bar{\xi})\bar{T}(\bar{\xi})A(z,\bar{z}) \;. \tag{B.12}$$

Likewise, let $\omega^a(z)$ and $\bar{\omega}^a(\bar{z})$ be analytic in z and $\bar{z}$, respectively, inside C. The corresponding Kac-Moody transformations are generated by the left and right isospin currents $J^a(z)$ and $\bar{J}^a(\bar{z})$, which are analytic functions in z and $\bar{z}$ respectively due to current conservation, $\partial_{\bar{z}} J^a(z) = \partial_z \bar{J}^a(\bar{z}) = 0$. The change in $\langle X\rangle$ due to such KM transformations is given by[6]

$$\langle \delta_{\omega,\bar{\omega}} X\rangle = -\oint_C \tfrac{d\xi}{2\pi i}\, \omega^a(\xi)\langle J^a(\xi)X\rangle \;+\; \oint_C \tfrac{d\bar{\xi}}{2\pi i}\, \bar{\omega}^a(\bar{\xi})\langle \bar{J}^a(\bar{\xi})X\rangle \;. \tag{B.13}$$

For a single (arbitrary) field $A_j(z,\bar{z})$, with left [right] isospin indices in the representations R $[\bar{R}]$ respectively, the currents J^a and $\bar{J}^a$ generate Kac-Moody transformations through

$$\delta_{\omega,\bar{\omega}} A_j(z,\bar{z}) = -\oint_C \tfrac{d\xi}{2\pi i}\, \omega^a(\xi)J^a(\xi)A_j(z,\bar{z}) \;+\; \oint_C \tfrac{d\bar{\xi}}{2\pi i}\, \bar{\omega}^a(\bar{\xi})\bar{J}^a(\bar{\xi})A_j(z,\bar{z}) \;. \tag{B.14}$$

In eq. (B.12) the functions $\varepsilon(z)$ and $\bar{\varepsilon}(\bar{z})$ are independent, and in (B.14) the functions $\omega^a(z)$ and $\bar{\omega}^a(\bar{z})$ are independent. This means that the z and $\bar{z}$

[4] We use the convention that both the $\oint d\xi$ and $\oint d\bar{\xi}$ integrations are counterclockwise around C. This means that $\oint_C \frac{d\xi}{2\pi i}\frac{f(\xi)}{\xi - z} = f(z)$, and $-\oint_C \frac{d\bar{\xi}}{2\pi i}\frac{f(\bar{\xi})}{\xi - \bar{z}} = f(\bar{z})$.

[5] Eq. (B.11) is derived for free fermions in section B.2. [Gins87], p.18, 19. explains lucidly how the contour integrals arise from the familiar commutation relations $\delta X = \varepsilon[T, X]$ of eq. (A.22).

[6] This is the analogue of the familiar relation $\delta X = -\omega^a[J^a, X]$ of eq. (A.12). We use sign-conventions for $J^a, \bar{J}^a$ in eq. (B.13) that are opposite to those of [KZ84], eq.(2.7) and [GW86], eq. (3.15); this choice is made in order to be consistent with the free-fermion representation of the current operators that is used in the rest of this thesis, namely $J^a(z) =: \psi^\dagger(z) T^a \psi(z) :$, with normalization $\langle \psi^\dagger(\xi)\psi(z)\rangle = (\xi - z)^{-1}$. Consequently, theWard identity eq. (B.24) and all related equations differ by a minus sign from those in [KZ84] and [GW86].

dependences actually separate, so that a field may be thought to "factorize" into a left- and right-handed component [Lud94a, eq.(6.12)]:

$$A_i(z,\bar{z}) \;=\; A_{iL}(z)A_{iR}(\bar{z})\,. \tag{B.15}$$

To be more precise, all correlation functions are sums of products of left and right factors [Lud94a, eq.(6.13)]:

$$\langle A_1(z_1,\bar{z}_1)\dots A_n(z_n,\bar{z}_n)\rangle = \tag{B.16}$$
$$\sum_{(a),(b)} \langle A_{1L}(z_1)\dots A_{nL}(z_n)\rangle_{(a)}\langle A_{1R}(\bar{z}_1)\dots A_{nR}(\bar{z}_n)\rangle_{(b)}\cdot M^{(a),(b)}\;.$$

However, a "correlation function" of purely left- or right-handed fields, a so-called "conformal block", is in general not completely specified by the fields themselves, and extra labels (a), (b) are needed. The reason is [KZ84, section 4] that such a pure L-handed correlation function typically has to satisfy a set of differential equations, known as the Knizhnik-Zamolodchikov equations, which have, in general, *several* independent solutions, labeled by the index (a). The matrix M in eq. (B.16), which specifies which linear combination of products of conformal blocks needs to be used, is determined by the requirement that the left-hand side of eq. (B.16) be single-valued [DF84,BPZ84].

Now consider correlation functions $\langle X\rangle$ of Virasoro primary fields, and $\langle Y\rangle$ of Kac-Moody primary fields:

$$\langle X\rangle = \langle \phi_1(z_1,\bar{z}_1)\dots\phi_n(z_n,\bar{z}_n)\rangle\;. \tag{B.17}$$

$$\langle Y\rangle = \langle \varphi_1(z_1,\bar{z}_n)\dots\varphi_n(z_n,\bar{z}_n)\rangle\;. \tag{B.18}$$

Then, using eq. (B.6) on the left-hand-side of eq. (B.11), and eq. (B.8) on the left-hand-side of eq. (B.13), we obtain

$$\oint_C \tfrac{d\xi}{2\pi i}\,\varepsilon(\xi)\langle T(\xi)X\rangle \;-\; \oint_C \tfrac{d\bar{\xi}}{2\pi i}\,\bar{\varepsilon}(\bar{\xi})\langle \bar{T}(\bar{\xi})X\rangle$$

$$= \sum_{i=1}^{n} \left[\Delta_{\phi_i} \varepsilon'(z_i) + \varepsilon(z_i)\partial_{z_i} + \bar{\Delta}_{\phi_i} \bar{\varepsilon}'(\bar{z}_i) + \bar{\varepsilon}(\bar{z}_i)\partial_{\bar{z}_i} \right] \langle X \rangle \; ; \tag{B.19}$$

$$- \oint_C \tfrac{d\xi}{2\pi i}\, \omega^a(\xi) \langle J^a(\xi) Y \rangle \; + \; \oint_C \tfrac{d\bar{\xi}}{2\pi i}\, \bar{\omega}^a(\bar{\xi}) \langle \bar{J}^a(\bar{\xi}) Y \rangle$$

$$= \sum_{i=1}^{n} \left[\omega^a(z_i) t_i^a + \bar{\omega}^a(\bar{z}_i) \bar{t}_i^a \right] \langle Y \rangle \; . \tag{B.20}$$

The notation in eq. (B.20) means that t_i^a $[\bar{t}_i^a]$ acts on the left [right] isospin indices of the field φ_i $[\bar{\varphi}_i]$ in $\langle Y \rangle$.

Since the functions $\varepsilon(z)$ and $\bar{\varepsilon}(\bar{z})$ are independent, and likewise $\omega(z)$ and $\bar{\omega}(\bar{z})$ are independent, the z and $\bar{z}$ dependences in eqs. (B.19) and (B.20) separate, as explained above:

$$\oint_C \tfrac{d\xi}{2\pi i}\, \varepsilon(\xi) \langle T(\xi) X \rangle \;=\; \sum_{i=1}^{n} \left[\Delta_{\phi_i} \varepsilon'(z_i) + \varepsilon(z_i)\partial_{z_i} \right] \langle X \rangle \; ; \tag{B.21}$$

$$- \oint_C \tfrac{d\xi}{2\pi i}\, \omega^a(\xi) \langle J^a(\xi) Y \rangle \;=\; \sum_{i=1}^{n} \omega^a(z_i) t_i^a \langle Y \rangle \; , \tag{B.22}$$

with similar equations for $\langle \bar{T}(\bar{\xi}) X \rangle$ and $\langle \bar{J}^a(\bar{\xi}) Y \rangle$. We henceforth do not display the right-handed expressions in $\bar{z}$, since they are entirely analogous to the left-handed ones in z.

Using Cauchy's theorem to write the right hand sides of these equations as contour integrals over $\oint_C d\xi$, and then noting that the resulting equations must hold for arbitrary $\varepsilon(\xi)$ and $\omega^a(\xi)$, one obtains the Ward identities for correlation functions of Virasoro and Kac-Moody primary fields, respectively:

$$\langle T(\xi) X \rangle \;=\; \sum_{i=1}^{n} \left[\frac{\Delta_{\phi_i}}{(\xi - z_i)^2} + \frac{1}{(\xi - z_i)} \partial_{z_i} \right] \langle X \rangle \; ; \tag{B.23}$$

$$\langle J^a(\xi) Y \rangle \;=\; \sum_{i=1}^{n} \frac{-\, t_i^a}{(\xi - z_i)} \langle Y \rangle \; , \tag{B.24}$$

with identical equations for $\bar{T}$ and $\bar{J}^a$, in terms of $\bar{\Delta}_\phi$ and $\bar{t}^a$. These relations imply the following operator product expansions of a Virasoro primary field with

T, and of a Kac-Moody primary field with J^a:

$$T(\xi)\phi_i(z,\bar{z}) = \frac{\Delta_{\phi_i}}{(\xi-z)^2}\phi_i(z,\bar{z}) + \frac{1}{(\xi-z)}\partial_z\phi_i(z,\bar{z}) + \quad \dots \tag{B.25}$$

$$J^a(\xi)\varphi_i(z,\bar{z}) = \frac{-\,t_i^a}{(\xi-z)}\varphi_i(z,\bar{z}) + \quad \dots \ , \tag{B.26}$$

where the ... represent terms that are regular as $\xi \to z$.

The energy momentum tensor has dimension $\Delta = 2$ but is not Virasoro primary; the currents are not Kac-Moody primary, but are Virasoro primary with dimension $\Delta = 1$. Their mutual OPE's are

$$T(\xi)T(z) = \frac{c/2}{(\xi-z)^4} + \frac{2}{(\xi-z)^2}T(z) + \frac{1}{(\xi-z)}T'(z) + \quad \dots \ ; \tag{B.27}$$

$$T(\xi)J^a(z) = \frac{1}{(\xi-z)^2}J^a(z) + \frac{1}{(\xi-z)}J^{a\prime}(z) + \quad \dots \ ; \tag{B.28}$$

$$J^a(\xi)J^b(z) = \frac{\frac{1}{2}k\delta^{ab}}{(\xi-z)^2} + \frac{f^{abc}}{(\xi-z)}J^c(z) + \quad \dots \ . \tag{B.29}$$

The definitions of T and J^a have to be supplemented with the asymptotic conditions[7]

$$T(z) \sim z^{-4} \ , \qquad J^a(z) \sim z^{-2} \ , \qquad \text{as } \ z \to \infty \ . \tag{B.30}$$

$T(z)$ and $J^a(z)$ can be expanded in Laurent series:

$$T(z) = \sum_{n=-\infty}^{\infty} L_n z^{-n-2} \ , \qquad\qquad J^a(z) = \sum_{n=-\infty}^{\infty} J_n^a z^{-n-1} \ . \tag{B.31}$$

The L_n and J_n^a may be though of as maps which act on the space of local fields through[8]

$$L_n A(z,\bar{z}) = \oint_C \tfrac{d\xi}{2\pi i}\, T(\xi)(\xi-z)^{n+1}A(z,\bar{z}) \ , \tag{B.32}$$

$$J_n^a A_j(z,\bar{z}) = \oint_C \tfrac{d\xi}{2\pi i}\, J^a(\xi)(\xi-z)^{n}A_j(z,\bar{z}) \ , \tag{B.33}$$

[7] See [KZ84, eq. (2.10)]; an explanation of this condition can be found in [CH93], after eq. (2.40).

[8] I believe that the extra t_j^a contained in eq. (B.3.20) of [GW86] and eq. (2.15) of [KZ84] relative to eq. (B.33) is a typo.

and due to the Ward identities eqs. (B.12) and (B.14) they generate the conformal and Kac-Moody transformations on the fields.

Due to eq. (B.27), the L_n obey the Virasoro algebra,

$$[L_n, L_m] = (n-m)L_{n+m} + \tfrac{1}{12}c(n^3-n)\delta_{n+m,0} \ , \tag{B.34}$$

in other words, the fields of the theory constitute a representation of the Virasoro algebra, where the Virasoro operators act on them as defined in eq. (B.32).

Likewise, eq. (B.29) implies that the J_n^a satisfy the Kac-Moody algebra (or current algebra):[9]

$$\left[J_n^a, J_m^b\right] = f^{abs}J_{n+m}^c + \tfrac{1}{2}kn\delta^{ab}\delta_{n+m,0} \ , \tag{B.35}$$

$$\left[J_n^a, \bar{J}_m^b\right] = 0 \ . \tag{B.36}$$

If one assumes that a primary field of the Kac-Moody algebra is also a primary field of the Virasoro algebra [this is true for all Wess-Zumino-Witten theories, which is sufficiently general for our purposes (see section B.3)], then under J_n^a and L_n the fields in the theory transform into one another. In particular, for Virasoro primary fields one has [from eqs. (B.25)]

$$L_n\phi_l = 0 \quad \text{for} \ \ n>0 \ , \qquad \text{and} \quad L_o\phi_l = \Delta_l\phi_l \ , \tag{B.37}$$

and for KM primary fields [from (B.26)]:

$$J_n^a\varphi_l = 0 \quad \text{for} \ \ n>0 \ , \qquad \text{and} \quad J_0^a\varphi_l = -t_l^a\varphi_l \ . \tag{B.38}$$

By repeatedly applying on a primary field operators from the Virasoro or Kac-Moody algebra, one obtains new local fields of the general form:

$$J_{-n_1}^{a_1}J_{-n_2}^{a_2}\ldots\bar{J}_{-\bar{n}_1}^{\bar{a}_1}\bar{J}_{-\bar{n}_2}^{\bar{a}_2}\ldots L_{-m_1}L_{-m_2}\ldots\bar{L}_{-\bar{m}_1}\bar{L}_{-\bar{m}_2}\ldots\phi(z,\bar{z}) \ . \tag{B.39}$$

[9] These relations were derived in a pedestrian manner in appendix A.

Mathematically, this field $\phi(z,\bar{z})$ generates a highest-weight representation of the combined Kac-Moody and Virasoro algebras. The highest-weight vector is the primary field ϕ and its weight is $(\Delta,\bar{\Delta})$ for $(L_o,\bar{L}_o)$, and the weights of the representations $(R,\bar{R})$ for the Kac-Moody algebra. This is due to the fact that all the positive operators (those with $n>0$) annihilate the primary field [eq. (B.37)].

Every local field in the theory will belong to some unique such highest-weight representation with a certain primary field sitting at the top. Thus, every field corresponds to some unique primary one. The Ward identities enable us to express any correlator of local fields in terms of those of primary fields. One simply needs to repeatedly apply the Ward identities. It is thus sufficient to focus attention on the correlators of primary fields, since they contain the full information about the theory.

The simplest example of relations satisfied by the correlators of primary fields follows from the general Ward identies of eqs. (B.23) and (B.24). The asymptotic behavior as $z\to\infty$ of the currents is $T(z)\to z^{-4}$ and $J^a(z)\to z^{-2}$ (this is understood to be valid when the currents are inside correlators; these relations follow from the requirement of regularity at infinity). Applying these to the Ward identities and integrating $\oint d\xi$ around a contour that encloses all the $\{z_i,\bar{z}_i\}$, one obtains

$$\sum_{i=1}^{n} t_i^a \langle \varphi_1(z_1,\bar{z}_1)\dots\varphi_n(z_n,\bar{z}_n)\rangle \;=\; 0\,, \qquad \text{(B.40)}$$

$$\sum_{i=1}^{n} t_i^a \left(z_i^{n+1}\partial_{z_i}+(n+1)\Delta_i z_i^n\right)\langle \varphi_1(z_1,\bar{z}_1)\dots\varphi_n(z_n,\bar{z}_n)\rangle \;=\; 0\,, \qquad \text{(B.41)}$$

where $n=-1,0,1$. These equations are the manifestations of invariance with respect to the subalgebras of projective conformal transformations and of global gauge transformations. They strongly constrain the correlators of primary fields,

enabling one to write them in terms of invariants of the algebra G and the projective transformations. The two- and three-point functions are completely determined by these equations, up to an overall constant [Gins87, section 2.1]: writing $z_{12} \equiv z_1 - z_2$ and $\bar{z}_{12} \equiv \bar{z}_1 - \bar{z}_2$

$$\langle \phi_1^{ij}(z_1, \bar{z}_1) \phi_2^{kl}(z_2, \bar{z}_2) \rangle = \frac{A_{ik-o} B_{jl,o}}{z_{12}^{2\Delta} \bar{z}_{12}^{2\bar{\Delta}}} \ , \tag{B.42}$$

for $\Delta_1 = \Delta_2 = \Delta$, and $\bar{\Delta}_1 = \bar{\Delta}_2 = \bar{\Delta}$, otherwise the correlator vanishes. Also (using the convention of [Gins87, eq. (2.5)])

$$\langle \phi_1^{ij}(z_1, \bar{z}_1) \phi_2^{kl}(z_2, \bar{z}_2) \phi_3^{mn}(z_3, \bar{z}_3) \rangle = \frac{F_{ik,m} G_{jl,n}}{z_{12}^{\Delta_{123}} z_{23}^{\Delta_{231}} z_{13}^{\Delta_{312}} \bar{z}_{12}^{\bar{\Delta}_{123}} \bar{z}_{23}^{\bar{\Delta}_{231}} \bar{z}_{13}^{\bar{\Delta}_{312}}} \tag{B.43}$$

where $\Delta_{abc} = \Delta_a + \Delta_b - \Delta_c$. The constants A, B, F, and G are proportional to the appropriate structure constants (Clebsch-Gordan coefficients) of the algebra.

Four-point functions, however, are not so fully determined just by conformal invariance. Invariance under the small conformal group allows the following general form [Pol70], [Gins87, eq. (2.6)]:

$$G^{(4)}(z_m, \bar{z}_m) = g(\xi, \bar{\xi}) \prod_{m<n} z_{mn}^{-(\Delta_m + \Delta_n) + \Delta_T/3} \prod_{m<n} \bar{z}_{mn}^{-(\bar{\Delta}_m + \bar{\Delta}_n) + \bar{\Delta}_T/3} \ , \tag{B.44}$$

where $\Delta_T = \sum_{i=n}^{4} \Delta_n$, $\bar{\Delta}_T = \sum_{i=n}^{4} \bar{\Delta}_n$, and the cross-ration ξ and its relatives are defined by:

$$\xi = \frac{z_{12} z_{34}}{z_{13} z_{24}} \ , \qquad 1 - \xi = \frac{z_{14} z_{23}}{z_{13} z_{24}}, \quad \frac{\xi}{1 - \xi} = \frac{z_{12} z_{34}}{z_{14} z_{23}} \ . \tag{B.45}$$

In general one cannot say more than that about the correlators, but there are some very important exceptions in which it is possible to obtain strong constraints on the correlators. They all stem form the fact that the various fields defined in eq. (B.39) are not linearly independent even though they formally appear to be

so. In particular there will be some combinations of (negative) operators from the Virasoro and Kac-Moody algebras which annihilate a particular primary field. The fields in eq. (B.39) which formally do not vanish, but in actuality do, are called *null vectors*. They play a crucial role both in the representation theory and in conformal field theory. The vanishing of a null vector implies the vanishing of a correlator containing it. In view of the Ward identities, this in turn gives rise to a constraint on the correlators of primary fields – typically, they have to satisfy some differential equations, such as the Knizhnik-Zamolodhcikov equations. By solving these differential equations, one can typically obtain exact analytic expressions for the correlators of primary fields, and hence for all correlators in the theory.

For an exploration of the constraints imposed by null vectors, see [GW86].

B.2 Example: Free Fermions

As an elementary example, we now illustrate how the familiar free fermion theory of appendix A (at $T = 0$) fits into the general theoretical framework summarized in section B.1. (The case of free bosons is *beautifully* treated by Polchinsky [Pol94, chapter 1].) In particular, we show from first principles how to derive, from the free-fermion Lagrangian, the Ward identities (B.19) and (B.20), and the stress-energy tensor $T, \bar{T}$ and currents $J^a, \bar{J}^a$ that appear therein. While the treatment below is by far not the most general possible, it is hoped that it will illustrate for the uninitiated reader the origin of some of the relations in section B.1; moreover, by acquiring a feeling for these relations via an explicit example, it is hoped that the reader will be able to appreciate better in which respects Cardy's *boundary* CFT, discussed in appendix C, differs from bulk CFT.

Consider N species each of free L- and R-moving fermions, $\psi^\alpha(z)$ and $\bar\psi^\alpha(\bar z)$, $\alpha = 1, \ldots, N$. The action is

$$\mathcal{S} = \int \tfrac{d\tau dx}{2\pi} \left[\psi^{\alpha\dagger}(\tau, ix) 2\partial_{\bar z} \psi^\alpha(\tau, ix) \; + \bar\psi^{\alpha\dagger}(\tau, ix) 2\partial_z \bar\psi^\alpha(\tau, ix) \right] , \tag{B.46}$$

where the integral goes over the complete complex plane, and the fields are normalized such that [see eq. (A.36) with $T = \mu_\alpha = 0$]

$$\langle \psi^\alpha(z) \psi^{\alpha\dagger}(z') \rangle = \frac{1}{z - z'} , \qquad \langle \bar\psi^\alpha(\bar z) \bar\psi^{\alpha\dagger}(\bar z') \rangle = \frac{1}{\bar z - \bar z'} . \tag{B.47}$$

Using ϕ_i as a shorthand for any of the fields $\psi^{\alpha_i}(z_i)$, $\psi^{\alpha_i\dagger}(z_i)$, $\bar\psi^{\alpha_i}(\bar z_i)$ or $\bar\psi^{\alpha_i\dagger}(\bar z_i)$, consider the correlation function

$$\langle X \rangle \equiv \langle \phi_i \ldots \phi_n \rangle \equiv \int \mathcal{D}\phi_1 \ldots \mathcal{D}\phi_n e^{-\mathcal{S}[\phi_i]} \phi_i \ldots \phi_n , \tag{B.48}$$

defined as a path integral (with the implicit assumption that th epath integral can be defined in a way consistent with all symmetries of the system, which is in general a highly non-trivial matter in the presence of gauge symmetries). Now consider an infinitesimal transformation, in which the ϕ_i are expressed in terms of new fields $\tilde\phi_i$ through

$$\phi_i \equiv \phi^\alpha(\tau, ix) = (1 - D_{\alpha\alpha'}(\tau, ix)) \, \tilde\phi_{\alpha'}(\tau, ix) \equiv (1 - D_i) \tilde\phi_i , \tag{B.49}$$

where D_i is an infinitesimal (c-number) operator acting on $\tilde\phi_i$. Under this transformation, the action can be rewritten, to leading order in D, as

$$\mathcal{S}[\phi_i] = \mathcal{S}[(1 - D_i)\tilde\phi_i] \equiv \mathcal{S}[\tilde\phi_i] - \delta\mathcal{S}[\tilde\phi_i] . \tag{B.50}$$

Assuming that the path-integral measure is invariant, $\int\mathcal{D}\phi = \int\mathcal{D}\tilde\phi$, the correlation

function can likewise be rewritten, to leading order in D, as[10]

$$\langle X\rangle \equiv \langle \phi_i \dots \phi_n\rangle \equiv \int \mathcal{D}\tilde{\phi}_1 \dots \mathcal{D}\tilde{\phi}_n e^{-\mathcal{S}[\tilde{\phi}_i]}(1+\delta\mathcal{S}[\tilde{\phi}_i])\sum_{i=1}^{n}(1-D_i)(\tilde{\phi}_i \dots \tilde{\phi}_n)\ . \tag{B.51}$$

Now, the leading term on the right hand side, $\langle\tilde{X}\rangle \equiv \langle\tilde{\phi}_i \dots \tilde{\phi}_n\rangle$, actually equals $\langle X\rangle$, because the actions $\mathcal{S}[\phi_i]$ and $\mathcal{S}[\tilde{\phi}_i]$ governing the $\langle X\rangle$ and $\langle\tilde{X}\rangle$ correlation functions have the same functional form in terms of the ϕ_i and $\tilde{\phi}_i$, respectively. What remains from eq. (B.51) is the identity

$$\langle \delta\mathcal{S}[\phi_i] X\rangle = \sum_{i=1}^{n} D_i\langle X\rangle\ , \tag{B.52}$$

where we have dropped the ~s, because any identity holding for the $\tilde{\phi}_i$ fields must also hold for the ϕ_i's. [Polchinski [Pol94] shows very nicely how the quantum version of Nöther's theorem can be derived from eq. (B.52).] Eq. (B.52) lies at the heart of eqs. (B.19) and (B.20), which we shall now derive from it by considering infinitesimal conformal and Kac-Moody transformations.

Under the conformal coordinate transformations $\xi = f(z)$, $\bar{\xi} = \bar{f}(\bar{z})$ (f and $\bar{f}$ arbitrary and unrelated holomorphic and anti-holomorphic functions of z and $\bar{z}$), the fermion fields transform according to eq. (B.2), with $(\Delta, \bar{\Delta}) = (1/2, 0)$ for ψ and $\psi^\dagger$, and $(0, 1/2)$ for $\bar{\psi}$ and $\bar{\psi}^\dagger$. Under $SU(N)$ Kac-Moody transformations, they transform according to [using the notation of eq. (A.7)]

$$\psi^\alpha(z) = \left[e^{-i\theta^X(z)T^X}\right]_{\alpha\alpha'}\tilde{\psi}^{\alpha'}(z)\ , \qquad \psi^{\dagger\alpha}(z) = \left[e^{i\theta^X T^{X*}}\right]_{\alpha\alpha'}\tilde{\psi}^{\alpha'\dagger}(z)\ , \tag{B.53}$$

$$\bar{\psi}^\alpha(\bar{z}) = \left[e^{-i\bar{\theta}^X(\bar{z})T^X}\right]_{\alpha\alpha'}\tilde{\bar{\psi}}^{\alpha'}(\bar{z})\ , \qquad \bar{\psi}^{\dagger\alpha}(z) = \left[e^{i\bar{\theta}^X(\bar{z})T^{X*}}\right]_{\alpha\alpha'}\tilde{\bar{\psi}}^{\alpha'\dagger}(\bar{z})\ , \tag{B.54}$$

Here $\theta(z)$ and $\bar{\theta}(\bar{z})$ are (arbitrary and unrelated) holomorphic and anti-holomorphic

[10] More generally, if the measure is not invariant, δS should be replaced by the change in (measure $\times\ e^{-S}$).

functions, that are real on the real axis (this condition is explained in footnote 5 of appendix A).

We now want to consider infinitesimal versions of such conformal and Kac-Moody transformations. However, since every non-constant analytic function always diverges somewhere in the complex plane, we have to restrict our attention to a limited domain, A. Let C be a closed contour enclosing all the points z_i and $\bar{z}_{\bar{j}}$ occuring in $\langle X \rangle$, and take A to be the domain enclosed by and including C, while denoting the rest of the complex plane by A' [see Fig. B.1]. Then consider an infinitesimal coordinate transformation of the form

$$\xi(\tau, ix) = z - \varepsilon(\tau, ix), \qquad \bar{\xi}(\tau, ix) = \bar{z} - \bar{\varepsilon}(\tau, ix) \ . \tag{B.55}$$

Likewise, for gauge transformations, take $\theta(\tau, ix)$ and $\bar{\theta}(\tau, ix)$ to be infinitesimal. In the notation of eq. (B.49), namely

$$\psi^{\alpha}(z) = (1 - D(\tau, ix))_{\alpha\alpha'} \tilde{\psi}^{\alpha'}(z) \ , \qquad \text{etc.}, \tag{B.56}$$

we obtain from eqs. (B.2) and (B.53):

$$D^{(\varepsilon)}_{\alpha\alpha'}(\tau, ix) = \left[\tfrac{1}{2}\partial_z \varepsilon(\tau, ix) + \varepsilon(\tau, ix)\partial_z\right] \delta_{\alpha\alpha'} \qquad \text{for } \psi \text{ and } \psi^{\dagger} \ ; \tag{B.57}$$

$$\bar{D}^{(\bar{\varepsilon})}_{\alpha\alpha'}(\tau, ix) = \left[\tfrac{1}{2}\partial_{\bar{z}} \bar{\varepsilon}(\tau, ix) + \bar{\varepsilon}(\tau, ix)\partial_{\bar{z}}\right] \delta_{\alpha\alpha'} \qquad \text{for } \bar{\psi} \text{ and } \bar{\psi}^{\dagger} \ ; \tag{B.58}$$

$$D^{(\theta)}_{\alpha\alpha'}(\tau, ix) = i\theta^X(\tau, ix) T^X_{\alpha\alpha'} \quad \text{for } \psi, \qquad \text{and } \left[D^{(\theta)}\right]^* \text{ for } \psi^{\dagger} \ ; \tag{B.59}$$

$$\bar{D}^{(\bar{\theta})}_{\alpha\alpha'}(\tau, ix) = i\bar{\theta}^X(\tau, ix) T^X_{\alpha\alpha'} \quad \text{for } \bar{\psi}, \qquad \text{and } \left[\bar{D}^{(\bar{\theta})}\right]^* \text{ for } \bar{\psi}^{\dagger} \ . \tag{B.60}$$

In the notation of eq. (B.5), we have

$$\begin{aligned} \omega^a t^a = i\theta^X T^X \quad &\text{for} \quad \psi \ , \qquad \text{and} \qquad (i\theta^X T^X)^* \quad \text{for} \quad \psi^{\dagger}, \\ \bar{\omega}^a \bar{t}^a = i\bar{\theta}^X T^X \quad &\text{for} \quad \bar{\psi} \ , \qquad \text{and} \qquad (i\theta^X T^X)^* \quad \text{for} \quad \bar{\psi}^{\dagger}. \end{aligned} \tag{B.61}$$

Now, since A is bounded, it is possible to choose ε and $\bar{\varepsilon}$ (or ω and $\bar{\omega}$) to be, for *all* $(\tau, ix) \in A$, both infinitesimal *and*, respectively, holomorphic and anti-holomorphic functions of z and $\bar{z}$. Outside A, i.e. for $(\tau, ix) \in A'$, we choose them to be arbitrary infinitesimal functions that vanish at ∞. In other words, we assume that D and $\bar{D}$ satisfy

$$\partial_{\bar{z}} D(\tau, ix) = \partial_z \bar{D}(\tau, ix) = 0 \quad \text{for} \quad (\tau, ix) \in A, \quad \text{and } D = \bar{D} = 0 \text{ at } \infty \ . \tag{B.62}$$

To find the corresponding $\delta\mathcal{S}[\tilde{\phi}_i]$, substitute eqs. (B.56) into eq. (B.50). Since the equations of motion are valid inside $\langle\ \rangle$, only those terms in $\langle \delta\mathcal{S}[\tilde{\phi}_i]\tilde{X}\rangle$ that don't contain any $\partial_{\bar{z}}\tilde{\psi}(z)$ $(= 0)$ and $\partial_z\tilde{\bar{\psi}}(\bar{z})$ $(= 0)$ survive, so that we get

$$\begin{aligned} \langle \delta\mathcal{S}[\tilde{\phi}_i]\tilde{X}\rangle \ &= \ \int\tfrac{d\tau dx}{2\pi} \Big\{ \langle \tilde{\psi}^{\alpha\dagger}(z)\,[2\partial_{\bar{z}} D_{\alpha\alpha'}(\tau, ix)]\,\tilde{\psi}^{\alpha'}(z)\tilde{X}\rangle & \text{(B.63)} \\ &\quad + \ \langle \tilde{\bar{\psi}}^{\alpha\dagger}(\bar{z})\,\big[2\partial_z \bar{D}_{\alpha\alpha'}(\tau, ix)\big]\,\tilde{\bar{\psi}}^{\alpha}(\bar{z})\tilde{X}\rangle \Big\} \ , & \text{(B.64)} \end{aligned}$$

where $\partial_{\bar{z}}$ and ∂_z act only on D and $\bar{D}$ respectively. Now comes the crucial point, which exploits the analiticity of D and $\bar{D}$: because of eq. (B.62), only the region outside A, namely A', makes a non-zero contribution to the integral. Furthermore, we can exploit the equations of motion to pull $\partial_{\bar{z}}$ and ∂_z out in front of the expectation values. Dropping the $\tilde{}$s, we get

$$\begin{aligned} \langle \delta\mathcal{S}[\phi_i]X\rangle \ &= \ \int_{A'}\tfrac{d\tau dx}{2\pi} \Big\{ 2\partial_{\bar{z}} \langle \psi^{\alpha\dagger}(z) D_{\alpha\alpha'}(\tau, ix)\psi^{\alpha'}(z)X\rangle & \text{(B.65)} \\ &\quad + \ 2\partial_z \langle \bar{\psi}^{\alpha\dagger}(\bar{z})\bar{D}_{\alpha\alpha'}(\tau, ix)\bar{\psi}^{\alpha}(\bar{z})X\rangle \Big\} \ , & \text{(B.66)} \end{aligned}$$

These integrals are of the form

$$\int_{A'}\tfrac{d\tau dx}{2\pi}\left[2\partial_{\bar{z}}F + 2\partial_z\bar{F}\right] = \int_{A'}\tfrac{d\tau dx}{2\pi}\vec{\partial}\cdot\vec{F} = \tfrac{1}{2\pi}\oint_C d\vec{S}\cdot\vec{F}\ , \tag{B.67}$$

where $\vec{\partial} = (\partial_\tau, \partial_x)$ and $\vec{F} = (F + \bar{F}, iF - i\bar{F})$. In the last equality we used Gauss' law to write the area integral over A' as a contour integral along the boundary

of A', namely C. Let $(d\tau, dx)$ be the tangent vector to C, whose direction we choose to be counter-clockwise. Then $d\vec{S}$, the normal vector to C that is oriented toward the outside of A' (i.e. inside of C) is given by $d\vec{S} = (-dx, d\tau)$ (see Fig. B.1]. Thus, Gauss' law implies $\binom{\partial_\tau}{\partial_x} \to \binom{-dx}{d\tau}$. To write the contour integral in terms of complex coordinates, note that

$$\binom{2\partial_{\bar{z}}}{2\partial_z} = \binom{1\ \ i}{1\ -i}\binom{\partial_\tau}{\partial_x} \overset{\text{Gauss}}{\longrightarrow} \binom{1\ \ i}{1\ -i}\binom{-dx}{d\tau} = \binom{1\ \ i}{1\ -i}\tfrac{1}{2}\binom{i\ -i}{1\ \ 1}\binom{dz}{d\bar{z}} = \tfrac{1}{i}\binom{-dz}{d\bar{z}} \ . \quad \text{(B.68)}$$

which implies that

$$\int_{A'} \tfrac{d\tau dx}{2\pi}\left[\partial_{\bar{z}}F + \partial_z \bar{F}\right] = -\oint_C \tfrac{dz}{2\pi i}F \ + \ \oint_C \tfrac{d\bar{z}}{2\pi i}\bar{F} \ . \quad \text{(B.69)}$$

Applying this general result to eq. (B.65), we obtain

$$\langle \delta\mathcal{S}[\phi_i]X\rangle = -\oint_C \tfrac{dz}{2\pi i}\langle \psi^{\alpha\dagger}(z)D_{\alpha\alpha'}(z)\psi^{\alpha'}(z)X\rangle + \oint_C \tfrac{d\bar{z}}{2\pi i}\langle \bar{\psi}^{\alpha\dagger}(\bar{z})\bar{D}_{\alpha\alpha'}(\bar{z})\bar{\psi}^{\alpha}(\bar{z})X\rangle \ , \quad \text{(B.70)}$$

where our notation $D(z)$ and $\bar{D}(\bar{z})$ makes explicit that, by eq. (B.62), these functions are holomorphic and anti-holomorphic along (and inside) C.

Finally, substitute the explicit forms of eqs. (B.57) to (B.60) into eq. (B.70); then eq. (B.52) gives

$$\oint_C \tfrac{dz}{2\pi i}\varepsilon(z)\langle T(z)X\rangle - \oint_C \tfrac{d\bar{z}}{2\pi i}\bar{\varepsilon}(\bar{z})\langle \bar{T}(\bar{z})X\rangle = \sum_{i\bar{j}}\left[D_i^{(\varepsilon)} + \bar{D}_{\bar{j}}^{(\bar{\varepsilon})}\right]\langle X\rangle \quad \text{(B.71)}$$

$$-\oint_C \tfrac{dz}{2\pi i}i\theta^X(z)\langle J^X(z)X\rangle + \oint_C \tfrac{d\bar{z}}{2\pi i}i\bar{\theta}^X(\bar{z})\langle \bar{J}^X(\bar{z})X\rangle = \sum_{i\bar{j}}\left[D_i^{(\theta)} + \bar{D}_{\bar{j}}^{(\theta)}\right]\langle X\rangle \quad \text{(B.72)}$$

where the sums on i and $\bar{j}$ go over all points z_i and $\bar{z}_{\bar{j}}$ occuring in $\langle X\rangle$, and

$$T(z) \ \equiv \ \tfrac{1}{2} : \left\{\left[\partial_z\psi^{\alpha\dagger}(z)\right]\psi^{\alpha}(z) - \psi^{\alpha\dagger}(z)\partial_z\psi^{\alpha}(z)\right\} : \ , \quad \text{(B.73)}$$

$$J^X(z) \ \equiv \ : \psi^{\alpha\dagger}(z)T^X_{\alpha\alpha'}\psi^{\alpha'}(z) : \ . \quad \text{(B.74)}$$

Identical equations give $\bar{T}(\bar{z})$ and $\bar{J}^X(\bar{z})$ in terms of $\bar{\psi}(\bar{z})$ and $\partial_{\bar{z}}\bar{\psi}(\bar{z})$.

These are the main results of this section. Eqs. (B.71) and (B.72) correspond to eqs. (B.19) and (B.20) (with the identifications made in eq. (B.61)), and the expressions for T and J^X that we derived in the process are just eqs. (A.21) and (A.8) of appendix A. The connection between the contour integrals of eqs. (B.71) and (B.72) and the canonical commutators of eqs. (A.12) and (A.22) is explained lucidly in [Gins87], p. 18,19.

As explained in section B.1 (just before eq. (B.23)), the operator product expansions of $T(z)\psi(w)$ and $J^X(z)\psi(w)$ [eqs. (B.25) and (B.26)] follow directly from eqs. (B.71) and (B.72).

To conclude this section, let us point out that for the present case of free fermions, all OPEs [also eqs. (B.27) to (B.29)] can actually be derived directly by simply using Wick's theorem, as illustrated in section A.5. For example, if in eq. (A.47) we choose the matrices A, B to be T^X, $T^{X'}$, then that equation yields the $J^X J^{X'}$ OPE of eq. (B.29).

As another example, we consider the OPE of $T(z)\psi(w)$, using eq. (B.47) to evaluate the Wick contractions:

$$\begin{aligned} T(z)\psi^\alpha(w) &= \tfrac{1}{2} : \Big\{ \Big[\partial_z \psi^{\beta\dagger}(z)\Big]\, \psi^\beta(z) - \psi^{\beta\dagger}(z)\partial_z\psi^\beta(z) \Big\} : \psi^\alpha(w) \qquad \text{(B.75)} \\ &= -\tfrac{1}{2}\psi^\alpha(z)\partial_z(z-w)^{-1} + \tfrac{1}{2}(z-w)^{-1}\partial_z\psi^\alpha(z) + \ldots \qquad \text{(B.76)} \\ &= \left[\frac{1/2}{(z-w)^2} \;+\; \frac{1}{(z-w)}\partial_z\right]\psi^\alpha(w) \;+\ldots\,, \qquad \text{(B.77)} \end{aligned}$$

where the last line is obtained by Taylor-expanding $\psi^\alpha(z) = \psi^\alpha(w) + (z - w)\partial_w\psi^\alpha(w) + \ldots$.

Finally, let us verify that the central charge for a single species ($N = 1$) of chiral Dirac fermions is $c = 1$, by using Wick's theroem to calculate the coefficient $c/2$ of the $(z-w)^{-4}$ term in the OPE (B.27) of $T(z)T(w)$. This term arises from

a double Wick contraction in each of the four terms of $T(z)T(w)$:

$$T(z)T(w) = \left[\tfrac{1}{2} : \partial_z\psi^\dagger\psi - \psi^\dagger\partial_z\psi : (z)\right] \left[\tfrac{1}{2} : \partial_w\psi^\dagger\psi - \psi^\dagger\partial_w\psi : (w)\right] \tag{B.78}$$

$$= \tfrac{1}{4}\Big[(1+1)\partial_z(z-w)^{-1}\partial_w(z-w)^{-1} - (1+1)(z-w)^{-1}\partial_z\partial_w(z-w)^{-1}\Big] + \dots \tag{B.79}$$

$$= \frac{1/2}{(z-w)^4} + \dots , \tag{B.80}$$

which implies that $c = 1$, as advertized. It is an instructive exercise to use the same method to obtain the other terms in the TT OPE (B.27).

B.3 Wess-Zumino-Witten theories

[For details, see [KZ84] and [Gins87, chapter 9].]

In the previous section, we have seen that for free fermions, all the results of section B.1 can be derived by elementary means. This is not the case, however, for the charge, spin and channel sectors into which free fermions are factorized in AL's treatment of the Kondo problem. This is so because the spin, flavor and channel fields, taken separately, do not obey Wick's theorem, since each represents a strongly interacting field theory. Each of the charge, spin and channel sectors is in fact described by a so-called *Wess-Zumino-Witten* (WZW) theory. In this section, we summarize some basic facts about WZW theories, again plagiarizing [GW86], section 3.

WZW theories can be described axiomatically by imposing the Sugawara form on the energy-momentum tensor, namely

$$T(z) = \tfrac{1}{2\kappa}\sum_a : J^a(z)J^a(z) : , \tag{B.81}$$

$$\bar{T}(\bar{z}) = \tfrac{1}{2\kappa}\sum_a : \bar{J}^a(\bar{z})\bar{J}^a(\bar{z}) : , \tag{B.82}$$

where κ is some constant. The Laurent series expansion of this relation is

$$L_n = \tfrac{1}{2\kappa} \sum_{-\infty}^{\infty} {}^{*}_{*} J^a_{n-k} J^{a\,*}_{k\,*} \,, \tag{B.83}$$

where the normal ordering means pushing to the right the "annihilation operators" J^a_k with $k > 0$. Let D be the dimension of the group, and let c_v be the Casimir of the adjoint representation [$f^{abc} f^{abd} = c_v \delta_{cd}$]. Then the normalization κ of the stress-energy tensor and the central charge c are given by

$$\kappa = \tfrac{1}{2}(c_v + k) \,, \qquad\qquad c = \frac{kD}{c_v + k} \,. \tag{B.84}$$

In these theories, any field φ that is a Kac-Moody primary field is also a Virasoro primary field. Suppose φ transforms in the representation R with Casimir c_φ [$t^a t^a = c_\varphi I$]. Then the dimension Δ_φ of φ is given by

$$\Delta_\varphi = \frac{c_\varphi}{c_v + k} \,. \tag{B.85}$$

For a discussions of the null-vector constraints of the theory, consult [GW86].

As an example, let us apply this to the $SU(\tilde{N})_k$ Kac-Moody algebra that we encountered in the $U(1) \times SU(\tilde{N}) \times SU(k)$ bosonization of $N = \tilde{N}k$ species of left-moving (i.e. chiral) free fermions.

The underlying Lie algebra is $SU(\tilde{N})$, which has dimension $D = \tilde{N}^2 - 1$ and Casimir $c_v = \tilde{N}$ in the adjoint representation. Hence, the normalization factor 2κ of the stress-energy tensor eq. (B.81) is $2\kappa = \tilde{N} + k$, as we found by pedestrian means in appedix A [see eq. (A.102)]. The central charge is $c = \frac{k(\tilde{N}^2-1)}{\tilde{N}+k}$, as stated (though not derived) on page 303. Finally, consider $\tilde{N} = 2$; then the Casimir of a field φ_j of spin j is $c_j = j(j+1)$, and hence the scaling dimension of this field is $\Delta_j = \frac{j(j+1)}{2+k}$. This agrees with eq. (7.29), since the scaling dimension Δ_φ of a

Virasoro primary field can be read off from the eigenvalue E_φ of the finite-size spectrum through $E_\varphi - E_o = \frac{\pi}{l}\Delta_\varphi$. This relation is derived in the next section [see eq. (B.94), with $\bar{\Delta}_\varphi, \bar{N} = 0$, since in appendix A we consider chiral fermions, and $N = 0$ for the primary state in the tower].

B.4 Relation between Bulk Scaling Dimensions and Transfer Matrix on Strip

[Car84a], [Car86a], section 2, [CH93], section 13.1.

There exists a very useful relation, due to Cardy ([Car84a] and [Car86a, section 2]), between the scaling dimensions $(\Delta, \bar{\Delta})$ of Virasoro primary fields $\phi(z, \bar{z})$ in a bulk conformal field theory, and the eigenvalues of a certain transfer matrix e^{-H_P} on a strip of finite width l. Cardy derived this relation by exploiting a conformal transformation, $z = e^{2\pi w/l}$, which maps the plane (parametrized by z) onto a strip of finite width l (parametrized by w). The 2-point function $\langle\phi(w, \bar{w})\phi(w', \bar{w}')\rangle$ on the strip can then be calculated in two ways: firstly by simply applying the conformal map to the corresponding two-point function in the plane, $\langle\phi(z, \bar{z})\phi(z', \bar{z}')\rangle$, and secondly in terms of the transfer matrix on the strip. Equating the resulting two expressions yields the desired relation, eq. (B.94) below.

We now derive this relation, following [Car86a, section 2]. Parametrize the full complex plane by $z = \tau + ix = re^{i\theta}$. The 2-point correlation function of any Virasoro primary field $\phi(z, \bar{z})$ with scaling dimensions $(\Delta, \bar{\Delta})$ is given by eq. (B.42):

$$\langle\phi(z, \bar{z})\phi(z', \bar{z}')\rangle = \frac{1}{(z - z')^{2\Delta}(\bar{z} - \bar{z}')^{2\bar{\Delta}}} , \tag{B.86}$$

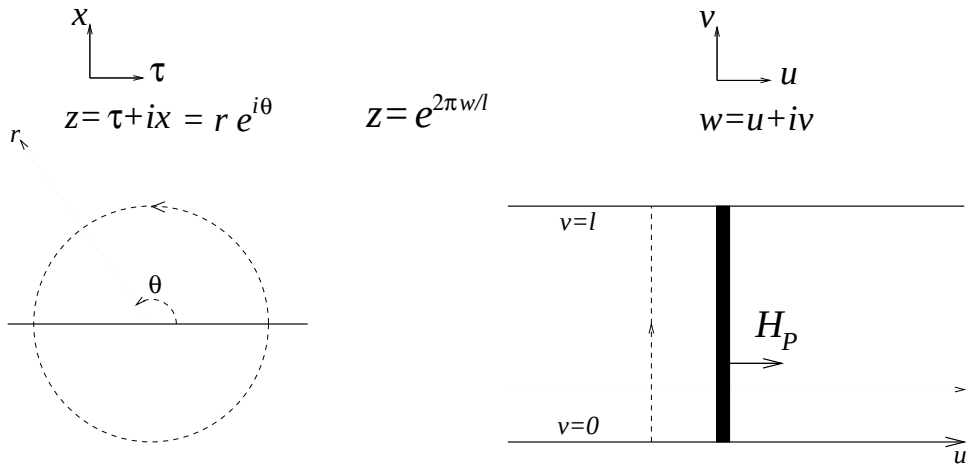

Figure B.2 The conformal transformation $z = e^{2\pi w/l}$ maps the plane, parametrized by $z = \tau + ix = re^{i\theta}$ onto a strip of width l, parametrized by $w = u + iv$, with periodic boundary condition at $v = 0, l$. H_P generates translations along the strip in the u-direction.

[To simplify our notation, we do not show here explicitly the "isospin indices" of the field ϕ^{ij} shown in eq. (B.42), and in eq. (B.86) have chosen unit normalization for each component of ϕ^{ij}.]

Now make a conformal transformation,

$$z = f(w) = e^{2\pi w/l} \,, \tag{B.87}$$

which maps the z-plane onto a strip of width l, parametrized by $w = u + iv$ (Fig. B.2).

This maps circles of constant radius r onto lines of constant $u = (l/2\pi)\ln r$, and lines of constant θ onto lines of constant $v = (l/2\pi)\theta$. In particular, the "upper side" ("lower side") of the positive τ-axis, i.e. $\theta = 0^+$ ($\theta = 2\pi - 0^+$) is mapped onto the lower (upper) edge of the strip, $v = 0$ ($v = l$); all fields that are single-valued at $\theta = 0, 2\pi$ in the plane [i.e. have integer $(\Delta, \bar{\Delta})$], are periodic at $v = 0, l$ on the strip.

Now, since $\phi(z, \bar{z})$ is a primary field, it transforms according to eq. (B.2),

which implies that the correlation function on the strip can be found from that on the plane (we use ˜s to distinguish strip- from plane fields):

$$\langle\phi(w,\bar{w})\phi(w',\bar{w}')\rangle \;=\; \left(\frac{\partial z}{\partial w}\frac{\partial z'}{\partial w'}\right)^{\Delta}\left(\frac{\partial \bar{z}}{\partial \bar{w}}\frac{\partial \bar{z}'}{\partial \bar{w}'}\right)^{\bar{\Delta}}\langle\phi(z,\bar{z})\phi(z',\bar{z}')\rangle \tag{B.88}$$

$$= \frac{(2\pi/l)^{2(\Delta+\bar{\Delta})}\, e^{2\pi/l\left[(w+w')\Delta+(\bar{w}+\bar{w}')\bar{\Delta}\right]}}{\left(e^{2\pi w/l}-e^{2\pi w'/l}\right)^{2\Delta}\left(e^{2\pi \bar{w}/l}-e^{2\pi \bar{w}'/l}\right)^{2\bar{\Delta}}} \tag{B.89}$$

$$= (\pi/l)^{2x}\left[\sinh\frac{\pi}{l}(w-w')\right]^{-2\Delta}\left[\sinh\frac{\pi}{l}(\bar{w}-\bar{w}')\right]^{-2\bar{\Delta}} \tag{B.90}$$

where $x \equiv \Delta+\bar{\Delta}$ is the scaling dimension of ϕ, and below we shall also use $s \equiv \Delta-\bar{\Delta}$, which is its spin. Now set $w = u+iv$ and $w' = u'+iv'$, and, for $u > u'$, expand in powers of $e^{-2\pi(u-u')/l}$, to obtain:

$$\langle\tilde{\phi}(w,\bar{w})\tilde{\phi}(w',\bar{w}')\rangle = \left(\tfrac{2\pi}{l}\right)^{2x}\sum_{N,\bar{N}=0}^{\infty} a_N a_{\bar{N}} e^{-2\pi/l(x+N+\bar{N})(u-u')} e^{-2\pi i/l(s+N-\bar{N})(v-v')} \tag{B.91}$$

where the coefficients are given by $a_N = \frac{\Gamma(2\Delta+N)}{\Gamma(2\Delta)N!}$ and $\bar{a}_{\bar{N}} = \frac{\Gamma(2\bar{\Delta}+\bar{N})}{\Gamma(2\bar{\Delta})\bar{N}!}$ (see [CH93, eq. (13.2)]).

Alternatively, this correlation function can be evaluated directly, in terms of the "transfer matrix" e^{-H_P} on a strip of width l and length $\beta \to \infty$. The terminology "transfer matrix" stems from statistical mechanics. In quantum field theory, H_P is simply the Hamiltonian of the system, which generates translations *along* the strip in the positive u-direction, and the subscript $_P$ indicates that all fields with integer $(\Delta,\bar{\Delta})$ satisfy periodic boundary conditions between the edges of the strip.[11] Thus, regarding u as time variable and v as space variable on the

[11] Since circles of constant r in the plane are mapped onto lines of constant u on the strip, the generators of scale transformations ($\tilde{r} = rb$) on the plane, namely $L_o+\bar{L}_o$, will be mapped onto the generator of translations ($\tilde{u} = u+\frac{bl}{2\pi}$) on the strip, namely $\frac{l}{2\pi}H_P$. Hence $H_P = \frac{2\pi}{l}(\tilde{L}_o+\tilde{\bar{L}}_o)$. See [Car86b, p.216] for a careful proof.

strip, represent $\tilde{\phi}(u,v)$ in a Heisenberg representation as

$$\tilde{\phi}(w,\bar{w}) = e^{uH_P}\tilde{\phi}(v)e^{-uH_P} \ , \tag{B.92}$$

and write the correlation function as

$$\begin{aligned}\langle\tilde{\phi}(w,\bar{w})\tilde{\phi}(w',\bar{w}')\rangle &= \lim_{\beta\to\infty}\frac{\sum_{n'k'}\langle n'k'|e^{-(\beta-u)H_P}\tilde{\phi}(v)e^{-(u-u')H_P}\tilde{\phi}(v')e^{-u'H_P}|n'k'\rangle}{\sum_{n'k'}\langle n'k'|e^{-\beta H_P}|n'k'\rangle} \\ &= \sum_{nk}\langle 0|\tilde{\phi}(v)|nk\rangle\langle nk|\tilde{\phi}(v')|0\rangle e^{-(E_n-E_o)(u-u')}\end{aligned} \tag{B.93}$$

Here $\{|nk\rangle\}$ denotes a complete set of eigenstates of H_P with energy E_n and momentum k (both quantized in units of $2\pi/l$ because of the periodic boundary conditions), so that the matrix elements in eq. (B.93) depend on v and v' as $e^{-ik(v-v')}$. In going from the first to the second line, we inserted a complete set of such states, $\sum_{nk}|nk\rangle\langle nk|$, and took the limit $\beta\to\infty$, so that only the state with $E_{n'}=E_o$ survived in the sum $\sum_{n'k'}$. Comparing our two expressions for the strip-correlation function, eqs. (B.91) and (B.93), we conclude that *to each primary operator of scaling dimensions* $(\Delta,\bar{\Delta})$ *in the infinite plane, there corresponds an infinite number of eigenstates of* H_P, labeled by $(\Delta,\bar{\Delta},N,\bar{N})$, with energy and momentum

$$\boxed{E_\phi(N,\bar{N}) - E_o = 2\pi(\Delta+\bar{\Delta}+N+\bar{N})/l} \tag{B.94}$$

$$k_\phi(N,\bar{N}) = 2\pi(\Delta-\bar{\Delta}+N-\bar{N}) \ . \tag{B.95}$$

These states together constitute the conformal tower T_ϕ associated with the Virasoro primary field $\tilde{\phi}$. The lowest state in the tower, called the *primary state*, must be non-degenerate [since $e^{-2\pi x/l}$ occurs only *once* in eq. (B.91)]; it has $N=\bar{N}=0$ and is denoted by $|\phi\rangle$, with

$$\langle 0|\tilde{\phi}(v)|\phi\rangle = (2\pi/l)^x \ e^{-i2\pi sv/l} \ . \tag{B.96}$$

The infinite number of states with N or $\bar{N} \neq 0$ are the descendent states in the tower.

Eq. (B.94) is the desired relation. *It allows one to read off from the finite-size spectrum of H_P the scaling dimensions of all Virasoro primary fields in the bulk theory.* In appendix C, section C.5 it is shown that a similar argument allows one to find all possible boundary operators for a boundary CFT from the finite-size spectrum of a certain related (but different) Hamiltonian on a strip.

Note that in the limit $u - u' \to \infty$ one can write eq. (B.91) in the form

$$\langle \tilde{\phi}(w, \bar{w}) \tilde{\phi}(w', \bar{w}') \rangle \sim e^{-(u-u')/\xi} \tag{B.97}$$

where the inverse correlation length is given by

$$\xi = \frac{l}{2\pi x} \, . \tag{B.98}$$

This limit corresponds to two points w and w' on the strip that are very far apart in the longitudinal direction (or two points in the plane with radii $r - r' \to \infty$). The fact that the correlation length in the longitudinal direction on the strip is proportional to the system size l in the transverse direction is to be expected, since a finite system size will always prevent ξ from becoming infinite. What is remarkable though (and was first pointed out by Cardy [Car84a]), is that the ratio l/ξ is *universal*, namely $l/\xi = 2\pi x$, and determined by the scaling dimension of the field $\tilde{\phi}$.[12]

[12]This is "one of the most important results for the application of conformal invariance to critical phenomena" [CH93, p. 48]. For a given lattice model, the ratio l/ξ can often readily be evaluated for various operators using numerical transfer matrix methods; this information can then be used to identify the conformal field theory corresponding to the lattice model (see [CH93] for an extensive discussion).

B.5 $T = 0$ to $T \neq 0$ Mapping of Plane to Cylinder

The Green's functions for a $T \neq 0$ theory can be found from those of the corresponding $T = 0$ CFT by mapping the complex plane onto a cylinder of radius $\beta = 1/T$. This was discussed in some detail in chapter 8, section 8.1. Here we would merely like to point out that eq. (B.94) of section B.4 can also be derived via this mapping, since a strip with periodic boundary conditions is topologically equivalent to a cylinder.

The infinite complex plane, be parametrized by $z = \tau + ix$, is mapped onto an infinite cylinder, parametrized by $\tilde{z} = \tilde{\tau} + i\tilde{x}$, by the conformal transformation [compare eq. (8.4)]

$$z = \tan \tfrac{\pi}{\beta}\tilde{z} \; . \tag{B.99}$$

Here $\tilde{x}$ parametrizes the longitudinal direction along the cylinder [see Fig. 8.1]. As shown in section 8.1, eq. (B.2) maps the two-point function of eq. (B.42) onto

$$\langle \tilde{\phi}_1^{ij}(\tilde{z}_1, \tilde{\bar{z}}_1)\tilde{\phi}_2^{kl}(\tilde{z}_2, \tilde{\bar{z}}_2)\rangle_T = \frac{A_{ik,o}B_{jl,o}}{\left[\frac{\beta}{\pi}\sin\frac{\pi}{\beta}(\tilde{z}_1 - \tilde{z}_2)\right]^{2\Delta}\left[\frac{\beta}{\pi}\sin\frac{\pi}{\beta}(\tilde{\bar{z}}_1 - \tilde{\bar{z}}_2)\right]^{2\bar{\Delta}}} \; . \tag{B.100}$$

Now, to rederive eq. (B.94), make the identification $\tilde{z} = iw = i(u + iv)$, i.e. $u = \tilde{x}$, $v = -\tilde{\tau}$, according to which u becomes the longitudinal parameter on the cylinder, as in section B.4. Then eq. (B.100) becomes

$$\langle \tilde{\phi}_1^{ij}(w_1, \bar{w}_1)\tilde{\phi}_2^{kl}(w_2, \bar{w}_2)\rangle_T = \frac{A_{ik,o}B_{jl,o}}{\left[i\frac{\beta}{\pi}\sinh\frac{\pi}{\beta}(w_1 - w_2)\right]^{2\Delta}\left[-i\frac{\beta}{\pi}\sinh\frac{\pi}{\beta}(\bar{w}_1 - \bar{w}_2)\right]^{2\bar{\Delta}}} \; , \tag{B.101}$$

which is analogous to eq. (B.90). This correlation function can also be evaluated in terms of the Hamiltonian H_P that generates translations in the longitudinal (u)

direction along the cylinder, in a way analogous to eqs. (B.92) and (B.93). The procedure is the same as that in section B.4, because both there and here periodic boundary conditions hold between the edges of the strip or around the circumference of the cylinder. Therefore, just as in section B.4, eqs. (B.94) follows, and so does (B.96).

Appendix C

Cardy's Boundary Conformal Field Theory

The development of *boundary conformal field theory*, in particular CFT in the upper half-plane with a boundary at Im(z)=0, is mainly due to Cardy [Car84a, Car84b,Car86a,Car86b,Car87,Car89,CL91]. In this appendix we introduce those features of Cardy's boundary CFT, and its generalization to theories that are invariant under a Kac-Moody current algebra, that are needed in Affleck and Ludwig's treatment of the Kondo problem. It is hoped that the presentation is sufficiently detailed and self-contained that the reader will be able to learn the material without recourse to Cardy's papers (though extensive and detailed references are given throughout).

The appendix is organized as follows. In section C.1, we discuss the cornerstone of Cardy's boundary CFT, namely how the R-handed generators $\bar{T}(z^*)$ and $\bar{J}^a(z^*)$ can be expressed in terms of the analytical continuations of $T(z)$ and $J^a(z)$ across the boundary, and the consequent elimination of all R-handed in

favor of L-handed fields. In section C.2, this is illustrated by considering in detail the two-point function $G^{(2)} = \langle \phi_i(z_1, z_1^*)\phi_i(z_2, z_2^*)\rangle$ and the related four-point function $G^{(4)} = \phi_{iL}(z_1)\phi_{iL}(z_2^*)\phi_{iR}(z_4^*)\phi_{iR}(z_3^*)\rangle$. By considering the boundary limit of these functions, the concept of boundary operators naturally arises, which we introduce in section C.3. In section C.4, we introduce the concept of a boundary state $|B\rangle$ and show how it determines the boundary conditions on the theory. We also derive Cardy's formula [eq. (C.64)] for the boundary state matrix elements $\langle a|B\rangle$, and show, for the case that the boundary condition is determined by a fusion principle, they can be calculated in terms of modular S-matrix elements [eq. (C.68)]. Finally, in section C.5 we derive a quick way for determining the complete boundary operator content of a BCFT in terms of the operator content of a strip theory, and show how the latter can be derived by "double fusion" if a fusion principle applies.

C.1 Relation between R- and L-moving fields in Boundary CFT

[Car84b], section 4, [AL91b], section 2.2

Throughout this section, we assume that the "physical section" of the theory (see footnote 1 of appendix B) has been taken, in which $z = \tau + ix$, and $\bar{z} = z^* = \tau - ix$. Consider a conformal field theory defined in the semi-infinite upper half of the complex plane, with a boundary along the real axis. In other words, all fields $A_i(z, z^*)$ are defined only for $x > 0$. The theory is assumed to be conformally invariant and, for some Lie Group G, Kac-Moody invariant in the bulk *and* along the boundary.[1]

[1] In [Car84b], section 4, Cardy only considered conformal invariance. However, the extension

Conformal and KM invariance in the *bulk* (upper half plane) implies that the theory has to be formulated in terms of a set of fields $A_i(z, z^*)$ which have all the local properties summarized in section B.1 of appendix B. In other words, they satisfy the transformations laws (B.2) and (B.3), and the OPEs (B.25) to (B.29). Furthermore, invariance of the bulk implies that under the infinitesimal conformal and KM transformations of eqs. (B.4) and (B.5), the action is invariant up to a *surface term*, $\delta\mathcal{S}$, which can be written as the sum of two contour integrals [as illustrated in section B.2 for free fermions, see eq. (B.70)]:

$$\begin{aligned} \delta_{\varepsilon,\varepsilon^*}\mathcal{S} &= \oint_{C_+} \tfrac{d\xi}{2\pi i}\, \varepsilon(\xi) T(\xi) \;-\; \oint_{C_+} \tfrac{d\xi^*}{2\pi i}\, \varepsilon^*(\xi^*) \bar{T}(\xi^*)\;, \\ \delta_{\omega,\bar{\omega}}\mathcal{S} &= -\oint_{C_+} \tfrac{d\xi}{2\pi i}\, \omega^a(\xi) J^a(\xi) \;+\; \oint_{C_+} \tfrac{d\xi^*}{2\pi i}\, \bar{\omega}^a(\xi^*) \bar{J}^a(\xi^*)\;. \end{aligned} \tag{C.1}$$

Here C_+ is a contour enclosing all the points (τ_i, ix_i) at which correlation functions of fields $A_i(z_i, z_i^*)$ are calculated, and lies entirely in the upper half-plane. It may be chosen to have the form shown in Fig. C.1, consisting of a straight portion C_+^r along the real axis, and a large semi-circle C_+^s.

"Invariance of the boundary" under conformal and KM transformations means, by definition, that the *boundary contribution* (due to the C_+^r portion of the contour C_+) to $\delta\mathcal{S}$ vanishes. The conditions under which this happens will be explored below.

The presence of a boundary at $x = 0$ implies three additional requirements on the theory:

(i) *Boundary conditions* have to be specified for $T, \bar{T}$ and $J^a, \bar{J}^a$ at $x = 0$.

(ii) Only a restricted class of conformal and KM transformations, namely those that *preserve the geometry and the boundary conditions*, can be considered.

---

of his theory to theories with KM invariance is self-evident, and was scetched, for example, in [AL91b, section 2.2].

(iii) A specific boundary condition [in addition to (i)] has to be imposed on the theory, which determines the behavior of correlation functions close to the boundary.

In the present section, we discuss (i) and (ii) and their consequences; (iii) is addressed in section C.2.2 [see eq. (C.30)].

C.1.1 Boundary Conditions on $T, \bar{T}$ and $J^a, \bar{J}^a$

The boundary condition on $T, \bar{T}$ and $J^a, \bar{J}^a$ that is imposed in all theories of interest to us is the following [AL91b, p.653]: *No energy or current density of any type may flow across the boundary.*[2] This is ensured by the requirement that

$$T(\tau) = \bar{T}(\tau) \ , \qquad J^a(\tau) = \bar{J}^a(\tau) \ , \tag{C.2}$$

be satisfied along the real axis. Intuitively, since T and J^a [or $\bar{T}$ and $\bar{J}^a$] depend on $z = \tau + ix$ [or $z^* = \tau - ix$], which becomes $i(t + x)$ [or $i(t - x)$] under $\tau \to it$, they carry energy and charge toward [or away from] the boundary. Thus the boundary conditions (C.2) ensure that as much energy and charge is carried away from as is carried toward the boundary, so that there is indeed zero flux across the boundary. More formally, in Cartesian coordinates one has (in the notation of [Gins87, p.17]) $T = \frac{1}{4}(T_{\tau\tau} - 2iT_{x\tau} + T_{xx})$, $\bar{T} = \frac{1}{4}(T_{\tau\tau} + 2iT_{x\tau} + T_{xx})$, and $J^a = J^a_\tau - iJ^a_x$, $\bar{J}^a = J^a_\tau + iJ^a_x$. Hence eq. (C.2) implies that at the boundary, the x-direction energy current density $T_{\tau x} = 0$, and likewise the x-direction charge current density $J^a_x = 0$.

The presence of a boundary further implies that only transformations may be

[2] It is shown in section C.1.3 that this is a necessary condition for the invariance of the boundary under restricted conformal and KM transformations of the form of eqs. (C.3) and (C.4).

considered that satisfy

$$\xi^*(\tau) = \xi(\tau)\,, \tag{C.3}$$

$$\bar{\omega}^a(\tau) = \omega^a(\tau)\,, \tag{C.4}$$

along the real axis. We shall call these *restricted* conformal and KM transformations. The reasons for these restrictions are as follows:

The condition (C.3) on ξ is necessary to *preserve the geometry*: it ensures that the boundary is mapped onto itself (i.e. that $\xi(\tau)$ is real).

The condition (C.4) on ω^a is necessary to *preserve the boundary conditions* (C.2): it ensures that along the boundary, the changes in $T, \bar{T}$ and $J, \bar{J}$ are

$$\delta_{\omega,\bar{\omega}} T(\tau + i\alpha) = \delta_{\omega,\bar{\omega}} \bar{T}(\tau - i\alpha), \qquad \delta_{\omega,\bar{\omega}} J^a(\tau + i\alpha) = \delta_{\omega,\bar{\omega}} \bar{J}^a(\tau - i\alpha)\,, \tag{C.5}$$

in the limit $\alpha \to 0$. To see this, calculate for example, $\delta_{\omega,\bar{\omega}} J^a$ and $\delta_{\omega,\bar{\omega}} \bar{J}^a$ from eq. (B.13): set $X \to J^a$ or $\bar{J}^a$ and use footnote 4 of appendix B and the OPE (B.29) for $J^a J^b$ (and a similar one for $\bar{J}^a \bar{J}^b$) to evaluate the contour integrals. One readily finds that

$$\delta_{\omega,\bar{\omega}} J^a(\tau + i\alpha) = -\tfrac{1}{2} k\, \partial_\tau \omega^a(\tau + i\alpha) - f^{bac}\, \omega^a(\tau + i\alpha)\, J^a(\tau + i\alpha) \tag{C.6}$$

$$\delta_{\omega,\bar{\omega}} \bar{J}^a(\tau - i\alpha) = -\tfrac{1}{2} k\, \partial_\tau \bar{\omega}^a(\tau - i\alpha) - f^{bac}\, \bar{\omega}^a(\tau - i\alpha)\, \bar{J}^a(\tau - i\alpha) \tag{C.7}$$

which implies that eq. (C.4) is necessary to ensure eq. (C.5).

More intuitively, condition (C.4) ensures that along the boundary one makes the *same* isospin transformation on the L and R indices of all KM primary fields, i.e. $\Omega^X(\tau) = \bar{\Omega}^X(\tau)$ in eq. (B.3), so that all boundary conditions between L and R primary fields will be preserved.[3]

[3]However, since J and T are not KM primary, this argument does not apply directly to them, which is why the argument involving eqs. (C.6) and (C.7) was given above.

C.1.2 Illustration of Boundary Conditions for Kondo Problem

Before proceeding with the formal development of the theory, let us recapitulate the reasons why the boundary conditions eq. (C.2) hold for the Kondo problem.

In the Kondo problem, $\psi(z) = \psi_L(z)$ and $\bar{\psi}(z^*) = \psi_R(z^*)$ describe, respectively, electrons incident and reflected from an impurity at $r = 0$ (r plays the role of x here). At zero-coupling ($\lambda_K = 0$), the 3D-1D mapping of chapter 4 ensures that $\psi_L(\tau + i0^+) = \psi_R(\tau - i0^+)$, which simply means that there is *no* electron scattering off the impurity. In this case, the boundary conditions (C.2) follow immediately from the definitions of $T, \bar{T}$ and $J^a, \bar{J}^a$, eqs. (B.73) and (B.74). Hence, by analytical continuation, the zero-coupling theory may be formulated completely in terms of L-moving fields, as discussed in section 7.2.

Turning on electron scattering off the impurity ($\lambda_K \neq 0$) in general causes $\psi_L(\tau + i0^+) \neq \psi_R(\tau - i0^+)$. In particular a discontinuity develops in the spin current, $\vec{J}_L(\tau + i0^+) \neq \vec{J}_R(\tau + i0^+)$, since due to impurity spin flips, the outgoing spin current need not be the same as the incident one.

However, at the strong-coupling fixed point, the impurity spin is *completely* absorbed, as described in section 7.4.1. In terms of the *total* spin current $\vec{\mathcal{J}}_L(\tau, ix) = \vec{J}_L(\tau, ix) + 2\pi\delta(x)\vec{S}$, the theory can be brought in the form of a *free* theory [see eq. (7.40)]. Therefore, as a simple consequence of the Heisenberg equations of motion, the total spin current is analytic at the boundary, $\vec{\mathcal{J}}_L(\tau + i0^+) = \vec{\mathcal{J}}_L(\tau - i0^+)$. Thus, the R-moving total spin currents can be reintroduced through $\vec{\mathcal{J}}_R(z^*) \equiv \vec{\mathcal{J}}_L(z^*)$ [see eq. (7.39)], so that for $z = z^* = \tau$, we recover eq. (C.2).

Thus, the boundary conditions (C.2) hold both for the zero-coupling and the strong-coupling Kondo problem (for a discussion of the strong-coupling boundary condition in terms of *fermion* fields (instead of currents), see appendix F).

Finally, to illustrate the need for the condition (C.4) for restricted KM transformations, note that it means the following for free fermions: The KM transformation laws for fermions are eqs. (B.53) and (B.54), and according to eq. (B.61), $\omega^a = i\theta^X$, $\bar{\omega}^a = i\bar{\theta}^X$. Thus the condition (C.4) implies that $\bar{\theta}^X(\tau) = \theta^X(\tau)$, i.e. along the real axis the *same* KM transformation has to be made on ψ_L and ψ_R. Clearly, this is a necessary condition if the zero-coupling boundary condition $\psi_L(\tau + i0^+) = \psi_R(\tau - i0^+)$, and consequently also $\vec{J}_L(\tau + i0^+) = \vec{J}_R(\tau + i0^+)$, are to be preserved.

C.1.3 Ward Identities for Boundary CFT

The boundary conditions (C.2) together with the restrictions (C.3) and (C.4) have profound consequences for the theory. Firstly, they imply that *the boundary is conformally and KM invariant* under restricted conformal and KM transformations. As mentioned above, this means that the *boundary contribution* (due to the C_+^r portion of the contour C_+) to the variation $\delta\mathcal{S}$ of the action [see eq. (C.1)] under such transformations vanishes:

$$\begin{aligned}
\int_{C_+^r} \tfrac{d\xi}{2\pi i}\, \varepsilon(\xi) T(\xi) - \int_{C_+^r} \tfrac{d\xi^*}{2\pi i}\, \varepsilon^*(\xi^*) \bar{T}(\xi^*) \; &= \int_{-\infty}^{\infty} \tfrac{d\tau}{2\pi i} \xi(\tau)[T(\tau) - \bar{T}(\tau)] = 0 \; ; \\
-\int_{C_+^r} \tfrac{d\xi}{2\pi i}\, \omega^a(\xi) J^a(\xi) + \int_{C_+^r} \tfrac{d\xi^*}{2\pi i}\, \bar{\omega}^a(\xi^*) \bar{J}^a(\xi^*) \; &= \int_{-\infty}^{\infty} \tfrac{d\tau}{2\pi i} \omega^a(\tau)[J^a(\tau) - \bar{J}^a(\tau)] = 0 \; .
\end{aligned}$$

We have derived this result as a consequence of the boundary condition (C.2). Of course, the converse is also true: eq. (C.2) can also be viewed as a necessary condition for the invariance of the boundary under restricted conformal and KM

transformations.

Secondly, the boundary conditions (C.2) together with the restrictions (C.3) and (C.4) imply that the separation of the theory into equations involving only T, J^a and $\bar{T}, \bar{J}^a$, respectively, no longer goes through. Instead, since analytic functions that are equal on an open domain (the real axis) must be analytical continuations of each other, they imply that

$$\bar{T}(z^*) = T(z^*)\,, \qquad \bar{J}^a(z^*) = J^a(z^*)\,, \qquad \text{for} \quad \text{Im}\, z < 0\,; \tag{C.8}$$

$$\xi^*(z^*) = \xi(z^*)\,, \qquad \bar{\omega}^a(z^*) = \omega^a(z^*)\,, \qquad \text{for} \quad \text{Im}\, z < 0\,. \tag{C.9}$$

Thus, $\bar{T}$ and $\bar{J}^a$ can be viewed as the analytic continuations of T and J^a into the lower half-plane. Furthermore, from eq. (B.31) it follows that $\bar{L}_n = L_n$ and $\bar{J}^a_n = J^a_n$, which means that there is only a single Virasoro algebra $\{L_n\}$ and only a single KM algebra $\{J^a_n\}$ [since the $\{\bar{L}_n\}$ and $\{\bar{J}^a_n\}$ are no longer independent of these, as they were in the bulk theory].

In the spirit of eq. (C.8), relabel all points z_i^* occuring in a correlation function $\langle X\rangle = \langle A_1(z_1, z_1^*)\ldots A_n(z_n, \bar{z}_n)\rangle$ as $z_i^* \equiv z_i'$, where the z_i' all lie in the lower half-plane, and write $\langle X'\rangle = \langle A_1(z_1, z_1')\ldots A_n(z_n, z_n')\rangle$. Using eqs. (C.8) and (C.9), the $\oint_{C_+} d\xi^*$ integrals in eqs. (B.11) and (B.13) may be rewritten as $-\oint_{C_+^*} d\xi$, where C_+^* is the complex conjugate contour of C_+, taken in the reverse direction, lying in the lower half-plane (see Fig. C.1). Thus, eqs. (B.11) and (B.13) become

$$\langle \delta_{\varepsilon,\varepsilon^*} X'\rangle = \oint_{C_+ + C_+^*} \tfrac{d\xi}{2\pi i}\, \varepsilon(\xi)\langle T(\xi) X'\rangle = \oint_C \tfrac{d\xi}{2\pi i}\, \varepsilon(\xi)\langle T(\xi) X'\rangle \tag{C.10}$$

$$\langle \delta_{\omega,\bar{\omega}} X'\rangle = -\oint_{C_+ + C_+^*} \tfrac{d\xi}{2\pi i}\, \omega^a(\xi)\langle J^a(\xi) X'\rangle = -\oint_C \tfrac{d\xi}{2\pi i}\, \omega^a(\xi)\langle J^a(\xi) X'\rangle \tag{C.11}$$

For the last equalities, we used the fact that the two straight portions of the

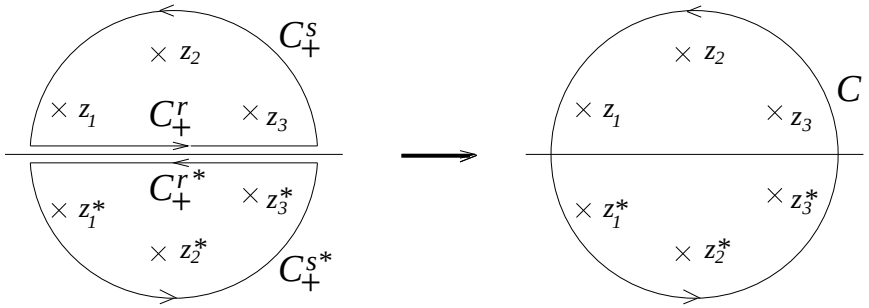

Figure C.1 Integration contours occuring in Cardy's boundary approach.

contours C_+ and C_+^* cancel, so that $C_+ + C_+^* = C$ is a large contour enclosing all the points z_i and z_i'.

If all the fileds ϕ_i in $\langle X' \rangle$ are Virasoro primary, or all fields φ_i in $\langle Y' \rangle$ are KM primary, we can carry the development a little further, as in section B.1. $\langle \delta_{\varepsilon,\varepsilon^*} X' \rangle$ and $\langle \delta_{\omega,\bar{\omega}} X' \rangle$ are also equal to the right hand sides of eqs. (B.19) and (B.20), which, using eq. (C.9), can be rewritten as

$$\langle \delta_{\varepsilon,\varepsilon^*} X' \rangle = \sum_{i=1}^{n} \left[\Delta_{\phi_i} \varepsilon'(z_i) + \varepsilon(z_i)\partial_{z_i} + \bar{\Delta}_{\phi_i} \varepsilon'(z_i') + \varepsilon(z_i')\partial_{z_i'} \right] \langle X' \rangle; \quad \text{(C.12)}$$

$$\langle \delta_{\omega,\bar{\omega}} Y' \rangle = \sum_{i=1}^{n} \left[\omega^a(z_i) t_i^a + \omega^a(z_i') \bar{t}_i^a \right] \langle Y' \rangle \; . \quad \text{(C.13)}$$

Use Cauchy's theorem to write the right hand sides of these equations as contour integrals over $\oint_C d\xi$, equate the results to eqs. (C.10) and (C.11), and note that the resulting equations must hold for arbitrary $\varepsilon(\xi)$ and $\omega^a(\xi)$. One thus obtains the Ward identities for correlation functions of Virasoro and Kac-Moody primary fields, respectively, in the presence of a boundary:

$$\langle T(\xi)\phi_1(z_1, z_1') \ldots \rangle \quad \text{(C.14)}$$
$$= \sum_{i=1}^{n} \left[\frac{\Delta_{\phi_i}}{(\xi - z_i)^2} + \frac{1}{(\xi - z_i)}\partial_{z_i} + \frac{\bar{\Delta}_{\phi_i}}{(\xi - z_i')^2} + \frac{1}{(\xi - z_i')}\partial_{z_i'} \right] \langle \phi_1(z_1, z_1') \ldots \rangle$$

$$\langle J^a(\xi)\varphi_1(z_1,z_1')\ldots\rangle \;=\; \sum_{i=1}^{n}\left[\frac{-\,t_i^a}{(\xi-z_i)} \;+\; \frac{-\,\bar{t}_i^a}{(\xi-z_i')}\right]\langle\varphi_1(z_1,z_1')\ldots\rangle\;. \qquad \text{(C.15)}$$

This is to be compared to eqs. (B.23) and (B.24) for the bulk case. Eq. (C.15) can be converted into a set of differential equations, known as the Knizhnik-Zamolodchikov equations, (see [KZ84, eq.(4.6)] or [AL94, eq.(B.8)]), whose form there depends only on bulk properties of the theory (such as bulk OPEs). These equations completely determine the behavior of $\langle\varphi_1(z_1,z_1')\ldots\rangle$, up to a small number of coefficients that depend on the boundary conditions on the theory.

Now, the short-distance OPEs should be independent of the presence of the boundary, so the rest of the analysis follows through as in the bulk. Hence we have arrived at the important result that the correlation function $\langle\phi_1(z_1,z_1^*)\phi_2(z_2,z_2^*)\ldots\phi_n(z_n,z_n^*)\rangle$ in the semi-infinite geometry, regarded as a function of $(z_1,z_2,\ldots,z_n;z_1^*,z_2^*,\ldots,z_n^*)$, satisfies the same differential equation as does the bulk correlation function $\langle\phi_1(z_1,z_1^*)\phi_2(z_2,z_2^*)\ldots\phi_{2n}(z_{2n},z_{2n}^*)\rangle$, regarded as a function of $(z_1,z_2,\ldots,z_{2n})$ only.[4]

This is Cardy's key conclusion for a boundary CFT: *n-point functions in the presence of a boundary are calculated as though they were bulk $2n$-point functions.* Quoting [AL94, p. 559], we have the following recipe: "Replace all R-fields in a *Green's function in the presence of the boundary* by L-fields, evaluated at the arguments of the R-fields in the lower half complex plane. The R-fields can be envisioned as sitting at mirror image points in the lower half plane. The resulting function, containing only L-fields, is a L-chiral function in the entire complex plane." Explicitly, in the notation of eqs. (B.15) and (B.16) (see also

[4]In this statement it is implicit that the left isospin indices of the field $\phi_{n+i}(z_{n+i},z_{n+i}^*)$ have the same KM transformation properties as the right isospin indices of the field $\phi_i(z_i,z_i^*)$, and that $\Delta_{\phi_{n+i}}=\bar{\Delta}_{\phi i}$ etc.

[AL91b, eq.(2.34)], [Lud94a, eq.(6.14)]):

$$A_i(z,z^*) \;=\; A_{iL}(z)A_{iR}(z^*) \;\to\; A_{iL}(z)A_{iL}(z^*) \tag{C.16}$$

$$\langle A_1(z_1,z_1^*)\dots A_n(z_n,z_n^*)\rangle \;=\; \sum_{(a)}\langle A_{1L}(z_1)\dots A_{nL}(z_n)A_{1L}(z_1^*)\dots A_{nL}(z_n^*)\rangle_{(a)}\cdot D^{(a)}\;. \tag{C.17}$$

As in eq. (B.16), the label (a) is needed because the Knizhnik-Zamolodchikov equations that determine the $2n$-point function in general have several independent solutions, known as *conformal blocks*. Note, however, that in general it is not true that $A_{iR}(z^*)$ is simply the analytic continuation of $A_{iL}(z_i^*)$ into the lower half-plane, as was the case for $\bar{T}$ and $\bar{J}^a$. Instead, in general, $A_{iR}(\tau - i0^+) \neq A_{iL}(\tau + i0^+)$, i.e. the field $A_{iL}(z)$, viewed as a L-chiral field defined in the entire complex plane, is *not* analytic at the real axis. This is because of the possibility of non-trivial boundary conditions, as will be discussed in section C.3.1 (after eq. (C.38)).

C.2 The Boundary 2-Point Function $G_s^{(2)}$

As an example of the above theory, Cardy considered [Car84b, p.524] the 2-point function of a Virasoro primary, Kac-Moody singlet, Hermition operator $\phi_i(z,z^*) = \phi_{iL}(z)\phi_{iL}(z^*)$ with scaling dimensions (Δ_i,Δ_i):

$$G_s^{(2)} = \langle\phi_i(z_1,z_1^*)\phi_i(z_2,z_2^*)\rangle = \langle\phi_{iL}(z_1)\phi_{iL}(z_1^*)\phi_{iL}(z_2)\phi_{iL}(z_2^*)\rangle\;. \tag{C.18}$$

We shall discuss this function in some detail, since it can be used to illustrate a number of important concepts in boundary CFT, and in particular leads naturally to the introduction of boundary operators and boundary operator product exapansions in section C.3. (Since any KM primary operator is also Virasoro

primary, the discussion for operators that are not KM singlets and/or not Hermitian is entirely analogous, modulo the appearance of isospin indices and or †'s. An example is given in our discussion of the Kondo problem, appendix D.)

C.2.1 General Functional Form of $G_s^{(2)}$

According to the previous section, $G_s^{(2)}$ satisfies the same equation as (the holomorphic factor of) the four-point function

$$G^{(4)} = \langle \phi_i(z_1, z_1^*)\phi_i(z_2, z_2^*)\phi_i(z_4, z_4^*)\phi_i(z_3, z_3^*)\rangle \tag{C.19}$$

in the bulk.[5] Invariance under the small conformal group fixes this to have the form [see eq. (B.44)[6]:[7]

$$G^{(4)}(z_1, z_2, z_3, z_4) = \left[\frac{(1-\xi)^{-1}}{z_{12}z_{43}}\right]^{2\Delta_i} F_b(\xi) \;=\; \left[\frac{(1-\eta)^{-1}}{z_{14}z_{32}}\right]^{2\Delta_i} F_b(1-\eta) \tag{C.20}$$

where $z_{ij} = z_i - z_j$ and the cross-ratios ξ and η are defined by

$$\xi = \frac{z_{12}z_{43}}{z_{13}z_{42}}\,, \qquad \eta = 1-\xi = \frac{z_{14}z_{32}}{z_{13}z_{42}}\,, \qquad \frac{1-\xi}{\xi} = \frac{z_{14}z_{12}}{z_{13}z_{43}}\,. \tag{C.21}$$

The function $F_b(\xi)$ is determined by a certain set of differential equations, known as the Knizhnik-Zamolodchikov equations, which is determined by bulk properties (such as bulk OPEs). According to the above analysis, the 2-point function in the surface geometry can be obtained from eq. (C.20) by replacing z_3 and z_4 by $z_3^* = z_2^*$ and $z_4^* = z_1^*$, and therefore has the form:

$$G_s^{(2)}(z_1, z_1^*; z_2, z_2^*) = \left[\frac{(1-\xi)^{-1}}{|z_{12}|^2}\right]^{2\Delta_i} F_s(\xi) \;=\; \left[\frac{(1-\eta)^{-1}}{4x_1x_2}\right]^{2\Delta_i} F_s(1-\eta) \tag{C.22}$$

[5]The dummy indices z_3 and z_4 in eq. (C.19) are written in this order purely for the sake of being notationally consistent with appendix D, where we need the limit $z_1 \to z_4^*$, $z_2 \to z_3^*$.

[6]This follows from eq. (B.44), since $\Delta_m = \Delta_i$ for $m = 1, \ldots, 4$, so that $\prod_{m<n} z_{mn}^{-(\Delta_m+\Delta_n)+\Delta_T/3} = [z_{12}z_{13}z_{14}z_{23}z_{24}z_{34}]^{-2\Delta/3} = [-\xi^{-1}(1-\xi)^2]^{2\Delta/3}[z_{13}z_{42}]^{-2\Delta}$.

[7]Cardy Compare this to [Car84b, eq.(4.11)].

where now

$$\xi = \frac{|z_1 - z_2|^2}{|z_1 - z_2^*|^2}\,, \qquad \eta = 1 - \xi = \frac{4x_1x_2}{|z_1 - z_2^*|^2}\,, \qquad \frac{1-\xi}{\xi} = \frac{4x_1x_2}{|z_1 - z_2|^2}\,. \tag{C.23}$$

The two alternative ways of writing $G_s^{(2)}$ are convenient in the limits $\xi \to 0^+$ and $\eta \to 0^+$, respectively. The limit $\xi \to 0^+$ is called the *bulk limit* [see Fig. C.2(a)] since it corresponds to the case $|z_{12}| \to 0$ relative to all other distances, or more generally, any limit in which the distances x_1 and x_2 of z_1 and z_2 to the boundary become infinite relative to the separation $|z_1 - z_2|$, i.e. $\xi \to 0^+$, so that bulk behavior is expected to dominate [see Fig. C.2(a), with $z_3^* = z_2^*$ and $z_4* = z_1^*$]. The limit $\eta \to 0^+$ is called the *boundary* or *surface limit* [see Fig. C.2(b)], since it corresponds to x_1 and/or $x_2 \to 0$, or more generally, any limit in which the distances x_1 and x_2 become small compared to the separation $|z_1 - z_2^*|$ i.e. $\eta \to 0^+$, so that boundary effects are expected to emerge.

The function $F_s(\xi)$ is determined by the same Knizhnik-Zamolodchikov equations as $F_b(\xi)$. The only difference between $G_b^{(4)}$ and $G_s^{(2)}$ lies in the different boundary conditions they must satisfy. These boundary conditions are specified by specifying the asymptotic behavior of $F_s(\eta)$ in the limits $\xi \to 0^+$ and/or $\eta \to 0^+$, i.e. the leading coefficients in the expansions

$$(1-\xi)^{-2\Delta_i} F_s(\xi) = \sum_n a_{in}^b\, \xi^{\Delta_n^b} \qquad \text{for} \quad \xi \to 0^+\,; \tag{C.24}$$

$$(1-\xi)^{-2\Delta_i} F_s(1-\eta) = \sum_n a_{in}^s\, (\eta)^{\Delta_n^s} \qquad \text{for} \quad \eta \to 0^+ \tag{C.25}$$

The superscripts b/s distinguish the bulk from the surface or boundary limit (see below). Since F_s satisfies the Knizhnik-Zamolodchikov equation, the number of coefficients $a_{in}^{b/s}$ that can be independently specified is limited, and equal to the number of independent conformal blocks in eq. (C.17). In particular, if sufficiently

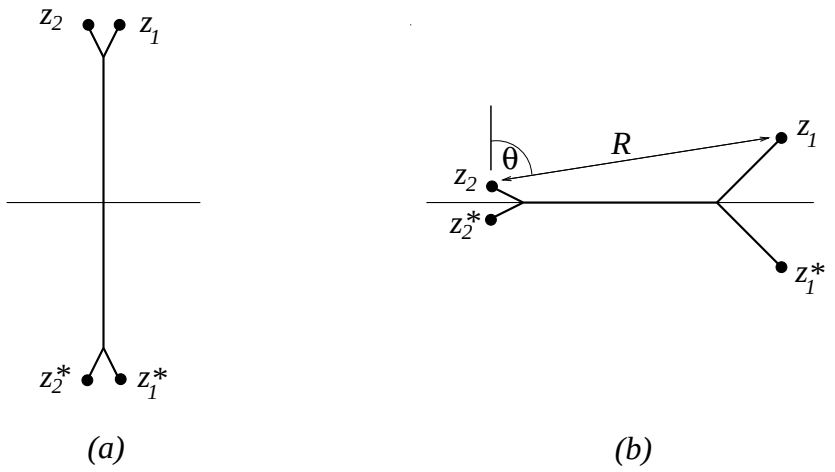

Figure C.2 (a) Bulk and (b) boundary limits for the two-point function $G_s^{(4)} = (z_1, z_1^*; z_2, z_2^*)$.

many bulk coefficients a_{in}^b are specified to determine F_s completely, all surface coefficients a_{in}^s and exponents Δ_n^s are automatically determined as well.

C.2.2 Bulk and Boundary Limits of $G_s^{(4)}$

For the sake of applicability in appendix D, we shall keep z_3^* and z_4^* distinct from z_2^* and z_1^* for the time being (but still in the lower half-plane), using the notation $z_{14}^* = z_1 - z_4^*$, etc., and study $G_s^4(z_1, z_2, z_3^*, z_4^*) = \phi_{iL}(z_1)\phi_{iL}(z_2^*)\phi_{iR}(z_4^*)\phi_{iR}(z_3^*)\rangle$, which is given by eq. (C.20) (with F_s instead of F_b). By eqs. (C.24) and (C.25), the *bulk* and *boundary limits* of $G_s^{(4)}$ are:

$$G_s^{(4)} \;=\; \begin{cases} (z_{12}z_{43}^{**})^{-2\Delta_i} \sum_n a_{in}^b \, \xi^{\Delta_n^b} \quad \text{for} \quad \xi \to 0 \; ; & \text{(C.26)} \\ (z_{14}^* z_{32}^*)^{-2\Delta_i} \sum_n a_{in}^s \, \eta^{\Delta_n^s} \quad \text{for} \quad \eta \to 0 \; . & \text{(C.27)} \end{cases}$$

The properties of ϕ_i in the bulk strongly constrain the freedom available in specifying the boundary conditions on F_s and $G_s^{(4)}$ [Car84b, section 4.1.1]. This

happens via the bulk OPE of $\phi_{iL}(z)$ with itself, which has the general form

$$\phi_{iL}(z_1)\phi_{iL}(z_2) = \sum_n \frac{C_{ii,n}\phi_{nL}(z_2)}{(z_{12})^{2\Delta_i-\Delta_n}} \ . \tag{C.28}$$

Inserting this into eq. (C.18) one obtains a representation for $G_s^{(4)}$ that is valid for $z_1 \to z_2$ and $z_3^* \to z_4^*$, i.e. in the bulk limit [see Fig. C.2(a)]:

$$G_s^{(4)} \ = \ \sum_{nn'} \frac{C_{ii,n}C_{ii,n'}\,\langle\phi_{nL}(z_2)\phi_{n'L}(z_4^*)\rangle}{(z_{12})^{2\Delta_i-\Delta_n}\,(z_{43}^{**})^{2\Delta_i-\Delta_{n'}}} \ , \qquad \text{for} \quad \xi \to 0^+ \ . \tag{C.29}$$

The correlation function $\langle\phi_{nL}(z_2)\phi_{n'L}(z_4^*)\rangle$ occuring here is shown in section C.3 to have the form (see eq. (C.38) below),

$$\langle\phi_{nL}(z)\phi_{n'L}(z^*)\rangle = \delta_{nn'}\frac{C_{no}^B}{[-i(z_2-z_4^*)]^{2\Delta_n}} \ , \tag{C.30}$$

where the coefficient C_{no}^B may be thought of as specifying a boundary condition, labeled by B, on this function. This implies that in the bulk limit,

$$G_s^{(4)} \ = \ (z_{12}z_{43}^{**})^{-2\Delta_i}\sum_n (C_{ii,n})^2\left(\frac{z_{12}z_{43}^{**}}{-(z_{24}^*)^2}\right)^{\Delta_n} \ , \qquad \text{for} \quad \xi \to 0^+ \ , \tag{C.31}$$

which, when compared with eq. (C.26) (in the limit $z_1 \to z_2$, $z_3^* \to z_4^a st$), immediately gives

$$a_{in}^b = (C_{ii,n})^2 C_{no}^B \ , \qquad \Delta_n^b = 2\Delta_i - \Delta_n \ . \tag{C.32}$$

Now, the coefficients $C_{ii,n}$ in the bulk OPE (C.28) are always *independent* of the particular boundary condition imposed at the boundary, and are known from bulk CFT. (Intuitively speaking, in the limit $\xi \to 0$ in which the bulk OPE may be used, one is so far away from the boundary relative to $z_1 - z_2$ that all boundary effects become irrelevant). Thus, eq. (C.32) implies that the a_{in}^b and Δ_n^b, and hence *the full behavior of* $F_s(\eta)$ *and* $G_s^{(4)}$*, are completely determined once the (first few)* C_{no}^B *have been specified.* In other words, "specifying a boundary

condition" B for a boundary CFT is equivalent to specifying the values of these coefficients C_{no}^B. In section C.4 it is shown that these C_{no}^B may be specified in a rather compact form in terms of a certain *boundary state* $|B\rangle$ [see eq. (C.54)].

The leading term in eq. (C.31) corresponds to $\phi_o = I$, the unit operator, for which $\Delta_o = 0$. Thus in the bulk limit, the leading term in $G_s^{(4)}$, namely $(z_{12}z_{43}^{**})^{-2\Delta_i}$, does not depend on $z_{24}^* = \tau_1 - \tau_2 + i(x_1 + x_2)$ (except if $C_{no}^B = 0$). This was to be expected, since deep enough in the bulk, translational invariance should be restored.[8]

Next consider the boundary limit: Take $z_3^* = z_3^*$ and $z_4^* = z_1^*$, and suppose that $x_1 \geq x_2$, so that we can write $x_1 = x_2 + R\cos\theta$, where $R = |z_1 - z_2|$ and $\theta \in [0, \pi/2]$ is the angle between the normal to the surface and the vector pointing from z_2 to z_1. When $R \to 0^+$ for fixed (small) x_2, the cases $\theta < \pi/2$ and $\theta = \pi/2$ correspond to surface-bulk and surface-surface correlation functions, respectively. Taking the limit $R \to \infty$ and $\eta \to \frac{4x_1x_2}{R^2} \to \infty$ in eq. (C.27), and denoting the leading (smallest) surface exponent by $\Delta_{\tilde{n}}^s$, we obtain

$$G_s^{(2)} = \begin{cases} a_{i\tilde{n}}^s (4x_2\cos\theta)^{-2\Delta_i + \Delta_{\tilde{n}}^s} R^{-(2\Delta_i + \Delta_{\tilde{n}}^s)} & \sim R^{-\Delta_\perp} \quad \text{for } \theta < \pi/2\,, \quad \text{(C.33)} \\ a_{i\tilde{n}}^s (4x_2x_2)^{-2\Delta_i + \Delta_{\tilde{n}}^s} R^{-2\Delta_{\tilde{n}}^s} & \sim R^{-\Delta_\parallel} \quad \text{for } \theta = \pi/2\,. \quad \text{(C.34)} \end{cases}$$

Hence we identify $\Delta_\perp = 2\Delta_i + \Delta_{\tilde{n}}^s$ and $\Delta_\parallel = 2\Delta_{\tilde{n}}^s$. The fact that $\Delta_\perp \neq \Delta_\parallel$ means that the decay of the 2-point function depends on the direction relative to the boundary. This is a well-known general feature of critical systems with boundaries, first found in [BH72], and is discussed at length in, e.g. [Die86].[9]

[8] This is simply a manifestation of the linked cluster theorem applied to eq. (C.17), according to which $G_s^{(4)} = \langle \phi_{iL}(z_1)\phi_{iL}(z_2)\rangle\langle \phi_{iL}(z_4^*)\phi_{iL}(z_3^*)\rangle = (z_{12}z_{43}^{**})^{-2\Delta_i}$ in this limit (see Fig. C.2).

[9] In the general theory of critical phenomena for semi-infinite systems with a boundary (see [Die86]), boundary effects such as $\Delta_\perp \neq \Delta_\parallel$ occur only if one of the points at which correlation functions are evaluated is within a correlation length ξ of the boundary. However, systems

What determines the boundary-limit exponents Δ_n^s and coefficients a_{in}^s? Once the C_{no}^B have been specified so that $G_s^{(4)}$ is completely determined, the Δ_n^s and a_{in}^s are also completely determined, and can be found by simply taking the boundary limit eq. (C.27) of $G_s^{(4)}$. This can be done in great generality, using very general (so-called "duality") properties of the function F_s, as was shown in [CL91, p.277]. Several explicit examples of this procedure, applied to the Kondo problem, can be found in [AL94], sections 3.3 and 4. In the next section, we give an "interpretation" of the Δ_n^s and a_{in}^s by showing that they also occur in the so-called *boundary OPE* that one obtains when taking a field very close to the boundary.

C.3 Boundary Operators

In the previous section we encountered the "cross-boundary" correlation function $\langle \phi_{nL}(z_2)\phi_{n'L}(z_4^*)\rangle$ of eq. (C.30), an example of a correlation function that contains arguments "on both sides of the boundary". The OPE of $\phi_{nL}(z_i)$ with $\phi_{n'L}(z_j^*)$ always involves the limit $z_i \to z_j^*$ (i.e. $x_i \to 0$, $x_j \to 0$) in which these operators are evaluated close to the boundary. Therefore, to understand equations such as eq. (C.30), and more generally, the behavior of fields close the boundary, it is convenient to introduce the concept of "boundary operators", to which this section is devoted.

C.3.1 Basic Properties of Boundary Operators

By definition, a *boundary operator* is an operator $\Phi(\tau)$ that lives on the boundary (a bulk operator evaluated at the boundary is also sometimes referred to as a

with conformal invariance are scale-invariant, and hence have $\xi = \infty$, so that the effect of the boundary becomes particularly pronounced and propagetes through the entire system.

boundary operator). A boundary operator $\Phi_k(\tau)$ with scaling dimension Δ_k obeys the conformal transformation law

$$\Phi_k(\tau) = \left(\frac{\partial f(\tau)}{\partial \tau}\right)^{\Delta_k} \tilde{\Phi}_k(\xi) \ , \tag{C.35}$$

under restricted [see eq. (C.3)] conformal transformations $\xi = f(z)$. Hence boundary operators have correlation functions (choosing unit normalization)

$$\langle \Phi_k(\tau_1)\Phi_l(\tau_2)\rangle = \frac{\delta_{kl}}{|\tau_1 - \tau_2|^{2\Delta_k}} \ . \tag{C.36}$$

Note the occurence of the absolute value, which is explained at the end of section C.3.2; it is sometimes paraphrased by saying that "boundary operators have no statistics" (since the correlation function does not pick up a phase under exchange of its arguments).

The only boundary operator with non-zero expectation value is the identity operator, $I = \Phi_o$, which has scaling dimension $\Delta_o = 0$: $\langle \Phi_k(\tau)\rangle = \delta_{ko}$.

Boundary operators enter the calculation of correlation functions via so-called *boundary operator product expansions* (BOPE), which supplement the usual bulk OPEs of a bulk CFT. A BOPE is a short-distance expansion which specifies the short-distance behavior of a given bulk field near the boundary in terms of boundary operators, and depends on the specific boundary condition imposed at the boundary, as explained below. Such boundary BOPEs were first written down (in a non-CFT context) by Diehl and Dietrich [DD81, eq.(IV.6)].

We shall only be interested in the BOPE of Virasoro primary fields $\phi_i(z, z^*)$ with scaling dimensions (Δ_i, Δ_i) (i.e. spin $\Delta_i - \Delta_i = 0$). Actually, since $\phi_i(z, z^*) = \phi_{iL}(z)\phi_{iL}(z^*)$, let us consider the slightly more general OPE of $\phi_{iL}(z_1)$ with $\phi_{iL}(z_2^*)$. Assuming that the boundary respects (restricted) confor-

mal symmetry, their OPE is necessarily of the form:[10]

$$\phi_{iL}(z_1)\phi_{iL}(z_2^*) \;=\; \sum_k \frac{C_{ik}^B}{[-i(z_1-z_2^*)]^{2\Delta_i-\Delta_k}}\Phi_k(\tau)\;. \tag{C.37}$$

This general form is the only one compatible with scale invariance, since it is the only one that is form-invariant under $z = b\tilde{z}$, $\phi_i(z,z^*) = b^{-2\Delta_i}\tilde{\phi}_i(\tilde{z},\tilde{z}^*)$, etc. The BOPE of $\phi_i(z,z^*)$ is obtained by simply taking $z_1 = z_2$ in eq. (C.37).

Eq. (C.37) immediately implies the result used in eq. (C.30) above, namely

$$\langle\phi_{iL}(z_1)\phi_{iL}(z_2^*)\rangle \;=\; \frac{C_{io}^B}{[-i(z_1-z_2^*)]^{2\Delta_i}}\;. \tag{C.38}$$

[The $\delta_{nn'}$ in eq. (C.30) follows from scale invariance, just as in eq. (B.42).] Contrast this with the case in which both arguments lie on the same side of the real axis, for which (using conventional normalization) one has:[11]

$$\langle\phi_{iL}(z_1)\phi_{iL}(z_2)\rangle = \frac{1}{(z_1-z_2)^{2\Delta_i}}\;. \tag{C.39}$$

The fact that in general $(-i)^{-2\Delta_i}C_{io}^B \neq 1$ means that $\langle\phi_{iL}(z_1)\phi_{iL}(z_2^*)\rangle$ is discontinuous as one of its arguments crosses the real axis. This is the reason why $\phi_{iL}(z^*)$ [or more correctly $\phi_{iR}(z^*)$] can not simply be regarded as the analytical continuation of $\phi_{iL}(z)$ across the real axis, as was emphasized above [after eq. (C.17)]. The special case in which $\langle\phi_{iL}(z_1)\phi_{iL}(z_2)\rangle$ *is* analytic across the boundary is called the *free* boundary condition, denoted by $B = F$, in which case we must have $C_{io}^F = (-i)^{2\Delta_i}$.

If we take $z_2^* = z_1^*$ in eq. (C.38), we obtain the result that the bulk operator $\phi_i(z,z^*)$ has the expectation value $\langle\phi_i(z,z^*)\rangle = C_{io}^B(2x)^{2\Delta_i}$. Note that due to

[10]The factor of $-i$ in the denominator, which ensures that the denominator is real in the limit $z_1 \to z_2^*$, is inserted in order to be consistent with the notation used in [CL91, eq.(1)].

[11]If both arguments z_1 and z_2 are taken infinitely far away from the boundary, the boundary can have no influence, and eq. (C.39) must hold. Since the functional form of $\langle\phi_{iL}(z_1)\phi_{iL}(z_2^*)\rangle$ is completely determined by conformal invariance, eq. (C.39) must therefore hold for arbitrary z_1 and z_2, as long as they are on the same side of the boundary.

the presence of a boundary, this is *not* zero if the BOPE contains the identity, in contrast to a bulk theory, where it is conventional to subtract constants such that $\langle\phi_i\rangle = 0$ for all operators. Note also that $\langle\phi_i(z,z^*)\rangle$ is independent of τ, as is to be expected by translational invariance along the boundary.

C.3.2 Relation between BOPE and $G_s^{(4)}$

To find out what determines the BOPE coefficients C_{ik}^B, consider the boundary limit $\eta \to 0$ of the function $G_s^{(4)}$, which has the form (C.27). An alternative expression for $G_s^{(4)}$ can be found by directly evaluating eq. (C.18) in the limit $z_1 \to z_4^*$, $z_2 \to z_3^*$ and $|z_1 - z_2| = |\tau_1 - \tau_2| \to \infty$, so that $\eta \to 0^+$ [see Fig. C.2(b)]. Using the BOPE (C.37) twice in eq. (C.18) and then eq. (C.36), one obtains

$$G_s^{(4)} \to \sum_{kl} \frac{C_{ik}^B C_{il}^B \langle\Phi_k(\tau_1)\Phi_l(\tau_2)\rangle}{(-iz_{14}^*)^{2\Delta_i-\Delta_k}(-iz_{23}^*)^{2\Delta_i-\Delta_l}} = \sum_k \frac{(C_{ik}^B)^2}{(z_{14}^* z_{32}^*)^{2\Delta_i-\Delta_k}|\tau_1-\tau_2|^{2\Delta_k}} \quad \text{(C.40)}$$

This has exactly the form of eq. (C.27), since $\eta \to \frac{z_{14}^* z_{32}^*}{(\tau_1-\tau_2)^2}$ in this limit, implying that

$$(C_{ik}^B)^2 = a_{ik}^s \,, \qquad \Delta_k = \Delta_k^s \,. \quad \text{(C.41)}$$

Thus each term Φ_k in the BOPE of $\phi_{Li}(z)\phi_{Li}(z^*)$ makes a contribution to the boundary-limit expression eq. (C.27) for $G_s^{(4)}$. In particular, *the exponents* Δ_k^s *are simply the scaling dimensions of the boundary operators* Φ_k *that occur in the BOPE of* $\phi_i(z,z^*)$. Conversely, *the structure of this BOPE* (i.e. the coefficients C_{ik}^B) *is determined by the boundary behavior of the 2-point function.* It follows that only the C_{io}^B are independent coefficients: as argued in the previous section, specifying these completely determines $G^{(4)}$, hence a_{ik}^s and Δ_k^s, and thus by eq. (C.41) also a_{ik}^s for $k \neq 0$.

This boundary limit also illustrates why eq. (C.36) features an absolute value $|\tau_2 - \tau_2|$: boundary-boundary 2-point function such as $\langle \Phi_k(\tau_1)\Phi_l(\tau_2)\rangle$ occur only when one takes a (double) boundary limit of some multi-point function such as $G_s^{(4)}$. In this limit, the only dependence of the multi-point function on $(\tau_1 - \tau_2)$ will be through some cross-ratio such as η, which, in this limit, always contains only the combination $(\tau_1 - \tau_2)^2 = |\tau_1 - \tau_2|^2$. Hence $\langle \Phi_k(\tau_1)\Phi_l(\tau_2)\rangle$ can also depend only on $|\tau_2 - \tau_2|$. It can easily be checked that this is also the case for more general functions than the one discussed here.

C.3.3 Two Examples: $\langle \psi_R \psi_L^\dagger \rangle$ and $\langle \psi_R \Phi_n \psi_L^\dagger \rangle$

As the previous subsection illustrates, BOPEs determine the overall amplitude of any correlation function that contains operators evaluated at points on opposite sides of the real axis, i.e. $\phi_i(z_i)$ and $\phi_j(z_j^*)$, because the OPE of two such operators is always a BOPE. We give two more examples involving fermion fields, of interest in chapters 7 and 8. In each, the functional form of a correlation function is determined by conformal invariance, but its amplitude has to be found using a BOPE.

(i) Consider the *L*-*R* fermion-fermion function $-G_{LR}(z_1, z_2^*) = \langle \psi_L(z_1)\psi_R^\dagger(z_2^*)\rangle$. According to eq. (C.17), this is given by $\langle \psi_L(z_1)\psi_L^\dagger(z_2^*)\rangle$ and hence, by conformal invariance [eq. (B.42)], has the functional form $c[-i(z_1 - z_2^*)]^{-1}$. To find the overall amplitude c, we should use the OPE of $\psi_L(z_1)\psi_L^\dagger(z_2^*)$ in the limit $z_1 \to z_2^*$, which must have the form of eq. (C.37), namely

$$\psi_L(z_1)\psi_L^\dagger(z_2^*) = \sum_k \frac{C_{\psi k}^B}{[-i(z_1 - z_2^*)]^{1-\Delta_k}} \Phi_k(\tau) \; . \tag{C.42}$$

Thus, the amplitude of G_{LR} is $c = C^B_{\psi o}$:

$$-G_{LR}(z_1, z_2^*) = \langle \psi_L(z_1)\psi_R^\dagger(z_2^*)\rangle = \frac{C^B_{\psi o}}{-i(z_1 - z_2^*)}. \tag{C.43}$$

(ii) Next, consider the insertion of a boundary operator Φ_n into G_{LR} (as needed in section 8.5, eq. (8.26)). The functional form of the 3-point function is completely determined by conformal invariance[12] [see eq. (B.43)]:

$$\langle \psi_L(z_1)\Phi_n(\tau')\psi_R^\dagger(z_2^*)\rangle = \frac{\tilde{c}}{(\tau' - z_1)^{\Delta_n}(\tau' - z_2^*)^{\Delta_n}[-i(z_1 - z_2^*)]^{1-\Delta_n}} . \tag{C.44}$$

To calculate the overall amplitude $\tilde{c}$, the BOPE (C.42) again has to be used: Evaluate $\langle \psi\Phi\psi\rangle$ in the limit $z_1 \to z_2^*$ (specifically, take $\tau_1 = \tau_2$ and $x_1 = x_2 \to 0$), using first eq. (C.42) and then eq. (C.36); this gives $\tilde{c} = C^B_{\psi m}$ for the overall amplitude. To find $C^B_{\psi m}$ explicitly, however, is rather cumbersome. As discussed in the previous subsection, one has to explicitly calculate the 4-point function $\langle \psi_{L1}\psi^\dagger_{L2}\psi_{R3}\psi^\dagger_{R4}\rangle$ in terms of $C^B_{\psi o}$, and then take the double boundary limit of eq. (C.40). AL did this in great detail for the Kondo problem [AL94]. We present their calculation in detail in appendix D, and derive a list of the first few Φ_n (with $\Delta_n \leq \frac{3}{2}$) for which $C^B_{\psi o} \neq 0$ in table D.1.

C.4 The Boundary State $|B\rangle$

In this section we introduce the concept of a boundary state $|B\rangle$, introduced by Cardy in [Car86b], which represents a very concise way of specifying the boundary condition for a boundary CFT. We follow the presentation of [CL91]. In section C.4.1 we show how the coefficients of the identity, C^B_{io}, in the BOPE of $\phi_i(z, z^*)$ can be calculated in terms of $|B\rangle$. In section C.4.2 we derive Cardy's

[12] As usual, the extra factor of $(-i)$ in the denominator of eq. (C.44) is inserted for the sake of convenience, to ensure that no extra overall phase occurs in eq. (C.44).

formula, which gives matrix elements of $|B\rangle$ explicitly in terms of modular S-matrices, and apply it to the case where the boundary condition is governed by a fusion principle.

C.4.1 Relation between $|B\rangle$ and BOPE coefficients

[CL91]

We have seen in appendix B that there is a 1-1 correspondence between bulk scaling operators $\phi_i(z, z^*)$ and the eigenstates of the transfer matrix e^{-H_P} of the theory defined on an infinitely long cylinder of radius β [section B.5] onto which the plane is mapped by $z = \tan \frac{\pi}{\beta} iw$ [eq. (B.99)]. Quoting [CL91], "roughly speaking, the eigenstate $|\phi_i\rangle$ corresponding to ϕ_i is the lowest state in the spectrum (of H_P) which is allowed to propagate when the operator is placed at minus infinity on the cylinder". However, when one starts with a boundary CFT in the upper *half*-plane, the corresponding infinite cylinder becomes a *semi*-infinite half-cylinder, with a boundary at one end, and the cylinder theory has to be modified accordingly.

Let B denote the boundary condition imposed at $x = 0$ of the half-plane (specifically, the set of coefficients C^B_{no}). Consider again the "finite-temperature" transformation eq. (B.99) (with $\tilde{z} = iw$)

$$z = \tan \tfrac{\pi}{\beta} iw \; . \tag{C.45}$$

which maps the upper half-plane, parametrized by $z = \tau + ix$ with $x \in [0, \infty]$, onto a semi-infinite cylinder of circumference β, parametrized by $w = u + iv$, with $u \in [0, \infty]$ and $v \in [-\beta/2, \beta/2]$ [see Fig. C.3]. The boundary at $x = 0$ is mapped onto the circular lower edge of the cylinder at $u = 0$, so that the

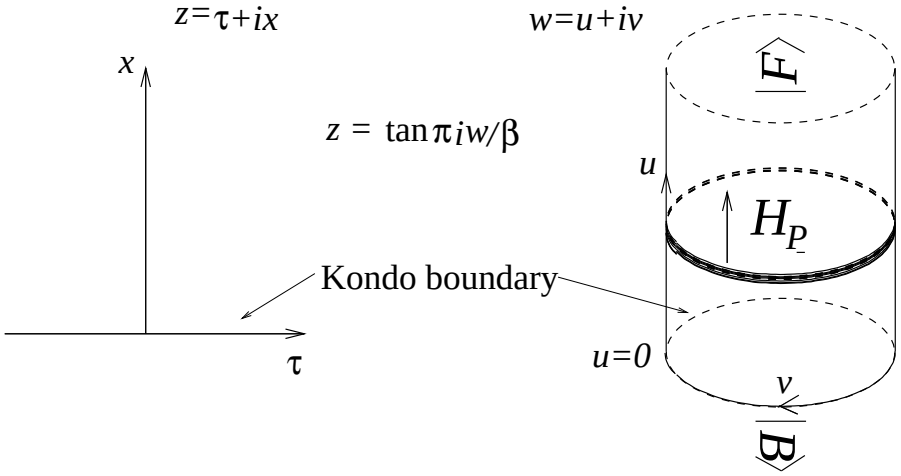

Figure C.3 The transformation $z = \tan\frac{\pi}{\beta}iw$ maps the upper half-plane ($z = \tau + ix$) onto a semi-infinite cylinder ($w = u + iv$). The boundary at $x = 0$ is mapped onto the lower edge of the cylinder at $u = 0$.

boundary condition B that holds at $x = 0$ for the half-plane also holds at $u = 0$ for the cylinder.

Regard u as the "time-variable" in the longitudinal direction along the cylinder. Imagine the cylinder to be canonically quantized along lines of constant u, and let H_P be the Hamiltonian that generates translations in the u-direction. Then H_P contains *no* information about the boundary condition B, because the latter acts only at $u = 0$; in fact, this is the same H_P as that in section B.5. Now consider the field $\tilde{\phi}_i(u, v)$ with scaling dimensions (Δ_i, Δ_i) [the $\tilde{}$ denotes the cylinder-version of half-plane field $\phi_i(\tau, x)$]. We would like to calculate the cylinder expectation value $\langle\tilde{\phi}_i(u, v)\rangle$ in terms of the cylinder transfer matrix e^{-H_P}, in analogy to eq. (B.93). In contrast to the bulk case, however, the presence of a boundary condition at $u = 0$ has to be accounted for here. This is done replacing

the traces $\sum_{n'k'}$ in eq. (B.93) by the following matrix element [CL91, eq.(2)]:

$$\langle\tilde{\phi}_i(u,v)\rangle \equiv \lim_{l\to\infty} \frac{\langle F|e^{-(l-u)H_P}\tilde{\phi}_i(v)e^{-uH_P}|B\rangle}{\langle F|e^{-lH_P}|B\rangle} \tag{C.46}$$

Here the so-called *boundary states* $|B\rangle$ and $|F\rangle$ live in the Hilbert space upon which H_P acts. They determine the "initial" and "final" states at $u = 0$ and $u = l \to \infty$ of the u-propagation, generated by H_P through $\tilde{\phi}(u,v) = e^{uH_P}\tilde{\phi}(v)e^{-uH_P}$ [as in eq. (B.92)]. $|B\rangle$ is determined by the boundary condition B, as is made explicit below, whereas $|F\rangle$ corresponds to a "free" boundary condition at $u = l \to \infty$, where the effect of the boundary at $u = 0$ has died out.

Upon taking the limit $l \to \infty$, only the ground state contribution $\langle 0|e^{-(l-u)E_o}$ to $\langle F|e^{-(l-u)H_P}$ survives in eq. (C.46), where $|0\rangle$ denotes the ground state of H_P, with eigenenergy E_o. Further, insert a complete set of states between $\tilde{\phi}_i(v)$ and e^{-uH_P}. Of the many eigenstates $|\phi_i, N\rangle$ in the conformal tower corresponding to $\tilde{\phi}_i$, only the (lowest-energy) primary state $|\phi_i\rangle$, with eigenenergy E_{ϕ_i}, will survive in the limit $u \to \infty$, so that we get

$$\langle\tilde{\phi}_i(u,v)\rangle \quad \stackrel{u\to\infty}{\longrightarrow} \quad \frac{e^{-(l-u)E_o}\langle 0|\tilde{\phi}_i(v)|\phi_i\rangle\langle\phi_i|B\rangle e^{-uE_{\phi_i}}}{e^{-lE_o}\langle 0|B\rangle} \tag{C.47}$$

$$= \quad (2\pi/i\beta)^{2\Delta_i}\frac{\langle\phi_i|B\rangle}{\langle 0|B\rangle}e^{-\frac{2\pi}{\beta}2\Delta_i u} \tag{C.48}$$

For the last step, we used $E_{\phi_i} - E_o = \frac{2\pi}{\beta}2\Delta_i$ [see eq. (B.94)] and $\langle 0|\tilde{\phi}_i(v)|\phi_i\rangle = (2\pi/i\beta)^{2\Delta_i}$ [see eq. (B.96), with an extra phase i].[13]

[13] As was shown in section B.5, the eqs. (B.96) and (B.94) that were used to obtain eq. (C.48) follow from mapping a *bulk* theory on the full complex plane onto an *infinite* cylinder of circumference β. The reasons why they also hold for the present case of a boundary theory in the upper half-plane, mapped onto a boundary theory on a semi-infinite cylinder, are as follows: Eq. (B.94) is a property of the Hamiltonian H_P on a cylinder (of circumference β) which, as emphasized above, is not influenced by the presence of a boundary. Eq. (B.96) is a consequence of the normalization of the bulk OPE $\phi(z_1,z_1^*)\phi(z_2,z_2^*) = 1/|z_1 - z_2|^{4\Delta_i} + \ldots$, which also holds for the boundary theory (see last sentence of section B.5). The extra phase i inserted in $(2\pi/i\beta)^{2\Delta_i}$ relative to Eq. (B.96) corresponds to the extra i occuring in eq. (B.101) relative to eq. (B.93).

The matrix elements in eq. (C.48) are of course related to the BOPE coefficients C_{io}^B introduced in eq. (C.37). This relation may be found by once again resorting to Cardy's trick of using the conformal map (C.45) to recalculate the cylinder expectation value $\langle\tilde{\phi}_i(u,v)\rangle$ in terms of the corresponding half-plane quantity $\langle\phi_i(\tau,x)\rangle$: Using the conformal transformation law eq. (B.2), we have

$$\langle\tilde{\phi}_i(u,v)\rangle \;=\; \left|\tfrac{\partial_z}{\partial_w}\right|^{2\Delta_i}\langle\phi_i(\tau,x)\rangle \;=\; \left|\tfrac{\partial_z}{\partial_w}\right|^{2\Delta_i}\tfrac{C_{io}^B}{(2x)^{2\Delta_i}}\;, \tag{C.49}$$

where eq. (C.38) (with $z_1 = z_2$) was used for the last equality. By elementary trigonometry we have

$$x = \mathrm{Im}(z) = \frac{\frac{1}{2}\sinh 2\frac{\pi}{\beta}u}{\cosh^2\frac{\pi}{\beta}u\cos^2\frac{\pi}{\beta}v + \sinh^2\frac{\pi}{\beta}u\sin\frac{\pi}{\beta}v} \tag{C.50}$$

$$\left|\tfrac{\partial_z}{\partial_w}\right| = \left|\tfrac{\beta}{\pi}\cosh^2\tfrac{\pi}{\beta}w\right|^{-1} = \left[\tfrac{\beta}{\pi}\left(\cosh^2\tfrac{\pi}{\beta}u\cos^2\tfrac{\pi}{\beta}v + \sinh^2\tfrac{\pi}{\beta}u\sin\tfrac{\pi}{\beta}v\right)\right]^{-1}\;, \tag{C.51}$$

so that eq. (C.49) reduces to the simple form

$$\langle\tilde{\phi}_i(u,v)\rangle = \frac{C_{io}^B}{\left(\frac{\beta}{\pi}\sinh\frac{\pi}{\beta}2u\right)^{2\Delta_i}}\;. \tag{C.52}$$

Note that this expression has the expected properties of (i) being translationally invariant around the cylinder (v-independent), and (ii) correctly reproducing the half-plane form $\frac{C_{io}^B}{(2u)^{2\Delta_i}}$ in the limit $u \to 0$ (where the curvature of the cylinder becomes unimportant). On the other hand, by comparing the limit $u \to \infty$

$$\langle\tilde{\phi}_i(u,v)\rangle \stackrel{u\to\infty}{\longrightarrow} (2\pi/\beta)^{2\Delta_i}e^{-\frac{2\pi}{\beta}2\Delta_i u}\,C_{io}^B\;, \tag{C.53}$$

to eq. (C.48), we deduce a simple but important expression for the coefficients C_{io}^B in terms of boundary state matrix elements [CL91, eq.(6)]:

$$\frac{C_{io}^B}{(-i)^{2\Delta_i}} = \frac{\langle\phi_i|B\rangle}{\langle 0|B\rangle}\;, \tag{C.54}$$

which implies

$$\boxed{\langle \phi_{Li}(z_1)\phi_{Ri}(z_2^*)\rangle = \frac{1}{(z_1 - z_2^*)^{2\Delta_i}} \frac{\langle \phi_i|B\rangle}{\langle 0|B\rangle}} \tag{C.55}$$

This important relation is used extensively in chapters 6 and 7.

Since we have argued in section C.2.2 that the C_{io}^B completely determine the behavior of the 2-point function $G_s^{(4)}$ and all BOPEs, we conclude that this information in equivalently contained in $|B\rangle$. In other words, the boundary matrix elements occuring in eq. (C.48) contain all information necessary to calculate correlation functions in the presence of a boundary via the cylinder-transfer matrix approach. Thus, *the boundary state* $|B\rangle$ *completely characterizes the boundary condition* B.

C.4.2 The Matrix Elements $\langle a|B\rangle$

[Lud94a, appendix A.1], [AL94, appendix F]

In this section we derive an important relation, known as Cardy's formula, which relates the matrix elements $\langle A|a\rangle\langle a|B\rangle$ to the operator content of a cyllinder with boundary conditions A and B at its two ends, and periodic boundary conditions around the circumference. This relation can be regarded as constraint on the possible values of the matrix elements, that is imposed by *modular invariance* of a CFT on a cylinder. Since the argument has been presented in quite some detail in chapter 6, we shall be rather brief here. The most complete and detailed derivation that I know of is given in [AL94, appendix F], a more concise version of which appears in [Lud94a], appendix A.1

Consider the same cylinder, of circumference β, as in the previous section, but now with a finite length l, and boundary conditions A and B imposed at $x = l$

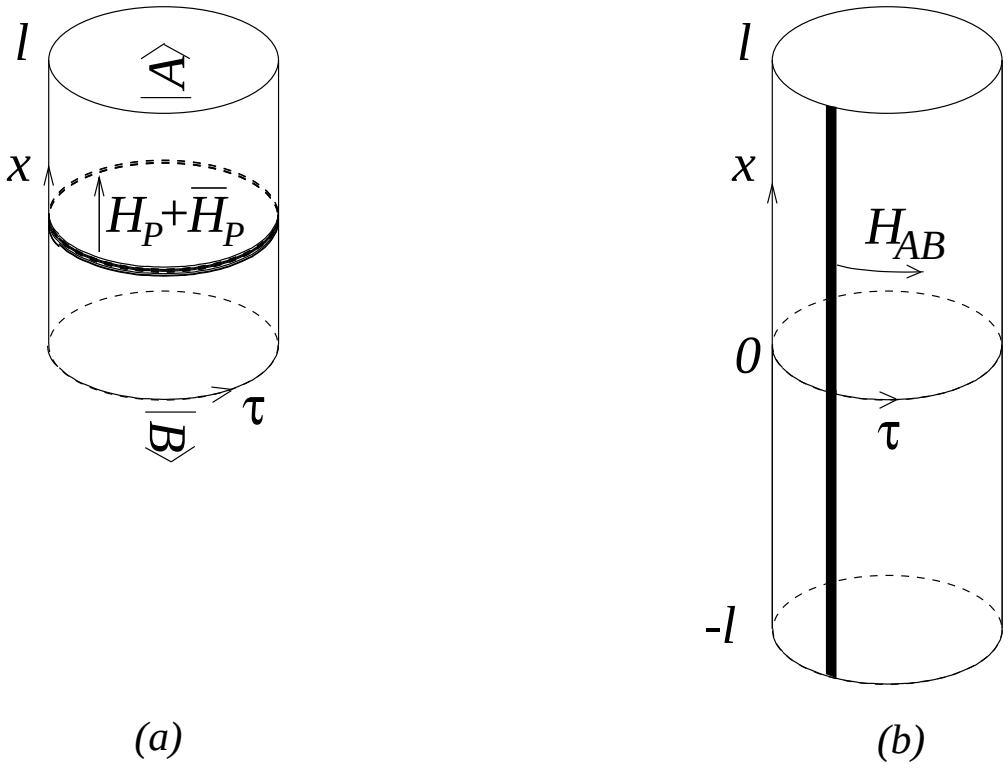

Figure C.4 (a) Closed string picture: the system is quantized along lines of constant x, translations in the x direction are generated by $H_P+\bar{H}_P$, which is periodic in the τ-direction. The boundary conditions A and B are encoded in the boundary states $|A\rangle$ and $|B\rangle$. (b) Open string picture: the system is quantized along lines of constant τ, translations in the τ-direction are generated by H_{AB}. The relations $\bar{T}(z^*) = T(z^*)$ $\bar{J}^a(z^*) = J^a(z^*)$ at $x = 0$ imply that $\bar{T}(z^*)$ and $\bar{J}^a(z^*)$ can be regarded as the analytic continuations of $T(z^*)$ and $J^a(z^*)$ into a "lower half-cyinder". The boundary conditions A and B determine the operator content, characterized by the integers $\{n^a_{AB}\}$, of the theory in the open string picture.

and $x = 0$, respectively. Let it be parametrized by $z = \tau + ix$ [corresponding to $z = iw = i(u + iv)$ in previous section], with $\tau \in [-\beta/2, \beta/2]$ and $x \in [0, l]$.

We would like to calculate the partition function Z_{AB} for this system. This will be done in two ways: firstly, by considering the theory to be quantized along lines of constant x and secondly along lines of constant τ [Fig. C.4].

This freedom to choose the quantization direction is a consequence of the Lorentz invariance of CFTs. The resulting two expressions for Z_{AB} must be equal

(this is obvious from a statistical mechanics point of view; in CFT it is called the principle of *modular invariance* on the cylinder). Equating the two expressions for Z_{AB} then gives Cardy's formula.

Closed String Picture

Start by considering the theory quantized along lines of constant x, (as in previous section), with periodic boundary conditions around the circumference [Fig. C.4(a)]. (This is called the "closed string picture" by string theorists.) For present purposes it is convenient to regard L- and R-moving fields as both living in the upper half-plane, as functions of z and z^*. The Hamiltonian that generates translations in the x-direction is then $H_P + \bar{H}_P$. Due to the conformal and KM invariance of both bulk and boundary, the Hilbert space on which $H_P + \bar{H}_P$ acts must carry a representation of the conformal and KM algebras, i.e. it must be a direct sum of complete conformal towers:

$$HS_P = \sum_{\oplus a} \sum_{\oplus \bar{a}} T^a \otimes \bar{T}^{\bar{a}} \ , \tag{C.56}$$

A typical state has the form $|a,m\rangle \otimes \overline{|a',m'\rangle}$, where m labels descendents within a tower, and energy $E = \frac{2\pi}{\beta}[\Delta_a + m + \bar{\Delta}_{a'} + m']$.

The boundary conditions A and B are represented by the boundary states $|A\rangle$ and $|B\rangle$, which can be shown to have the following structure[14]

$$|B\rangle = \sum_a B_a \sum_m |a,m\rangle \otimes \overline{|a,m\rangle} \ , \tag{C.57}$$

(note that the L- and R-sectors are linked in this sum).

[14]The origin of eq. (C.57) is the fact that conformal invariance of the boundary requires that $T(\tau) - \bar{T}(\tau) = 0$ and $J^a(\tau) - \bar{J}^a(\tau) = 0$ at both boundaries [eq. (C.2)]. This implies that the Fourier components of $T - \bar{T}$ and $J^a - \bar{J}^a$ vanish [see for example eq. (6.70)], which means, for the cylinder, that for all n, $L_n - \bar{L}_{-n}$ and $J^a_n - \bar{J}^a_{-n}$ must annihilate $|A\rangle$ and $|B\rangle$. This condition can be shown [Ishi89] to lead to the requirement that boundary states have the form eq. (C.57).

In the closed string picture, the system starts in the initial state $|B\rangle$ at "time" $x = 0$, and propagates to the final state $|F\rangle$ at $x = l$. Therefore, the partition function is:

$$Z_{AB} = \langle A|e^{-l(H_P+\bar{H}_P)}|B\rangle \ . \tag{C.58}$$

Inserting a complete set of states, and exploiting the special structure of eq. (C.57), this reduces to

$$Z_{AB} = \sum_{\tilde{a}} \langle A|\tilde{a}\rangle\langle\tilde{a}|B\rangle\chi_{\tilde{a}}(\tilde{q}^2) \ , \qquad \tilde{q}^2 = e^{-4\pi l/\beta} \ , \tag{C.59}$$

where $|\tilde{a}\rangle$ represents a primary state and $\chi_{\tilde{a}}(\tilde{q}) = \sum_m \langle \tilde{a}, m|e^{-lH_P}|\tilde{a}, m\rangle$ is the *character* for the $\tilde{a}$-th (chiral) tower (the $\tilde{q}^2$ arises because L- and R-movers both contribute the same energies).

Open String Picture

Now consider the theory quantized along lines of constant τ (called the "open string picture" by string theorists) [Fig. C.4(b)]. First note that the conditions $\bar{T}(z^*) = T(z)$ and $\bar{J}^a(z^*) = J^a(z)$ at the boundary at $x = 0$ [eq. (C.2)] can be used to regard $\bar{T}(z^*)$ and $\bar{J}^a(z^*)$ as the analytic continuations of $T(z^*)$ and $J^a(*)$ into a "lower half-cylinder" [see eqs. (C.8) and (C.9)]. One therefore has only a single set of chiral generators $T(z)$ and $J^a(z)$ of conformal and KM transformations, defined on a cylinder of length $2l$, with $x \in [-l, l]$, so that the corresponding Hilbert space will contain only L-states [see eq. (C.60) below]. Moreover, the condition $\bar{T}(z^*) = T(z)$ and $\bar{J}^a(z^*) = J^a(z)$ at the boundary at $x = l$ implies that T and J^a are periodic between $x = \pm l$: $T(\tau - il) = T(\tau + il)$, etc.

Let H_{AB} be the Hamiltonian that generates translations *around* the cylinder, in the τ-direction, and HS_{AB} the Hilbert space on which H_{AB} acts. The structure of HS_{AB} will depend on the boundary conditions A and B imposed at $x = l$ and

0 of the cylinder.[15] Now, since A and B are assumed not to break conformal and KM invariance, HS_{AB} too must necessarily always decompose into a sum over complete conformal towers T_a of states:

$$HS_{AB} = \sum_{\oplus a} n^a_{AB} T_a \ , \tag{C.60}$$

where a typical state is $|a, m\rangle$ with energy (note the length $2l$): $E = \frac{2\pi}{2l}[\Delta_a + m]$.

The set of integers $\{n^a_{AB}\}$ characterize the operator content of the theory in the open string picture. They depend on the boundary condition: different boundary conditions will allow or forbid different towers to occur. The fact that the $\{n^a_{AB}\}$ must always be integers can be regarded as a constraint on the structure of any boundary states $|A\rangle$ and $|B\rangle$ in the closed string picture. Conversely, one can start by defining a theory with prescribed operator content $\{n^a_{AB}\}$ in the open string picture, and deduce the corresponding $|A\rangle$ and $|B\rangle$ from there (as shown below); in other words, *a particular boundary condition can be imposed by specifying a particular set of integers* $\{n^a_{AB}\}$. This is in fact the strategy followed in the Kondo problem, as explained in section 7.4.2.

The partition function in the open string picture will be simply:

$$Z_{AB} = \sum_{a,m} \langle a, m | e^{-\beta H_{AB}} | a, m \rangle = \sum_a n^a_{AB} \chi_a(q) \ , \qquad q \equiv e^{-\pi\beta/l} \tag{C.61}$$

$$= \sum_{\tilde{a}} n^a_{AB} S^{\tilde{a}}_a \chi_{\tilde{a}}(\tilde{q}^2) \ . \tag{C.62}$$

For the second line we exploited a mathematical identity satisfied by the

[15] Intuitively speaking, this is so because in the constant-τ quantization scheme, every eigenstate $|n\rangle$ of H_{AB} with eigenfunction $a_n(\tau, x)$, is created from the vacuum by an operator of the form $a_n(\tau) = \int_0^l dv\, a^*_n(\tau, x)\tilde{\phi}(\tau, x)$, and hence depends on the behavior of the quantum fields $\tilde{\phi}(u, v)$ at the edges of the cylinder.

characters[16]

$$\chi_a(q) = \sum_{\tilde{a}} S_a^{\tilde{a}} \chi_{\tilde{a}}(\tilde{q}^2) \ . \tag{C.63}$$

to rewrite $\chi(q)$ in terms of $\chi(\tilde{q})$. The matrix $S_a^{\tilde{a}}$ is known as the modular S-matrix; it depends on the KM symmetry group under consideration, and for various groups can be looked up in math texts.

Cardy's Formula and Fusion

Comparing eq. (C.62) with eq. (C.59), we deduce[17] a very important result, called Cardy's formula:

$$\langle A|\tilde{a}\rangle\langle\tilde{a}|B\rangle = \sum_{\tilde{a}} n_{AB}^a S_a^{\tilde{a}} \ . \tag{C.64}$$

This expresses the boundary matrix elements in terms of the boundary operator content $\{n_{AB}^a\}$ in the open string picture, and the modular matrices $S_a^{\tilde{a}}$, which are known. Thus specification of the boundary condition has been narrowed down to specification of the integers $\{n_{AB}^a\}$.

To write down the $\{n_{AB}^a\}$ for a specific physical problem, physical insight is needed. It turns out that in many cases of interest, including the Kondo problem, they are given by a so-called "fusion principle". Consider as given a trivial, free boundary CFT on the cylinder, characterized by free boundary conditions at both ends of the cylinder, $A = B = F$, with given operator content $\{n_{FF}^a\}$ corresponding to a free theory (the $\{n_{FF}^a\}$ can be found by elementary arguments). Then one can define a non-trivial boundary CFT with boundary

[16]The characters form a representation of the modular group. Eq. (C.63) specifies how they transform under modular transformations.

[17]Actually, this step requires the characters to be linearly independent. In case they are not (as for the Kondo problem), the derivation has to be generalized somewhat: then one has to calculate a "grand canonical partition function", in terms of "non-specialized characters", which *are* linearly independent. This is done in [AL94, appendix F], and also in chapter 6, see eq. (6.52). The result is the same, namely eq. (C.64).

conditions F at $x = l$ and B at $x = 0$ by a *fusion Ansatz*, which defines the corresponding $\{n_{FB}^a\}$ through

$$n_{FB}^a = \sum_b n_{FF}^b N_{bc}^a \,, \tag{C.65}$$

Here N_{bc}^a are the conformal fusion rule coefficients that determine which conformal fields ϕ_a can occur in the OPE of ϕ_b and ϕ_c (hence the $\{n_{FB}^a\}$ depend on the (fixed) indix c). AL solved the Kondo problem by means of such a construction, as discussed at great length in section 7.4.2 (where the remaining steps of this section are repeated for the Kondo problem).

It so happens that the fusion rule coefficients and the modular S-matrix are related by a mathematical identity, known as Verlinde's formula [Ver88]:

$$\sum_a N_{bc}^a S_a^{\tilde{a}} = \frac{S_b^{\tilde{a}} S_c^{\tilde{a}}}{S_0^{\tilde{a}}} \,, \tag{C.66}$$

(where $a = 0$ denotes the tower built on the identity operator). Eqs. (C.65) and (C.66) can be used to eliminate n_{BF}^a from eq. (C.64):

$$\langle \tilde{a}|B\rangle = \frac{1}{\langle F|\tilde{a}\rangle} \frac{S_c^{\tilde{a}}}{S_0^{\tilde{a}}} \sum_b n_{FF}^b S_b^{\tilde{a}} = \frac{S_c^{\tilde{a}}}{S_0^{\tilde{a}}} \langle \tilde{a}|F\rangle \,, \tag{C.67}$$

where in the second equality we used the Cardy formula for $A = B = F$ to eliminate n_{FF}^b. Now divide this formula by a similar formula, with $|\tilde{a}\rangle = |0\rangle$ (corresponding the identity operator). Since $\frac{\langle \tilde{a}|F\rangle}{\langle 0|F\rangle} = 1$ for all $\tilde{a}$ (this follows from eq. (C.55), which must reduce to a free Green's function, i.e. unit normalization, for $B = F$), we find

$$\frac{\langle \tilde{a}|B\rangle}{\langle 0|B\rangle} = \frac{S_c^{\tilde{a}}/S_0^{\tilde{a}}}{S_c^0/S_0^0} \,. \tag{C.68}$$

Thus, if a fusion principle can be invoked to determine the n_{FB}^a, the boundary matrix elements, the boundary condition B and consequently the entire boundary CFT are completely determined.

C.5 Boundary Operator Content from H_{BB} on Strip

[Car84a,Car84b]

Sometimes it is convenient to have a quick way of determining the *boundary operator content* of a theory, i.e. the set of all allowed boundary operators, without being interested in BOPE coefficients. In this section, we show how this information can be directly extracted from $|B\rangle$.

C.5.1 Mapping Half-Plane to Strip

Consider the semi-infinite upper half-plane, with a certain conformally invariant boundary condition B imposed at the boundary, the properties of which are encoded in the boundary state $|B\rangle$.

It was shown in section B.4 that for a *bulk* CFT on the full complex plane, the bulk operator content could be specified in terms of the finite-size spectrum of a certain transfer matrix e^{-H_P} for a strip with periodic boundary conditions, by using the transformation $z = e^{2\pi w/l}$, to map the plane onto the strip. We now show that for a boundary CFT, the boundary operator content can be similarly specified in terms of the finite-size spectrum of a different transfer matrix, $e^{-H_{BB}}$, corresponding to —em a strip for which the boundary condition B is imposed along both edges.

Parametrizing the half-plane as usual by $z = \tau + ix$, $x > 0$, consider the conformal map

$$z = e^{\pi w/l} \,, \tag{C.69}$$

which maps the half-plane onto a semi-infinite strip, parametrized by $w = u + iv$,

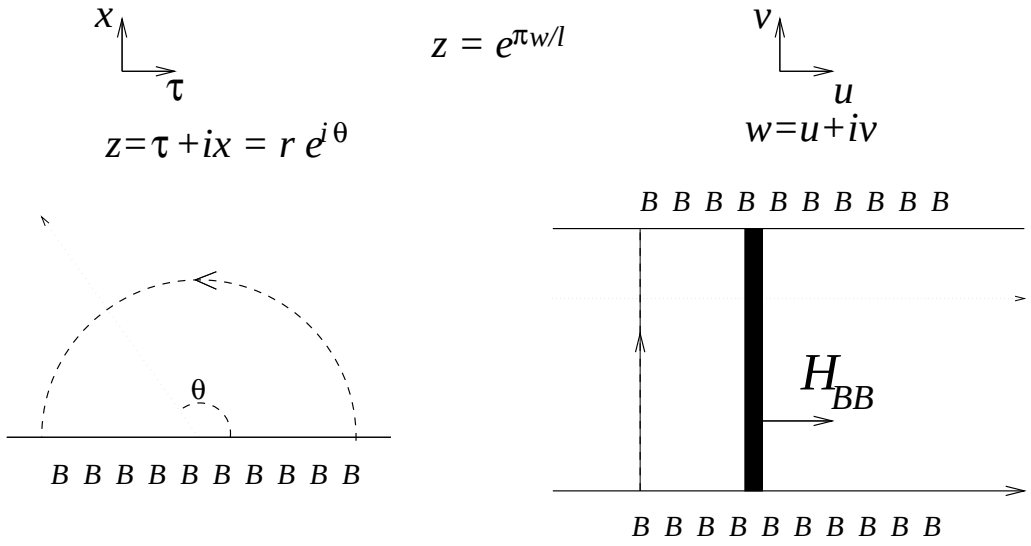

Figure C.5 The conformal transformation $z = e^{\pi w/l}$ maps the half-plane, parametrized by $z = \tau + ix = re^{i\theta}$ and boundary condition B along the real axis, onto a strip of width l, parametrized by $w = u + iv$, with the boundary condition B at both boundaries $v = 0, l$. The Hamiltonian H_{BB} generates translations along the strip in the u direction. The operator content on the strip is characterized by the integers $\{n^a_{BB}\}$, which also determine the boundary operator content of the half-plane.

with $u \in [-\infty, \infty]$ and $v \in [0, l]$ [Fig. C.5].

Since the positive and negative τ-axes are mapped onto the lower ($v = 0$) and upper ($v = l$) edges of the strip, respectively, one has the *boundary condition B along both edges of the strip.*

The situation is thus analogous to that in section C.4.2, where we had boundary conditions A and B at two edges of a cylinder, but now we have $A = B$. Let H_{BB} be the Hamiltonian that generates translations *along* the strip in the τ-direction. Since both boundaries and the bulk are conformally and KM invariant, the Hilbert space HS_{BB} on which H_{BB} acts will be a direct sum over complete conformal towers, [analogous to eq. (C.60)]:

$$HS_{BB} = \sum_{\oplus a} n^a_{BB} T_a \ . \tag{C.70}$$

The integers n^a_{BB}, which characterize the strip operator content, are related to $|B\rangle$ through Cardy's formula C.64, and hence are known if $|B\rangle$ has been specified.

The way in which the operator content $\{n^a_{BB}\}$ for the strip theory termines the *boundary* operator content of the half-plane theory is through the finite-size spectrum of H_{BB}, which determines the decay of 2-point functions along the strip. The argument is exactly analogous to the bulk case of section B.4. Let $\phi_i(z, z^*)$ be a Virasoro primary field in the half-plane with scaling dimensions (Δ_i, Δ_i), and consider the corresponding 2-point function $\widetilde{G}^{(2)}_s = \langle\tilde{\phi}_i(w_1, w_1^*)\tilde{\phi}_i(w_2, w_2^*)\rangle$ on the strip. In the limit of a very large separation $(u_1 - u_2) \to \infty$ along the strip, it will decay like

$$\widetilde{G}^{(2)}_s = \langle\tilde{\phi}_i(w_1, w_1^*)\tilde{\phi}_i(w_2, w_2^*)\rangle \to e^{-(E_a - E_o)(u_1 - u_2)} \ , \tag{C.71}$$

where E_a is the eigenvalue of that primary (i.e. lowest-energy) state $|a\rangle$ for which $\langle a|\tilde{\phi}_i|0\rangle \neq 0$ [see eq. (B.93)]. However, $\widetilde{G}^{(2)}$ can also be calculated by using the conformal map (C.69) from the semi-infinite half-plane [eq. (B.88)]:

$$\widetilde{G}^{(2)}_s = \langle\tilde{\phi}_i(w_1, w_1^*)\tilde{\phi}_i(w_2, w_2^*)\rangle = \left|\frac{\partial z_1}{\partial w_1}\right|^{2\Delta_i}\left|\frac{\partial z_2}{\partial w_2}\right|^{2\Delta_i}\langle\phi_i(z_1, z_1^*)\phi_i(z_2, z_2^*)\rangle \ , \tag{C.72}$$

where in the right-hand side we now have to insert the half-plane 2-point function $G^{(2)}_s$ calculated in the presence of the boundary, as given by eq. (C.22). However, instead of repeating in detail the steps analogous to eq. (B.88) to (B.91), a short-cut is possible here, since in the end only the limit $u_1 \gg u_2$, i.e. $|z_1| \gg |z_2|$, is needed: Take $z_1 = r_1 e^{i(\pi/2 - \theta)}$ with $r_1 \to \infty$ and $|\theta| < \pi/2$, and $z_2 = ix_2$ with $x_2 \sim O(1)$, so that

$$R = |z_1 - z_2| \simeq r_1 \ , \qquad e^{\pi u_1/l} = |z_1| = r_1 \simeq R \ , \qquad e^{\pi u_2/l} = |z_2| = x_2 \ . \tag{C.73}$$

In this limit, $G_s^{(2)}$ is given by the limiting expression (C.33), which, when inserted in the right hand side of eq. (C.72), gives

$$\widetilde{G}_s^{(2)} \;\sim\; e^{\pi(u_1+u_2)2\Delta_i/l} R^{-(2\Delta_i+\Delta_{\tilde{n}}^s)} x_2^{-(2\Delta_i-\Delta_{\tilde{n}}^s)} \;\sim\; e^{-\pi(u_1-u_2)\Delta_{\tilde{n}}^s/l} \; . \tag{C.74}$$

Comparing with eq. (C.71), we conclude that

$$E_a - E_o = \tfrac{\pi}{l}\Delta_{\tilde{n}}^s \; . \tag{C.75}$$

Now, we already know from section C.3.3 that each boundary exponent Δ_s corresponds to some boundary operator $\Phi_{\tilde{k}}$ in the half-plane theory. Hence, *to each primary state $|a\rangle$ in the strip Hilbert space HS_{BB}, there corresponds a boundary operator $\Phi_{\tilde{k}}$ on the boundary of the half-plane* whose scaling dimension is related through eq. (C.75) to the eigenenergy E_a of $|a\rangle$ [likewise, the descendents of $|a\rangle$ correspond to τ-derivatives of $\Phi_{\tilde{k}}(\tau)$ with scaling dimensions $\Delta_s + N$, as can be verified by considering the subleading terms of eq. (C.74)]. Thus, *the integers $\{n_{BB}^a\}$, which specify all primary states for the strip-geometry, also completely specify the list of all allowed boundary operators $\Phi_{\tilde{k}}$, i.e. the boundary operator content, of the half-plane theory.*

C.5.2 $\{n_{BB}^a\}$ from Double Fusion

Next we need a way to extract the $\{n_{BB}^a\}$ from $|B\rangle$. If the boundary condition B has been specified through a fusion principle, as explained in section C.4.2, this can be done by judiciously juggling with Cardy and Verlinde's formulas:

$$\sum_{a'} n_{BB}^{a'} S_{a'}^{\tilde{a}} \;=\; \langle B|\tilde{a}\rangle\langle\tilde{a}|B\rangle \tag{C.76}$$

$$\;=\; \left(S_c^{\tilde{a}}/S_0^{\tilde{a}}\right)^2 \langle F|\tilde{a}\rangle\langle\tilde{a}|F\rangle \tag{C.77}$$

$$= \left(S_c^{\tilde{a}}/S_0^{\tilde{a}}\right)^2 \sum_b n_{FF}^b S_b^{\tilde{a}} \tag{C.78}$$

$$= \sum_{b,d} n_{FF}^b N_{bc}^d N_{dc}^{a'} S_{a'}^{\tilde{a}} \ . \tag{C.79}$$

Here the first line is Cardy's formula (C.64) for $A = B$, the second follows from eq. (C.67), the third from Cardy's formula for $A = B = F$, and the fourth from using Verlinde's formula (C.66) twice. Finally, inverting this result by matrix-multiplying[18] from right by $(S^{-1})_{\tilde{a}}^{a}$, we obtain the so-called *double fusion formula* [Lud94a, eq.(A.14)]

$$n_{BB}^a = \sum_{b,d} n_{FF}^b N_{bc}^d N_{dc}^a \ . \tag{C.80}$$

This formula states that *if a fusion principle, starting from* $\{n_{FF}^a\}$*, is used to specify a boundary condition* B (more precisely the operator content $\{n_{FB}^a\}$ of the theory on a cylinder of finite length with boundary conditions F and B at its edges) *then the* **boundary operator content** *of the theory at the* B*-boundary, characterized by* $\{n_{BB}^a\}$*, can be obtained by "double fusion".* It gives a convenient and quick way of deriving a list of all possible boundary operators.

In section 7.4.3 this has been done for the Kondo problem, eq. (C.80) taking the form of eq. (7.53). Table 7.1 contains a list of all possible KM-primary boundary operators for the Kondo problem.

[18] The modular S-matrix is unitary, and hence invertible.

Appendix D

The Function $G^{(4)} = \langle \psi_L \psi_L^\dagger \psi_R \psi_R^\dagger \rangle$

In this appendix we show explicitly how Affleck and Ludwig calculated the 4-point function

$$G^{(4)} = \langle \psi_{L\alpha i}(z_1) \psi_L^{\bar{\beta}\bar{j}\dagger}(z_2) \psi_{R\beta j}(z_3^*) \psi_R^{\bar{\alpha}\bar{i}\dagger}(z_4^*) \rangle \ . \tag{D.1}$$

for the case $\tilde{N} = 2$, $k = 2$ and an $s = 1/2$ impurity that is relevant for the 2-channel Kondo problem. We go through this exercise for two reasons: firstly, to illustrate the general theory of appendix C with a concrete example; and secondly, because this calculation is essential to verify that the leading irrelevant operator $\vec{J}_{-1} \cdot \vec{\phi}_s$ (that gives rise to the $T^{1/2}$ on which the entire thesis hinges!, and discussed in section D.5), indeed does occur in the boundary operator product expansion of $\psi_R \psi_L^\dagger$.

This calculation has already been done in complete detail in a formidable and remarkably explicit paper by Affleck and Ludwig [AL94] (in this appendix equations from that paper will be referred to by subscripts $_{AL}$, e.g. $(2.16)_{AL}$. However, that paper is written in great generality, for the case of a Kondo problem with $U(1) \times SU(\tilde{N}) \times SU(k)$ symmetry, and all possible 4-fermion correlation

functions are calculated (the one in eq. (D.1) is called a Green's function "of Class (c), First type", and defined on p. 550 of [AL94]). Moreover, the information relevant to the calculation at hand is spread evenly throughout the entire 64 pages of [AL94], which makes it difficult to locate unless one has read the entire paper in detail. It is hoped that by presenting an example of the simplest non-trivial case, namely $\tilde{N} = k = 2$, in explicit detail here, the essentials of the calculation will become more accessible to the reader who does not have the time or interest to go through the most general calculation.

D.1 $G^{(4)}$ for Free Fermions

For the case of free fermions, i.e. with a trivial, free boundary condition at $x = 0$, it is trivial to find $G^{(4)}$: Simply substitute $\psi_R(z^*) \to \psi_L(z^*)$ [Cardy's recipe eq. (C.16)] and use the free-fermion, bulk OPE for $\psi_L\psi_L^\dagger$ in the limits $z_1 \to z_2$, $z_3* \to z_4^*$ and $z_1 \to z_4^*$, $z_2 \to z_3^*$. Since the only singular term in the OPE of $\psi_L(z_1)\psi^\dagger(z_2)$ is z_{12}^{-1}, we conclude that the only singular terms in $G_F^{(4)}$ must be $[(2.16)_{AL}]$:

$$G_F^{(4)} = \frac{I_1\tilde{I}_1}{z_{12}z_{34}^{**}} + \frac{I_2\tilde{I}_2}{z_{14}^{*}z_{23}^{*}} + g_{anal} \ . \tag{D.2}$$

Here $z_{14}^{*} = z_1 - z_4^*$, etc, and we introduced the KM-invariant tensors $[(2.20)_{AL}]$:

$$(I_1)_{\alpha\beta}^{\bar{\alpha}\bar{\beta}} = \delta_\alpha^{\bar{\beta}}\,\delta_\beta^{\bar{\alpha}} \ , \qquad (I_2)_{\alpha\beta}^{\bar{\alpha}\bar{\beta}} = \delta_\alpha^{\bar{\alpha}}\,\delta_\beta^{\bar{\beta}} \ , \tag{D.3}$$

$$(\tilde{I}_1)_{ij}^{\bar{i}\bar{j}} = \tilde{\delta}_i^{\bar{j}}\,\tilde{\delta}_j^{\bar{i}} \ , \qquad (\tilde{I}_2)_{ij}^{\bar{i}\bar{j}} = \tilde{\delta}_i^{\bar{i}}\,\tilde{\delta}_j^{\bar{j}} \ . \tag{D.4}$$

(We distinguish tensors in the spin and flavor sectors by putting a ˜ on the latter.) The function g_{anal} has to be analytic in the entire complex plane, and hence a constant. However, $G^{(4)} \to 0$ as $z_{12} \to \infty$, hence $g_{anal} = 0$.

D.2 General form of $G^{(4)}$

In this section we discuss the general form of $G^{(4)}$ for any general KM-invariant boundary condition, denoted by B, specializing to $B = F$ for free or $B = K$ for Kondo boundary conditions in the next section.

For a general B, $G^{(4)}$ will reduce to the free form of eq. (D.2) only in the extreme bulk limit, and exhibit unusual, non-Fermi liquid behavior (in the form of anomalous exponents) in the boundary limit. The key to calculating $G^{(4)}$ in this general case is to exploit the fact that KM-invariance is respected in both the bulk and the boundary, so that $G^{(4)}$ can throughout be expressed in KM-invariant form.

According to table 7.1 (left part) a free fermion field ψ can be thought of as a triplet of charge, spin and flavor fields, with $(Q, j, f) = (-1, \frac{1}{2}, \frac{1}{2})$. Moreover, for both the free and the over-screened Kondo fixed points, the Hamiltonian can be written as the sum of three commuting pieces, $H = H_c + H_s + H_f$. This suggests that in general, a fermion field operator can be written as a product of a charge, a spin and a flavor factor [$(3.6)_{AL}$]:

$$\psi_{L\alpha i}(z) \;\rightarrow\; e^{\frac{-i}{2}\phi_{cL}(z)}\mathbf{g}_{L\alpha}(z)\mathbf{h}_{Li}(z)\;, \tag{D.5}$$

$$\psi_{R\alpha i}(z^*) \;\rightarrow\; e^{\frac{-i}{2}\phi_{cR}(z)}\mathbf{g}_{R\alpha}(z^*)\mathbf{h}_{Ri}(z^*)\;. \tag{D.6}$$

For the over-screened fixed point, ψ here is not the usual free-fermion field ψ_{free}, but is understood to be the field into which the initial free field ψ_{free} renormalizes as one flows to the fixed point. [In particular, bilinear currents formed from this field (see eq. (D.21) below) correspond to the *analytic* currents $\mathcal{J}^X$ introduced in section 7.4.1, see eq. (7.39).]

Let us discuss some of the properties of the charge, spin and flavor fields. $\phi_c(z) = \phi_{cL}(z) + \phi_{cR}(z^*)$ is a free massless boson field (see appendix E) with action $S_{\phi_c} = \frac{1}{8\pi}\int_{-\infty}^{\infty} d\tau \int_0^{\infty} dx\, [(\partial_\tau \phi_c)^2 + (\partial_x \phi_c)^2]$, so that $e^{\frac{i}{2}\phi_{cL}}$ is a $Q = -1$ *charge* field of scaling dimension $\Delta_c = \frac{1}{8}$ (see below).

The spin and flavor sectors are both described in terms of $SU(2)_s$ WZW theories (some properties of which are summarized in section B.3). The spin sector is described by $\mathbf{g}_\alpha(z)$, a $j = \frac{1}{2}$, $SU(2)_2$ KM-primary *spin* field, and the flavor sector by $\mathbf{h}_i(z)$ a $f = \frac{1}{2}$, $SU(2)_2$ KM-primary *flavor* field. $j = \frac{1}{2}$ and $f = \frac{1}{2}$ means that under $SU(2)$ transformations in the spin and channel sectors, $\mathbf{g}_\alpha$ and $\mathbf{h}_i$ transform as spin-$\frac{1}{2}$ fields [just as the fermions of section B.2, compare eq. (B.56)]:

$$\mathbf{g}_\alpha = \left(\delta_\alpha^\beta - i\theta^a (T^a)_\alpha^\beta\right) \tilde{\mathbf{g}}_\beta \,, \qquad \mathbf{h}_i = \left(\delta_i^j - i\tilde{\theta}^A (\tilde{T}^A)_i^j\right) \tilde{\mathbf{h}}_j \,. \tag{D.7}$$

Here[1] $(T^a)_\alpha^{\bar\beta} = \frac{1}{2}(\sigma^a)_\alpha^{\bar\beta}$ and $(\tilde{T}^A)_i^{\bar j} = \frac{1}{2}(\sigma^A)_i^{\bar j}$ are the $SU(2)$ generators, in the spin and channel sectors, normalized to $\mathrm{Tr} T^a T^b = \frac{1}{2}\delta^{ab}$.

Being KM primary, the fields $e^{\frac{-i}{2}\phi_{cL}}$, $\mathbf{g}_\alpha$ and $\mathbf{h}_i$ are also Virasoro primary, with scaling dimensions $\Delta_c = \frac{1}{8}$, $\Delta_g = \frac{3}{16}$ and $\Delta_h = \frac{3}{16}$, respectively,[2] which correctly add up[3] to $\Delta_\psi = \frac{1}{2} = \Delta_c + \Delta_g + \Delta_h$. Finally, we mention that both $\mathbf{g}$ and $\mathbf{h}$ have fractional statistics,[4] which combine in such a way as to produce

[1] In this appendix, the notation $T_\alpha^{\bar\beta}$ corresponds to $T_{\alpha\bar\beta}$ of the other appendices, i.e. the lower and upper indices label rows and columns.

[2] This follows from table 7.1 and eq. (B.94), or, for Δ_g, Δ_h, directly from eq. (B.85), which gives $\Delta_j = \frac{j(j+1)}{2+k} = \frac{3}{16}$ for $j = \frac{1}{2}$, $k = 2$.

[3] Of course, the scaling dimensions will *always* (for arbitrary $\tilde{N}, k$) add up correctly, if one glues the charge, spin and flavor fields together using free-fermion gluing conditions, since these are purposefully constructed in such a way as to reproduce the free fermion spectrum. In particular, the singly occupied free-fermion level has energy $\frac{2\pi}{l}\frac{1}{2} = E_{Qo} + E_{so} + E_{fo}$, which translates, via eq. (B.94), to $\frac{1}{2} = \Delta_c + \Delta_g + \Delta_h$.

[4] By definition, $\langle \mathbf{g}_\alpha(z_1) \mathbf{g}^{\bar\beta\dagger}(z_2)\rangle \equiv \frac{\delta_\alpha^{\bar\beta}}{(z_1 - z_2)^{1/2}} \equiv \langle \mathbf{g}^{\bar\beta\dagger}(z_1) \mathbf{g}_\alpha(z_2)\rangle$ [Lud95], which implies that

Fermi statistics for ψ.

Since H_c, H_s and H_f commute, any multi-point correlation function factorizes [$(3.9)_{AL}$]:

$$G^{(4)} = \langle e^{-\frac{i}{2}\phi_{cL}(z_1)} e^{\frac{i}{2}\phi_{cL}(z_2)} e^{-\frac{i}{2}\phi_{cL}(z_3^*)} e^{\frac{i}{2}\phi_{cL}(z_4^*)} \rangle \tag{D.8}$$

$$\times \sum_{p,q} \langle\, a_{p,q}\, \mathbf{g}_{L\alpha}(z_1) \mathbf{g}_L^{\bar{\beta}\dagger}(z_2) \mathbf{g}_{L\beta}(z_3^*) \mathbf{g}_L^{\bar{\alpha}\dagger}(z_4^*) \rangle_{(p)} \tag{D.9}$$

$$\times \langle \mathbf{h}_{Li}(z_1) \mathbf{h}_L^{\bar{j}\dagger}(z_2) \mathbf{h}_{Lj}(z_3^*) \mathbf{h}_L^{\bar{i}\dagger}(z_4^*) \rangle_{(q)} \,. \tag{D.10}$$

Here we have implemented Cardy's prescription (C.17) of replacing R- by L-moving fields, evaluated in the lower half-plane. However, eq. (D.8) illustrates an important subtlety of the "factorization" (D.5): the functions $\langle \mathbf{g}\mathbf{g}^\dagger \mathbf{g}\mathbf{g}^\dagger \rangle_{(p)}$ and $\langle \mathbf{h}\mathbf{h}^\dagger \mathbf{h}\mathbf{h}^\dagger \rangle_{(q)}$, the so-called *conformal blocks* in the spin and flavor sectors, are determined by the Knizhnik-Zamolodchikov differential equations, which have two independent solutions, labeled by p (or q) $= 1, 2$. (There is only one conformal block for the charge fields.) $G^{(4)}$ is therefore a *linear combination of 4 independent functions*. The coefficients $a_{p,q}$, which determine how the conformal blocks are "glued together", depend on the boundary conditions on $G^{(4)}$ [they play the role of the coefficients a^b_{in} in eq. (C.26)]. Each boundary condition selects a particular set of coefficients $a_{p,q}$ (made explicit in eq. (C.32), or eq. (D.27) below); in particular, the free Green's function $G_F^{(4)}$ of eq. (D.2) can also be represented in this way. Therefore, eq. (D.5) is not a true factorization into independent factors: the factors have to be glued together in a very specific way, dependent on boundary

$\mathbf{g}_\alpha(z_1)\mathbf{g}^{\bar{\beta}\dagger}(z_2) = \pm i \mathbf{g}^{\bar{\beta}\dagger}(z_2)\mathbf{g}_\alpha(z_1)$. The best way to keep track of such phases is to extract the mutual exchange properties of these fields from explicit expressions for their multi-point correlation functions, since theses are known exactly from [KZ84]. For the present calculation, where we do work only with a well-defined 4-point function, we therefore need not worry about the statistics of $\mathbf{g}$ and $\mathbf{h}$. For recent developments regarding the statistics of such fields, see [BLS94].

conditions.

The charge conformal block is simply given by

$$\langle e^{-\frac{i}{2}\phi_{cL}(z_1)} e^{\frac{i}{2}\phi_{cL}(z_2)} e^{-\frac{i}{2}\phi_{cL}(z_3^*)} e^{\frac{i}{2}\phi_{cL}(z_4^*)} \rangle = \left[\frac{(1-\xi)^{-1}}{z_{12} z_{34}^{**}}\right]^{2\Delta_c} = \left[\frac{(1-\eta)^{-1}}{z_{14}^{*} z_{23}^{*}}\right]^{2\Delta_c} , \quad \text{(D.11)}$$

where

$$\xi = \frac{z_{12} z_{34}^{**}}{z_{13}^{*} z_{24}^{*}} , \qquad \eta = 1 - \xi = \frac{z_{14}^{*} z_{23}^{*}}{z_{13}^{*} z_{24}^{*}} . \quad \text{(D.12)}$$

Reason: the charge sector is unaffected by the boundary condition imposed in the spin sector, and always corresponds to a free theory. Hence, the charge conformal block must reduce to eq. (D.12), the only expression that is consistent with the general form (B.44) for a 4-point function and correctly reduces to $(z_{12} z_{34}^{**})^{-2\Delta_c}$ and $(z_{14}^{*} z_{23}^{*})^{-2\Delta_c}$ in the limits[5] $z_1 \to z_2$, $z_3^* \to z_4^*$ and $z_1 \to z_4^*$, $z_2 \to z_3^*$, in which $\xi \to 0^+$ and $\eta \to 0^+$, respectively.

The spin (and flavor) conformal blocks have the following general structure, (discussed at length in [AL94, app.B]) [$(B.4)_{AL}$]:

$$\langle \mathbf{g}_{L\alpha}(z_1) \mathbf{g}_L^{\bar{\beta}\dagger}(z_2) \mathbf{g}_{L\beta}(z_3^*) \mathbf{g}_L^{\bar{\alpha}\dagger}(z_4^*) \rangle_{(p)} = \left[\frac{(1-\xi)^{-1}}{z_{12} z_{34}^{**}}\right]^{2\Delta_g} \sum_{A=1,2} (I_A)_{\alpha\beta}^{\bar{\alpha}\bar{\beta}} g_A^{(p)}(\xi) . \quad \text{(D.13)}$$

The prefactor has the same origin [eq. (B.44)] in eq. (D.11), and the tensor structure $\sum_{A=1,2} I_A$ is enforced by KM invariance [KZ84, eq.4.4] (I_1 and I_2 are the only KM-invariant tensors).

The functions $g_A^{(p)}(\xi)$ ($p = 0, 1$; $A = 1, 2$) are determined completely by the Knizhnik-Zamolodchikov equations[6] [$(D.4)_{AL}$ or $(B.8)_{AL}$]. To find them explicitly,

[5] These limits are always understood to be taken in such a way that the ξ or η are real and positive. For ξ, whose phase can of course be arbitrary, this convention is a matter of convenience, to avoid having to deal with extra phases. For η, it happens automatically, since $\eta \to \frac{4x_1 x_2}{|\tau_1 - \tau_2|}$ = real in the limit $z_1 \to z_4^*$, $z_2 \to z_3^*$.

[6] For the present case, they are $\partial_\xi[(1-\xi)^{-2\Delta_g} g_A(\xi)] = \sum_{B=1,2} \left[\frac{P_{A,B}}{\xi} + \frac{Q_{A,B}}{\xi - 1}\right] (1 -$

some straightforward solving of differential equations is needed, done in [KZ84]. For the case $\tilde{N} = k = 2$ of present interest, they turn out to be [see after $(4.1)_{AL}$]:

$$\begin{aligned}
\mathbf{g}_1^{(0)}(\xi) &= \tfrac{1}{2}(1-\xi)^{1/2}[\ \ F_+(\xi) + F_-(\xi)] \quad \stackrel{\xi\to 0^+}{\longrightarrow} \quad 1 \\
\mathbf{g}_1^{(1)}(\xi) &= \tfrac{1}{2}(1-\xi)^{1/2}[-F_+(\xi) + F_-(\xi)] \quad \stackrel{\xi\to 0^+}{\longrightarrow} \quad -\tfrac{1}{2}\xi^{1/2} \\
\mathbf{g}_2^{(0)}(\xi) &= \tfrac{1}{2}\xi^{1/2}[F_+(\xi) - F_-(\xi)] \quad \stackrel{\xi\to 0^+}{\longrightarrow} \quad \tfrac{1}{2}\xi \\
\mathbf{g}_2^{(1)}(\xi) &= \tfrac{1}{2}\xi^{1/2}[F_+(\xi) + F_-(\xi)] \quad \stackrel{\xi\to 0^+}{\longrightarrow} \quad \xi^{1/2}
\end{aligned} \tag{D.14}$$

where[7]

$$F_\pm(\xi) = (1 \pm \xi^{1/2})^{1/2} \ . \tag{D.15}$$

The flavor conformal blocks $\langle \mathbf{h}\mathbf{h}^\dagger\mathbf{h}\mathbf{h}^\dagger\rangle_{(q)}$ have exactly the same structure as eq. (D.13), and for $\tilde{N} = k = 2$ we have $\Delta_h = \Delta_g = \frac{3}{16}$ and $\mathbf{h}_A^{(p)}(\xi) = \mathbf{g}_A^{(p)}(\xi)$.

Inserting eq. (D.11) and eq. (D.13) into eq. (D.8), we obtain

$$G^{(4)} \ = \ \frac{(1-\xi)^{-1}}{z_{12}z_{34}^{**}} \sum_{A,\tilde{A}=1,2} \sum_{p,q=1,2} I_A\tilde{I}_{\tilde{A}}\ a_{p,q}\ \mathbf{g}_A^{(p)}(\xi)\,\mathbf{h}_{\tilde{A}}^{(q)}(\xi) \ . \tag{D.16}$$

Clearly $G^{(4)}$ is completely determined once the $a_{p,q}$ have been specified.

D.3 Bulk limit of $G^{(4)}$

In this section we shall find the coefficients $a_{p,q}$ of eq. (D.16), for both free and Kondo boundary conditions $B = F$ and K, by exactly the same strategy as that used to find eq. (C.32) in appendix C. One calculates $G^{(4)}$ in two ways: firstly, by simply taking the bulk limit $\xi \to 0^+$ explicitly in eq. (D.16); and secondly,

$\xi)^{-2\Delta_g} g_B(\xi)$, where $P_{A,B} = \frac{1}{8}\left(\begin{smallmatrix} 3 & 2 \\ 0 & -1 \end{smallmatrix}\right)$ and $Q_{A,B} = \frac{1}{8}\left(\begin{smallmatrix} -1 & 0 \\ 2 & 3 \end{smallmatrix}\right)$. Knizhnik and Zamolodchikov have shown [KZ84, section 4] that explicit expressions for general $\tilde{N}$ and k can be given in terms of hypergeometrical equations, see $(B.12)_{AL}$.

[7] The branch cut of the square root is chosen as usual along the negative real axis [AL94, footnote 51, p.594]. This means that $(-\xi)^{1/2} = e^{\pm i\pi/2}\xi^{1/2}$ for $\mathrm{Im}\xi \gtrless 0$.

by using considering the limit $z_1 \to z_2$ and $z_3^* \to z_4^*$ [Fig. D.1(a)], in which one can use the *bulk* OPEs for $\psi(z_1)\psi^\dagger(z_2)$ and $\psi(z_3^*)\psi^\dagger(z_4^*)$ in eq. (D.1), and then eq. (C.55) to evaluate the resulting cross-boundary $(z_2 - z_4^*)$ two-point functions. The latter explicitly depend on the boundary conditions via the known matrix elements $\frac{\langle\phi_i|B\rangle}{\langle 0|B\rangle}$. Equating the two expressions for the bulk limit of $G^{(4)}$ then uniquely determines the $a_{p,q}$ in terms of the $\frac{\langle\phi_i|B\rangle}{\langle 0|B\rangle}$.

D.3.1 Bulk OPE of $\psi_L\psi_L^\dagger$

In order to proceed, we need the bulk OPE of $\psi_{L\alpha i}(z_1)\psi_L^{\bar\beta\bar\jmath\dagger}(z_2)$. Since in the limit $\xi \to 0^+$ under consideration this OPE is taken asymptotically far away from the boundary, where all boundary effects have died out, it is in fact the trivial OPE of *free* fermions, which may be calculated using Wick's theorem:

$$\psi_{L\alpha i}(z_1)\psi_L^{\bar\beta\bar\jmath\dagger}(z_2) \;=\; \frac{\delta_\alpha^{\bar\beta}\delta_i^{\bar\jmath}\mathbf{1}(z_2)}{z_{12}} \;+\; :\psi_{L\alpha i}(z_1)\psi_L^{\bar\beta\bar\jmath\dagger}(z_2): + \ldots \tag{D.17}$$

Now, it is essential to decompose $:\psi\psi^\dagger:$ into $SU(2)\times SU(2)$-invariant form. A short-cut for finding the necessary Clebsch-Gordan coefficients is to use the following identities (which follow from eq. (A.73), with $T_\alpha^{\bar\beta}$ here $\equiv T_{\alpha\bar\beta}$ there),

$$\begin{aligned}(T^a)_\alpha^{\bar\beta}(T^a)_\beta^{\bar\alpha} &= \tfrac{1}{2}\left[(I_2)_{\alpha\beta}^{\bar\alpha\bar\beta} - \tfrac{1}{2}(I_1)_{\alpha\beta}^{\bar\alpha\bar\beta}\right]\\ (\tilde T^A)_i^{\bar\jmath}(\tilde T^A)_j^{\bar\imath} &= \tfrac{1}{2}\left[(\tilde I_2)_{ij}^{\bar\imath\bar\jmath} - \tfrac{1}{2}(\tilde I_1)_{ij}^{\bar\imath\bar\jmath}\right]\ ,\end{aligned} \tag{D.18}$$

which imply

$$(I_2)_{\alpha\beta}^{\bar\alpha\bar\beta}(\tilde I_2)_{ij}^{\bar\imath\bar\jmath} = \left[2(T^a)_\alpha^{\bar\beta}(T^a)_\beta^{\bar\alpha} + \tfrac{1}{2}(I_1)_{\alpha\beta}^{\bar\alpha\bar\beta}\right]\left[2(\tilde T^A)_i^{\bar\jmath}(\tilde T^A)_j^{\bar\imath} + \tfrac{1}{2}(\tilde I_1)_{ij}^{\bar\imath\bar\jmath}\right] \tag{D.19}$$

Contracting this with $-:\psi_L^{\beta j\dagger}\psi_{L\bar\alpha\bar\imath}:$ we obtain for eq. (D.17):

$$\begin{aligned}\psi_{L\alpha i}(z_1)\psi_L^{\bar\beta\bar\jmath\dagger}(z_2) \;=\; \frac{\delta_\alpha^{\bar\beta}\delta_i^{\bar\jmath}\mathbf{1}(z_2)}{z_{12}} \;-\; \Big[\,2(T^a)_\alpha^{\bar\beta}(\tilde T^A)_i^{\bar\jmath}\,O_L^{a,A}(z_2)\\ +\,(T^a)_\alpha^{\bar\beta}\delta_i^{\bar\jmath}\,\mathcal{J}_s^a(z_2) + \delta_\alpha^{\bar\beta}(\tilde T^A)_i^{\bar\jmath}\,\mathcal{J}_f^A(z_2) \;+\; \tfrac{1}{4}\,\delta_\alpha^{\bar\beta}\delta_i^{\bar\jmath}\,\mathcal{J}_c^o(z_2)\,\Big] \;+\; O(z_{12}\ ,\end{aligned} \tag{D.20}$$

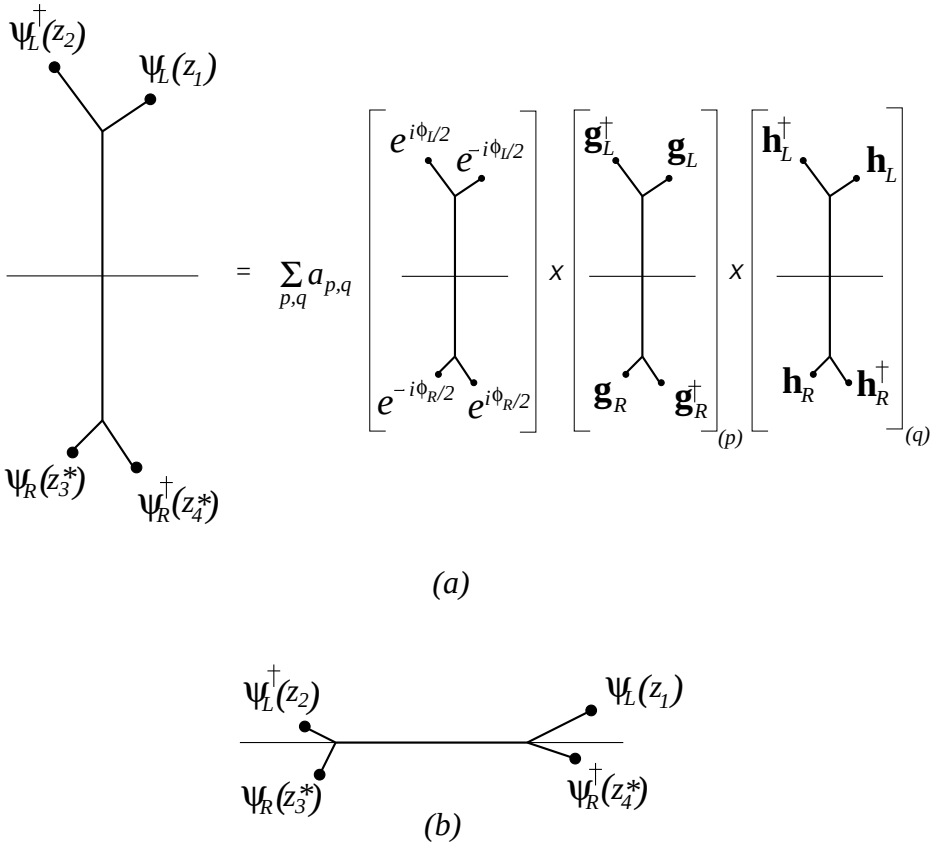

Figure D.1 (a) Bulk and (b) boundary limits of the four- point function $G^{(4)} = \langle \psi_{L\alpha i}(z_1)\psi_L^{\bar{\beta}\bar{j}\dagger}(z_2)\psi_{R\beta j}(z_3^*)\psi_R^{\bar{\alpha}\bar{i}\dagger}(z_4^*)\rangle$. $G^{(4)}$ can be expressed as a particular linear combination of products of conformal block functions, of charge, spin and flavor fields, as in eq. (D.8), characterized by coefficients $a_{p,q}$. These can be determined (see section D.3.2) by considering the bulk limit, shown in (a). The boundary limit, shown in (b), can be used to determine the boundary operator product expansion of $\psi_{L\alpha i}(z_1)$ and $\psi_R^{\bar{\alpha}\bar{i}\dagger}(z_4^*)$ (see section D.4.1).

where the charge ($\mathcal{J}_c$), spin ($\mathcal{J}_s^a$), flavor ($\mathcal{J}_f^A$) and "spin-flavor" ($O^{a,A}$) currents are defined by ($N_{\tilde{a}}$ is the normalization[8]):

$$\begin{aligned}
\mathcal{J}_c^0(z) &= :\psi^{\bar{\alpha}\bar{i}\dagger}\,\psi_{\bar{\alpha}\bar{i}}:(z)\,, & N_c &= 4\,,\\
\mathcal{J}_s^a(z) &= :\psi^{\bar{\beta}\bar{i}\dagger}\,(T^a)^{\bar{\alpha}}_{\bar{\beta}}\psi_{\bar{\alpha}\bar{i}}:(z)\,, & N_s &= 1\,,\\
\mathcal{J}_f^A(z) &= :\psi^{\bar{\alpha}j\dagger}\,(\tilde{T}^A)^{\bar{i}}_{j}\psi_{\bar{\alpha}\bar{i}}:(z)\,, & N_f &= 1\,,\\
O^{a,A}(z) &= 2:\psi^{\beta j\dagger}\,(T^a)^{\bar{\alpha}}_{\bar{\beta}}\,(\tilde{T}^A)^{\bar{i}}_{j}\,\psi_{\bar{\alpha}\bar{i}}:(z)\,, & N_O &= 1\,.
\end{aligned} \tag{D.21}$$

This decomposition of $:\psi_{L\alpha i}(z_1)\psi_L^{\bar{\beta}\bar{j}\dagger}(z_2):$ reflects the fact that since ψ and $\psi^\dagger$ have quantum numbers $(Q,j,f)=(\pm1,\frac{1}{2},\frac{1}{2})$, $:\psi\psi^\dagger:$ decomposes into 4 pieces, with quantum numbers $(0,1,1)$, $(0,1,0)$, $(0,0,1)$ and $(0,0,0)$. The charge, spin and flavor currents are not KM primary,[9] since they are KM generators of $U(1)_c\times SU(2)_s\times SU(2)_f$ transformations. However, we see from (the left part of) table 7.1 that a free-fermion theory a $(0,1,1)$ KM primary[10] field of scaling dimension $\Delta_{1,1}=1$ does occur, which we can therefore identify with $O^{a,A}(z)$. Under $SU(2)_s\times SU(2)_f$ transformations, $O^{a,A}$ transforms in the spin-adjoint, flavor-adjoint representation.[11]

D.3.2 Determination of $a_{p,q}$

Now we are ready to carry through the strategy outlined at the beginning of this section in order to find the coefficients $a_{p,q}$, namely to compare two alternative

[8]For any of these currents $\mathcal{J}_L^{\tilde{a}}$, the normalization $N_{\tilde{a}}$ in $\langle\mathcal{J}_L^{\tilde{a}}(z_1)\mathcal{J}_L^{\tilde{a}}(z_2)\rangle=\frac{N_{\tilde{a}}}{(z_1-z_2)^2}$ can be calculated with Wick's theorem from the right-hand sides of eq. (D.21), using eq. (A.47). For $O^{a,A}$, $N_O=1$ by construction.

[9]The currents can be regarded as KM descendents of unity $\mathbf{1}$, since, by eq. (B.33), we have $\mathcal{J}^{\tilde{a}}(z)=\mathcal{J}^{\tilde{a}}_{-1}\mathbf{1}(z)$.

[10]Note that the $O^{a,A}(z)$ are among the KM generators of $SU(4)$ transformations on the four fields $\psi^{\alpha i\dagger}$. Hence they are not $SU(4)$-KM primary. However, with respect to the smaller $U(1)_c\times SU(2)_s\times SU(2)_f$ symmetry to which $SU(4)$ is broken down for the Kondo problem by the coupling to an impurity, $O^{a,A}$ is KM primary.

[11]Explicitly, using eq. (B.56) in eq. (D.21), it can be checked that $O^{a,A}=\left[\delta^{ac}-i\theta^b(\boldsymbol{T}^b)^a_{\ c}\right]\left[\delta^{AC}-i\tilde{\theta}^B(\widetilde{\boldsymbol{T}}^B)^A_{\ C}\right]\tilde{O}^{c,C}$, where $(\boldsymbol{T}^b)^a_{\ c}=-i\varepsilon^{bac}$ and $(\widetilde{\boldsymbol{T}}^B)^A_{\ C}=-i\varepsilon^{BAC}$.

expressions for the bulk limit of $G^{(4)}$ to each other. The first part of the strategy is simple enough: inserting the $\xi \to 0^+$ limits of eq. (D.14) into eq. (D.16) (with $\mathbf{g} = \mathbf{h}$) gives:

$$G^{(4)} \overset{\xi\to 0^+}{\longrightarrow} \frac{1}{z_{12} z_{34}^{**}} \left[I_1 \tilde{I}_1 \, a_{0,0} + \left(I_1 \tilde{I}_2 a_{0,1} + I_2 \tilde{I}_1 a_{1,1} \right) \tfrac{1}{2} \xi^{1/2} + I_2 \tilde{I}_2 \, a_{1,1} \, \xi \; + \ldots \right] , \tag{D.22}$$

where we displayed *only the leading coefficient* for each $I_a \tilde{I}_{\tilde{A}}$. [Clearly, the $a_{p,q}$ play the role of the a_{in}^b in eq. (C.26).]

For the second part of the strategy, we consider the limit $z_1 \to z_2$ and $z_3^* \to z_4^*$ [Fig. D.1(a)] and insert the bulk OPE (D.20), and an identical one for $\psi_{R\beta j}(z_3^*)\psi_R^{\bar{\alpha}\bar{i}\dagger}(z_4^*)$, into eq. (D.1) to obtain the following alternative expression for $G^{(4)}$, valid in the bulk limit $\xi \to 0^+$:

$$\begin{aligned} G^{(4)} \quad \overset{\xi\to 0^+}{\longrightarrow} \quad & \frac{I_1 \tilde{I}_1}{z_{12} z_{34}^{**}} \; + \; \frac{1}{(z_{24}^*)^2} \Bigg[(I_2 - \frac{1}{2} I_1)(\tilde{I}_2 - \tfrac{1}{2}\tilde{I}_1) \; \frac{\langle O^{a,A} | B \rangle}{\langle 0 | B \rangle} \\ & + \tfrac{1}{2}(I_2 - \tfrac{1}{2} I_1)\tilde{I}_1 + I_1 \tfrac{1}{2}(\tilde{I}_2 - \tfrac{1}{2}\tilde{I}_1) + \tfrac{4}{16} I_1 \tilde{I}_1 \Bigg] . \end{aligned} \tag{D.23}$$

Here we have used the identities eq. (D.18) to rewrite the tensor products, and used the L-R Green's functions

$$\langle \mathcal{J}_{L\Upsilon}^{\tilde{a}}(z_2) \mathcal{J}_{R\Upsilon}^{\tilde{a}'}(z_4^*) \rangle \;\; = \;\; \frac{N_\Upsilon \delta_{\tilde{a}\tilde{a}'}}{(z_{24}^*)^2} , \qquad \text{for} \quad \Upsilon = c, s, f, \tag{D.24}$$

$$\langle O_L^{a,A}(z_2) \, O_R^{a',A'}(z_4^*) \rangle \;\; = \;\; \frac{\delta^{a,a'} \delta^{A,A'}}{(z_{24}^*)^2} \; \frac{\langle O^{a,A} | B \rangle}{\langle 0 | B \rangle} . \tag{D.25}$$

Eq. (D.24) for the currents $\mathcal{J}_c$, $\mathcal{J}_s^a$ and $\mathcal{J}_f^A$ is obtained by analytic continuation ($z_4 \to z_4^*$) from the corresponding L-L correlation functions, a procedure that is valid because all KM currents are analytic at the boundary [see eq. (C.8)]. $O^{a,A}$, on the other hand, is not a $U(1)_c \times SU(2)_c \times SU(2)_f$ KM current, and hence not necessarily analytic at the boundary. However, it is KM primary, and hence its L-R function is given by eq. (C.55), which gives (D.25).

We see that the only place where the boundary condition B on the theory enters into $G^{(4)}$ is through the matrix elements $\frac{\langle O^{a,A}|B\rangle}{\langle 0|B\rangle}$. For a free theory ($B = F$) they are equal to 1, since in that case all fields must be analytic at the boundary. For the Kondo boundary condition ($B = K$), they can by found by using eqs. (7.67) and (7.66). Therefore,

$$\frac{\langle O^{a,A}|B\rangle}{\langle 0|B\rangle} = \left\{ \begin{array}{l} 1 \\ \\ \frac{S^1_{1/2}/S^1_0}{S^0_{1/2}/S^0_0} = -1 \end{array} \right\} = \pm 1 \quad \text{for} \quad B = F/K \; . \tag{D.26}$$

Now compare eq. (D.23) with eq. (D.22), our two equivalent expressions for $G^{(4)}$. Since $\xi \to \frac{z_{12} z^{**}_{34}}{(z^*_{24})^2}$ in this limit, we immediately deduce[12] that [this corresponds to eq. (C.32)]:

$$a_{0,0} = 1, \quad a_{1,0} = a_{0,1} = 0, \quad a_{1,1} = \frac{\langle O^{a,A}|B\rangle}{\langle 0|B\rangle} \; = \; \pm 1 \; , \qquad \text{for} \quad B = F/K \; . \tag{D.27}$$

Thus, the goal of determining the $a_{p,q}$ has been achieved, and $G^{(4)}$ is now fully determined. It has turned out that the sole difference between the free and Kondo boundary conditions is one little ± 1 in eq. (D.27)!! However, this difference has profound consequences for $G^{(4)}$, in particular in the boundary limit, as we shall see in section D.4.1.

D.3.3 Explicit Expressions for $G^{(4)}$

We are now ready to obtain an explicit expression for $G^{(4)}$. By using eqs. (D.27) and (D.14) in the general expression eq. (D.16) for $G^{(4)}$, straightforward direct computation gives:

$$G^{(4)} \;\; = \;\; \frac{(1-\xi)^{-1}}{z_{12} z^{**}_{34}} \Big[I_1 \tilde{I}_1 \left(g^{(0)}_1 g^{(0)}_1 \pm g^{(1)}_1 g^{(1)}_1 \right) \; + \; I_2 \tilde{I}_2 \left(g^{(0)}_2 g^{(0)}_2 \pm g^{(1)}_2 g^{(1)}_2 \right)$$

[12]Note that in eq. (D.23) only the leading terms $\frac{I_1 \tilde{I}_1}{z_{12} z^{**}_{34}}$ and $\frac{I_2 \tilde{I}_2}{(z^*_{24})^2}$ need to be known to fix the $a_{p,q}$'s.The subleading terms in $I_1 \tilde{I}_2$, $I_2 \tilde{I}_1$ and $I_1 \tilde{I}_1$ can be used as a check on the final answer: indeed, eqs. (D.29) and (D.30) agree to order $\xi/(z_{12} z^{**}_{34})$ with eq. (D.23).

$$+ \left(I_1\tilde{I}_2 + I_2\tilde{I}_1\right)\left(g_1^{(0)}g_2^{(0)} \pm g_2^{(1)}g_1^{(1)}\right)\Big] \ , \qquad \text{(D.28)}$$

which simplifies to[13]

$$G_F^{(4)} = \frac{1}{z_{12}z_{34}^{**}}\left[I_1\tilde{I}_1 + \tfrac{\xi}{1-\xi}I_2\tilde{I}_2\right] , \qquad \text{(D.29)}$$

$$G_K^{(4)} = \frac{(1-\xi)^{1/2}}{z_{12}z_{34}^{**}}\left[I_1\tilde{I}_1 + \tfrac{\xi}{1-\xi}\left(-I_2\tilde{I}_2 + I_1\tilde{I}_2 + I_2\tilde{I}_1\right)\right] . \qquad \text{(D.30)}$$

These are the final results for $G_F^{(4)}$ and $G_K^{(4)}$, corresponding to free (F) and (K) Kondo boundary conditions. Eq. (D.29) for $G_F^{(4)}$ agrees with eq. (D.2). Eq. (D.30) for $G_K^{(4)}$ deserves to admired with due respect for a few moments: exact, explicit expressions for 4-point functions for a strongly interacting electron system are rather rare in condensed matter physics! This function clearly has a more complex structure, with an additional $(1-\xi)^{1/2}$ and $I_1\tilde{I}_2$, $I_2\tilde{I}_1$ terms. While they vanish in the bulk limit $\xi \to 0$, they become extremely important in the boundary limit $\eta = 1-\xi \to 0$, which we discuss next.

D.4 Boundary Limit for $G^{(4)}$

With explicit expressions for $G^{(4)}$ in hand, the full boundary boundary OPE of $\psi_{L\alpha i}(z_1)\psi_R^{\bar{\alpha}\bar{i}\dagger}(z_4^*)$ can now be extracted (eq. (D.36) below). This is done (following the strategy of section C.3.2) by calculating the *boundary limit* of $G^{(4)}$ in two ways: firstly, take the boundary limit $\eta \to 0$ explicitly in eqs. (D.29) and (D.30) (this gives the coefficients a_{in}^s in eq. (C.27)); secondly, evaluate $G^{(4)}$ in the limit $z_1 \to z_4^*$, $z_2 \to z_3^*$ [Fig. D.1(b)] using the boundary OPE of $\psi_L\psi_R^\dagger$ twice in eq. (D.1)

[13]Note that the square root in eq. (D.30) causes no discontinuities: $(1-\xi)^{1/2} = \eta^{1/2} = \left(\frac{z_{14}^* z_{23}^*}{z_{13}^* z_{24}^*}\right)^{1/2}$, and since z_1, z_2 are in the upper half-plane whereas z_3^*, z_4^* are in the lower half-plane, the discontinuity in $(z_i - z_j)^{1/2}$ that always occurs (at the branch cut of the square root) when z_i is moved right around z_j, never occur for $\eta^{1/2}$. (AL alway choose the branch cut of the square root such that $0 < \arg(z^* - z')^* < \pi/2$ [AL94, p.577].)

(as in eq. (C.40)). Comparing the two limiting expressions for $G^{(4)}$ gives the BOPE coefficients $|C^B_{\psi k}|^2$ (as in eq. (C.41)).

D.4.1 Boundary Form of $G^{(4)}$

The first step of the strategy is straightforward: in terms of $\eta = 1-\xi$, eqs. (D.29) and (D.30) can trivially be rewritten as:

$$G_F^{(4)} = -\frac{1}{z_{14}^* z_{32}^*}\Big[\delta^2\tilde{\delta}^2 \; + \; \tfrac{\eta}{1-\eta}\left(4T^2\tilde{T}^2+T^2\tilde{\delta}^2+\delta^2\tilde{T}^2+\tfrac{1}{4}\delta^2\tilde{\delta}^2\right)\Big] \tag{D.31}$$

$$G_K^{(4)} = -\frac{\eta^{1/2}}{z_{14}^* z_{32}^*}\Big[2T^2\tilde{\delta}^2+2\delta^2\tilde{T}^2 \; + \; \tfrac{\eta}{1-\eta}\left(4T^2\tilde{T}^2+T^2\tilde{\delta}^2+\delta^2\tilde{T}^2+\tfrac{1}{4}\delta^2\tilde{\delta}^2\right)\Big] \tag{D.32}$$

Here we have rewritten the tensors $I_A\tilde{I}_{\tilde{A}}$ in a way more useful for comparison with eq. (D.42) below, by using the identities (following from eq. (D.18), with switched indices $\bar{\alpha} \leftrightarrow \bar{\beta}$ and $\bar{i} \leftrightarrow \bar{j}$):

$$\begin{aligned} I_1\tilde{I}_1 \;&=\; 4T^2\tilde{T}^2 + T^2\tilde{\delta}^2 + \delta^2\tilde{T}^2 + \tfrac{1}{4}\delta^2\tilde{\delta}^2 \,, \qquad I_2\tilde{I}_2 \;=\; \delta^2\tilde{\delta}^2 \,, \\ -I_2\tilde{I}_2 + I_1\tilde{I}_2 + I_2\tilde{I}_1 \;&=\; 2T^2\tilde{\delta}^2 + 2\delta^2\tilde{T}^2 \,, \end{aligned} \tag{D.33}$$

where

$$\begin{aligned} (\delta^2)^{\bar{\alpha}\bar{\beta}}_{\alpha\beta} = \delta^{\bar{\alpha}}_{\alpha}\,\delta^{\bar{\beta}}_{\beta} = (I_2)^{\bar{\alpha}\bar{\beta}}_{\alpha\beta} \,, \qquad & (T^2)^{\bar{\alpha}\bar{\beta}}_{\alpha\beta} = (T^a)^{\bar{\alpha}}_{\alpha}\,(T^a)^{\bar{\beta}}_{\beta} \,, \\ (\tilde{\delta}^2)^{\bar{i}\bar{j}}_{ij} = \tilde{\delta}^{\bar{i}}_{i}\,\tilde{\delta}^{\bar{j}}_{j} = (\tilde{I}_2)^{\bar{i}\bar{j}}_{ij} \,, \qquad & (\tilde{T}^2)^{\bar{i}\bar{j}}_{ij} = (\tilde{T}^A)^{\bar{i}}_{i}\,(\tilde{T}^A)^{\bar{j}}_{j} \end{aligned} \,. \tag{D.34}$$

D.4.2 General Form of BOPE of $\psi_L\psi_R^\dagger$

For the second part of the strategy, we need the BOPE of

$$\begin{aligned} \psi_{L\alpha i}(z_1)\psi_R^{\bar{\alpha}\bar{i}\dagger}(z_4^*) = 2(T^a)^{\bar{\alpha}}_{\alpha}(\tilde{T}^A)^{\bar{i}}_{i}\left[\psi_{L1}T^a\tilde{T}^A\psi^\dagger_{R4^*}\right] \; + \; \tfrac{1}{4}\delta^{\bar{\alpha}}_{\alpha}\delta^{\bar{i}}_{i}\left[\psi_{L1}\psi^\dagger_{R4^*}\right] \\ + (T^a)^{\bar{\alpha}}_{\alpha}\delta^{\bar{i}}_{i}\left[\psi_{L1}T^a\tilde{\psi}^\dagger_{R4^*}\right] \; + \; \delta^{\bar{\alpha}}_{\alpha}(\tilde{T}^A)^{\bar{i}}_{i}\left[\psi_{L1}\tilde{T}^A\psi^\dagger_{R4^*}\right] \,. \end{aligned} \tag{D.35}$$

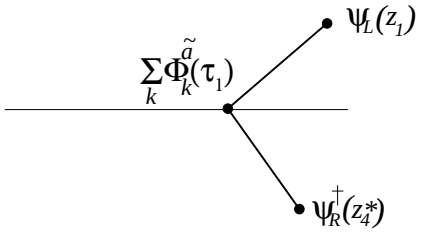

Figure D.2 The boundary operator product expansion [see eq. (D.36)] of $\psi_{L\alpha i}(z_1)$ and $\psi_R^{\bar{\alpha}\bar{i}\dagger}(z_4^*)$ in terms of the boundary operators $\Phi_k^{\tilde{a}}(\tau_1)$.

where we have used eq. (D.19) (with $\bar{\alpha} \leftrightarrow \bar{\beta}$ and $\bar{i} \leftrightarrow \bar{j}$, and contracted with $\psi_{L\bar{\beta}\bar{j}}\psi_R^{\beta j\dagger}$) to make explicit the tensor structure of the OPE. Evidently, it must have the following general form (see Fig. D.2):

$$\psi_{L\alpha i}(z_1)\psi_R^{\bar{\alpha}\bar{i}\dagger}(z_4^*) \;=\; \sum_k \frac{C^B_{\psi k}}{(-iz_{14}^*)^{1-\Delta_k}} \left(X_k^{\tilde{a}}\right)_{\alpha i}^{\bar{\alpha}\bar{i}} \Phi_k^{\tilde{a}}(\tau_1)\;, \tag{D.36}$$

with Hermitian conjugate[14]

$$\psi_{R\beta j}(z_3^*)\psi_L^{\bar{\beta}\bar{j}\dagger}(z_2) \;=\; \sum_k \frac{(C^B_{\psi k})^*}{(iz_{32}^*)^{1-\Delta_k}} \left(X_k^{\tilde{a}}\right)_{\beta j}^{\bar{\beta}\bar{j}} \Phi_k^{\tilde{a}}(\tau_1)\;. \tag{D.37}$$

Here $\Phi_k^{\tilde{a}}(\tau_1)$ is a (hermitian) boundary operator[15] with scaling dimension Δ_k and normalization

$$\langle \Phi_k^{\tilde{a}} \Phi_{k'}^{\tilde{b}} \rangle \;=\; \frac{\delta_{kk'}\delta^{\tilde{a}\tilde{b}} N_k}{|\tau_1 - \tau_2|^{2\Delta_k}}\;, \tag{D.38}$$

and $\left(X_k^{\tilde{a}}\right)_{\alpha i}^{\bar{\alpha}\bar{i}}$ is one of the four tensors (playing the role of Clebsch-Gordan coefficients):

$$\left(X_k^{\tilde{a}}\right)_{\alpha i}^{\bar{\alpha}\bar{i}} \;=\; \delta_\alpha^{\bar{\alpha}}\,\tilde{\delta}_i^{\bar{i}}\;, \qquad (T^a)_\alpha^{\bar{\alpha}}\,\tilde{\delta}_i^{\bar{i}}\;, \qquad \delta_\alpha^{\bar{\alpha}}\,(\tilde{T}^A)_i^{\bar{i}}\;, \quad \text{or} \quad (T^a)_\alpha^{\bar{\alpha}}\,(\tilde{T}^A)_i^{\bar{i}}\;, \tag{D.39}$$

[14]Upon taking the Hermitian conjugate, one also has to take $z_{23}^* \to -z_{23}^*$, because $z = \tau + ix$ becomes $i(t+x)$ after a Wick rotation back to real times, i.e. purely imaginary. This is consistent with "$\left(\frac{1}{z_{12}}\right)^\dagger$" $= [\psi(z_1)\psi^\dagger(z_2)]^\dagger = \psi(z_2)\psi^\dagger(z_1) = \frac{1}{z_{21}}$.

[15]From eq. (D.35) it follows that all boundary operators $\Phi_k^{\tilde{a}}(\tau_1)$ that occur in combination with the tensor $\left(X_k^{\tilde{a}}\right)_{\alpha i}^{\bar{\alpha}\bar{i}}$ in eq. (D.36) must correspond to the operators that occur when taking the limit $z_1 \to z_4^*$ in the object $\psi_{L\bar{\beta}\bar{j}}(z_1)\left(X_k^{\tilde{a}}\right)_{\beta j}^{\bar{\beta}\bar{j}}\psi_R^{\beta j\dagger}(z_4^*)$, or equivalently, in its hermitian conjugate $-\psi_L^{\bar{\beta}\bar{j}\dagger}(z_1)\left(X_k^{\tilde{a}}\right)_{\bar{\beta}\bar{j}}^{\beta j}\psi_{R\beta j}(z_4^*)$.

For future reference, their "squares" are [in the notation of eq. (D.34)]:

$$\sum_{\tilde{a}} \left(X_k^{\tilde{a}}\right)_{\alpha i}^{\bar{\alpha}\bar{i}} \left(X_k^{\tilde{a}}\right)_{\beta j}^{\bar{\beta}\bar{j}} = (\delta^2)_{\alpha\beta}^{\bar{\alpha}\bar{\beta}} (\tilde{\delta}^2)_{ij}^{\bar{i}\bar{j}} , \quad (T^2)_{\alpha\beta}^{\bar{\alpha}\bar{\beta}} (\tilde{\delta}^2)_{ij}^{\bar{i}\bar{j}} , \tag{D.40}$$

$$(\delta^2)_{\alpha\beta}^{\bar{\alpha}\bar{\beta}} (\tilde{T}^2)_{ij}^{\bar{i}\bar{j}} , \quad \text{or} \quad (T^2)_{\alpha\beta}^{\bar{\alpha}\bar{\beta}} (\tilde{T}^2)_{ij}^{\bar{i}\bar{j}} . \tag{D.41}$$

Now, what KM primary fields can potentially occur in $\psi_L \psi_R^\dagger$? The only KM primary fields that can occur in the OPE of two fields with $(Q, j, f) = (\pm 1, \frac{1}{2}, \frac{1}{2})$ must have quantum numbers $(0,0,0)$, $(0,1,0)$, $(0,0,1)$ and $(0,1,1)$. Are such fields allowed on the Kondo boundary? We see from table 7.1 (right part, rows 1,2,5 and 6) that the list of all possible boundary operators for the Kondo boundary indeed does contain four operators with these quantum numbers. They are denoted by $\Phi_k^{\tilde{a}} = \mathbf{1}$, ϕ_s^a, ϕ_{fl}^A and $O^{a,A}$, respectively [AL94, p.568], and have scaling dimensions $\Delta_k = 0, \frac{1}{2}, \frac{1}{2}, 1$, with normalization chosen to be $N_k = 1$ (but $N_k \neq 1$ for some of their descendents,[16] see table D.1). Under $SU(2)$ transformations, ϕ_s^a and ϕ_f^A transform in the adjoint (spin-1) representations[17] in the spin and flavor sectors, respectively, analogous to $O^{a,A}$. The descendents of these fields, obtained by acting on them [in a way defined in eq. (B.32)] with a Fourier component of a current, $\mathcal{J}_{-n}^{\tilde{a}}$ $(n > 0)$, have scaling dimension $\Delta_k + n$, and are also allowed boundary operators. The fields $\mathbf{1}$, ϕ_s^a, ϕ_f^A and $O^{a,A}$ and their first few descendents[18] are listed in table D.1, together with the corresponding Δ_k, $X_k^{\tilde{a}}$ and N_k.

[16] The normalization of a descendent operator can be found as follows (see [AL91b], footnote on p.665): Let $\langle|\rangle$ denote the scalar product defined in [BPZ84]), and assume unit normalization for ϕ_s^a: $\langle\phi_s^a|\phi_s^b\rangle = \delta^{ab}$. Then $\langle\mathcal{J}_{-1}^a\phi_s^a|\mathcal{J}_{-1}^b\phi_s^b\rangle = \langle\phi_s^a|[\mathcal{J}_{+1}^a, \mathcal{J}_{-1}^b]|\phi_s^b\rangle = \langle\phi_s^a| \left(i\varepsilon^{abc}\mathcal{J}^c + \frac{1}{2}2\delta^{ab}\right)|\phi_s^b\rangle$ $= \langle\phi_s^a|i\varepsilon^{abc}i\varepsilon^{cbd}|\phi_s^d\rangle + 3 = 9$. For the third equality we used eq. (A.105), and for the fourth eq. (B.38), which reads $\mathcal{J}^c|\phi_s^b\rangle = -(\boldsymbol{T}^c)^b{}_d|\phi_s^d\rangle$, where $(\boldsymbol{T}^c)^b{}_d = -i\varepsilon^{cbd}$ for the spin-1 representation of ϕ_s^a, see footnote 17.

[17] Explicitly, under $SU(2)$ transformations in the spin and channel sectors, we have (compare footnote 11): $\phi_s^a = \left[\delta^{ac} - i\theta^b(\boldsymbol{T}^b)^a{}_c\right]\tilde{\phi}_s^c$, where $(\boldsymbol{T}^b)^a{}_c = -i\varepsilon^{bac}$, and similarly $\phi_f^A = \left[\delta^{AC} - i\tilde{\theta}^B(\widetilde{\boldsymbol{T}}^B)^A{}_C\right]\tilde{\phi}_f^C$, where $(\widetilde{\boldsymbol{T}}^B)^A{}_C = -i\varepsilon^{BAC}$.

[18] According to footnote 9, entries 4 to 6 of table D.1 can be regarded as descendents of unity, $\mathbf{1}$; their normalizations are given in eq. (D.21).

The fact that a boundary operator can potentially occur in a BOPE certainly does not mean that it actually does occur. Whether it occurs or not can be learned from the boundary limit of $G^{(4)}$, to which we now turn.

D.4.3 Determination of BOPE coefficients $|C^B_{\psi k}|^2$

To determine the BOPE coefficients $|C^B_{\psi k}|^2$, we comparing two equivalent expressions for the boundary limit of $G^{(4)}$: In the limit $z_1 \to z_4^*$, $z_2 \to z_3^*$ [Fig. D.1(b)], we can use eqs. (D.36) to (D.38) in eq. (D.1) to obtain the following expression for $G^{(4)}$ in the boundary limit (the overall sign results from $\psi_2\psi_3^\dagger = -\psi_3^\dagger\psi_2$):

$$G^{(4)} \overset{\eta\to 0^+}{\longrightarrow} \frac{-\sum_k |C^B_{\psi k}|^2 N_k \;\; \sum_{\tilde a} \left(X_k^{\tilde a}\right)^{\bar\alpha\bar\imath}_{\alpha i} \left(X_k^{\tilde a}\right)^{\bar\beta\bar\jmath}_{\beta j}}{(z_{14}^* z_{32}^*)^{1-\Delta_k} |\tau_1-\tau_2|^{2\Delta_k}} \tag{D.42}$$

Since $\eta \to \frac{z_{14}^* z_{32}^*}{|\tau_1-\tau_2|^2}$ when $z_1 \to z_4^*$, $z_2 \to z_3^*$, we can directly compare eqs. (D.31) and (D.32) with eq. (D.42) (using eq. (D.40) in the latter), to read off all the coefficients $|C^B_{\psi k}|^2$. For example, the $k=3$ term in eq. (D.42) gives $\frac{-|C^B_{\psi 3}|^2 T^2 \tilde T^2}{(z_{14}^* z_{32}^*)}\,\eta$. Comparing this to eqs. (D.31) and (D.32) implies that $|C^B_{\psi 3}|^2 = 4$ or 0, for $B=F$ or K, respectively. The coefficients $|C^B_{\psi k}|^2$ obtained in this way for all boundary operators with $\Delta_k \le \frac{3}{2}$ are listed in table D.1, with separate columns for the free and Kondo cases.

Actually, from the present correlation function $\langle \psi_L \psi_L^\dagger \psi_R \psi_R^\dagger \rangle$, one can not obtain $|C^B_{\psi k}|^2$ separately for $k=7,8$ and 11,12, but only the combinations:[19]

$$|C^B_{\psi 7}|^2 + |C^B_{\psi 8}|^2 = \begin{cases} 0 \\ \\ \frac{1}{9\times 4} \end{cases}, \qquad |C^B_{\psi 11}|^2 + |C^B_{\psi 12}|^2 = \begin{cases} 0 \\ \\ 4 \end{cases}, \quad \text{for} \quad B = F/K\ , \tag{D.43}$$

[19] This is $[(4.7)_{AL}]$, with $C^B_{\psi 7} = C/4$ and $C^B_{\psi 8} = C'/4$. The 1/4 arise since AL introduce the C and C' in the *contracted* BOPE of $\psi_{L\alpha i}(z_1)\psi_R^{\alpha i\dagger}(z_4^*)$, see $(4.6)_{AL}$.

Table D.1 List of all boundary operators $\Phi_k^{\tilde{a}}(\tau_1)$ of dimension $\Delta_k \leq 3/2$ in the boundary operator product expansion of $\psi_{L\alpha i}(z_1)\psi_R^{\bar{\alpha}\bar{i}\dagger}(z_4^*)$ [see eq. (D.36)] for both free (F) and Kondo (K) boundary conditions. The tensors $\left(X_k^{\tilde{a}}\right)_{\alpha i}^{\bar{\alpha}\bar{i}}$ and their "squares" [needed in eq. (D.42)] are given explicitly in eqs. (D.39) and (D.40). The values for $|C_{\psi k}^F|^2$ and $|C_{\psi k}^K|^2$ are found by comparing (power by power in η) eq. (D.42) to the boundary limit $\eta \to 0^+$ of the exact expressions (D.31) and (D.32) for $G_F^{(4)}$ and $G_K^{(4)}$, respectively.

k	Δ_k	$\Phi_k^{\tilde{a}}(\tau_1)$	$\left(X_k^{\tilde{a}}\right)_{\alpha i}^{\bar{\alpha}\bar{i}}$	N_k	$\lvert C_{\psi k}^F\rvert^2$	$\lvert C_{\psi k}^K\rvert^2$
0	0	$\mathbf{1}$	$\delta\,\tilde{\delta}$	1	1	0
1	$\frac{1}{2}$	ϕ_s^a	$T^a\,\tilde{\delta}$	1	0	2
2	$\frac{1}{2}$	ϕ_f^A	$\delta\,\tilde{T}^A$	1	0	2
3	1	$O^{a,A}$	$T^a\tilde{T}^A$	1	4	0
4	1	$\mathcal{J}_c^o$	$\delta\tilde{\delta}$	4	$\frac{1}{16}$	0
5	1	$\mathcal{J}_s^a$	$T^a\tilde{\delta}$	1	1	0
6	1	$\mathcal{J}_f^A$	$\delta\tilde{T}^A$	1	1	0
7	$\frac{3}{2}$	$\mathcal{J}_{-1}^a\phi_s^a$	$\delta\,\tilde{\delta}$	9	0	$\frac{1}{72}$
8	$\frac{3}{2}$	$\mathcal{J}_{-1}^A\phi_f^A$	$\delta\,\tilde{\delta}$	9	0	$\frac{1}{72}$
9	$\frac{3}{2}$	$\mathcal{J}_{-1}^o\phi_s^a$	$T^a\,\tilde{\delta}$	1	0	1
10	$\frac{3}{2}$	$\mathcal{J}_{-1}^o\phi_f^A$	$\delta\,\tilde{T}^A$	1	0	1
11	$\frac{3}{2}$	$\mathcal{J}_{-1}^A\phi_s^a$	$T^a\,\tilde{T}^A$	1	0	2
12	$\frac{3}{2}$	$\mathcal{J}_{-1}^a\phi_f^A$	$T^a\,\tilde{T}^A$	1	0	2

since the $\Phi_7^{\tilde{a}}, \Phi_8^{\tilde{a}}$ (and $\Phi_{11}^{\tilde{a}}, \Phi_{12}^{\tilde{a}}$) terms have the same tensor structure. However, by also considering the correlation function $\langle \psi_L \psi_R^\dagger \psi_L \psi_R^\dagger \rangle$, AL showed by an entirely analogous calculation that $[(4.14)_{AL}]$

$$\left(C_{\psi 7}^B\right)^2 + \left(C_{\psi 8}^B\right)^2 = 0 \,, \qquad \left(C_{\psi 11}^B\right)^2 + \left(C_{\psi 12}^B\right)^2 = 0 \,, \tag{D.44}$$

which implies the values[20] listed in table D.1:

$$|C_{\psi 7}^B|^2 = |C_{\psi 8}^B|^2 = \begin{cases} 0 \\ \\ \frac{1}{9\times 8} \end{cases} \,, \qquad |C_{\psi 11}^B|^2 = |C_{\psi 12}^B|^2 = \begin{cases} 0 \\ \\ 2 \end{cases} \,, \quad \text{for} \quad B = F/K \,. \tag{D.45}$$

Thus, we now have succeeded in constructing a complete list of all boundary operators with $\Delta_k \leq 3/2$ occuring in the BOPE of $\psi_L \psi_R^\dagger$.

The last two columns of table D.1 illustrate the dramatic difference between the free and the Kondo cases: *none* of the boundary operators that occur in the free case occur in the Kondo case, and vice versa. Although the two theories become identical in the extreme bulk limit, they are totally "orthogonal" to each other in the extreme boundary limit! Note in particular the emergence of anomalous exponents $\Delta_k = \frac{1}{2}$ and $\frac{3}{2}$ in the Kondo case, but absent in the free theory. These are examples of the non-Fermi-liquid exponents for which the multi-channel Kondo problem is famous. In this calculation they are shown to arise as a result of boundary operators that occur in the Kondo but not in the free theory.

Note also that the identity does not occur in the BOPE for Kondo boundary conditions: $C_{\psi 0}^K = 0$, which means $\langle \psi_L(z_1) \psi_R^\dagger(z_4^*) \rangle = 0$. This result was also be

[20] Using arguments involving the discrete symmetries of time-reversal and charge-conjugation, AL showed furthermore (see [AL94], p. 586, and in particular footnote 42) that $C_{\psi 7}^B$ and $C_{\psi 8}^B$ differ by a factor i. This factor of i is verified in appendix F, footnotefoot:bosoni, page 417.

found directly in section 7.5.2 by using eq. (7.67) with $j = \frac{1}{2}$, as explained there [compare eq. (7.69)]. This means that the amplitude for an incident free electron to be "scattered from the boundary" into an outgoing free electron is strictly 0!! This is known as the unitarity paradox, whose resolution, due to [ML95], is sketched in section 7.5.2 and in more detail in appendix F.

D.5 Leading Irrelevant Operator $\mathcal{J}^a_{-1} \cdot \phi^a_s$

[AL91b, p.657,682], [AL93, p.7304], [AL94, p.586]

It is important to determine the leading irrelevant boundary operator that can appear in the effective Hamiltonian at the overscreened fixed point, since it determines the critical behavior of physical quantities such as the conductivity, magnetization and specific heat (see chapter 8).

The right part of table table 7.1 gives the list of all possible KM primary boundary operators that can occur on the Kondo boundary. The *leading irrelevant boundary operator* is the boundary operator with smallest scaling dimension that has the same symmetries as the initial weak-Hamiltonian (else it cannot be generated under the RG flow from the weak-coupling limit to the overscreened fixed point). The isotropic Kondo Hamiltonian of eq. (7.2) studied by AL is a KM singlet, with quantum numbers $(Q, j, f) = (0, 0, 0)$.

Now, from table 7.1, right part, we see that the only KM primary boundary operator with these quantum numbers is the identity. Hence the the leading irrelevant operator must be a KM descendent. The lowest dimension KM singlets are, in the notation of table D.1, $\Phi_7 = \mathcal{J}^a_{-1}\phi^a_s$ and $\Phi_8 = \tilde{\mathcal{J}}^A_{-1}\phi^A_f$, with scaling

dimensions[21] $\Delta_7 = \Delta_8 = \frac{3}{2}$ (since, by footnote 2, ϕ_s^a and ϕ_f^A have scaling dimensions $\frac{1}{2}$).

Furthermore, AL showed that the weak-coupling Hamiltonian is *even* under the discrete symmetries of time-reversal ($\boldsymbol{T}$) and, assuming particle-hole symmetry, charge conjugation ($\boldsymbol{C}$), and hence also under ($\boldsymbol{CT}$) [the precise meaning of these symmetry transformations is defined in eqs. $(4.43)_{AL}$ and $(4.44)_{AL}$ of [AL94]]. They also showed [AL94, p.586] that $\mathcal{J}_{-1}^a \phi_s^a$ and $\tilde{\mathcal{J}}_{-1}^A \phi_s^A$ are even and odd under ($\boldsymbol{CT}$), respectively. Therefore, assuming particle-hole symmetry, $\tilde{\mathcal{J}}_{-1}^A \phi_s^A$ cannot occur in the effective overscreened Hamiltonian. Thus, AL concluded [AL91b, p.657] that there is only a single leading irrelevant operator, namely $\mathcal{J}_{-1}^a \phi_s^a$, with scaling dimension $\frac{3}{2}$ (and normalization 9, see footnote 16).

The fact that the leading irrelevant operator *does* occur in the BOPE of $\psi_R \psi_L^\dagger$, as verified in section D.4.3 and table D.1, is crucial for the calculation of the temperature dependence of the self-energy, and hence the bulk conductivity or point-contact conductance. The reason is that, as shown in [AL93], the leading $T \neq 0$ correction to the self-energy is governed by $\langle \psi_R \mathcal{J}_{-1}^a \phi_s^a \psi_L^\dagger \rangle$; the anomalous, non-Fermi-liquid $T^{1/2}$ scaling behavior of the self-energy arises from the non-Fermi-liquid scaling dimension of $\frac{3}{2}$ of $\mathcal{J}_{-1}^a \phi_s^a$, as shown in sections 8.4 and 8.5 [see eq. (8.33)].

For the arguments of those sections, it is assumed that the boundary operators Φ_n occuring in $\langle \psi_R \Phi_n \psi_L^\dagger \rangle$ is Virasoro primary, since the $T \neq 0$ version of this function is calculated by a conformal map of the plane to a cylinder, assuming

[21] For general $\tilde{N}$ and k, the scaling dimensions are $\Delta_7 = 1 + \frac{\tilde{N}}{\tilde{N}+k}$ and $\Delta_8 = 1 + \frac{k}{\tilde{N}+k}$. This follows because according to eq. (B.85), the scaling dimension of the KM primary fields ϕ_s^a and ϕ_f^A are given by $\Delta_\phi = \frac{c_\phi}{\tilde{N}+k}$, where for the adjoint representations of $SU(\tilde{N})$ and $SU(k)$, we have $c_\phi = \tilde{N}$ and k, respectively.

that all operators involved are Virasoro primary [compare eq. (8.35)]. Now, $\mathcal{J}^a_{-1}\phi^a_s$ is in fact Virasoro primary, though this is not a priori obvious, since it is not KM primary. To verify this, note that an operator ϕ_i is Virasoro primary if it satisfies [eq. (B.37)] the condition $L^s_n\phi_i = 0$ for all $n > 0$, which does hold for $(\mathcal{J}^a_{-1}\phi^a_s)$:

$$L^s_1(\mathcal{J}^a_{-1}\phi^a_s) = \left(\mathcal{J}^a_{-1}L^s_1 + \mathcal{J}^a_0\right)\phi^a_s = 0 - (\boldsymbol{T}^a)^a_{\ b}\phi^b_s = 0\ . \tag{D.46}$$

Here eq. (A.104) was used for the first equality, eq. (B.37)[22] and eq. (B.38) for the second and footnote 17 for the third, according to which $(\boldsymbol{T}^a)^a_{\ b} = -i\varepsilon^{aab} = 0$. Similarly, $L^s_1(\mathcal{J}^a_{-1}\phi^a_s) = 0$ for all $n > 0$.

[22]Since ϕ^a_s, being KM primary, *is* Virasoro primary, $L^s_1\phi^a_s = 0$.

Appendix E

Free Bosons

In this appendix we give some standard results from the theory of free massless bosons in two dimensions, that are needed for the bosonization of fermions used in chapter 6 and appendix F. For a detailed discussion, refer to the lectures by Shankar [Sha91]; for a more concise and elegant treatment, to those by Polchinski [Pol94, chapter 1].

E.1 Boson Basics

The Lagrangian action for a free boson on an infinite line ($x \in [-\infty, \infty]$) is [Sha91,Pol94] (with normalization $\varphi_{here} = \sqrt{4\pi}\varphi_{Shankar}$)

$$\mathcal{S} \equiv \tfrac{1}{8\pi}\int d\tau \int dx \left[(\partial_\tau \varphi(\tau,x))^2 + (\partial_x \varphi(\tau,x))^2\right] \;=\; -\tfrac{1}{2\pi}\int d\tau \int dx\, \varphi(\tau,x)\partial_z\partial_{z^*}\varphi(\tau,x)\;, \tag{E.1}$$

where $z = \tau + ix$ and $\partial_z = \frac{1}{2}(\partial_\tau - i\partial_x)$. This action leads to the equation of motion $\partial_z\partial_{z^*}\varphi = 0$, implying that $\varphi(z,z^*)$ decomposes into L- and R-moving components:

$$\varphi(z,z^*) = \varphi_{_L}(z) + \varphi_{_R}(z^*)\;. \tag{E.2}$$

For a line of infinite length, $\varphi_{L/R}$ can be expressed in terms of $\varphi(\tau, x)$ through

$$\varphi_{L/R}(\tau \pm ix) = \tfrac{1}{2}\left[\varphi(\tau, x) \mp \int_x^\infty dx'\, i\partial_\tau \varphi(\tau, x')\right] . \tag{E.3}$$

The canonical equal-time commutation relation for φ and its conjugate field $\frac{i\partial\mathcal{L}}{\partial(\partial_\tau\varphi)} = \frac{i}{4\pi}\partial_\tau\varphi(\tau, x')$ is

$$[\varphi(\tau, x), \tfrac{i}{4\pi}\partial_\tau\varphi(\tau, x')] = i\frac{\kappa/\pi}{(x-x')^2+\kappa^2} \;\simeq\; i\delta(x-x') , \tag{E.4}$$

where $1/\kappa$ is a large ultra-violet cut-off in momentum integrals.[1] Eq. (E.4) implies via eq. (E.3) that

$$[\varphi_L(\tau + ix), \varphi_R(\tau - ix')] \;=\; i\pi \tag{E.5}$$

$$\begin{aligned} [\varphi_{L/R}(\tau + ix), \varphi_{L/R}(\tau - ix')] &= \mp i2 \lim_{\kappa\to o} \tan^{-1}\left(\frac{x-x'}{\kappa}\right) \\ \equiv\; \mp i\pi\varepsilon(x-x') &= \begin{cases} 0 & \text{if} \quad x = x' , \\ \mp i\pi & \text{if} \quad x \gtrless x' . \end{cases} \end{aligned} \tag{E.6}$$

Eq. (E.5) can be ensured by requiring that $[\varphi_{0L}, \varphi_{0R}] = i\pi$, where φ_{0L} (φ_{0R}) is the z- (z^*)-independent part of $\varphi_L(z)$ ($\varphi_R(z^*)$), the so-called zero-mode.

If one considers bosons on a finite interval, say $x \in [0, l]$, the representation of eq. (E.3) is no longer applicable (and eqs. (E.5) and (E.5) can consequently be modified). Instead, one has to carefully make mode expansions for $\varphi_{L/R}$, whose detailed properties depend on the boundary conditions on the fields $\varphi_{L/R}$. [For detailed examples of boundary-condition-dependent mode expansions, see, e.g. [GSW87, p.66], [WA94,EA92].]

[1] The ultra-violet cut-off κ is on the order of the lattice spacing. In CFT, one implicitly takes $\alpha \to 0$, and the divergences that arise as $z \to z'$ play a central role in the theory, via operator product expansions.

The correlation functions for $\varphi_L(z)$ and $\varphi_R(z^*)$ are[2]

$$\langle\varphi_L(z_1)\varphi_L(z_2)\rangle = -\ln[(z_1-z_2+\kappa)/\Lambda]\,, \tag{E.7}$$

$$\langle\varphi_R(z_1^*)\varphi_R(z_2^*)\rangle = -\ln[(z_1^*-z_2^*+\kappa)/\Lambda]\,, \tag{E.8}$$

where $\Lambda^{-1} \to 0$ is an infra-red cut-off in momentum integrals (discussed in [GSW87, p.139]), that cancels from all relevant expressions.[3]

Below we shall consider a number of independent boson fields φ_α, labeled by an index α, with

$$\langle\varphi_\alpha\varphi_\beta\rangle = 0 \quad \text{and} \quad [\varphi_\alpha,\varphi_\beta] = [\varphi_\alpha,\partial_\tau\varphi_\beta] = 0 \qquad \text{if} \quad \alpha\neq\beta\,. \tag{E.9}$$

E.2 Vertex Operators

The normal-ordered form of an exponential operator is defined as follows:[4]

$$:e^A: \equiv \frac{e^A}{\langle e^A\rangle} = \frac{e^A}{e^{\frac{1}{2}\langle A^2\rangle}}\,, \tag{E.10}$$

so that $\langle :e^A:\rangle = 1$. When manipulating with exponential operators, the following identities [derived in [Sha91], see eq.(3.22)] are useful:

$$e^Ae^B = e^{A+B}e^{[A,B]/2}\,; \qquad :e^A::e^B: = :e^{A+B}:\,e^{\langle AB\rangle}\,. \tag{E.11}$$

[2]Actually, eqs. (E.7) and (E.8) hold only modulo additive constants $\pm i\pi$. The reason is (see [GSW87, eq. (3.2.41)] or [Pol94, eq. (1.4.25)]) that they are derived from $\langle\varphi(z_1,z_1^*)\varphi(z_2,z_2^*)\rangle = -\ln[(z_1-z_2+\kappa)/\Lambda] - \ln[(z_1^*-z_2^*+\kappa)/\Lambda] = \langle(\varphi_L+\varphi_R)(\varphi_L+\varphi_R)\rangle$. Therefore, the functions $\langle\varphi_L\varphi_L\rangle$ and $\langle\varphi_R\varphi_R\rangle$ can be determined from this only to within the constant $\langle\varphi_L\varphi_R+\varphi_R\varphi_L\rangle$, which need not be zero, since $[\varphi_L,\varphi_R] = i\pi \neq 0$. However, extra contributions $\pm i\pi$ in eqs. (E.7) and (E.8) can be ignored for our purposes: since the infra-red cut-off $\ln\Lambda$ cancels from all relevant formulae, so will the combination $\ln\Lambda \pm i\pi = \ln(\Lambda e^{\pm i\pi})$.

[3]Typically, the cancelation of Λ happens via $\langle\varphi(z)\varphi(0)\rangle - \langle\varphi(0)\varphi(0)\rangle = \ln(z+\kappa)/\kappa$. However, we display Λ explicitly because of the role it plays in eq. (E.15) below.

[4]For a discussion of normal ordering of exponentials, see [Sha91, eq.(3.22)], where eq. (E.11) is derived, [GSW87, p.89] or the particularly elegant treatment of [Pol94, eq.(1.1.18)].

The normal-ordered exponential of a free boson is called a *vertex operator*:[5]

$$V^{(\alpha)}_{L,\lambda}(z) \;\equiv\; \Lambda^{-\lambda^2/2}\;{:}e^{i\lambda\varphi_{L\alpha}(z)}{:}\,, \qquad V^{(\alpha)}_{R,\lambda}(z^*) \;\equiv\; \Lambda^{-\lambda^2/2}\;{:}e^{i\lambda\varphi_{R\alpha}(z^*)}{:}\,, \tag{E.12}$$

[the normalization factor $\Lambda^{-\lambda^2/2}$ is needed to ensure proper normalization of the two-point function (E.15) below]. Evidently $\langle V^{(\alpha)}_{L,\lambda}(z)\rangle = \delta_{\lambda,0}$ in the limit $\Lambda^{-1}\to 0$. Using the second of eq. (E.11) together with eq. (E.7), one finds the following vertex operator OPEs (note that *singular* terms occur only for $\alpha=\beta$):

$$V^{(\alpha)}_{L,\lambda_1}(z_1)\,V^{(\beta)}_{L,\lambda_2}(z_2) \;=\; \frac{\delta_{\alpha\beta}\,V^{(\alpha)}_{L,\lambda_1+\lambda_2}(z_2)}{(z_1-z_2)^{-\lambda_1\lambda_2}}\Big(1+\lambda_1(z_1-z_2)\,i\partial_{z_2}\varphi(z_2)+\ldots\Big) \tag{E.13}$$

$$i\partial_z\varphi_{L\alpha}(z_1)\,V^{(\beta)}_{L,\lambda_2}(z_2) \;=\; \frac{\delta_{\alpha\beta}\,\lambda_2}{z_1-z_2}\,V^{(\beta)}_{L,\lambda_2}(z_2)\;+\ldots\;\;. \tag{E.14}$$

It follows that the two-point function

$$\langle V^{(\alpha)}_{L,\lambda_1}(z_1)V^{(\beta)}_{L,\lambda_2}(z_2)\rangle \;=\; \frac{\delta_{\alpha\beta}\Lambda^{-\frac{1}{2}(\lambda_1+\lambda_2)^2}}{(z_1-z_2)^{-\lambda_1\lambda_2}}\,. \tag{E.15}$$

is non-zero in the limit $\Lambda^{-1}\to 0$ only if $\lambda_1+\lambda_2=0$, which implies its invariance under $\varphi\to\varphi+const$, as expected. [This is the reason for including the factor $\Lambda^{-\lambda^2/2}$ in the definition (E.12).]

The vertex operator $V^{(\alpha)}_{L,\lambda}(z)$ is a Virasoro primary field, with scaling dimension $\lambda^2/2$ (for a proof, see [GSW87, p.89]).

Similar properties hold for right-movers, with $L\to R$ and $z\to z^*$.

E.3 Bosonization of Free Fermions

A single species of spinless, L- and R-moving free fermions (with linear dispersion) can be expressed in terms of a single species of bosons through vertex operators

[5] One often sees the form $V^{(\alpha)}_{L,\lambda}(z) \;\equiv\; \kappa^{-\lambda^2/2}e^{i\lambda\varphi_{L\alpha}(z)}$, which is equivalent to eq. (E.12), since $\langle e^{i\lambda\varphi_{L\alpha}(z)}\rangle = e^{\frac{1}{2}\lambda^2\ln\kappa/\Lambda} = (\kappa/\Lambda)^{\lambda^2/2}$.

with $\lambda = \pm 1$: Explicitly, $\psi_{L}(z) \equiv \Lambda^{-1/2} :e^{-i\varphi_{L}(z)}:$ and $\psi_{R}(z^*) \equiv \Lambda^{-1/2} :e^{-i\varphi_{R}(z^*)}:$ (here eqs. (E.5) and (E.11) ensure that ψ_{L} and ψ_{R} anti-commute). It is evident from eq. (E.15) that this identification reproduces the correct fermion Green's function, including the correct statistics [which can also be checked on an operator level by using eq. (E.11) in combination with eq. (E.6)].

The same method can be used to bosonize a set of $2N$ independent fermions $\psi_{L\alpha}$, $\alpha = 1, \ldots, 2N$, in terms of $2N$ independent boson fields $\varphi_{L\alpha}$. However, one has to take care that different species of fermions anti-commute.[6] There are several ways to do this, one of which is to make the bosonization Ansatz

$$\psi_{L\alpha}(z) \equiv a_\alpha \Lambda^{-1/2} :e^{-i\varphi_{L\alpha}(z)}: \qquad \psi_{L}^{\alpha\dagger}(z) \equiv a_\alpha \Lambda^{-1/2} :e^{i\varphi_{L\alpha}(z)}: \quad , \tag{E.16}$$

$$\psi_{R\alpha}(z^*) \equiv a_\alpha \Lambda^{-1/2} :e^{-i\varphi_{R\alpha}(z^*)}: \qquad \psi_{R}^{\alpha\dagger}(z^*) \equiv a_\alpha \Lambda^{-1/2} :e^{i\varphi_{R\alpha}(z^*)}: , \tag{E.17}$$

where the different φ_α commute [as in eq. (E.9)] and we have introduced [Lud95, ML95] a set of $2N$ anti-commuting, hermitian constants a_α (sometimes called *cocycles* in the string theory literature) satisfying

$$\{a_\alpha, a_\beta\} = 2\delta_{\alpha\beta} \, . \tag{E.18}$$

Since $a_\alpha^2 = 1$, all relations involving bilinears of a single fermion species ψ_α are unaffected by the a_α. The sole role of the a_α's is to ensure that $\{\psi_{L\alpha}, \psi_{L\beta}\} = 0$ if $\alpha \neq \beta$ [recall eq. (E.9)], i.e. to serve as a mnemonic to remind us to include $-$ signs when permuting fermion fields. The a_α's are otherwise trivial constants, and for definiteness may be thought of as a set of (hermitian) matrices that realize the Clifford algebra eq. (E.18).

[6] This matter is not discussed in the literature that treats the the 2-channel Kondo model via bosonization [EK92,SG94,SH95a]. However, for our application in appendix F, it will be important to treat this with care.

Note that the combination $a_{2N+1} \equiv -(-i)^N a_1 a_2 \ldots a_{2N}$ satisfies the relations

$$\{a_\alpha, a_{2N+1}\} = 0, \qquad [a_\alpha a_\beta, a_{2N+1}] = 0, \qquad a_{2N+1}^2 = 1 \; . \tag{E.19}$$

The third relation (ensured by the phase $-(-i)^N$) implies that one can classify states as having even or odd "parity" according to their eigenvalues $\eta = \pm 1$ under a_{2N+1}. Let $|0\rangle_\eta$ be a ground state with $a_{2N+1}|0\rangle_\eta = \eta|0\rangle_\eta$. Then a m-fermion state, $|m\rangle_\eta \equiv (\psi)^{m'}(\psi^\dagger)^{m+m'}|0\rangle_\eta$, has parity $(-)^m\eta$. When working on a subspace of definite m, one may thus make the replacement $a_{2N+1} \to (-)^m\eta$.

Eq. (E.16) and eq. (E.13) imply the following bosonic expressions for normal-ordered fermion currents (the first by expanding the exponential in the right-hand side of eq. (E.13)):

$$:\psi_L^{\alpha\dagger}(z)\psi_{L\beta}(z): = \begin{cases} :i\partial_z\varphi_{L\alpha}(z): & \text{for} \quad \alpha = \beta \; , \\ a_\alpha a_\beta \, \Lambda^{-1} \; :e^{i(\varphi_{L\alpha}-\varphi_{L\beta})(z)}: & \text{for} \quad \alpha \neq \beta \; . \end{cases} \tag{E.20}$$

Let $(T^A)_\alpha^\beta$ be any $N \times N$ matrix, and define a corresponding current through:

$$J_L^A(z) =: \psi_L^{\alpha\dagger}(z)(T^A)_\alpha^\beta \psi_{L\beta}(z): \quad . \tag{E.21}$$

Then, using eqs. (E.14) and (E.13), it is instructive to check that the bosonic expressions (E.20) and (E.16) reproduce[7] the OPEs expected from using Wick's theorem for fermions [compare eq. (B.26) and (A.47)]:

$$J^A(z_1)\psi_L^{\gamma\dagger}(z_2) \;\; = \;\; \frac{\psi_L^{\alpha\dagger}(z_2)(T^A)_\alpha^{\;\gamma}}{z_1 - z_2} \; + \ldots \quad , \tag{E.22}$$

$$J^A(z_1)J^B(z_2) \;\; = \;\; \frac{\mathrm{Tr}T^AT^B}{z_1 - z_2} + \; :\psi_L^{\alpha\dagger}(z_2)\left([T^A, T^B]\right)_\alpha^{\;\beta}\psi_{L\beta}(z_2): \; + \ldots \tag{E.23}$$

where the dots represent terms which are less singular [e.g., in eq. (E.22), a term $e^{i(\varphi_{L\alpha}-\varphi_{L\beta}+\varphi_{L\gamma})}$ with $\gamma \neq \beta$, which is less singular because the leading term in eq. (E.13) is absent for $\gamma \neq \beta$].

[7] Note that the a_α's play an essential role in ensuring the requisite $-$ signs for forming the commutator in eq. (E.23).

As an example (of interest in section 6.3), consider the case of two spinless fermions fields, $\alpha = (1,2) = (+,-)$. In this case it is convenient to introduce linear combinations of the bosons φ_{L1} and φ_{L2}:

$$X^0_L(z) = \tfrac{1}{\sqrt{2}}(\varphi_{L1} + \varphi_{L2})(z)\ , \qquad X^3_L(z) = \tfrac{1}{\sqrt{2}}(\varphi_{L1} - \varphi_{L2})(z)\ . \tag{E.24}$$

Then we have

$$\psi_\alpha(z) = a_\alpha\, \Lambda^{-1/2}\ :e^{-i\varphi_{L\alpha(z)}} = a_\alpha\, \Lambda^{-1/2}\ :e^{-i\frac{1}{\sqrt{2}}[X^0_L(z)+\alpha X^3_L(z)]}:\ , \tag{E.25}$$

$$\begin{aligned}
\tfrac{1}{2}\sum_\alpha :\psi^{\alpha\dagger}_L(z)\psi_\alpha(z): &= \tfrac{1}{\sqrt{2}}\ :i\partial_z X^0(z)\ :, && \text{(E.26)}\\
\sum_{\alpha\alpha'} :\psi^{\alpha\dagger}(z)\tfrac{1}{2}\sigma^1_{\alpha\alpha'}\psi_{\alpha'}(z): &= a_3\,\Lambda^{-1}\ :\sin\sqrt{2}X^3(z)\ :\ , && \text{(E.27)}\\
\sum_{\alpha\alpha'} :\psi^{\alpha\dagger}(z)\tfrac{1}{2}\sigma^2_{\alpha\alpha'}\psi_{\alpha'}(z): &= -a_3\,\Lambda^{-1}\ :\cos\sqrt{2}X^3(z):\ , && \text{(E.28)}\\
\sum_{\alpha\alpha'} :\psi^{\alpha\dagger}(z)\tfrac{1}{2}\sigma^3_{\alpha\alpha'}\psi_{\alpha'}(z): &= \tfrac{1}{\sqrt{2}}\ :i\partial_z X^3(z):\ . && \text{(E.29)}
\end{aligned}$$

where $a_3 = ia_1a_2$. If explicit representations for a_α ($\alpha = 1,2,3$) are desired, one can choose the Pauli matrices: $a_\alpha = \sigma^\alpha$, with the "η-parity" ground state $|0\rangle_\eta$ being proportional to $\binom{1}{0}$ or $\binom{0}{1}$ for $\eta = 1$ or -1, respectively.

Appendix F

Bosonic Description of Overscreened Fixed Point for 2-channel Kondo Problem

In this appendix we describe how Maldacena and Ludwig [ML95] reformulated the AL theory for the overscreened fixed point, for $k = 2$ channels (and $\tilde{N} = 2$), in terms of *free bosons* (!). This approach not only achieved its initial goal of resolving the unitarity paradox [see section 7.5.2]; in addition, it lead to a very transparent description of the overscreened fixed point in terms of very simple boundary conditions satisfied by the free bosons. In particular, the origin of the anomalous non-Fermi-liquid exponents $\Delta = \frac{1}{2}$ becomes very clear [section F.4], as does the nature of the corresponding boundary operators ϕ_s^a and ϕ_f^A [section F.6].

The reader not familiar with all the intricacies of AL's CFT approach is nevertheless encouraged to read on: the only input from AL's CFT needed here are eqs. (F.5) to (F.7). Once these are assumed, the rest follows purely from

applying results from the theory of free bosons. In fact, the approach is similar in spirit to that used by Emery and Kivelson [EK92] to address the anisotropic 2-channel Kondo problem, although the details are quite different.

As always, our presentation is considerably more pedestrian than that used in [ML95]. In particular, we avoid the group theoretic arguments by which the approach was discovered, since *a posteriori* one can get by without them, and instead merely describe how it works. In addition, we show explicitly [section F.6] how the boundary operators ϕ_s^a and ϕ_f^A, introduced in appendix D, can also be expressed in terms of the boson fields (a matter addressed only in passing in [ML95]).

F.1 Statement of the Unitarity Paradox

Let us recall what the "unitarity paradox" is. Consider the fermion field ψ that the free-fermion field ψ_{free} renormalizes into as one flows towards the over-screened fixed point. It was shown in section 7.5.2 (and emphasized again at the end of section D.4.3), that for the Kondo problem, the fermion field $\psi_{\scriptscriptstyle R}(z^*)$ is not simply proportional to the analytic continuation of $\psi_{\scriptscriptstyle L}(z^*)$ into the lower half-plane:

$$\psi_{\scriptscriptstyle R}(z^*) \neq c\, \psi_{\scriptscriptstyle L}(z^*)\ . \tag{F.1}$$

Instead, for $k = 2$, $\tilde{N} = 2$, one actually finds the dramatic result that their two-point function vanishes [see eq. (7.69)]:

$$\langle \psi_{\alpha i {\scriptscriptstyle R}}(z^*) \psi_{\scriptscriptstyle L}^{\dagger \alpha' i'}(z') \rangle \ = \ 0\ . \tag{F.2}$$

This seems to violate unitary: when a free electron scatters off the boundary (the impurity), the amplitude for a free electron to emerge is zero [if $k > 2$, the

amplitude is not zero, but still < 1, compare eq. (7.68)].

The resolution of this paradox by Maldacena and Ludwig (ML) rests on the following realization: the fact that a free electron does not scatter into a free electron does not mean that it disappears; according to the dictates of unitary, it must simply mean that $\psi_L^{\alpha i\dagger}$ scatters into some other (non-Fermi-liquid) excitation, with the same quantum numbers $(Q, j_z, f_z) = (1, \alpha\frac{1}{2}, i\frac{1}{2})$, $(\alpha, i = \pm)$ that does not occur in a theory of free fermions, but does in the overscreened Kondo theory.

Let this other excitation, which we call a *spinor-electron* (ML simply call it a "spinor"), be described by a field $S^{\alpha i\dagger}$. *By definition*, this is the field into which an electron scatters at the boundary, and hence by definition $S_R^{\alpha i\dagger}$ is the analytic continuation of $\psi_L^{\alpha i\dagger}$ into the lower half-plane:

$$S_R^{\alpha i\dagger}(z^*) \equiv \psi_L^{\alpha i\dagger}(z^*) \; . \tag{F.3}$$

The challenge is to find the properties of $S^{\alpha i\dagger}$.

Now, although the electron fields $\psi_L^\dagger$ and $\psi_R^\dagger$ do not obey simple boundary conditions, bilinear combinations of $:\psi^\dagger\psi:$ do: The familiar charge ($\mathcal{J}_c^o$), spin ($\mathcal{J}_s^a$), flavor ($\mathcal{J}_f^A$) and "spin-flavor" ($O^{a,A}$) currents, to be generically denoted by $\mathcal{J}_Y^{\tilde{a}}$, are defined by eqs. (D.21) (N_Y being the normalization):

$$\begin{aligned}
\mathcal{J}_c^0(z) &= :\psi^{\alpha i\dagger}\,\psi_{\alpha i}:(z) \; , & N_c &= 4 \; , \\
\mathcal{J}_s^a(z) &= :\psi^{\beta i\dagger}\,(T^a)_\beta^{\ \alpha}\psi_{\alpha i}:(z) \; , & N_s &= 1 \; , \\
\mathcal{J}_f^A(z) &= :\psi^{\alpha j\dagger}\,(\tilde{T}^A)_j^{\ i}\psi_{\alpha i}:(z) \; , & N_f &= 1 \; , \\
O^{a,A}(z) &= 2:\psi^{\beta j\dagger}\,(T^a)_\beta^{\ \alpha}\,(\tilde{T}^A)_j^{\ i}\,\psi_{\alpha i}:(z) \; , & N_O &= 1 \; .
\end{aligned} \tag{F.4}$$

They have the L-R two-point functions [eqs. (D.24) and (D.25)],

$$\langle \mathcal{J}^{\tilde{a}}_{LY}(z_1)\mathcal{J}^{\tilde{a}'}_{RY}(z_2^*)\rangle = \frac{\eta_Y\, N_Y\, \delta_{\tilde{a}\tilde{a}'}}{(z_1 - z_2^*)^2}\ , \tag{F.5}$$

$$\eta_c = \eta_s = \eta_f = -\eta_O = 1\ , \tag{F.6}$$

which imply that

$$\mathcal{J}^{\tilde{a}}_{RY}(z^*) = \eta_Y \mathcal{J}^{\tilde{a}}_{LY}(z^*) \tag{F.7}$$

when acting on the ground state $|0\rangle$.

Since eqs. (F.5) to (F.7) completely determine all that follows (and are the only point at which input from AL's CFT approach is needed), their origin is worth recapitulating: For $_Y = c, s, f$, eq. (F.7) stipulates that the $U(1)_c \times SU(2)_s \times SU(2)_f$ generators $\mathcal{J}^0_c$, $\mathcal{J}^a_s$ and $\mathcal{J}^A_f$ be analytic at the boundary, which is the condition [eqs. (7.39) or eq. (C.8)] that ensures that the boundary is $U(1)_c \times SU(2)_s \times SU(2)_f$ KM-invariant (see section C.1). [This is the fundamental assumption on which AL's theory of the over-screened fixed point is based (see section 7.4.1); it is the technically precise statement of the loose statement that "the impurity is screened in such a way that the $U(1)_c \times SU(2)_s \times SU(2)_f$ symmetry is completely restored."] The $O^{a,A}$'s, however, are not generators of a KM symmetry and hence not necessarily analytic at the boundary. However, they *are* KM primary (see footnote 10 on page 382); hence their boundary conditions are governed by Cardy's result for L-R functions, eqs. (D.25) and (D.26), which imply $\eta_O = -1$.

The strategy followed by ML is straightforward: they *bosonize* the fermion-fields $\psi^{\alpha i\dagger}$ in terms of a set of boson fields $\varphi_{\alpha i}$, make a transformation to a new set of boson fields ϕ_Y, and then determine what boundary conditions the ϕ_Y

fields have to satisfy in order that eqs. (F.7) hold. Once these are known, it is straightforward to define the spinor-electron field $S^{\alpha i\dagger}$ in terms of the ϕ_Y-bosons, and deduce all its properties.

F.2 Bosonization of $\psi^{\alpha i\dagger}$

We bosonize according to the method outlined in appendix E. Introduce four independent, commuting, boson fields $\varphi_{\alpha i}$, each with the properties described in section E.1, and a set of four anti-commuting hermitian constants $a_{\alpha i}$ (sometimes called *cocycles* in the string theory literature) satisfying[1]

$$\{a_\alpha, a_\beta\} = 2\delta_{\alpha\beta}\ , \qquad \{a_\alpha, a_5\} = 0\ , \qquad a_5^2 = 1 \qquad \text{where} \quad a_5 = a_{11}a_{21}a_{12}a_{22}\ . \tag{F.8}$$

Then the fermion fields can be represented as:

$$\psi_{L\alpha i}(z) \equiv a_{\alpha i}\Lambda^{-1/2}\,{:}e^{-i\varphi_{L\alpha i}(z)}{:} \qquad \psi_L^{\alpha i\dagger}(z) \equiv a_{\alpha i}\Lambda^{-1/2}\,{:}e^{i\varphi_{L\alpha i}(z)}{:} \tag{F.9}$$

$$\psi_{R\alpha i}(z^*) \equiv a_{\alpha i}\Lambda^{-1/2}\,{:}e^{-i\varphi_{R\alpha i}(z^*)}{:} \qquad \psi_R^{\alpha i\dagger}(z^*) \equiv a_{\alpha i}\Lambda^{-1/2}\,{:}e^{i\varphi_{R\alpha i}(z^*)}{:} \tag{F.10}$$

Henceforth, if we do not display the subscripts L/R and arguments z/z^* explicitly, the formulas are understood to apply to both cases. Also, the normal ordering symbols and the normalization $\Lambda^{-1/2}$ will not be displayed, but understood.

According to eqs. (F.4) and the first of (E.20), the following four (commuting)

[1] An explicit realization of the $a_{\alpha i}$'s in terms of 4×4 matrices is, for example: $a_{11} = \begin{pmatrix} 1_2 & 0 \\ 0 & -1_2 \end{pmatrix}$; $(a_{21}, a_{12}, a_{22}) \equiv \vec{a} \equiv \begin{pmatrix} 0 & -i\vec{\sigma} \\ i\vec{\sigma} & 0 \end{pmatrix}$, and $a_5 = \begin{pmatrix} 0 & 1_2 \\ 1_2 & 0 \end{pmatrix}$, where $1_2 = \begin{pmatrix} 1 & 0 \\ 0 & 1 \end{pmatrix}$. A ground state $|0\rangle_{\eta_5}$ with a_5-parity of $\eta_5 = \pm 1$ then is proportional to $\begin{pmatrix} 1 \\ 1 \\ \eta_5 \\ \eta_5 \end{pmatrix}$.

currents $\mathcal{J}_c$, $\mathcal{J}_s^3$, $\mathcal{J}_f^3$ and $O^{3,3}$ are linear in the boson fields $\varphi_{\alpha i}$:

$$\begin{aligned}
\tfrac{1}{2}\mathcal{J}_c &= i\partial_z \tfrac{1}{2}\sum_{\alpha i} \varphi_{\alpha i} &&\equiv i\partial_z \phi_c \\
\mathcal{J}_s^3 &= i\partial_z \tfrac{1}{2}\sum_{\alpha i} (\sigma^3)^{\alpha}_{\alpha}\varphi_{\alpha i} &&\equiv i\partial_z \phi_s \\
\mathcal{J}_f^3 &= i\partial_z \tfrac{1}{2}\sum_{\alpha i} (\sigma^3)^{i}_{i}\varphi_{\alpha i} &&\equiv i\partial_z \phi_f \\
O^{3,3} &= i\partial_z \tfrac{1}{2}\sum_{\alpha i} (\sigma^3)^{\alpha}_{\alpha}(\sigma^3)^{i}_{i}\varphi_{\alpha i} &&\equiv i\partial_z \phi_x
\end{aligned} \tag{F.11}$$

On the right-hand side, we have introduced a new set of boson fields, which we collectively denote by ϕ_Y,

$$\phi_Y \equiv \begin{pmatrix} \phi_c \\ \phi_s \\ \phi_f \\ \phi_x \end{pmatrix} \equiv \tfrac{1}{2}\begin{pmatrix} 1 & 1 & 1 & 1 \\ 1 & -1 & 1 & -1 \\ 1 & 1 & -1 & -1 \\ 1 & -1 & -1 & 1 \end{pmatrix}\begin{pmatrix} \varphi_{11} \\ \varphi_{21} \\ \varphi_{12} \\ \varphi_{22} \end{pmatrix} . \tag{F.12}$$

Because this transformation is orthogonal, the ϕ_Y satisfy the same commutation relations as the $\varphi_{\alpha i}$ [compare eq. (E.6)].

$$\begin{aligned}
\Big[\phi_{Y\,L}(\tau,x), \phi_{Y'\,R}(\tau,x')\Big] &= i\pi\,\delta_{YY'} , \\
\Big[\phi_{Y\,L/R}(\tau,x), \phi_{Y'\,L/R}(\tau,x')\Big] &= \mp i\pi\varepsilon(x-x')\,\delta_{YY'} ,
\end{aligned} \tag{F.13}$$

Thus, they are also mutually independent and commuting, so that $e^{i\phi_Y}e^{i\phi_{Y'}} = e^{i(\phi_Y+\phi'_Y)}$ if ${}_Y \neq {}_{Y'}$.

It turns out to be convenient to express all fields and currents in terms of these new bosons:

$$\begin{pmatrix} \psi^{11\dagger} \\ \psi^{21\dagger} \\ \psi^{12\dagger} \\ \psi^{22\dagger} \end{pmatrix} = \begin{pmatrix} a_{11}\, e^{i\varphi_{11}} \\ a_{21}\, e^{i\varphi_{21}} \\ a_{12}\, e^{i\varphi_{12}} \\ a_{22}\, e^{i\varphi_{22}} \end{pmatrix} = \begin{pmatrix} a_{11}\, e^{\frac{i}{2}(\phi_c+\phi_s+\phi_f+\phi_x)} \\ a_{21}\, e^{\frac{i}{2}(\phi_c-\phi_s+\phi_f-\phi_x)} \\ a_{12}\, e^{\frac{i}{2}(\phi_c+\phi_s-\phi_f-\phi_x)} \\ a_{22}\, e^{\frac{i}{2}(\phi_c-\phi_s-\phi_f+\phi_x)} \end{pmatrix} , \tag{F.14}$$

$$\text{i.e.} \qquad \psi^{\alpha j\dagger} = a_{\alpha j} e^{\frac{i}{2}(\phi_c+\alpha\phi_s+j\phi_f+\alpha j\phi_x)} \tag{F.15}$$

and

$$\begin{aligned}
\mathcal{J}_s^\eta &= \eta\, a_{11}a_{21}\, e^{\eta i\phi_s}\left(e^{\eta i\phi_x} - a_5\, e^{-\eta i\phi_x}\right) , \\
\mathcal{J}_f^\eta &= \eta\, a_{11}a_{12}\, e^{\eta i\phi_f}\left(e^{\eta i\phi_x} + a_5\, e^{-\eta i\phi_x}\right) , \\
O^{\eta,3} &= \eta\, a_{11}a_{21}\, e^{\eta i\phi_s}\left(e^{\eta i\phi_x} + a_5\, e^{-\eta i\phi_x}\right) , \\
O^{3,\eta} &= \eta\, a_{11}a_{12}\, e^{\eta i\phi_f}\left(e^{\eta i\phi_x} - a_5\, e^{-\eta i\phi_x}\right) , \\
O^{\eta,\eta} &= 2\,\eta\, a_{11}a_{22}\, e^{\eta i(\phi_s+\phi_f)} , \\
O^{\eta,-\eta} &= 2\,\eta\, a_{11}a_{22}a_5\, e^{\eta i(\phi_s-\phi_f)} .
\end{aligned} \tag{F.16}$$

for $\eta = \pm$, with $\mathcal{J}_Y^\eta \equiv \mathcal{J}_Y^1 + \eta i \mathcal{J}_Y^2$; e.g. $\mathcal{J}_s^+ =: \psi^{1i\dagger}\psi_{2i} :$ and $\mathcal{J}_s^- =: \psi^{2i\dagger}\psi_{1i} :$. Here the a_5's arise from writing $a_{12}a_{22} = -a_{11}a_{21}a_5$, $a_{21}a_{22} = a_{11}a_{12}a_5$ and $a_{12}a_{21} = a_{11}a_{22}a_5$. We shall denote a ground state[1] with " a_5-parity" eigenvalue of $\eta_5 = \pm 1$ by $|0\rangle_{\eta_5}$, i.e. $a_5|0\rangle_{\eta_5} = \eta_5|0\rangle_{\eta_5}$. The two choices for η_5 are equivalent for our purposes (we continue to display the η_5-dependence, though, to verify explicitly that the value of η_5 does not matter).

F.3 Boundary Conditions for the ϕ_Y Bosons

Now, the boundary conditions (F.7) for $\mathcal{J}_c^0$, $\mathcal{J}_s^3$, $\mathcal{J}_f^3$ and $O^{3,3}$ immediately determine, via eq. (F.11), the following boundary conditions on the corresponding

boson fields:[2]

$$\phi_{cR} = \phi_{cL} + c_c\pi \ , \quad \phi_{sR} = \phi_{sL} + c_s\pi \ , \quad \phi_{fR} = \phi_{fL} + c_f\pi \ , \quad \phi_{xR} = -\phi_{xL} + c_x\pi \ . \tag{F.17}$$

The shifts parameterized by the constants c_Y are allowed, because they do not affect $i\partial_z\phi_{YL/R}(\tau \pm ix)$ for $x \neq 0$. The c_Y's are determined by the requirement that expressions (F.16) should be consistent with the two-point functions (F.5), or equivalently with the boundary conditions eq. (F.7), *when acting on the ground state* $|0\rangle_{\eta_5}$, i.e. when a_5 is replaced by η_5 in eq. (F.16). Thus, $\mathcal{J}_s^\eta$ and $\mathcal{J}_f^\eta$ pick up a factor $-\eta_5$ and η_5 when ϕ_x is replaced by $-\phi_x$. It is readily apparent that these factors can be neutralized and the relations (F.7) satisfied for *all* the currents in (F.16) by choosing the c_Y such that

$$e^{i\eta\pi(c_s+\eta' c_x)} = -\eta_5, \quad e^{i\eta\pi(c_f+\eta' c_x)} = \eta_5, \quad e^{i\eta\pi(c_s+\eta' c_f)} = -1 \ , \quad \text{for} \quad \eta,\eta' = \pm \ . \tag{F.18}$$

This can be realized by taking, for example,

$$c_s = \begin{cases} 1 \\ 0 \end{cases} , \quad c_f = \begin{cases} 0 \\ 1 \end{cases} , \qquad c_c = c_x = 0 \ , \qquad \text{for} \quad \eta_5 = \begin{cases} 1 \\ -1 \end{cases} \tag{F.19}$$

(which is the choice made by ML, who also implicitly take $\eta_5 = 1$). Thus, the ϕ_Y boson fields have extremely simple boundary conditions! As a check, ML

[2]Strictly speaking, the relation $\phi_{xR}(z^*) = -\phi_{xL}(z^*) + c_x\pi$ involves a somewhat sloppy notation, and the $-$ sign is to be understood as applying only to the z^*-*dependent* parts of the fields $\phi_{xL/R}$ [this is all that is required by the boundary condition $i\partial_{z^*}\phi_{xR} = -i\partial_z\phi_{xL}$]. The $-$ sign need not apply to the z^*-*independent* zero-modes $\phi_{xL,0}$ and $\phi_{xR,0}$. In fact, we shall choose them to be unaffected by the extra $-$ sign, so that in particular $[\phi_{xL}(\tau,x), \phi_{xR}(\tau,x')] = i\pi$ continues to hold, as in the second of eqs. (F.13). This is important to ensure that $\{\psi_L^{\alpha i\dagger}, \psi_s R^{\beta j}\} = 0$ continues to hold. – In general, questions of how various fields commute with each other can be tricky when fields with anomalous scaling dimensions are considered (compare footnote 4 on page 376), and are best settled by investigating the behavior of an explicitly known correlation function. That $\{\psi_L^{\alpha i\dagger}, \psi_s R^{\beta j}\} = 0$ follows, for example, from eq. (D.42) for $G^{(4)}$, in which the overall $-$ sign [needed to get agreement with the general expression (D.32)] arises from $\psi_{L2}\psi_{R3}^\dagger = -\psi_{R3}^\dagger\psi_{L2}$ [see the comment above eq. (D.42)].

calculated [ML95, appendix B] the exact partition function for the system in terms of these bosons, and found exact agreement with the result they had obtained previously by using the finite-size spectrum obtained through their fusion hypothesis.

As an aside, note that if one refermionizes by introducing a new set of fermion fields through $\tilde{\psi}^\dagger_Y \equiv a_Y e^{i\psi_Y}$ (this is done, for example, in Emery and Kivelson's treatment of the anisotropic 2-channel Kondo problem [EK92,SH95a]), they too have very simple boundary conditions:

$$\tilde{\psi}_{cL} = \tilde{\psi}_{cR} \ , \quad \tilde{\psi}_{sL} = e^{-i\pi c_s}\, \tilde{\psi}_{sR} \ , \quad \tilde{\psi}_{fL} = e^{-i\pi c_f}\, \tilde{\psi}_{fR} \ , \quad \tilde{\psi}_{xL} = e^{-i\pi c_x}\, \tilde{\psi}^\dagger_{xR} \ . \quad \text{(F.20)}$$

In fact, for the anisotropic 2-channel Kondo problem, the result that $\tilde{\psi}_{xL} \propto \tilde{\psi}^\dagger_{xR}$ was also found by Schiller and Hershfield [SH95b], using the Emery-Kivelson theory.

F.4 Origin of Non-Fermi-Liquid Exponent $\Delta = \frac{1}{2}$

The fact that ϕ_{xR} has a $-$ relative to ϕ_{xL} immediately explains the mysterious "orthogonality" of $\psi^{\alpha j\dagger}_L(z_1)$ and $\psi_{R\bar{\alpha}\bar{j}}(z_2^*)$ at the boundary: consider the following OPE,

$$\begin{aligned} \psi^{\alpha j\dagger}_L(z_1)\psi_{L/R\bar{\alpha}\bar{j}}(z_2^*) \ &\propto \ e^{\frac{i}{2}(\phi_c+\alpha\phi_s+j\phi_f+\alpha j\phi_x)_L(z_1)}\ e^{-\frac{i}{2}(\phi_c+\bar{\alpha}\phi_s+\bar{j}\phi_f\pm\bar{\alpha}\bar{j}\phi_x)_L(z_2^*)} \\ &= \ \frac{e^{\frac{i}{2}\left[(\phi_c+\alpha\phi_s+j\phi_f+\alpha j\phi_x)_L(z_1)-(\phi_c+\bar{\alpha}\phi_s+\bar{j}\phi_f\pm\bar{\alpha}\bar{j}\phi_x)_L(z_2^*)\right]}}{(z_1-z_2^*)^{\frac{1}{4}(1+\alpha\bar{\alpha}+j\bar{j}\pm\alpha\bar{\alpha}j\bar{j})}} + \ldots \ , \end{aligned} \quad \text{(F.21)}$$

where we used eq. (F.15), and the vertex operator OPE (E.13). Whereas for $\psi^{\alpha j\dagger}_L\psi_{L\bar{\alpha}\bar{j}}$, one gets the usual leading term $\delta^\alpha_{\bar{\alpha}}\delta^j_{\bar{j}}(z_1-z_2^*)^{-1}$, for $\psi^{\alpha j\dagger}_L\psi_{R\bar{\alpha}\bar{j}}$ the leading term is always proportional to $(z_1-z_2^*)^{-1/2}$, for all combinations of $\alpha, \bar{\alpha}, j, \bar{j}$

(actually, it even is $(z_1 - z_2^*)^{1/2}$ for $\alpha \neq \bar{\alpha}$ and $j \neq \bar{j}$). Thus, the $-$ sign in $\phi_{xR} = -\phi_{xL} + c_x\pi$ is responsible for the fact that identity operator cannot occur in the BOPE of $\psi_L^{\alpha j\dagger}$ and $\psi_{R\bar{\alpha}\bar{j}}$.

In addition, we see from this argument that since they all occur together with $(z_1 - z_2^*)^{-1/2} \equiv (z_1 - z_2^*)^{-(1-\Delta)}$, *all the leading operators that* **do** *occur in the BOPE of* $\psi_L^{\alpha j\dagger}$ *and* $\psi_{R\bar{\alpha}\bar{j}}$ *have scaling dimension* $\Delta = \frac{1}{2}$, *which is precisely the anomalous non-Fermi-liquid exponent* for which the 2-channel Kondo problem is famous, and which plays such an important role in this thesis. This is the simplest argument I know of for understanding the origin of the $\Delta = \frac{1}{2}$ exponent. In section F.6, we derive explicit expressions for these boundary operators.

F.5 The Spinor-Electron field $S^{\alpha i\dagger}$

With the boundary conditions for the ϕ_Y-bosons in hand, we are now able to define in an explicit way a field $S^{\alpha i\dagger}$ that has the desired property (F.3), namely:

$$S^{\alpha j\dagger}[\phi_c, \phi_s, \phi_f, \phi_x] \equiv \psi^{\alpha j\dagger}[\phi_c,\ \phi_s - c_s\pi,\ \phi_f - c_f\pi,\ -\phi_x + c_x\pi] \tag{F.22}$$

$$= e^{-\frac{i}{2}\pi(\alpha c_s + j c_f - \alpha j c_x)} a_{\alpha j} e^{\frac{i}{2}(\phi_c + \alpha\phi_s + j\alpha_f - \alpha j\phi_x)} ,$$

$$= -i \begin{pmatrix} a_{11}\, e^{\frac{i}{2}(\phi_c+\phi_s+\phi_f-\phi_x)} \\ -\eta_5\, a_{21}\, e^{\frac{i}{2}(\phi_c-\phi_s+\phi_f+\phi_x)} \\ \eta_5\, a_{12}\, e^{\frac{i}{2}(\phi_c+\phi_s-\phi_f+\phi_x)} \\ -\, a_{22}\, e^{\frac{i}{2}(\phi_c-\phi_s-\phi_f-\phi_x)} \end{pmatrix} = -i \begin{pmatrix} a_{11}\, e^{\frac{i}{2}(\phi_{11}+\phi_{21}+\phi_{12}-\phi_{22})} \\ -\eta_5\, a_{21}\, e^{\frac{i}{2}(\phi_{11}+\phi_{21}-\phi_{12}+\phi_{22})} \\ \eta_5\, a_{12}\, e^{\frac{i}{2}(\phi_{11}-\phi_{21}+\phi_{12}-\phi_{22})} \\ -\, a_{22}\, e^{\frac{i}{2}(-\phi_{11}+\phi_{21}+\phi_{12}-\phi_{22})} \end{pmatrix} \tag{F.23}$$

where for eq. (F.23) we implemented the choices eq. (F.19). The definition (F.22) is purposefully constructed in such a way that the boson boundary conditions eq. (F.17) imply the desired relation eq. (F.3), namely

$$S_R^{\alpha i\dagger}(z^*) = \psi_L^{\alpha i\dagger}(z^*) , \qquad \text{and also} \qquad S_L^{\alpha i\dagger}(z) = -\psi_R^{\alpha i\dagger}(z) . \tag{F.24}$$

[where $S_{L/R} \equiv S[\phi_{YL/R}]$, etc.]. Note that when expressed in terms of the original $\varphi_{\alpha i}$ bosons, $S^{\alpha i\dagger}$, in contrast to $\psi^{\alpha i\dagger}$ [see eq. (F.14)] does not reduce to a simple form.[3] This means that $S^{\alpha i\dagger}$ cannot be expressed in terms of free fermions (in a sense, it is a product of "square roots" of fermion fields). Nevertheless, it is a well-defined object, not any more esoteric than the fields used in Emery and Kivelson's approach to the anisotropic 2-channel Kondo problem [EK92].

What are the properties of $S^\dagger$?

Quantum numbers: First and foremost, since the only essential difference between $S^{\alpha j\dagger}$ and $\psi^{\alpha j\dagger}$ is $\phi_x \to -\phi_x$, they have the *same* (Q, j_z, f_z) quantum numbers [eigenvalues of $(\mathcal{J}_c^o, \mathcal{J}_s^3, \mathcal{J}_f^3)$, obtainable via the OPE (E.14)], namely $(1, \alpha\frac{1}{2}, j\frac{1}{2})$, with $\alpha, j = \pm$ [compare eqs. (F.14) and (F.23)]. Thus $S^{\alpha j\dagger}$ *carries the same units of charge, spin and flavor as a free fermion* (even though in a way that is not possible in a free fermion theory). This, then, is the key to the resolution to the unitarity paradox: the free electron simply scatters into a "non-free-electron" excitation with the same charge, spin and flavor quantum numbers. Merely the

[3]The second equality in (F.23) is responsible for the name "spinor" that ML chose for $S^\dagger$. Let $\vec{H} \equiv (H_1, H_2, H_3, H_4)$ be four Cartan (i.e. mutually commuting) generators of the group $SU(4)$ that mixes the components of $\psi^{\alpha i\dagger}$ among themselves. A representation in which the states have $\vec{H}$-eigenvalues (called "weights") of the form $(1,0,0,0), \ldots, (0,0,0,1)$ is called a *vector* representation of $SU(4)$, whereas one with eigenvalues of the form $\frac{1}{2}(\eta_1, \eta_2, \eta_3, \eta_4)$, where $\eta_i = \pm 1$, is called a *spinor* representation. (Actually, two different spinor representations are possible, distinguished by $\eta_1\eta_2\eta_3\eta_4 = \pm 1$.) If one chooses as Cartan generators the four currents $i\partial_z(\varphi_{11}, \varphi_{21}, \varphi_{12}, \varphi_{22})$, then eqs. (F.14) and (F.23) show that $\psi^\dagger$ and $S^\dagger$ transform respectively in the vector and spinor representations (the latter with $\eta_1\eta_2\eta_3\eta_4 = -1$) of $SU(4)$. This is why $S^\dagger$ was christened a "spinor" by ML (actually, they considered the larger group $SO(8)$ of transformations of the eight components of $(\psi^{\alpha i\dagger}, \psi^{\alpha i})$, which has $SU(4)$ as a subgroup – a thorough discussion of the properties of $SO(8)$ and related groups can be found in [Geo82]). — On the other hand, if one chooses as Cartan generators the four currents $\vec{H} = i\partial_z(\phi_c, \phi_s, \phi_f, \phi_x)$, then eqs. (F.14) and (F.23) show that *both* $\psi^\dagger$ and $S^\dagger$ transform in spinor representations (with $\eta_{11}\eta_{21}\eta_{12}\eta_{22} = +1$ and -1, respectively). This is the underlying reason for eq. (F.25) below, which shows that $S^\dagger$ and $\psi^\dagger$ transform (almost) identically under $U(1)_c \times SU(2)_s \times S(2)_f$; the essential difference between the two, namely ϕ_x vs. $-\phi_x$, only shows up for the non-$U(1)_c \times SU(2)_s \times S(2)_f$ transformations of $SU(4)$, namely those generated by $O^{a,A}$.

$i\partial_z\phi_x$ quantum number changes, which is not associated with a physically relevant observable.

Transformation properties: Also of interest are the transformation properties of $S^\dagger$ under $U(1)_c \times SU(2)_s \times S(2)_f$ transformations. These can be read off, according to eq. (B.26), from the most singular term of the OPEs of the various generators $\mathcal{J}^{\tilde{a}}_{YR}$ of this group with $S^\dagger_R$. These OPEs can be obtained from those of $\mathcal{J}^{\tilde{a}}_{YL}$ with $\psi^\dagger_L$ [given in eq. (E.22)] as follows,[4] for $_Y = s, f$:

$$\mathcal{J}^{\tilde{a}}_{RY}(z_1^*)S^{\alpha i\dagger}_R(z_2^*) = \eta^{\tilde{a}}\mathcal{J}^{\tilde{a}}_{LY}(z_1^*)\psi^{\alpha i\dagger}_L(z_2^*) \;= \frac{\eta^{\tilde{a}}\psi^{\beta j\dagger}_L(z_2^*)(T^{\tilde{a}}_Y)^{\alpha i}_{\beta j}}{z_1^*-z_2^*} = \frac{\eta^{\tilde{a}}(T^{*\tilde{a}}_Y)^{\alpha i}_{\beta j}\; S^{\beta j\dagger}_R(z_2^*)}{z_1^*-z_2^*} \tag{F.25}$$

where $\eta^{\tilde{a}} = (\eta^1,\eta^2,\eta^3) = (-1,-1,1)$. For the first equality, we used firstly $S^\dagger_R = \psi^\dagger_L$ [eq. (F.24)] and secondly the fact that when acting on the subspace $a_{\alpha i}|0\rangle_{\eta_5}$ (applicable for $S^\dagger$ and $\psi^\dagger$), eq. (F.7) becomes modified to $\mathcal{J}^{\tilde{a}}_{RY}(z^*) = \eta^{\tilde{a}}\eta_Y\mathcal{J}^{\tilde{a}}_{LY}(z^*)$ (with $\eta_s = \eta_f = 1$). The extra factor $\eta^{\tilde{a}}$ deserves explanation: the phase factors $e^{ic_Y\pi}$ were chosen in such a way that the currents $\mathcal{J}^\eta_{LY}$ and $\mathcal{J}^\eta_{RY}$ (for $\eta = \pm, _Y = s, f$) are equal at the boundary when acting on the groundstate $|0\rangle_{\eta_5}$, where $a_5 = \eta_5$. However, here they act on the subspace $a_{\alpha i}|0\rangle_{\eta_5}$, on which a_5 has eigenvalue $-\eta_5$ [see discussion after eq. (E.19)]. Hence there is an extra $-$ sign between $\mathcal{J}^\pm_{YL}$ and $\mathcal{J}^\pm_{YR}$ in eq. (F.16) when acting on this subspace [and hence too for $\mathcal{J}^{1,2}_Y$, but not for $\mathcal{J}^3$] which is the reason for the factor $\eta^{\tilde{a}}$ in eq. (F.25).

[4]The result (F.25) can also be checked directly by calculating these OPEs using eqs. (F.16) and (E.13). For example, consider $\mathcal{J}^-_s = \mathcal{J}^1_s - i\mathcal{J}^2_s$, for which $\eta^{\tilde{a}} = -1$: writing eqs. (F.16) and (F.23) in the notation of eqs. (E.12) to (E.14), and setting $a_5 = -\eta_5$, we have:

$$\begin{aligned}\mathcal{J}^-_{Rs}(z_1^*)S^{11\dagger}_R(z_2^*) &= -a_{11}a_{21}V^{(s)}_{-1}\Big(V^{(x)}_{-1} - a_5V^{(x)}_{+1}\Big)_R(z_1^*)\;(-ia_{11})\Big(V^{(c)}_{\frac12}V^{(s)}_{\frac12}V^{(f)}_{\frac12}V^{(x)}_{-\frac12}\Big)_R(z_2^*)\\ &= \;-i\,a_{21}\eta_5\frac{1}{[(z_1^*-z_2^*)^{\frac12}]^2}\Big(V^{(c)}_{\frac12}V^{(s)}_{-\frac12}V^{(f)}_{\frac12}V^{(x)}_{\frac12}\Big)_R(z_2^*) + \ldots \;=\; \frac{-S^{21\dagger}_R(z_2^*)}{(z_1^*-z_2^*)} + \ldots\,,\end{aligned}$$

which agrees with eq. (F.25), as do all other such calculations.

For the second equality in eq. (F.25), we used the standard OPE of $\mathcal{J}_Y^{\tilde{a}}$ with $\psi^\dagger$, namely eq. (E.22), and again $S_R^\dagger = \psi_L^\dagger$ for the third.

The extra factor of $\eta^{\tilde{a}}$ in eq. (F.25) implies that $S^\dagger$ does not quite transform in a "standard" way, but it is easy to construct an object that does: Using the Pauli-matrix identities

$$\eta^a \tilde{\varepsilon}_{\bar{\alpha}\alpha} (\sigma^{a*})^\alpha_{\ \beta} \tilde{\varepsilon}^{\beta\bar{\beta}} = -(\sigma^a)^{\ \bar{\beta}}_{\bar{\alpha}} \qquad \text{where} \quad \tilde{\varepsilon}_{\bar{\alpha}\alpha} = \begin{pmatrix} 0 & 1 \\ 1 & 0 \end{pmatrix}_{\bar{\alpha}\alpha} , \tag{F.26}$$

and a similar one for $(\sigma^{a*})^i_{\ j}$, we conclude from eq. (F.25) that the object $\tilde{\varepsilon}_{\bar{\alpha}\alpha}\tilde{\varepsilon}_{\bar{i}i} S^{\alpha i\dagger}$ *does* transform in a standard way:

$$\begin{aligned} \mathcal{J}^a_{sR}(z_1^*) \left[\tilde{\varepsilon}_{\bar{\alpha}\alpha}\tilde{\varepsilon}_{\bar{i}i} S_R^{\alpha i\dagger}(z_2^*)\right] &= -\tfrac{1}{z_1^* - z_2^*} (T^a)^{\ \bar{\beta}}_{\bar{\alpha}} \left[\tilde{\varepsilon}_{\bar{\beta}\alpha}\tilde{\varepsilon}_{\bar{i}i} S_R^{\alpha i\dagger}(z_2^*)\right] , \\ \mathcal{J}^a_{fR}(z_1^*) \left[\tilde{\varepsilon}_{\bar{\alpha}\alpha}\tilde{\varepsilon}_{\bar{i}i} S_R^{\alpha i\dagger}(z_2^*)\right] &= -\tfrac{1}{z_1^* - z_2^*} (T^a)^{\ \bar{j}}_{\bar{i}} \left[\tilde{\varepsilon}_{\bar{\alpha}\alpha}\tilde{\varepsilon}_{\bar{j}i} S_R^{\alpha i\dagger}(z_2^*)\right] . \end{aligned} \tag{F.27}$$

Finally, this result allows us to establish how $S^{\alpha i\dagger}$ can be represented in terms of the charge, spin and flavor fields $e^{i\phi_c/2}$, $\mathbf{g}$ and $\mathbf{h}$ introduced in appendix D, where, according to eq. (D.5), $\psi^{\alpha i\dagger} = e^{i\phi_c/2}\mathbf{g}^{\alpha\dagger}\mathbf{h}^{i\dagger}$. We merely have to form a combination of these fields that has the same $U(1)c \times SU(2)_s \times SU(2)_f$ transformation properties as $S^{\alpha i\dagger}$. Now, since $e^{i\phi_c/2}\mathbf{g}_{\bar{\alpha}}\mathbf{h}_{\bar{\imath}}$ in fact transforms precisely according to eq. (F.27), we conclude that $S^{\alpha i\dagger}$ can be represented as

$$S^{\alpha i\dagger} = -i\, \tilde{\varepsilon}^{\alpha\beta}\tilde{\varepsilon}^{ij}\, e^{i\phi_c/2} g_\beta h_j \ . \tag{F.28}$$

These expressions again illustrate the non-free-fermion nature of $S^{\alpha i\dagger}$ rather dramatically. Since $\mathbf{g}$ and $\mathbf{h}$ are annihilation operators, $S^{\uparrow 1\dagger}$ can evidently be represented as a combination of a "channel-particle" excitation $e^{i\phi_c/2}$, a "spin $\downarrow$-hole" excitation $\tilde{\varepsilon}^{\alpha\bar{\alpha}}\mathbf{g}_{\bar{\alpha}}$ (which gives it spin $\uparrow$) and a "flavor-2 hole" excitation $\tilde{\varepsilon}^{i\bar{i}}\mathbf{g}_{\bar{i}}$ (which gives it flavor 1). Such "particle-hole-hole" fields cannot exist in a theory of free fermions.

Correlation Functions: Since $S^\dagger$ is known explicitly in terms of free bosons, all correlation functions in which it appears can be calculated. However, a number of such functions can directly be obtained from the one already calculated in appendix D, namely

$$G^{(4)}(z_1, z_2, z_3^*, z_4^*) \equiv \langle \psi_{L\alpha i}(z_1) \psi_L^{\bar{\beta}\bar{j}\dagger}(z_2) \psi_{R\beta j}(z_3^*) \psi_R^{\bar{\alpha}\bar{i}\dagger}(z_4^*) \rangle \ , \tag{F.29}$$

which, by eq. (F.24), can also be written as

$$G^{(4)}(z_1, z_2, z_3^*, z_4^*) = \langle \psi_{L\alpha i}(z_1) \psi_L^{\bar{\beta}\bar{j}\dagger}(z_2) S_{L\beta j}(z_3^*) S_L^{\bar{\alpha}\bar{i}\dagger}(z_4^*) \rangle \ . \tag{F.30}$$

For example, consider the following function:

$$\begin{aligned} \tilde{G}^{(4)}(z_1, z_2, z_3^*, z_4^*) &\equiv \langle \psi_{L\alpha i}(z_1) S_L^{\bar{\alpha}\bar{i}\dagger}(z_2) S_R^{\bar{\beta}\bar{j}\dagger}(z_3^*) \psi_{R\beta j}(z_4^*) \rangle & \text{(F.31)} \\ &= -\langle \psi_{L\alpha i}(z_1) S_L^{\bar{\alpha}\bar{i}\dagger}(z_2) \psi_L^{\bar{\beta}\bar{j}\dagger}(z_3^*) S_{L\beta j}(z_4^*) \rangle & \text{(F.32)} \\ &= -G^{(4)}(z_1, z_3^*, z_4^*, z_2) \ , & \text{(F.33)} \end{aligned}$$

Here eq. (F.24) was used to obtain the second line, and comparison with eq. (F.30) yields the third. Thus $\tilde{G}^{(4)}$ is completely determined by $G^{(4)}$. In particular, the bulk limit $z_1 \to z_2$ for $\tilde{G}^{(4)}(z_1, z_2, z_3^*, z_4^*)$ yields the bulk OPE of $\psi_L(z_1)$ and $S_L^\dagger(z_2^*)$. This corresponds to the boundary limit $z_1 \to z_4^*$ for $G^{(4)}(z_1, z_2, z_3^*, z_4^*)$, which does not contain the identity operator (see eq. (D.36) and table D.1). Hence, ψ_L and $S_L^\dagger$ are "orthogonal" in the bulk limit. On the other hand, the boundary limit $z_1 \to z_3^*$ for $\tilde{G}^{(4)}(z_1, z_2, z_3^*, z_4^*)$ corresponds to the bulk limit $z_1 \to z_2$ for $\tilde{G}^{(4)}(z_1, z_2, z_3^*, z_4^*)$. Since in the latter the OPE of $\psi_L(z_1)$ and $\psi_L^\dagger(z_2)$ does contain unity, so does the BOPE of $\psi_L(z_1)$ and $S_R^\dagger(z_3^*)$; this, of course, simply reflects the requirement (F.3) according to which $S_R^\dagger$ was constructed.

F.6 The Boundary Operators Φ_s^a and Φ_f^A

Having found explicit expressions for $\psi_L^\dagger$ and $\psi_R^\dagger$ in terms of the ϕ_Y bosons, it is straightforward to also express the boundary operators $\phi_s^a(\tau)$ and $\phi_f^A(\tau)$, introduced in appendix D, in terms of the ϕ_Y. To avoid confusion with the boson fields, we denote them here by Φ_s^a and Φ_f^A.

The strategy is simple: by contracting the BOPE (D.36) with $(T^a)_\beta^\beta \delta_{\bar{j}}^{\ j}$ or $\delta_{\bar{\beta}}^\beta (\tilde{T}^A)_{\bar{j}}^{\ j}$ [or according to footnote 15 on page 387] it follows that the boundary operators Φ_s^a and Φ_f^A must be given by the leading non-zero terms in the boundary limit $z_1 \to z_2^*$ of the following two expressions:

$$\psi_L^{\bar{\beta}j\dagger}(z_1)\,(T^a)_{\bar{\beta}}^{\ \beta}\,\psi_{R\beta j}(z_2^*) \;=\; \frac{-(C_{\psi s}^K)^*}{(iz_{12}^*)^{(1-\Delta_s)}}\Phi_s^a(\tau_1) \;+\ldots\,, \tag{F.34}$$

$$\psi_L^{\beta\bar{j}\dagger}(z_1)\left(\tilde{T}^A\right)_{\bar{j}}^{\ j}\,\psi_{R\beta j}(z_2^*) \;=\; \frac{-(C_{\psi f}^K)^*}{(iz_{12}^*)^{(1-\Delta_f)}}\Phi_f^a(\tau_1) \;+\ldots\,, \tag{F.35}$$

where the constants $C_{\psi s}^K$ and $C_{\psi f}^K$ are to be chosen such that Φ_s^a and Φ_f^A are hermitian and normalized to unity, and $\Delta_{s/f}$ are their scaling dimensions.

These expressions can be evaluated by simply inserting into them the explicit expressions (F.14) for $\psi_L^\dagger$ and ψ_R in terms of the ϕ_{YL} and ϕ_{YR} bosons and using boundary condition (F.17) to express the ϕ_{YR}'s in terms of the ϕ_{YL}'s. The limit $z_1 \to z_2^*$ can then be evaluated with the aid of the vertex operator OPE (E.13). As shown in eq. (F.21), this always produces a factor $(z_{12}^*)^{-\frac{1}{4}(1+1+1-1)} = (z_{12}^*)^{-\frac{1}{2}}$ [the all-important change in sign for the fourth exponent from $-\frac{1}{2}$ to $\frac{1}{2}$ is a consequence of $\phi_{xR} = -\phi_L + c_x\pi$], and implies that $\Delta_s = \Delta_f = \frac{1}{2}$, in agreement with the results of appendix D (see table D.1). One readily finds the following explicit expressions, where $\Phi_Y^\pm \equiv \Phi_Y^1 \pm i\Phi^2$:

$$
\begin{aligned}
\Phi_s^3 &= p\,\tfrac{1}{\sqrt{2}}\left(e^{i\phi_{xL}} + \eta_5\, e^{-i\phi_{xL}}\right) , \\
\Phi_s^+ &= -p\,\eta_5 a_{11} a_{21}\,\tfrac{1}{\sqrt{2}}(1 - a_5\eta_5) e^{i\phi_{sL}} , \\
\Phi_s^- &= -p\, a_{11} a_{21}\,\tfrac{1}{\sqrt{2}}(1 - a_5\eta_5) e^{-i\phi_{sL}} , \\
\Phi_f^3 &= ip\,\tfrac{1}{\sqrt{2}}\left(e^{i\phi_{xL}} - \eta_5\, e^{-i\phi_{xL}}\right) , \\
\Phi_f^+ &= ip\,\eta_5 a_{11} a_{12}\,\tfrac{1}{\sqrt{2}}(1 - a_5\eta_5) e^{i\phi_{fL}} , \\
\Phi_f^- &= -ip\, a_{11} a_{12}\,\tfrac{1}{\sqrt{2}}(1 - a_5\eta_5) e^{-i\phi_{fL}} .
\end{aligned}
\tag{F.36}
$$

The normalization factor $\frac{1}{\sqrt{2}}$ that has been inserted implies $|C^B_{\psi k}|^2 = |C^B_{\psi k}|^2 = 2$, in agreement with table D.1. The phases p and ip have to ensure that Φ^a_s and Φ^A_f are hermitian,[5] and can be chosen, for example, to be $p = 1$ or i for $\eta_5 = 1$ or -1.

Note the peculiar fact that $\Phi^\pm_Y \neq 0$ only when acting on a subspace for which $a_5 = -\eta_5$. This turns out to be an inevitable consequence of the relations (F.18) [i.e. independent of specific choice (F.19)], which in turn are an inevitable consequence of the L-R 2-point functions eq. (F.5), as argued after eq. (F.17). However, for the correlation functions of interest to us, namely $\langle \psi_L \psi^\dagger_L \psi_R \psi^\dagger_R \rangle$ in appendix D and $\langle \psi_R \vec{\mathcal{J}}_s \cdot \vec{\Phi}_s \psi^\dagger_L \rangle$ in chapter 8, $\Phi^{\tilde{a}}_Y$ indeed *does* act on the subspace $a_{\alpha i}|0\rangle_{\eta_5}$ where $a_5 = -\eta_5$, so that this peculiarity is not something to be concerned about.

The boundary fields Φ^a_s and Φ^A_f should transform as spin-1, flavor-singlet and spin-singlet, flavor-1 fields, respectively, under $SU(2)_s \times SU(2)_f$ transformations. This means that they should have the following OPEs with the currents $\mathcal{J}^a_{sL}$ and

[5] Note that the extra factor of i in p vs. ip for Φ^a_s and Φ^A_f implies that $C^B_{\psi s}$ and $C^B_{\psi f}$ differ by a factor i, in agreement with footnote 20 on page 391.

$\mathcal{J}^A_{fL}$:[6]

$$\begin{aligned}
\mathcal{J}^3_{YL}(z)\Phi^\pm_Y(\tau') &= \tfrac{\pm 1}{z-\tau'}\Phi^\pm_Y(\tau')\,, \qquad \mathcal{J}^3_{YL}(z)\Phi^3_Y(\tau') = \mathcal{J}^\pm_{YL}(z)\Phi^\pm_Y(\tau') = 0\,, \\
\mathcal{J}^\pm_{YL}(z)\Phi^3_Y(\tau') &= \tfrac{\mp 1}{z-\tau'}\Phi^\pm_Y(\tau')\,, \qquad \mathcal{J}^\pm_{YL}(z)\Phi^\mp_Y(\tau') = \tfrac{\pm 2}{z-\tau'}\Phi^3_Y(\tau')\,.
\end{aligned} \tag{F.37}$$

It can readily be verified (using the method of footnote 4) that for $a_5 = -\eta_5$, the expressions (F.36) for Φ^a_Y and (F.16) for $\mathcal{J}^a_Y$ (using the ϕ_{YL} bosons in the latter) do indeed give precisely these OPEs, which is a satisfying consistency check.

Finally, note that the descendents $\left(\mathcal{J}^{\tilde{a}}_{-nY}\Phi^{\tilde{a}'}_Y\right)$ of the boundary operators can be obtained just as easily. According to eq. (B.33) (and Cauchy's theorem), the n-th descendent is simply the term proportional to $(z-\tau')^{-(n+1)}$ in the OPE of $\mathcal{J}^{\tilde{a}}_Y(z)$ with $\Phi^{\tilde{a}'}_Y(\tau')$. The most important descendents for the Kondo problem are the leading irrelevant operators $\mathcal{J}^a_{-1s}\Phi^a_s$ and $\mathcal{J}^a_{-1f}\Phi^a_f$ of dimension $\frac{3}{2}$ (see section D.5). From eqs. (F.16), (F.36) and the subleading term in the general vertex operator OPE (E.13), one readily finds[7]

$$\begin{aligned}
\left(\mathcal{J}^a_{-1s}\Phi^a_s\right)(\tau) &= 3\,i\partial_z\phi_{sL}\,\Phi^a_s(\tau) = 3\,i\partial_z\phi_{sL}\,p^{\frac{1}{2}}\left(e^{i\phi_{xL}} + \eta_5\,e^{-i\phi_{xL}}\right)(\tau)\,, \\
\left(\mathcal{J}^A_{-1f}\Phi^A_f\right)(\tau) &= 3\,i\partial_z\phi_{fL}\,\Phi^a_f(\tau) = 3\,i\partial_z\phi_{fL}\,ip^{\frac{1}{2}}\left(e^{i\phi_{xL}} - \eta_5\,e^{-i\phi_{xL}}\right)(\tau)\,.
\end{aligned} \tag{F.38}$$

Thus, these important operators, too, have simple representations in terms of the ϕ_Y boson fields.

In conclusion, it is worth emphasizing that the approach described above is essentially a reduction of the Kondo problem to a problem of free bosons

[6]The relations eq. (F.37) follow from eq. (B.26) and the standard relations for the spin-1 representation of $SU(2)$; alternatively, they can be obtained directly from the general OPE eq. (A.47) for two bilinear fermionic currents, using the definitions (F.4) for the currents, (F.34) and (F.35) for Φ^a_s and Φ^A_f, and the property $[T^a, T^b] = i\varepsilon^{abc}T^c$.

[7]Alternatively, one can check that the sum $\left(\mathcal{J}^a_{-1s}\Phi^a_s\right) + \left(\mathcal{J}^A_{-1f}\Phi^A_f\right)$ is the leading term in $\psi^{\beta j\dagger}_L(z_1)\psi_{R\beta j}(z_2^*)$ in the limit $z_1 \to z_2$, in agreement with table D.1, according to which these are the first operators in the BOPE of $\psi^{\bar{\beta}\bar{j}\dagger}_L(z_1)\psi_{R\beta j}(z_2^*)$ with tensor structure $\delta^{\bar{\beta}}_{\beta}\delta^{\bar{j}}_{j}$.

with known boundary conditions. This is a very remarkable simplification. All operators of interest have simple representations in terms of the free bosons, and hence the problem of calculating correlation functions is reduced to an exercise in free-boson theory. (In practice, though, such exercises are often most conveniently dealt with by using conformal methods nevertheless, for example by exploiting conformal invariance when calculating a 3-point function such as $\langle \psi_R \vec{\mathcal{J}}_s \cdot \vec{\Phi}_s \psi_L^\dagger \rangle$.)

References

[Aff86a] I. Affleck, Phys. Rev. Lett. **56**, 746 (1986).

[Aff86a] I. Affleck, Nucl. Phys. B **265**, 409 (1986).

[Aff90] I. Affleck, Nucl. Phys. **B336**, 517 (1990).

[AL91a] I. Affleck and A. W. W. Ludwig, Nucl. Phys. **B352**, 849 (1991).

[AL91b] I. Affleck and A. W. W. Ludwig, Nucl. Phys. **B360**, 641 (1991).

[AL91c] I. Affleck and A. W. W. Ludwig, Phys. Rev. Lett. **67**, 161 (1991).

[AL91d] I. Affleck and A. W. W. Ludwig, Phys. Rev. Lett. **67**, 3160 (1991).

[AL92a] I. Affleck and A. W. W. Ludwig, Phys. Rev. Lett. **68**, 1046 (1992).

[AL92b] I. Affleck, A. W. W. Ludwig, H.-B. Pang and D. L. Cox, Phys. Rev. **B45**, 7918 (1992).

[AL93] I. Affleck and A. W. W. Ludwig, Phys. Rev. **B48**, 7297 (1993).

[AL94] I. Affleck and A. W. W. Ludwig, Nucl. Phys. **B428**, 545 (1994).

[ABI90] D. Altschüler, M. Bauer and C. Itzykson, Comm. Math. Phys. **132**, 349 (1990).

[AS89] B. L. Al'tshuler and B. Z. Spivak, Pis'ma Zh. Eksp. Teor. Fiz. **49**, 671 (1989) [JETP Lett. **49**, 772 (1989)].

[And70] P. W. Anderson, J. Phys. C., **3**, 2436 (1970), P. W. Anderson and G. Yuval, *Magnetism*, Vol. **5**, Chapter 7, G.T. Rado and H. Suhl, eds. Academic Press, New York, (1973).

[AHV72,Phil72] P. W. Anderson, B. I. Halperin and C. M. Varma, Philos. Mag. **25**, 1 (1972); W. A. Phillips, J. Low Temp. Phys. **7**, 351 (1972).

[AYH70] P. W. Anderson, G. Yuval and D.R. Hamann, Phys. Rev. B **1**, 4464 (1970).

[AT91] B. Andraka and A. M. Tsvelik, Phys. Rev. Lett. **67**, 2886 (1991)

[AD84] N. Andrei and C. Destri, Phys. Rev. Lett. **52**, 364 (1984).

[Bate54] Bateman Manuscript Project, Tables of Integral Transforms, Vol. 1, Mc Graw Hill (1954).

[Berg84] G. Bergmann, Phys. Rep. **107**, 1 (1984).

[BH72] K. Binder and P. C. Hohenberg, Phys. Rev. B **6**, 3461 (1972).

[Bic87] N. E. Bickers, Rev. Mod. Phys. **59**, 845 (1987).

[BPZ84] A. A. Belavin, A. M. Polyakov and A. B. Zamolodchikov, Nucl. Phys. **B241**, 333 (1984).

[BVZ82] J. L. Black, K. Vladàr and A. Zawadowski, Phys. Rev. B **26**, 1559 (1982).

[BCN86] H. W. J. Blöte, J. L. Cardy and M. P. Nightingale, Phys. Rev. Lett. **56**, 742 (1986).

[Born64] M. Born, *Principles of Optics,* MacMillan Company, N.Y. (1964), p. 396.

[BLS94] P. Bouwknegt, A. W. W. Ludwig and K. Schoutens, (a) "Affine and Yangian Symmetries in $SU(2)_1$ Conformal Field Theory", Lectures given at the 1994 Trieste Summer School on High Energy Physics and Cosmology, Trieste, July 1994, hep-th/9412199; (b) Phys. Lett. **338B**, 448 (1994); (c) "Spinon basis for higher level SU(2) WZW models", hep-th/9412108; (d) "Spinon basis for $\hat{sl}_2$ integrable highest weight modules and new character formulas", hep-th/9504074.

[CKLM94] C. G. Callan, I. G. Klebanov, A. W. W. Ludwig and J. M. Maldacena, Nucl. Phys. **B422**, 417 (1994).

[Car84a] J. L. Cardy, J. Phys. A **17**, L385 (1984).

[Car84b] J. L. Cardy, Nucl. Phys. **B240**, 514 (1984).

[Car86a] J. L. Cardy, Nucl. Phys. **B270**, 186 (1986).

[Car86b] J. L. Cardy, Nucl. Phys. **B275**, 200 (1986).

[Car87] J. L. Cardy, in "Phase Transitions", **11**, ed. Domb. and Lebowitz), p. 55 (1987), Academic Press, London.

[Car89] J. L. Cardy, Nucl. Phys. **B324**, 581 (1989).

[CL91] J. L. Cardy and D. C. Lewellen, Phys. Lett. B, **259**, 274 (1991).

[CH93] P.Christe and M. Henkel, "Introduction to Conformal Field Theory and Its Applications to Critical Phenomena" (1993), Springer Verlag, New York.

[Cox87] D. L. Cox, Phys. Rev. Lett. **59**, 1240 (1987); Physica (Amsterdam) **153-155C**, 1642 (1987); J. Magn. Magn **76 &77**, 53 (1988).

[CR93] D. L. Cox and A. E. Ruckenstein, Phys. Rev. Lett. **71**, 1613 (1993).

[Cox95] D. L. Cox, private communication.

[CJJ89] D. L. Cox, M. Jarrell, C. Jayaprakash, H. R. Krishna-murthy, and J. Deisz, Phys. Rev. Lett. **B62**, 2188 (1989).

[CZ95] D. L. Cox and A. Zawadowski, Review Article: "Exotic Kondo Effects in Real Materials", to be published (1995).

[CLN80] D. M. Cragg, P. Lloyd and P. Nozières, J. Phys. **13**, 245 (1980).

[Die86] H. W. Diehl, in *Phase Transitions and Critical Phenomena*, Vol. 10, eds. C. Domb and J. L. Lebowitz, Academic Press, N.Y., (1986).

[DD81] H. W. Diehl and S. Dietrich, Z. Phys. B **42**, 65 (1981).

[DF84] V. S. Dotsenko and V. A. Fateev, Nucl. Phys. **B240**, 312 (1984).

[DJW89] A. M. Duif, A. G. Jansen and P. Wyder, J. Phys.: Cond. Matt. **1**, 3157 (1989).

[EA92] S. Eggert and I. Affleck, Phys. Rev. B **46**, 10866 (1992).

[EK92] V. J. Emery and S. Kivelson, Phys. Rev. B **46**, 10 812 (1992); Phys. Rev. Lett. **71**, 3701 (1993).

[EKP92] P. Esquinazi, R. Konig and F. Pobell, Z. Phys. B **87**, 305 (1992).

[Gan94] J.-W. Gan, J. Phys. Condens. Matter, **6**, 4547 (1994).

[Geo82] H. Georgi, *Lie Algebras in Particle Physics*, Benjamin/Cummings Publishing Comp. (1982).

[Gep87] D. Gepner, Nucl. Phys. **B287**, 111 (1987).

[GW86] D. Gepner and E. Witten, Nucl. Phys. **B278**, 493 (1986).

[GVR93] T. Giamarchi, C. M. Varma, A. E. Ruckenstein and P. Nozières, Phys. Rev. Lett. **70**, 3967 (1993).

[Gins87] Paul Ginsparg, in "Fields, Strings and Critical Phenomena", ed. by E. Brézin and J. Zinn-Justin, Elsevier Science Publishers B.V. (1989).

[GZC92] G. Golding, N. M. Zimmerman, S. N. Coppersmith, Phys. Rev. Lett. **68**, (1992).

[GSW87] M. B. Green, J. H. Schwarz and E. Witten, *Superstring Theory*, Vol. 1, Cambridge University Press (1987).

[GW78] G. Grüner and A. Zawadowski, in *Progress in Low Temperature Physics, Vol. VIIB*, ed. D. F. Brewer (North-Holland, 1978).

[HMG84] V. Hakim, A. Muramatsu and F. Guinea, Phys. Rev. B **30**, 464 (1984); A. J. Leggett *et al.*, Rev. Mod. Phys. **59**, 1 (1987).

[Hew93] A. C. Hewson, *The Kondo Problem to Heavy Fermions*, Cambridge University Press, 1993.

[Hers93] Selman Hershfield, Phys. Rev. Lett., **70**, 2134 (1993).

[HKH94] M. H. Hettler, J. Kroha, and S. Hershfield, Phys. Rev. Lett. **73**, 1967 (1994).

[HKH95] M. H. Hettler, J. Kroha, and S. Hershfield, unpublished. I thank these authors for their kind permission to included unpublished results of theirs in my thesis.

[HR86] S. Hunklinger and A. K. Raychaudhuri, in *Progress in Low Temperature Physics Vol. IX*, ed. D. F. Brewer (North-Holland, 1986).

[Ishi89] N. Ishibashi, Mod. Phys. Lett. **A4**, 251 (1989); T. Onogi and N. Ishibashi, Nucl. Phys., **B318**, 239 (1989).

[Jack75] J.D. Jackson, *Classical Electrodynamics,* 2nd Ed., John Wiley & Sons, N.Y. (1975), p. 427.

[JvGW80] A. G. M. Jansen, A. P. van Gelder and P. Wyder, J. Phys. C. **13**, 6073 (1980).

[KP84] V. G. Kac and K. Peterson, Adv. Math. **53**, 125 (1984).

[KB62] L. P. Kadanoff and G. Baym, *Quantum Statistical Mechanics,* Benjamin, New York (1962).

[Kel64] L. V. Keldysh, Zh. Eksp. Teor. Fiz. **47**, 1515 (1964) [Sov. Phys. JETP **20**, 1018 (1965)].

[KZ84] V. G. Knizhnik and A. B. Zamolodchikov, Nucl. Phys. **B247**, 83 (1984).

[KV60] W. Kohn and S. H. Vosko, Phys. Rev. **119**, 912 (1960).

[Kon64] J. Kondo, Prog. Theor. Phys. **32**, 37 (1964).

[KWW80] H. R. Krishnamurthy, H.R. Wilkins, K. G. Wilson, Phys. Rev. B**21**, 1003 & 1044, (1980).

[KOS77] I. O. Kulik, A. N. Omelyanchouk and R. I. Shekhter, Fiz. Nizk. Temp. **3**, 1543 (1977) [Sov. J. Low. Temp. Phys. **3**, 740 (1977)].

[KSO77] I. O. Kulik, R. I. Shekhter and A. N. Omelyanchouk, Solid State Comm. **23**, 301 (1977).

[LR85] P.A. Lee and T. V.Ramakrishnan, Rev. Mod. Phys. **57**, 287 (1985).

[Lud94a] A. W. W. Ludwig, Int. J. Mod. Phys. **B8**, 347 (1994).

[Lud94b] A. W. W. Ludwig, "Methods of Conformal Field Theory in Condensed Matter Physics — An Introduction to Non-Abelian Bosonization", Lecture Notes, Trieste 1992 (to be published).

[Lud95] A. W. W. Ludwig, private communication.

[LYSN80] A. A. Lysykh, I. K. Yanson, O.I. Shklyarevskii and Yu. G. Naydyuk, Solid State Comm. **35**, 987 (1980).

[ML95] J. M. Maldacena and A. W. W. Ludwig, preprint con-mat/9502109 (1995).

[MWL93] Y. Meir, N. S. Wingreen and P. A. Lee, Phys. Rev. Lett. **70**, 2601 (1993).

[WM94] N. S. Wingreen and Y. Meir Phys. Rev. B, **49**, 11040 (1994).

[Merz70] E. Merzbacher, *Quantum Mechanics,* 2nd. Ed., John Wiley & Sons (1970).

[MF95] A. L. Moustakas and D. S. Fisher, preprint cond-mat/9508011 (1995); see also Phys. Rev. B **51**, 6908 (1995).

[MG86] A. Muramatsu and F. Guinea, Phys. Rev. Lett. **57**, 2337 (1986).

[NO88] J. W. Negele and H. Orland, *Quantum Many-Particle Systems*, Addison-Wesley (1988).

[Noz74] P. Nozières, *J. Low. Temp. Phys.*, **17**, 31 (1974).

[Noz75] P. Nozières, *Proceedings of LT14*, Vol. **5**, North Holland (1975).

[Noz78] P. Nozières, J. Physique, **39**, 1117 (1978).

[NB80] P. Nozières and A. Blandin, J. Phys. (Paris) **41**, 193 (1980).

[OKS77] A. N. Omelyanchuk, I. O. Kulik and R. I. Shekhter, Pis'ma Zh. eksp. Teor. Fiz. **25**, 465 (1977) [JETP Lett., **25**, 437 (1977).

[PC91] H.-B. Pang, Ph.D. dissertation, The Ohio State University, unpublished (1992); H.-B. Pang and D. L. Cox, Phys. Rev. B **44**, 9454 (1991).

[Amb69] V. Ambegaokar, "The Green's Function Method", in *Superconductivity*, ed. R. D. Parks, Marcell Dekker (1969).

[Phil81] W. A. Phillips, ed., *Amorphous Solids: Low-Temperature Properties*, (Springer-Verlag, Berlin, 1981).

[Phil87] W. A. Phillips, Rep. Prog. Phys. **50**, 1657 (1987).

[Pol94] J. Polchinski, "What is String Theory", Lectures presented at the 1994 Les Houches Summer School "Fluctuating Geometries in Statistical Mechanics and Field Theory", hep-th/9411028 (1994).

[PT94] J. Polchinski and L. Thorlacius, Phys. Rev. **D50**, R622 (1994).

[Pol70] A. M. Polyakov, Pisma ZhETP **12**, 538 (1970) [JETP Lett. **12** 381 (1970)].

[RB88] K. S. Ralls and R. A. Buhrman, Phys. Rev. Lett. **60**, 2434 (1988); Phys. Rev. B **44**, 5800 (1991).

[RRB89] K. S. Ralls, D. C. Ralph and R. A. Buhrman, Phys. Rev. B **40**, 11561 (1989); Phys. Rev. B **47**, 10509 (1993).

[Ralph93] D. C. Ralph, Ph.D. dissertation, Cornell University (1993).

[RB92] D. C. Ralph and R. A. Buhrman, Phys. Rev. Lett. **69**, 2118 (1992).

[RB95] D. C. Ralph and R. A. Buhrman, Phys. Rev. B **51**, 3554 (1995).

[RLvDB94] D. C. Ralph, A. W. W. Ludwig, J. von Delft, and R. A. Buhrman, Phys. Rev. Lett. **72**, 1064 (1994).

[RLvDB95] D. C. Ralph, A. W. W. Ludwig, J. von Delft, and R. A. Buhrman, Phys. Rev. Lett. **75**, 771 (1995).

[RS86] J. Rammer and H. Smith, Rev. Mod. Phys. **58**, 323 (1986).

[Sak85] J. J. Sakurai, *Modern Quantum Mechanics,* Addison-Wesley (1985).

[SH95a] A. Schiller and S. Hershfield, Phys. Rev. B **51**, 12896 (1995). I thank these authors for showing me their results prior to publication.

[SH95b] A. Schiller and S. Hershfield, private communication.

[SML91] C. L. Seaman, M. B. Maple, B. W. Lee, S. Ghamaty, M. S. Torikachvili, J.-S. Kang, L. Z. Liu, J. W. Allen and D. L. Cox, Phys. Rev. Lett. **67**, 2882 (1991).

[SG94] A. M. Sengupta and A. Georges, Phys. Rev. B **49**, 10020 (1994).

[Sha91] R. Shankar, Lectures given at the BCSPIN School, Katmandu, May 1991, published in *Condensed Matter and Particle Physics*, Eds. Y. Lu, J. Pati and Q. Shafi, World Scientific (1993).

[Som54] A. Sommerfeld, *Optics,* Academic Press, N.Y. (1954), p.227.

[Theo91] N. D. Theodore, Ph.D. thesis, Cornell University, 1991 (unpublished).

[Ver88] E. Verlinde, Nucl. Phys. **B300**, 360 (1988).

[VZ83] K. Vladar and A. Zawadowski, Phys. Rev. B **28**, (a) 1564; (b) 1582; (c) 1596 (1983).

[VZZ86] K. Vladar, G. T. Zimányi and A. Zawadowski, Phys. Rev. B **56** 286 (1986).

[VZZ88] K. Vladar, A. Zawadowski and G. T. Zimànyi, Phys. Rev. B **37**, 2001, 2015 (1988).

[VZ85] K. Vladar and G. T. Zimányi, J. Phys. C **18**, 3755 (1985).

[vDLA95] J. von Delft, A. W. W. Ludwig and V. Ambegaokar, unpublished.

[WT85] P. B. Wiegmann and A. M. Tsvelick, Z. Physik **B54**, 201 (1985).

[Wil75] K. G. Wilson, Rev. Mod. Phys., **47**, 773 (1975).

[WAM95] N. S. Wingreen, B. L. Altshuler and Y. Meir, Phys. Rev. Lett. **75**, 770 (1995).

[WA94] E. Wong and I. Affleck, Nucl. Phys. B **417**, 403 (1994).

[YS86] I. K. Yanson and O. I. Shklyarevskii, Fiz. Nizk. Temp. **12**, 899 (1986) [Sov. J. Low. Temp. Phys. **12**, 509 (1986)].

[YA70] G. Yuval and P. W. Anderson, Phys. Rev. B **1**, 1522 (1970).

[YA84] C. C. Yu and P. W. Anderson, Phys. Rev. B **29**, 6165 (1984).

[Zar93] G. Zaránd, Solid St. Comm. **86**, 413 (1993).

[Zar95] G. Zaránd, Phys. Rev. B **51**, 273 (1995).

[ZZ94a] G. Zaránd and A. Zawadowski, Phys. Rev. Lett. **72**, 542 (1994).

[ZZ94b] G. Zaránd and A. Zawadowski, Phys. Rev. B **50**, 932 (1994).

[Zaw80] A. Zawadowski, Phys. Rev. Lett. **45**, 211 (1980).

[ZV92] A. Zawadowski and K. Vladar, in *Quantum Tunneling in Condensed Media,* ed. Yu. Kagan and A. J. Leggett (Elsevier, 1992) p. 427.

[Ziman] J. M. Ziman, *Principles of the Theory of Solids,* 2nd Ed., Cambridge University Press (1972).

[ZGH91] N. W. Zimmerman, B. Golding, W. H. Haemmerle, Phys. Rev. Lett. **67**, 1322 (1991).